8-24-2012

Synthesis and Catalytic Applications of Platinum(II) and Palladium(II)-PTA and DAPTA Complexes

Sitaram Acharya
University of Missouri-St. Louis, saxd6@mail.umsl.edu

Synthesis and Catalytic Applications of Platinum(II) and Palladium(II)-PTA and DAPTA Complexes

---

A dissertation submitted in partial fulfillment of the requirements for the degree

Doctor of Philosophy in Chemistry

Sitaram Acharya

M. S., Chemistry, University of Missouri-St. Louis, St. Louis, Missouri, 2009
M. Sc., Chemistry, Tribhuvan University, Kathmandu, Nepal, 1995
B. Sc., Science, Tribhuvan University, Kathmandu, Nepal, 1993

Advisory Committee

Janet Braddock-Wilking, Ph. D. (Chairperson)

James S. Chickos, Ph. D.

Wesley R. Harris, Ph. D.

Eike Bauer, Ph. D.

University of Missouri-St. Louis, St. Louis, Missouri

July-2012

Abstract

The cage-like tertiary phosphine, 1,3,5-triaza-7-phosphaadamantane (PTA) has recently received interest because of its water-solubility, air-stability, non-ionic, non-surfactant, and basic nature. These properties can solubilize transition metal complexes in the aqueous phase. A related air-stable derivative, *N,N'*-diacetyl-1-3-5-triaza-7-phosphaadamantane (DAPTA) has greater water-solubility than PTA, however, its coordination chemistry has not been significantly explored.

This study involved the synthesis and characterization of a series of novel air-stable and water-soluble four-coordinated dialkyl, dialkynyl, dihalo, and halo(alkyl) complexes of platinum and palladium bearing PTA and DAPTA ligands. The alkyl complexes of the type $MX(R)P_2$ (M = Pt, Pd; X = Cl, Br, I; R = Me, Et; P = PTA, DAPTA) were obtained as the *trans*-isomers whereas the dialkyl or dihalo complexes of the type MX'_2P_2 (X' = Me, Br) were isolated as *cis*-isomers except *trans*-MI_2P_2. The complexes were characterized by multinuclear NMR, IR, MS, and elemental analysis experiments. X-ray crystallographic studies were performed on some of the complexes and confirmed a square planar geometry.

The complex, *cis*-$PtMe_2(PTA)_2$ was found to be a very effective catalyst in hydrosilylation reactions of alkenes, alkynes, and a ketone using a variety of tertiary hydrosilanes including siloles and silafluorenes, with good regioselectivity and relatively low catalyst loading. The hydrosilylation reaction of terminal alkynes formed the *β-trans* isomer as the major product and the *α*-isomer as a minor product. This study is the first example of using a transition metal PTA complex as a pre-catalyst for hydrosilylation reactions.

III

The Suzuki-Miyaura and Sonogashira cross-coupling reactions are some of the most common C-C bond forming reactions. The complex, *trans*-$PdCl(Me)(PTA)_2$ was found to be effective in catalyzing Suzuki-Miyaura cross-coupling reactions of a series of haloarenes with phenylboronic acid with minimal homo-coupling, especially in isopropanol solvent. The previously reported complex, *cis*-$PdCl_2(PTA)_2$ was found to catalyze Sonogashira cross-coupling reactions of haloarenes with terminal alkynes effectively with minimal side reactions in piperidine in the absence of Cu(I) salts. The effects of substituents and leaving groups in both kinds of cross-coupling reactions have been investigated.

Acknowledgment

First and foremost I offer my sincerest gratitude to my advisor, Dr. Janet Braddock-Wilking, who has supported me throughout my thesis with her patience and knowledge whilst allowing me the room to work in her research lab. Because of her understanding, encouragement, and personal guidance, one simply could not wish for a better or friendlier advisor.

My thanks and appreciation goes to my thesis committee members, Dr. James S. Chickos, Dr. Wesley R. Harris, and Dr. Eike Bauer for their valuable suggestions and comments. I wish to thank Dr. Joyce Y. Corey for her useful suggestions related to my research.

I would like to thank Dr. Nigam P. Rath for solving the X-ray crystal structures and Dr. Rensheng Luo for assisting me in NMR experiments. My thanks also go to Dr. Rudolf E. K. Winter and Mr. Joe Kramer for their assistance in mass spectrometry, Dr. Dan Zhou and Dr. David Osborn for SEM and EDS, and Dr. Kevin J. Koeller for HPLC-MS experiments.

All my labmates, who always created an excellent working environment in the laboratory through mutual cooperation, are highly acknowledged. My special thanks also go to Professors Mohan B. Gewali and Jay K. Shrestha from Tribhuvan University, Kathmandu (Nepal) for their motivation towards my graduate study. All the folks who directly / indirectly inspired or supported me during my doctoral study are also thankful.

This dissertation is simply impossible without the physical and moral support of my family members; especially my parents, my wife; Bina, and my daughters; Ishika and Ishma.

The financial support from National Science Foundation to our research project is gratefully acknowledged. Finally, I would like to express my thanks to the Department of Chemistry and Biochemistry and Center for Nanoscience, University of Missouri-St. Louis for providing me an opportunity for my doctoral study.

Table of Contents

List of Abbreviations

COD	1,5-cyclooctadiene
cp	Cyclopentadienyl
DAPTA	*N,N'*-diacetyl-1,3,5-triaza-7-phosphaadamantane
DFPTA	*N,N'*-diformyl-1,3,5-triaza-7-phosphaadamantane
DFT	Density Functional Theory
dmPTA	*N,N'*-dimethyl-1,3,5-triaza-7-phosphaadamantane
DMSO	Dimethylsulfoxide
dppa	1,2-bis(diphenylphosphino)acetylene
dppe	1,2-bis(diphenylphosphino)ethane
dppf	1,1-bis(diphenylphosphino)ferrocene
dppm	1,1-bis(diphenylphosphino)methane
dppp	1,3-bis(diphenylphosphino)propane
EDS	Energy-dispersive X-ray spectroscopy
EI-MS	Electron ionization-mass spectrometry
ESI-MS	Electron spray ionization-mass spectrometry
FAB-MS	Fast atom bombardment-mass spectrometry
GC	Gas chromatography
GC-MS	Gas chromatography-mass spectrometry
HOMO	Highest occupied molecular orbital
HPLC	High performance liquid chromatography
HRMS	High resolution mass spectrometry
IR	Infra red
LUMO	Lowest unoccupied molecular orbital

mPTA	*N*-methyl-1,3,5-triaza-7-phosphaadamantane
nbe	norbornene
NHC	*N*-heterocyclic carbene
NMR	Nuclear magnetic resonance
py	Pyridine
pyrim	Pyrimidine
OTf	OSO_2CF_3
PTA	1,3,5-triaza-7-phosphaadamantane
PtNps	Platinum nanoparticles
SEM	Scanning electron microscopy
THF	Tetrahydrofuran
THMP	Tris(hydroxymethyl)phosphine
TMEDA	*N*,*N*, *N'*,*N'*-(tetramethyl)ethylenediamine
TPPDS	Doubly *meta*-sulfonated triphenylphosphine
TPPMS	Mono *meta*-sulfonated triphenylphosphine
TPPTS	Triply *meta*-sulfonated triphenylphosphine
TON	Turn over number
Ts	$CH_3C_6H_4SO_2$

Alkyl and aryl radicals: R (alkyl), Ar (aryl), Me (methyl), Et (ethyl), ^{n}Pr (*n*-propyl), ^{i}Pr (isopropyl), ^{t}Bu (tertiary butyl), Ph (phenyl), Bz (benzyl), tol (tolyl), Mes (mesityl).

1. General Introduction

This section provides an introduction to the PTA and PTA-derivatized ligands and their coordination chemistry with the Group 10 metals, platinum and palladium. A brief overview on the catalytic applications of the PTA complexes of platinum and palladium is also given. At the end of the section, the main objective of the research project is described.

1.1 Platinum and Palladium-PTA and DAPTA Complexes

Transition metal complexes are widely known for their catalytic applications in a variety of reactions. Late transition metal complexes, especially those of Group 10 metals, have significant applications in catalysis because of their ability to form coordination compounds in various oxidation states which is essential for the catalytic cycle.[1, 2, 3]

1.1.1 PTA: a water-soluble phosphine

Organophosphines are one of the most common ligands used in organometallic chemistry due to their ability to stabilize metals in low oxidation states and the ability to influence both steric and electronic properties of the catalyst. An advantage of utilizing phosphines as ligands for metal complexes is that the electronic and steric effects can be tuned through modification of the substituents.[1] As a result, this can be beneficial for homogeneous catalysis whereby the activity or selectivity of the catalyst can be modified. In addition, water-solubility can be enhanced by modifying the phosphine by

incorporation of polar or ionic groups such as hydroxyl or amine units as well as sulfonate, carboxylate, and ammonium groups. Water-soluble transition metal complexes can be generated by complexation with such kind of hydrophilic phosphines.[1] Examples of water-soluble monodentate aryl phosphine derivatives that are widely used are the sulfonated analogues of PPh_3 such as monosulfonated TPPMS and tris-sulfonated TPPTS. Despite their higher water-solubility, the sulfonated phosphines are known to be good surfactants (Figure 1.1.1a).[1b]

One such monodentate system, 1,3,5-triaza-7-phosphatricyclo-[3.3.1.1]decane (or 1,3,5-triaza-7-phosphaadamantane, PTA) (Figure 1.1.1b), has recently received considerable attention due to its ease of synthesis, high water-solubility (235 mg/mL), resistance to oxidation, non-ionic nature, and air-stability.[1]

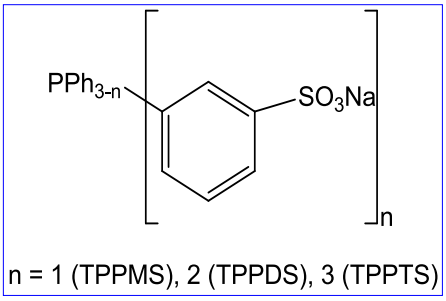

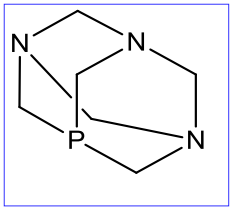

(PTA)

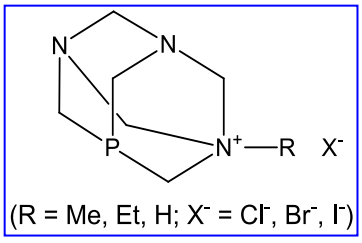

(RPTA$^+$X$^-$)

Figure 1.1.1a. Some sulfonated phosphines. **Figure 1.1.1b.** Structure of PTA. **Figure 1.1.1c.** Structure of RPTA$^+$X$^-$.

The PTA ligand is also soluble in a number of organic solvents such as methanol, ethanol, dimethyl sulfoxide, tetrahydrofuran, methylene chloride, and chloroform.[1, 2] Moreover, owing to its basic character (protonation p*K*a = 5.70) it is able to coordinate with a number of transition metals, especially with the metals which act as soft bases such as Pt, Pd, Co, Rh, and Ir.[3] Unlike the sulfonated phosphines, it is a poor surfactant.

The most widely used method to determine the steric behavior of a ligand when coordinated to a metal center utilizes the Tolman cone angle (Table 1.1.1 and Figure 1.1.2).[4] The effective cone angle 118° for the PTA in the Pt complexes,[5a] which is the same as that of PMe_3,[4] illustrates the rigidness and a small steric size of the ligand. However, Alyea *et al.* have reported the cone angle of PTA to be 102° in a five-coordinated molybdenum complex.[5b] These electronic and steric factors make PTA a unique ligand in transition metal complexes.[5]

Table 1.1.1. Tolman cone angle values of different phosphines.

Ligand	Tolman cone angle[4]
$Me_2P(CH_2)_2PMe_2$	107
$P(OEt)_3$	109
PMe_3	118
PTA	118[5a]
$Ph_2P(CH_2)_2PPh_2$	127
PEt_3	132
P^nPr_3	132
$P(CF_3)_3$	137
PPh_3	145
PCy_3	170
P^tBu_3	182

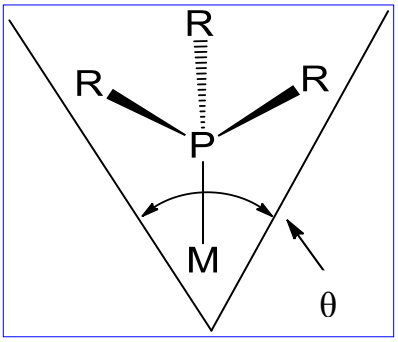

Figure 1.1.2. Tolman cone angle of a tertiary phosphine.

1.1.2 Importance of transition metal PTA complexes

Transition metal PTA complexes have mainly three types of applications: catalytic, biological, and photoluminescence.[1] Many electron-rich transition metal complexes,

especially those containing Group 10 metals in low oxidation states containing ligands such as tertiary phosphines and olefins display efficient catalytic activity.[6] Tertiary phosphines, PR_3, are important ligands since their electronic and steric properties are readily tunable by varying the nature of the R group (R = alkyl, aryl).[1, 6] The PTA ligands may be a good alternative to the traditionally used alkyl or aryl substituted tertiary phosphines. The PTA complexes of the electron-rich Group 10 metals, such as platinum and palladium, have great potential in applications as organometallic-based catalysts because of the ease in preparation and their resistance to reactivity with air and moisture. Due to the water-solubility of the PTA ligand, these complexes can also form a biphasic reaction mixture which may possibly aid the separation and recycling of the catalyst, a major concern in homogeneous catalysis.[7-9] Due to these factors, PTA has been employed as a ligand in catalytic hydroformylation reactions,[7a] hydrogenation reactions,[7b] cross-coupling reactions,[8] and ethylene polymerization reaction,[9] in aqueous-organic biphasic and monophasic systems. The carbonylation reaction of benzyl chloride has also been shown to be catalyzed by water-soluble phosphine complexes of palladium in a biphasic system.[10] Krogstad *et al.* have investigated intramolecular hydroamination reactions in aqueous and organic media catalyzed by some palladium(II) and platinum(II)-PTA complexes.[2c, 11]

Additionally, Ru,[12] Rh, Os,[13] Cu, Au,[14] and Pt[15] complexes of PTA have also been shown to exhibit cytotoxic properties. For illustration, the antitumor activity of the ruthenium(II) arene PTA complexes (abbreviated RAPTA), $[RuCl_2(\eta^6\text{-arene})(PTA)]$, (arene = *p*-cymene, toluene, benzene, benzo-15-crown-5, 1-ethylbenzene-2,3-dimethylimidazolium tetrafluoroborate, ethyl benzoate, hexamethylbenzene) has been

evaluated.[12] These compounds are found to be active toward the TS/A mouse adenocarcinoma cancer cell line, however cytotoxicity on the HBL-100 human mammary (non-tumor) cell line was not found with concentrations up to 0.3 mM indicating good selectivity of the ruthenium(II) arene complexes to certain cancer cells. Derivatives of the RAPTA compounds, with the methylated PTA ligand, have been synthesized and these have proved to be cytotoxic toward both cell lines according to *in vitro* experiments.[12] A related ligand resembling PTA, 1-adamantamine, shows good antitumour activity against angio- and pancreatic carcinoma whereas the complex, $PtCl_2$(DAA) (DAA = 1,2-diaminoadamantane) is presently used in Japan as a therapeutic anti-cancer drug.[16] Complexes of platinum(II) containing water-soluble ligands in a *cis*-arrangement are of significant importance for their potential use in drug design due to their similarity to cisplatin. It is often assumed that a β-hydrogen is a prerequisite for biological activity,[17a] however, a recent study showed biological activity of the complexes without a β-hydrogen atom.[17b] This indicates the importance of additional studies involving platinum(II) complexes containing alternate ligand systems, such as water-soluble phosphines. Additionally, photoluminescence properties of gold PTA complexes (PTA)AuBr, (PTA)AuI, and [(PTAH)AuI][AuI_2] have also been investigated.[18]

1.1.3 DAPTA and other PTA-derivatized ligands

It is also possible to alkylate or protonate one of the nitrogen bases in PTA to afford the ionic ligands $PTAMe^+$ and $PTAH^+$, respectively, thus providing additional solubility properties in water (Figure 1.1.1c).[19a] Most of the modifications involving PTA have concerned the triazacyclohexane ring known as the *lower rim* and in particular the

nitrogen atoms. First of all, due to the basicity of PTA (protonation p*K*a = 5.70), in aqueous solution at pH lower than 6.5, PTA can be *N*-protonated giving the corresponding phosphonium complex, $[PTAH]^+X^-$. Additional *N*-protonation is not favoured as demonstrated by a combined study involving experimental data and *ab initio* calculations. It has been shown that the increase in ring cage strain of the PTA ligand determines the decrease of its stability arising from a change in the hybridization of the nitrogen centers.[19]

The PTA can be alkylated at one nitrogen atom by performing the reactions with several electrophiles such as CH_3I, C_2H_5I, $PhCH_2Cl$, or $(CH_2)_4I$ in water, acetone, or methanol under reflux conditions.[19b-d] Bis-methylation on the lower rim of PTA can be achieved by reacting PTA with 2 molar equivalents of MeOTf under reflux in dry acetone.**Error! Bookmark not defined.** The reaction led to a formation of a dicationic erivative of PTA, *N*,*N*'-dimethyl-1,3,5-triaza-7-phosphadamantane [dmPTA] as the triflate salt, $[dmPTA](OTf)_2$ (Equation 1.1.1) which has a cone angle (steric behavior) and electronic properties similar to PTA and shows a good water-solubility ($S_{25\ °C}$ = 12 mg/mL).[20]

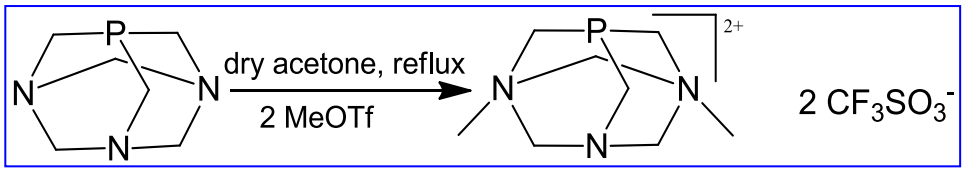

Equation 1.1.1. Synthesis of N'N'-dimethylPTA triflate (dmPTA triflate).

The bis(phosphine) derivatives linking two PTA molecules *via* the N atoms have been prepared by the reaction of PTA with differently substituted dibenzyl bromides (Scheme 1.1.1). Depending on the position of the substituents on the aromatic ring, the

resulting *ortho*-, *para*-, and *meta*-substituted ligands presented a remarkable difference in water-solubility. The *ortho*-derivative was found to have the highest solubility in water ($S_{25\,°C}$ = 2000 mg/mL). The *meta*-phosphine also showed a very good water-solubility ($S_{25\,°C}$ = 810 mg/mL), while the water-solubility of the *para*-analogue was found to be very low compared to the other isomers ($S_{25\,°C}$ = 12.5 mg/mL).[21]

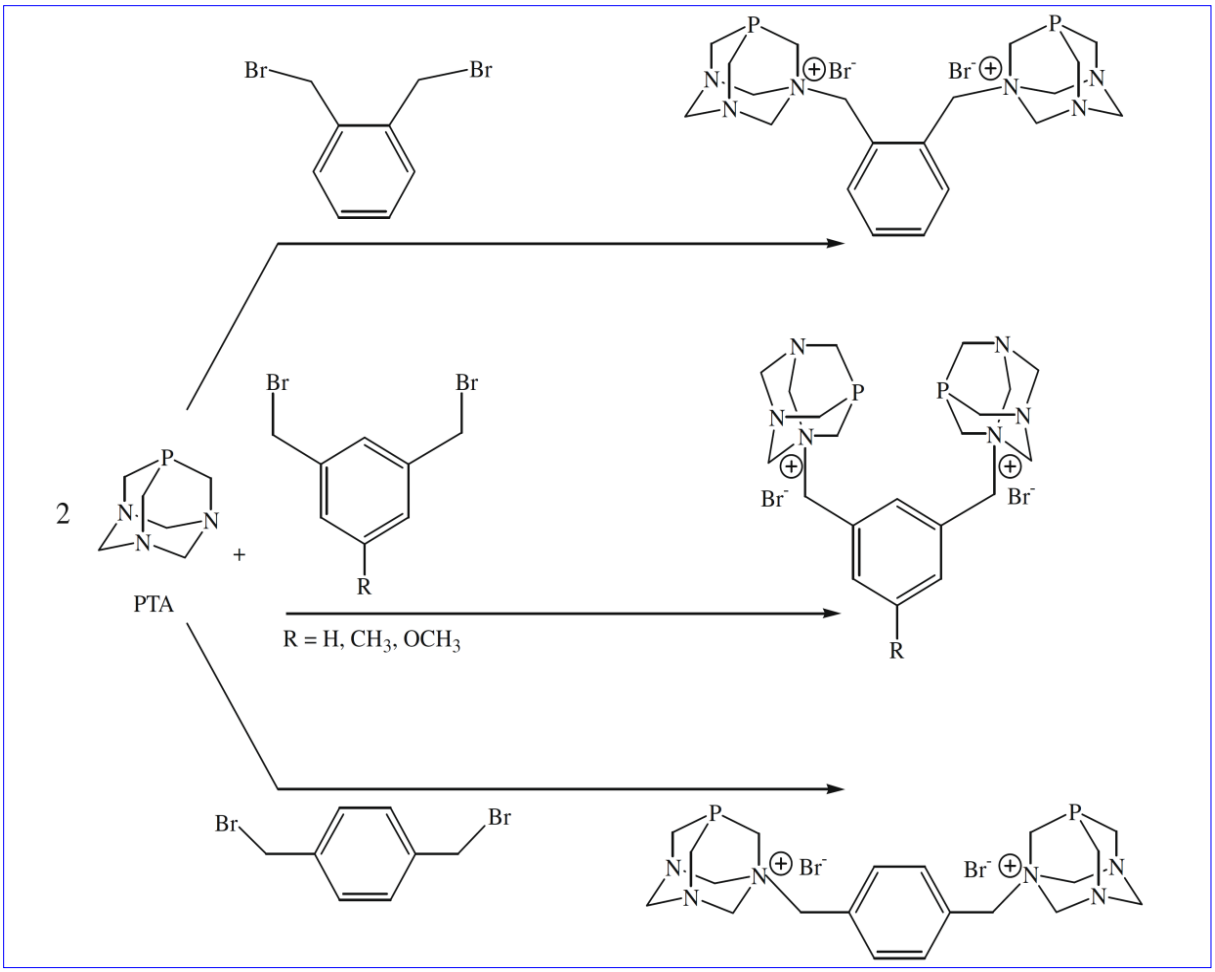

Scheme 1.1.1. Synthesis of bidentate bis(PTA) ligands.

Selective open-cage derivatives of PTA can be prepared by cleaving a C-N bond of the triazacyclohexane ring. The diacetyl derivative of PTA, called DAPTA (DAPTA = *N,N'*-diacetyl-1,3,5-triaza-7-phosphaadamantane), has been recently reported.[22] To date,

only a small number of complexes containing this ligand are known.[22] Reaction of water or acetone solution of PTA and PTA(O) with *ca.* 3 molar equivalents of acetic anhydride at 0 °C provided the corresponding acylated products DAPTA and its oxide DAPTA=O, respectively (Equation 1.1.2).[22] More importantly, the water-solubility of DAPTA was found to be excellent ($S_{25\,°C}$ = 7.4 M)[22a] and its binding ability toward a variety of metal centers such as Ni, Pt, Pd, and Au was shown to be comparable to that of PTA.[22]

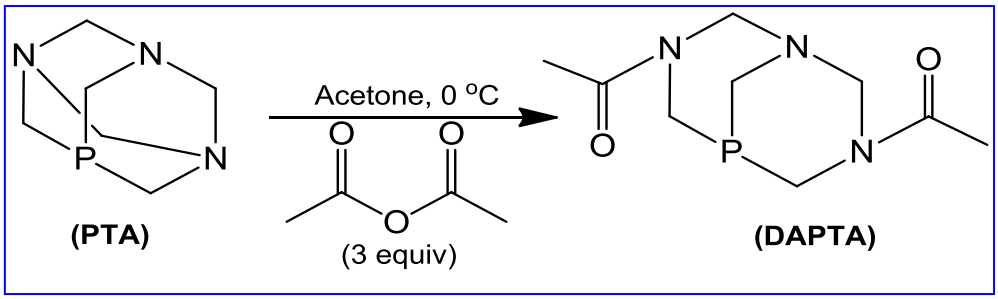

Equation 1.1.2. Synthesis of DAPTA.

The formyl analogue of DAPTA, *N,N'*-diformyl-1,3,5-triaza-7-phosphaadamantane (DFPTA), was prepared from the reaction of formic anhydride (pepared *in situ*) with an aqueous solution of PTA at -5 °C.[23] After the solvent removal and extraction with ethanol, DFPTA was obtained as an air-stable solid. Surprisingly, its solubility in a variety of solvents, including water, was found to be considerably less than that of the DAPTA ligand.[23]

A cavity is created within the cage structure of the rigid DAPTA ligand (Figure 1.1.3) as evident from the space-filling model.[22a] The clearly exposed phosphorus atom

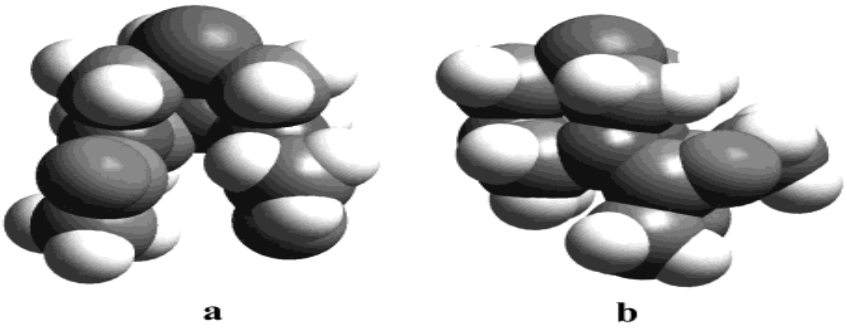

Figure 1.1.3. Space-filing model of DAPTA showing (a) front and (b) side view.[22a]

facilitates binding to a metal center. Additionally, the exposed acyl-free nitrogen and oxygen atoms also facilitate hydrogen bonding to the surrounding aqueous environment. The calculated cone angle was found to be similar to that reported for PTA (~ 118^{o}).[5a] Because of its water-solubility, the υ(C=O) vibration of aqueous solution of DAPTA appears at 1608 cm^{-1}, which is *ca.* 34 cm^{-1} lower energy than that observed in weakly interacting organic solvents. This is indicative of a strong interaction of the C=O bond dipoles with water. The binding ability of DAPTA toward a variety of transition metal centers was shown to be very much comparable to that of the parent PTA ligand, which in turn compares favorably with the air-sensitive PMe_3 ligand.[22a] The M-P bond distances observed in corresponding metal complexes of PTA and DAPTA also support this fact. For example, the W-P bond distances in $(CO)_5W(PTA)$, $(CO)_5W(DAPTA)$, and $(CO)_5W(PMe_3)$ are found to be 2.4976(15), 2.492(3), and 2.516(3) Å, respectively. Further evidence for the relative binding abilities of the PTA and DAPTA ligands was provided by the similarities in the υ(C=O) stretching frequencies in $M(CO)_5L$ complexes (M = Cr, W and L = PTA, DAPTA).[22a, 24]

On the other hand, a number of transition metal PTA and DAPTA complexes do not reflect the solubility trend of the corresponding ligands. For instance, $Ni(DAPTA)_4$ is highly soluble in organic solvents and insoluble in water, whereas the $Ni(PTA)_4$ analogue

is highly water-soluble.[22a] Similarly, a number of new platinum(II)-DAPTA complexes synthesized during the current study have been found to possess poorer solubility in water than their PTA analogues; which will be discussed in detail in the "*Results and Discussion*" section.

1.1.4 Characterization of PTA and DAPTA

Infrared (IR) spectroscopy is poorly diagnostic for the PTA ligand showing two characteristic absorption bands at 452 and 405 cm^{-1} in the far-IR spectrum.[25] The ^{1}H NMR spectrum of PTA in D_2O shows an AB quartet signal at 4.42 ppm ($^{2}J_{HH}$ = 12.5 Hz) corresponding to the six protons of NCH_2N and a doublet at 3.89 ppm ($^{2}J_{PH}$ = 9.0 Hz) corresponding to the hydrogens of the -CH_2 groups bound to phosphorus.[2a] The derivatization of both the *lower* and *upper rim* of the PTA core causes a decrease of molecular symmetry giving rise to highly complex ^{1}H NMR spectra.[20, 22] On the contrary, the $^{31}P\{^{1}H\}$ NMR spectrum for PTA in D_2O shows a singlet at -98.7 ppm[2a] whereas the $^{31}P\{^{1}H\}$ NMR spectrum for DAPTA in $CDCl_3$ shows a singlet at -78.5 ppm.[22a] This is an important method to investigate the coordination chemistry of the PTA and DAPTA ligands, and to study the *in situ* mechanism of the reactions catalyzed by PTA or DAPTA complexes of the transition metals. All ^{1}H NMR resonances associated with the -CH_2 carbons in DAPTA exhibit the ^{1}H-^{31}P couplings around 13 Hz.[22] The -CH_3 hydrogens on the [C(O)CH_3] functionality are observed as a singlet at 1.96 ppm in the ^{1}H NMR spectrum . On the contrary to what is expected for the *anti* conformation (*vide infra*), a single resonance for the acyl carbons is displayed at 168.9 ppm in the $^{13}C\{^{1}H\}$ NMR spectrum of DAPTA in $CDCl_3$.[22a]

On the other hand, both the ^{13}C and ^{1}H NMR spectra of DAPTA indicate a mixture of the *syn* and *anti* conformers present in aqueous solution. The $^{13}C\{^{1}H\}$ NMR resonances of the acyl carbon, [N*C*(O)CH_3] occur at 172.2 and 171.7 ppm, with the latter being about one-fourth the intensity of the former.[22] The two acyl groups adopt an *anti* conformation in the solid state (*vide infra*), with the experimental barrier of rotation of the N-C(O) bond *ca.* 18-19 kcal/mol which is generally ascribed to the σ-electronic resonance model of an amide. A large part of the rotational stability of the N-C bond is assigned to a Coulombic interaction *via* the σ-system between the N atom and C atom of the amide group according to *ab initio* calculations.[22a]

1.1.5 Coordination chemistry of PTA and DAPTA

The coordination chemistry of PTA and DAPTA involves either the phosphorus atom which coordinates to the transition metals acting as soft bases or nitrogen atoms which coordinate preferentially to the metals acting as hard bases.[1] Fewer examples of *N*-coordinated PTA complexes are described in the literature.[26] Owing to the hard nature of manganese(II) as well as N atoms of PTA, the *N*-coordinated complexes such as [MnX_2(PTA-κN)$_2$(H_2O)$_2$] (X = Cl, Br) have been prepared from the reaction of the hydrated MnX_2 salts and PTA.[26a] Another *N*-coordinated PTA complex, $ZnCl_2$(PTA)$_2$ was recently prepared by the reaction of $ZnCl_2$ with 2 molar equivalents of PTA which is also the first zinc complex bearing a PTA ligand.[26b] An increasing number of examples of P- and N-coordinated PTA complexes are appearing in the literature.[1] The PTA complexes coordinated by phosphorus are more numerous and have several applications.[1]

Some examples of the PTA complexes coordinated by phosphorus and nitrogen atom are given in Figure 1.1.4.[22, 26]

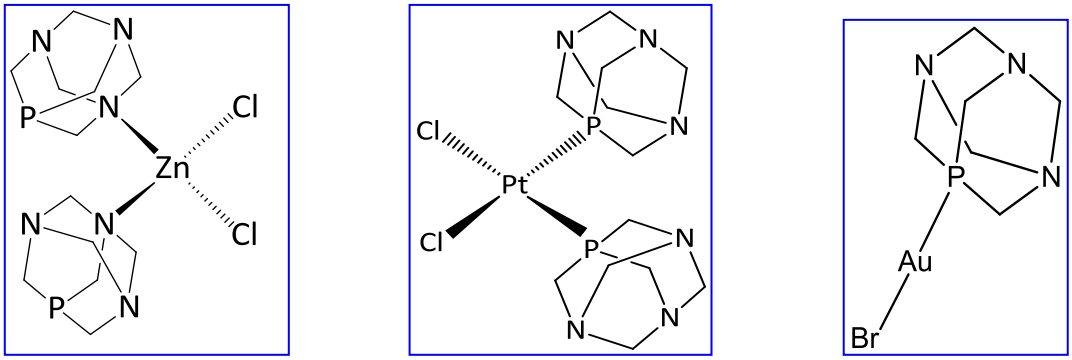

Figure 1.1.4. Some N- and P-coordinated transition metal PTA complexes.[2c, **Error! Bookmark not**

a ligand exchange reaction by heating PTA with $Mo(CO)_6$ in dry diglyme or alternatively, by the reaction of the THF adduct of $Mo(CO)_5$ with PTA.[24] This procedure, was also applied to obtain $Cr(CO)_5$(PTA) and $W(CO)_5$(PTA) from $Cr(CO)_6$ and $W(CO)_6$, respectively.[24]

1.1.6 PTA and DAPTA complexes of Group 10 metals

A variety of late transition metal PTA and DAPTA complexes, including those of platinum and palladium, have been synthesized from their amines or phosphine analogues.[1] These complexes are known for their catalytic and medicinal applications. For example, the reaction of the dimeric complex, [Pd(dmba)(μ-Cl)$_2$ [dmba = N,C-chelating 2-(dimethylaminomethyl)phenyl] with 2 equivalents of PTA in CH_2Cl_2 yielded the air-stable monomeric complex, [Pd(dmba)Cl(PTA)] (Equation 1.1.3).[8] This complex

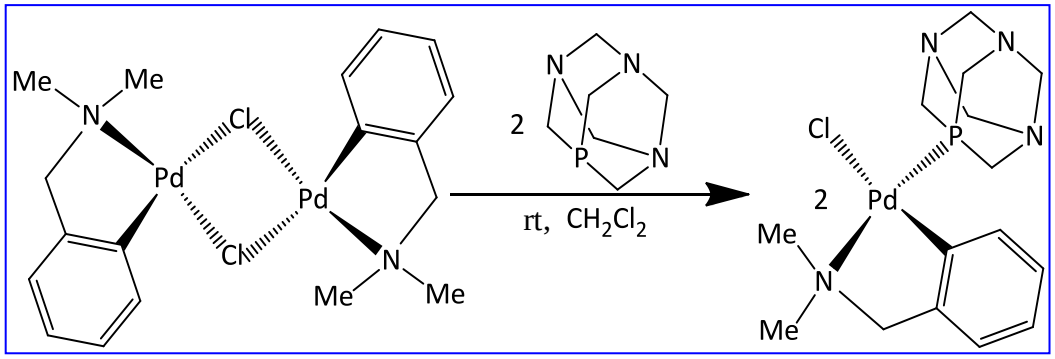

Equation 1.1.3. Synthesis of [Pd(dmba)Cl(PTA)].[8]

was used as a catalyst in copper- and amine-free Sonogashira cross-coupling reactions.[8] The more stable *cis*-$PtCl_2(PPh_3)$(PTA) was synthesized using a ligand displacement method by the reaction of *cis*-$PtCl_2(PPh_3)_2$ with PTA in 1 : 1 molar ratio. This complex was investigated in cell growth inhibition tests.[27]

A palladium DAPTA complex, [Pd(salicylaldiminato-κ^2-N,O)(DAPTA)(Me)] was prepared by the reaction of $PdMe_2$(TMEDA) with DAPTA and salicylaldimine in toluene at -30 °C.[22a] Some of the Pd complexes that act as fluorination catalysts, *trans*-$PdX(Ph)(PTA)_2$ (X = Br, I), were synthesized by treating *trans*-$PdX(Ph)(PPh_3)_2$ with 2 molar equivalents of PTA in CH_2Cl_2. These complexes showed the expected two signals in the $^{31}P\{^1H\}$ NMR spectra with chemical shifts of -68.3 and -66.3 ppm, respectively.[28] The dichloro palladium(II) complex containing the open-cage DAPTA ligand, *cis*-$PdCl_2(DAPTA)_2$ was prepared by the reaction of $PdCl_2$ with 2 molar equivalents of DAPTA.[22b] Similarly, *trans*-$Pd(SR)_2P_2$ (R = py, pyrim; P = PTA, DAPTA) complexes were prepared when *cis*-$PdCl_2P_2$ was added to a solution of the sodium salt of the thiol derivatives in absolute EtOH which was prepared *in situ* from the reaction of the thiol derivative and NaOEt. The complexes displayed two bands in the far-IR spectrum corresponding to υ(Pd-P) and υ(Pd-Cl) stretches; consistent with the *trans*-geometry.[22b]

1.1.7 Cyclooctadiene complexes as precursors for the synthesis of PTA complexes

The most efficient method for the synthesis of late transition metal phosphine complexes is the ligand substitution method using the corresponding COD (COD = η^4-1,5-cyclooctadiene) complex. The ligands such as COD, PhCN, or TMEDA are often

labile and can easily be replaced by tertiary phosphines which leads to the formation of thermodynamically stable M-P bonds (M = Pt, Pd etc.) and stable COD, PhCN, or TMEDA molecules.[11, 22, 29a,b] The PTA complexes *cis*-[$PtX_2(PTA)_2$] (X = Cl, Br, I) were prepared bythe reaction of the corresponding *cis*-PtX_2(COD) precursor with 2 equivalents of PTA in CH_2Cl_2.[2c] The $^{31}P\{^1H\}$ NMR spectra exhibited a singlet with platinum satellites having about the 1/3rd intensity of the main signal due to the coupling of ^{31}P nucleus with another spin ½ nucleus, ^{195}Pt which has *ca.* 33% of natural abundance. The $^1J_{PtP}$ values of the chloro-, bromo-, and iodo-derivative (3350, 3432, and 2509 Hz, respectively) clearly showed a *cis*-phosphine configuration.[2c] Although the *cis* iodo-complex has a significantly lower $^1J_{PtP}$ value (2509 Hz) than the bromo- and chloro-analogues, the $^1J_{PtP}$ value for the *trans*-$PtI_2(PTA)_2$ complex which was prepared by treating *cis*-$PtCl_2(PTA)_2$ with NaI was reported to be 2316 Hz.[29c] The PTA complexes, *cis*-$PdX_2(PTA)_2$ (X = Cl, Br) were prepared in a similar way, by reacting the corresponding *cis*-PdX_2(COD) precursor with 2 molar equivalents of PTA in CH_2Cl_2.[11]

The complexes, *cis*-$MX_2(PTA)_2$ (M = Pt, Pd) were used as catalysts for intramolecular hydroamination reactions of terminal alkynylamines in water.[2c, 11] Recently, cycloisomerization (or heteroannulation) reaction of (*Z*)-enynols into furans in green solvents such as water and glycerol catalyzed by the *cis*-$PdCl_2L_2$ (L = PTA, DAPTA) complexes has also been reported.[29d] The crystal structure of another square planar platinum(II)-PTA complex, *trans*-$Pt(CN)_2(PTA)_2$ was reported; the bond length data suggested that the PTA ligand has a higher *trans*-influence than the nitrile group.[29]

The $^1J_{PtP}$ coupling constants of a variety of platinum(II)-PTA and the related triphenylphosphine complexes in the $^{31}P\{^1H\}$ NMR spectra are listed in Table 1.1.2.

Table 1.1.2. $^{1}J_{PtP}$ values for different Pt(II) phosphine complexes.

Complex	**$^{1}J_{PtP}$, Hz**	**Reference**
cis-$PtCl_2(PTA)_2$	3350	2c
cis-$PtBr_2(PTA)_2$	3432	2c
cis-$PtI_2(PTA)_2$	2509	2c
trans-$PtI_2(PTA)_2$	2316	29c
cis-$PtPh_2(PTA)_2$	1560	35
cis-$PtCl_2(PPh_3)_2$	2627	29f
trans-$Pt(CN)_2(PTA)_2$	2060	29e

1.1.8 Platinum(II) and palladium(II) alkynyl phosphine complexes

There is considerable current interest in transition metal σ-bonded alkynyl complexes because of their synthetic, catalytic, and material applications.[30, 31] The alkynyl ligand has been reported to be a good σ- and π-donor ligand, but a poor π-acceptor.[30, 31] The platinum(II) or palladium(II) alkynyl complexes are synthesized by the reaction of an alkynyl anion or a main group covalent alkynyl compound with a platinum(II) or palladium(II) precursor. Formation of these complexes also takes place by the oxidative-addition of a terminal alkyne or chloroalkyne to a platinum(0) or palladium(0)

precursor.[30] Such complexes are generally stabilized by good σ-donors such as phosphine ligands.[31]

Platinum σ-bonded ethynyl complexes were first prepared by Hagihara and coworkers in 1977.[31a] For the Group 10 alkynyl systems, the majority of the studies have been concentrated on *trans*-platinum bis(phosphine) complexes. Platinum alkynyl bis(phosphine) complexes that have a *cis* configuration have been studied less. This is partly because the *cis*-isomer is thermodynamically unstable compared to the *trans*-isomer in solution, particularly when monodentate phosphines are present as the auxiliary ligands.[31] Therefore, the complexes of the type, $MX(C{\equiv}CR)L_2$ and $M(C{\equiv}CR)_2L_2$ (M = Pt, Pd; L = phosphine) are usually *trans* at room temperature. Use of chelating phosphine or diimine groups overcomes the thermodynamic instability.[31b] Introduction of air-stable and relatively basic monodentate PTA or DAPTA ligands can be a good option for the synthesis of stable *cis*- and *trans*-alkynyl complexes of platinum and palladium.

Alkynyl complexes of the type, *trans*-$Pd(C{\equiv}CR)_2(PEt_3)_2$ (R = Ph, CF_3, *p*-$O_2NC_6H_4$) were first prepared by the reaction of *cis*-$PdBr_2(PEt_3)_2$ with the related alkynyl Grignard reagents in diethyl ether.[31c, e] The X-ray crystal structures of *trans*-$Ni(C{\equiv}CR)_2(PEt_3)_2$ and *trans*-$Pt(C{\equiv}CR)_2(PEt_3)_2$ were also reported.[31c-e] When *cis*-$PdCl_2(PEt_3)_2$ was reacted with ($PhC{\equiv}CH$) in the presence of triethylamine (NEt_3), *trans*-$Pd(C{\equiv}CPh)_2(PEt_3)_2$ was formed as a white solid.[31f]

Krogstad *et al.* reported an alkynyl platinum(II) complex bearing a PTA ligand, *trans*-$[Pt\{C{\equiv}C(CH_2)_3NH_3\}_2(PTA)_2]Br_2$ which was synthesized by heating *cis*-$PtBr_2(PTA)_2$ with 4-pentyn-1-amine at 50 ^oC for 5 days. This complex showed a singlet resonance at δ -58.9 ppm in the $^{31}P\{^1H\}$ NMR spectrum in D_2O with ^{195}Pt satellites ($^1J_{PtP}$ = 2305 Hz).

The *cis*-[Pt{C≡C(CH$_2$)$_3$NH$_2$}$_2$(PTA)$_2$] complex reported in the same literature was obtained by heating *cis*-PtCl$_2$(PTA)$_2$ with 4-pentyn-1-amine at 50 ^{o}C for 2 h, which exhibited a singlet resonance at the chemical shift of -64.5 ppm in the ^{31}P{^{1}H}NMR spectrum in D$_2$O with ^{195}Pt satellites ($^{1}J_{PtP}$ = 2167 Hz). The X-ray crystal structure of the *trans*-complex revealed a slight distortion from the ideal square planar geometry as shown in Figure 1.1.5. The P(1)–Pt–P(1A) [180.00(14)^{o}] and C(1)–Pt–C(1A)

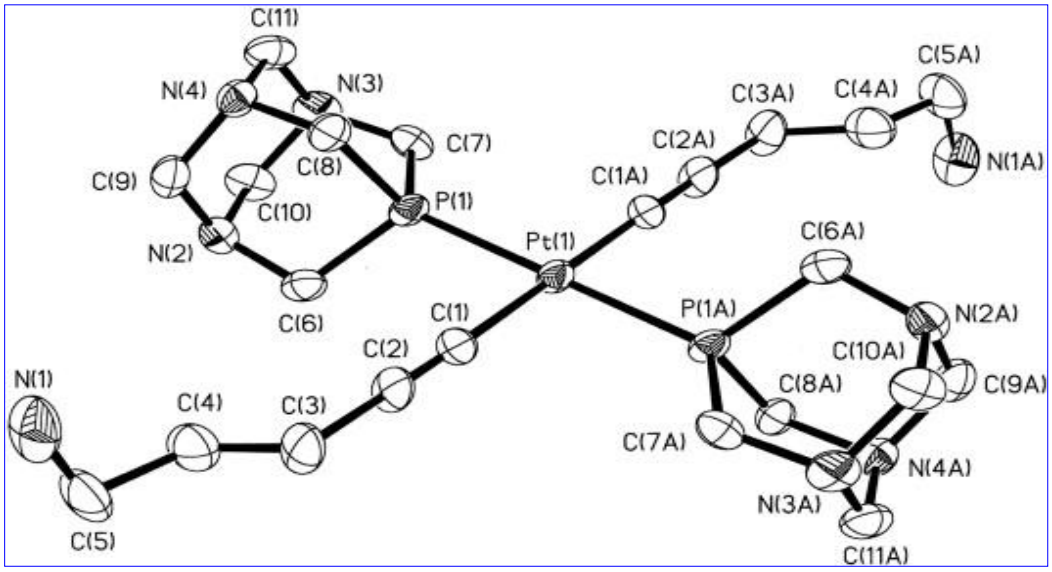

Figure 1.1.5. Molecular structure of *trans*-[Pt{C≡C(CH$_2$)$_3$NH$_3$}$_2$(PTA)$_2$]Br$_2$.[11] Thermal ellipsoids are drawn at the 50% probability level. Anions are omitted for clarity.

[180.000(5)^{o}] bond angles were found to be perfectly linear while the C(1)–Pt–P(1) [85.9(4)^{o}] and C(1)–Pt–P(1A) [94.1(4)^{o}] bond angles were deviated from the expected values. The distorted geometry is assumed to promote the hydrogen bonding between the bromide counter-anion and σ-alkynyl ligand.[11]

1.1.9 Platinum(II) and palladium(II) alkyl phosphine complexes

Transition metal alkyl complexes are known to play an important role in a variety of important organometallic reactions such as olefin polymerization, hydroformylation reactions, and hydrogenation reactions.[32a] Early efforts to synthesize these complexes were not successful and originally it was thought that such species were unstable due to weak metal-carbon bonds. Since the M-C bond dissociation energies are generally 40-60 kcal/mol, the issue is not the thermodynamic stability of the metal alkyl complexes but their kinetic instability. Metal alkyl complexes may also undergo decomposition due to β-hydride elimination.[32] Based on experimental observations, the general relative stability of different alkyl ligands follows the order as: 1-norbornyl > benzyl > trimethylsilyl > neopentyl > Ph ~ Me > > Et (1^o R) > 2^o, 3^o R (R = alkyl).[32a] In addition to this, fluoroalkyl complexes are found to be more stable than alkyl complexes.[32a] Furthermore, introduction of strong electron-donating ligands such as phosphines increases the stability of the alkyl complexes.[32a] Chatt and Shaw predicted that platinum(II) alkyl and aryl complexes could be stabilized by the presence of ligands such as substituted phosphines that produce a large crystal field stabilizing energy (CFSE).[32b]

A stable four-coordinated alkyl metallacycle of platinum bearing the PPh_3 ligand, $[Pt(CH_2)_4(PPh_3)_2]$ was reported by Whitesides *et al.* which was synthesized by substitution of PPh_3 for the corresponding COD complex.[32c] Several other monodentate square planar Group 10 alkyl phosphine complexes including *trans*-$PtCl(C_2H_5)(PPh_3)_2$, and *trans*-$PtX(CH_3)(PPh_3)_2$ (X = Cl, Br, I) were also reported.[32d] To the best of our knowledge, dialkyl or non-chelated monoalkyl complexes of platinum or palladium bearing PTA ligands have not yet been reported.

A palladium alkyl complex ligated with the bidentate analogue of PTA, [PdCl(Me)(κ^2-P,N-PTN)], was synthesized by the reaction of [PdCl(Me)(COD)] with PTN (PTN = 7-phospha-3,7-dimethyl-1,3,5-triazabicyclo[3.3.1]nonane) in 1 : 1 molar ratio.[32e] The ^{1}H NMR signal of the Pd-Me unit appears as a doublet at 0.50 ppm with a coupling constant $^3J_{PH}$ of 13.4 Hz, as expected for a *cis*-(Me-Pd-P) geometry. The chelate behavior of the PTN can be implied from the resonances belonging to the P-CH_3 (δ 1.20, d, $^2J_{PH}$ = 10.8 Hz) and N-CH_3 groups (δ 2.40, s).[32e] Komiya *et al.* have reported the synthesis of some stable water-soluble *cis*-dialkylplatinum(II) complexes bearing sulfonated phosphine and hydroxyphosphine ligands. When $PtMe_2$(COD) was treated with 2 molar equivalents of a phosphine ligand (L) in ethanol (L = TPPMS, TPPTS, THMP), the corresponding platinum(II) alkyl phosphine complex was obtained in a good yield whereas the analogous diethyl complexes were found to undergo β-hydride elimination.[33]

An organometallic synthesis of platinum nanoparticles (PtNps) and their transfer into water using PTA as a stabilizer has been reported for the first time. The PtNps were prepared by hydrogenation of $PtMe_2$(COD) in the presence of 0.8 molar equivalents of PTA per platinum in THF at 70 ^{o}C.[34] The signals from the PCH_2N protons were not observed in the ^{1}H NMR spectrum which can be explained by the close vicinity to the surfaces of the particles whereas the enhancement of the signal (δ 4.6-4.5 ppm) was indicated corresponding to the NCH_2N protons of the PTA ligands bound to the surfaces of the particles. This suggests the absence of any free PTA ligand and the presence of the PTA oxide. The absence of peaks at about -98 ppm in the ^{31}P{^{1}H}MAS NMR spectrum established the absence of free PTA ligand. The observed signals were assigned to the

PTA ligands bound to the surfaces of the nanoparticles through the P-atoms rather than through the N-atoms.[34b]

The platinum(II) diaryl PTA complex, *cis*-$PtPh_2(PTA)_2$ has been prepared utilizing a ligand substitution method by treating $PtPh_2(COD)$ in CH_2Cl_2 with 2 molar equivalents of PTA in methanol at room temperature (Equation 1.1.4), which is the first example of a square planar diphenyl platinum(II) complex with a *cis* geometry containing non-bridging phosphine ligands.[35] This complex is also the first platinum(II)-PTA complex bearing either two alkyl or two aryl ligands.

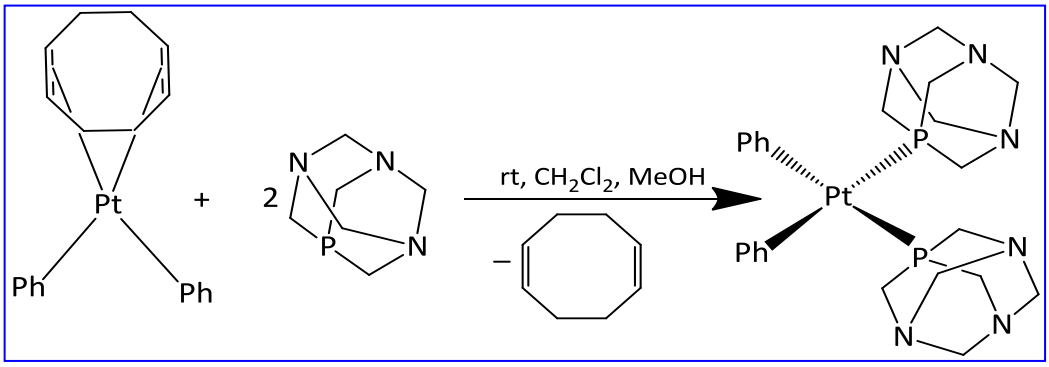

Equation 1.1.4. Synthesis of *cis*-$PtPh_2(PTA)_2$.[35]

The $^{31}P\{H\}$ NMR spectrum of *cis*-$PtPh_2(PTA)_2$ in $CDCl_3$ displayed a single resonance at -77.2 ppm with ^{195}Pt satellites ($^1J_{PtP}$ = 1560 Hz). The complex was also characterized by X-ray crystallography confirming the *cis* orientation of the PTA ligands. The molecule displayed a slightly distorted square planar geometry.[35]

Very few other Group 10 metal monoalkyl complexes bearing PTA ligand have been reported.[22] On the other hand, air-stable and watr-soluble dialkyl, dialkynyl, and halo(alkyl) complexes of platinum and palladium bearing PTA and DAPTA ligands have not been reported yet. Therefore, the current study is focused on the syntheses and

characterizations of such types of complexes of platinum and palladium and the investigation of their catalytic activity in the hydrosilylation reactions and cross-coupling reactions.

1.1.10 References

[1] (a) Phillips, A. D.; Gonsalvi, L.; Romerosa, A.; Vizza, F.; Peruzzini, M. *Coord. Chem. Rev.* **2004**, *248*, 955. (b) Verspui, G. *Chem. Commun.* **1998**, 401. (c) Bravo, J.; Bolaño, S.; Gonsalvi, L.; Peruzzini, M. *Coord. Chem. Rev.* **2010**, *254*, 555.

[2] (a) Daigle, D. J.; Darensbourg, M. Y. *Inorg. Synth.* **1998**, *32*, 40. (b) Alyea, E.; Ferguson, G.; Kannan, S. *Polyhedron* **1998**, *17*, 2727. (c) Krogstad, D. A.; Owens, S.; Halfen, J. A.; Young, V. G. *Inorg. Chem. Commun.* **2005**, *8*, 65.

[3] (a) Darensbourg, D. J.; Robertson, J. B.; Larkins, D. L.; Reibenspies, J. H. *Inorg. Chem.* **1999**, *38*, 2473. (b) Jaremko, L.; Kirilov, A. M.; Smoleński, P.; Lis, T.; Pombeiro, A. J. *Inorg. Chem.* **2008**, *47*, 2922. (c) Smoleński, P. *J. Organomet. Chem.* **2011**, *696*, 3867.

[4] Tolman, C. A. *Chem Rev.* **1977**, *3*, 313.

[5] (a) Otto, S.; Roodt, A. *Inorg. Chem. Commun.* **2001**, *4*, 49. (b) Alyea, E. C.; Fisher, K. J.; Foo, S.; Philip, B. *Polyhedron* **1993**, *12*, 489.

[6] Rauchfuss, T. B. *Platinum Met. Rev.* **1980**, *24*, 95 and references therein.

[7] (a) Smolenski, P.; Pruchnik, F. P.; Ciunik, Z.; Lis, T. *Inorg. Chem.* **2003**, *42*, 3318. (b) Darensbourg, D. J.; Joó, F.; Kannisto, M.; Kathó, A.; Reibenspies, J. H. *Organometallics* **1992**, *11*, 1990.

[8] Ruiz, J.; Cutillas, N.; López, F.; López, G.; Bautista, D. *Organometallics* **2006**, *25*, 5768.

[9] Korthals, B.; Gottker-Schnetmann, I.; Mecking, S. *Organometallics* **2007**, *26*, 1311.

[10] Okano, T.; Uchida, I.; Nakagaki, T.; Konishi. H.; Kiji, J. *J. Mol. Catal.* **1989**, *54*, 65.

[11] Krogstad, D. A.; Cho, J.; DeBoer, A. J.; Klitzke, J. A.; Sanow, W. R.; Williams, H. A.; Halfen J. A. *Inorg. Chim. Acta* **2006**, *359*, 136.

[12] Egger, A. E.; Hartinger, C. G.; Renfrew, A. K.; Dyson, P. J. *J. Biol. Inorg. Chem.* **2010**, *15*, 919.

[13] Dorcier, A.; Hartinger, C. G.; Scopelliti, R.; Fish, R. H.; Keppler, B. K.; Dyson, P. J. *J. Inorg. Biochem.* **2008**, *102*, 1066.

[14] Santini, C; Pallei, M.; Papini, G.; Morresi, B.; Galassi, R.; Ricci, S.; Tisato, F.; Porchia, M.; Rigobello, M. P.; Gandin, V.; Marzano, C. *J. Inorg. Biochem.* **2011**, *105*, 232.

[15] Miranda, S.; Vergara, E.; Mohr, F.; de Vos, D.; Cerrada, E.; Mendia, A.; Laguna, M. *Inorg. Chem.* **2008**, *47*, 5641.

[16] Shionogi and Co. Ltd. Jpn Kokai Tokyo Koho JP58 79994 (1983).

[17] (a) Reedijk, J. *Inorg. Chim. Acta* **1992**, *198*, 873. (b) Bloemink, M. J.; Engelking, H.; Karentzopoulos, S.; Krebs, B.; Reedijk, J. *Inorg. Chem.* **1996**, *35*, 619.

[18] Assefa, Z.; McBurnett, B. G.; Staples, R. J.; Fackler, J. P.; John, P. *Inorg. Chem.* **1995**, *34*, 4965.

[19] (a) Darensbourg, D. J.; Decuir, R. J.; Reibenspies, J. H. In *Aqueous Organometallic Chemistry and Catalysis*; Horvart, I. T.; Joó, F. Eds.; Kluwer, Dordrecht: 1995, p 61. (b) Daigle, D. J. *Inorg. Synth.* **1998**, *32*, 43. (c) Forward, J. M.; Staples, R. J.; Liu, C. W.; Fackler, J. P. *Acta Crystallogr.* **1997**, *C53*, 195. (d) Fluck, E.; Förster, J. E.; Weidlein, J.; Hädicke, E. *Z. Naturforsch.* **1997**, *32*, 499.

[20] Mena-Cruz, A.; Lorenzo-Luis, P.; Romerosa, A.; Saoud, M.; Serrano-Ruiz, M. *Inorg. Chem.* **2007**, *46*, 6120.

[21] Krogstad, D. A.; Gohmann, K. E.; Sunderland, T. L.; Geis, A. L.; Bergamini, P.; Marvelli, L.; Young Jr., V. G. *Inorg. Chim. Acta* **2009**, *362*, 3049.

[22] (a) Darensbourg, D. G.; Ortiz, C. G.; Kamplain, J. W. *Organometallics* **2004**, *23*, 1747. (b) Elena Vergara, E.; Miranda, S.; Mohr, F.; Cerrada, E.; Tiekink, E. R. T.; Romero, P.; Mendía, A.; Laguna, M. *Eur. J. Inorg. Chem.* **2007**, 2926. (c) Darensbourg, D. G.; Ortiz, C. G.; Yarbrough, J. C. *Inorg. Chem.* **2003**, *42*, 6915. (d) For the synthesis of DAPTA, we used acetone in place of water to make the work-up process easier.

[23] Krogstad, D. A.; Ellis, G. S.; Gunderson, A. K.; Hammirich, A. J.; Rudolf, J. W.; Halfen, J. A. *Polyhedron* **2007**, *26*, 4093.

[24] Darensbourg, M. Y.; Daigle, D. J. *Inorg. Chem.* **1975**, *5*, 1217.

[25](a) Alyea, E. C.; Fisher, K. J.; Johnson, S. *Can. J. Chem.* **1989**, *67*, 1319. (b) Fluck, E.; Förster, J. E.; Weidlein, J.; Hädicke, E. *Z. Naturforsch.* **1977**, *32*, 499.

[26] (a) Frost, B. J.; Bautista, C. M.; Huang, R.; Shearer, J. *Inorg. Chem.* **2006**, *45*, 3481. (b) Smoleńsky, P.; Benisvy, L.; Fátima, M.; da Silva, C. G.; Pombeiro, A. J. L. *Eur. J. Inorg. Chem.* **2009**, 1181.

[27] Bergamini, P.; Bertolasi, V.; Marvelli, L.; Canella, A.; Gavioli, R.; Mantovani, N.; Mañas, S.; Romerosa, A. *Inorg. Chem.* **2007**, *46*, 4267.

[28] Grushin, V. V.; Marshall, W. J. *Organometallics* **2008**, *27*, 4825.

[29] (a) Kistner, C. R.; Hutchinson, H.; Doyle, J. R.; Storlie, J. C. *Inorg. Chem.* **1963**, *2*, 1255. (b) Otto, S. *Inorg. Chim. Acta* **2010**, *363*, 3316. (c) Otto, S.; Roodt, A. *Acta Crystallogr.* **2001**, *C57*, 540. (d) Francos, J.; Cadierno, V. *Green Chem.* **2010**, *12*, 1552. (e) Smoleński, P.; Mukhopadhyay, S.; da Silva, C. G.; Charmier, M. A. J.; Pombeiro, A. J. L. *Dalton Trans.* **2008**, 6546. (f) Otto, S.; Johansson, M. *Acta Crystallogr.* **2000**, *C56*, e12.

[30] Canty, A. J. "Palladium Carbon δ-Bonded Complexes." In *Comprehensive Organometallic Chemistry II*; Abel, E. W.; Stone, F. G. A.; Wilkinson, G. Eds.; Pergamon: Exeter, 1995; Vol. 9, pp 225-290.

[31] (a) Sonogashira, K.; Takahashi, S.; Hagihara, N. *Macromolecules* **1977**, 10, 879. (b) Sonogashira, K.; Takahashi, S.; Hagihara, N.; Fujikura, Y.; Yatake, T.; Toyoshima, N. *J. Organomet. Chem.* **1978**, *145*, 101. (c) Calvin, G.; Coates, G. E. *J. Chem. Soc.* **1960**, 2008. (d) Spofford, W. A., III; Carfagna, P. D.; Amma, E. L. *Inorg. Chem.* **1967**, *6*, 1553. (e) Bruce, M. I.; Harbourne, D. A.; Waugh, F.; Stone, F. G. A. *J. Chem. Soc.* (*A*) **1968**, 356. (f) Kim, H.-J.; Lee, S. W. *Bull. Korean Chem. Soc.* **1999**, *20*, 1089.

[32] (a) Hager, E.; Sivaramakrishna, A.; Clayton, H. S.; Mogorosi, M. M.; Moss, J. R. *Coord. Chem. Rev.* **2008**, *252*, 1668. (b) Chatt, J.; Shaw, B. L. *J. Chem. Soc.* **1961**, 285.

(c) McDermott, J. X.; White, J. F.; Whitesides, G. M. *J. Am. Chem. Soc.* **1976**, *98*, 6521. (d) Bardi, R.; Piazzesi, A. M. *Inorg. Chim. Acta* **1981**, *47*, 249. (e) Caporali, M.; Bianchini, C.; Bolaño, S.; Bosquain, S. S.; Gonsalvi, L.; Oberhauser, W.; Rossin, A.; Peruzzini, M. *Inorg. Chim. Acta* **2008**, *361*, 3017.

[33] Komine, N.; Ikuine, M.; Sato, K.; Hirano, M.; Komiya, S. *Bull. Chem. Soc. Jpn.* **2003**, *76*, 183.

[34] (a) Debouttière, P.-J.; Martinez, V.; Philippot, K.; Chaudret, B. *Dalton Trans.* **2009**, 10172. (b) Debouttière, P.-J.; Coppel, Y.; Denicourt-Nowicki, A.; Roucoux, A.; Chaudret, B.; Philippot, K. *Eur. J. Inorg. Chem.* **2012**, 1229.

[35] Muller, A.; Roodt, A. *Acta Crystallogr.* **2004**, *C60*, 266.

1.2 Platinum Catalyzed Hydrosilylation Reactions

Activation of Si-H bonds by late transition metal complexes such as those of platinum and palladium is regarded as the most common synthetic method for the preparation of new complexes containing a metal-silicon bond.[1] When late transition metals are used, the process is generally believed to proceed by an oxidative-addition pathway (Scheme 1.2.1).[1c] The oxidative-addition takes place by non-classical interactions as shown in the second and third steps in Scheme 1.2.1. The metal can back-bond to the σ*-orbital of the Si-H unit. This results in weakening of the Si-H bond and the formation of the σ-complex which is like an incomplete or arrested oxidative-addition. The bonding interaction partially depletes the Si-H bond. The electrons are now delocalized over the metal which results in the formation of the three-center two-electron (3c-2e) bonds. When the weakening of the Si-H bond is severe, then the final oxidative-addition product is formed.[1]

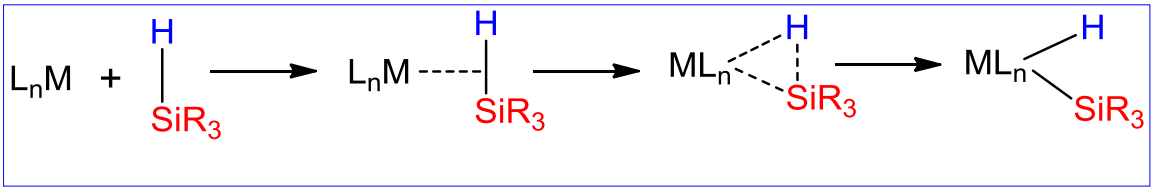

Scheme 1.2.1. Oxidative-addition in Si-H bond activation by late transition metal complexes.[1c]

The complexes with good electron-donor ligands such as phosphines will undergo π-back bonding to the σ*-orbital on the Si-H unit and promote oxidative-addition (Figure 1.2.1). Additionally, the use of electron-withdrawing groups at silicon also promotes oxidative-addition. Hydrosilanes containing various numbers of Si-H bonds are known to react with a range of transition metal precursors. The secondary (R_2SiH_2) and primary

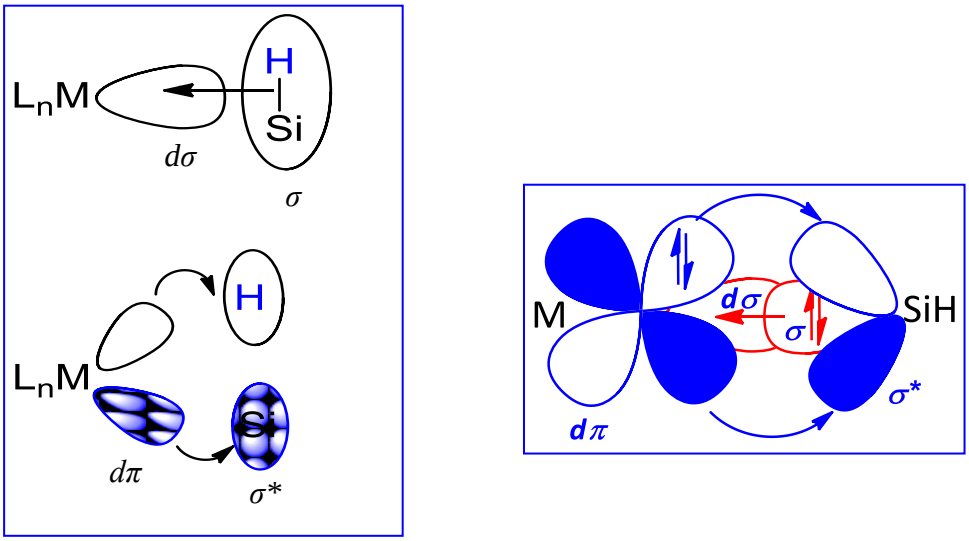

Figure 1.2.1. Orbital interaction to promote oxidative-addition in Si-H bond activation.

($RSiH_3$) hydrosilanes are of great interest because of the presence of additional potential sites of reactivity at the silicon center.[1] Unlike the E-H bond activation for late transition metal precursors, the E-H bond activation for early transition metal precursors, many of which are in their highest oxidation state, proceed through a four-centered transition state in a sigma-bond metathesis step (Scheme 1.2.2).[1e, f]

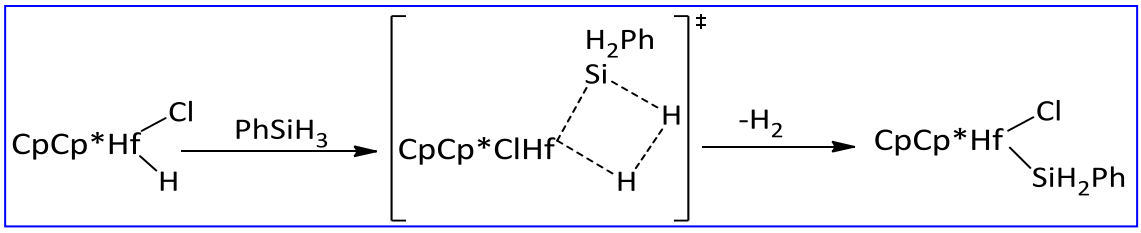

Scheme 1.2.2. Sigma-bond metathesis in Si-H bond activation by early transition metal complexes.[1f]

1.2.1 Hydrosilylation reaction

The Si-H bond activation can be a stoichiometric or catalytic process. Transition metal catalyzed Si-H bond activation can be carried out by either hydrosilylation or dehydrogenative coupling reactions (Scheme 1.2.3).[2] Hydrosilylation reaction is the metal catalyzed addition of a Si-H bond in a hydrosilane to an unsaturated substrate such

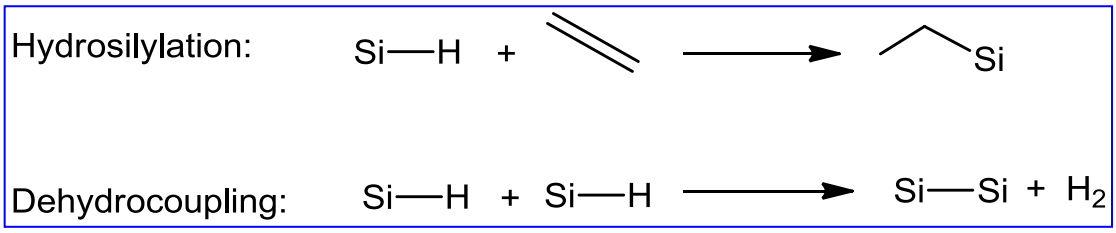

Scheme 1.2.3. Hydrosilylation vs dehydrogenative coupling reactions.

as a C=C double bond of an alkene or alkadiene, C≡C triple bond of an alkyne or alkadiyne, C=O bond of an aldehyde or a ketone, C=N bond of an imine, and C≡N bond of a nitrile compound.[3] The hydrosilylation reaction is the most common method to form a Si-C bond. In general, the hydrosilylation reactions are used for the industrial production of organosilicon compounds such as those used for polymers, coupling agents, adhesives, binders, and many other organosilicon reagents.[4] The corresponding germanium and tin reactions, hydrogermylation and hydrostannylation reaction, respectively, are also known but much less studied.[5] In fact, platinum catalyzed hydrosilylation reactions have been known since 1965.[6] The homogeneous catalyzed hydrosilylation reactions of alkenes or alkynes bear an interest from a mechanistic as well as a synthetic point of view.[4, 6]

1.2.2 Mechanism of hydrosilylation reaction

1.2.3 Mechanism of hydrosilylation reaction

The widely accepted mechanisms for hydrosilylation reactions are the Chalk-Harrod and the modified Chalk-Harrod mechanisms.[6, 7] These mechanisms follow a series of oxidative-addition, migratory insertion, and reductive-elimination pathways (Scheme 1.2.4). Both mechanisms involve oxidative-addition of a Si-H bond to the metal center

as a key step in the catalytic cycle. Therefore, many electron-rich transition metal complexes, especially those containing Group 10 metals in low oxidation states

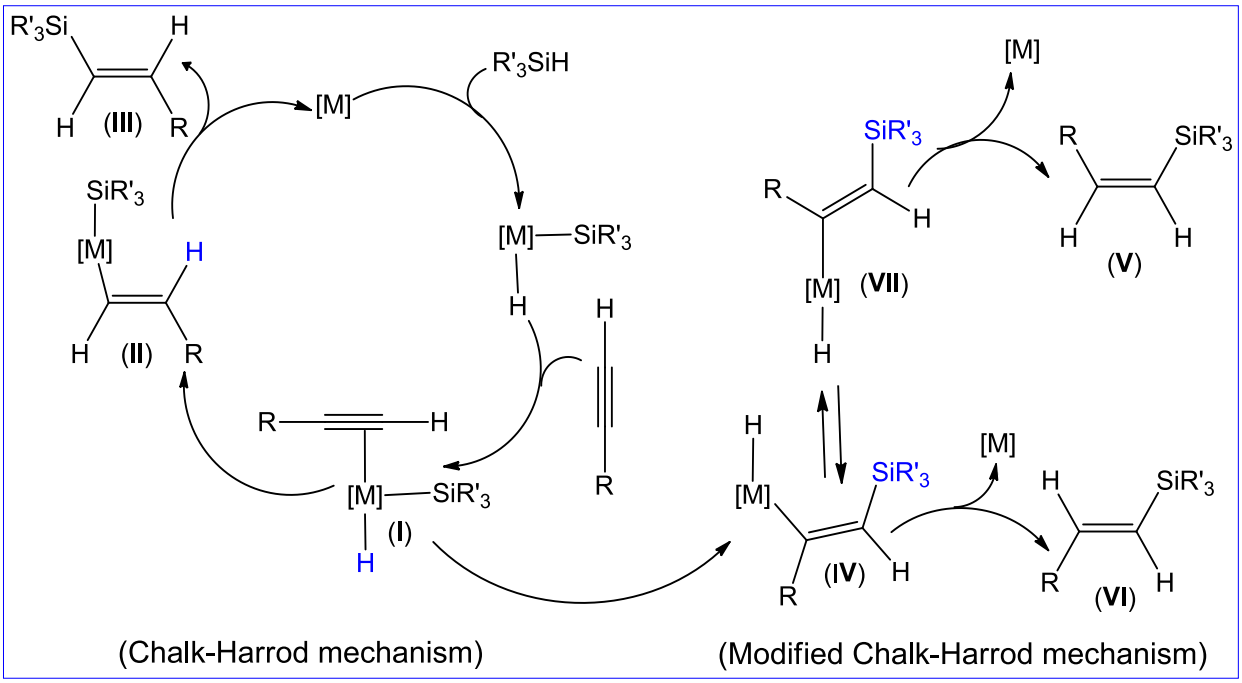

Scheme 1.2.4. Mechanism of hydrosilylation reaction.

containing good donor ligands such as tertiary phosphines and olefins display efficient catalytic activity. A variety of Pt(0) and Pt(II) complexes with such ligands have been used as well-established homogeneous hydrosilylation reaction catalysts. The conventional hydrosilylation reaction of alkenes catalyzed by Speier's catalyst ($H_2PtCl_6 \cdot 6H_2O$) is generally assumed to proceed by the Chalk-Harrod mechanism which is also applicable to the hydrosilylation reaction of alkynes catalyzed by the Pt complexes.[6] Initial oxidative-addition of the hydrosilane to the metal center of the catalyst followed by the coordination of the alkyne generates complex **I**, which undergoes alkyne insertion into the M-H bond (*hydrometallation*) to furnish the vinyl

organometallic complex (**II**). Finally, reductive-elimination produces the *E*-vinylsilane (**III**) and regenerates the catalyst.

This mechanism accounts for Pt catalyzed hydrosilylation reactions, however, it does not account for the formation of the *Z*-vinylsilanes (**V**) as well as dehydrogenative silylated products from the Co, Ru, Rh, and Ir catalyzed hydrosilylation reactions of alkynes. To explain the formation of the observed products, a different hydrosilylation mechanism has been proposed, which involves preferentially an alkyne insertion into the M-Si bond (*silylmetallation*) to form the *β*-silylalkyl hydrido intermediate (**IV**), has been proposed. Direct reductive-elimination from **IV**, on which the metal and silyl group are oriented *cis*, gives the *E*-vinylsilane (**VI**). Alternatively, the complex (**IV**) could undergo a metal-assisted isomerization to **VII** through a zwitterionic carbene-like intermediate[7] which leads to the formation of thermodynamically less stable *Z*-vinylsilane (**V**). The ease of steric strain between the metal and the adjacent silane is the driving force for this isomerization. The formation of the dehydrogenative silylated products as shown in Scheme 1.2.3 takes place by *β*-hydrogen elimination from the complex **VII**.[7]

Prignato and Trogler experimentally investigated that Si-H oxidative-addition occurs not to a Pt(0) alkene complex but to a Pt(0) bis(phosphine) complex when a platinum bis(phosphine) complex was used as a catalyst.[8] Theoretical calculations were carried out to investigate the mechanistic details and the nature of the hydrosilylated product formed in a Pt catalyzed hydrosilylation reaction.[9] During this study, $Pt(PH_3)_2$ was modeled as a catalyst for the hydrosilylation reaction of ethylene in the presence of a tertiary hydrosilane, $H\text{-}SiR_3$.[9] The results of this investigation suggested that ethylene is more readily inserted into the Pt-H bond than into the $Pt\text{-}SiH_3$ bond. Furthermore, the

investigations showed that the rate-determining step is the isomerization of the ethylene insertion product, $Pt(SiR_3)(C_2H_5)(PH_3)$ in the Chalk-Harrod mechanism and its barrier (*E*a) is 22 kcal/mol for R = H, 26 kcal/mol for R = Cl, and 23 kcal/mol for R = Me.[9] Similarly, in the modified Chalk-Harrod mechanism, the rate-determining step is the ethylene insertion, independent of the kind of substituent on Si (*E*a = 44 kcal/mol for R = H and Me and 60 kcal/mol for R = Cl). These activation barriers are much higher than that of the rate-determining step of the Chalk-Harrod mechanism. Thus, it should be clearly concluded that the Pt(0) catalyzed hydrosilylation reaction of ethylene proceeds through the Chalk-Harrod mechanism.[9]

1.2.4 Selectivity of products in hydrosilylation reaction

It is worthy of note that hydrosilanes exhibit a wide range of reactivity in the oxidative-addition depending on the nature of the metal catalyst, solvent, and substituents on the silicon atom. The platinum complexes tolerate essentially any hydrosilane, such as $HSiCl_nMe_{3-n}$ (n = 1-3), $HSi(OR)_3$, or H_nSiR_{4-n} (n = 1-3; R = alkyl or Ph) in the hydrosilylation reaction, while palladium complexes are reactive mostly with $HSiCl_nR_{3-n}$ (n = 2, 3), and Rh complexes preferably with $HSiR_3$.[3a] The rate and selectivity of the hydrosilylation reactions is adversely affected by certain combinations of hydrosilanes and/or unsaturated groups.[10, 11] For example, addition of a variety of tertiary hydrosilanes (R_3SiH) to styrenes gives a 60 : 40 mixture of β- and α-products (according to Markovnikov and anti-Markovnikov addition of the hydrosilane, respectively) as opposed to the high selectivity for β-addition normally achieved with other alkenes.[10] The rate of the hydrosilylation reaction is also affected by the electronic nature of the R groups on the hydrosilane. For example, the rate of the reaction is dramatically enhanced by the

electron-withdrawing R groups.[3, 12, 13] Additionally, it is well-known that internal double bonds and substituted double bonds are reluctant to add R_3SiH; for example, cyclohexene will add R_3SiH only at drastic conditions.[11]

The hydrosilylation reaction of terminal alkynes with tertiary hydrosilanes (R_3SiH), generally results in the formation of three kinds of products: *β-trans*, *β-cis*, and *α*-isomers; usually the *β-trans* isomer being a major product (Scheme 1.2.5).[12, 13] However, the observed selectivity depends upon several factors including the substituent on the hydrosilane and/or alkyne, nature of the catalyst, as well as the reaction conditions (temperature, solvent, and catalyst loading).[12, 13, 15] When relatively sterically hindered hydrosilanes such as tertiary hydrosilanes (R_3SiH) are used, the silicon unit of the hydrosilane (R_3Si) cannot easily approach the second carbon atom of the substrate and consequently, the *β*-isomer is selectively formed. The hydrosilylation reaction favors the *syn* addition of the Si-H bond to the unsaturated systems (Si and H atoms at the *cis*-position), and thus the corresponding *trans*-isomers are selectively formed.[12, 13]

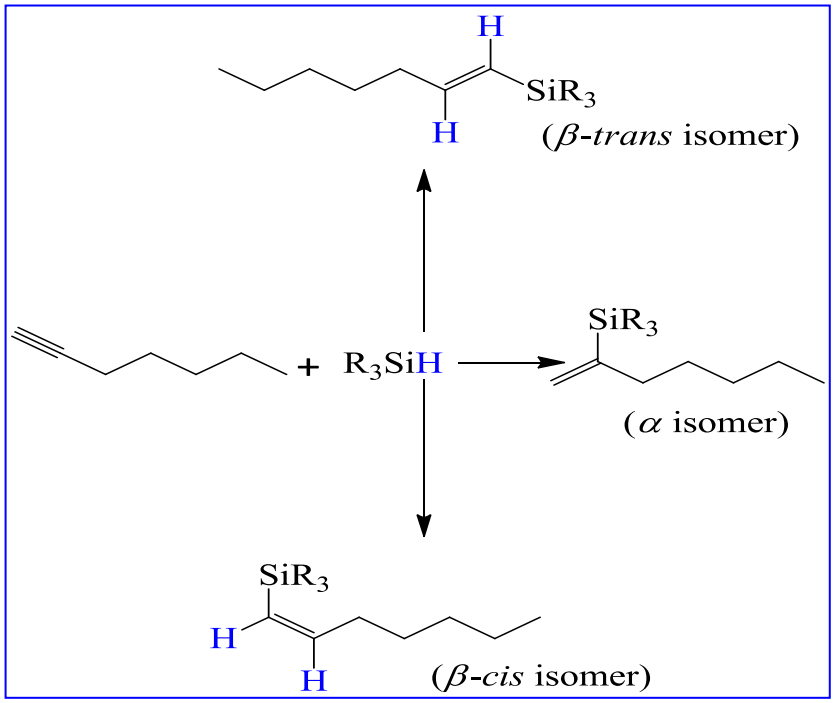

Scheme 1.2.5. Nature of the products formed in hydrosilylation reaction of terminal alkynes.

The α-isomer can be the major product when less sterically hindered primary ($RSiH_3$) and secondary (R_2SiH_2) hydrosilanes are used or when the silicon atom contains electron-withdrawing groups. Because of the presence of additional potential reacting sites (Si-H unit), the hydrosilylation reactions with primary and secondary hydrosilanes are often accompanied with multiple side-reactions.[3a] Lewis *et al.* suggested that the hydrosilylation reaction of an olefin proceeds *via* a nucleophilic attack of the olefin on an activated R_3SiH-Pt complex. Thus, the higher activity of alkynes vs alkenes could be due to the higher degree of nucleophilicity of alkynes than that of alkenes. Therefore, three possible hydrosilylated products, instead of two for alkenes, may result from addition of R_3SiH to terminal alkynes. Another difference between the addition of R_3SiH to alkynes vs alkenes is that a number of structural and electronic factors that impede the hydrosilylation reactions of alkenes have a minimal impact on the hydrosilylation reactions of alkynes.[10, 12] Moreover, formation of the α-product in alkynes may become a lower energy process than for alkenes due to the lower steric bulk around the unsaturated group in alkynes.[10, 12]

1.2.5 Some examples of Pt catalyzed hydrosilylation reactions

Alkenylsilanes have been proved to be valuable intermediates in a number of catalytic organic reactions, such as the vinylation of aryl halides, recently adapted by some research groups to aqueous conditions.[14, 15] Therefore, the preparation of alkenylsilanes by the hydrosilylation reactions of alkynes in aqueous conditions would be highly desirable. In this respect, although Wilkinson's catalyst [$Rh(PPh_3)_3Cl$],[14a] Karstedt's catalyst [$Pt_2(dvtms)_3$] (dvtms = 1,3-divinyl-1,1,3,3-tetramethyldisiloxane) (Figure

1.2.2),[14b, c] and Speier's catalyst ($H_2PtCl_6 \cdot 6H_2O$ in $^{i}PrOH$)[6, 12a , e] are widely used in industry, Wilkinson's catalyst usually selectively forms the *β-cis* or *α*-product and the latter two form colloidal Pt particles during the course of the reaction.[12, 14]

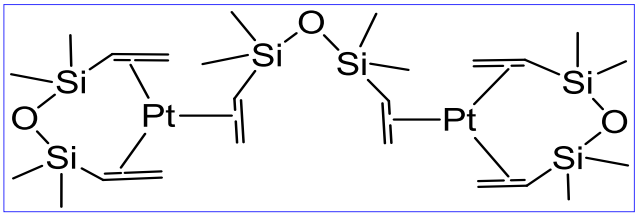

Figure 1.2.2. Karstedt's catalyst.

Also, these platinum catalysts become corrosive in the system due to the formation of HCl that can be removed by treatment with a suitable base. However, under these conditions, a storage stability and reduction of the catalytic activity occurs. Furthermore, the active catalytic species in the Speier's catalyst is still ambiguous.[6, 12, 14]

Markó and co-workers have investigated the sterically-controlled hydrosilylation reactions of alkynes using Pt(0) NHC complexes (NHC = *N*-heterocyclic carbene), [(IPr)Pt(diene)] [IPr = 1,3-bis(2,6-diisopropylphenyl)imidazolium] as catalysts (Figure 1.2.3a).[15a] The pre-catalysts functioned with remarkable efficiency and regioselectivity as well as avoided the formation of Pt colloids. The reaction was found to be effective at 1 mole% catalyst loading.[15a] Recently, the hydrosilylation reactions of terminal alkynes catalyzed by water-soluble Pt(0) NHC complexes (Figure 1.2.3b) have been reported for

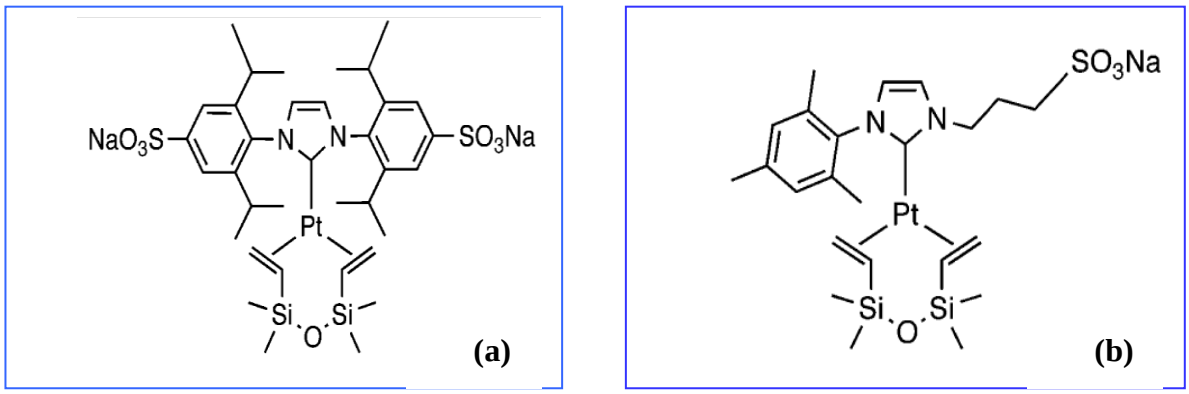

Figure 1.2.3. Water-soluble Pt NHC complexes used as pre-catalysts in hydrosilylation reactions. (a) [(IPr)Pt(diene)][15a] (b) A water-soluble Pt(0) NHC complex.[15b]

the first time by de Jesús *et al.* These catalysts are active at room temperature and highly recyclable. These properties can be linked to the stability of the platinum-carbene carbon bond under aqueous reaction conditions. These catalytic reactions yielded the products with very good regioselectivity, forming the *β-trans* hydrosilylated product as the major product and the *α*-isomer as a minor product.[15b] The regioselectivity of the *β-trans* isomer with respect to the *α*-isomer was determined by the ^{1}H NMR spectroscopy and found to be comparable to that found with another catalyst, $Pt(PCy)_3$ for the same substrate. However, the regioselectivity was found to be lower than that reported for other phosphine or NHC complexes.[15]

Denmark *et al.* reported that [($^{t}Bu_3P$)Pt(DVDS)] (DVDS = 1,3-divinyl-1,1,3,3-tetramethyldisiloxane) was found to be the most active and regioselective catalyst for the selective *β-trans* isomer formation in the hydrosilylation reaction of 1-heptyne with arylsilanes and alkenylsilanes.[16a] One of the limitations of this procedure is the unwanted formation of disiloxanes which results in lower yields of the hydrosilylated products. However, milder hydrosilylation conditions can be applied with ruthenium and rhodium catalysts such as [Ru(H)Cl(CO)($P^{i}Pr_3$)$_2$],[16b] [$RhCl(PPh_3)_3$],[14a] [Rh(COD)Cl]$_2$,[16c] and [$RuCl_2$(*p*-cymene)]$_2$,[16d] that have all been reported to generate the *Z*-vinylsilanes (*β-cis* isomers) selectively (as shown in Scheme 1.2.5) with Et_3SiH under a variety of specialized conditions.

The Lewis group investigated the catalytic hydrosilylation reaction of alkynes using a variety of tertiary hydrosilanes in the presence of the Karstedt's catalyst. Gentle heating the reaction mixture for about 5 min to initiate the reaction led to an exothermic reaction and complete conversion to the products in less than 1 h. Mostly, only the *β*-product was

formed with a sterically bulky group near the α-position whereas some reactions resulted in the formation of the α-isomer as well. The reaction of the tertiary hydrosilane, $Ph_{3-x}Me_xSiH$ (x = 0-2) to 1-pentyne was independent of variations of the ratio of Ph/Me substitution on the silicon center. Therefore, all three hydrosilanes resulted in roughly the same proportion of β- and α-products. A trend was observed favoring the formation of the α-product with more electron-withdrawing groups on the silicon center. The highest degree of the α-product was obtained with the $(EtO)_3SiH$ reagent.[13] Selected results from hydrosilylation reactions of terminal alkynes with different tertiary hydrosilanes, as described by Lewis *et al.* are given in Table 1.2.1.

Table 1.2.1. Regioselectivity of the products formation from hydrosilylation reactions of terminal alkynes with different tertiary hydrosilanes catalyzed by Karstedt's catalyst.[13] .

Hydrosilane	**Alkyne**	**Ratio of isomers (*β-trans* : *α* : *β-cis*)**
Ph_3SiH	1-pentyne	77 : 23 : traces
Ph_3SiH	phenylacetylene	78 : 7 : 15
Ph_2MeSiH	1-pentyne	78 : 20 : 2
$PhMe_2SiH$	1-pentyne	70 : 25 : 5
$(EtO)_3SiH$	1-pentyne	55.5 : 38.5 : 6
$(EtO)_3SiH$	phenylacetylene	70 : 30 : 0

During these investigations, Ph_2MeSiH and 1-pentyne were combined with Karstedt's catalyst (3 μL**,** 0.8 μmol of Pt). Analysis of the entire product mixture was carried out by GC and ^1H NMR spectroscopy. The ^1H NMR spectral analysis of the product mixture showed two large resonances at 6.16 ppm and 5.95 ppm (doublet of triplets with $^3J_{HH}$ =

18.5 Hz) for the *β-trans* isomer, with a smaller multiplet at 6.30 ppm for the *β-cis* isomer, and a pair of multiplets at 5.83 and 5.40 ppm for the *α*-isomer. The ratio of the products *β-trans : β-cis : α* was found to be 78 : 2 : 20, respectively, as detected by the ^{1}H NMR spectroscopy. A similar type of reaction was carried out between another tertiary hydrosilane, Ph_3SiH and phenylacetylene. After adding Karstedt's catalyst with the same catalyst loading, the reaction mixture was heated to *ca.* 60 ^{o}C for 2 min. The ^{1}H NMR spectral analysis of the product mixture showed a large resonance at 6.98 ppm (doublet with J = 18.0 Hz) for the *β-trans* isomer, with a smaller singlet at 7.16 for the *β-cis* isomer, and a pair of doublets at 6.28 and 5.69 (J = 2.0 Hz) for the *α*-isomer. As detected by GC, the ratio of the products (*β-trans : β-cis : α*) was found to be 78 : 15 : 7, respectively. It is important to note that the reaction of Ph_3SiH with 1,7-octadiyne in the presence of the Karstedt's catalyst with the same catalyst loading yielded the disilylated *β-trans* isomer with 100% regioselectivity.[13] The product distribution (*β-trans : α*) obtained for the reaction between Ph_3SiH and 1-pentyne was found to be 77 : 23, respectively, when the Karstedt's catalyst was used and this ratio did not change when the Speier's catalyst was used.[13]

Ojima *et al.* published the first report on the hydrosilylation reaction of terminal alkynes with tertiary hydrosilanes catalyzed by $RhCl(PPh_3)_3$ (Wilkinson's catalyst), in which *cis*-(1-silylalkenes) (*β-cis* isomers) were formed as the major products which are believed to be formed *via* the *anti* addition.[14a] Haszeldine and co-workers reported a *trans* to *cis* isomerization in the hydrosilylation reaction of l-hexyne with Et_3SiH catalyzed by $RhCl(PPh_3)_3$ and proposed a mechanism including the first *syn* addition of

the hydrosilane to l-hexyne, giving the *trans*-product followed by isomerization to the *cis*-product *via* the formation of a zwitter-ionic carbene complex intermediate.[17a]

In another investigation related to Rh catalyzed hydrosilylation reactions, Ojima *et al.* reported that the *β-cis* : *β-trans* ratio of the reaction product of Et_3SiH and 1-pentyne catalyzed by $(Ph_3P)_3RhC1$ was found to be 69 : 31, respectively.[17b] Lewis *et al.* obtained no *cis*-product (*β-trans* : α = 89 : 11) when this reaction was catalyzed by Pt using Karstedt's catalyst and $PtCl_2(COD)$.[13] The reaction was rerun utilizing $(Ph_3P)_3RhCl$ in place of Pt catalysts and a *β-cis* : *β-trans* : α product ratio of 72 : 22 : 6 was observed. When the reaction was rerun with $RhC1_3$ in ^{i}PrOH, nearly identical results were obtained. Thus, it appeared that a different mechanism was operative in the Rh catalyzed reaction. These results again support the fact that Pt catalyzed hydrosilylation reaction of alkynes is characterized by the *syn* addition giving mainly the *β-trans* product whereas Rh catalyzed hydrosilylation reactions of alkynes is characterized by the *anti* addition giving mainly the *β-cis* product. On the basis of the supporting experiments carried out by the Lewis group, the Rh catalyzed reaction between Et_3SiH and l-pentyne apparently resulted in a kinetic product mixture assuming that the *cis*-alkenyl product is thermodynamically less stable than the *trans*-analogue. Similarly, a mechanism by which the kinetically favored *cis*-product formed and then subsequently converted to the *trans*-isomer in the presence of *in situ* generated active Pt catalyst is ruled out.[13]

The reaction mixture of Et_3SiH and 1-hexyne was heated for 24 h in toluene at 55 ^{o}C in the presence of Wilkinson's catalyst (1-hexyne/catalyst = $1/10^4$). Analysis of the entire product mixture was carried out by GC and ^{1}H NMR spectroscopy. The ^{1}H NMR spectrum of the product mixture displayed two large resonances at 6.38 ppm (doublet of

triplets with $^{3}J_{HH}$ = 14.1 Hz) and 5.38 ppm (doublet with $^{3}J_{HH}$ = 14.1 Hz) for the *β-cis* isomer, two smaller resonances at 6.03 ppm (doublet of triplets with $^{3}J_{HH}$ = 18.7 Hz) and 5.53 ppm (doublet with $^{3}J_{HH}$ = 18.7 Hz) for the *β-trans* isomer, and a pair of multiplets at 5.60 and 5.30 ppm for the *α*-isomer. The ratio of the products *β-cis : β-trans : α* was found to be 96 : 2 : 2, respectively as determined by the ^{1}H NMR spectroscopy. In some of these Rh catalyzed reactions such as those involving $PhMe_2SiH$, the *α*-isomer usually displayed a pair of doublets (in some cases singlets) in between 5.30-5.80 ppm; the coupling (*J*) values ranged between 1.5-3.0 Hz. [17b] In all of the reported Pt or Rh catalyzed hydrosilylation reactions, the $^{3}J_{HH}$ value of the alkenyl protons for the *β-trans* isomer was found to fall between 16.5 to 20 Hz and whereas that for the *β-cis* isomer ranged from 8.5 to 14.5 Hz.[13, 17]

Generally, the chemical shifts of the alkenyl hydrogens of the *β-cis* isomers were found to occur about 0.5 ppm upfield of those on the *β-trans* isomers. The vinylidene hydrogen resonances in the *α*-isomer were also often found upfield of the olefinic protons in the *β-trans* isomers.[13, 17] Several characteristic features were noticed in the $^{13}C\{^{1}H\}$ NMR spectra of the hydrosilylated products reported by the Lewis group. The olefinic carbon nearest to the silicon gave a downfield resonance in the $^{13}C\{^{1}H\}$ NMR spectrum, in contrast to the olefinic proton nearest to the silicon in the ^{1}H NMR spectrum. The carbon attached to the silicon atom in the *β-trans* and *α*-isomers was shifted considerably downfield compared to the corresponding carbon in the *β-cis* isomers.[13]

Another platinum complex, $[Pt(PPh_3)_2\{\eta^2\text{-}(H_2C{=}CH_2)\}]$ was reported to catalyze the hydrosilylation reactions of a variety of alkenes with diethylsilane, trialkoxysilanes, and trichlorosilane. Mostly, the *β*-isomer was formed as the major product.[18a] A platinum(II)

phosphine complex, *cis*-$PtCl_2(PhCH{=}CH_2)_2$, was utilized as a pre-catalyst for the hydrosilylation reaction of 1-hexene and phenylacetylene using a tertiary hydrosilane, $PhMe_2SiH$. Though 1-hexene was found to undergo minimal isomerization to an internal olefin, the β-isomer and the α-isomer were found to be the major and minor products, respectively.[18b] It had been reported previously that *cis-trans* isomerization of the hydrosilanes occurs on prolonged reaction times and such isomerization can be reduced by the addition of free alkenes or alkynes to the system.[3a]

1.2.6 Hydrosilylation reaction using siloles and silafluorenes

Silafluorenes and siloles (1-silacyclopentadienes) (Figure 1.2.4a-c) as well as their oligomers are attractive as a fluorophore because of their unique photoluminescence and ability to sense a wide range of explosive analytes.[19] Polymers having a *p*-vinylene unit

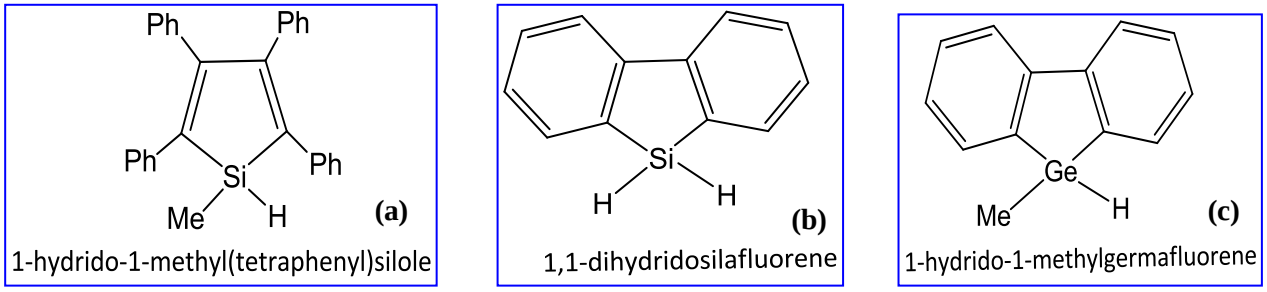

Figure 1.2.4a-c. Some examples of silole and silafluorene and germanium analogue.

exhibit strong emissive properties.[20] Silicon-doped poly(vinylenes) are also promising organic light-emitting diodes (OLEDs) and preceramic materials.[21] Silole (or silafluorene)-vinylene polymers or dimers can be formed by a hydrosilylation reaction of an alkyne system with the corresponding silole or silafluorene which gives the regioselective product according to the literature reports.[22, 23] The germanium analogue

can be obtained by a hydrogermylation reaction of an alkyne using a corresponding germole or germafluorene.

Trogler *et al.* have reported the luminescent poly- or disilylated/germylated products synthesized by hydrosilylation or hydrogermylation reactions of a variety of alkynes using siloles and silafluorenes and their germanium analogues (Equation 1.2.1).[22] These

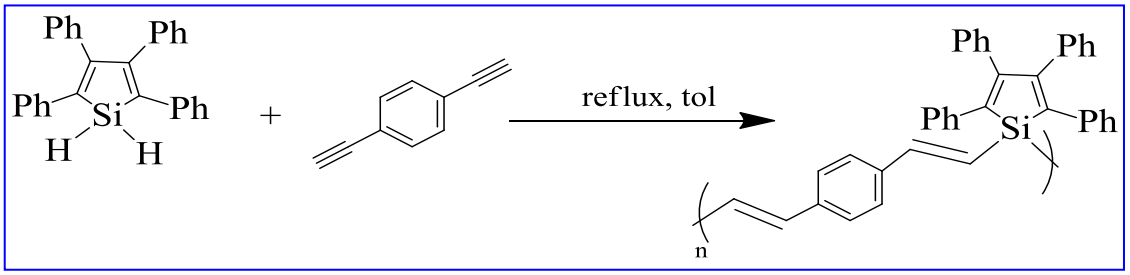

Equation 1.2.1. Formation of silole-vinylene polymer by catalytic hydrosilylation reaction.[22]

copolymers or disilylated/germylated products take advantage of σ^*-π^* conjugation between the σ^* orbital on the silicon centers of the polymer backbone and the π^* molecular orbital of the alkadiene moiety in the metallole ring and can exhibit chemical sensing properties.[22, 23]

Trogler's group reported using UV-emitting silafluorene materials featuring a high-energy ^{1}SOMO (singlet singly occupied molecular orbital) that lies above the LUMO energy of a larger range of explosives than for the previously reported fluorescence sensors.[23] Silafluorenes are able to sense a range of analytes without green emission (g-band) and provide thermal stability. The good sensitivity of the silafluorene-containing polymers or dimers is attributed largely to the orbital energy matching between the excited state (HOMO) of the polymeric material and LUMO of the analyte.[22, 23]

An important feature in such poly- or disilylated products is the Lewis acidity on the silicon center that can interact with lone pairs nitrogen or oxygen atoms (Lewis bases) of the explosive analyte, which is not observed in other luminescent organic polymers.[23] The Lewis acid-base interaction is more convenient due to the larger intramolecular distances between silafluorene units.[23] The strained silacycle of both the (tetraphenyl)silole and silafluorene co-monomers act as hard Lewis acid centers that promote binding of the hard bases such as nitrogen or oxygen atoms present in nitro- and nitrate-containing explosive analytes. The incorporation of flexible phenylene-divinylene units maintains delocalization for fluorescence quenching which prevents the self-quenching processes in thin films.[20, 22, 23]

The silafluorene hydrosilylated products revealed a better alignment for conjugation of the bridging organic π-system and the Si-C σ*-orbitals. The plane of the vinylene unit in the disilylated product formed by the hydrosilylation reaction of 1-hydrido-1-methylsilafluorene and 1,4-diethynylbenzene is tilted by 71.0^{o} with respect to that of the silafluorene unit (Figure 1.2.5).[22] This allows the π-orbitals of the vinylene unit to better face the silacyclopentadiene unit and partial overlap of the former with the σ*-orbitals of the silicon-exocyclic substituent unit.

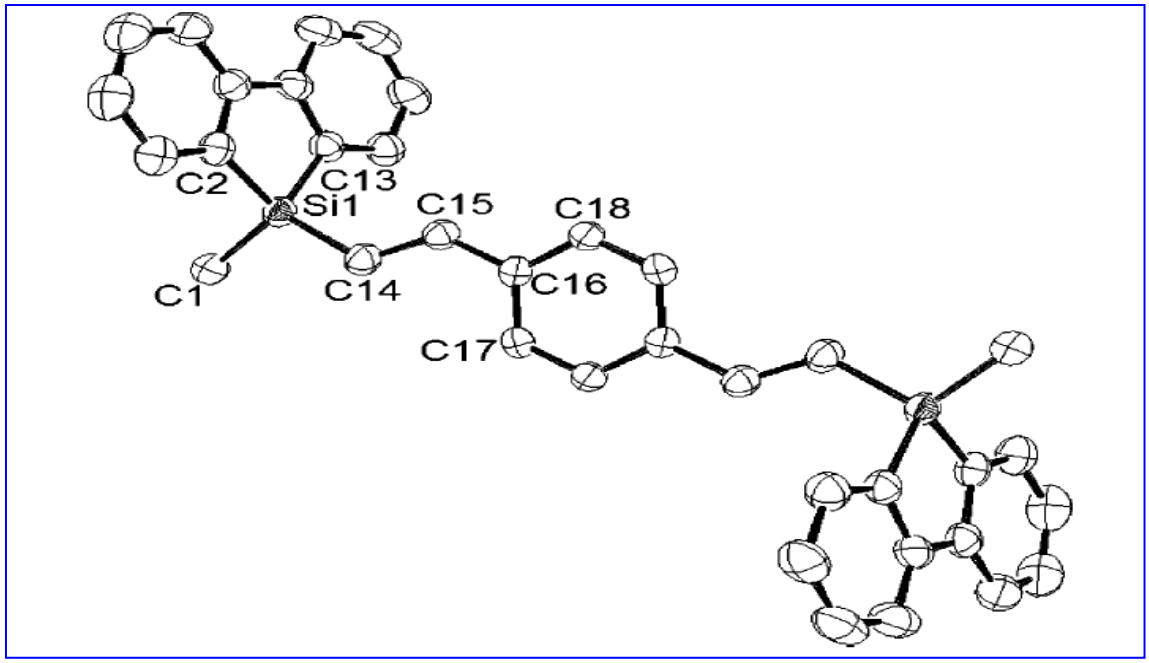

Figure 1.2.5. Molecular structure of the hydrosilylated product of 1-hydrido-1-methylsilafluorene and 1,4-diethynylbenzene. Thermal ellipsoids are drawn at the 50% probability level. Hydrogen atoms are omitted for clarity. Selected bond lengths (Å): Si1-C14 = 1.848(2), C14-C15 = 1.337(3), C15-C16 = 1.476(3) and angles (deg): C2-Si1-C13 = 91.08(9), Si1-C14-C15 = 123.14(16), C14-C15-C16 = 126.13(18).[22]

The conjugation in the silafluorene poly- or disilylated products is expected to be better than in the (tetraphenyl)silole analogue since the σ*-orbitals at silicon make a major contribution to the LUMO of the disilylated photoluminescent substance. The fluorescence emission of the disilylated products is red-shifted by *ca.* 5 nm compared to the parent silafluorene. Therefore, copolymerization of silafluorene with an unsaturated organic conjugated system in the 1,1-position offers the possibility of a new type of stable blue emitting materials.[22, 23]

Trogler and co-workers investigated catalytic hydrosilylation or hydrogermylation reactions with a variety of siloles and silafluorenes (or their germanium analogues) in the presence of the traditional Pt/Pd catalysts such as $Pd(PPh_3)_4$, Speier's catalyst, Karstedt's catalyst, and Wilkinson's catalyst. The hydrosilylation reaction of 1,4-diethynylbenzene

and trimethylsilylacetylene catalyzed by the Speier's catalyst (chloroplatinic acid, CPA) was separately carried out with 1-hydrido-1-methyl(tetraphenyl)silole by refluxing in toluene, with a catalyst loading of *ca.* 0.5 mole% (analogous to Equation 1.2.1). The starting material was consumed within 10 min, as indicated by the disappearance of the Si-H proton resonance and the appearance of vinylic protons in the ^{1}H NMR spectrum. The crystal structure of the product obtained in the latter reaction revealed exclusive *syn*-*β* addition (yielding the *trans*-*β* product) to the trimethylsilylacetylene group, which is promoted by steric crowding between the silicon center and the 2,5-phenyl groups on the silole unit.[22]

The hydrosilylation reaction of 1,4-diethynylbenzene was also carried out with 1-hydrido-1-methylsilafluorene in the presence of 0.5 mole% of CPA by stirring the starting materials in toluene at room temperature for 12 h. The (*β-trans*)-only vinyl disilylated product (Figure 1.2.5) was obtained in 79% yield. The ^{1}H NMR spectrum of the *trans*-alkenyl product exhibited two doublets for the alkenyl hydrogens at 7.07 and 6.51 ppm, with J = 19.2 Hz for both doublets. The effect of reaction temperature on the stereochemistry and regioselectivity of the disilylated product can be explained by the sterically less demanding environment at silicon for the silafluorene moiety as compared to the (tetraphenyl)silole. On oxidative-addition to the platinum center, 1,2-insertion of the Si-H bond across the coordinated triple bond of 1,4-diethynylbenzene exhibits reduced steric control in the case of the silafluorene as compared to the (tetraphenyl)silole. Therefore, a reduced temperature is necessary to form the kinetically favored *trans*-product selectively.[22]

In addition to all of these studies on the Pt catalyzed hydrosilylation reactions involving siloles and silafluorenes, Murakami's group have investigated some ruthenium catalyzed hydrosilylation reactions with siloles and silafluorenes.[24] A double *trans* hydrosilylation reaction of 1,3-diynes was carried out by the reaction of silafluorenes with *m*-bis(diynyl)benzene in 1,2-dichloroethane in the presence of 6-7 mole% of a cationic ruthenium catalyst, $[Cp^*Ru(MeCN)_3]PF_6$. The photophysical properties of the resulting hydrosilylated oligomers were studied and these products were found to exhibit a very good fluorescence behavior.[24]

1.2.7 Transition metals-PTA complexes in hydrosilylation reactions

Only a few researchers have investigated homogeneous catalytic hydrosilylation reactions involving transition metals complexes with P,N-ligand systems.[25] There are a number of literature examples for the hydrogenation reactions of alkenes, alkynes, aldehydes, or ketones catalyzed by the transition metal PTA complexes.[26] The PTA-stabilized platinum nanoparticles were recently found to catalyze an aqueous biphasic hydrogenation reaction.[26d] To the best of our knowledge, however, essentially none of the transition metal PTA complexes has been reported to catalyze hydrosilylation reactions. Berk *et al.* have investigated the catalytic hydrosilylation reactions of butanone with Et_3SiH using a variety of rhenium PTA complexes such as $[Re(PTA)_2Br_2(NO)(CH_3CN)]$, $[Re(PTA)_3Br_2(NO)]$, $[Re(PTAH)_2Br_2(NO)(CH_3CN)][Br]_2$, and $[Re(PTAH)(PTA)Br_2(NO)(CH_3CN)][Br]$. However, either these complexes were not able to catalyze the hydrosilylation reaction at all or the yield of the hydrosilylated product was very poor.[27] Therefore, current study is focused on the investigation of the catalytic hydrosilylation reactions catalyzed by the novel platinum(II)-PTA complexes.

1.2.8 References

[1] (a) Braddock-Wilking, J.; Corey, J. Y.; Trankler, K. A.; Xu, H.; French, L. M.; Praingam, N.; White, C.; Rath, N. P. *Organometallics* **2006**, *25*, 2859. (b) Braddock-Wilking, J.; Corey, J. Y.; Trankler, K. A.; Dill, K. M.; French, L. M.; Rath, N. P. *Organometallics* **2004**, *23*, 4576. (c) Corey, J. Y.; Braddock-Wilking, J. *Chem. Rev.* **1999**, *99*, 175. (d) Corey, J. Y. *Chem. Rev*. **2011**, *111*, 863. (e) Sadow, A. D.; Tilley, T. D. *J. Am. Chem. Soc.* **2003**, *125*, 9462. (f) Tilley, T. D**.** *Acc. Chem. Res.* **1993**, *26*, 22.

[2] For the examples of dehydrocoupling reactions, see: (a) Harrison, D.; Edwards, D.; McDonald, R.; Rosenberg, L. *Dalton Trans.* **2008**, 3401. (b) Chandrasekhar, V.; Krishnan, V.; Sasikumar, P.; Murthy, V. *J. Inorg. Organomet. Polym. Mater.* **2007**, *17*, 439. (c) Maddocks, A.; Hook, J.; Stender, H.; Harris, A. *J. Mater. Sci.* **2008**, *43*, 2666. (d) Miller, R. D.; Michl, J. *Chem. Rev*. **1989**, *89*, 1359.

[3] (a) Marciniec, B. *Silicon Chem. 1* **2002**, *1*, 155. (b) Crabtree, R. H. In *The Organometallic Chemistry of Transition Metals*; Eds.; Wiley-Interscience: New York, 2005; p 99.

[4] For instance, see: (a) Speier, J. L. *Adv. Organomet. Chem.* **1979**, *17*, 407. (b) Harrod, J. F.; Chalk, A. J. In *Organic Synthesis via Metal Carbonyls*; Wender, I., Pino, P., Eds.; John Wiley & Sons Ltd.: New York, 1977; Vol. 2, p 673. (c) Tilley, T. D. In *The Chemistry of Organic Silicon Compounds*; Patai, S., Rappoport, Z., Eds.; John Wiley & Sons Ltd.: New York, 1989; p 1415. (d) Ojima, I. In *The Chemistry of Organic Silicon Compounds*; Patai, S., Rappoport, Z., Eds.; John Wiley & Sons Ltd.: New York, 1989; p 1479.

[5] Voronkov, M. G.; Adamovich, S. N.; Khramtsova, S. Y.; Shternberg, B. Z.; Rakhlin, V. I.; Mirskov, R. G. *Russ. Chem. Bull.* **1991**, 2520.

[6] Chalk, A. J.; Harrod, J. F. *J. Am. Chem. Soc.* **1965**, *87*, 16.

[7] Schroeder, M. A.; Wrighton, M. S. *J. Organomet. Chem.* **1977**, *128*, 345.

[8] Prignato, A. L.; Trogler, W. C. *J. Am. Chem. Soc.* **1987**, *109*, 3586.

[9] Sakaki, S.; Mizoe, N.; Sugimoto, M. *Organometallics* **1998**, *17,* 2510.

[10] Lewis, L. N. *J. Am. Chem. Soc.* **1990**, *112, 6998.*

[11] Eaborn, C.; Bott, R. W. In *The Bond* to *Carbon;* MacDiarmid, A. G., Ed.; Marcel Dekker: New York, 1968; Vol. 1.

[12] (a) Speier, J. L. *Adv. Organomet. Chem.* **1979**, *17*, 407. (b) Itami, K.; Mitsudo, K.; Nishino, A.; Yoshida, J. *J. Org. Chem.* **2002**, *67*, 2645. (c) Boudjouk, P.; Hauck, B. J.; Chauhan, M.; Keller, L. P. *J. Organomet. Chem.* **2002**, *645*, 1. (d) Lewis, L. N.; Uriarte, R. J. *Organometallics* **1990**, *9*, 621. (e) Speier, J. L.; Webster, J. A.; Bernes, G. H. *J. Am. Chem. Soc.* **1957**, *79*, 974. (f) Motoda, D.; Shinokubo, H.; Oshima, K. *Synlett* **2002**, *9*, 1529.

[13] Lewis, L. N.; Sy, K. G.; Bryant, Jr., G. L.; Donahue, P. E. *Organometallics* **1991**, *10*, 3750.

[14] (a) Ojima, I.; Kumagai, M. *J. Organomet. Chem.* **1974**, *66*, C14. (b) Karstedt, B. D. *US Patent* 3 775 452 (**1973**). (c) Lewis, L. N.; Lewis, N.; Uriarte, R. J. In *Homogeneous Transition Metal Catalyzed Reactions*; Adv. Chem. Ser. 230, Eds.; Mose, W. R.; Slocum, D. W. American Chemical Society: Washington, D. C., 1992; p. 541.

[15] (a) Berthon-Gelloz, G.; Schumers, J.-M.; De Bo, G.; Markó, I. E. *J. Org. Chem.* **2008**, *73*, 4190. (b) Silvestri, G. F.; Flores, J. C.; de Jesús, E. *Organometallics* **2012**, *31*, 3355. (c) De Bo, G.; Berthon-Gelloz, G.; Tinant, B.; Markó, I. E. *Organometallics* **2006**, *25*, 1881. (d) Blug, M.; Le Goff, X.-F.; Mézailles, N.; Le Floch, P. *Organometallics* **2009**, *28*, 2360.

[16] (a) Denmark, S. E; Wang, Z. *Org. Lett.* **2001**, *3*, 1073. (b) Esteruelas, M. A.; Herrero, J.; Oro, L. A. *Organometallics* **1993**, *12*, 2377. (c) Takeuchi, R.; Tanouchi, N. *J. Chem. Soc., Perkin Trans. 1* **1994**, 2909. (d) Na, Y.; Chang, S. *Org. Lett.* **2000**, *2*, 1887.

[17](a) Dickers, H. M.; Haszeldine, R. **N.;** Mather, A**.** P.; Parish, R. V. *J. Organomet. Chem.* **1978**, *161*, 91. (b) Ojima, I.; Clos, N.; Donovan, R. J.; Ingallina, P. *Organometallics* **1990**, *9*, 3129. (c) Brady, K. A.: Nile, T. A. *J. Organomet. Chem.* **1981**, *206*, 299.

[18] (a) Marciniec, B.; Gulinski, J.; Urbaniak, W.; Nowicka, T.; Mirecki, J. *Appl. Organomet. Chem.* **1990**, *4*, 27. (b) Caseri, W.; Pregosin, P. S. *Organometallics* **1988**, *7*, 1373.

[19] (a) West, R.; Sohn, H.; Bankwitz, U.; Calabrese, J.; Apeloig, Y.; Mueller, T. *J. Am. Chem. Soc.* **1995**, *117*, 11608. (b) Yu, G.; Yin, S.; Liu, Y.; Chen, J.; Xu, X.; Sun, X.; Ma, D.; Zhan, X.; Peng, Q.; Shuai, Z.; Tang, B.; Zhu, D.; Fang, W.; Luo, Y. *J. Am. Chem. Soc.* **2005**, *127*, 6335. (c) Sanchez, J. C.; DiPasquale, A. G.; Mrse, A. A.; Trogler, W. C. *Anal. Bioanal. Chem.* **2009**, *395*, 387.

[20] (a) Johansson, D. M.; Theander, M.; Srdanov, G.; Yu, G.; Inganas, O.; Andersson, M. R. *Macromolecules* **2001**, *34*, 3716-3719. (b) Fan, C.; Plaxico, K. W.; Heeger, A. J. *J. Am. Chem. Soc.* **2002**, *124*, 5642.

[21] (a) Benfaremo, N.; Sandman, D. J.; Tripathy, S.; Kumar, J.; Yang, K.; Rubner, M. F.; Lyons, C. *Macromolecules* **1998**, *31*, 3595. (b) Kim, D.-J.; Kim, S.-H.; Zyung, T.; Kim, J.-J.; Cho, I.; Choi, S. K. *Macromolecules* **1996**, *29*, 3657.

[22] Sanchez, J. C.; Urbas, S.; Toal, S.; DiPasquale, A. G.; Rheingold, A. L.; Trogler, W. C. *Macromolecules* **2008**, *41*, 1237.

[23] (a) Sanchez, J. C.; Trogler, W. C. *Macromol. Chem. Phys.* **2008**, *209*, 1527. (b) Sanchez, J. C.; DiPasquale, A. G.; Rheingold, A. L.; Trogler, W. C. *Chem. Mater.* **2007**, *19*, 6459. (c) Sanchez, J. C.; Trogler, W. C. *J. Mater. Chem.* **2008**, *18*, 3143.

[24] Matsuda, T.; Kadowaki, S.; Murakami, M. *Chem. Commun.* **2007**, 2627.

[25] (a) Gavrilov, K. N.; Polosukhin, A. I. *Russ. Chem. Rev.* **2000**, *69*, 661. (b) McKay, I. D.; Payne, N. C. *Can. J. Chem.***1986**, *64*, 1930.

[26] (a) Smolenski, P.; Pruchnik, F. P.; Ciunik, Z.; Lis, T. *Inorg. Chem.* **2003**, *42*, 3318. (b) Csabai, P.; Joó, F. *Organometallics* **2004**, *23*, 5640. (c) Bolaño, S.; Gonsalvi, L.; Zanobini, F.; Vizza, F.; Bertolasi, V.; Romerosa, A.; Peruzzini, M. *J. Mol. Catal. A* **2004**, *224*, 61. (d) Debouttière, P.-J.; Coppel, Y.; Denicourt-Nowicki, A.; Roucoux, A.; Chaudret, B.; Philippot, K. *Eur. J. Inorg. Chem.* **2012**, 1229.

[27] Dong, H.; Berke, H. *Adv. Synth. Catal.* **2009**, *351*, 1783.

1.3 Palladium Catalyzed Cross-Coupling Reactions

Metal catalyzed carbon-carbon and carbon-heteroatom bond formation reactions are highly important reactions in synthetic chemistry.[1] Palladium catalyzed cross-coupling reaction of an electrophile C-X unit (X is mainly Br, I, OTf) and an organometallic species C-M (M is mainly Mg, Zn, Sn, and B) or an alkene/alkyne is a versatile method for the C-C bond formation (Equation 1.3.1). The principle of nickel or palladium catalyzed cross-coupling reactions is that two molecules are brought together on the metal *via* the metal-carbon bonds formation and the carbon atoms bound to the metal are brought very close to one another. In the next step, the coupling of the two carbon atoms leads to the formation of a new carbon-carbon single bond. The catalytic cross-coupling reactions often use readily available starting materials and are able to tolerate a wide range of functional groups. The efficiency of the Pd center originates from its ability to activate the C-X bonds (X = I, Br, Cl, O) by an oxidative-addition to the metal center which provides an organopalladium complex that can be reactive towards nucleophiles.[1]

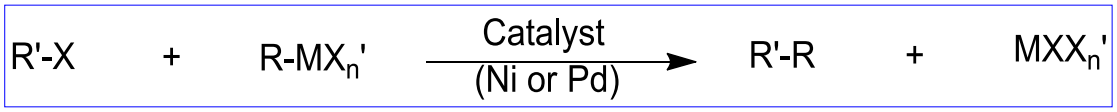

Equation 1.3.1. Metal catalyzed cross-coupling reaction.

1.3.1 Catalytic cycle followed by cross-coupling reactions

The mechanism of the cross-coupling reactions has been studied intensively over the years.[1, 2] The generally accepted catalytic cycle in Pd catalyzed cross-coupling reactions follows a pathway through oxidative-addition, transmetallation, and reductive-elimination. The palladium species introduced as the catalyst precursor is considered to be converted to a catalytically active species of low coordination number enabling the

oxidative-addition of the organic substrate (i.e. an aryl halide) to the metal center. This is followed by transmetallation (ligand metathesis) of the organic groups. Finally, reductive-elimination of the cross-coupled product leads to regeneration of the catalytically active species (Scheme 1.3.1). Palladium still remains the metal of choice for cross-coupling processes. Recent efforts on increasing the efficiency of a catalyst such as reactivity, selectivity, and longevity has resulted more detailed mechanistic studies being performed for key reactions catalyzed by a number of highly active catalysts.[2]

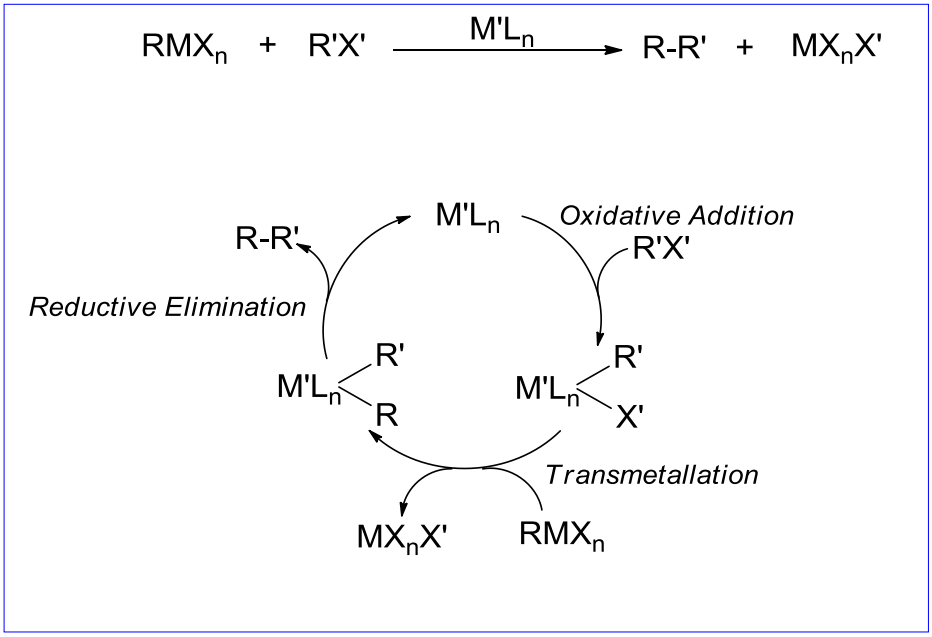

Scheme 1.3.1. General catalytic cycle followed by cross-coupling reactions.[1, 2]

1.3.2 Suzuki -Miyaura cross-coupling reaction

The Suzuki-Miyaura cross-coupling reaction is a highly versatile approach for the generation of carbon-carbon bonds.[3, 4] This is a reaction of an aryl- or vinylboronic acid with an alkyl-, aryl-, allyl- or a vinyl halide catalyzed by palladium complexes (Scheme 1.3.2). It is widely used to synthesize poly-olefins, styrenes, and substituted biphenyls.[3, 4]

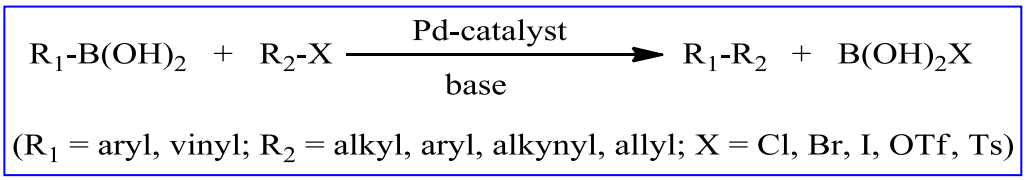

Scheme 1.3.2. Suzuki-Miyaura cross-coupling reaction.

The reaction was first reported by Suzuki and co-workers in 1979.[3a] It was reported that the reaction between an equimolar amount of (*E*)-1-hexenyldisiamyl borane in THF and (*E*)-1-bromo-2-phenylethene along with 1 mol% of $Pd(PPh_3)_4$ catalyst in the presence of a base such as sodium methoxide, ethoxide, acetate, or hydroxide gave (*E*,*E*)-1-phenyl-1,3-octadiene in good yields.[3] The reaction proceeded with complete retention of stereochemistry for the alkenyl halide but with inversion of stereochemistry for the allylic and benzylic halides.[3b]

The mechanism for the Suzuki-Miyaura reaction is similar to that for other cross-coupling reactions (Scheme 1.3.3).[4] Oxidative-addition is often the rate limiting step in

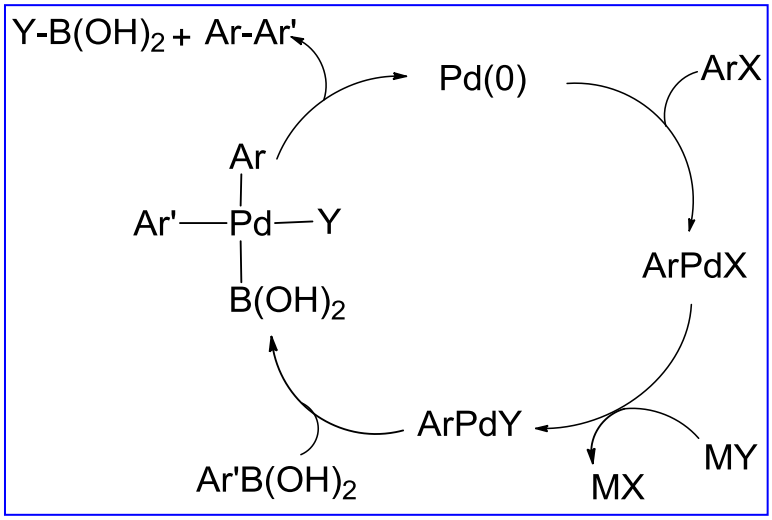

Scheme 1.3.3. Catalytic cycle in Suzuki-Miyaura cross-coupling reaction.

the catalytic cycle.[3, 4] The transmetallation of the organoborane to palladium occurs with retention of stereochemistry.[3b, c] Due to the low nucleophilicity of the organic group on the boron atom, the transmetallation step between the organoboron compound and the organopalladium(II) complex does not usually proceed in the absence of a base. The nucleophilicity can be enhanced by the quarternization of the boron center with a negatively charged base and the resulting borate complex undergoes an efficient coupling reaction with the aryl halide. It has been suggested that the transmetallation step takes place on a charged $[Ar'B(OH)_3]^-$ species rather than on the neutral arylboronic acid.[3] Reductive-elimination occurs directly from the *cis*-complex whereas the *trans*-complex reacts after isomerization to the corresponding *cis*-complex during one of the steps in the catalytic cycle, mainly after the transmetallation step.[3]

1.3.3 Side reactions in Suzuki -Miyaura cross-coupling reaction

The major problem in Suzuki-Miyaura cross-coupling reactions is homo-coupling which results in the formation of symmetrical biaryls.[5] Marcuccio and co-workers have found that coupling of arylboronic acids with the phenyl group from the triphenylphosphine ligand is a side reaction to the desired coupling of the arylboronic acid with an aryl bromide.[5a] Homo-coupling also takes place because of aryl-aryl exchange between the aryl halide(s) and coordinated phosphine ligand(s).[5b] Additionally, self-coupling of aryl groups of the arylboronic acids may occur to give the side products, usually biphenyl.[5c]

Homo-coupling occurs especially when the substrate (aryl halide) is less active and/or the reaction is in contact with some source of oxidant such as air (oxidative coupling). In oxidative coupling, the catalytic cycle follows an alternative path to yield the homo-

coupled product (Scheme 1.3.4).[5d-f] To avoid homo-coupling, ligand-free palladium(II)-assisted coupling reactions and perfectly anaerobic environments are desirable.

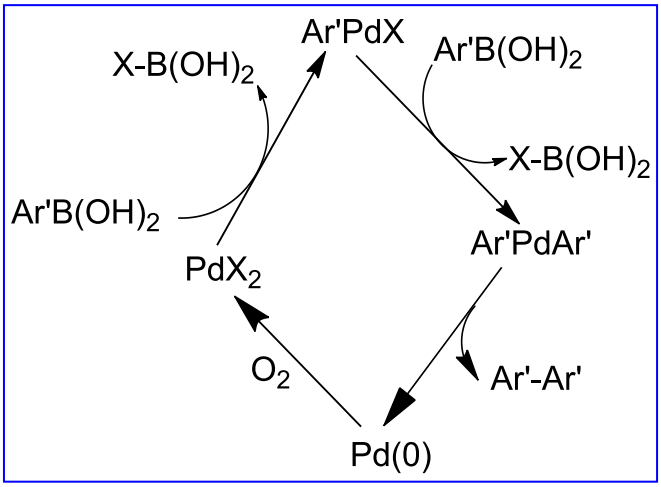

Scheme 1.3.4. Mechanism for homo-coupling in Suzuki-Miyaura cross-coupling reaction.[5d-f]

In the palladium catalyzed cross-coupling reaction, the order of reactivity of the substrate based on the halogen atom is usually I > Br > > Cl.[5e] The lower activity of aryl bromides or chlorides compared to aryl iodides makes homo-coupling of the arylboronic acids more significant significant for the former. Furthermore, the amount of the reagent or substrate, the solvent, and the nature of catalyst may have significant control over homo-coupling and other side reactions occurring in Suzuki-Miyaura cross-coupling reactions, which will be discussed below. Homo-coupling is also observed in other types of cross-coupling reactions such as Stille,[5g] Heck,[5h] and Sonogashira cross-coupling reactions.[5i]

A large variety of palladium(0) catalysts bearing various ligands can be used for the Suzuki-Miyaura cross-coupling reactions. Phosphine complexes are widely used because of their ease in preparation and air-stability. One of the drawbacks in catalytic cross-

coupling reactions, including the Suzuki-Miyaura cross-coupling reaction, is the formation of a side product as a result of β-hydride elimination when a substrate is used that contains β-hydrogen atoms (Scheme 1.3.5). When the metal is coordinated to good donor ligands such as phosphines, especially ligands with a greater bite angles such as many bidentate phosphines, the energy of the empty orbital of the metal (LUMO) is

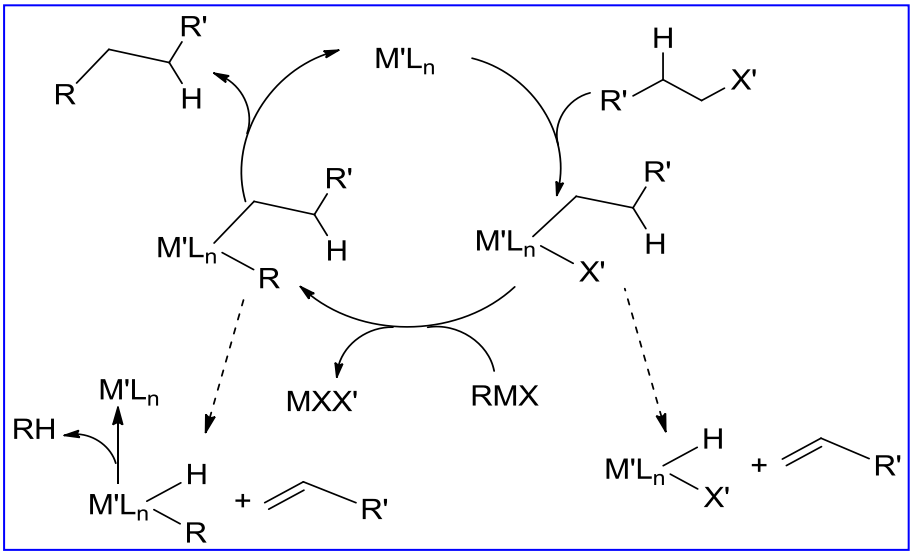

Scheme 1.3.5. Catalytic cycle for cross-coupling reaction along with β-hydride elimination.

raised. Therefore, the β-hydrogen cannot approach the vacant coordination site of the metal easily. Moreover, the sterically hindered hydrogen will not be able to approach the metal center easily. For this reason, the reductive-elimination is preferred to the β-hydride elimination after the transmetallation step.[6]

1.3.4 Suzuki -Miyaura cross-coupling reactions catalyzed by some Pd complexes

Colacot *et al.* systematically compared the catalytic activities of the Pd(II)-phosphine complexes such as (dppf)PdX_2 (X = Cl, Br, I) in the Suzuki-Miyaura cross-coupling reaction of 4-bromoacetophenone with phenylboronic acid in toluene as a function of

respective (X-Pd-X) bond angles and (P-Pd-P) bite angles, which is the ligand-metal-ligand chelation angle (P-M-P bond angle) for the bidentate phosphines (Figure 1.3.1). With 1 mole% catalyst loading, the reaction mixture was stirred at 70 ^{o}C for 2 h in the presence of K_2CO_3. Both (dppf)$PdCl_2$ and (dppf)$PdBr_2$ showed the highest activity under identical conditions which was expected, based on their similar bite angles and (X-Pd-X) bond angles. The conversion of the aryl halide into the products, as determined by GC, was found to be 94% and 93%, respectively. However, (dppf)PdI_2 displayed lower

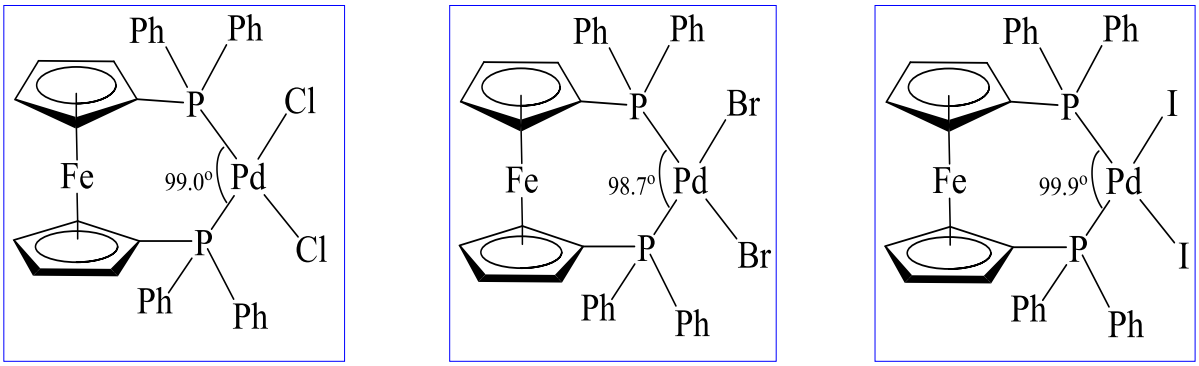

Figure 1.3.1. Structures of PdX_2(dppf) complexes with (P-Pd-P) bite angles.[7]

activity (69% yield) due to its lower solubility in toluene. Actually, most of the catalysts with smaller (X-Pd-X) bond angles and larger (P-Pd-P) bite angles were found to be more effective. The rate of conversion was found to be lower for the $PdCl_2(PPh_3)_2$ catalyzed reaction than for the reactions catalyzed by $PdCl_2$(dppe) and PdX_2(dppf) (X = Cl, Br). In most cases, the homo-coupled product, biphenyl, was also detected in the range between 2–10% yield. On the other hand, the Ph_3P-$Pd(OAc)_2$ catalyst system gave lower yield although the amount of the side products was minimized.[7]

Dong *et al.* have reported an efficient system to carry out Suzuki-Miyaura cross-coupling reactions of aryl bromides with [*p*-(un)substituted phenyl] boronic acids in

refluxing isopropanol using ligand-free $PdCl_2$ as a catalyst (0.3 mole% catalyst loading) and K_2CO_3 base.[5f] It was found that the $PdCl_2$/isopropanol system could inhibit the homo-coupling of phenylboronic acid efficiently and give the cross-coupled products in the range of 80-99% of isolated yields. When *p*-iodotoluene was reacted with phenylboronic acid for 4 h in refluxing ^{i}PrOH in the presence of K_2CO_3, the conversion of the iodotoluene was found to be > 99% with the ratio of cross-coupled and homo-coupled products being 99.7 : 0.3, respectively. This reaction system tolerated a variety of functional groups. In other refluxing solvent systems such as toluene, methanol, dimethylformamide (DMF), ethyl acetate, and 1,4-dioxane, the reactions were found to be less effective, forming a greater amount of biphenyl. A possible mechanism for isopropanol activation of the catalyst was also proposed by Dong and co-workers (see Scheme 2.3.2 in *"Results and Discussion"*).[5f] It had been found that the substituted aryl halides containing electron-withdrawing groups gave better yields of cross-coupled products than those containing electron-donating groups.[5j]

The use of aryl bromides and iodides was described in the original publications on Pd catalyzed cross-coupling reactions and there were no efficient catalysts for the most of the aryl chlorides for a number of years.[1, 2, 5] This correlates with the strength of the Ar-X bond, which increases as: I < Br < Cl (65, 81, and 96 kcal mol^{-1}, respectively) and results in the oxidative-addition step becoming increasingly difficult.[1, 8] However, Suzuki-Miyaura cross-coupling reactions of activated aryl chlorides have been possible in the presence of a wide range of catalysts. For example, Shen *et al.* proposed that the PCy_3 ligand may promote the oxidative-addition of the aryl chloride. Additionally, it had been proposed that the the steric demands of the ligand might promote the formation of a

monophosphine complex as the active catalyst during the reaction and aid reductive-elimination.[8a] Hartwig *et al.* investigated the catalytic role of a dimeric palladium(I) complex, $[PdBr\{P(^tBu)_3\}]_2$ which was supposed to generate highly active monophosphine species *via* dissociation.[8b]

Frech and Bolliger have recently reported the catalytic activities of the palladium(II) aminophosphine complexes of the type, $[P\{(NC_5H_{10})_{3-n}(C_6H_{11})_n\}_2PdCl_2]$ in Suzuki-Miyaura cross-coupling reactions performed with various aryl bromides and showed that they are highly active and reliable catalysts with exceptional functional group tolerance.[9] The reactions were carried out in refluxing toluene with 0.2 mole% catalyst loading with respect to the aryl halide. Aminophosphines were expected to be excellent ligand systems for these transformations since they undergo slow degradation in the presence of water and they promote the formation of palladium nanoparticles which function as the active catalysts. Moreover, the formation of the nanoparticles was accompanied by the generation of easily separable side products.[9] However, the catalytic reactions need multiple and lengthier work-up processes to get the pure cross-coupled products.

1.3.5 Catalytic role of PTA in Suzuki-Miyaura cross-coupling reactions

Frost *et al.* have reported the Suzuki-Miyaura cross-coupling reaction of substituted aryl halides with phenylboronic acid in a water and acetonitrile biphasic solvent system in the presence of 5 mole% of a palladium(II) catalyst, $Pd(OAc)_2$ or $PdCl_2$, in combination with 10 mole% of a PTA-derivatized ligand such as DAPTA and RO-PTA (RO-PTA = ring opened-PTA, also known as PTN) (Figure 1.3.2).[10] The reaction mixture was heated at 80 ^oC for 6 h in the presence of the base, Na_2CO_3. The combination of RO-PTA and $Pd(OAc)_2$ or $PdCl_2$ generated an effective catalyst for the

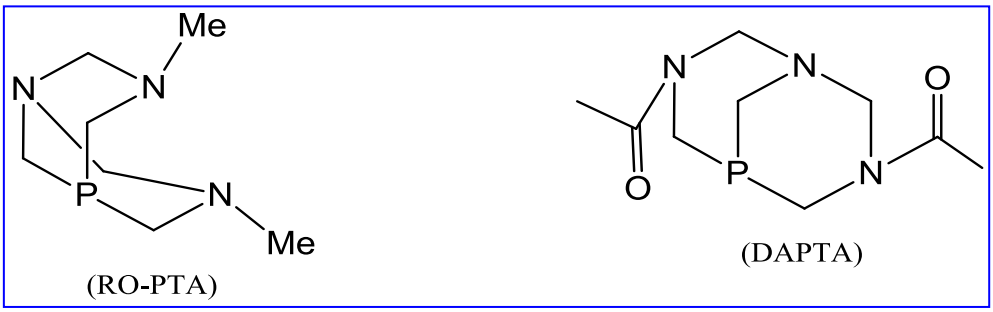

Figure 1.3.2. Structures of RO-PTA and DAPTA ligands.

Suzuki-Miyaura cross-coupling reaction. Electron-neutral and electron-deficient aryl bromide substrates coupled well with phenylboronic acid giving the cross-coupled products in 77-90% yields. The catalytic system was modestly effective in the Suzuki-Miyaura cross-coupling reactions of electron-rich and sterically hindered aryl bromides.[10] None of the transition metal complexes bearing a PTA or PTA-derivatized ligand have been utilized yet as a pre-catalyst in Suzuki-Miyaura cross-coupling reaction.

1.3.6 Sonogashira cross-coupling reaction

One of the most straightforward methods for the preparation of arylalkynes is the palladium catalyzed sp^2-sp coupling of aryl or alkenyl halides or triflates with terminal alkynes which was reported initially by Sonogashira *et al.* in 1975 (Equation 1.3.2).[11]

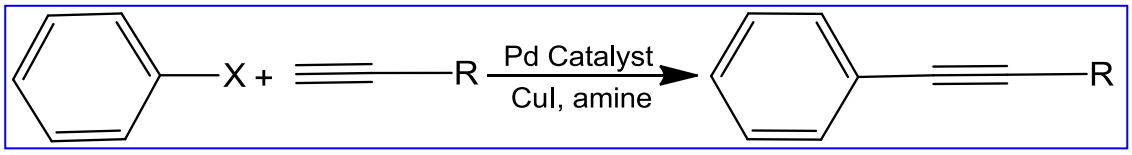

Equation 1.3.2. Sonogashira cross-coupling reaction.

A Sonogashira cross-coupling reaction can be carried out with or without the presence of a copper(I) co-catalyst and a base such as a secondary or tertiary amine to neutralize the halogen acid generated during the reaction. The Sonogashira cross-coupling reaction has become the exceptional method to prepare arylalkynes and

conjugated π-systems, enynes which can act as precursors for the synthesis of natural products, pharmaceuticals, and many other organic materials.[12] It is necessary to note that even primary alkyl bromides or iodides,[13a] and secondary alkyl bromides[13b] can be alkynylated using a Sonogashira protocol.

As in Suzuki-Miyaura cross-coupling reactions, Sonogashira cross-coupling reactions are also interfered by the formation of side products due to β-hydride elimination[14a] and oxidative homo-coupling reactions.[14b, c] Usually, Sonogashira cross-coupling reactions are carried out in the presence of copper(I) co-catalysts such as CuI to activate the alkyne molecules. Copper iodide abstracts the acidic hydrogen from the terminal alkyne and produces a copper(I) acetylide, which serves as an activated species for the Sonogashira cross-coupling reactions (Scheme 1.3.6).

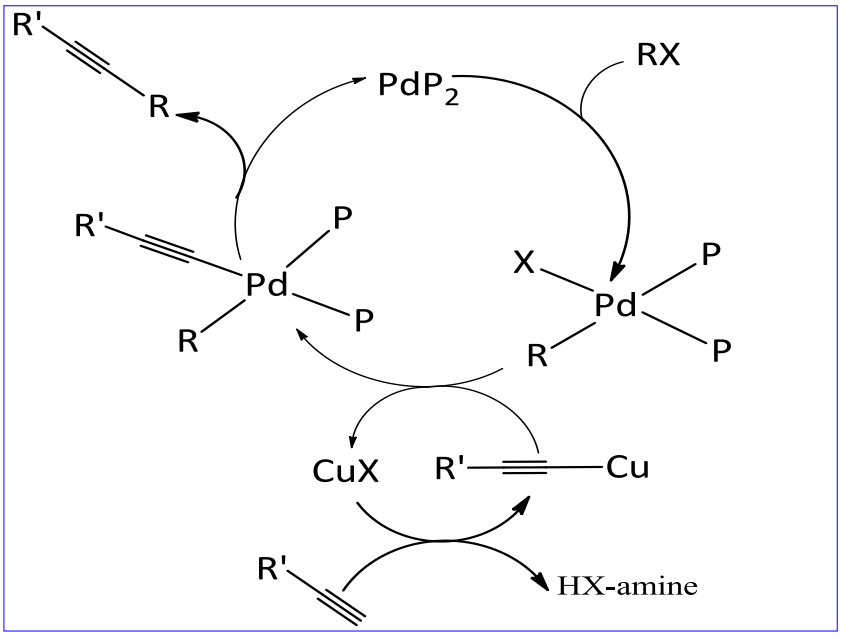

Scheme 1.3.6. Role of copper(I) halide in the catalytic cycle of Sonogashira cross-coupling reaction; P = phosphine.

1.3.7 Copper-free Sonogashira cross-coupling reaction

Although a copper co-catalyst is added to the reaction to enhance the reactivity, it also has drawbacks apart from adding another difficult to recover and environmentally unfriendly reagent to the reaction mixture. The presence of copper salt can promote the formation of alkyne dimers.[15] This gives rise to the Glaser coupling reaction, which involves the formation of undesired homo-coupled products of acetylene derivatives upon oxidation.[15] As a result, it is necessary to run a Sonogashira cross-coupling reaction with a copper co-catalyst in a strictly anaerobic environment to minimize the dimerization. Most of the Pd catalyzed Sonogoshira cross-coupling reactions are high temperature reactions. At higher temperatures, the copper salt such as CuI is able to catalyze one or more of the side reactions mentioned above. Additionally, the separation of CuI from the product mixture is also not an easy task.[15] Nowadays, a significant number of copper-free variations of the Sonogashira cross-coupling reaction have been developed to minimize the formation of the homo-coupled products.[16]

The mechanism of the copper-free Sonogashira coupling reaction is not well-known. After oxidative-addition of aryl halides (Ar-X) to the metal center, it is speculated that loss of one ligand from the Pd(0) catalyst system occurs to create an intermediate complex. Subsequently, this new intermediate can then promote the deprotonation of the terminal alkyne hydrogen followed by ligand exchange with the leaving group X. Then reductive-elimination generates the desired cross-coupled product.[17] If a stronger base such as piperidine or pyrrolidine is used, it will also assist in deprotonation of alkynes to generate the activated substrate species ready to coordinate to the metal.[18]

1.3.8 Some examples of Pd catalyzed Sonogashira cross-coupling reactions

Distinct amines need to be added as a solvent or in excess for the reaction to progress because of the crucial role of a base. The secondary amines including piperidine, pyrrolidine, morpholine, or diisopropylamine have been found to react effectively and reversibly with *trans*-$PdX(R)(PPh_3)_2$ (R = Me, Ph; X = Cl, Br, I, OTf) complexes by substituting one PPh_3 ligand. The equilibrium constant of this reaction depends on the nature of R and X, p*K*a of the protonated amine, and steric hindrance of the amine.[19] This result is a competition involving the alkyne and the amine groups for the ligand exchange process. Therefore, the amine is usually added in excess to encourage preferential substitution.

A problem with palladium(0) complexes as pre-catalysts is that the formation of the active palladium(0) catalyst is hindered by the certain coordinating properties of the ligands which are required to stabilize palladium(0) species. Also, palladium(II) complexes exhibit greater stability than palladium(0) complexes over an extended period of time because the oxidation of palladium(II) into palladium(IV) is relatively difficult. The palladium(II) pre-catalyst is reduced to palladium(0) in the reaction by either an amine, a reactant, or a phosphine ligand, thus enabling the reaction to progress.[19 -21] Many effective palladium(II) catalysts have been explored in Sonogashira cross-coupling reactions.[20-22] Krause *et al.* developed methods for the synthesis of arylacetylenes by Sonogashira cross-coupling reaction of substituted aryl bromides with terminal alkynes including phenylacetylene and trimethylsilylacetylene in THF in the presence of Et_3N. The pre-catalyst employed in the reaction was 5 mole% of $PdCl_2(PPh_3)_2$ with 1 mole% of CuI based on the aryl halides. The cross-coupled products were obtained in modest to high yields. GC-MS showed that only traces (< 5%) of homo-coupled products were

formed. The reduced homo-coupling could partly be due to slow addition of the alkyne to the reaction mixture. However, these reactions involved only the aryl halides containing electron-withdrawing substituents.[20]

Leadbeater's group investigated copper-free Sonogashira cross-coupling reactions of a variety of substituted aryl bromides and aryl iodides with phenylacetylene and trimethylsilylacetylene using piperidine, pyrrolidine, and triethylamine as the solvents.[21] With 2-4 mole% catalyst loading, $PdCl_2(PPh_3)_2$ was used as a pre-catalyst. No additional base was required and the reactions were usually complete within an hour. The results for the reactions heated in piperidine at 70 ^oC are listed in Table 1.3.1. It was observed that the aryl halides containing electron-withdrawing substituents gave better yields of cross-coupled products than those containing electron-donating substituents. Moreover, the reaction was found to be more effective for aryl iodides than for aryl bromides as the I group is more labile than the Br group (C-I bond is weaker than C-Br bond).[21]

Table 1.3.1. Results from copper-free Sonogashira cross-coupling reactions in piperidine catalyzed by $PdCl_2(PPh_3)_2$.[21] Reaction temp. = 70 ^oC. [a]Catalyst loading and yield are based on the haloarenes.

Catalyst loading[a]	Time	Aryl halide	Alkyne	% Yield, GC
4 mole%	10 min	4-bromoacetophenone	phenylacetylene	94
2 mole%	10 min	4-bromoacetophenone	trimethylsilylacetylene	75
4 mole%	10 min	4-bromotoluene	phenylacetylene	16
1 mole%	30 min	4-bromoacetophenone	phenylacetylene	73
0.5 mole%	20 min	4'-iodoanisole	phenylacetylene	79
0.5 mole%	20 min	4'-iodoacetophenone	phenylacetylene	96
2 mole%	10 min	4-iodotoluene	trimethylsilylacetylene	99

Another Pd(II) phosphine complex, *cis*-$PdCl_2(PCy_3)_2$ showed high catalytic activity in the copper-free cross-coupling reaction of aryl chlorides with a variety of terminal alkynes in DMSO at 100-120 ^oC with Cs_2CO_3 as the base.[22] The benefit of a copper-free process included readily available and easy to use catalysts and with a high catalytic activity for electron-deficient, electron-neutral, and electron-rich aryl chlorides in which the catalytic turn over number (TON) ranged from 28 to 33.[22] A range of functional groups such as alcohols, ketones, and esters were utilized under these conditions.

1.3.9 Sonogashira cross-coupling reaction catalyzed by Pd-PTA complexes

Ruiz *et al.* in 2006 reported conditions for an efficient copper- and amine-free catalyzed Sonogashira cross-coupling reaction of aryl bromides and chlorides with terminal alkynes by the chelated complex, [Pd(dmba)Cl(PTA)] [dmba = N,C-chelating 2-(dimethylaminomethyl)phenyl] (Equation 1.1.3). This complex is one of the palladacycle complexes that are found to be active in the Sonogashira cross-coupling reactions. This is the only Sonogashira cross-coupling reaction reported that uses a palladium PTA complex.[23] The unique adamantane-type phosphine that had been used until then in coupling reactions was the palladium complex, [Pd(PA-Ph)$_2$·dba] (PA-Ph = 1,3,5,7-tetramethyl-2,4,8-trioxa-6-phenyl-6-phosphaadamantane; dba = dibenzylideneacetone).[24] Ruiz's group first studied the reaction of 4-bromoacetophenone and phenylacetylene at 60 °C in the presence of 2 mol% of [Pd(dmba)Cl(PTA)] based on the aryl bromide. The solvents screened were toluene, CH_3CN, acetone, and THF. The best conversion was obtained when acetonitrile was used. Commonly used tertiary amine bases such as triethylamine gave inferior results whereas alkali metals carbonates, Cs_2CO_3 and K_2CO_3 were found to be more effective. Another notable observation was that the presence of

copper co-catalyst added at the beginning of the reaction had a deleterious effect on the desired transformation.[23]

After preliminary optimization of the reaction conditions, the catalytic activity of the palladium PTA complex was explored in the reaction of aryl bromides with terminal alkynes in acetonitrile at 80 °C in the presence of Cs_2CO_3, while the reaction was carried out for 24 h. The catalyst loading was 2.5 mole% with respect to the aryl bromides. The reactions were found to be very effective with minimal homo-coupling and excellent yields. Because of greater extent of homo-coupling, the yield of the cross-coupled product was observed to be *ca.* 70% when phenylacetylene was used. The reaction was also carried out with aryl chlorides under similar reaction conditions except the use of 3 mole% of the pre-catalyst with respect to the aryl chlorides. Again, the catalytic activity was found to be very good.[23] However, the synthesis of this pre-catalyst complex is not straightforward. Despite the water-solubility of a number of palladium PTA, NHC, and sulfonated phosphine complexes, very few biphasic and aqueous-phase catalysis have been investigated in the Sonogashira cross-coupling reactions.[25]

In this regard, the current study is focused on the investigation of the catalytic activity of some palladium(II)-PTA complexes in the Suzuki-Miyaura and copper-free Sonogashira cross-coupling reactions using different solvent systems.

1.3.10 References

[1] (a) Ananikov, V. P.; Musaev, D. G.; Morokuma, K. Organometallics **2005**, *24*, 715. (b) Colacot, T. J. *Platinum Met. Rev.* **2001**, *45*, 22. (c) Jana, R.; Pathak, T. P.; Sigman, M. S. *Chem. Rev.* **2011**, *111*, 1417.

[2] (a) Barnard, C. *Platinum Met. Rev.* **2008**, *52*, 38. (b) Crisp, G. T. *Chem. Soc. Rev.* **1998**, *27*, 427. (c) Tamao, K.; Sumitani, K.; Kumada, M. *J. Am. Chem. Soc.* **1972**, *94*, 4374.

[3] (a) Miyaura, N.; Yamada, K.; Suzuki, A. *Tetrahedron Lett.* **1979**, *20*, 3437. (b) Miyaura, N.; Suzuki, A. *Chem. Rev.* **1995**, *95*, 2457. (c) Ridgway, B. H.; Woerpel, K. A. *J. Org. Chem*. **1998**, *63*, 458.

[4] Miyaura, N.; Yamada, K.; Suginome, H.; Suzuki, A. *J. Am. Chem. Soc*. **1985**, *107*, 972.

[5] (a) O'Keefe, D. F.; Dannock, M. C.; Marcuccio, S. M. *Tetrahedron Lett.* **1992**, *33*, 6679. (b) Kong, K. C.; Cheng, C. H. *J. Am. Chem. Soc*. **1991**, *113*, 6313. (c) Song, Z. Z.; Wong, H. N. C. *J. Org. Chem*. **1994**, *59*, 33. (d) Blackburn, T. F.; Schwartz, J. *J. Chem. Soc., Chem. Commun*. **1977**, 157. (e) Moreno-Manax, M.; Perez, M.; Pleixats, R. *J. Org. Chem.* **1996**, *61*, 2346. (f) Xiao-Chun, T.; Yue-Ping, Z.; Tian-Xiong, H.; Dong, S. *Chin. J. Chem.* **2007**, *25*, 1326. (g) Segelstein, B. E.; Butler, T. W.; Chenard, B. L. *J. Org. Chem*. **1995**, *60*, 12. (h) Hunt, A. R.; Stewart, S. K.; Whiting, A. *Tetrahedron Lett*. **1993**, *34*, 3599. (i) Li, J. H.; Liang, Y.; Xie, Y. X. *J. Org. Chem.* **2005**, *70*, 4393. (j) Kotha, S.; Lahiri, K.; Kashinath, D. *Tetrahedron* **2002**, *58*, 9633.

[6] Ney, J. E.; Wolfe, J. P. *J. Am. Chem. Soc.* **2005**, *127*, 8644.

[7] Colacot, T. J.; Qian, H.; Cea-Olivares, R.; Hernandez-Ortega, S. *J. Organomet. Chem.* **2001**, *637*, 691.

[8] (a) Shen, W. *Tetrahedron Lett.* **1997**, *38*, 5575. (b) Stambuli, J. P.; Kuwano, R.; Hartwig, J. F. *Angew. Chem., Int. Ed.* **2002**, *41*, 4746.

[9] Bolliger, J. L.; Frech, C. M. *Chem. Eur. J.* **2010**, *16*, 4075.

[10] Weeden, J. A.; Huang, R.; Galloway, K. D.; Gingrich, P. W.; Frost, B. J. *Molecules* **2011**, *16*, 6215.

[11] (a) Sonogashira, K.; Tohda, Y.; Hagihara, N. *Tetrahedron Lett.* **1975**, *16*, 4467. (b) Chinchilla. R.; Najera, C. *Chem. Rev.* **2007,** *107*, 874.

[12] For examples, see: (a) Sonogashira, K. In *Comprehensive Organic Synthesis*; Trost, B. M., Fleming, I., Eds.; Pergamon Press: New York, 1991; Vol. 3, pp 521-549. (b) Rossi, R.; Carpita, A.; Bellina, F. *Org. Prep. Proced. Int.* **1995**, *27*, 129. (c) Nicolaou, K. C.; Dai, W.-M. *Angew. Chem.* **1991**, *103*, 1453.

[13] (a) Eckhardt, M.; Fu, G. C. *J. Am. Chem. Soc.* **2003**, *125*, 13642. (b) Altenhoff, G.; Würtz, S.; Glorius, F. *Tetrahedron Lett.* **2006**, *47*, 2925.

[14] (a) Vechorkin, O.; Barmaz, D.; Proust, V.; Hu, X. *J. Am. Chem. Soc.* **2009**, *131*, 12078. (b) Siemsen, P.; Livingston, R. C.; Diederich, F. *Angew. Chem., Int. Ed.* **2000**, *39*, 2632. (c) Li, J.-H.; Liang, Y.; Zhang, X.-D. *Tetrahedron* **2005**, *61*, 1903.

[15] (a) Austin, W. B.; Bilow, N.; Kelleghan, W. J.; Lau, K. S. Y. *J. Org. Chem.* **1981**, *46*, 2280. (b) Siemsen, P.; Livingston, R. C.; Diederich, F. *Angew. Chem., Int. Ed.* **2000**, *39*, 2632.

[16] For examples, see: (a) Uozumi, Y.; Kobayashi, Y. *Heterocycles* **2003**, *59*, 71. (b) Fukuyama, T.; Shinmen, M.; Nishitani, S.; Sato, M.; Ryu, I. *Org. Lett.* **2002**, *4*, 1691. (c)

Böhm, W. P. W.; Herrmann, W. A. *Eur. J. Org. Chem.* **2000**, 3679. (d) Heidenreich, R. G.; Köhler, K.; Krauter, J. G. E.; Pietsch, J. *Synlett.* **2002**, 1118.

[17] (a) Soheili, A.; Albaneze-Walker, J.; Murry, J. A.; Dormer, P. G.; Hughes, D. L. *Org. Lett.* **2003**, *5*, 4191. (b) Amatore, C.; Bensalen, S.; Ghalem, S.; Jutand, A. *J. Organomet. Chem.* **2004**, *689*, 4642.

[18] Alami, M.; Ferri, F.; Linstrumelle, G. *Tetrahedron Lett*. **1993**, *34*, 6403.

[19] Jutand, A.; Ne´gri, S.; Principaud, A. *Eur. J. Org. Chem.* **2005**, 631.

[20] Thorand, S.; Krause, N. *J. Org. Chem.* **1998**, *63*, 8551.

[21] Leadbeater, N. E.; Tominack, B. J. *Tetrahedron Lett.* **2003**, *44*, 8653.

[22] Yi, C.; Hua, R. *J. Org. Chem.* **2006**, *71*, 2535.

[23] Ruiz, J.; Cutillas, N.; López, F.; López, G.; Bautista, D. *Organometallics* **2006**, *25*, 5768.

[24] Abjabeng, G.; Brenstrum, T.; Frampton, C.; Robertson, A. J.; Hilhouse, J.; McNulty, J.; Capretta, A. *J. Org. Chem.* **2004**, *69*, 5082.

[25] For examples, see: (a) Anderson, K. W.; Buchwald, S. L. *Angew. Chem., Int. Ed.* **2005**, *44*, 6173. (b) Nájera, C.; Gil-Moltó, J.; Karlström, S.; Falvello, L. R. *Org. Lett.* **2003**, *5*, 1451. (c) Köllhofer, A.; Plenio, H. *Chem. Eur. J.* **2003**, *9*, 1416. (d) DeVasher, R. B.; Moore, L. R.; Shaughnessy, K. H. *J. Org. Chem.* **2004**, *69*, 7919. (e) Tzschucke, C. C.; Markert, C.; Glatz, H.; Bannwarth, W. *Angew. Chem., Int. Ed.* **2002**, *41*, 4500.

1.4 Statement of Problem

Many catalytically active transition metals phosphine complexes are not air-stable. Moreover, the synthetic procedure for these complexes is not easy. In this regard the focus of this study has been concentrated on the synthesis and characterization of platinum(II) and palladium(II) phosphine complexes bearing air-stable and water-soluble PTA and DAPTA ligands by a simple ligand substitution method utilizing the respective cyclooctadiene precursor complexes. These complexes can be synthesized by room temperature reactions. The dialkyl platinum or palladium complexes bearing PTA or DAPTA ligands have not yet been reported. To the best of our knowledge, no mononuclear alkyl or alkynyl complexes for any of the transition metals bearing DAPTA ligands have been reported. A primary goal of the project is concentrated on synthesizing such complexes because of their stability and water-solubility and potential applications as catalysts.

As they exhibit similar electronic and steric behavior to several alkyl-phosphines, the investigation of Group 10 metal PTA and DAPTA complexes in catalytic hydrosilylation reactions, in Si-C bond formation, and catalytic cross-coupling reactions, in C-C bond formation, are of great interest. Many of such catalytic systems are interfered by side reactions and require higher catalyst loading while many of the hydrosilylation reactions fail to give the products regioselectively. Utilization of platinum or palladium complexes containing PTA or DAPTA ligands for metal-mediated hydrosilylation, hydrogermylation, or hydrostannylation reactions and stoichiometric E-H bond activation (E = Si, Ge, Sn) has not yet been fully investigated. The hydrosilylation and hydrogermylation reactions of a variety of terminal alkenes and alkynes with different

tertiary hydrosilanes including some siloles and silafluorenes and their germanium analogues catalyzed by a novel air-stable and water-soluble platinum(II)-PTA complex, *cis*-dimethylbis(1,3,5-triaza-7-phosphaadamantane) platinum(II) [*cis*-$Pt(CH_3)_2(PTA)_2$] is described in the current study.

None of the palladium(II) complexes bearing PTA or PTA-derivatized ligands have been utilized yet as a pre-catalyst in C-C bond formation such as Suzuki-Miyaura and Sonogashira cross-coupling reactions. The Suzuki-Miyaura cross-coupling reaction catalyzed by a novel palladium-PTA complex, *trans*-chloro(methyl)bis(1,3,5-triaza-7-phosphaadamantane) palladium(II) [*trans*-$PdCl(CH_3)(PTA)_2$] is described. Additionally, the copper-free Sonogashira cross-coupling reaction catalyzed by a palladium PTA complex, *cis*-dichlorobis(1,3,5-triaza-7-phosphaadamantane) palladium(II) [*cis*-$PdCl_2(PTA)_2$] is described. These reactions are found to be effective with minimal side reactions. Additionally, very few biphasic and aqueous-phase conditions have been investigated in Sonogashira cross-coupling reactions. The water-soluble palladium PTA and DAPTA complexes have their potential applications in such kinds of biphasic or aqueous-phase catalytic systems in cross-coupling reactions and hydrosilylation reactions in green chemistry. Such reactions can also be applied for the purpose of efficient recycling of the catalyst in homogeneous catalysis.

In this regard, the focus of this study was to synthesize and characterize a number of novel air-stable and water-soluble platinum(II) and palladium(II) alkyl, alkynyl, halo(alkyl), and halide complexes bearing PTA and DAPTA ligands and utilize them in such kinds of catalytic reactions as well as in stoichiometric reactions. The synthesis of new PTA- and DAPTA-containing platinum(II) and palladium(II) complexes and the

study of their catalytic role in the catalyzed addition reaction of Group 14 E-H (E = Si, Ge) bonds to unsaturated substrates as well as catalyzed Suzuki-Miyaura cross-coupling reactions and copper-free Sonogashira cross-coupling reactions are described in the current study.

2. Results and Discussion

This section describes the results and discussion for the synthesis of a variety of PTA and DAPTA complexes of Pt and Pd and their catalytic applications in hydrosilylation reactions and cross-coupling reactions.

2.1 Synthesis of Platinum(II) and Palladium(II)-PTA and DAPTA Complexes

The synthesis of a number of water-soluble platinum(II) and palladium(II)-PTA and DAPTA complexes bearing alkyl, alkynyl, or halide ligands was carried out. These complexes were characterized by multinuclear NMR spectroscopy, IR spectroscopy, mass spectrometry, elemental analysis, and X-ray crystallography. The following sections describe the synthesis and characterization of these complexes.

2.1.1 Synthesis of Pt(II) and Pd(II) alkyl complexes bearing PTA ligands

The reaction between *cis*-$PtMe_2(COD)$, (COD = 1,5 -cyclooctadiene), and PTA was carried out in 1 : 2 molar ratio, respectively at room temperature for 14 h to produce *cis*-dimethylbis(1,3,5-triaza-7-phosphaadamantane)platinum(II) [*cis*-$PtMe_2(PTA)_2$] (**1a**) as a white solid in 90% yield (Scheme 2.1.1).

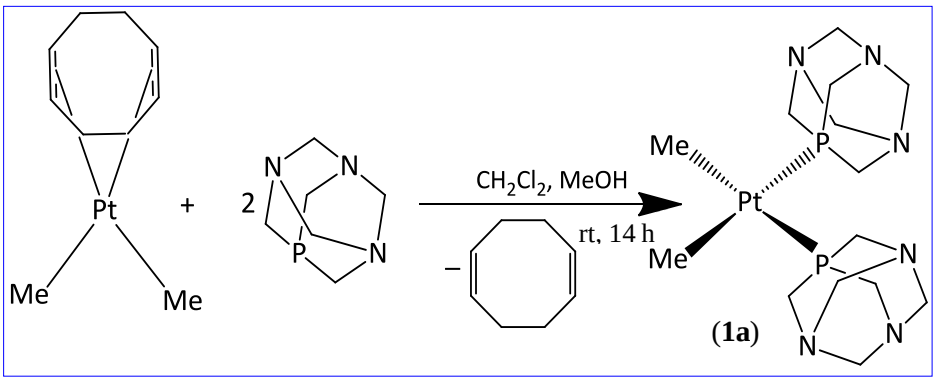

Scheme 2.1.1. Synthesis of *cis*-$PtMe_2(PTA)_2$ (**1a**).

Complex **1a** was characterized by ^{1}H, $^{13}C\{^{1}H\}$, and $^{31}P\{^{1}H\}$ NMR spectroscopy, mass spectrometry (MS), elemental analysis (EA), and X-ray crystallography. The $^{31}P\{^{1}H\}$ NMR spectrum of **1a** exhibited a resonance at -63.4 ppm with a $^{1}J_{PtP}$ coupling constant of 1608 Hz (Figure 2.1.1); consistent with a *cis* orientation of the phosphine groups at the platinum center.[1]

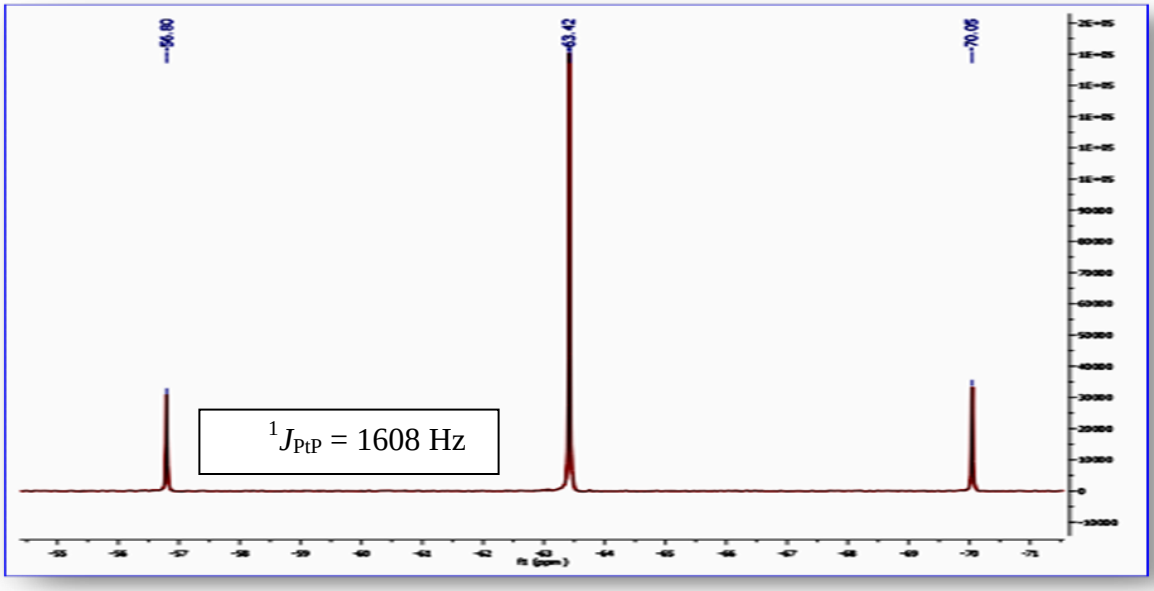

Figure 2.1.1. $^{31}P\{^{1}H\}$ NMR spectrum of *cis*-$Pt(CH_3)_2(PTA)_2$ (**1a**).

The related diphenyl complex, *cis*-$Pt(C_6H_5)_2(PTA)_2$, exhibited a resonance at -77.2 ppm with a similar $^{1}J_{PtP}$ coupling constant of 1560 Hz[1] whereas the related dibromo complex, *cis*-$PtBr_2(PTA)_2$, showed a downfield resonance at -49.7 ppm in the $^{31}P\{^{1}H\}$ NMR spectrum with a $^{1}J_{PtP}$ coupling constant of 3432 Hz due to a weaker *trans*-influence of the bromo-group.[2a] The ^{1}H NMR spectrum of **1a** showed an AB quartet at 4.52 ppm for two inequivalent diastereotopic NCH_2N hydrogens and a broad resonance corresponding to the PCH_2N hydrogens at 4.08 ppm. A similar pattern of an AB quartet was observed corresponding to the NCH_2N hydrogens for the related complex, *cis*-

$Pt(N_3)_2(PTA)_2$.[3] The formation of the *cis*-complex **1a** is expected due to the *cis* arrangement of the COD ligand in the platinum precursor and the small cone angle of the PTA ligand ($\theta = 118^o$)[4a] which is similar to that of PMe_3.[4b] On extending the reaction time to 20 h, complex **1a** appears to undergo slow isomerization to give a mixture of **1a** and *trans*-$PtMe_2(PTA)_2$, **1b** in approximately 16 : 1 ratio, respectively. The $^{31}P\{^1H\}$ NMR spectrum of **1b** in $CDCl_3$ exhibits a singlet peak at -60.4 ppm with a coupling value of $^1J_{PtP} = 2777$ Hz.

X-ray quality crystals of **1a** were obtained by slow diffusion of Et_2O to a $CHCl_3$ solution of **1a** at low temperature (< 0 ^oC). Complex **1a** crystallizes as triclinic crystals in a P-1 space group. The X-ray crystallographic data of **1a** showed that it has a slightly distorted square planar geometry which is possibly due to small steric repulsion caused by two *cis* oriented PTA ligands (Figure 2.1.2a). The (C14-Pt-P1) and (C13-Pt-P2) bond angles were found to be 172.4(4)^o and 171.4(4)^o, respectively. The larger PTA ligands compared to the methyl groups result in smaller (C-Pt-C) and larger (P-Pt-P) bond angles, which are 85.1(6)^o and 98.13(9)^o, respectively. These values are comparable with those of the related complex, *cis*-$Pt(C_6H_5)_2(PTA)_2$ for which the (C-Pt-C) and (P-Pt-P) bond angles were determined to be 84.6(2)^o and 99.28(6)^o, respectively.[1] These are also closely related to the (Br-Pt-Br) and (P-Pt-P) angles of the related complex, *cis*-$PtBr_2(PTA)_2$, which are 85.25(10)^o and 94.95(17)^o, respectively.[2a] The higher steric demand of Br in comparison to Ph and Me has not been a significant factor since larger (Br-Pt-Br) and smaller (P-Pt-P) angles are expected in *cis*-$PtBr_2(PTA)_2$.[2a]

The Pt-P(1), Pt-P(2), and Pt-C(13) bond distances in **1a** are 2.246(3) Å, 2.260(3) Å, and 2.097(13) Å, respectively. The average Pt-P bond lengths in the analogous dibromo

and diphenyl complexes are 2.231(3) Å and 2.288(16) Å, respectively. The difference in Pt-P bond distances in these three complexes also suggests that the *trans*-influence capability of the ligands follows the order: Ph > Me > Br (Table 2.1.1).[1, 2]

Figure 2.1.2b shows the molecular structure of (**3a**). The discussion of the structure is below after the Table 2.1.2.

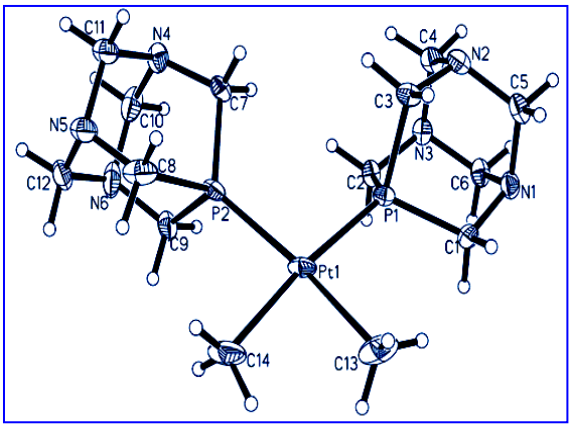

Figure 2.1.2a. Molecular structure of (**1a**). Solvent molecules are omitted for clarity. Thermal ellipsoids are drawn at the 50% probability level.

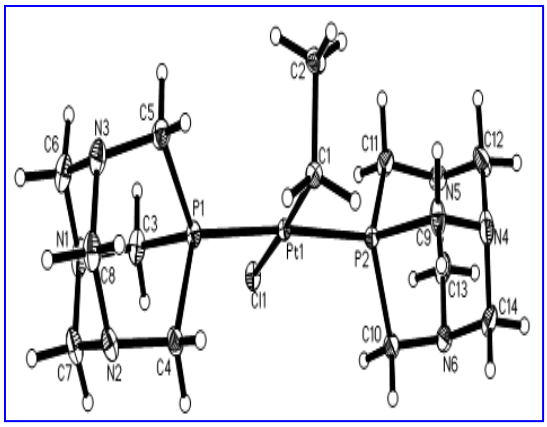

Figure 2.1.2b. Molecular structure of (**3a**). Solvent molecules are omitted for clarity. Thermal ellipsoids are drawn at the 50% probability level.

Table 2.1.1. Selected bond lengths and bond angles for **1a**, **3a**, and related complexes.

Complex	C-Pt-C/Br-Pt-Br, deg	P-Pt-P, deg	Pt-P, Å	Pt-C, Å	Pt-Cl, Å
1a	85.1(6)	98.13(9)	2.246(3)	2.097(13)	-
cis-$PtPh_2(PTA)_2$[1]	84.6(2)	99.28(6)	2.288(16)	2.064(6)	-
cis-$PtBr_2(PTA)_2$[2a]	85.25(10)	94.95(17)	2.231(3)	-	-
3a	-	175.29(3)	2.2672(10)	2.069(4)	2.4500(9)
trans-$PtCl(Me)(PPh_3)_2$[6a]	-	174.31(1)	2.295(3) 2.298(3)	2.08(1)	2.431(3)

The syntheses of *trans*-halo(alkyl)bis(1,3,5-triaza-7-phosphaadamantane) platinum(II) and palladium(II) complexes, *trans*-MX(R)$(PTA)_2$ (M = Pt, Pd) were performed by a room temperature reaction of respective COD precursor with 2 molar equivalents of PTA (Scheme 2.1.2). The complexes formed were characterized by ^{1}H, $^{13}C\{^{1}H\}$, and $^{31}P\{^{1}H\}$ NMR, mass spectrometry, elemental analysis, and X-ray crystallography. For the phosphorus-ligated complexes of the type PtX(R)$(PTA)_2$ (R = alkyl, H; X = halides, solvent), the *trans*-isomers are generally known to be more stable than the *cis*-isomers. This is partly due to the fact that the bonding of strong σ-donors (R) is maximized when they are *trans* to the relatively weaker σ-donors (X) rather than to the relatively stronger σ-donor PTA.[5]

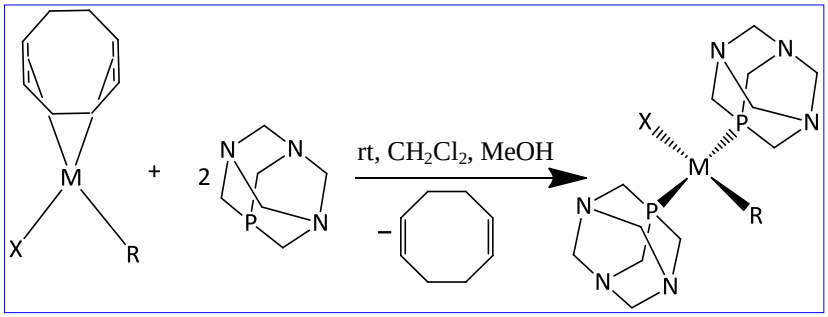

M = Pt: R = Me, X = Cl (**2a**);
R = Me, X = Br (**2b**);
R = Me, X = I (**2c**);
R = Et, X = Cl (**3a**);
R = Et, X = Br (**3b**);
R = Et, X = I (**3c**).
M = Pd: R = Me, X = Cl (**5a**);
R = Me, X = Br (**5b**);
R = Me, X = I (**5c**).

Scheme 2.1.2. Synthesis of *trans*-MX(R)$(PTA)_2$ complexes.

The reaction between *cis*-PtX(R)(COD) and PTA was carried out in 1 : 2 molar ratio, respectively, at room temperature to give the corresponding products with the general formula, *trans*-PtX(R)$(PTA)_2$ [R = Me; X = Cl (**2a**), X = Br (**2b**), X = I (**2c**)] and [R = Et; X = Cl (**3a**), X = Br (**3b**), X = I (**3c**)] in moderate to high yields (Table 2.1.2). It is important to note that complex **3** was obtained pure in good yields without any side reactions caused by β-hydride elimination. Analysis of complexes **2** and **3** by $^{31}P\{^{1}H\}$ NMR spectroscopy showed chemical shift values which ranged from -67.8 to -60.3 ppm,

respectively, but now much larger $^1J_{PtP}$ values between 2681-2949 Hz were observed which is consistent with a *trans* geometry of the PTA ligands at the platinum center (Scheme 2.1.2).[6] The complexes **2a** and **3a** have the highest and complexes **2c** and **3c** have the lowest $^1J_{PtP}$ coupling constants. This can be attributed to the difference in *s*-character of the Pt-P bond which falls in the order: I < Br < Cl.[2] On the other hand, the $^1J_{PtP}$ value for the ethyl complex **3** is larger than that for the methyl complex **2**, partly due to the higher electron-donating capability of the ethyl vs methyl group. Two broad resonances, in addition to the resonances for the alkyl protons, were observed in the ^{1}H NMR spectrum for PCH_2N and NCH_2N hydrogens as displayed by many of the Group 10 metal PTA complexes.[2, 4] The ^{1}H NMR spectrum for **3c** was found to be more complicated.

Table 2.1.2 lists the ^{31}P{^{1}H} NMR spectroscopic data for complexes **2a-c**, **3a-c**, and **5a-c** along with associated J_{PtP} values and percent yields.

Table 2.1.2. ^{31}P{^{1}H} NMR spectral data and yields for *trans*-MX(R)(PTA)$_2$ complexes.

Complex	M	X	R	^{31}P{^{1}H} NMR, δ	J_{PtP}, Hz	% Yield
2a	Pt	Cl	Me	-60.4	2779	86
2b	Pt	Br	Me	-63.4	2748	93
2c	Pt	I	Me	-67.9	2690	88
3a	Pt	Cl	Et	-60.3	2961	76
3b	Pt	Br	Et	-63.1	2926	76
3c	Pt	I	Et	-67.7	2867	63
5a	Pd	Cl	Me	-62.2	-	77
5b	Pd	Br	Me	-64.6	-	88
5c	Pd	I	Me	-66.9	-	68

X-ray quality crystals of **3a** were obtained by slow diffusion of diethyl ether to a methylene chloride solution of **3a** at low temperature (< 0 ^{o}C). Complex **3a** crystallized as monoclinic crystals in a $P2_1/n$ space group analogous to the related complex, *trans*-$PtCl(Me)(PPh_3)_2$.[6] Complex **3a** showed a slightly distorted square planar geometry with a *trans*-orientation of the two PTA ligands and the expected connectivity (Figure 2.1.2b). The distortion from the ideal square planar geometry is probably due to steric repulsion that takes place between the Cl and PTA ligands and/or the C_2H_5 and PTA ligands.

The (P-Pt-P) and (Cl-Pt-C) angles are 175.29(3)^{o} and 175.75(11)^{o}, respectively (Table 2.1.1). The (Cl-Pt-P1) and (Cl-Pt-P2) bond angles are 92.36(3)^{o} and 87.81(3)^{o}, respectively whereas the (C1-Pt-P1) and (C1-Pt-P2) bond angles are 88.40(10)^{o} and 91.77(10)^{o}, respectively. The Pt-C and Pt-Cl bond lengths are 2.069(4) Å and 2.4500(9) Å, respectively while the Pt-P bond lengths are 2.2667(10) Å and 2.2672(10) Å. The bond lengths and bond angles of **3a** are in close proximity to those reported for the related complex, *trans*-$PtCl(Me)(PPh_3)_2$ [Pt-Cl = 2.431(3) Å, Pt-C = 2.08(1) Å, Pt-P = 2.295(3) Å and 2.298(3) Å; (P-Pt-Cl) = 88.1(1)°, (P-Pt-C) = 92.3(4)° and 91.6(4)°].[6a] The difference in the Pt-P bond lengths in **3a** and *trans*-$PtCl(Me)(PPh_3)_2$ can be attributed to the difference in the nature of the phosphine ligand.

Crystal data parameters of **3a** and the other related PTA and DAPTA complexes **1a**, **4**, **6b**, and **12d** are given in Table 2.1.3.

Table 2.1.3. Crystal data parameters for complexes **1a, 3a, 4, 6b,** and **12d**.

Complexes	**1a**	**3a**	**4**	**6b**	**12d**
Crystal system	Triclinic	Monoclinic	Monoclinic	Triclinic	Triclinic
Space group	P-1	$P2_1/n$	$P2_1/n$	P-1	P-1
a Å	10.7357(10)	7.5269(13)	5.9009(8)	6.1536(3)	7.1506(2)
α deg	73.542(5)	90	90	99.093(3)	101.537(2)
b Å	10.9909(11)	9.8831(16)	24.185(4)	13.7686(7)	7.8076(2)
β deg	84.327(5)	91.341(10)	104.100(6)	92.238(3)	96.0190(10)
c Å	17.4623(17)	29.718(5)	6.2474(13)	17.6651(9)	13.0720(4)
γ deg	76.911(4)	90	90	98.096(3)	105.8880(1)
Volume $Å^3$	1923.4(3)	2210.1(6)	864.7(2)	1460.28(13)	677.80(3)
Density (calcd) mg/m^3	2.069	1.980	2.229	1.691	2.300
Absorption coefficient	7.682 mm^{-1}	6.871 mm^{-1}	8.615 mm^{-1}	8.948 mm^{-1}	7.615 mm^{-1}
Temperature	100(2) K	100(2) K	100(2) K	296(2) K	100(2) K
Goodness-of-fit on F^2	1.046	1.094	1.155	1.329	1.040
Final R indices	R1 = 0.0346	R1 = 0.0284	R1 = 0.0433	R1 = 0.0845	R1 = 0.0201
	wR2 = 0.1021	wR2 = 0.0648	wR2 = 0.0882	wR2 = 0.188	wR2 = 0.0395

When **2a** was subjected to crystallization in CH_2Cl_2 solution by slow diffusion of *n*-pentane at low temperature below 0 ^oC for several days, unexpectedly X-ray quality crystals of *trans*-dichlorobis(PTA) platinum(II) [*trans*-$PtCl_2(PTA)_2$] (**4**) were obtained.

A possible explanation for how **2a** was converted into **4** upon crystallization in CH_2Cl_2 may be due to the presence of a trace amount of HCl in the solvent or glassware.

Complex **4** crystallized as monoclinic crystals in a $P2_1/n$ space group. X-ray crystallography of **4** revealed the slightly distorted square planar geometry of the molecule with (Cl-Pt-P) bond angles of 87.29(10)° and 92.71(10)° (Figure 2.1.3 and Table 2.1.4). The (Cl-Pt-Cl) and (P-Pt-P) bond angles are perfectly linear. The Pt-P and Pt-Cl bond lengths are 2.257(2) Å and 2.345(4) Å, respectively.

The Pt-P and Pt-Cl bond distances in the related complex, *trans*-$PtCl_2(PPh_3)_2$[7] were reported as 2.3163(11) Å and 2.2997(11) Å, respectively, whereas these values for the *cis*-analogue, *cis*-$PtCl_2(PTA)_2 \cdot H_2O$,[8] were observed to be 2.2263(14) Å and 2.365(2) Å, respectively (Table 2.1.4), indicative of greater *trans*-influence behavior of PTA compared to Cl. The $^{31}P\{^1H\}$ NMR spectrum of **4** showed a single peak at -60.4 ppm with ^{195}Pt satellites and a coupling value of $^1J_{PtP} = 2778$ Hz. The $^1J_{PtP}$ coupling value has been reported to be 3350 Hz for the corresponding *cis*-analogue, *cis*-$PtCl_2(PTA)_2$[2] and 2627 Hz for *trans*-$PtCl_2(PPh_3)_2$.[7]

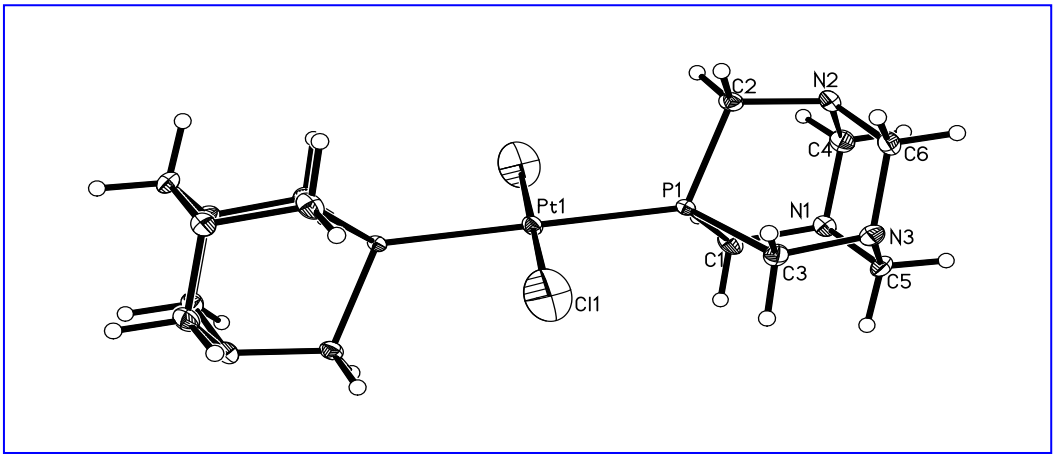

Figure 2.1.3. Molecular structure of (**4**). Thermal ellipsoids are drawn at the 50% probability level.

Table 2.1.4. Selected bond lengths and bond angles for (**4**) and related complexes.

Complex	Pt-P, Å	Pt-Cl, Å	P-Pt-Cl	Cl1-Pt-P1-C1
4	2.257(2)	2.345(4)	87.29(10)° 92.71(10)°	128.2(3)°
trans-$PtCl_2(PPh_3)_2$[7]	2.3163(11)	2.2997(11)	87.88(4)° 92.12(4)°	136.03(12)°
cis-$PtCl_2(PTA)_2 \cdot H_2O$[8]	2.2263(14)	2.365(2)	89.44(5)° 176.47(4)°	-

Likewise, the synthesis of the related PTA-ligated palladium alkyl complexes, *trans*-halo(methyl)bis(1,3,5-triaza-7-phosphaadamantane) palladium(II), *trans*-PdX(Me)$(PTA)_2$ [X = Cl (**5a**), X = Br (**5b**), X = I (**5c**)] were carried out starting with the respective COD complex (Scheme 2.1.2) . The syntheses of complexes **5a-c** were carried out using a ligand substitution reaction by treating the corresponding PdX(Me)(COD) with 2 molar equivalents of PTA at room temperature. The complexes **5a-c** were found to undergo slow decomposition at room temperature. The ^{1}H NMR spectra of these complexes exhibited two broad singlet resonances for the PCH_2N and NCH_2N hydrogens and an upfield triplet resonance for the methyl proton as a result of ^{1}H-^{31}P coupling ($^3J_{PH}$ = 6.7-6.9 Hz). A single resonance was observed in the ^{31}P{^{1}H} NMR spectra, the chemical shifts lying between -66.9 to -62.2 ppm, indicating the *trans* orientation of the PTA ligands (Table 2.1.2). Despite the instability, we were able to perform an elemental analysis for **5c** whereas elemental analysis results could not be obtained for **5a** and **5b** owing to their instability. Attempt to synthesize the Pd(II)-PTA complexes with an ethyl ligand were not successful because of the instability of the corresponding COD precursor.

2.1.2 Synthesis of some Pt(II) and Pd(II) alkynyl complexes bearing PTA ligands

The complex, *cis*-di(phenylethynyl)bis(PTA)platinum(II) [*cis*-Pt(C≡CPh)$_2$(PTA)$_2$] (**6a**) was obtained in 86% yield when a CH_2Cl_2 solution of Pt(C≡CPh)$_2$(COD)[9b] was stirred with 2 molar equivalents of PTA in methanol for about 1 h (Scheme 2.1.3). The NMR spectral data indicated the presence of both isomers **6a** (major) and *trans*-Pt(C≡CPh)$_2$(PTA)$_2$, **6b** (minor), however when the reaction was run for a longer period of time **6b** was the major isomer produced, as indicated by the $^{31}P\{^1H\}$ NMR spectrum.

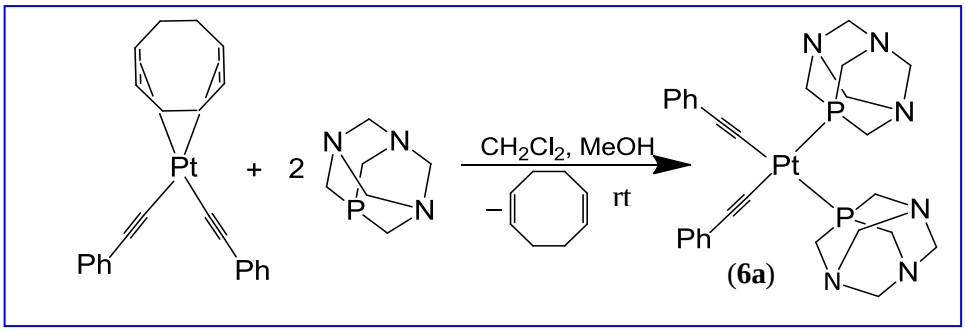

Scheme 2.1.3. Synthesis of *cis*-Pt(C$_2$Ph)$_2$(PTA)$_2$.

The ^1H NMR spectral data for both the products were essentially identical and thus the ratio of the isomers could not be determined from the peak integration. Attempts to crystallize **6a** by slow diffusion of diethyl ether into a methylene chloride solution of **6a** resulted in the isolation of crystals of *trans*-Pt(C≡CPh)$_2$(PTA)$_2$ (**6b**).

The $^{13}C\{^1H\}$ NMR spectrum of the alkynyl carbon showed an AXX' type of virtual triplet at 99.7 ppm and a doublet of doublets at 98.0 ppm due to ^{13}C-^{31}P coupling. The J_{PtC} coupling was not well-resolved. In addition, a couple of minor peaks for the alkynyl carbons of **6b** were also observed. Such kind of AXX' spectra were also observed in the

related complexes *cis*-Pt(C≡CPh)$_2$(PPh$_2$H)$_2$ and *cis*-Pt(C≡C^{t}Bu)$_2$(PPh$_2$H)$_2$.[9a] However, the ^{31}P{^{1}H} NMR spectrum displayed only one resonance at -69.9 ppm corresponding to **6a** with $^1J_{PtP}$ = 2071 Hz which is diagnostic for a *cis*-alkynyl phosphine complex.[2b, 9] The $^1J_{PtP}$ value for the related Pt alkynyl complex bearing PTA ligands, *cis*-[Pt{C≡C(CH$_2$)$_3$NH$_3$}$_2$(PTA)$_2$]Br$_2$ was reported as 2167 Hz.[2b] The $^1J_{PtP}$ value for **6a** is slightly lower than the reported $^1J_{PtP}$ values for the related *cis*-complexes, probably because of the different alkynyl group and/or phosphine. The appearance of two peaks at 2103 and 2042 cm^{-1} in the IR spectra represent symmetric and antisymmetric stretches of the C≡C group. These IR stretching frequencies are lower in comparison to that for the free alkyne (which is 2119 cm^{-1} for uncoordinated phenylacetylene) which indicates the M→L π-back bonding between the metal and the alkynyl carbon to some extent in these complexes. This is supported by the fact that alkynyl carbons displayed downfield resonances in the ^{13}C{^{1}H} NMR spectrum compared to the free alkyne.

Usually, the *cis*-isomer of platinum or palladium alkynyl phosphine complexes prepared from respective dichloro complex is thermodynamically unstable with respect to the *trans*-isomer in solution, particularly when monodentate phosphines are present as the auxiliary ligands. For example, the reaction of *cis*-Pt(P^{t}Bu$_3$)$_2$Cl$_2$ with phenylacetylene (PhC≡CH) below -20 ^{o}C gave *cis*-Pt(P^{t}Bu$_3$)$_2$(C≡CPh)$_2$, while above this temperature a mixture of the *cis*- and *trans*-isomers was obtained. Therefore, the complexes of the type MX(C≡CR)L$_2$ and M(C≡CR)$_2$L$_2$ (M = Pt, Pd) are usually *trans* at the temperatures above -5 ^{o}C.[9d, e] The isomerization of **6a** into **6b** during the crystallization of former below 0 ^{o}C is consistent with this fact.

When *cis*-$MCl_2(PTA)_2$ (M = Pt, Pd)[2] was stirred with an excess of phenylacetylene in absolute ethanol in the presence of triethylamine for an extended period of time followed by washing the residue with dry methanol, the corresponding complexes **6b** or *trans*-$Pd(C{\equiv}CPh)_2(PTA)_2$, **7** were obtained in good yields (Scheme 2.1.4).

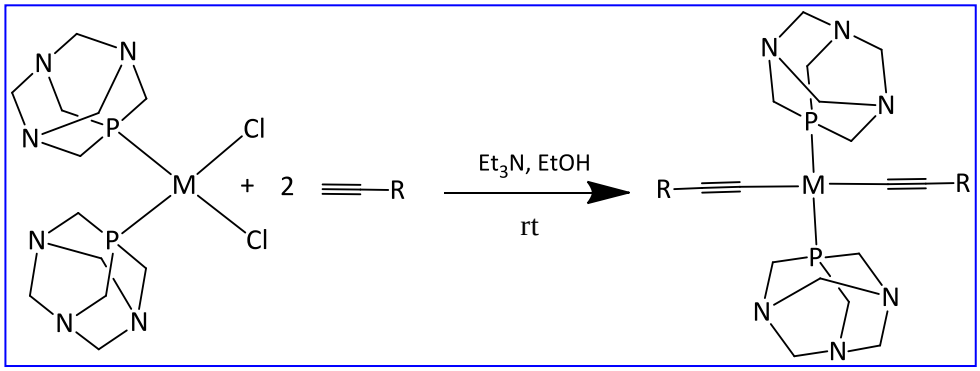

Scheme 2.1.4. Synthesis of *trans*-$M(C_2Ph)_2(PTA)_2$ complexes.

The $^{31}P\{^1H\}$ NMR spectrum showed a single resonance at -64.3 ppm for **6b** with a coupling value of $^1J_{PtP}$ = 2309 Hz which is diagnostic for *trans*-alkynyl phosphine complexes.[2b, 9d] The $^1J_{PtP}$ value for the related Pt alkynyl complex bearing PTA ligands, *trans*-$[Pt\{C{\equiv}C(CH_2)_3NH_3\}_2(PTA)_2]Br_2$ was reported as 2305 Hz.[2b] However, the $^1J_{PtP}$ values in **6b** are slightly lower than the reported $^1J_{PtP}$ values for some of the related *trans*-complexes bearing other phosphines, probably because of the difference in the nature of phosphines in the complexes.[9] The $^{31}P\{^1H\}$ NMR spectrum of the complex **7** showed a singlet at -56.3 ppm. Complex **6b** slowly undergoes isomerization to give a mixture with the *cis*-isomer **6a** upon standing for long periods in solution at room temperature whereas complex **7** was also found to be unstable in solution upon standing for extended periods of time due to its decomposition.

Crystals of **6b** suitable for X-ray crystallography were obtained by slow diffusion of diethyl ether to a methylene chloride solution of **6b** below 0 ^oC. Complex **6b** crystallizes

as triclinic crystals in a P-1 space group. The crystallization occurs with two crystallographically independent molecules in the asymmetric unit. Both molecules have identical absolute configurations and very similar conformations. The geometries of the two independent platinum centers are essentially the same. The PTA ligands have the *trans* configuration in **6b** although the precursor complex has a *cis* configuration (Figure 2.1.4a). The change in the relative orientation of the phosphine ligands (PTA) from *cis* to *trans* during the reaction suggests that the reaction might have proceeded through a dissociation of the phosphine ligand. The molecular structure of **6b** obtained from **6a** is shown in Figure 2.1.4a and is discussed below. Selected bond lengths and bond angles of **6b** obtained from **6a** are mentioned in Table 2.1.5.

The crystal structure of **6b** shows that the molecule has nearly square planar geometry with (C-Pt-C) and (P-Pt-P) bond angles of 179.999(3)^{o} and 180.000(1)^{o}, respectively. The (C-Pt-P) bond angles are 90.2(3)^{o} and 89.8(3)^{o}, demonstrating the linearity of the ethynylplatinum units and negligible distortion from the ideal geometry. The average Pt-C(1) and Pt-P(1) bond distances of **6b** are 1.985(10) Å and 2.268(3) Å, respectively. Both the Pt-P bond distances are equal because of crystal symmetry. The Pt-P bond distance is slightly longer than the corresponding distance of related *cis*-$PtX_2(PTA)_2$ complexes [2.219(5)–2.236(3) Å].[2a, 8] This indicates that PTA has a greater *trans*-influence than X. The C(2)-C(3) and C(16)-C(17) bond distances are the same [1.450(15)] Å which is shorter than the standard C-C single bond. The C(1)-C(2) and C(15)-C(16) bond distances are 1.189(15)^{o} and 1.190(15)^{o}, respectively which is in the range for a normal C≡C bond length. These results indicate that complex **6b** is a σ-alkynyl complex and not a vinylidene complex. The average Pt-C, Pt-P, and C≡C bond

lengths for the related complex, *trans*-$Pt(C{\equiv}CPh)_2(PEt_3)_2$ as reported by Carpenter and Lukehart were found to be 1.98(1) Å, 2.289(3) Å, and 1.21(1) Å, respectively.[10] The values for the related complex, *trans*-$[Pt\{C{\equiv}C(CH_2)_3NH_3\}_2(PTA)_2]Br_2$ were reported to be 2.032(15) Å, 2.264(3) Å, and 1.19(2) Å, respectively,[2b] which are close in value to each other.

On the other hand, the crystal structure of **6b** obtained by slow diffusion of diethyl ether to a CH_2Cl_2 solution of **6b** below 0 °C was found to be more distorted with Pt-C(9), Pt-C(1), C(9)-C(10), and C(1)-C(2) bond distances of 1.967(14) Å, 2.042(16) Å, 1.14(2) Å, 1.24(2) Å, respectively (Figure 2.1.4b).

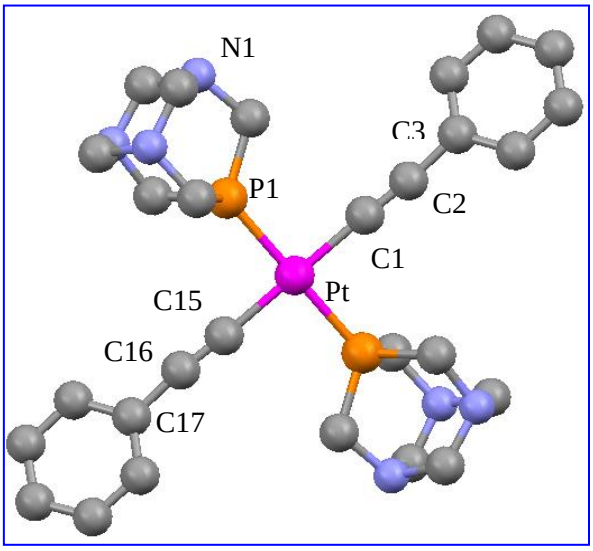

Figure 2.1.4a. Crystal structure of (**6b**) obtained from isomerization of (**6a**), hydrogen atoms are omitted for clarity (50% probability ellipsoids).

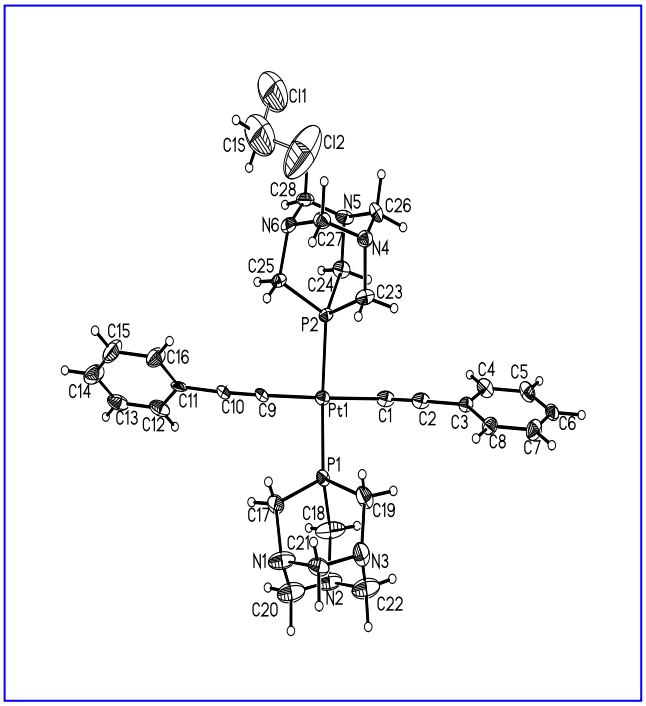

Figure 2.1.4b. Molecular structure of (**6b**). Thermal ellipsoids are drawn at the 50% probability level. Solvent molecules are omitted for clarity.

Table 2.1.5. Selected bond length and bond angle values for (**6b**).

Pt-C1	C1-Pt-P1	C1-Pt-C1 P1-Pt-P1	Pt-P1	C1-C2	C2-C3
1.985(10) Å	90.2(3)° 89.8(3)°	179.999(3)° 180.000(1)°	2.265(3) Å	1.189(15) Å	1.450(15) Å

For the synthesis of other PTA-ligated alkynyl complexes of platinum and palladium, another alkyne, trimethylsilylacetylene was employed. The syntheses of *trans*-$M(C_2SiMe_3)_2(PTA)_2$ [M = Pt (**8a**); M = Pd (**8b**)] were carried out by stirring *cis*-$MCl_2(PTA)_2$ with an excess of trimethylsilylacetylene in absolute ethanol at room temperature in the presence of triethylamine for an extended period of time (Scheme 2.1.4). The formation of **8b** was very slow and took *ca.* 76 h compared to *ca.* 16 h for complex **8a**. When the reaction was monitored after 72 h, only one molecule of trimethylsilylethynyl ligand was found to be coordinated to the metal center, as predicted by ^{1}H NMR spectrum analysis of the $SiMe_3$ hydrogens at 0.20 ppm which integrates only 9 protons instead of 18 (compared to PTA protons). Complexes **8a** and **8b** were obtained in 69% and 60% yields, respectively. Both the complexes were found to undergo slow decomposition at room temperature.

Complex **8a** showed an AB quartet in the ^{1}H NMR spectrum at 4.51 ppm corresponding to the NCH_2N protons, and two broad resonances at 4.30 and 0.15 ppm corresponding to the PCH_2N and CH_3 hydrogens, respectively, while complex **8b** displayed three broad resonances at 4.53, 4.33, and 0.15 ppm in the ^{1}H NMR spectrum. Similar types of AB quartets were also reported in the literature for the *trans*-bis(PTA) complexes of platinum and palladium.[3] The ^{31}P{^{1}H} NMR spectrum of **8a** displayed a

single peak at -66.4 ppm with a coupling of $^{1}J_{PtP}$ = 2343 Hz (comparable to **6a**), diagnostic for the *trans*-orientation of the PTA ligands, whereas that of **8b** showed a single peak at -58.8 ppm. As expected, the $^{29}Si\{^{1}H\}$ NMR spectrum of both complexes displayed a single resonance at -24.0 ppm (**8a**) and -24.3 ppm (**8b**). Two resonances corresponding to the symmetric and antisymmetric stretches of the C≡C group were observed in the IR spectra of **8a** and **8b**. The C≡C stretching frequencies in the IR were found to be 2112 and 2054 cm^{-1} for **8a** and 2108 and 2042 cm^{-1} for **8b** which is not significantly different from that of the uncoordinated $Me_3SiC{\equiv}CH$ (~ 2050 cm^{-1}) and similar to the related Pt alkynyl PTA complexes.[2b] The $^{13}C\{^{1}H\}$ NMR spectra for these complexes could not be obtained because of their low solubility in most of the deuterated solvents and their instability in the solvents such as DMSO-d_6 and D_2O in which they are soluble.

2.1.3 Synthesis of alkylbis(DAPTA) complexes of platinum and palladium

A similar kind of ligand exchange method was applied for the synthesis of a variety of platinum(II) and palladium(II)-DAPTA (DAPTA = *N,N'*-diacetyl-1,3,5-triaza-7-phosphaadamantane) complexes bearing alkyl or alkynyl groups. By stirring $PtMe_2(COD)$ in CH_2Cl_2 with DAPTA in methanol in a 1 : 2 molar ratio, respectively, overnight at room temperature yielded *cis*-$PtMe_2(DAPTA)_2$, **9a** as a white solid in 91% yield with respect to $PtMe_2(COD)$ (Scheme 2.1.5). The $^{31}P\{^{1}H\}$ NMR spectrum of **9a** displayed two resonances at -37.8 and -38.2 ppm with approximately the same intensity and almost the same $^{1}J_{PtP}$ coupling values, 1634 Hz and 1635 Hz, respectively. The appearance of two phosphorus signals can be attributed to the existence of **9a** as an equilibrium mixture of two conformers in solution.

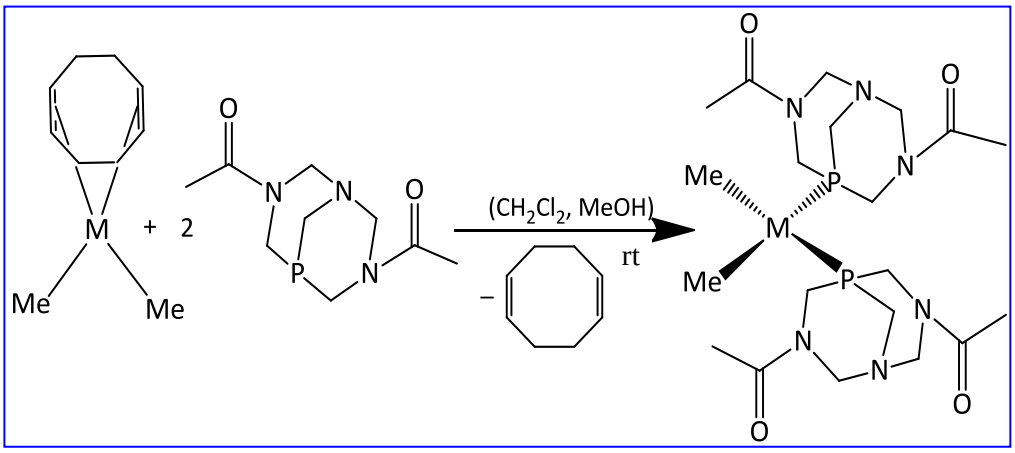

Scheme 2.1.5. Synthesis of *cis*-$PtMe_2(DAPTA)_2$ (**9a**).

The ^{1}H NMR spectrum showed four broad signals, too far away for coupling to other nuclei, corresponding to the COC*H*$_3$ hydrogens at 2.15, 2.12, 2.11, and 2.09 ppm (two of them were of almost equal intensity) whereas the ^{13}C{^{1}H} NMR spectrum displayed two signals for the methyl carbon of the acyl group (CO*C*H$_3$) at 21.7 and 21.3 ppm as well as two signals for the carbonyl carbon of the acyl group (*C*OCH$_3$) at 170.1 and 170.0 ppm. This possibly arises due to the fact that all acyl groups of the DAPTA ligand undergo a *syn* orientation in one of the conformers whereas in another conformer, the acyl groups have a *syn* orientation in one of the ligands and an *anti* orientation in another ligand. The ^{1}H NMR spectrum showed a number of resonances corresponding to the PC*H*$_2$N, NC*H*$_2$N, PC*H*$_2$NC, COC*H*$_3$, and C*H*$_3$ hydrogens which are consistent with the presence of diastereotopic hydrogens in the PC*H*$_2$N, NC*H*$_2$N, and PC*H*$_2$NC units of the ligand. Most of the ligand proton resonances integrated as two protons but some of them as four protons, which is due to the non-symmetry of the compound. The splitting pattern of the resonances was found to be almost the same as that of the free ligand.[11a] The signal for

the methyl protons suggests a ^{1}H-^{195}Pt coupling of $^{2}J_{PtH}$ = 71 Hz. However, the ^{1}H-^{31}P coupling could not be resolved.

Similarly, the $^{13}C\{^{1}H\}$ NMR spectrum exhibited a pair of doublet of doublets resonance at 2.69 ppm with $^{1}J_{PtC}$ *ca.* 580 Hz, $^{2}J_{PC(trans)}$ = 9.0 Hz, and $^{2}J_{PC(cis)}$ = 3.7 Hz and at 1.43 ppm with $^{1}J_{PtC}$ *ca.* 580 Hz, $^{2}J_{PC(trans)}$ = 9.8 Hz, and $^{2}J_{PC(cis)}$ = 3.7 Hz; indicating coupling of the ^{13}C nucleus with the other spin ½ nuclei of ^{31}P and ^{195}Pt. Heating a solution of **9a** in CH_2Cl_2 for 2 h appears to promote isomerization to give *trans*-$PtMe_2(DAPTA)_2$, **9b** assigned as the major product along with trace amounts of unassigned products. The $^{31}P\{^{1}H\}$ NMR spectral analysis of the mixture of products displayed a single resonance at -36.8 ppm ($^{1}J_{PtP}$ = 2938 Hz) corresponding to the possible *trans*-isomer (**9b**) and other small resonances for the unassigned products.

In order to synthesize *trans*-halo(alkyl)bis(DAPTA) platinum(II) complexes, the reaction between *cis*-PtX(Me)(COD) and DAPTA was carried out in 1 : 2 molar ratio, respectively, at room temperature to give the corresponding products with the general formula, *trans*-$PtX(Me)(DAPTA)_2$ [X = Cl (**10a**), X = Br (**10b**), X = I (**10c**)] in 81-91% yields (Scheme 2.1.6 and Table 2.1.6).

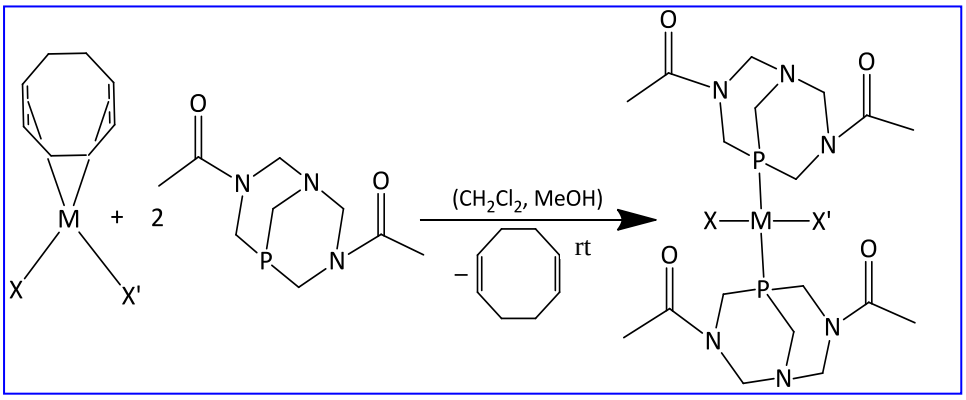

Scheme 2.1.6. Synthesis of *trans*-$MX(X')(DAPTA)_2$ complexes.

M = Pt; X' = Me:
X = Cl, **10a**;
X = Br, **10b**;
X = I, **10c**.
M = Pt;
X = X' = I, **12d**.
M = Pd; X' = Me:
X = Cl, **11a**;
X = Br, **11b**;
X = I, **11c**.

Table 2.1.6. Yields and $^{31}P\{^{1}H\}$ NMR spectral data for *trans*-$MX(X')(DAPTA)_2$ complexes.

Complex	M	X	X'	% Yield	$^{31}P\{^{1}H\}$ NMR, δ	J_{PtP}, Hz
10a	Pt	Cl	Me	91	-36.8	2937
10b	Pt	Br	Me	86	-39.0	2901
10c	Pt	I	Me	81	-42.2	2849
11a	Pd	Cl	Me	78	-38.7	-
11b	Pd	Br	Me	81	-39.9	-
11c	Pd	I	Me	61	-41.4	-
12d	Pt	I	I	88	-50.3	2369

The $^{1}J_{PtP}$ coupling constants in the $^{31}P\{^{1}H\}$ NMR spectrum were found to be 2937, 2901, and 2849 Hz, respectively, for the complexes **10a**, **10b**, and **10c** (Table 2.1.6) and are larger than those for the analogous PTA complexes **2a**, **2b**, and **2c**. As in the analogous PTA complexes, the chloro-ligated DAPTA complex has the highest $^{1}J_{PtP}$ coupling constant. These coupling constant values and the appearance of a single resonance in the $^{31}P\{^{1}H\}$ NMR spectrum is diagnostic for the *trans* orientation of the DAPTA ligands.[6a] The appearance of two resonances of the acyl hydrogens in the ^{1}H NMR spectrum for **10a** and **10b** is evident for the *anti* orientation of the acyl groups in DAPTA ligand, whereas a single resonance for **10c** suggests their *syn* orientation. Another feature is the methyl proton showed coupling with the ^{31}P and ^{195}Pt nuclei in the ^{1}H NMR spectrum, however the coupling with ^{31}P could not be resolved in **10c**.

The analogous palladium(II)-DAPTA complexes, *trans*-PdX(Me)(DAPTA)$_2$ [X = Cl (**11a**), X = Br (**11b**), X = I (**11c**)] were synthesized in 61-81% yields from the PdX(Me)(COD) precursors (Scheme 2.1.6). The appearance of a single resonance in the $^{31}P\{^1H\}$ NMR spectrum is diagnostic for the *trans* orientation of the DAPTA ligands (Table 2.1.6). The appearance of two resonances for the acyl hydrogens in the ^1H NMR spectrum is evident for the *anti* orientation of the acyl groups in the DAPTA ligand whereas an additional small resonance was also observed in the case of **11c**. The complexes were found to be unstable in solutions but remained stable at room temperature in solid state for several days. On extending the reaction time to 48 h, **11c** appears to undergo partial isomerization to give *cis*-PdI(Me)(DAPTA)$_2$, **11d** resulting in a mixture containing the *cis*- and *trans*-isomers in approximately 9 : 1 ratio, respectively, as determined by the $^{31}P\{^1H\}$ NMR spectroscopy. The $^{31}P\{^1H\}$ NMR spectrum of the product mixture showed two singlet peaks corresponding to two isomers at -41.3 (**11c**) ppm and -47.5 ppm (**11d**).

2.1.4 Synthesis of dihalobis(DAPTA)platinum(II) or palladium(II) complexes

Only a limited number of platinum and palladium-DAPTA complexes have been reported in the literature which also include *cis*-MCl$_2$(DAPTA)$_2$.[11] Analogous bromo-complexes, *cis*-MBr$_2$(DAPTA)$_2$ (M = Pt; **12a** and M = Pd; **12c**) were synthesized by reacting the respective MBr$_2$(COD) complex with 2 molar equivalents of DAPTA at room temperature (Scheme 2.1.7). Complex **12a** was obtained as an off-white solid in 71% yield. The $^{31}P\{^1H\}$ NMR spectrum in DMSO-d_6 showed two resonances, as in the

case of complex **9a**, at -31.5 ppm ($^1J_{PtP}$ = 3307 Hz) and -31.6 ppm ($^1J_{PtP}$ = 3311 Hz) in an equimolar ratio in the form of a mixture of two conformers in solution. The $^1J_{PtP}$ value is

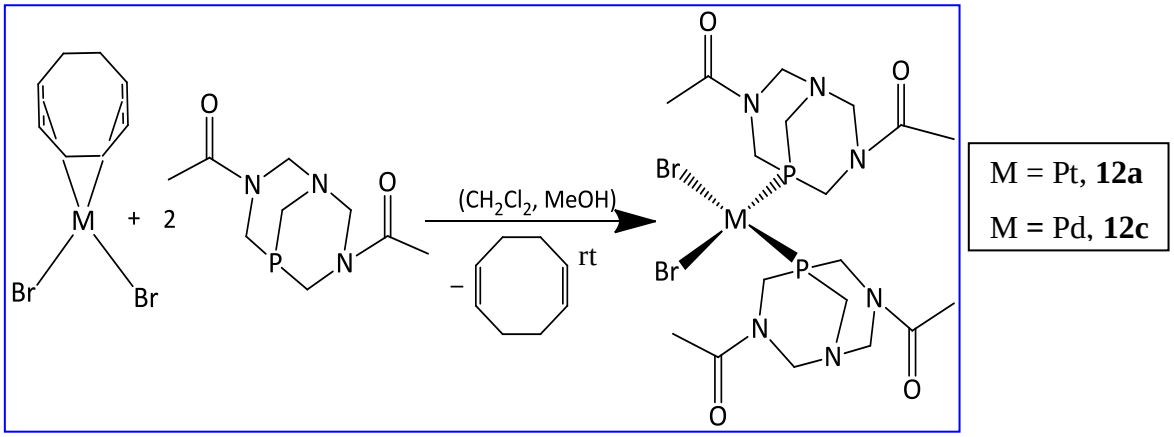

Scheme 2.1.7. Synthesis of *cis*-$MBr_2(DAPTA)_2$ complexes.

characteristic of *cis*-complexes of this type.[2a] Additionally, a similar resonance pattern was observed corresponding to a trace amount of an unassigned conformer mixture and possibly, *trans*-$PtBr_2(DAPTA)_2$ (**12b**) conformer mixture in the product mixture. The approximate ratio of **12a** : unassigned product : **12b** was detected to be 1 : 0.11 : 0.08, respectively, by the integration of the $^{31}P\{^1H\}$ NMR peaks. On the other hand, the ^1H NMR spectrum of **12a** showed two resonances in 1 : 1 ratio corresponding to the acyl protons.

On extending the reaction time to 15 h, complex **12a** appears to undergo slow isomerization to give a mixture of **12a** and *trans*-$PtBr_2(DAPTA)_2$, **12b** in approximately 11 : 1 ratio, respectively. The $^{31}P\{^1H\}$ NMR spectrum in DMSO-d_6 displayed a pair of peaks of **12a** at -31.6 and -31.7 ppm but with a higher coupling constant ($^1J_{PtP}$ = 3363 Hz)

as well as another pair of peaks of **12b** at -33.0 and -33.1 ppm. The ^{195}Pt satellites for **12b** could not be resolved since it was present in a trace amount in the product mixture.

The Pd analogue, complex **12c**, was obtained as a yellow powder in 84% yield. Complex **12c** was found to have better solubility than complex **12a** in organic solvents but found to undergo decomposition in solution. The $^{31}P\{^{1}H\}$ NMR spectrum of **12c** displayed a single resonance at -38.9 ppm. The appearance of a single resonance for the acyl protons in the ^{1}H NMR spectrum accounts for the same orientation of the acyl groups (i.e. *syn*) in the ligand.

The complex, *trans*-$PtI_2(DAPTA)_2$ (**12d**) was obtained as a yellow powder in 88% yield by the reaction of $PtI_2(COD)$ with 2 molar equivalents of DAPTA (Scheme 2.1.6). Owing to the larger size of I vs Br, the repulsion caused between I and the DAPTA ligands resulted in *trans* orientation of the DAPTA ligands in **12d**. The $^{31}P\{^{1}H\}$ NMR spectrum of **12d** in DMSO-d_6 showed a peak at -50.3 ppm with $^{1}J_{PtP}$ = 2369 Hz, which is diagnostic for the *trans* orientation of the DAPTA ligands. The ^{1}H NMR spectrum displayed two peaks for the acyl protons indicating the *anti* orientation of the acyl groups in the ligand. Complex **12d** was found to undergo slow decomposition in DMSO-d_6 solution at room temperature over *ca.* 3 h. On extending the reaction time to 24 h, **12d** and a mixture of two conformers of its isomer, *cis*-$PtI_2(DAPTA)_2$, **12e** as well as trace amounts of other unassigned products were obtained. The $^{31}P\{^{1}H\}$ NMR spectrum displayed two resonances corresponding to **12e** at -35.1 ppm ($^{1}J_{PtP}$ = 3141 Hz) and -35.2 ppm ($^{1}J_{PtP}$ = 3144 Hz), a resonance at -49.4 corresponding to **12d** ($^{1}J_{PtP}$ = 2369 Hz), and some other unassigned minor peaks.

X-ray quality crystals of **12d** were obtained by slow diffusion of methylene chloride to a methanol solution of **12d** at low temperature (below 0 ^{o}C). To the best of our knowledge, this is the first crystallographically characterized Pt or Pd-DAPTA complex bearing a halogen ligand. Complex **12d** was crystallized as triclinic crystals in a P-1 space group. The crystal structure shows a nearly ideal square planar geometry (Figure 2.1.5). The accuracy of the crystal structure of the molecule is supported by a small value of the final R indices (R1 = 0.0201). Selected bond lengths and bond angles of **12d** are given in Table 2.1.7.

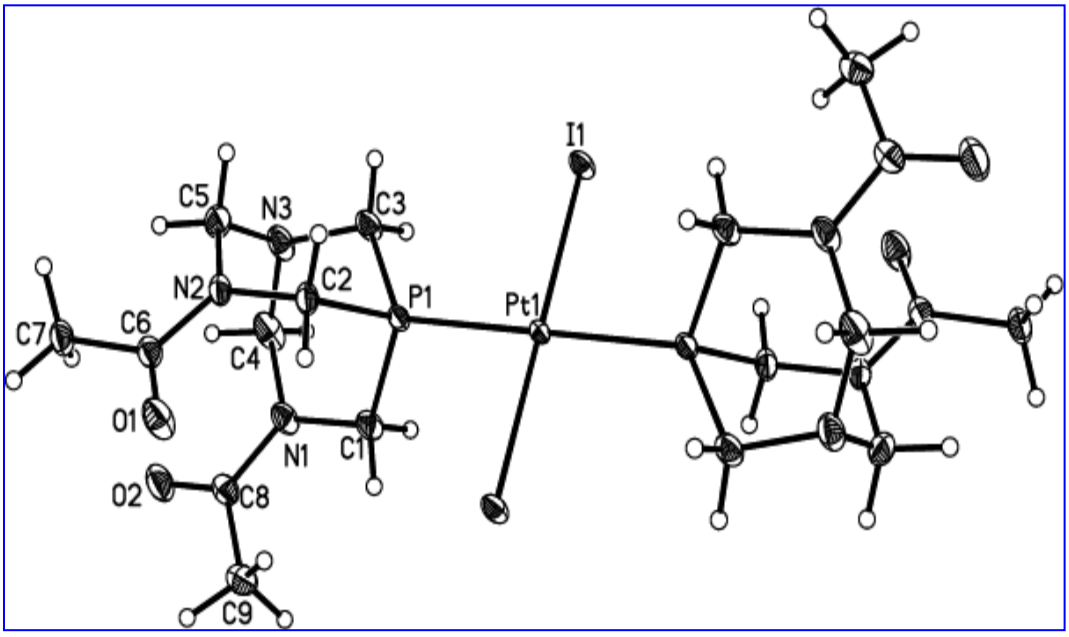

Figure 2.1.5. Molecular structure of *trans*-$PtI_2(DAPTA)_2$ (**12d**). Solvent hydrate molecule is omitted for clarity. Thermal ellipsoids are drawn at the 50% probability level.

Table 2.1.7. Selected bond length and bond angle values for (**12d**) and the related complex.

Complex	Pt-P, Å	Pt-I, Å	P-Pt-P	I-Pt-I	I-Pt-P	I1-Pt-P1-C1
12d	2.3027(4)	2.61175(10)	180.0°	180.0°	90.992(9)° 89.007(9)°	-55.36(6)° 124.65(6)°
trans-$PtI_2(PTA)_2$[12a]	2.3128(12)	2.6022(6)	180.0°	180.0°	90.94(3) 89.06(3)	-

The (P-Pt-P) and (I-Pt-I) bond angles are exactly 180.0° whereas the (I-Pt-P) bond angles are observed to be 90.992(9)° and 89.007(9)°. The (I-Pt-P-C1) torsion angle of 124.65(6)° also suggests only a small deviation from planarity. Both the Pt-P and both the Pt-I bond distances are equal due to crystal symmetry. The average Pt-P and Pt-I bond lengths are 2.3027(4) Å and 2.61175(10) Å, respectively, while these bond distances for the analogous PTA complex, *trans*-$PtI_2(PTA)_2$ were reported as 2.3128(12) Å and 2.6022(6) Å, respectively.[12a] These bond distances are virtually identical to those found in the analogous PMe_3 complex of 2.315(4) Å and 2.599(2) Å, respectively, indicative of the similar electronic properties of these ligand systems.[12b] The Pt-P bond distances are comparable with the distance of 2.318(2) Å found for the corresponding PPh_3 complex,[12c] while they are shorter than those found for the bulkier PCy_3 complexes.[12d] The Pt-P bond distances of the title compound are very similar to those found in other Pt complexes containing two PTA ligands in a *trans* orientation.[12a]

2.1.5 Synthesis of some alkynyl complexes bearing DAPTA ligands

The dialkynylbis(DAPTA) complexes were synthesized following the same procedure applied for the synthesis of the PTA-analogues (Scheme 2.1.8). When *cis*-$MCl_2(DAPTA)_2$ (M = Pt, Pd)[2a, 11] was stirred with an excess of phenylacetylene in absolute ethanol in the presence of triethylamine for 14-15 h, the corresponding complexes, *cis*-$Pt(C_2Ph)_2(DAPTA)_2$, **13a** or *trans*-$Pd(C_2Ph)_2(DAPTA)_2$, **14** were obtained in good yields. Complex **13a** was obtained as an off-white solid in 68% yield. The $^{31}P\{^1H\}$ NMR spectrum of **13a** in DMSO-d_6 showed a single peak at δ -41.6 with a coupling value of $^1J_{PtP}$ = 2145 Hz characteristic for the *cis*-complex. Three peaks at 2108, 2038 cm^{-1}, corresponding to two C≡C stretches, and at 1634 cm^{-1}, corresponding to a C=O stretch, were observed in the IR spectrum. However, three broad signals corresponding to the COCH_3 protons were observed at 2.06, 1.99, and 1.87 ppm in the ^1H NMR spectrum. This is probably due to the fact that in a solution of **13a**, acyl groups undergo a *syn* orientation in one of the ligands (1 peak) and an *anti* orientation in another ligand (2 peaks).

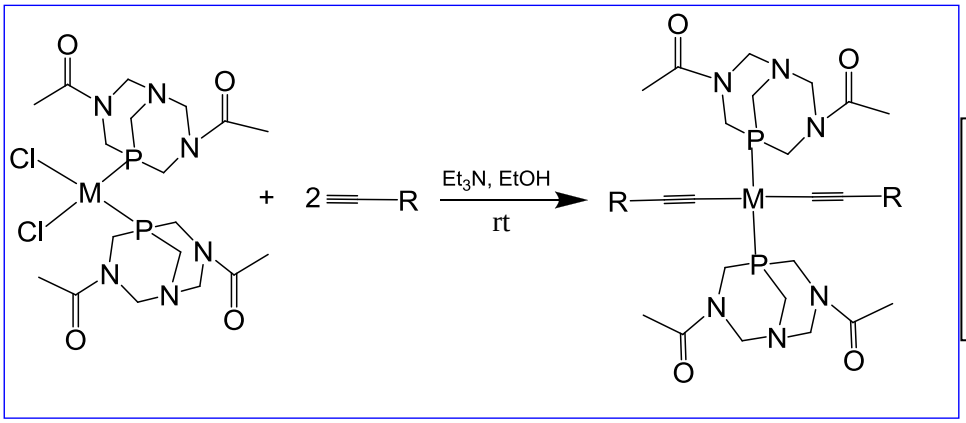

Scheme 2.1.8. Synthesis of *trans*-dialkynylbis(DAPTA) complexes.

When the reaction was monitored after 5 h, the starting material, *cis*-$MCl_2(DAPTA)_2$ was not consumed completely and an unassigned product was identified as the only product in a small amount. The $^{31}P\{^1H\}$ NMR spectrum of the reaction mixture displayed a single peak at -40.8 ppm, corresponding to the unassigned product along with another single peak at -79.4 ppm, corresponding to the uncoordinated phosphorus ligand. Surprisingly, when the reaction was extended over *ca.* 6 h, a mixture of **13a** and the unassigned product was obtained in approximately 4 : 1 ratio, respectively. The $^{31}P\{^1H\}$ NMR spectrum of the product mixture in DMSO-d_6 showed two singlets at δ -40.3 ppm (unassigned product) and δ -41.5 ppm with $^1J_{PtP}$ = 2144 Hz (**13a**). However, Pt satellites could not be resolved for the unassigned product. The signal for the unassigned product completely disappeared after 14 h. When **13a** was heated in $CDCl_3$ solution, isomerization occurred and *trans*-$Pt(C_2Ph)_2(DAPTA)_2$, **13b** was obtained as a major product with trace amounts of some unassigned products. The $^{31}P\{^1H\}$ NMR spectrum showed a broad singlet peak at -41.9 ppm with $^1J_{PtP}$ = 2444 Hz (**13b**) along with minor unassigned resonances. On the other hand, on heating a solution of **13a** in DMSO-d_6, only the unassigned resonances were observed in the $^{31}P\{^1H\}$ NMR spectrum.

Complex **13a** was also obtained in 71% yield starting from the $Pt(C_2Ph)_2(COD)$[9b] precursor by following a similar procedure used for the synthesis of complex **6a** (Scheme 2.1.9). In addition to the better yield of the product, the superiority of this method is that formation of none of the *trans*-isomer, **13b** was noticed on monitoring the reaction periodically.

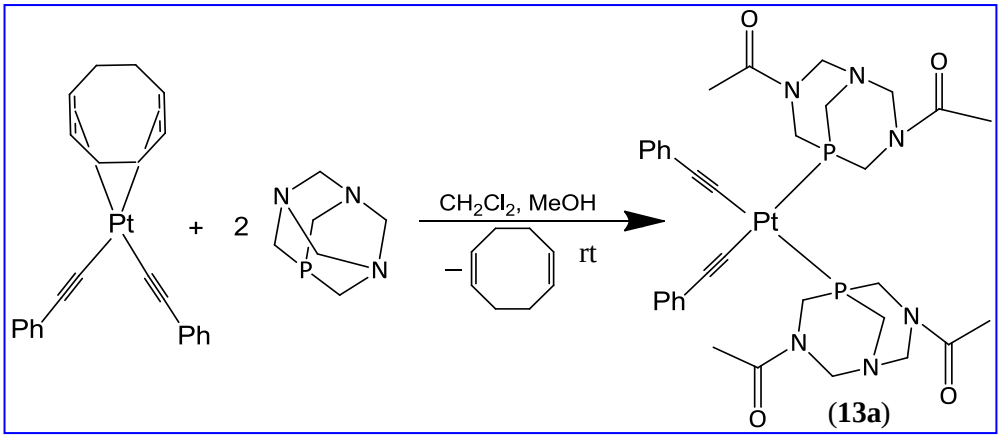

Scheme 2.1.9. Synthesis of *cis*-$Pt(C_2Ph)_2(DAPTA)_2$, **13a**.

Complex **14** was obtained as a yellow solid in 65% yield. Its acyl protons showed two resonances in the ^1H NMR spectrum and a singlet peak was observed at -35.2 ppm in the $^{31}P\{^1H\}$ NMR spectrum. The reaction was monitored periodically and two singlet resonances were observed at -35.2 and -79.1 ppm after 3 h until the completion of the reaction which means **14** is resistant to undergo isomerization unlike **13b**.

As their PTA analogues, the syntheses of bis(trimethylsilylethynyl)bis(DAPTA) complexes, *trans*-$M(C_2Me_3Si)_2(DAPTA)_2$ [M = Pt (**15a**); M = Pd (**15b**)] were carried out by stirring *cis*-$MCl_2(DAPTA)_2$[2a, 11] with an excess of trimethylsilylacetylene in absolute ethanol at room temperature in the presence of Et_3N for 14-15 h (Scheme 2.1.8). Complexes **15a** and **15b** were obtained as a white solid (68% yield) and an off-white solid (61% yield), respectively. Complex **15b** was found to undergo slow decomposition at room temperature while solutions of both the complexes were found to undergo slow decomposition at room temperature over a period of time. The ^1H NMR spectra of both the complexes displayed two broad peaks for the acyl hydrogens whereas an upfield singlet was observed corresponding to the Me_3Si protons. The $^{29}Si\{^1H\}$ NMR spectra of

15a and **15b** displayed a single resonance at -23.4 and -23.5 ppm, respectively. A peak at -43.3 ppm in the $^{31}P\{^{1}H\}$ NMR spectrum of **15a** with a coupling constant of $^{1}J_{PtP} = 2498$ Hz suggests a *trans*-orientation of the DAPTA ligands whereas as for the complex **14**, the $^{31}P\{^{1}H\}$ NMR spectrum of **15b** showed a singlet peak at -35.1 ppm.

2.1.6 Synthesis of additional dialkynyl PTA and DAPTA complexes of Pt and Pd

In order to add more complexes to the library of alkynyl PTA and DAPTA complexes of platinum and palladium, we undertook the challenge of synthesis and characterization of a number of platinum(II) and palladium(II) PTA and DAPTA complexes bearing a variety of alkynyl ligands, including nitrogen donors. The synthesized complexes were characterized by ^{1}H, $^{13}C\{^{1}H\}$, and $^{31}P\{^{1}H\}$ NMR spectroscopy, IR spectroscopy, mass spectrometry, elemental analysis, and in some cases X-ray crystallography.

The synthesis of one of such complex, *cis*-[Pt{C_2(*p*-tol)}$_2$(PTA)$_2$] (**16**) was carried out by stirring a CH_2Cl_2 solution of [Pt{C_2(*p*-tol)}$_2$(COD)] overnight with 2 molar equivalents of PTA in methanol at room temperature (Scheme 2.1.10). Complex **16** was obtained as an off-white solid in 89% yield.

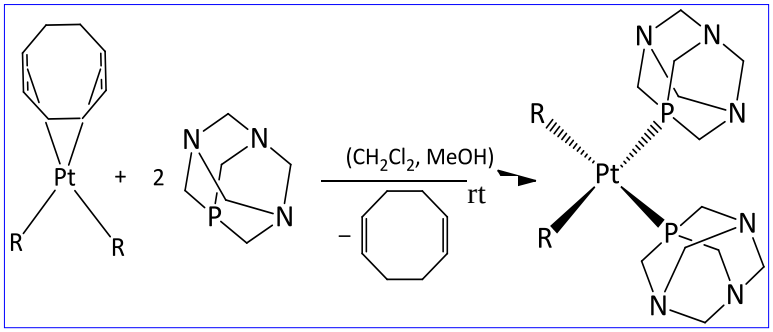

R = C_2(*p*-tol), **16**;
R = C_2(*m*-py), **18a**;
R = C_2(*o*-py), **19a**;
R = C_2(*m*-$C_6H_4NH_2$), **20**

Scheme 2.1.10. Synthesis of *cis*-dialkynylbis(PTA) complexes of platinum.

The $^{1}J_{PtP}$ value in the $^{31}P\{^{1}H\}$ NMR spectrum was determined to be 2070 Hz, which is similar to that shown by other *cis*-alkynyl PTA complexes such as **6a** and **13a**. The $^{1}J_{PtP}$ value for the related Pt alkynyl complex bearing PTA ligands, *cis*-[Pt{C≡C$(CH_2)_3NH_3$}$_2$(PTA)$_2$]Br_2 was reported as 2167 Hz.[2b] The ^{1}H NMR spectrum also showed the expected signals. Complex **16** displayed only one C≡C stretch at 2120 cm^{-1} in the IR spectrum.

Complex **16** was also prepared by following an alternative procedure which required an extended reaction time. On stirring *cis*-$PtCl_2(PTA)_2$ with an excess of 4-ethynyltoluene in absolute ethanol at room temperature in the presence of triethylamine for *ca.* 72 h, complex **16** was obtained as an off-white solid in 80% yield, which is lower than that obtained by applying the previous method (89%). The reaction was monitored periodically. After 6 h, a minor peak corresponding to **16** and two other major signals including that corresponding to free PTA were observed in the $^{31}P\{^{1}H\}$ NMR spectrum. After 48 h, a major signal corresponding to **16** and an additional minor signal (which could probably be due to the *trans*-isomer of **16**) were observed. However, $^{1}J_{PtP}$ for other signals could not be observed.

The reaction of the palladium precursor, *cis*-$PdCl_2(PTA)_2$[2b] with 4-ethynyltoluene under the same conditions used in the preparation of **16** for 6 h led to the formation of *trans*-[Pd{C_2 (*p*-tol)}$_2$(PTA)$_2$] (**17**) as an off-white solid in 81% yield (Scheme 2.1.11). The reaction was monitored after 3 h while no additional signals in the $^{31}P\{^{1}H\}$ NMR spectrum other than those for **17** and the free PTA were observed. Complex **17** was found to be unstable in solution on standing for long time periods at room temperature. The $^{31}P\{^{1}H\}$ NMR spectrum showed a singlet peak at -56.9 ppm, comparable to the

analogous complexes **7** and **8b**. Expected signals were observed in the ^{1}H NMR spectrum including two broad peaks at 4.55 and 4.44 ppm corresponding to the NC*H*$_2$N and PC*H*$_2$N hydrogens, respectively.

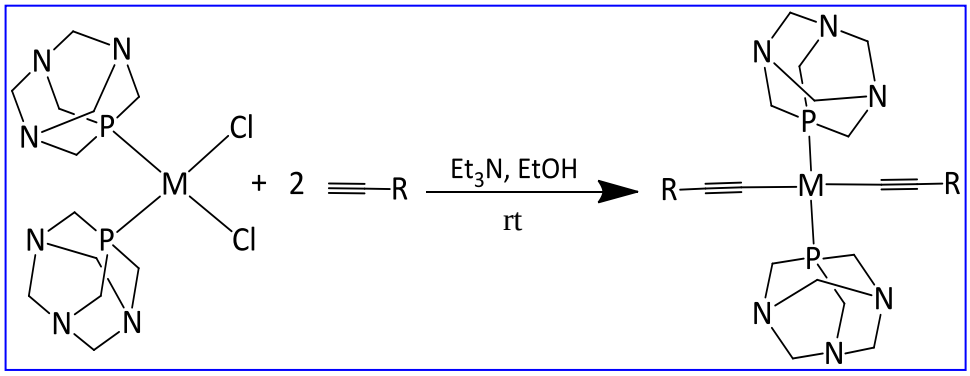

M = Pd:
R = *p*-tol, **17**;
R = *m*-py, **21**;
R = *o*-py, **22**;
R = *m*-$C_6H_4NH_2$, **23**;
M = Pt:
R = *m*-py, **18b**;
R = *o*-py, **19b**;
R = Bz, **24**

Scheme 2.1.11. Synthesis of *trans*-dialkynylbis(PTA) complexes of Pt and Pd.

X-ray quality crystals of **16** were obtained by the layering of methanol to a CH_2Cl_2 solution of **16** at a lower temperature below 0 ^{o}C. Complex **16** was crystallized as orthorhombic crystals in a Pbca space group. The crystal structure of **16** revealed a distorted square planar geometry of the molecule (Figure 2.1.6). Selected bond lengths and bond angles are given in Table 2.1.8.

The (C1-Pt-P2) and (C10-Pt-P10) bond angles are 176.72(7)^{o} and 171.42(7)^{o}, respectively. The average Pt-P bond length is 2.2759(6) Å whereas the average Pt-C(1) and Pt-C(10) bond distances are 2.011(3) Å and 1.993(16) Å, respectively. The C(1)-C(2) and C(10)-C(11) bond lengths representing the C≡C bond are 1.205(4) Å and 1.210(3) Å, respectively. The average Pt-C, Pt-P, and C≡C bond lengths for the related complex, *trans*-[Pt(C≡CPh)$_2$(PEt$_3$)$_2$] as reported by Carpenter and Lukehart were found to be 1.98(1) Å, 2.289(3) Å, and 1.21(1) Å, respectively.[10]

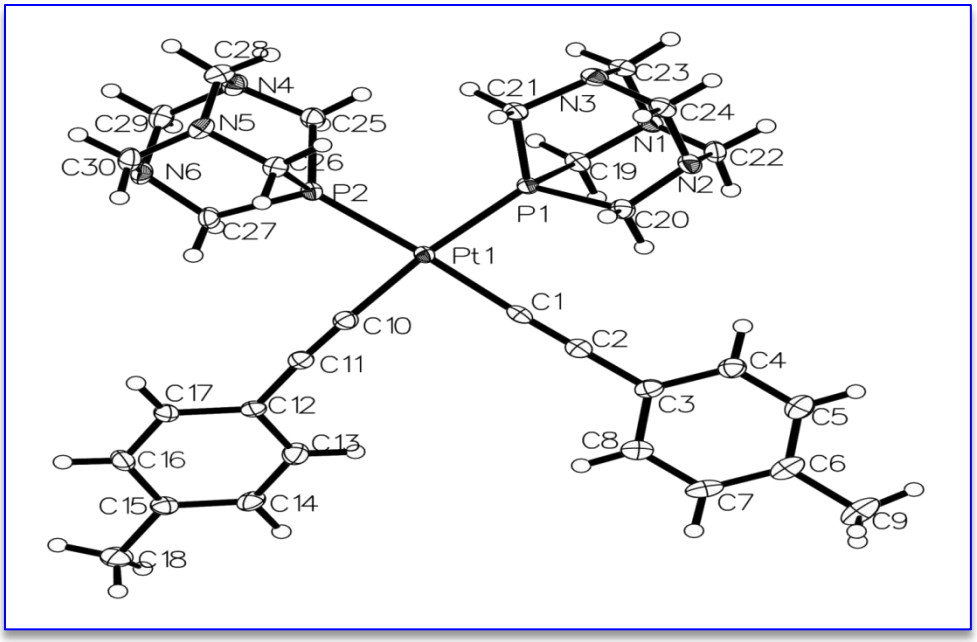

Figure 2.1.6. Molecular structure of *cis*-[Pt{C_2(*p*-tol)}$_2$(PTA)$_2$], **16**. Solvent molecules are omitted for clarity. Thermal ellipsoids are drawn at the 50% probability level.

Table 2.1.8. Selected bond length and bond angle values for (**16**).

Pt-C1	Pt-C10	P1-Pt-P2 C1-Pt-C10	C1-Pt-P2	C10-Pt-P1	Pt-P1	C1-C2 C10-C11	C2-C3 C11-C12
2.011(3) Å	1.993(16) Å	97.95(2)° 88.64(10)°	176.72(7)°	171.42(7)°	2.2759(6) Å	1.205(4) Å 1.210(3) Å	1.438(4) Å 1.436(3) Å

These bond length values are very similar to those of other related *cis*-platinum alkynyl complexes bearing phosphines including Pt(C≡CH)$_2$(dppe) [Pt–C = 2.025(5) Å, Pt–P = 2.2851(12) Å, and C≡C = 1.164(8) Å].[9d] The C(2)-C(3) and C(11)-C(12) bond lengths in **16** are 1.438(4) Å and 1.436(3) Å, respectively which are significantly shorter than the standard carbon-carbon single bond length (~ 1.54 Å) because of the binding of the sp^2 carbon atom to the ethynyl group. The distortion from the ideal geometry in **16** is probably due to steric repulsion caused by the *cis* oriented PTA ligands to some extent. This is the reason why the (P1-Pt-P2) bond angle [97.95(2)°] undergoes a larger deviation

from the ideal value (90°) in comparison to the (C1-Pt-C10) bond angle [88.64(10)°]. The larger size of PTA than 4-ethynyltoluene leads to larger (P1-Pt-P2) and smaller (C1-Pt-C10) angles.

Crystal data parameters of **16** and other related dialkynylbis(PTA) complexes of platinum and palladium, **19b** and **22** are given in Table 2.1.9.

Table 2.1.9. Crystal data parameters for **16**, **19b**, and **22**.

Complexes	**16**	**19b**	**22**
Crystal system	Orthorhombic	Triclinic	Monoclinic
Space group	Pbca	P-1	$P2_1/c$
a Å	11.3678(5)	6.3135(3)	5.9965(15)
α deg	90	110.424(2)	90
b Å	20.2126(10)	9.9760(5)	22.542(5)
β deg	90	91.205(2)	102.123
c Å	25.9026(14)	10.8270(5)	12.990(3)
γ deg	90	96.390(2)	90
Volume $Å^3$	5951.7(5)	633.77(5)	1716.7(7)
Density (calcd) mg/m^3	1.746	1.870	1.671
Absorption coefficient	4.945	5.695	1.136
Temperature	100(2) K	100(2) K	100(2) K
Goodness-of-fit on F^2	1.058	1.027	1.031
Final R indices	R1 = 0.0270, wR2 = 0.0492	R1 = 0.0207, wR2 = 0.0396	R1 = 0.0388, wR2 = 0.0747

The synthesis of a complex bearing the 3-ethynylpyridine ligand, *cis*-[Pt{C_2(*m*-py)}$_2$(PTA)$_2$] (**18a**) was carried out by ligand exchange of [Pt{C_2(*m*-py)}$_2$(COD)][9, 10] with PTA in 1 : 2 molar ratio, respectively (Scheme 2.1.10). Complex **18a** was obtained as a white solid in 86% yield. As in the other alkynyl complexes discussed above, the $^{31}P\{^1H\}$ NMR spectrum showed a singlet at -71.5 ppm with a coupling value of $^1J_{PtP}$ = 2075 Hz. On the other hand, the ^1H NMR spectrum displayed an AB quartet at 4.54 ($^2J_{HH}$ = 13 Hz) as in the complex **1a** and a broad signal at 4.33 ppm which represents the NC*H*$_2$N and PC*H*$_2$N protons, respectively. Both the C≡C stretch (2112 cm^{-1}) and C=N stretch (1613 cm^{-1}) were observed in the IR spectrum, and the reduced C≡C stretching frequency compared to that in the free alkyne suggesting π-back bonding to some extent.[13]

On the other hand, the synthesis of the 2-ethynylpyridine analogue of **18a**, *cis*-[Pt{C_2(*o*-py)}$_2$(PTA)$_2$], **19a** was carried out by a similar reaction through the ligand exchange of [Pt{C_2(*o*-py)}$_2$(COD)] with PTA in 1 : 2 molar ratio, respectively (Scheme 2.1.10). Complex **19a** was obtained as a white solid in 82% yield. Two broad signals, in addition to other downfield signals, were observed in the ^1H NMR spectrum at 4.53 and 4.41 ppm for the NC*H*$_2$N and PC*H*$_2$N protons, respectively. The $^{31}P\{^1H\}$ NMR spectrum for **19a** was nearly identical to that of **18a** showing a singlet at -70.5 ppm with a coupling value of $^1J_{PtP}$ = 2069 Hz. Like **18a**, notable in the IR spectra of **19a** are the C≡C stretch (2108 cm^{-1}) and C=N stretch (1605 cm^{-1}).

Complex **19a** was also prepared in a relatively lower yield (76%) through an alternative procedure by stirring *cis*-$PtCl_2(PTA)_2$[2a] with an excess of 2-ethynylpyridine for *ca.* 72 h in absolute ethanol in a basic medium. An incomplete reaction after 60 h

resulted in the formation of a mixture of *trans*-[Pt{C_2 (*o*-py)}$_2$(PTA)$_2$] (**19b**) and an unassigned product in approximately 5 : 1 ratio, respectively. The $^{31}P\{^1H\}$ NMR spectrum of the product mixture exhibited a single singlet peak, along with a minor resonance of the unassigned product, corresponding to **19b** at -64.3 ppm with acoupling constant of $^1J_{PtP}$ = 2287 Hz .

Complex **19b** was selectively obtained in pure form (81% yield) when the reaction was stopped after 16 h. The ^1H NMR spectrum for **19b** was essentially identical to that for **19a** whereas the $^1J_{PtP}$ coupling constant in the $^{31}P\{^1H\}$ NMR spectrum was found to be 2281 Hz (δ -64.3 ppm). The chemical shift and coupling constant values are comparable to that of the related diethynyl complex, **6b** ($^1J_{PtP}$ = 2309 Hz; δ -64.3 ppm) whereas the $^1J_{PtP}$ value ($^1J_{PtP}$ = 2305 Hz; δ -58.9 ppm) is also comparable to that of the related complex, *trans*-[Pt{C≡C(CH$_2$)$_3$NH$_3$}$_2$(PTA)$_2$]Br$_2$.[2b] A more downfield chemical shift for the latter is as expected because of possible deshielding effect in the cationic species.[2] The C≡C stretching frequency (2103 cm^{-1}) in the IR spectrum is comparable to that of the uncoordinated 2-ethynylpyridine (2110 cm^{-1}) and the related complex, *trans*-[Pt{C≡C(CH$_2$)$_3$NH$_3$}$_2$(PTA)$_2$]Br$_2$ (2122 cm^{-1}).[2b] Additionally, the C=N stretch was also observed in the IR spectrum at 1617 cm^{-1}.

X-ray quality crystals of **19b** were obtained by layering of methanol to a $CHCl_3$ solution of **19b** below 0 ^oC. Complex **19b** was crystallized as a triclinic crystal in a P-1 space group and the crystal structure exhibited a square planar geometry (Figure 2.1.7). The final R indices, R1 = 0.0207 is evidence for an excellent crystal structure. The PTA ligands are oriented *trans* to each other. The alkynylplatinum units are linear. Selected

bond length and bond angles of complex **19b** are listed in Table 2.1.10 and the crystal structure is described below.

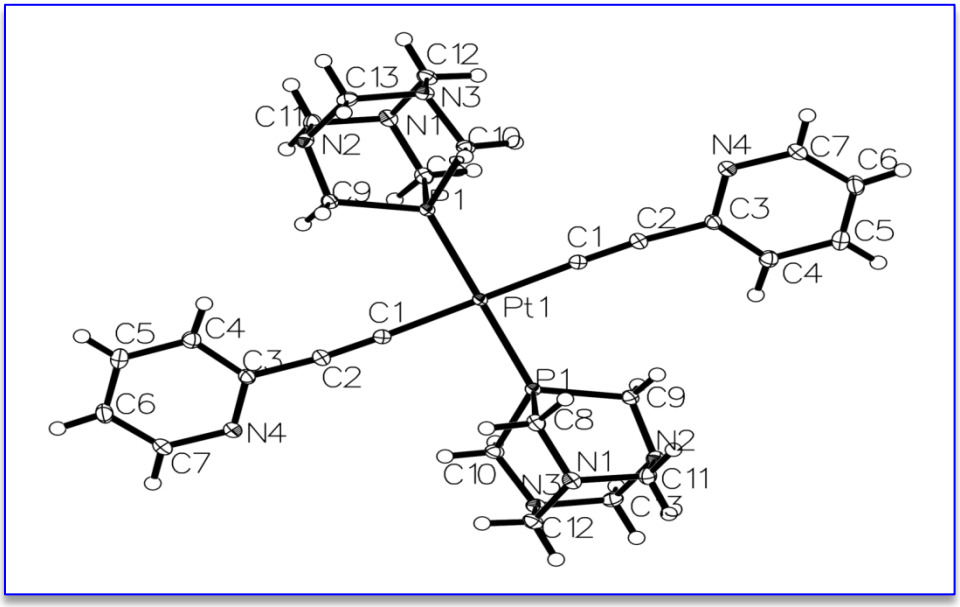

Figure 2.1.7. Molecular structure of *trans*-[Pt{C_2(*o*-py)}$_2$(PTA)$_2$], **19b**. Thermal ellipsoids are drawn at the 50% probability level.

Table 2.1.10. Selected bond lengths and bond angles for (**19b**).

Pt-C1	P1-Pt-P1	C1-Pt-C1	Pt-P1	C1-C2	C2-C3	Cl-Pt-P1
1.9955(11) Å	179.999(15)°	179.999(1)°	2.2782(3) Å	1.2165(15) Å	1.4317(15) Å	89.25(3)° 90.75(3)°

Both the (P-Pt-P) and (C-Pt-C) bond angles are the same [179.999(15)° and 179.999(1)°, respectively] while the (C-Pt-P) bond distances are 89.25(3)° and 90.75(3)°. The (P1-Pt-C1-C2) torsion angle values of 180(100)° and 0(3)° also show that there is little deviation from planarity. The average Pt-P, Pt-C(1), and C(1)-C(2) bond distances are 2.2782(3) Å, 1.9955(11) Å, and 1.2165(15) Å, respectively. These values for the

related complex, *trans*-[Pt{C≡C$(CH_2)_3NH_3$}$_2$$(PTA)_2$]$Br_2$ were reported to be 2.264(3) Å, 2.032(15) Å, and 1.19(2) Å, respectively,[2b] which are in close proximity to each other. The Pt-P bond distance is slightly longer than the corresponding distance of related *cis*-$PtX_2(PTA)_2$ (X = Cl, Br, I) complexes [2.219(5)–2.236(3) Å].[2a] This indicates that the PTA ligand has a greater *trans*-influence than X. The average C(2)-C(3) bond length is 1.4317(15) Å which is significantly shorter than the standard C-C single bond length (~ 1.54 Å). Laguna *et al.* reported very similar Pt-P, Pt-C, and C≡C bond length values [2.2896(15) Å, 2.006(6) Å, and 1.191(9) Å, respectively] for the related *trans*-alkynyl complex, *trans*-[Pt(C≡C$CH_2R)_2(PPh_3)_2$] (R = pyrazolyl).[14] These bond length values are also in a close agreement to those reported for other related alkynyl complexes such as *trans*-[Pt{C≡C$(C_6H_4$-4-$NH_2)$}$_2$$(PPh_3)_2$] [Pt–P = 2.310(1) Å, Pt–C = 2.005(4) Å, and C≡C =1.206(6) Å].[15] Additionally, the average Pt-C, Pt-P, and C≡C bond lengths for the related complex, *trans*-$Pt(C_2Ph)_2(PEt_3)_2$ as reported by Carpenter and Lukehart were found to be 1.98(1) Å, 2.289(3) Å, and 1.21(1) Å, respectively which are in close agreement to those found for **19b**.[10]

The syntheses of *trans*-[M{C_2 (*m*-py)}$_2$$(PTA)_2$] (M = Pt; **18b** and M = Pd; **21**) were carried out by stirring a suspension of *cis*-$MCl_2(PTA)_2$ in abs. ethanol with an excess of 3-ethynylpyridine for *ca.* 12-16 h in absolute ethanol in the presence of Et_3N (Scheme 2.1.11). Complexes **18b** and **21** were obtained as white solids in 84% and 79% yield, respectively. The appearance of an AB quartet (J_{HH} = 13 Hz), as demonstrated by some of the *trans*-PTA complexes,[3] at 4.54 ppm and a broad signal at 4.40 ppm in the ^{1}H NMR spectrum of **18b** indicate the presence of the NCH_2N and PCH_2N protons, respectively. On the other hand, **21** shows two broad signals for these hydrogens at 4.56 and 4.43 ppm,

respectively. While complex **18b** appears to undergo isomerization on standing for long time periods in $CDCl_3$ and DMSO-d_6 solutions, complex **21** was also found to be unstable in solution on standing for long time periods.

The $^{13}C\{^1H\}$ NMR spectrum of **18b** showed two triplets at 73.5 ppm ($^1J_{PC}$ = 3.4 Hz) and 53.4 ppm ($^1J_{PC}$ = 11.6 Hz) corresponding to the N*C*H_2N and P*C*H_2N carbons, respectively, along with the aromatic carbon signals as well as some signals due to the possibly isomerized products. However, the $^2J_{PtC}$ coupling could not be resolved. The downfield resonance of the alkynyl carbon (δ 107.5 and 102.5 ppm) suggest some degree of π-back bonding from the metal σ-orbitals to the alkynyl π*-orbitals. However, the C≡C stretching frequency of **18b** and **21** (2108 cm^{-1}) in the IR region is not significantly different from that of the free 3-ethynylpyridine (2112 cm^{-1}). The $^{31}P\{^1H\}$ NMR spectrum of **18b** showed a resonance at -65.3 ppm with a coupling constant of $^1J_{PtP}$ = 2282 Hz; as comparable to **19b** whereas **21** showed a resonance at -56.9 ppm comparable to **8b**. As stated earlier in this section, the $^1J_{PtP}$ value for the related Pt alkynyl complex bearing PTA ligands, *trans*-$[Pt\{C{\equiv}C(CH_2)_3NH_3\}_2(PTA)_2]Br_2$ was reported as 2305 Hz.[2b]

The palladium analogue of **19b**, *trans*-$[Pd\{C_2(o\text{-py})\}_2(PTA)_2]$ (**22**) was synthesized using *cis*-$PdCl_2(PTA)_2$[2b] and following the same procedure used for the synthesis of **19b** (Scheme 2.1.11). Complex **22** was obtained as a white solid in 83% yield and was found to be unstable in solution on standing for few hours at room temperature. As in the case of **18b**, the ^1H NMR spectrum of **22** displayed an AB quartet resonance at 4.53 ppm (J_{HH} = 12 Hz) corresponding to the NC*H*$_2$N protons and a broad signal at 4.45 corresponding to the PC*H*$_2$N protons while a single resonance appeared at δ -56.2 ppm in the $^{31}P\{^1H\}$ NMR spectrum, as in the *m*-ethynylpyridine analogue, **21**. The C≡C and C=N stretching

frequencies in **22** were found to be a little bit higher in energy (2120 and 1629 cm^{-1}, respectively) in the IR spectrum than those in the ethynylpyridine complexes of platinum described above.

Despite its instability in solution, X-ray quality crystals of **22** were obtained by layering of methanol over a $CHCl_3$ solution of **22** at low temperature. Pale yellow crystals were obtained after cooling below 0 ^oC for 2 days. Complex **22** was crystallized as monoclinic crystals in a $P2_1/c$ space group.

Complex **22** was found to have a slightly distorted square planar geometry (Figure 2.1.8) with a *trans* orientation of the PTA ligands. The change in relative orientation of the phosphine ligands (PTA) from *cis* to *trans* during the reaction suggests that the reaction might have proceeded with a prior dissociation of the phosphine. This type of reactivity has frequently been observed for Pd(II) complexes of the type PdR_2L_2 that lose one of the phosphine ligands before reductive-elimination.[16] Selected bond lengths and bond angles of **22** are listed in Table 2.1.11.

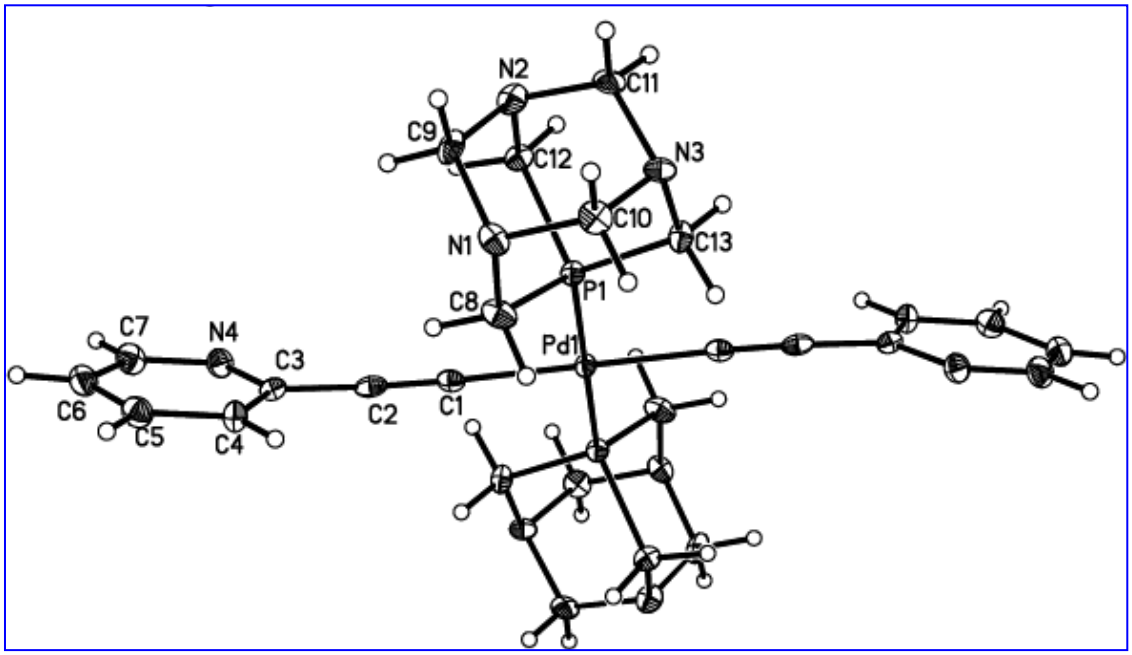

Figure 2.1.8. Molecular structure of *cis*-[Pd{C_2(*o*-py)}$_2$(PTA)$_2$], **22**. Solvent molecules are omitted for clarity. Thermal ellipsoids are drawn at the 50% probability level.

The alkynylpalladium unit in **22** is linear which is evident from the (P-Pd-P), (C-Pd-C), and (Pd-C1-C2) bond angles; 180.0(0)^o, 180.0(2)^o, and 175.9(4)^o, respectively (Table 2.1.11). This is as expected for the *sp*-hybridized carbons. The (C-Pd-P) bond angles, 86.25(12)^o and 93.75(12)^o, are slightly deviated from the ideal values. The average Pd-P, Pd-C, and C(1)-C(2) bond lengths are 2.2614(11) Å, 2.016(4) Å, and 1.188(6) Å, respectively, which are in the close proximity to those reported for the related complexes. The Pd-P, Pd-C, and C≡C bond lengths in a related phenylethynyl complex, *trans*-[Pd(C≡CPh)$_2$(PEt$_3$)$_2$] were reported as 2.3009(7) Å, 1.998(3) Å, and 1.202(4) Å, respectively.[13] As in the complexes **16** and **19b**, the C(2)-C(3) bond length in **22**, 1.453(6) Å, is found to be shorter than the normal C-C single bond which was also found to be shorter, 1.437(3) Å, in the related complex, *trans*-Pd(C≡CPh)$_2$(PEt$_3$)$_2$.**Error! ookmark not defined**

Table 2.1.11. Selected bond lengths and bond angles for (**22**) and the related complex, *trans*-Pd(C$_2$Ph)$_2$(PEt$_3$)$_2$.

Complex	Pd-C1-C2	Pd-C1, Å	C1-Pd-P1	C1-Pd-C1 P1-Pd-P1	Pd-P1, Å	C1-C2, Å	C2-C3, Å
22	175.9(4)°	2.016(4)	93.75(12)° 86.25(12)°	180.0(2)° 180.0°	2.2614(11)	1.188(6)	1.453(6)
trans-Pd(C$_2$Ph)$_2$(PEt$_3$)$_2$[16]	177.7(2)°	1.998(3)	92.18(8)° 87.82(2)°	180.0° 180.0°	2.3009(7)	1.202(4)	1.437(3)

The ethynyl-substituted aniline ligated PTA complex of platinum, *cis*-[Pt{C_2(*m*-$C_6H_4NH_2$)}$_2$(PTA)$_2$] (**20**), was prepared by treating [Pt{C_2 (*m*-$C_6H_4NH_2$)}$_2$(COD)] with PTA at room temperature in 1 : 2 molar ratio, respectively (Scheme 2.1.10). Complex **20** was obtained as an off-white solid in 78% yield. The ^{1}H NMR spectrum of **20** in DMSO-d_6 demonstrated a broad signal for the PCH_2N hydrogens and a multiplet due to possible virtual or long-range coupling of the NCH_2N hydrogens. A resonance diagnostic to the *trans*-alkynyl complex was observed in the ^{31}P{^{1}H} NMR spectrum at -70.5 ppm with the $^1J_{PtP}$ coupling constant of 2064 Hz, which is comparable to a related *cis*-complex such as **16**. Complex **20** could also be synthesized in a relatively lower yield (71%) by the reaction of *cis*-$PtCl_2(PTA)_2$ with an excess of 3-ethynylaniline over an extended period of time (*ca.* 76 h) in absolute ethanol in the presence of Et_3N. A comparison of yields of different *cis*-dialkynylbis(PTA) complexes along with their ^{31}P{^{1}H} NMR data are shown in Table 2.1.12.

Table 2.1.12. Yields and ^{31}P{^{1}H} NMR spectral data for *cis*-dialkynylbis(PTA) complexes.

Complex	**C≡CR**	**% Yield**	**^{31}P{^{1}H} NMR, δ**	**J_{PtP}, Hz**
6a	C≡CPh	86	-69.9	2057
19a	C≡C(*o*-py)	86	-70.5	2069
16	C≡C(*p*-tol)	89	-70.2	2070
18a	C≡C(*m*-py)	82	-71.5	2075
20	C≡C(*m*-$C_6H_4NH_2$)	78	-70.5	2064

The palladium analogue of **20**, *trans*-[Pd{C_2(*m*-$C_6H_4NH_2$)}$_2$(PTA)$_2$] (**23**) was obtained in 74% yield by an overnight reaction of *cis*-$PdCl_2(PTA)_2$ with an excess of 3-ethynylaniline in absolute ethanol in the presence of Et_3N (Scheme 2.1.11). In addition

to the aromatic and amine proton signals, two broad resonances were observed in the ^{1}H NMR spectrum of **23** at 4.55 ppm (NCH_2) and 4.42 ppm (PCH_2) whereas a resonance at -56.9 ppm was observed in the $^{31}P\{^{1}H\}$ NMR spectrum. Complex **23** was found to be unstable in solution on standing for few hours at room temperature. It is important to note that a significantly lowering of the C≡C stretching frequency for **20** and **23** (2095 and 2099 cm^{-1}, respectively) was noticed in the IR spectrum. Attempts to synthesize the *cis*-isomer of **23** were not successful. Attempts to determine the accurate mass of **20** and **23** failed because of formation of the cluster of M^+ and $(M+H)^+$ ions while analyzing by mass spectrometry.

Another alkynyl PTA complex, *trans*-$Pt(C_2Bz)_2(PTA)_2$ (**24**) (Bz = $C_6H_5CH_2$) was obtained in 78% yield by the reaction of *cis*-$PtCl_2(PTA)_2$ with an excess of 3-phenyl-1-propyne for *ca.* 36 h in absolute ethanol in the presence of Et_3N (Scheme 2.1.11) at room temperature. A multiplet (a virtual doublet of doublets) at 4.48-4.22 ppm (NCH_2) and a broad signal at 4.16 ppm (PCH_2) appeared in the ^{1}H NMR spectrum of **24** along with the aromatic and methylene protons resonances. This clearly implies the presence of two inequivalent NCH_2N hydrogens. The appearance of a resonance in the $^{31}P\{^{1}H\}$NMR spectrum with a coupling value of $^{1}J_{PtP}$ = 2335 Hz suggests the *trans* disposition of the PTA ligands which is closely related to the $^{1}J_{PtP}$ value (2305 Hz) reported for the related complex, *trans*-$[Pt\{C{\equiv}C(CH_2)_3NH_3\}_2(PTA)_2]Br_2$.[2b] An incomplete reaction of the *cis*-$PtCl_2(PTA)_2$ after 12 h resulted in the formation of a mixture of **24** (-64.4 ppm, $^{1}J_{PtP}$ = 2335 Hz) and an unassigned *trans*-product (-61.2 ppm, $^{1}J_{PtP}$ = 2376 Hz) in approximately 1 : 1 ratio. Complex **24** appears to undergo slow conversion to an unassigned product on leaving its $CDCl_3$ solution at room temperature for several days.

Table 2.1.13 summarizes the yields and the $^{31}P\{^{1}H\}$ NMR spectral data of different *trans*-alkynyl PTA complexes, *trans*-$M(C_2R)_2(PTA)_2$. Some Pd complexes have been prepared in lower yields due to their instability. As expected, phosphorus of the Pd complexes is more deshielded than that of the Pt analogues.

Table 2.1.13. Yields and $^{31}P\{^{1}H\}$ NMR spectral data for *trans*-dialkynylbis(PTA) complexes.

Complex	M	R	% Yield	$^{31}P\{^{1}H\}$ NMR, δ	J_{PtP}, Hz
6b	Pt	Ph	81	-64.3	2301
7	Pd	Ph	86	-56.3	-
8a	Pt	$SiMe_3$	69	-66.4	2343
8b	Pd	$SiMe_3$	60	-58.8	-
17	Pd	*p*-tol	81	-56.9	-
19b	Pt	*o*-py	81	-64.3	2281
18b	Pt	*m*-py	84	-65.3	2282
22	Pd	*o*-py	83	-56.2	-
21	Pd	*m*-py	79	-56.9	-
23	Pd	*m*-$C_6H_4NH_2$	74	-56.9	-
24	Pt	Bz	78	-64.4	2335

The DAPTA analogues of **16** and **20**, *cis*-$[Pt\{C_2(p\text{-tol})\}_2(DAPTA)_2]$ (**25**) and *cis*-$[Pt\{C_2(m\text{-}C_6H_4NH_2)\}_2(DAPTA)_2]$ (**26**), respectively, were prepared by a ligand exchange reaction of the respective COD complexes with 2 molar equivalents of the DAPTA ligand (Scheme 2.1.12). The complexes **25** and **26** were obtained in 79% and 68% yields, as an off-white solid and a yellow solid, respectively. Complex **25** could

also be prepared in slightly lower yield (75%) by carrying out the reaction between *cis*-$PtCl_2(DAPTA)_2$ and an excess of 4-ethynyltoluene over an extended period of time (*ca.* 65 h). The C≡C stretching frequency of **25** was found to be higher (2140 cm^{-1}) than that of **16** (2120 cm^{-1}) in the IR spectrum whereas the C≡C stretching frequency of **26** (2103 cm^{-1}) is comparable to that of **20** (2095 cm^{-1}). Complex **26** exhibited some unprecedented additional peaks in the mass spectrum due to cluster formation with the matrix.

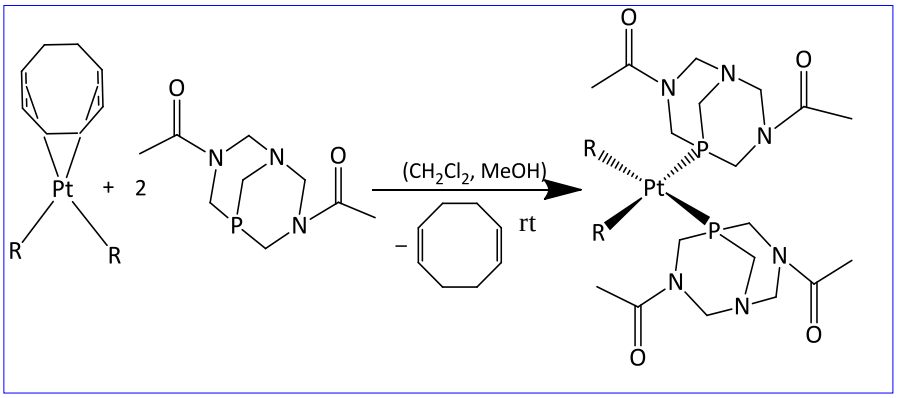

R = C_2(*p*-tol), **25**;
R = C_2(*m*-$C_6H_4NH_2$), **26**;
R = C_2(*m*-py), **27**.

Scheme 2.1.12. Synthesis of *cis*-dialkynylbis(DAPTA) complexes of Pt.

A single resonance was observed in the $^{31}P\{^1H\}$ NMR spectra for **25** and **26** each in DMSO-d_6 solution at -41.5 ($^1J_{PtP}$ = 2143 Hz) and -41.2 ($^1J_{PtP}$ = 2141 Hz) ppm, respectively, which is identical to the $^{31}P\{^1H\}$ NMR spectral results for the related complex **13a** in DMSO-d_6 (δ -41.6 ppm, $^1J_{PtP}$ = 2145 Hz) (Table 2.1.14). The ^1H NMR spectrum of **25** was observed to be similar to that of the related alkynyl DAPTA complex, **13a**. The splitting pattern of the ligand proton resonances was the same as that of **13a**. In complex **26**, however, an overlap of the NH_2 proton resonances and a resonance due to the two protons of the NCH_2N group resulted in a broad multiplet at ~ 5.0 ppm. The appearance of two broad singlet peaks corresponding to the CH_3CO protons (1.99, 1.88

ppm for **25** and 1.99, 1.92 ppm for **26**) indicates the *anti* conformation of each DAPTA ligand with respect to the acyl group.

Table 2.1.14. Yields and $^{31}P\{^{1}H\}$ NMR spectral data for *cis*-dialkynylbis(DAPTA) complexes.

Complex	C≡CR	% Yield	$^{31}P\{^{1}H\}$ NMR, δ	J_{PtP}, Hz
13a	C≡CPh	76	-41.6	2145
25	C≡C(*p*-tol)	79	-41.5	2143
27	C≡C(*m*-py)	80	-45.0, -45.2	2123, 2124
26	C≡C(*m*-$C_6H_4NH_2$)	68	-41.2	2141

The DAPTA analogues of **18b** and **19b**, *cis*-[Pt{C_2(*m*-py)}$_2$(DAPTA)$_2$] (**27**) and *trans*-[Pt{C_2(*o*-py)}$_2$(DAPTA)$_2$] (**28**), respectively were synthesized by the reaction between *cis*-$PtCl_2$(DAPTA)$_2$ and an excess of 3-ethynylpyridine and 2-ethynylpyridine, respectively, in absolute EtOH in the presence of Et_3N at room temperature. The synthesis of complex **28** is shown in Scheme 2.1.13. Complexes **27** and **28** were formed after *ca.* 48 h as an off-white solid in 80% and 82% yield, respectively. A prolonged reaction time (*ca.* 76 h) did not result in the isomerization of **28** unlike other related complexes such as **19b**. On the other hand, attempt to synthesize *trans*-isomer of **27** by altering the reaction time was unsuccessful.

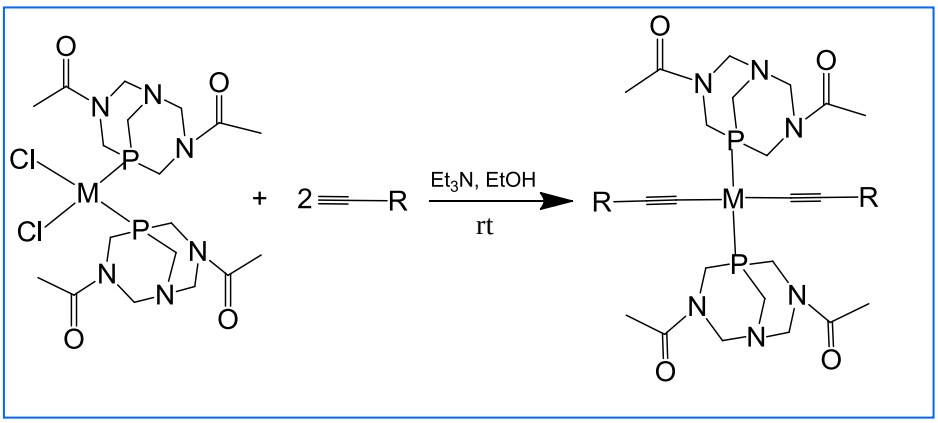

Scheme 2.1.13. Synthesis of *trans*-dialkynylbis(DAPTA) complexes.

Complexes **27** (Scheme 2.1.12) and **28** could also be prepared in very good yields (84% and 83%, respectively) by an overnight reaction of the respective COD precursor with 2 molar equivalents of the DAPTA ligand. We are in the process of exploring the reason for such kind of change of stereochemistry of the metal complex on changing the isomeric alkynyl ligand under the same reaction conditions.

As seen in other DAPTA complexes, the chemical shifts in **27** and **28** appeared as a downfield shift in the $^{31}P\{^{1}H\}$NMR spectrum compared to the corresponding PTA complexes **18b** and **19b**, respectively. The appearance of two signals at -45.0 and -45.2 ppm in approximately 1 : 1 ratio with almost the same ^{31}P-^{195}Pt ($^{1}J_{PtP}$ = 2123 and 2124 Hz) coupling value in the $^{31}P\{^{1}H\}$NMR spectrum of **27** (Table 2.1.14) in $CDCl_3$ suggests that **27** exists as a mixture of two conformers in solution in which the ligand orientation is *cis* to each other.[11b] The appearance of many broad signals corresponding to the C*H*$_3$CO hydrogens in the ^{1}H NMR spectrum of **27** is consistent with this fact.

As described for the related complex **9a**, it seems that all of the acyl groups of the DAPTA ligand undergo a *syn* orientation in one of the conformers whereas in another conformer, the acyl groups have a *syn* orientation in one of the ligands and an *anti* orientation in another ligand. The ^{1}H NMR spectra, as they appeared in other related DAPTA complexes such as **13a**, showed a number of resonances corresponding to the PC*H*$_2$N, NC*H*$_2$N, PC*H*$_2$NC, COC*H*$_3$, and C*H*$_3$ hydrogens and were consistent with the presence of diastereotopic hydrogens in PC*H*$_2$N, NC*H*$_2$N, and PC*H*$_2$NC fragments of the

ligand. The splitting pattern of the resonances was almost the same as that of the free ligand.[11a] The ^{1}H NMR spectrum of **28** looked similar to that of the related complex, **15a** except that the signals corresponding to the C*H*$_3$CO hydrogens were found to be more complicated because of the appearance of multiple broad singlet signals. In contrast to the results for **27**, the ^{31}P{^{1}H} NMR spectrum of **28** showed a single resonance at -41.5 ppm with a coupling value of $^{1}J_{PtP}$ = 2441 Hz, consistent with the single conformation and *trans* orientation of the DAPTA ligands. These results are comparable with that exhibited by the related *trans*-DAPTA complex, **15a** and related *trans*-alkynyl PTA complex, *trans*-[Pt{C≡C(CH$_2$)$_3$NH$_3$}$_2$(PTA)$_2$]Br$_2$.[2b]

The DAPTA analogue of **17**, *trans*-[Pd{C$_2$(*p*-tol)}$_2$(DAPTA)$_2$] (**29**) was obtained as a yellow solid (80% yield) by the room temperature reaction of *cis*-PdCl$_2$(PTA)$_2$[2b] with an excess of 4-ethynyltoluene in absolute EtOH and triethylamine for *ca.* 18 h (Scheme 2.1.13). Complex **29** was found to be unstable in solution on standing for long periods at room temperature. The ^{31}P{^{1}H} NMR spectrum showed a singlet peak at -35.0 ppm, the chemical shifts being similar to those for the related alkynyl DAPTA complexes such as **14** (-35.2 ppm) and **15b** (-35.1 ppm). As with the PTA complexes **20** and **23**, attempts for the determination of the accurate mass of some of the DAPTA complexes (**25**, **26**, and **29**) also failed because of the formation of M^{+} and $(M+H)^{+}$ clusters while analyzing by mass spectrometry. The ^{1}H NMR spectrum was found to be almost identical to that of the related complexes **14** and **15b**. Two broad resonances for the acyl protons suggest an *anti* orientation of the acyl groups in the DAPTA ligand. In comparison to the platinum alkynyl DAPTA complexes **27** (2123 cm^{-1}) and **28** (2120 cm^{-1}), complex **29** has a lower C≡C stretching frequency (2103 cm^{-1}) in the IR spectrum. The ^{31}P{^{1}H} NMR spectral

data and isolated yields of different *trans*-dialkynylbis(DAPTA) complexes, *trans*-$Pt(C_2R)_2(DAPTA)_2$ are summarized in Table 2.1.15.

Table 2.1.15. Yields and $^{31}P\{^1H\}$ NMR spectral data for *trans*-dialkynylbis(DAPTA) complexes.

Complex	M	R	% Yield	$^{31}P\{^1H\}$ NMR, δ	J_{PtP}, Hz
14	Pd	Ph	65	-35.2	-
15a	Pt	$SiMe_3$	68	-43.3	2492
15b	Pd	$SiMe_3$	61	-35.1	-
28	Pt	*o*-py	82	-41.5	2441
29	Pd	*p*-tol	80	-35.0	-

2.1.7 Investigation of water-solubility of PTA and DAPTA complexes

Since the water-solubility of transition metals complexes has nowadays been more important, especially in the field of aqueous phase or biphasic catalysis,[17] we were interested in investigating the water-solubility of the platinum and palladium PTA and DAPTA complexes described herein. Darensbourg *et al.* have reported the water-solubility of some of the sulfonated phosphines and measured the water-solubility of the DAPTA ligand. The water-solubility of DAPTA has been found to be excellent as compared to that of the water-soluble sulfonated phosphines as well as PTA.[11b] We have further measured the solubility of a variety of PTA and DAPTA complexes described

above by adding the respective compex into a fixed volume of distilled water followed by stirring until a supersaturated solution is formed..

Preliminary data suggest that the dialkyl and dialkynyl DAPTA complexes, **9a** and **14** were found to have slightly better water-solubility than their PTA analogues **1a** and **7**, respectively (Figure 2.1.9a).

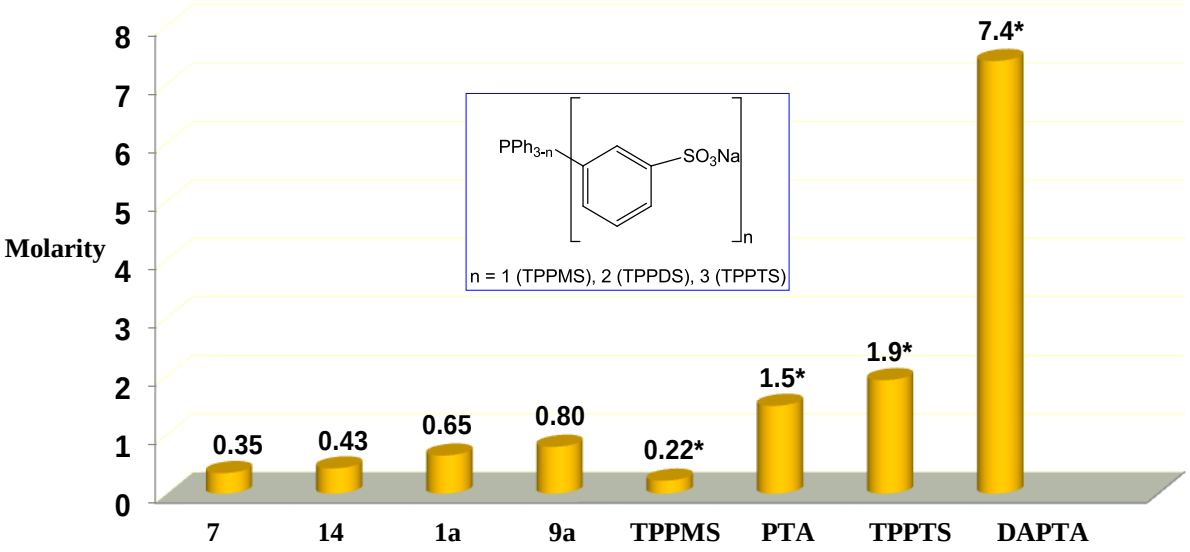

Figure 2.1.9a. Water-solubility of some phosphines and their complexes (*reported in the ref.[11b]).

However, this was not necessarily found to be consistent for all of the complexes. For instance, the PTA complexes, **2a**, **2b**, and **20** were found to more soluble in water than their DAPTA analogues, **10a**, **10b**, and **26**, respectively (Figure 2.1.9b).

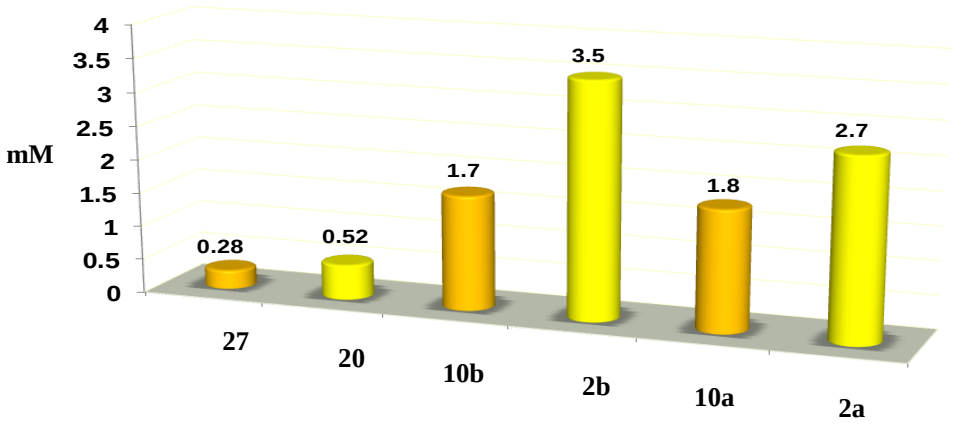

Figure 2.1.9b. Water-solubility of PTA and DAPTA complexes.

2.1.8 Synthesis and characterization of some additional PTA complexes

We were interested in adding to the library of water-soluble complexes containing the bidentate version of PTA ligands by synthesizing a tetramethyl bidentate-PTA complex, *cis,cis*-[$PtMe_2(\mu$-P, P$)_2PtMe_2$] Br_4 (**30**) by an overnight reaction of $PtMe_2$(COD) in dry dichloromethane with a dry methanol solution of 1,1'-[1,3-phenylenebis(methylene)]bis-3,5-diaza-1-azonia-7-phosphatricyclo[3.3.1.1]decane dibromide in a 1 : 1 molar ratio (Scheme 2.1.14). The dinuclear complex, **30** was obtained as a white solid in 54% yield.

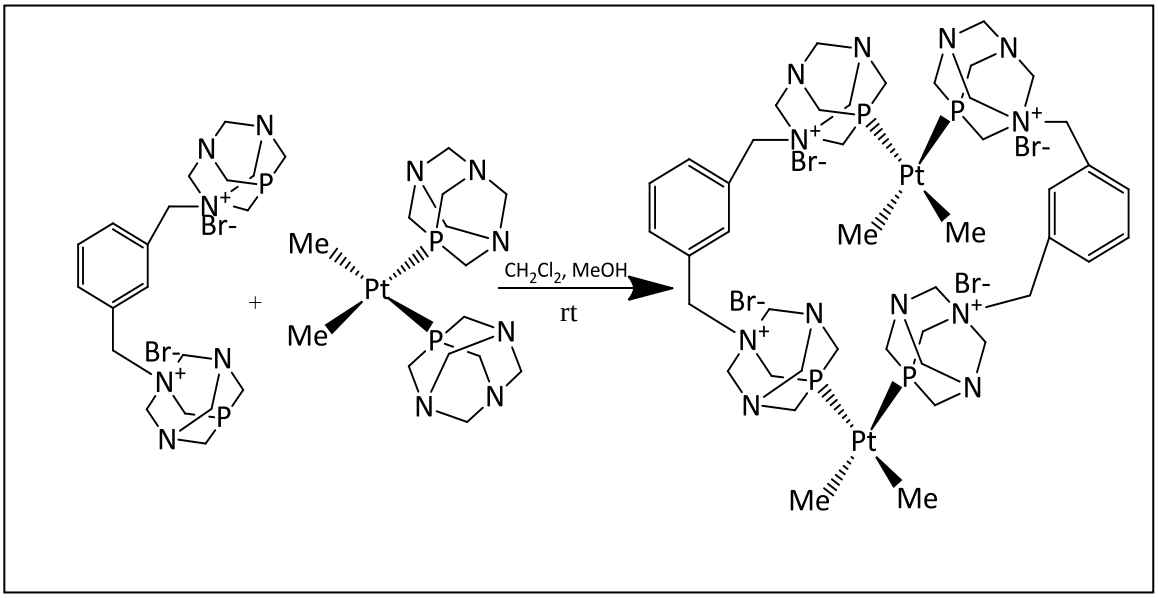

(**30**)

Scheme 2.1.14. Synthesis of *cis,cis*-[$PtMe_2(\mu$-P, P$)_2PtMe_2]Br_4$, **30**.

The $^{31}P\{^1H\}$NMR spectrum of **30** in D_2O exhibited a pair of doublets with ^{195}Pt satellites, observed at -35.9 ppm (d, $^1J_{PtP}$ = 1694 Hz, $^2J_{PP}$ = 9.5 Hz) and -38.0 ppm (d, $^1J_{PtP}$ = 1701 Hz, $^2J_{PP}$ = 9.3 Hz). The related dibromo-complex reported recently by Krogstad *et al.*, *cis,cis*-[$PtBr_2(\mu$-P, P$)_2PtBr_2]Br_4$ displayed a similar kind of pattern in the $^{31}P\{^1H\}$NMR spectrum ($^1J_{PtP}$ ~ 3500 Hz).[18] HPLC/MS analysis of **30** displayed a peak at *m/z* = 1011.9 corresponding to the mass of the fragment $[M - \{(P, P) + CH_3\}]^+$. The fact that the coupling constants in the $^{31}P\{^1H\}$ NMR spectrum were exactly the same implied that the R group of the phenyl backbone had little impact on the basicity of the (P, P) ligands. Based on the multiplicity of the phosphorus peaks, the phosphorus atoms seem to be inequivalent on the NMR time-scale and hence that the bridging scaffold was rigid upon coordination, as reported for the related dibromo-complex.[18] The ^1H NMR spectrum of **30** was highly complex making it difficult to assign the resonances.

In an attempt to synthesize **2c**, the incompletely dried PtI(Me)(COD) precursor on treating with 2 molar equivalents of PTA unexpectedly resulted in the formation of the oxidized product, *cis*- or *trans*-PtI(Me)$(OPTA)_2$ (**31**) as the only product. The MS analysis of the product enabled us to identify it as **31**. The ^1H NMR spectrum of **31** displayed two broad signals for the NCH_2N and PCH_2N protons as well as an upfield triplet due to the CH_3 protons with a coupling value of $^2J_{PtH}$ = 39 Hz, which is smaller than the $^2J_{PtH}$ for **2c** (79 Hz). The $^{31}P\{^1H\}$NMR spectrum showed a resonance at -12.2

ppm corresponding to the OPTA ligand but the J_{PtP} coupling constant could not be resolved. Therefore, the coordination mode of the phosphine in **31** is still ambiguous.

The synthesis and crystal structure for *trans*-$PdI_2(PTA)_2$ (**32**) has been reported in the literature.[19] However, to the best of our knowledge, no NMR characterization for **32** has yet been reported elsewhere. For the synthesis of **32** in an improved yield, we employed a modified literature procedure[20] and treated PdI_2(TMEDA) (TMEDA = tetramethylethylenediamine) with PTA in 1 : 2 molar ratio at 0 ^oC. Complex **32** was obtained as a yellow solid in 68% yield. The ^1H NMR spectrum showed two broad signals whereas a signal at -68.5 ppm was observed in the $^{31}P\{^1H\}$NMR spectrum. The HRMS analysis of **32** also provided confirmation of its identity.

2.1.9 Synthesis of ipac mPTA triflate

The coordination chemistry of many PTA-derivatized ligands remains relatively unexplored because their metal complexes are not strongly water-soluble.[13, 20] The synthesis of new water-soluble PTA-derivatized phosphines to serve as ligands for lower valence metal complexes rendering them water-soluble is required.[14, 20] In this regards, we have investigated the synthesis and characterization of a novel water-soluble PTA-derivatized ligand, *N*-methyl-3,5-diaza-1-azonia-7-phosphatricyclo[3.3.1.1]decane-7-(4-methylpentan-2-one) triflate (**L1**) which we also call as "ipac mPTA triflate" (ipac mPTA = isopropylacetonate *N*-methyl-1,3,5-triaza-7-phosphaadamantane).

The novel water-soluble phosphine, **L1** was synthesized by refluxing a mixture of PTA and methyl triflate (1 : 2 molar ratio) for 2 h in bulk acetone or an acetone/water mixture (~ 20 : 1, respectively). Compound **L1** was obtained as a white solid in 60% yield (Scheme 2.1.15). Although the same reaction in dry acetone led to the formation of

dmPTA triflate (dmPTA = *N,N'*-dimethylPTA) as reported by Mena-Cruz *et al.*, use of bulk acetone resulted in the formation of **L1**.[21]

Scheme 2.1.15. Synthesis of ipac mPTA triflate.

The ^{1}H NMR spectrum of **L1** in DMSO-d_6 showed the appearance of four doublets at 4.98 (J = 15.0 Hz), 3.17 (J = 21.0 Hz), 2.89 (J = 6.3 Hz), and 1.31 (J = 19.2 Hz) ppm which correspond to the NCH_2N, CH_2, NCH_3, and CH_3 hydrogen atoms, respectively. A broad signal corresponding to NCH_2NC protons appeared at 5.10 ppm whereas a multiplet corresponding to the PCH_2N protons was observed at ~ 4.70 ppm. The acyl protons exhibited a singlet at 2.23 ppm. The appearance of a doublet of doublets at 4.45 ppm (J = 45.0 Hz, 13.8 Hz) suggested that the PCH_2NC hydrogens are magnetically inequivalent.

The ^{13}C{^{1}H} NMR spectrum of **L1** showed the expected signals for all carbons including that of the triflate anion. The doublets at 53.8 (J_{CP} = 32.2 Hz), 45.0 (J_{CP} = 28.5 Hz), 42.2 (J_{CP} = 22.5 Hz), and 33.1 (J_{CP} = 22.5 Hz) ppm represent the PCH$_2$NC, PCH$_2$N, CH$_2$, and C carbons, respectively, in all of which ^{13}C-^{31}P couplings were observed. Furthermore, the ^{13}C-^{19}F coupling (J_{CF} = 315 Hz) was observed for the CF$_3$ carbon. The splitting pattern observed for **L1** in the ^{1}H and ^{13}C{^{1}H} NMR spectra were almost identical to that reported for dmPTA triflate.[22] A more downfield resonance was seen at -

14.0 ppm (compared to -81.7 ppm for dmPTA triflate)[22] in the $^{31}P\{^{1}H\}$ NMR spectrum of **L1** in DMSO-d_6.

X-ray quality crystals of **L1** were obtained by layering methanol over an acetone solution of **L1** below 0 ^{o}C. **L1** was crystallized in a P-1 space group in dicationic form along with two moles of the ($CF_3SO_3^-$) counter-anion (Figure 2.1.10). The geometry around the phosphorus center is nearly tetrahedral, however, it is somewhat distorted having smaller angles around the adamantane cage.

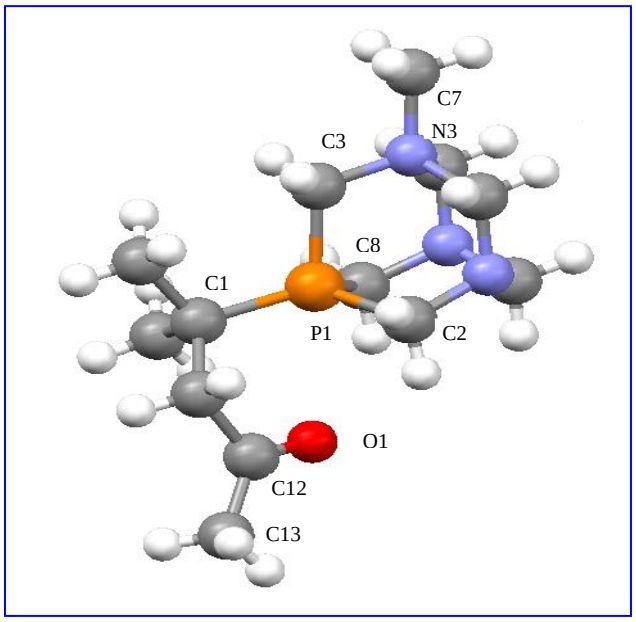

Figure 2.1.10. Crystal structure of ipac mPTA, **L1**, anion molecules are omitted for clarity (50% probability ellipsoids).

Selected bond lengths and bond angles are listed in Table 2.1.16. The average P(1)-C(8) bond length in **L1** is 1.849(3) Å which is close to the P-C bond length reported for dmPTA [1.840(5) Å].[22] The (C8-P1-C1), (C8-P1-C2), and (C8-P1-C3) bond angles are 117.8(1)^{o}, 122.5(1)^{o}, and 108.8(1)^{o}, respectively. The N(3)-C(5) and N(3)-C(6) bond lengths are identical which are 1.543(3) Å and 1.543(4) Å, respectively, whereas the

N(3)-C(3) and N-C_{methyl} [N(3)-C(7)] bond lengths are predicted to be 1.508(4) Å and 1.504(3) Å, respectively. As described in the previous works,[20-22] it appears that the (N)C-N bond lengths are the most affected upon alkylation of the PTA nitrogen atoms. The geometry about the methylated nitrogen is tetrahedral with all the (C-N3-C) angles falling between 107.5(2)°-110.4(2)°. The C(12)-C(13) bond is significantly shorter [1.493(4) Å] than the typical C-C single bond (~ 1.54 Å) which is possibly due to inductive effect and/or existence of the molecule partially in the 'enolic' form.

Table 2.1.16. Selected bond lengths and bond angles for **L1**.

P1-C8	C12-C13	C8-P1-C3	C8-P1-C2	C8-P1-C1	C7-N3-C5	N3-C5	N3-C7	N3-C3
1.849(3) Å	1.493(4) Å	108.8(1)°	122.5(1)°	117.8(1)°	109.5(2)°	1.543(3) Å	1.504(3) Å	1.508(4) Å

Although the mechanism for the formation of **L1** is not clear, it is anticipated that this is primarily due to hydrolysis of MeOTf (Scheme 2.1.16). Triflic acid formed during the

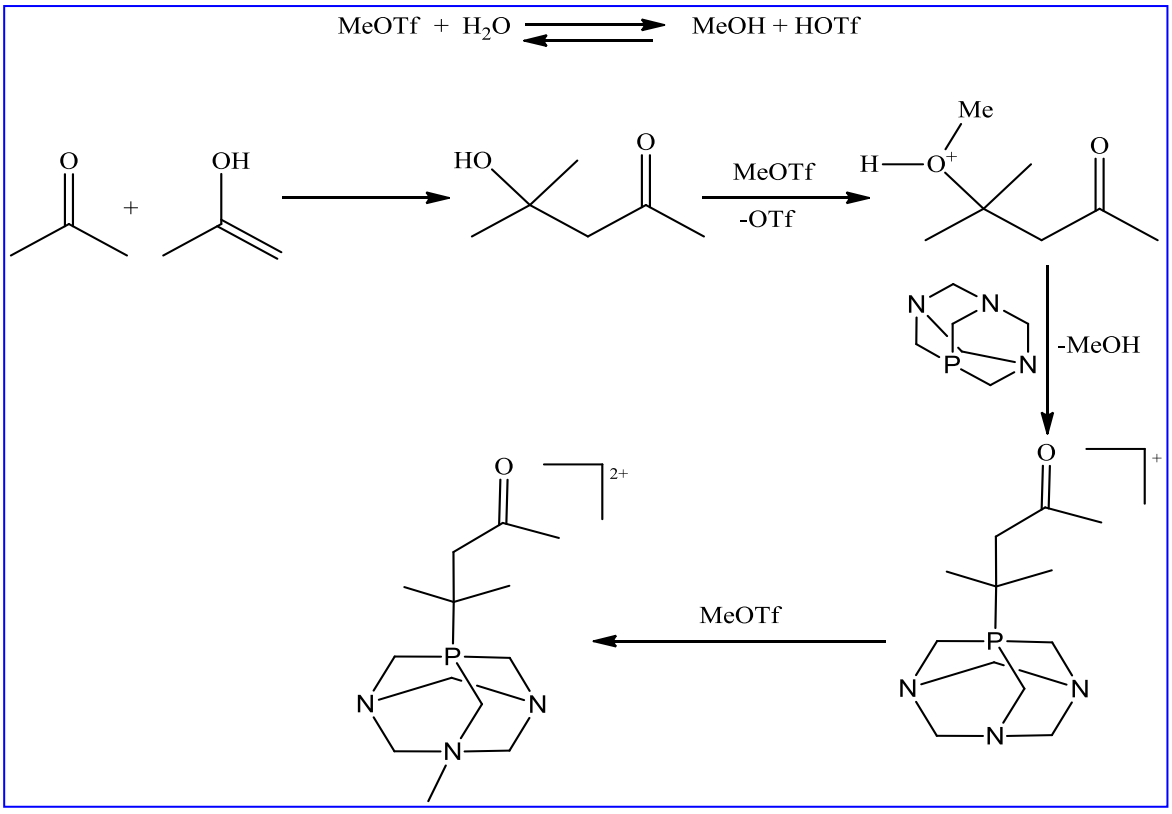

Scheme 2.1.16. Proposed mechanism for the formation of **L1**.

reaction promotes the formation of the 'enol' from acetone which then reacts with another molecule of acetone to give 4-hydroxy-4-methyl-pentan-2-one. The hydroxide substituent is then methylated from another molecule of MeOTf making it a good leaving group which is followed by nucleophilic attack by phosphorus. Finally, *N*-methylation takes place to yield **L1**.

2.2 Hydrosilylation Reactions Catalyzed by cis-$PtMe_2(PTA)_2$

The utilization of platinum or palladium complexes containing the PTA or DAPTA ligands for metal-mediated hydrosilylation reactions has not yet been fully investigated. We investigated the catalytic hydrosilylation reactions of different terminal alkenes and alkynes with a variety of tertiary hydrosilanes including siloles and silafluorenes utilizing the complex, *cis*-$PtMe_2(PTA)_2$ (**1a**) (Figure 2.2.1a) as a pre-catalyst. The catalytic activity of *cis*-$PtCl_2(PTA)_2$[2a] (**M2**) (Figure 2.2.1b) was also investigated, however, it was not found to be an effective catalyst in hydrosilylation reaction.

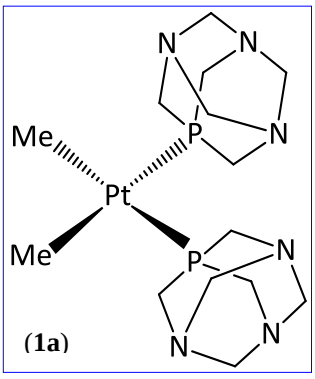

Figure 2.2.1a. Structure of (**1a**).

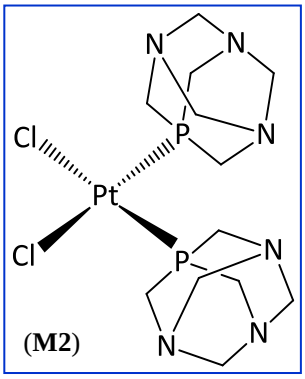

Figure 2.2.1b. Structure of (**M2**).

2.2.1 Hydrosilylation reaction of alkynes

Our research efforts began with the platinum catalyzed reaction of the tertiary hydrosilane, Ph_2MeSiH (**S1**) with a variety of terminal alkynes in a 1 : 1 molar ratio to examine the effect of steric and electronic factors on the selectivity of the products that were produced. In the presence of the pre-catalyst (**1a**), the reaction solutions were refluxed in *n*-hexane under an inert atmosphere of argon with 0.5 mole % catalyst loading with respect to **S1**. The reaction was monitored by GC periodically. Analysis of the entire product mixture was carried out by GC and ^{1}H NMR spectroscopy. The formation of the products was indicated by the disappearance of the Si-H proton resonance and appearance of vinylic protons in the ^{1}H NMR spectrum. The products were characterized by ^{1}H, ^{13}C{^{1}H}, and ^{29}Si{^{1}H} NMR spectroscopy and GC-MS after purification through a silica gel column. The key diagnostic vinylic (olefinic) resonances in the NMR spectra observed in the hydrosilylation and hydrogermylation reactions are indicated in the following sections below.

Due to the presence of two fairly sterically bulky phenyl groups at the silicon center in **S1** near the α-position, the β-product was selectively formed as the major isomer but generally two isomers were formed. The two isomers that were generated from the reaction mixture were found to be the *β-trans* isomer (major product) and the α-isomer (minor product) which are formed as a result of Markovnikov and anti-Markovnikov addition, respectively (Scheme 2.2.1). Formation of the *β-cis* isomer occurs because of *trans* addition of the hydrosilane to the metal center in the catalytic cycle[23] whereas the *β-trans* isomer is formed due to *cis* addition. The formation of the *β-cis* isomer was not observed in any of the reactions.

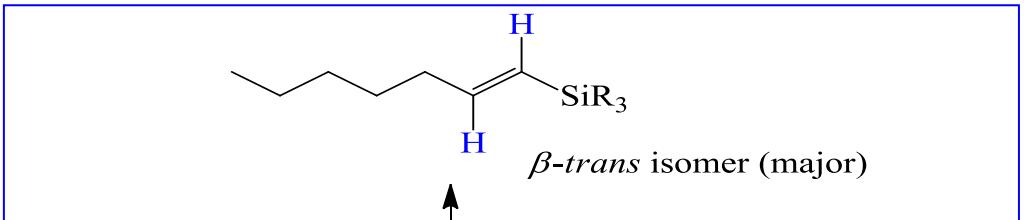

Whe

Scheme 2.2.1. Nature of the products formed in hydrosilylation reaction of a terminal alkyne with **S1** catalyzed by (**1a**).

product

spectral analysis of the product mixture **H1** after separation of the starting materials by Kugelrohr distillation and silica gel column chromatography showed two large resonances for the alkenyl protons at the chemical shifts of 6.40 ppm (doublet of triplets with $^{3}J_{HH}$ = 18.5 Hz and $^{4}J_{HH}$ = 6.0 Hz) and 6.18 ppm (doublet of triplets with $^{3}J_{HH}$ = 18.5 Hz and $^{4}J_{HH}$ = 1.0 Hz) corresponding to the *β-trans* isomer and a pair of multiplets (minor peaks) at 6.03 and 5.30 ppm corresponding to the *α*-isomer. However, these peaks did not appear to be in the first order pattern. The ratio of these products *β-trans : α* was found to be 87 : 13, respectively, as determined by integration of the ^{1}H NMR spectrum. This is consistent with the appearance of two resonances at -11.0 and -14.8 ppm in the ^{29}Si{^{1}H} NMR spectrum. The ^{13}C{^{1}H} (DEPT) NMR spectrum showed several minor peaks corresponding to the *α*-product.

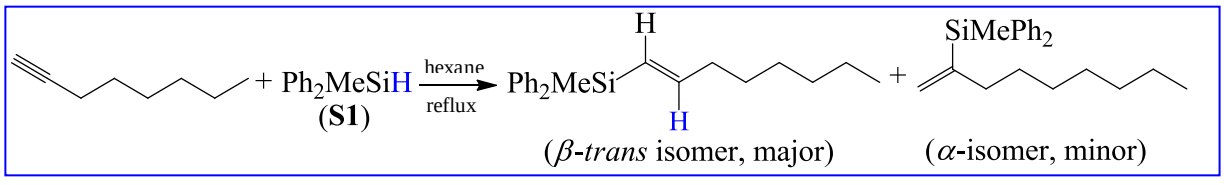

Scheme 2.2.2. Hydrosilylation reaction of 1-octyne with **S1** in the presence of **1a** to give **H1**.

Our results are consistent with that reported by Lewis *et al.* for the hydrosilylation reaction of 1-pentyne with **S1** in the presence of the Karstedt's catalyst (3 μL**,** 0.8 μmol of Pt)[24] except that the formation of *β-cis* isomer was not observed and the regioselectivity of the products was better in the majority of our reactions. The ^{1}H NMR spectrum of the product mixture as reported by Lewis *et al.* showed two large resonances at 6.16 ppm and 5.95 ppm (doublet of triplets with $^3J_{HH}$ = 18.5 Hz) for the *β-trans* isomer, with a smaller multiplet at 6.30 ppm for the *β-cis* isomer, and a pair of multiplets at 5.83 and 5.40 ppm for the *α*-isomer. The ratio of the products *β-trans : β-cis : α* was found to be 78 : 2 : 20, respectively, as determined by the integration of the ^{1}H NMR spectrum.[24]

In another Rh catalyzed reaction of Et_3SiH and 1-hexyne as reported by Ojima *et al.*, the ^{1}H NMR spectrum of the product mixture displayed two large resonances at 6.38 ppm (doublet of triplets with $^3J_{HH}$ = 14.1 Hz) and 5.38 ppm (doublet with $^3J_{HH}$ = 14.1 Hz) for the *β-cis* isomer, a smaller resonance at 6.03 ppm (doublet of triplets with $^3J_{HH}$ = 18.7 Hz) and 5.53 ppm (doublet with $^3J_{HH}$ = 18.7 Hz) for the *β-trans* isomer, and a pair of multiplets at 5.60 and 5.30 ppm for the *α*-isomer.[25] In all of the reported Pt or Rh catalyzed hydrosilylation reactions, the reported $^3J_{HH}$ value of the alkenyl protons for the *β-trans* isomer falls between 16.5 to 20 Hz whereas that for the *β-cis* isomer ranges from 8.5 to 14.5 Hz.[25, 26]

The hydrosilylation reaction of **S1** and 1-octyne was also investigated using a Pd catalyst, *cis*-$PdCl_2(PTA)_2$[2b] (**M1**), however, no reaction took place at all even at 6 mole% of catalyst loading. We have also investigated the hydrosilylation reaction of 1-octyne with **S1** using 0.5-3 mole% of *cis*-$PtCl_2(PTA)_2$[2a] (**M2**) (Figure 2.2.1b) as the catalyst

under the same reaction conditions with varying the solvents from *n*-hexane to toluene and THF; however the reaction was found to be too slow compared to the reaction using **1a**. This is probably due to lower solubility of **M2** in all of the solvents in comparison to that of **1a**.

A similar type of reaction of **S1** was carried out separately with two aromatic alkynes; phenylacetylene and 3-phenyl-1-propyne. The reaction of **S1** with phenylacetylene (Scheme 2.2.3a) was found to be relatively slow and resulted in 56% of combined NMR yields [turn over number (TON) = 112]. The ^{1}H NMR spectrum analysis of the product mixture **H3** after separation of **S1** by silica gel column chromatography showed two large resonances at 6.93 and 6.72 ppm (doublets with $^{3}J_{HH}$ = 19.1 Hz) for the *β-trans* isomer and a small pair of doublets at 6.11 and 5.55 ppm ($^{2}J_{HH}$ = 2.7 Hz) for the *α*-isomer. As detected by the ^{1}H NMR integration, the ratio of the products *β-trans : α* was found to be 88 : 12, respectively.

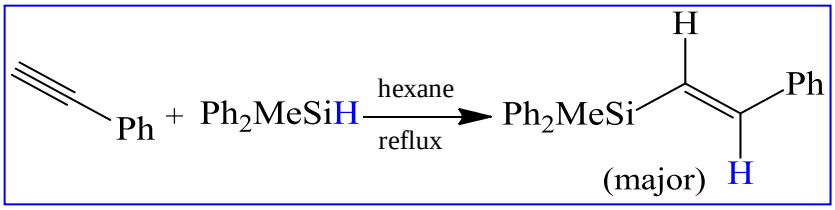

Scheme 2.2.3a. Hydrosilylation reaction of phenylacetylene with **S1** to give **H3**.

This regioselectivity is slightly better than the GC ratio described by Pannell *et al.* (*β-trans : β-cis : α* = 82 : traces: 18) for the same reaction carried out in toluene using Speier's catalyst.[27] A similar type of reaction was carried out by Lewis *et al.* between another tertiary hydrosilane, Ph_3SiH, and phenylacetylene in the presence of the Karstedt's catalyst.[24] The ^{1}H NMR analysis of the product mixture showed a large resonance at 6.98 ppm (doublet with $^{3}J_{HH}$ = 18.0 Hz) for the *β-trans* isomer, with a

smaller singlet at 7.16 ppm for the *β-cis* isomer, and a pair of doublets at 6.28 and 5.69 ppm ($^2J_{HH}$ = 2.0 Hz) for the *α*-isomer. As detected by GC, the ratio of the products *β-trans : β-cis : α* was found to be 78 : 15 : 7, respectively.

The comparison of the catalytic activity of **1a** with that of some of the traditional catalysts is given in Table 2.2.1.

Table 2.2.1. Comparison of the catalytic activity of **1a** and traditional catalysts in hydrosilylation reaction.

Catalyst	**Hydrosilane**	**Alkyne**	**Catalyst loading**	**Time (h)**	***β-trans* : *α* : *β-cis***	**Conditions**
(**1a**)	Ph_2MeSiH	1-heptyne phenylacetylene	0.5 mole%	16 34	89 : 11 : 0 88 : 12 : 0	reflux, hexane
Speier's catalyst [27]	Ph_2MeSiH	phenylacetylene	10^{-5} mole%	< 1	82 : 18 : traces	reflux, toluene
Karstedt catalyst[24]	Ph_2MeSiH	1-pentyne	0.04 mole%	1	78 : 20 : 2	rt , no solvent

The $^{13}C\{^1H\}$ NMR spectrum results for **H3** were found to be consistent with the ^1H NMR spectrum results. The $^{13}C\{^1H\}$(DEPT) NMR spectrum displayed the expected number of major peaks for CH_2, CH, and CH_3 carbons for the *β-trans* product. A resonance was observed at -15.3 ppm corresponding to the *β-trans* isomer and at -10.8 ppm for the *α*- isomer were observed in the $^{29}Si\{^1H\}$ NMR spectrum.

The reaction of **S1** was carried out with another terminal alkyne, 3-phenyl-1-propyne, which shows different steric behavior compared to phenylacetylene, to give **H4**. The reaction with 3-phenyl-1-propyne (Scheme 2.2.3b) was also found to be slower (95% conversion in 25 h, TON = 130) compared to the reaction shown in Scheme 2.2.2. The

product ratio (*β-trans* : *α*) was found to be 86 : 14, respectively, as determined by the integration of the ^{1}H NMR spectrum.

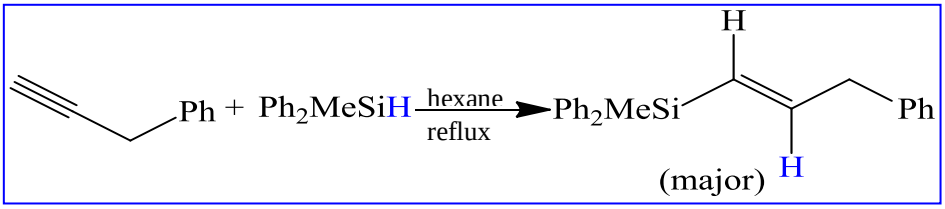

Scheme 2.2.3b. Hydrosilylation reaction of 3-phenyl-1-propyne with **S1** to give **H4**.

The ^{1}H Cl_3 exhibited two sets of doublet of triplets at 6.40 ppm (J = 18.4 Hz, 6.2 Hz) and 6.12 ppm (J = 18.4 Hz, 1.4 Hz) which corresponded to the *β-trans* product. A pair of minor broad doublets were also observed at ~ 5.55 and 5.39 ppm ($^{2}J_{HH}$ = 1.3 Hz), which corresponded to the *α*-product. The ^{13}C{^{1}H} and ^{29}Si{^{1}H} NMR results were consistent with this, the latter spectrum showing two signals at -11.2 and -15.3 ppm. A ^{1}H-^{1}H COSY NMR experiment also confirmed the coupling of the two olefinic hydrogens with each other as well as that of one of the olefinic hydrogens with the =CCH_2 hydrogen. Moreover, it also showed the coupling of the olefinic hydrogen with the =CH_2 hydrogens of the *α*-product. HRMS analysis of **H4** also confirmed the formation of the desired product. When the secondary hydrosilane PhMeSiH_2 was utilized in the hydrosilylation reactions with 1-octyne and phenylacetylene in the presence of **1a**, multiple isomers were formed and these were difficult to separate. This is obvious for the reactions with such kinds of hydrosilanes as well as primary hydrosilanes because of the presence of a greater number of potential reacting Si-H units.

The reaction of **S1** was performed with a dialkyne molecule, 1,7-octadiyne by employing the reacting substances in 2 : 1 molar ratio, respectively (Scheme 2.2.4). As

expected, the reactants converted into a disilylated product and a mixture of disilylated *β-trans* isomer and *α*-isomer (**H5**) was obtained in 71% of combined yield after purification by silica gel column chromatography.

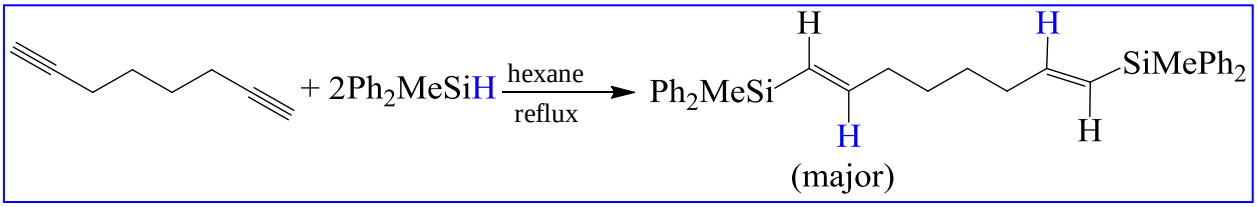

Scheme 2.2.4. Hydrosilylation reaction of 1,7-octadiyne with **S1** in the presence of (**1a**) to give **H5**.

found to be 87 : 13, respectively as determined by the ^{1}H NMR spectrum integration. The *m/z* value in the MS (FAB) spectrum was also consistent with the disilylated product displaying a $(M+2H)^{+}$ peak at *m/z* = 505. The ^{1}H NMR spectrum exhibited a pair of doublet of triplets at 6.27 ppm (*J* = 18.6 Hz, 6.0 Hz) and 6.07 ppm (*J* = 18.6 Hz, 1.3 Hz), each integrating to two protons (*β-trans* product) and two sets of broad multiplets as the minor peaks at 5.77 and 5.31 ppm (*α*-product). Two peaks were seen at -11.5 and -15.3 ppm in the ^{29}Si{^{1}H} NMR spectrum for the two isomers. The ^{13}C{^{1}H} NMR spectral data for **H5** were consistent with the ^{1}H and ^{29}Si{^{1}H} NMR spectral data.

In further understanding the role of the groups bonded to the silicon atom in the catalytic hydrosilylation reaction, the hydrosilylation reactions of a terminal alkyne, 1-heptyne (**A1**), with a variety of sterically hindered tertiary hydrosilanes in the presence of 0.5 mole% of **1a** as a pre-catalyst were carried out (Figure 2.2.2).

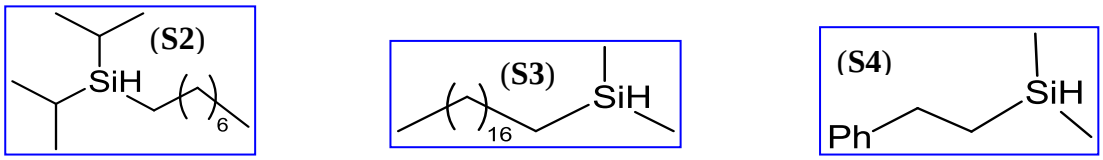

Figure 2.2.2. Some sterically hindered hydrosilanes.

When the sterically hindered hydrosilanes **S2**, **S3**, and **S4** as were used, the silicon unit of the hydrosilane (R_3Si) could not easily approach the second (secondary) carbon atom of the substrate and consequently the *β-trans* isomer was formed selectively. As expected, the *β-trans* : *α* ratio was found to be better in these reactions. To the best of our knowledge, hydrosilylation reactions using these hydrosilanes have not been explored before. All of these reactions were performed in refluxing *n*-hexane and monitored periodically by GC-MS.

An overnight reaction of **A1** with diisopropyloctylsilane (**S2**) resulted in 88% conversion of **S2**. The *β-trans* : *α* ratio in the crude product mixture as detected by the ^{1}H NMR integration was found to be 93 : 7, respectively, whereas after column chromatography, the *β-trans* isomer was obtained as the only product, [1-diisopropyloctylsilyl-1-heptene, **H7**), in a 77% isolated yield. The appearance of a pair of doublet of triplets at the chemical shifts of 5.95 ppm (olefinic proton, J_{HH} = 18.7 Hz, 6.3 Hz) and 5.41 ppm (olefinic proton, J_{HH} = 18.7 Hz, 1.4 Hz), and a multiplet at 2.08-1.96 ppm (=CC*H*$_2$ protons) in the ^{1}H NMR spectrum is consistent with the *β-trans* isomer. No resonances were observed for the *α*-isomer. A set of ^{29}Si satellites were observed due to ^{29}Si-^{1}H$_{olefinic}$ coupling with $^2J_{SiH}$ = 114 Hz for the *β-trans* isomer. The ^{29}Si{^{1}H} NMR (singlet at -1.5 ppm) and the ^{13}C{^{1}H} NMR spectra also support the formation of the single isomer, **H7**. The ^{29}Si-^{13}C coupling could also be detected in the ^{13}C{^{1}H} NMR spectrum for the carbon bonded to the silicon center.

An overnight reaction of **A1** with dimethyloctadecylsilane (**S3**) resulted in 85% combined NMR yield based on **S3**. The product mixture, **H8** after purification through silica gel column chromatography using hexane/dichloromethane as the eluent (1 : 1)

contains both *β-trans* and *α*-isomers in 97 : 3 ratio, respectively, with an improved regioselectivity. The $^{29}Si\{^{1}H\}$ NMR spectrum displayed two peaks at the chemical shifts -3.8 and -7.0 ppm, consistent with the presence of two isomers in **H8**. As compared to **H7**, the silylated product mixture **H8** showed a pair of doublet of triplets for the olefinic hydrogens with $^{3}J_{HH}$ = 18.5 Hz in the ^{1}H NMR spectrum. Additionally, a virtual doublet corresponding to the *α*-product was seen as a minor peak at 5.31 ppm (multiplet) with a coupling value of $^{2}J_{HH}$ = 3.0 Hz.

In a similar way, an overnight reaction of **A1** with dimethylphenethylsilane (**S4**) resulted in a 67% combined NMR yield of the purified hydrosilylated product, **H9** (Scheme 2.2.5). The *β-trans* : *α* product ratio was 14 : 1, respectively, as determined by the ^{1}H NMR spectrum integration. Similar to **S2** and **S3**, the reaction was found to have very good selectivity.

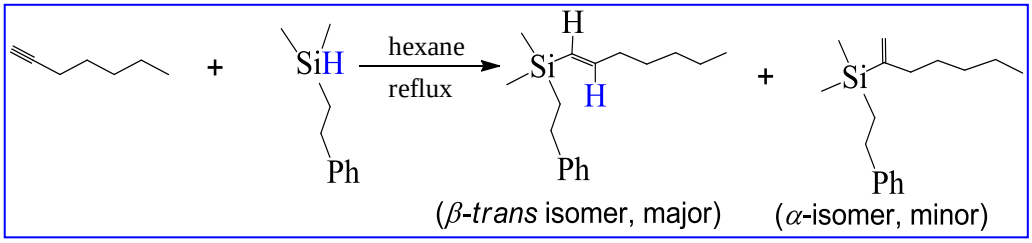

Scheme 2.2.5. Hydrosilylation reaction of 1-heptyne (**A1**) with **S4** in the presence of **1a** to give **H9**.

The ^{1}H NMR splitting pattern and chemical shifts for the olefinic protons of **H9** are similar to that of **H7** or **H8** with $^{3}J_{HH}$ = 18.5 Hz. The presence of two isomers in **H9** was again evident from the appearance of two signals at -3.5 and -6.6 ppm in the $^{29}Si\{^{1}H\}$ NMR spectrum. In addition to this, some minor resonances corresponding to the *α*-isomer, that is, a multiplet at 5.83 ppm (overlapping with the olefinic hydrogens' signals

of the *β-trans* isomer) and a virtual doublet at 5.57 ppm ($^2J_{HH}$ = 1.5 Hz) were also observed in the ^{1}H NMR spectrum.

The reaction of tris(phenylethynyl)silane [HSi(C≡CPh)$_3$, **S5**)] with **A1** resulted in the hydrosilylated product, **H10** which was obtained as a colorless solid in 55% yield (TON = 110). The products were formed in approximately 2 : 1 ratio (*β-trans* : *α*, respectively) with relatively poor regioselectivity. This can be attributed to the presence of the *sp*-hybridized linear ethynyl group bound to the Si center that results in **S5** being less sterically hindered. For this reason, the Si atom may approach to the second carbon atom of **A1** more easily to form the *α*-product. The appearance of two doublet of triplets at the chemical shift of 6.77 ppm (=C*H* proton, *J* = 18.2 Hz, 6.2 Hz) and 5.81 ppm (=C*H* proton, *J* = 18.3 Hz, 1.5 Hz), and a quartet at 2.30 ppm (=CCH_2 protons, *J* = 7.2 Hz) in the ^{1}H NMR spectrum of **H10** is consistent with the *β-trans* isomer. The resonances at 6.08 (br m, =C*H*), 5.93 (br m, =CH_2), and 2.51 (t, J_{HH} = 7.5 Hz, =CCH_2) correspond to the *α*-product. Interestingly, the =CH_2 signals appeared more downfield than one of the =C*H* signals. Unexpectedly, the ^{29}Si{^{1}H} NMR (DEPT) spectrum showed only one signal at -70.0 ppm. Another signal was observed as a virtual phase-down peak at -72.2 ppm.

In all of the hydrosilylation reactions of alkynes described above, the olefinic carbon nearest to the silicon gave a downfield resonance in the ^{13}C{^{1}H} NMR spectra, in contrast to the olefinic proton nearest to the silicon in the ^{1}H NMR spectrum. This is consistent with the results described for products obtained from similar hydrosilylation reactions.[25-27]

2.2.2 Hydrosilylation reactions of alkenes

The hydrosilylation reaction of 1-hexene was carried out overnight under the same conditions with 98% of **S1** converted into the products. Extending the reaction time did not significantly change the reactant to product ratio. Several peaks corresponding to unassigned products as well as the hydrosilylated addition product were observed upon GC analysis of the product mixture. The hydrosilylated product (**H2**) which was isolated as a colorless oil (62% yield) after column chromatography on silica gel using *n*-hexane as the eluent contained mainly the *β*-isomer, [$H_3C(CH_2)_4CH_2SiMePh_2$] with traces of the *α*-isomer [2-(methyldiphenylsilyl)hexane]. The $^{29}Si\{^1H\}$ NMR spectrum in $CDCl_3$ showed only one resonance at -7.1 ppm for the *β*-isomer. The regioselectivity of the products was consistent with that in the related $Pt(PPh_3)_2[\eta^2\text{-}(H_2C{=}CH_2)]$ catalyzed hydrosilylation reaction of alkenes using a variety of tertiary hydrosilanes.[28a] The hydrosilylation reaction of 1-hexene using $PhMe_2SiH$ catalyzed by another platinum(II) phosphine complex, *cis*-$PtCl_2(PhCH{=}CH_2)_2$ (*ca.* 0.05 mole%) resulted in the *β*-isomer as the major product with *ca.* 4% of the isomerized product 2-hexene.[28b]

The reaction of **S1** with 1,9-decadiene was relatively sluggish and found to undergo only 45% conversion with respect to **S1**. Although **S1** and the alkyne were employed in 2 : 1 molar ratio, unlike **H5**, formation of a monosilylated product took place which was found to be consistent with the appearance of the "=*C*H_2 and =*C*H" carbon peaks in the $^{13}C\{^1H\}$ NMR spectrum. However, GC-MS analysis showed the molecular ion peak with a very weak intensity. After purification through silica gel column, the *β*-product (**H6**) was only obtained which was confirmed by the appearance of a single resonance at -7.1 ppm in the $^{29}Si\{^1H\}$ NMR spectrum. The ^1H NMR spectrum of **H6** was found to be more complicated.

It has been reported previously that *cis-trans* isomerization of the hydrosilanes occurs on prolonged reaction times and such isomerization can be reduced by the addition of free alkenes or alkynes to the system.[29] No such isomerization occurred in our systems when the reactions were run for the extended period of time. Furthermore, the addition of PTA or copper salts such as CuI and $CuSO_4$ to the reaction mixture also did not alter the nature and regioselectivity of the products. The hydrosilylation activity of variety of tertiary hydrosilanes with different alkenes or alkynes in the presence of **1a** is summarized in Table 2.2.2. The results have shown a very good regioselectivity of the hydrosilylated products, especially when a sterically hindered hydrosilane was used.

Table 2.2.2. Results from the hydrosilylation reactions of alkynes with different hydrosilanes in the presence of **1a**. [a]Monitored by GC, conversion with respect to the silane. Combined NMR yields ([b]isolated yield of the major product), 0.5 mole% of (**1a**), refluxed. **S6** = 1-hydrido-1,2,5-triphenylsilole.

Entry	Hydrosilane	Alkene/Alkyne	Time (h)	% Conversion[a]	% Yield	*β-trans* : *α*
1	**S1**	1-octyne	16	96	85	87 : 13
2	**S1**	phenylacetylene	34	96	56	88 : 12
3	**S1**	3-phenyl-1-propyne	25	95	65	86 : 14
4	**S2**	1-heptyne	16	88	77[b]	93 : 7
5	**S3**	1-heptyne	16	91	85	97 : 3
6	**S4**	1-heptyne	16	86	67	96 : 4
7	**S1**	1,7-octadiyne	26	85	71	87 : 13
8	**S6**	1-heptyne	26	91	61	84 : 16
9	**S1**	1-hexene	26	98	62[b]	*β*-only
10	**S5**	1-heptyne	18	84	55	67 : 33

2.2.3 Comparison of catalytic activity of 1a with the other phosphines of platinum

Chelating bisphosphine complexes are less widely used in catalytic reactions.[30] We investigated the hydrosilylation reaction of 1-heptyne (**A1**) with Ph_2MeSiH (**S1**) in the presence of a variety of mono-, di-, and trinuclear bidentate phosphines of platinum such as $Pt_2(\mu\text{-dppm})_3$ (**B1**),[31a] $Pt_3(nbe)_2(dppa)_4$ (**B2**), $PtMe_2(dppp)$ (**B3**),[31b] and $PtMe_2(dppe)$ (**B4**)[31b, c] as pre-catalysts (Figure 2.2.3). To the best of our knowledge, hydrosilylation reactions utilizing **B1** and **B2** as pre-catalysts have not been investigated yet.

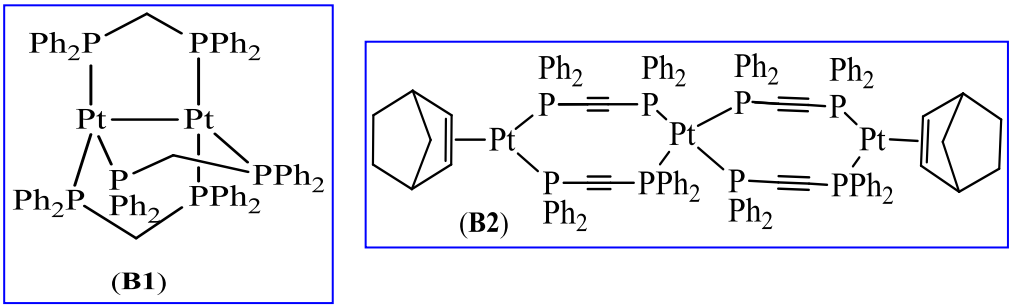

Figure 2.2.3. Some polynuclear chelating phosphines.

The reactions were run at the similar conditions, that is, in refluxed *n*-hexane overnight in the presence of 0.5 mole% of the catalyst. The reaction was monitored periodically by GC and the products after purification by column chromatography were analyzed by ^{1}H, $^{13}C\{^{1}H\}$, $^{13}C\{^{1}H\}$ DEPT, and $^{29}Si\{^{1}H\}$ NMR spectroscopy and GC-MS. The regioselectivity and the yield of the products in the hydrosilylation reaction of **A1** and **S1** using **1a** as a pre-catalyst (Scheme 2.2.1) were comparable to that when the chelating bisphosphine complexes were used as pre-catalysts (Table 2.2.3).

Table 2.2.3. Comparison of catalytic activity of (**1a**) and some chelating phosphines of Pt in the hydrosilylation reaction of Ph_2MeSiH, **S1** and 1-heptyne, **A1**. Catalyst loading = 0.5 mole%; refluxed (hexane); conversion and yields are based on the silane.

Catalyst	**time, h**	**% Conversion (GC)**	**Combined NMR yield (%)**	**Ratio of products (*β-trans* : *α*)**

B1	16	95	75	89 : 11
B2	16	95	74	90 : 10
B3	16	90	72	87 : 13
B4	16	95	84	90 : 10
1a	16	100	85	89 : 11

As expected, the colorless oily product mixture, **H11** obtained in these reactions consists of two isomeric products *viz. β-trans* and *α*-products. The regioselectivity of these products in **H11** involving **B1** and **B2** was found to be 89 : 11 and 90 : 10, respectively, whereas that involving **B3** and **B4** was detected to be 87 : 13 and 90 : 10, respectively. Under similar circumstances, the regioselectivity of the products on using **1a** was found to be 89 : 11, respectively. The combined NMR yield of **H11**was determined to be the highest (84%) when **B4** was used as a pre-catalyst which is comparable to that with **1a**. The ^{1}H NMR spectrum of **H11** obtained from each of these reactions showed a pair of broad multiplet as a minor peak at 5-6 ppm, which suggests the existence of *α*-isomer as a minor product in **H11**.

These results suggest that these chelated phosphine complexes can also act as effective catalysts in hydrosilylation reactions. One of the possible reasons for the catalytic activity of the complexes such as **B1** and **B2** is their larger bite angles (> 120^{o})[31a] which eventually facilitate the oxidative-addition, a key step in the catalytic cycle. Larger bite angles promote the electron donation from **A1** to platinum, which would result in an accumulation of electron density on the metal center.[31] This increases

the availability of the electron density on the metal for π-back donation into the antibonding orbitals of other ligands, which could potentially weaken other bonds within the catalytic complex, leading to faster reactivity.[31] However, the steric characteristics of the diphosphine ligand and the structure of the metal phosphine complex do not appear to be the leading factor for the regioselectivity of the products in our study. For example, **B4** has displayed relatively better catalytic activity in spite of its relatively smaller bite angle (95^{o}).[31b, c] This can be explained in light of reaction kinetics. Due to hemi-labile nature of dppe ligand in the complex, it provides a potential site for the reversible binding of analytes to a transition metal center because of their dynamic chelating ability.[31]

2.2.4 Hydrosilylation reaction of terminal alkynes using siloles and silafluorenes

To find whether the unsaturated systems can undergo hydrosilylation using hindered siloles or silafluorenes, we have performed the reaction of 1-heptyne with 1-hydrido-1,2,5-triphenylsilole (**S6**), 1-hydrido-1-methyltetraphenylsilole (**S7**), and 1-hydrido-1-methylsilafluorene (**S8**) with 1-heptyne (**A1**), trimethylsilylacetylene (hindered system, **A2**), and 1,4-diethynylbenzene (with the less hindered ethynyl group, **A3**), respectively, in the presence of **1a**. While Trogler *et al.* have reported the hydrosilylation reactions of **S7** and **S8** with some alkynes using Speier's catalyst,[32] we have investigated the hydrosilylation reactions of **S7** and **S8** with the same alkynes using the water-soluble platinum(II) phosphine complex, **1a**.

The hydrosilylation reaction activity of **S6** has not been reported elsewhere. The reaction of **S6** with **A1** was carried out in refluxing benzene under argon with 0.5 mole% of **1a** (Scheme 2.2.6). The reaction with **S6** was found to be relatively slow compared to

S1 which could probably be due to the bulkiness around the Si-H bond. The reation resulted in the formation of a yellow solid (**H12**) after 26 h in 61% of combined yield as the *β- trans* and *α*-products; the ratio of which was detected to be 84 : 16, respectively, by the ^{1}H NMR spectrum integration. The appearance of two signals in the ^{29}Si{^{1}H} NMR spectrum at -10.0, -12.2 ppm also support the fact that **H12** is a mixture of two isomers. The coupling constants with respect to the major alkenyl signals at 6.38 ppm (doublet of triplets, $^{3}J_{HH}$= 18.5 Hz, 6.2 Hz, 1H) and 6.07 ppm (m, 1H) resemble that of the *β-trans* products.

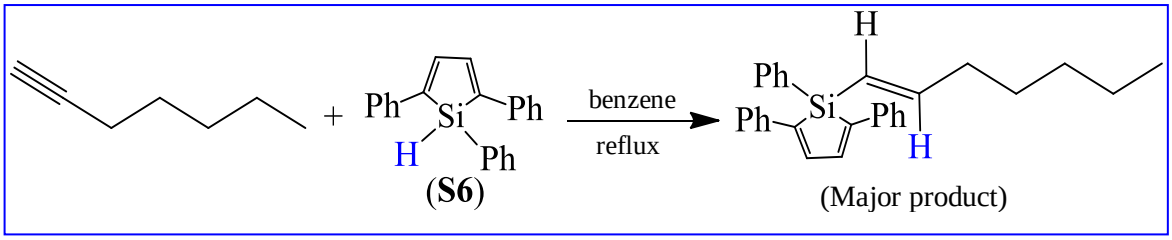

Scheme 2.2.6. Hydrosilylation reaction of 1-heptyne (**A1**) with the silole **S6** in the presence of (**1a**) to give **H12**.

The silafluorene moiety has a sterically less demanding environment at silicon, therefore, upon oxidative-addition to the platinum center, the 1,2-insertion of the Si-H bond across the coordinated dialkyne triple bond reduces the steric constraints. For this reason, a lower temperature is required in the reaction with **S8** to obtain the kinetically favored *trans*-product.[32] Therefore, the reaction of **S7** was performed in refluxing toluene under argon while the reaction with **S8** was carried out in toluene at room temperature (Scheme 2.2.7a-b).

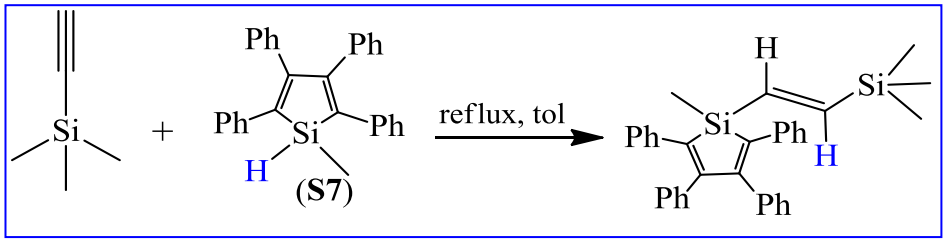

Scheme 2.2.7a. Hydrosilylation reaction of trimethylsillacetylene (**A2**) with 1-hydrido-1-methyl(tetraphenyl)silole (**S7**) catalyzed by (**1a**) to give **H13**.

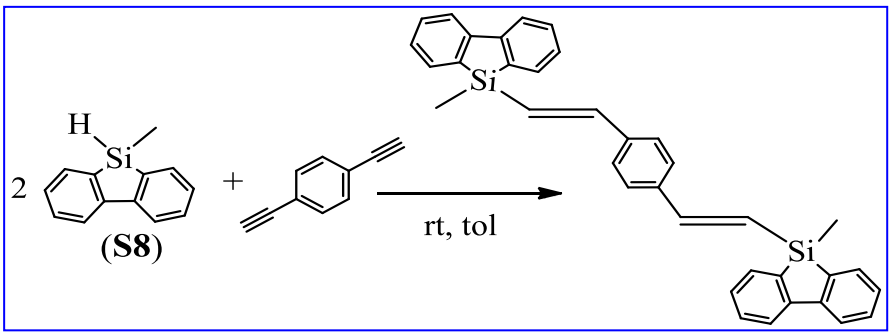

Scheme 2.2.7b. Hydrosilylation reaction of 1,4-diethynylbenzene (**A3**) with 1-hydrido-1-methylsilafluorene (**S8**) catalyzed by (**1a**) to give **H14**.

T
mole
loading. With **S7**, the hindered alkyne system prevented poly-addition resulting in the formation of the *β-trans* isomer as confirmed by ^{1}H NMR spectroscopy (Scheme 2.2.7a). The reaction of **S7** and **A2** was performed in 1 : 1 molar ratio for 24 h. After purification through a silica gel column followed by reprecipitation with a minimal amount of THF, the (*β-trans*)-only product (**H13**) was obtained as a yellow powder in 50% yield. GC-MS data were consistent with the formation of the desired hydrosilylated product.

The signals for the olefinic protons overlapped with those for the ring hydrogens in the ^{1}H NMR spectrum of **H13**. Two single resonances at 0.40 and 0.07 ppm were observed which correspond to silole-methyl and alkyne-methyl protons, respectively. Trogler *et al.* have reported the appearance of the silole-methyl proton signal at 0.55 ppm.[32] The crude mixture of **H13** with the *α*-product, however, showed two signals for the silole-methyl protons at 0.60 (*α*-product) and 0.37 ppm (*β-trans* product) in *ca.* 1 : 2 ratio, respectively. The $^{3}J_{HH}$ coupling constant value was observed to be 18.9 Hz which is consistent with the *β-trans* isomer. However, the $^{3}J_{HH}$ coupling for the minor product (*α*-isomer) could not be resolved. The ^{29}Si{^{1}H} (DEPT) NMR spectrum of **H13** showed

two resonances at -1.0 and -7.4 ppm, consistent with the presence of two different chemically inequivalent silicon atoms. The fluorescence measurements of **H13** showed the emission and excitation peaks at 416 and 345 nm, respectively.

The reaction of **A3** with **S8** was first carried out in a 1 : 2 molar ratio, respectively, in refluxing toluene with a lower catalyst loading (1 mole%) (Scheme 2.2.7b), however it was difficult to resolve the multiple isomers formed during this reaction. Upon heating the reaction mixture, a number of isomers were formed including *β-cis* (doublet for alkenyl protons at 6.39 ppm, $^{3}J_{HH}$ = 12.1 Hz), *gem* or *α* (two doublets at 6.03 and 5.83 ppm, $^{2}J_{HH}$ = 1.2 Hz), and *β-trans* vinyl (two doublets at 7.05 and 6.50 ppm, $^{3}J_{HH}$ = 18.8 Hz) isomeric products, which was similar as reported by Trogler *et al.* for the same reaction in the presence of 0.5 mole% of Speier's catalyst,[32] as well as some other signals corresponding to unidentified products were also observed. However, by stirring the starting materials in the same molar ratio at room temperature for 20 h (Scheme 2.2.7) followed by reprecipitation with THF, a mixture of two disilylated isomers, **H14**, was obtained as an off-white powder (52% yield). The ratio of the *β-trans* : *α* isomers in **H14**, as determined by the ^{1}H NMR integration after purification through silica gel column chromatography, was found to be 87 : 13, respectively. The ^{1}H NMR spectrum of **H14** in $CDCl_3$ showed a pair of doublets at 7.06 ppm ($^{3}J_{HH}$ = 18.9 Hz, 2H) and 6.50 ppm ($^{3}J_{HH}$ = 18.9 Hz, 2H), corresponding to the *β-trans* product. In addition to this, two minor broad peaks were observed at 6.02 and 5.79 ppm corresponding to the *α*-product. Moreover, two signals corresponding to the Si-C*H*$_3$ protons, which also integrated in the same ratio (87 : 13), were observed at ~ 0.6 ppm (major) and ~ 0.4 ppm (minor); consistent with the presence of the two isomers in **H14**. The ^{29}Si{^{1}H} and ^{13}C{^{1}H} NMR spectral results are

consistent with the ^{1}H NMR spectral results displaying two resonances at -4.9 and -12.9 ppm in the former while displaying a required number of signals for the =*C*H and *C*H_3 carbons in the latter.

In a similar way, 1 : 1 reactions of the 1,1-dihydrido(tetraphenyl)germole (**S9**) with the same terminal dialkyne, **A3**, were carried out in the presence of 1-4 mole% of **1a** which did not show the disappearance of the Ge-H signal in the ^{1}H NMR spectrum even after prolonged reaction time. When the reaction mixture was refluxed in toluene for 24 h with 0.25 mole % of chloroplatinic acid or 6 mole% of **1a**, a polymeric substance, **H15** formed (Scheme 2.2.8) with an acetylinic end group and the presence of the =CH group, as identified by IR spectroscopy (ν = 2251 cm^{-1}). The product was reprecipitated with a minimal amount of THF to remove low molecular weight oligomers.

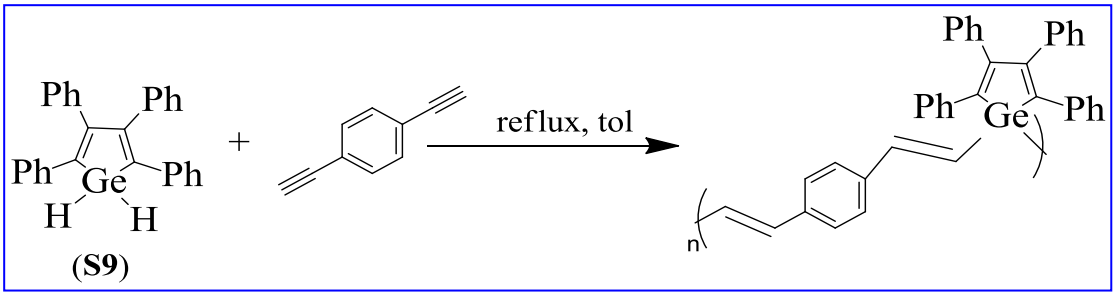

Scheme 2.2.8. Hydrogermylation reaction of 1,4-diethynylbenzene with 1,1-dihydrido(tetraphenyl)germole (**S9**) to give **H15**.

A broad resonance was seen in the aromatic region in the ^{1}H NMR spectrum of **H15**. The NMR and IR spectroscopy results are consistent with that of the previously reported hydrosilylated oligomeric product of **A3** obtained with the silicon analogue, 1,1-dihydrido(tetraphenyl)silole in the presence of some traditional catalysts such as chloroplatinic acid (0.2 mole%), Wilkinson's catalyst (2 mole%), Karstedt's catalyst (1 mole%), or $Pd(PPh_3)_4$ (1 mole%). However, the end group in the poly(silafluorene-

phenylenedivinylene) obtained by the reaction of 1,1-dihydridosilafluorene and **A3** was a terminal Si-H and not a C≡CH group, as detected by IR spectroscopy.[32] Fluorescence excitation and emission wavelengths for **H15** were recorded to be 358 and 420 nm, respectively, which are comparable to that of **H13**. Such kinds of poly- or disilylated products obtained by hydrosilylation/hydrogermylation reactions of siloles and silafluorenes and their germanium analogues have the potential applications as sensors for nitroaromatic explosives which take advantage of σ^*-π^* conjugation between the σ^* orbital on the silicon and germanium centers of the polymer backbone and the π^* molecular orbital of the metallole moiety, HOMO-LUMO energy match of silylated/germylated products and analytes, respectively, and the Lewis acidity on the silicon center that can interact with lone pairs on oxygen or nitrogen of the nitroaromatic explosive analyte.[32]

2.2.5 Attempted hydrosilylation reactions of ketones

Hydrosilylation reactions of a carbon-heteroatom unsaturated system have been of great interest over recent decades.[33] A hydrosilylation reaction of such a system with siloles or silafluorenes has not been reported yet. We have attempted to carry out hydrosilylation reactions of several compounds with C=O bonds which include acetophenone, 1-phenyl-1,2-propanedione, and 2,4-pentanedione using **S8**. The reactions were found to be very slow in the presence of **1a** as a pre-catalyst, therefore Speier's catalyst and Wilkinson's catalyst were used due to their known efficiency for catalyzing hydrosilylation reactions. The hydrosilylation reaction of 2,4-pentanedione and **S8** was performed in refluxing toluene under argon with 1 mole% of Speier's catalyst or 2 mole % of Wilkinson's catalyst (Scheme 2.2.9) and the reaction was monitored by GC-MS.

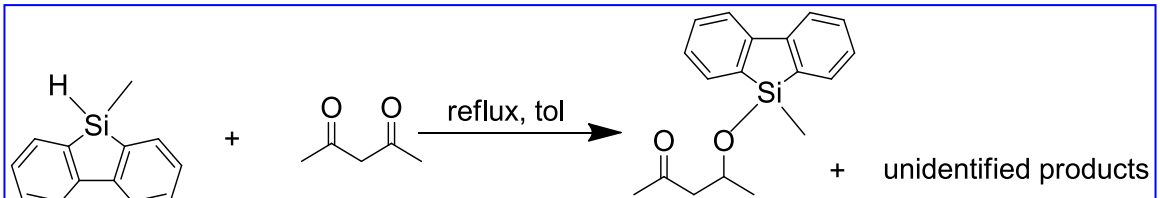

Scheme 2.2.9. Attempted hydrosilylation reaction of 2,4-pentanedione with (**S8**) catalyzed by traditional catalysts.

We have noticed that due to possible keto-enol tautomerism, the hydrosilylation reaction of ketones gives a number of isomers including a monosilylated silyl ether as a major isomer as identified by a -CH signal in the ^{1}H NMR spectrum of the crude product. The reaction was accompanied by the formation of siloxanes. The other products formed could not be identified conclusively. The reaction was also run at room temperature, however, no products were formed even at prolonged reaction time. In previously reported hydrosilylation reactions of mono- and diketones with Ph_2MeSiH and Ph_2SiH_2, a silyl ether product was obtained as the major isomer and the addition was observed to proceed at both the C=O bonds of the diketone.[33]

2.3 Palladium(II)-PTA Complexes Catalyzed Cross-Coupling Reactions

We have investigated Suzuki-Miyaura cross-coupling reactions and copper-free Sonogashira cross-coupling reactions using a variety of aryl halides in the presence of palladium(II)-PTA complexes. Utilizing relatively low catalyst loading, we were able to obtain the cross-coupled products in moderate to high yields with minimal side reactions such as homo-coupling reactions. The products were purified by column chromatography using silica gel and dichloromethane/MeOH or hexane/dichlorometane as the eluent(s) and were characterized by GC-MS and ^{1}H, $^{13}C\{^{1}H\}$, $^{29}Si\{^{1}H\}$NMR, and IR spectroscopy.

2.3.1 Pd-PTA complexes catalyzed Suzuki-Miyaura cross-coupling reactions

We began the Suzuki-Miyaura cross-coupling reactions of *p*-bromoacetophenone (**R1**) with phenylboronic acid (**T1**) in 1 : 1 molar ratio in the presence of 0.5 mole% of *cis*-$PdCl_2(PTA)_2$ (**M1**)[2b] (Figure 2.3.1) as a pre-catalyst and a base, K_2CO_3 (Scheme 2.3.1).

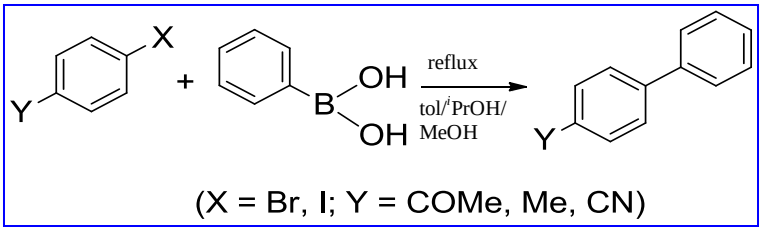

Scheme 2.3.1. Suzuki-Miyaura cross-coupling reactions catalyzed by (**5a**).

The reaction mixture was refluxed in toluene, however, the reaction was found to be too slow. Then the reaction was monitored with a higher catalyst loading (1-5 mole%).

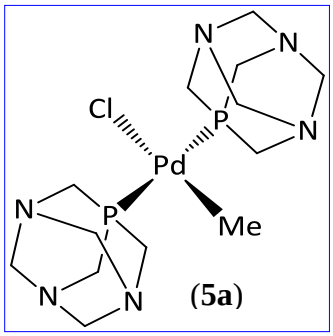

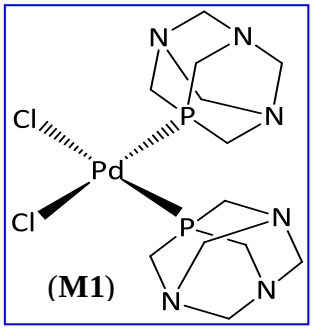

Figure 2.3.1. Structures of *trans*-PdCl(Me)$(PTA)_2$, (**5a**) and *cis*-$PdCl_2(PTA)_2$, (**M1**).

When the reaction was rerun with 5 mole% of **M1**, an 88% conversion with respect to the **R1** was observed by GC after 14 h to form a product mixture, which consists of 18% of the homo-coupled product, that is, biphenyl (Table 2.3.1).

Table 2.3.1. Results for Suzuki-Miyaura cross-coupling reaction of 4-bromoacetophenone (**R1**) with $PhB(OH)_2$ (**T1**) catalyzed by *cis*-$PdCl_2(PTA)_2$ (**M1**) [refluxed; 5 mole% of (**M1**)]. [a]GC yields.

Solvent	Time	% Conversion	% Biphenyl	% Yield[a]
Toluene	30 min 1 h 2 h 14 h	70 85 86 88	20 20 22 18	50 65 64 70
MeOH	30 min 1 h 2 h 14 h	67 80 88 90	25 21 18 16	42 59 70 74

The reactions were rerun in different solvent systems such as methanol and isopropanol, however, the yield of the cross-coupled product and side product did not change significantly. Since **M1** was found to be insoluble in most of the solvents, we presumably thought that low solubility of the catalytic species could be the leading factor for its lower catalytic activity.

Owing to this fact, **M1** was replaced by another more soluble Pd(II)-PTA complex, *trans*-PdCl(Me)$(PTA)_2$ (**5a**) as a pre-catalyst (Figure 2.3.1). The reaction of **R1** and **T1**was carried out in different solvent systems in the presence of 3 mole% of **5a** and the most common and inexpensive base, K_2CO_3. Since the reactions were found to be too slow in toluene and methanol, the catalyst loading was increased to 5 mole%. To our surprise, in toluene and methanol, as the reaction progressed the yield of the cross-coupled product decreased whereas that of the homo-coupled product increased (Table 2.3.2).

We do not have a valid explanation for this anomaly at this time. However, it can be anticipated that preferential conversion of the reacting substances into biphenyl may take

place from multiple sources, that is, homo-coupling not only takes place from aryl halide but also from unreacted phenylboronic acid; which were employed in approximately 1 : 1.3 ratio, respectively. This eventually results in lowering of the overall yield of the desired product as the reaction progresses.

On the other hand, refluxing **R1** and **T1** in ^{i}PrOH with 3 mole% of **5a** resulted in completion of the reaction in 3 h giving 4'-phenylacetophenone, **P1** (99% GC yield) with minimal homo-coupling (Table 2.3.2). After purification through column chromatography, **P1** gave the expected signals in the ^{1}H and ^{13}C{^{1}H} NMR spectra. The C=O stretching frequency for **P1** in the IR spectrum was detected to be 1674 cm^{-1}, which is expectantly higher than that for **R1** (1659 cm^{-1}).

Table 2.3.2. Results for Suzuki-Miyaura cross-coupling reaction of 4-bromoacetophenone, **R1** with $PhB(OH)_2$, **T1** catalyzed by (**5a**); refluxed; [a]GC yields (isolated yield is in parentheses). Refluxed; catalyst loading: b= 5 mole%, c and d = 3 mole% based on **R1**.

Solvent	Time	% Biphenyl	% Yield[a]
Toluene[b]	30 min.	20	45
	1 h	22	48
	2 h	32	39
	4 h	43	36
MeOH[c]	30 min.	9	83
	1 h	7	92
	2 h	20	79
	4 h	25	74
	14 h	36	63
^{i}PrOH[d]	30 min.	4	92
	1 h	3	96
	3 h	1	99 (82)

2.3.2 Substituent effect in Suzuki-Miyaura cross-coupling reactions

To understand the role of substituents in the aryl halides examined in the Suzuki-Miyaura cross-coupling reaction catalyzed by **5a** described herein, a variety of substrates were introduced. The reaction of **T1** was carried out with 4-iodotoluene, **R2** and in refluxing isopropanol in the presence of 3 mole% of **5a** and K_2CO_3. After 1 h, the reaction was found to undergo 99% conversion with respect to **R2** and further heating did not significantly change the product yield. The cross-coupled product **P2** was obtained as a white solid in 86% of isolated yield. Formation of **P2** was also confirmed by ^{1}H and $^{13}C\{^{1}H\}$ NMR spectroscopy and GC-MS.

When **T1** and 4-bromotoluene, **R3** were reacted with each other under the same conditions, the reaction was too slow. On increasing the catalyst loading to 8 mole% with respect to **R3**, only 41% of **R3** was found to be converted into the product **P2** with 7% of biphenyl formation (Table 2.3.3). Therefore, the change in substituent (Br vs I) in the haloarene ring has made a significant difference in the catalytic activity of **5a**.

Table 2.3.3. Results for Suzuki-Miyaura cross-coupling reaction of 4'-halotoluene (**R2** and **R3**) with $PhB(OH)_2$, **T1** catalyzed by (**5a**); refluxed in $^{i}PrOH$; [a]GC yields (isolated yields are in parentheses). Catalyst loading: b = 3 mole%, c = 8 mole%.

Substrate	Time	% Conversion	% Biphenyl	% Yield[a]
4'-iodotoluene[b]	30 min 1 h 3 h	93 99 99	4 3 3	89 96 96 (86)
4'-bromotoluene[c]	30 min 1 h 3 h 14 h 48 h	2 8 10 25 41	10 8 22 17 7	(34)

The reaction of **R2** and **T1** was also carried out in other solvent systems as well. The reaction was less effective in toluene and MeOH. The substrate was switched to 4-bromobenzonitrile (**R4**) and the reaction was carried out in ^{i}PrOH in the presence of 3 mole% of **5a**. The reactivity was better with minimal homo-coupling (7%) and a shorter reaction time (3 h) when isopropanol was used, however **5a** was equally effective in MeOH as well (Table 2.3.4). After purification by the silica gel column chromatography, the cross-coupled product 4'-phenylbenzonitrile, **P3** was obtained as a pale yellow solid in 80% yield. Expected signals were observed in the ^{1}H and ^{13}C{^{1}H} NMR spectra of **P3**.

Table 2.3.4. Results for Suzuki-Miyaura cross-coupling reaction of 4-bromobenzonitrile, **R4** with $PhB(OH)_2$, **T1** catalyzed by 3 mole% of (**5a**); refluxed; [a]GC yields (isolated yield is in parentheses).

Solvent	Time	% Conversion	% Biphenyl	% Yield[a]
MeOH	30 min.	87	11	76
	1 h	90	14	76
	2 h	95	15	80
	4 h	99	13	86
^{i}PrOH	30 min.	85	6	79
	1 h	95	8	87
	3 h	99	7	92 (80)

Based on the observations during the investigation of Suzuki-Miyaura cross-coupling reactions, following conclusions can be drawn:

(a) Electron-withdrawing substituent in the haloarenes resulted in minimal homo-coupling and better yields than electron-donating substituent (**R4** vs **R3**). In fact, the presence of the electron-withdrawing substituent facilitates the oxidative-addition of the haloarenes to the metal center.

(b) With the more labile iodo-group, iodoarenes possessed greater reactivity towards cross-coupling reactions than bromoarenes (**R2** vs **R3**).

(c) The use of ^{i}PrOH as a solvent prevented homo-coupling and consequently increased the yield of the cross-coupled product which is largely due to the higher solubility of **5a** in ^{i}PrOH. Additionally, ^{i}PrOH is a cost-effective and an environmentally-friendly solvent. It is also a lower boiling solvent (82.5 ^{o}C) compared to toluene (110.6 ^{o}C) which results in the reaction as well as the work-up process being easier.

A similar kind of reactivity trend was observed in other reported Pd catalyzed Suzuki-Miyaura cross-coupling reactions.[34-35] Dong *et al.* have proposed a pathway for catalyst

($PdCl_2$) activation by isopropanol (Scheme 2.3.2).[35] The PdX_2 complex can react with isopropanol in the presence of a base to generate a palladium isopropanolate intermediate.[36] A β-H elimination reaction from the intermediate can form a [HPdX] species and acetone. Reductive-elimination of HX from the [HPdX] produces the catalytically active Pd(0) species, which is available for the catalytic reaction. However, it is assumed that the coordination of Pd to oxygen seems less likely for **5a**. This is because of the presence of only one Cl group in **5a** which results in generation of a less electrophilic palladium center in **5a** as compared to $PdCl_2$. As described earlier in this section, the isopropanol-promoted catalytic activity of **5a** is probably due to its enhanced solubility.

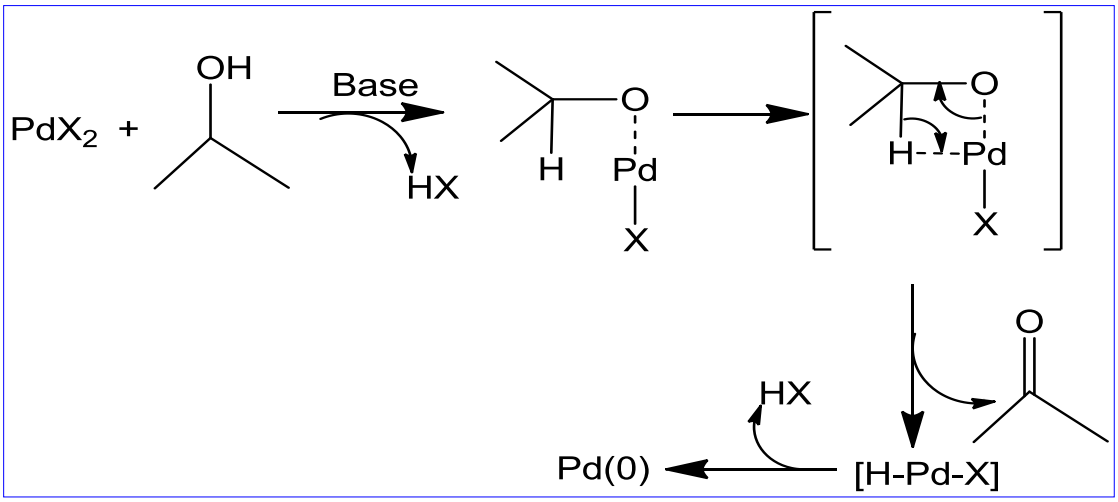

Scheme 2.3.2. Proposed catalytic cycle in isopropanol activated Suzuki-Miyaura cross-coupling reactions catalyzed by PdX_2.[35]

A comparison of results from Suzuki-Miyaura cross-coupling reaction of **R1** and **T1** utilizing various palladium(II) catalysts and solvent systems is given in Table 2.3.5.

Table 2.3.5. Comparison of catalytic activity of different Pd(II)-phosphines in Suzuki-Miyaura cross-coupling reaction of **R1** and **T1**. Catalyst loading is based on **R1**; K_2CO_3 was used as a base; refluxed.

Catalyst	Catalyst loading[a]	Time	% Conversion	Yield, GC (%)	Solvent	Reference
5a	3 mole%	3 h	100	99	^{i}PrOH	this work
trans-$PdCl_2(PPh_3)_2$	1 mole%	2 h	83	73-81	toluene	34c
5a	3 mole%	1 h	99	92	MeOH	this work
$PdCl_2$(dppf)	1 mole%	2 h	94	92	toluene	34c
$PdCl_2$(dppe)	1 mole%	2 h	84	82	toluene	34c

2.3.3 Analysis of residual Pd species in Suzuki-Miyaura cross-coupling reaction

To understand the status of the PTA ligand in the catalytic reaction, we analyzed a part of the reaction mixture of **R1**and **T1** in ^{i}PrOH by the $^{31}P\{^{1}H\}$ NMR spectroscopy after completion of the reaction. A major signal at -10.5 ppm along with a minor peak at -66.3 ppm were seen in approximately 3 : 1 ratio, respectively. The reaction mixture was then filtered through a silica gel column. When the resulting filtrate was analyzed by the $^{31}P\{^{1}H\}$ NMR spectroscopy, a weaker resonance was observed at -7.3 ppm. Moreover, since the $^{31}P\{^{1}H\}$ NMR spectrum displayed no signal for the pure cross-coupled products they should not have any P centers in them. It is more likely that the ligand part of the reaction mixture stayed with the metal-base residue during filtration.

For this reason, a part of the reaction mixture which consists of the metal-base residue and product was washed with CH_2Cl_2, MeOH, and water after filtration. The scanning

electron microscopy (SEM) analysis of the dry residue displayed coarse colloidal sized particles (Appendix III.1). This is most likely to be the Pd(0) species generated during catalysis. The energy dispersive X-ray spectroscopy (EDS) results of the crude residual species showed the presence of elements such as P, Pd, Cl, K, C, and O. On the other hand, the EDS spectrum of the residue after washing with water displayed a very weak signal of P which is possibly because the water-soluble phosphine has been washed away from the phosphine-containing residue (Appendix III.2). Based on these observations, it can be inferred that mostly, the PTA part of the catalyst in our cross-coupling reactions stays with the residue and does not go along with the product. This is very important as it makes the separation of the product and catalytic species easier.

2.3.4 Pd(II) catalyzed copper-free Sonogashira cross-coupling reactions

We have investigated Sonogashira cross-coupling reactions of a variety of aryl halides with some terminal alkynes (Scheme 2.3.3). These catalytic reactions were begun with the reaction of 4-bromoacetophenone, **R1** and phenylacetylene, **A4** in the presence of **5a** as a pre-catalyst (3 mole%) and CuI (4 mole%) based on **R1**. The reaction mixture was refluxed in isopropanol, however, only 5% of **R1** was found to be converted into the desired cross-coupled product after 24 h. No significant change in reactivity was observed even when the catalyst loading was increased to 5 mole%. No cross-coupled product formation was detected when the reaction was carried out in toluene as well.

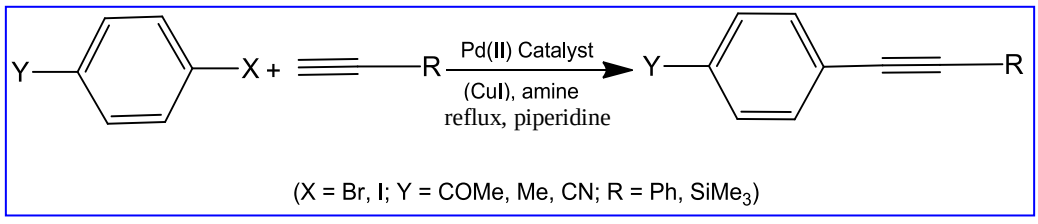

Scheme 2.3.3. Sonogashira cross-coupling reactions of substituted haloarenes.

A new palladium(II)-PTA complex, *cis*-$PdCl_2(PTA)_2$ (**M1**), which has been reported by Krogstad *et al.*,[2b] was introduced as a pre-catalyst for the reaction of **R1** and **A4** in the presence of triethylamine. The reaction mixture was refluxed in THF and isopropanol, separately in the presence of 3 mole% of **M1** and 4 mole% of CuI with respect to **R1**. In both the reactions, a significant amount of the dimeric product of phenylacetylene corresponding to *m/z* = 202 was formed, as detected by GC-MS, whereas even a prolonged reaction time was unable to improve the amount of the cross-coupled product. Assuming that CuI is responsible for dimerization of phenylacetylene, the reaction was screened with a lower CuI loading. However, the formation of the homo-coupled product could not be avoided. The reactions were carried out at room temperature and lower as well as with higher catalyst loading (5 mole%) while no cross-coupling took place. This led to following conclusions:

(a) Sonogashira cross-coupling reaction of **R1** and **A4** requires higher temperature.

(b) The reaction takes place only in the presence of catalyst as well as a deprotonating substance such as CuI (which forms Cu acetylide) as a co-catalyst.

(c) At higher temperature, use of CuI catalyzes the side reactions such as homo-coupling or dimerization of **A4** which possibly takes place through the pathway as proposed in Scheme 2.3.4.

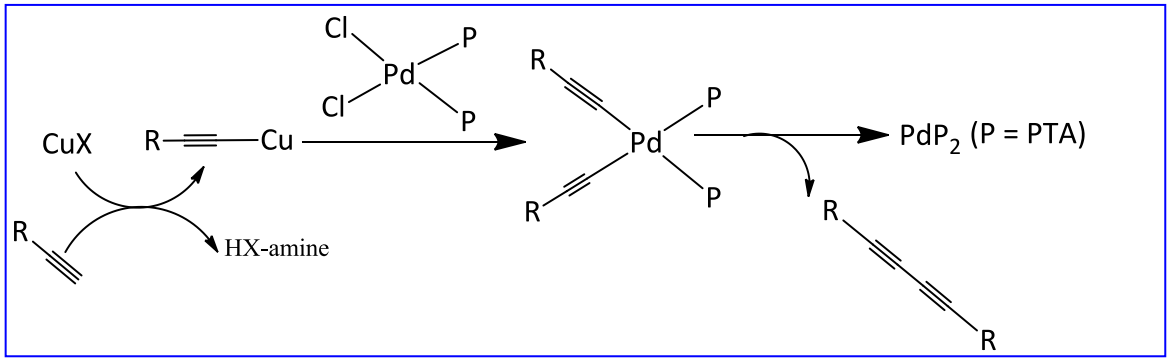

Scheme 2.3.4. Proposed alkyne-dimerization pathway in Sonogashira cross-coupling reactions.

In this regard, the Sonogashira cross-coupling reactions of phenylacetylene (**A4**) and trimethylsilylacetylene (**A2**) were carried out in the presence of **M1** as a pre-catalyst in piperidine, which is a good deprotonating solvent with a relatively higher basic character (p*K*a ~ 11.3). Piperidine not only can be a good alternative for CuI but also it functions as both a solvent and base.

In one such reaction, **A4** was slowly added to **R1** in piperidine containing 3 mole% of **M1**, and then the reaction mixture was refluxed under argon for 3 h. The GC analysis showed 99% conversion of **R1** with 97% yield of the cross-coupled product. For the same reaction in piperidine, Leadbeater and Tominack have reported a 94% GC yield of the cross-coupled product when 4 mole% of traditional Sonagashira cross-coupling catalyst, $PdCl_2(PPh_3)_2$ was used as a pre-catalyst.[37] Therefore, the catalytic turn over numbers (TON) for the majority of the reactions in our system (~ 32) appears slightly better than in the Leadbeater-Tominack's system (23.5). Similarly, Krause and Thorand reported that the room temperature reaction of **R1** and **A4** in THF in the presence of $PdCl_2(PPh_3)_2$ resulted in 87% yield after 16 h (Table 2.3.7).[38a] These results are also comparable to that from the reaction catalyzed by a Pd-PTA complex, [Pd(dmba)Cl(PTA)].[38b]

After purification by silica gel column chromatography, the cross-coupled product, 4-(phenylethynyl)acetophenone, **P4** was obtained as a pale yellow solid in 72% isolated yield. The C=O stretching frequency in the IR spectrum of **P4** was found to be 1671 cm^{-1}, which is higher in comparison to that of **R1**. However, no peak corresponding to a C≡C stretch could be observed in the IR spectrum. The ^{1}H and $^{13}C\{^{1}H\}$ NMR spectra displayed the expected signals; the splitting pattern and chemical shifts are comparable to

those reported in the literature.[39] The results from these optimized reactions are summarized in Table 2.3.6.

Table 2.3.6. Results for copper-free Sonogashira cross-coupling reactions of substituted haloarenes and alkynes using 3 mole% of *cis*-$PdCl_2(PTA)_2$ (**M1**); refluxed in piperidine. [a]Isolated yields (GC yields are in parentheses).

Entry	Substrate	Alkyne	Time, h	% Conversion	% Yield[a]
1	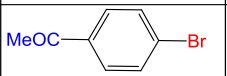	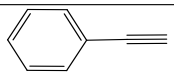	3	99	72 (97)
2	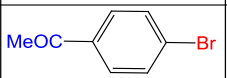		3	96	61 (87)
3	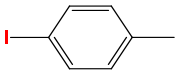	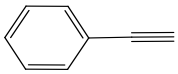	4	97	76 (95)
4	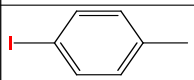		4	96	81 (91)
5	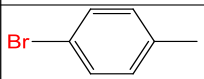	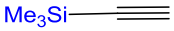	18	66	43 (54)
6	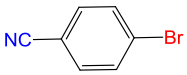	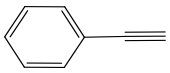	5	89	71 (83)
7	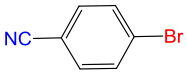	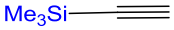	5	84	63 (76)

On the other hand, trimethylsilylacetylene, **A2** was found to dimerize more easily. The reaction of **R1** with **A2** resulted in 96% conversion of **R1** in 3 h with 87% GC yield of the cross-coupled product, 4-[(trimethylsilyl)ethynyl]acetophenone (**P5**) which was isolated in a relatively low (61%) yield. We do not have a valid explanation for a wide difference in isolated and GC yields of **P5**. The GC-MS and ^{1}H and $^{13}C\{^{1}H\}$NMR spectral data were consistent with **P5**, except that the $SiMe_3$ protons showed a more downfield resonance (0.35 ppm) in the ^{1}H NMR spectrum than that reported (0.25 ppm) in the literature.[39] The reactions of **R1** with **A2** and **A4** were also carried out in piperidine

in the presence of **5a** as a pre-catalyst, however, the reactions were found to be too slow resulting in poorer yields.

For further investigation of copper-free Sonogashira cross-coupling reactions, 4-iodotoluene, **R2** and 4-bromotoluene, **R3** were separately treated with **A4** with the same catalyst loading (3 mole% of **M1** with respect to **R2** or **R3**). The reaction of **R2** and **A4** led to the formation of 4-(phenylethynyl)toluene, **P6** which was isolated as a white solid in 76% yield. The GC analysis of the crude product showed a 97% conversion of **R2** with only 2% of the homo-coupled product formation.

The reaction of **R2** and **A2** was found to be sluggish even with 5 mole% of **M1**. Only 34% of **R2** was found to be converted into the products while 18% of the cross-coupled product was observed by GC. The reactions of **R2** and **R3** with **A2** resulted in 96% (4 h) and 66% (18 h) conversion, respectively. The cross-coupled product, 4-[(trimethylsilyl)ethynyl]toluene, **P7** was obtained as a yellow oily liquid. The GC yields of the crude product with **R2** and **R3** were recorded as 91% and 54%, respectively, whereas the isolated yields were found to be 81% and 43%, respectively. Expected signals were observed in the ^{1}H and $^{13}C\{^{1}H\}$ NMR spectra, however, GC-MS was found to be more diagnostic. The presence of the less labile Br group and electron-donating CH_3 group accounts for lower reactivity of **R3** compared to **R2**. In such conditions, the coupling carbon becomes less nucleophilic and consequently, nucleophilic attack becomes more unlikely.

To investigate the effect of the substituent in the substrate molecule, 4-bromobenzonitrile, **R4** was treated with **A4** under similar reaction conditions. After 5 h, **R4** was found to undergo 89% conversion with 6% of the homo-coupled product being

formed. Therefore, the effectiveness of the reaction is found to be better than that with **R3** though both of the substrates contain the Br leaving group. This is largely due to the presence of electron-withdrawing group in **R4**. The cross-coupled product, 4-(phenylethynyl)benzonitrile, **P8** was obtained as an off-white solid (71% yield).

The reaction of **R4** and **A2** in refluxing piperidine in the presence of 3 mole% of **M1** yielded the cross-coupled product, 4-[(trimethylsilyl)ethynyl]benzonitrile, **P9** (76% yield) with 84% conversion with respect to **R4**. As in other reactions involving **A2**, the extent of homo-coupling was observed to be higher than in the reactions involving **A4**. Again the efficiency of this reaction is higher in comparison to the reaction of **A2** and **R3** due to substituent effect (electron-withdrawing vs electron-donating substituent). Similar kinds of reactivity trends have been described in the literatures.[38, 40]

The ^{1}H and $^{13}C\{^{1}H\}$ NMR spectra of **P8** and **P9** displayed the expected signals. Unlike in other products in our study, the C≡C stretching frequency of **P9** could be detected by IR spectroscopy which was found to be higher (2153 cm^{-1}) than that in **A2** (~ 2050 cm^{-1}).[41] This can be attributed to the conjugation effect in **P9**.

The results from Sonogashira cross-coupling reactions utilizing **M1** and other pre-catalysts are summarized in Table 2.3.7.

Table 2.3.7. Results from Sonogashira cross-coupling reactions of **R1** with terminal alkynes using different Pd complexes as pre-catalysts. [a]Catalyst loading is based on haloarenes; [b]isolated yields are in parentheses; [c]4 mole% of CuI was used as a co-catalyst; [d]1.5 equiv of Cs_2CO_3 was also used; [e]heated over oil-bath at 70 ^oC; other reactions were refluxed.

Catalyst	Catalyst loading[a]	Time	Alkyne	% Yield, GC[b]	Solvent	Reference
$PdCl_2(PPh_3)_2$	2 mole%	10 min	**A2**	75	piperidine	37[e]
$PdCl_2(PPh_3)_2$	4 mole%	10 min	**A4**	94	piperidine	37[e]
M1	3 mole%	3 h	**A4**	97 (72)	piperidine	this work
M1	3 mole%	3 h	**A2**	87 (61)	piperidine	this work
$PdCl_2(PPh_3)_2$	2 mole%[c]	16 h	**A4**	87	THF	38a
Pd(dmba)Cl(PTA)	2 mole%[d]	24 h	**A4**	92	CH_3CN	38b

We also investigated the reactions of other substrates containing electron-donating substituent such as 4-bromoanisole with **A2** and **A4**, but the reactions were found to be too slow even with higher catalyst loading. The reactions were screened in different solvents and temperatures, and none of them gave better results. The reactions of **A2** and **A4** with the substituted chlorobenzene containing the electron-withdrawing groups did not form the cross-coupled products at all.

2.4 Conclusions

We have been able to synthesize a number of four-coordinated water-soluble platinum(II) and palladium(II)-PTA complexes bearing alkyl ligands in moderate to high yields following a ligand substitution method. The respective platinum(II) and palladium(II)-cyclooctadiene precursors were treated with 2 molar equivalents of PTA at room temperature in 1 : 1 solvent mixture of methanol and CH_2Cl_2. Additionally, we have also synthesized several other water-soluble platinum(II) and palladium(II) alkyl and halide complexes bearing an acyl derivative of PTA, that is, DAPTA ligand. These complexes were synthesized by room temperature reactions of the respective cyclooctadiene precursors with 2 equivalents of DAPTA. The complexes of the type, MX_2P_2 (P = PTA, DAPTA; X = Me, Br; M= Pt, Pd), except MI_2P_2, were isolated as the *cis*-isomers whereas the complexes of the type, $MX(R)P_2$ (X = Cl, Br, I; R = Me, Et) were obtained as *trans*-isomers. These complexes were characterized by various techniques which include multinuclear NMR spectroscopy, IR spectroscopy, mass spectrometry, elemental analysis, melting point determination, and X-ray crystallography. The X-ray crystal structures of the complexes **1a**, **3a**, **4**, and **12d** showed the square planar geometry with expected connectivities. The bond lengths, bond distances, and other structural parameters were comparable to that of of the related phosphine complexes.

The *cis*-$PtMe_2(DAPTA)_2$ (**9a**) and *cis*- $PtBr_2(DAPTA)_2$(**12a**) were obtained as an approximately 1 : 1 mixture of two conformers whereas the rest of the complexes were synthesized as a single isomer. Some of the palladium complexes were found to be unstable at room temperature while most of the platinum and palladium complexes

possessed fairly thermal- and air-stability. Some of the complexes were found to undergo isomerization on prolonged reaction time and/or heating. The dialkyl, PtR_2P_2 or halo(alkyl), $MX(R)P_2$ complexes bearing PTA, DAPTA, and any other PTA-derivatized ligands have been reported for the first time.

We have also carried ot the syntheses of the four-coordinated platinum(II) and palladium(II) dialkynylbis(PTA) or (DAPTA) complexes. The alkynyl complexes of the transition metals bearing such kinds of PTA or PTA-derivatized ligands have not been reported elsewhere previously. The *cis*-PTA or DAPTA complexes ligated with the alkynyl (C_2R) goups such as phenylethynyl, trimethylsilylethynyl, ethynylaniline, ethynylpyridine, benzylethynyl, and tolylethynyl were synthesized by room temperature reactions of respective cyclooctadiene precursors, $M(C_2R)_2(COD)$ with 2 molar equivalents of the PTA or DAPTA in 1 : 1 methanol and CH_2Cl_2 mixture. The *trans*-analogues were prepared by treating the suspension of respective *cis*-MCl_2P_2 complexes in absolute ethanol with excess of corresponding alkyne at room temperature in the presence of triethylamine. Some of the *cis*-alkynyl complexes could also be prepared through the isomerization of *trans*-analogues on carrying out the reaction for extended period of time whereas some of the *cis*-alkynyl complexes were found to undergo isomerization in solutions to the respective *trans*-analogues. For example, *cis*-$Pt(C_2Ph)_2(PTA)_2$ (**6a**) upon recrystallization at low temperature gave the crystals of its *trans*-analogue (**6b**) and *cis*-$[Pt\{C_2(m\text{-py})\}_2(PTA)_2]$ (**19a**) isomerized to its *trans*-anlaogue (**19b**) upon standing long in $CDCl_3$ or CH_2Cl_2 solutions at room temperature.

The novel dialkynyl complexes synthesized were characterized by multinuclear NMR spectroscopy, IR spectroscopy, mass spectrometry, elemental analysis, melting point

determination, and X-ray crystallography. The molecular geometry associated with the alkynyl PTA complexes **6b**, **16**, **19b**, and **22** as determined by X-ray crystallography was found to be identical to that of the related σ-alkynyl phosphine complexes; consistent with the square planar geometry with expected bond connectivities. The complex, *cis*-[Pt{C_2(*m*-py)}$_2$(DAPTA)$_2$] (**27**) was obtained as an approximately 1 : 1 mixture of two conformers whereas other dialkynyl complexes were isolated as a single isomer. We have carried out the synthesis and structural and other characterizations of a novel PTA-derivatized water-soluble dicationic ligand, ipac mPTA (**L1**). The coordination chemistry of ipac mPTA has yet to be identified.

The catalytic activity of one of the platinum(II)-PTA complexes, *cis*-$PtMe_2(PTA)_2$ (**1a**) was investigated in the metal catalyzed hydrosilylation reactions of a variety of alkynes, alkenes, and ketones with tertiary hydrosilanes. The hydrosilylated products were purified and characterized by multinuclear NMR spectroscopy, IR spectroscopy, GC-MS, and/or mass spectrometry. Complex (**1a**) exhibited a very good catalytic activity in a lower catalyst loading forming the regioselective products upon hydrosilylation reaction of terminal alkenes and alkynes. Hydrosilylation reaction of alkenes gave two products as a result of Markovnikov (β-product) and anti-Markovnikov (α-product) addition whereas the reaction of alkynes also resulted in two isomeric products, *β-trans* isomer and α isomer. The *β-trans* isomer was found to be the major product; usually with > 80% regioselectivity. When sterically hindered hydrosilanes were used, the regioselectivity improved in the favor of the *β-trans* product. The J_{HH} coupling constant values for the olefinic hydrogens in the ^{1}H NMR spectra of the hydrosilylated products was found to be *ca.* 18-19 Hz which is diagnostic for the *β-trans*

product. Similarly, hydrosilylation reactions of alkenes yielded the β-product as a major product. Since all of these hydrosilylation reactions produced moderate to high yields of products with 0.5 mole% of (**1a**), the catalytic turn over number (TON) in most of the reactions was found to be very good. The mechanistic detail of these reactions has not been investigated, however, based on the nature of the products formed it is anticipated that these reactions, like other platinum catalyzed hydrosilylation reactions, follow the Chalk-Harrod mechanism.

The hydrosilylation reaction of the terminal alkynes was also carried out with some siloles and silafluorenes. These reactions resulted in the formation of mono- and disilylated products. The hydrogermylation reaction of 1,4-diethynylbenzene using a secondary germole, 1,1-dihydrido(tetraphenyl) germole resulted in the formation of an oligomer. Such kinds of di- or polysilylated (germylated) products have their potential applications as chemical sensors.[32] Owing to the water-solubity of PTA and DAPTA complexes, the synthesized complexes have the potential applications in aqueous-phase or biphasic catalytic reactions. This eventually facilitates the recycling of the catalyst; a major concern in homogeneous catalysis. The PTA and DAPTA complexes also contribute to the green chemistry-based reactions.

The Suzuki-Miyaura cross-coupling reaction and copper-free Sonogashira cross-coupling reaction were investigated utilizing palladium(II)-PTA complexes as pre-catalysts. Suzuki-Miyaura cross-coupling reaction of a variety of substituted haloarenes and phenylboronic acid was found to be effectively catalyzed by *trans*-PdCl(Me)$(PTA)_2$ (**5a**) with minimal catalyst loading. The efficiency of the catalyst was detected to be

higher with minimal side reaction such as homo-coupling when isopropanol was used as a reaction solvent.

While analyzing the residual palladium species through scanning electron microscopy (SEM) and energy-dispersive X-ray spectroscopy (EDS), the presence of the elements from the catalytic species such as P, Pd, and Cl were detected in the coarse colloidal residual particles. On the other hand, the phosphorus signals could hardly be detected in the $^{31}P\{^{1}H\}$ NMR spectrum of the crude cross-coupled product. This implies that the residual palladium species contains most of the phosphine of the pre-catalyst (**5a**) which is one of the advantages of using (**5a**) as a pre-catalyst over other phophine complexes in such kinds of cross-coupling reactions.

Another palladium(II)-PTA complex, *cis*-$PdCl_2(PTA)_2$ (**M1**)[2b] was found to be an effective catalyst in copper-free Sonogashira coupling reations of terminal alkynes with a variety of substituted haloarenes. The cross-coupled products were purified and characterized by NMR spectroscopy, IR spectroscopy, and GC-MS experiments. Very good yields of the cross-coupled products were obtained with minimal side reactions when the reactions were carried out in refluxed piperidine.

Apart from the solvent, the catalytic activity of both types of cross-coupling reactions, that is, Suzuki-Miyaura and Sonogashira cross-coupling reactions, was also found to be dependent upon the nature of the substrates. Generally, haloarenes with electron-withdrawing substituents were found to be more reactive to form the cross-coupled product than that with electron-donating substituents. Furthermore, iodoarenes were more reactive than bromoarenes.

Finally, in addition to the catalytic activity of the platinum(II) and palladium(II)-PTA and DAPTA complexes in a variety of monophasic or biphasic reactions, these complexes can be applied in stoichiometric reactions such as E-H bond activation (E = Si, Ge, Sn) of the hydrosilanes, hydrogermanes, and hydrostananes. In addition to this, the *cis*-dialkyl (dialkynyl or dihalo)bis(PTA/DAPTA) complexes of platinum and palladium can be the potential candidates for their cytotoxic activity because of their structural resemblance with cisplatin.

2.5 References

[1] Mulle, A.; Roodt, A. *Acta Crystallogr.* **2004**, *C60*, 266.

[2] (a) Krogstad, D. A.; Owens, S.; Halfen, J. A.; Young, V. G. *Inorg. Chem. Commun.* **2005**, *8*, 65. (b) Krogstad, D. A.; Cho, J.; DeBoer, A. J.; Klitzke, J. A.; Sanow, W. R.; Williams, H. A.; Halfen J. A. *Inorg. Chim. Acta* **2006**, *359*, 136.

[3] Fleischer, A.; Roller, A.; Arion, V. B.; Keppler, B. K.; Mohr, F. *Can. J. Chem.* **2009**, *87*, 146.

[4] (a) Otto, S.; Roodt, A. *Inorg. Chem. Commun.* **2001**, *4*, 49. (b) Tolman, C. A. *Chem Rev.* **1977**, *3*, 313.

[5] Crispini, A.; Harrison, K. N.; Orpen, A. G.; Pringle, P. G.; Wheatcroft, J. R. *J. Chem. Soc., Dalton Trans.* **1996**, 1069.

[6] (a) Bardi, R.; Piazzesi, A. M. *Inorg. Chim. Acta* **1981**, *47*, 249. (b) Otto, S.; Roodt, A.; Leipoldt, J. G. *S. Afr. J. Chem.* **1994**, *48*, 114.

[7] Otto, S.; Johansson, M. *Acta Crystallogr.* **2000**, *C56*, e12.

[8] Otto, S.; Roodt, A.; Purcell, W. *Inorg. Chem. Commun.* **1998**, *1*, 415.

[9] (a) Falvello, L. R.; Forniés, J.; Gómez, J.; Lalinde, E.; Martín, A.; Moreno, M. T.; Sacristán, J. *Chem. Eur. J.* **1999**, *5*, 474. (b) Cross, R. J.; Davidson, M. F. *J. Chem. Soc., Dalton Trans.* **1986**, 1987. (c) Saha, R.; Qaium, M. A.; Debnath, D.; Younus, M.; Chawdhury, N.; Sultana, N.; Kociok-Köhn, G.; Ooi, L.; Raithby, P. R.; Kijima, M. *Dalton Trans.* **2005**, 2760. (d) Janka, M.; Anderson, G. K.; Rath, N. P. *Organometallics*

2004, *23*, 4382. (e) Sonogashira, K.; Takahashi, S.; Hagihara, N. *Macromolecules* **1977**, 10, 879.

[10] Carpenter, J. P.; Lukehart, C. M. *Inorg. Chim. Acta* **1991**, *190*, 7.

[11] (a) Vergara, E.; Miranda, S.; Mohr, F.; Cerrada, E.; Tiekink, E. R. T.; Romero, P.; Mendía, A.; Laguna, M. *Eur. J. Inorg. Chem.* **2007**, 2926. (b) Darensbourg, D. J.; Ortiz, C. G.; Kamplain, J. W. *Organometallics* **2004**, *23*, 1747.

[12] (a) Otto, S.; Roodt, A. *Acta Crystallogr.* **2001**, *C57*, 540 and references therein. (b) Hitchcock, P. B.; Jacobson, B.; Pidcock, A. *J. Chem. Soc., Dalton Trans.* **1977**, 2038. (c) Boag, N. M.; Rao, M. K.; Terrill, N. J. *Acta Crystallogr.* **1991**, *C47*, 1064. (d) Alcock, N. W.; Leviston, P. G. *J. Chem. Soc., Dalton Trans.* **1971**, 1834.

[13] Kim, H.-J.; Lee, S. W. *Bull. Korean Chem. Soc.* **1999**, *20*, 1089.

[14] Mohr, F.; Mendía, C.; Laguna, M. *Eur. J. Inorg. Chem.* **2007**, 3115.

[15] Deeming, A. J.; Hogarth, G.; Lee, M. Y.; Saha, M.; Redmond, S. P.; Phetmung, H.; Orpen, A. G. *Inorg. Chim. Acta* **2000**, *309*, 109.

[16] Crabtree, R. H. In *The Organometallic Chemistry of the Transition Metals*, 2nd Ed.; John Wiley & Sons: 1994; pp 151-158.

[17] (a) Darensbourg, D. J.; Joo´, F.; Na´dasdi, L.; Be´nyei, A. Cs. *J. Organomet. Chem.* **1996**, *512*, 45. (b) Darensbourg, D. J.; Joo´, F.; Kannisto, M.; Katho´, A.; Reibenspies, J. H.; Daigle, D. J. *Inorg. Chem.* **1994**, *33*, 200.

---

[18] Krogstad, D. A. http:/acswebcontent.acs.org/prfar/2009/reports/P9848.html *Unpublished Results*

[19] Meij, A. M. M.; Otto, S.; Roodt, A. *Inorg. Chim. Acta* **2005**, *358*, 1005.

[20] Frost, B. J.; Bautista, C. M.; Huang, R.; Shearer, J. *Inorg. Chem.* **2006**, *45*, 3481.

[21] Mena-Cruz, A.; Lorenzo-Luis, P.; Romerosa, A.; Saoud, M.; Serrano-Ruiz, M. *Inorg. Chem.* **2007**, *46*, 6120.

[22] (a) Phillips, A. D.; Gonsalvi, L.; Romerosa, A.; Vizza, F.; Peruzzini, M. *Coord. Chem. Rev.* **2004**, *248*, 955. (b) Darensbourg, D. J.; Yarbrough, J. C.; Lewis, S. J. *Organometallics* **2003**, *22*, 2050.

[23] Chalk, A. J.; Harrod, J. F. *J. Am. Chem. Soc.* **1965**, *87*, 16.

[24] Lewis, L. N.; Sy, K. G.; Bryant, Jr., G. L.; Donahue, P. E. *Organometallics* **1991**, *10*, 3750.

[25] Ojima, I.; Clos, N.; Donovan, R. J.; Ingallina, P. *Organometallics* **1990**, *9*, 3129.

[26] (a) Dickers, H. M.; Haszeldine, R. **N.;** Mather, A**.** P.; Parish, R. V. *J. Organomet. Chem.* **1978**, *161*, 91. (b) Brady, K. A.; Nile, T. A. *J. Organomet. Chem.* **1981**, *206*, 299.

[27] Rivera-Claudio, M.; Rozell, J.; Ramirez-Oliva, E.; Cervantes, J.; Pannell, K. H. *J. Organomet. Chem.* **1996**, *521*, 267.

[28] (a) Marciniec, B.; Gulinski, J.; Urbaniak, W.; Nowicka, T.; Mirecki, J. *Appl. Organomet. Chem.* **1990**, *4*, 27. (b) Caseri, W.; Pregosin, P. S. *Organometallics* **1988**, *7*, 1373.

[29] Marciniec, B. *Silicon Chem. 1* **2002**, *1*, 155.

[30] (a) Kiso, Y.; Kumada, M.; Tamao, K.; Umeno, M. *Inorg. Chim. Acta* **1973**, *50*, 297. (b) Wang, X.; Chakrapani, H.; Madine, J. W.; Keyerleber, M. A.; Widenhoefer, R. A. *J. Org. Chem.* **2002,** *67*, 2778. (c) Xueran, L.; Zhenlin, Z.; Yuanyin, C.; Yezhi, Y. *Chin. J. Appl. Chem.* **1990**, *4*, 65.

[31] (a) Spivak, G. J.; Holah, D. G.; Hughes, A. N.; Krysa, E.; Havighurst, M. D.; Magnuson,V. R. *Polyhedron* **1997**, *16*, 2353. (b) Romeo, R.; D'Amico, G. *Organometallics* **2006**, *25*, 3435. (c) Procelewska, J.; Zahl, A.; Liehr, G.; van Eldik, R.; Smythe, N. A.; Williams, B. S.; Goldberg, K. I. *Inorg. Chem.* **2005**, *44*, 7732.

[32] Sanchez, J. C.; Urbas, S.; Toal, S.; DiPasquale, A. G.; Rheingold, A. L.; Trogler, W. C. *Macromolecules* **2008**, *41*, 1237.

[33] (a) Ojima, I.; Nihonyanagi, M.; Kogure, T.; Kumagai, M.; Horiuchi, S.; Nakatsugawa, K. *J. Organomet. Chem.* **1975**, *94*, 449. (b) Reznikov, A. N.; Lobadyuk, V. I.; Spevak, V. N.; Skvortsov, N. K. *Russ. J. Gen. Chem.* **1998**, *68*, 910. (c) Hashimoto, H.; Aratani, I.; Kabuto, C.; Kira, M. *Organometallics* **2003**, *22*, 2199.

[34] (a) Moreno-Manax, M.; Perez, M.; Pleixats, R. *J. Org. Chem.* **1996**, *61*, 2346. (b) Kotha, S.; Lahiri, K.; Kashinath, D. *Tetrahedron* **2002**, *58*, 9633. (c) Colacot, T. J.; Qian, H,; Cea-Olivares, R.; Hernandez-Ortega, S. *J. Organomet. Chem.* **2001**, *637*, 691.

[35] Xiao-Chun, T.; Yue-Ping, Z.; Tian-Xiong, H.; Dong, S. *Chin. J. Chem.* **2007**, *25*, 1326.

[36] (a) Nalesnik, T. E.; Holy, N. L. *J. Org. Chem.* **1977**, *42*, 372. (b) Blackburn, T. F.; Schwartz, J. *J. Chem. Soc., Chem. Commun.* **1977**, 157. (c) Bellosta, V.; Benhaddou, R.; Czernecki, S. *Synlett.* **1993**, 861.

[37] Leadbeater, N. E.; Tominack, B. J. *Tetrahedron Lett.* **2003**, *44*, 8653.

[38] (a) Thorand, S.; Krause, N. *J. Org. Chem.* **1998**, *63*, 8551. (b) Ruiz, J.; Cutillas, N.; López, F.; López, G.; Bautista, D. *Organometallics* **2006,** *25,* 5768.

[39] Bo-Nan, L.; Shao-Hsien, H.; Wei-Yi, W.; Chung-Yuan, M.; Fu-Yu, T. *Molecules* **2010**, *15*, 9157.

[40] (a) Liu, N.; Liu, C.; Xu, Q.; Jin, Z. *Eur. J. Org. Chem.* **2011**, *23*, 4422. (b) Gottardo, C.; Aguirre, A. *Tetrahedron Lett.* **2002**, *43*, 7091.

[41] Holmes, A. B.; Sporikou, C. N. *Org. Synth., Coll.* **1987**, *65*, 61.

3. Experimental Section

General remarks. All reactions were performed under an inert atmosphere of argon using flame or oven dried glassware on a dual-manifold Schlenk line unless otherwise indicated. The solvents; diethyl ether, methylene chloride, methanol, acetone, pentane, and hexane were purchased from Fisher Chemical Co, and distilled over appropriate drying agents under nitrogen prior to use then stored over activated molecular sieves. Chloroform-*d*, deuterium oxide, dimethyl sulfoxide-d_6, and benzene-d_6 were purchased from Cambridge Isotopes Inc. and dried over activated molecular sieves before use. All the other chemicals were purchased from Sigma-Aldrich Chemical Co. Phenylacetylene, 3-phenyl-1-propyne, 4-ethynyltoluene, and piperidine were distilled prior to use. Absolute ethanol, 3-ethynylaniline, 2-ethynylpyridine, 3-ethynylpyridine, and other commercially available reagents were used as received.

Most of the dialkynyl cyclooctadiene precursor complexes were synthesized following a modified literature procedure.[1] The following compounds were prepared according to a literature (or modified) procedure: PtX(Me)(COD) (X = Cl, Br, I) [COD = η^4-(1,5-cyclooctadiene)],[2] PtCl(Et)(COD),[3, 4] PtX(Et)(COD) (X = Br, I),[4, 5] $PdCl_2$(COD),[5] PdX(Me)(COD) (X = Cl, Br),[4, 5] PdI(Me)(COD),[4] $Pt(C_2Ph)_2$(COD),[5] *cis*-$PtCl_2(PTA)_2$,[6] *cis*-$PdCl_2(PTA)_2$,[7] *cis*-$PtCl_2(DAPTA)_2$,[6, 7, 8] *cis*-$PdCl_2(DAPTA)_2$,[7, 8] MX_2(COD) (M = Pt, Pd; X = Br, I).[9] *N,N'*-diacetyl-1,3,5-triaza-7-phosphaadamantane (DAPTA) was prepared following a modified literature procedure.[10] $Pt_3(nbe)_2(dppa)_4$, $Pt_2(dppm)_3$,[11a] $PtMe_2$(dppp),[11b] $PtMe_2$(dppe),[11c] 1-hydrido-1-methyl(tetraphenyl)silole,[12a] 1,1-dihydrido(tetraphenyl)germole,[12b] and 1-hydrido-1-methylsilafluorene[12c] were also

synthesized by using literature procedures. The following compounds were reported in the literatures: **H1**,[13a] **H2**,[13b] **H3**,[13c] **H11**,[13a] **H13**,[13d] **H14**,[13d] **H15**,[13d] **P1**,[14a] **P2**,[14b] **P3**,[14c] **P4**,[14d] **P5**,[14e] **P6**,[14d] **P7**,[14f] **P8**,[14d] and **P9**[14g].

NMR spectra were recorded on a Bruker Avance-300 MHz or Bruker ARX-500 MHz instrument at ambient temperature. Spectroscopic data were recorded at 300 MHz or 500 MHz, respectively for ^{1}H, 75 MHz or 125 MHz, respectively for ^{13}C, 121 or 202 MHz, respectively for ^{31}P, and 99 MHz for ^{29}Si. Unless otherwise stated, chloroform-*d* was used as the NMR solvent. Proton, carbon, phosphorus, and silicon chemical shifts (δ) are reported relative to the residual protio and deuterio solvent resonances, external H_3PO_4, and external tetramethylsilane respectively. Chemical shifts are reported in ppm and the coupling constants in Hertz (Hz). Melting point determinations were obtained on a Mel-Temp melting point apparatus and are uncorrected. Gas chromatography experiment was performed on a Shimadzu gas chromatograph (GC-14A) and GC-MS analysis was carried out on a Hewlett Packard-Model 5988A GC-MS instrument. Mass spectral data were obtained in FAB or EI mode with nitrobenzyl alcohol (NBA) on a JEOL MStation-JMS700. Infrared spectra were recorded on a Thermo-Nicolet Avatar 360-FT IR spectrometer. HPLC-MS (ESI) spectral data were recorded on an Agilent HPLC-MS instrument. UV-Vis and Fluorescence spectra were recorded on a Cary 50 Bio UV-Vis Spectrophotometer and Cary Eclipse Fluorescence Spectrophotometer, respectively. SEM images were acquired on a JEOL JSM-6320F instrument and EDS spectra were recorded on an Oxford EDS instrument. Elemental analysis determinations were performed by Atlantic Microlabs, Inc., Norcross, GA. The X-ray crystallographic data were collected on a Bruker Apex II diffractometer equipped with a CCD area detector.

3.1. Synthesis of Platinum and Palladium PTA and DAPTA Complexes

3.1.1 Synthesis and characterization of some Pt(II) and Pd(II)-COD complexes

Synthesis of $PdMe_2$(COD), C1. $PdMe_2$(COD) (COD = 1,5-cyclooctadiene) was prepared by a modified literature procedure.[15] In a three-necked 100 mL round bottom flask was placed $PdCl_2$(COD) (0.288 g, 1.00 mmol) and 15 mL of dry Et_2O was added to form a yellow suspension. The reaction mixture was cooled to -78 ^oC and a methyllithium (1.3 mL, 208 mmol, 1.6 M) solution in ether was added dropwise through a syringe with continuous stirring. The mixture was stirred at -41 ^oC for 1 h and the volatiles were removed *in vacuo* at 0 ^oC. The resulting residue was extracted with 20 mL of *n*-pentane at 0 ^oC to yield a clear colorless extract. The volatiles were removed *in vacuo* at 0 ^oC to yield a white powder of **C1** (0.140 g, 58% yield). The product was stored below -30 ^oC. ^1H NMR (300 MHz, $CDCl_3$): δ 5.43 (br, 4H), 2.51-2.35 (m, 8H), 0.34 (s, 6H). The product was found to be too unstable for other characterizations.

Synthesis of [Pt{C_2(*m*-$C_6H_4NH_2$)}$_2$(COD)], C2. A representative synthesis is described as follows. In a 100 mL three-necked round bottom flask equipped with a 25 mL addition funnel and a magnetic stir bar was placed $PtCl_2$(COD) (0.100 g, 0.267 mmol). Absolute ethanol (30 mL) was added to the flask and the resulting suspension was stirred for 5 min. Triethylamine (0.080 g, 0.801 mmol) was added to the suspension followed by the dropwise addition of 3-ethynylaniline (0.309 g, 2.67 mmol) over 5 min with stirring. Absolute ethanol (5 mL) was added and the solution was stirred over 16 h and a white precipitate gradually formed. The resulting mixture was filtered using a sintered glass frit. The white solid was washed with methanol (3 x 5 mL) and dried in a

vacuum desiccator for 6 h. The solid was dissolved in a minimal amount of CH_2Cl_2 and filtered. The filtrate containing **C2** was evaporated and the resultant precipitate was then washed with 5 mL of diethyl ether and dried *in vacuo*. **C2** was obtained as an off-white solid (0.111 g, 78% yield). ^{1}H NMR (300 MHz): δ 7.03 (t, J = 7.8 Hz, 2H), 6.84 (m, 2H), 6.77 (m, 2H), 6.53 (m, 2H), 5.69 (br, J_{PtH} = 45.0 Hz, 4H), 3.58 (br, 4H, NH_2), 2.58 (br, 8H).

[Pt{C_2(*p*-tol)}$_2$(COD)], C3. Reagents used: $PtCl_2$(COD) (0.100 g, 0.267 mmol, triethylamine (0.080 g, 0.801 mmol), and 4-ethynyltoluene (0.307 g, 2.67 mmol). **C3** was obtained as a white solid (0.121 g, 85% yield). ^{1}H NMR (300 MHz): δ 7.32-7.23 (m, 4H), 7.07-6.98 (m, 2H), 5.66 (br, J_{PtH} = 44 Hz, 4H), 2.54 (br, 8H), 2.28 (s, 6H).

[Pt{C_2(*o*-py)}$_2$(COD)], C4. Reagents used: $PtCl_2$(COD) (0.100 g, 0.267 mmol, triethylamine (0.080 g, 0.801 mmol), and 2-ethynylpyridine (0.275 g, 2.67 mmol). **C4** was obtained as an off-white solid (0.107 g, 79% yield). ^{1}H NMR (300 MHz, $CDCl_3$): δ 8.48 (m, 2H), 7.53 (dt, J = 7.7 Hz, 1.8 Hz, 2H), 7.40 (m, 2H), 7.08-7.03 (m, 2H), 5.78 (br, J_{PtH} = 45 Hz, 4H), 2.56 (br, 8H).

[Pt{C_2(*m*-py)}$_2$(COD)], C5. Reagents used: $PtCl_2$(COD) (0.100 g, 0.267 mmol), triethylamine (0.080 g, 0.801 mmol), and 3-ethynylpyridine (0.275 g, 2.67 mmol). **C5** was obtained as an off-white solid (0.110 g, 81% yield). ^{1}H NMR (300 MHz, $CDCl_3$): δ 8.64 (d, J = 1.3 Hz, 2H), 8.41 (dd, J = 4.8 Hz, 1.6 Hz, 2H), 7.68 (dt, J = 6.0 Hz, 1.8 Hz, 2H), 7.18-7.12 (m, 2H), 5.76 (br, J_{PtH} = 43 Hz, 4H), 2.63 (br, 8H).

3.1.2 Synthesis of Platinum(II) and Palladium(II)-PTA and DAPTA Complexes

Synthesis of *cis*-$PtMe_2(PTA)_2$ (1a). A solution of *cis*-$PtMe_2(COD)$ (0.217 g, 0.651 mmol) in dichloromethane (45 mL) was placed in a 100 mL round bottom flask equipped with a 25 mL addition funnel and a magnetic stir bar. A solution of 1,3,5-triaza-7-phosphaadamantane (PTA) (0.204 g, 1.30 mmol) in methanol (45 mL) was added dropwise with stirring over 10 min. The reaction solution was stirred for 14 h at room temperature. The colorless reaction mixture was then evaporated to dryness on a rotary evaporator and the resulting white residue was washed with diethyl ether (3 x 20 mL). The solid was filtered and dried under vacuum at room temperature for 10 min. Complex **1a** was obtained as a white solid (0.316 g, 90% yield), Mp 231-233 ^{o}C. X-ray quality crystals of **1a** were obtained by slow diffusion of Et_2O to $CHCl_3$ solution of **1a** at low temperature (below 0 ^{o}C). ^{1}H NMR (300 MHz): δ 4.59, 4.54, 4.49, and 4.45 (br, 12H, NCH_2), 4.08 (br, 12H, PCH_2), 0.47 (m, $^{2}J_{PtH}$ = 68 Hz, 6H, Pt-CH_3). $^{13}C\{^{1}H\}$ NMR (75 MHz): δ 73.6 (vt, NCH_2, $^{3}J_{PC}$ = 3 Hz), 52.7 (m, $^{1}J_{PC}$ = 8.6 Hz, PCH_2), -0.01 (dd, $^{1}J_{PtC}$ = 581 Hz, $^{2}J_{PC(trans)}$ = 94.8 Hz, $^{2}J_{PC(cis)}$ = 9.5 Hz, Pt-CH_3). $^{31}P\{^{1}H\}$ NMR (121 MHz): δ -63.4 ($^{1}J_{PtP}$ = 1608 Hz). MS (FAB): *m/z (%)* 539 (10, M^+), 524 (30, -CH_3), 307 (100), 289 (51). HRMS (FAB): *m/z* calcd for $C_{13}H_{27}N_6P_2Pt$, 524.1420; found: 524.1422 **[**$(M\text{-}CH_3)^+$]. Anal. Calcd for $C_{14}H_{30}N_6P_2Pt$: C, 31.17; H, 5.61. Found: C, 31.26; H, 5.64.

On extending the reaction time to 20 h, complex **1a** appears to undergo slow isomerization to give a mixture of **1a** and *trans*-$PtMe_2(PTA)_2$, **1b** in approximately in 16:1 ratio, respectively. $^{31}P\{^{1}H\}$ NMR (121 MHz): δ -60.4 ($^{1}J_{PtP}$ = 2777 Hz, **1b**), -63.4 ($^{1}J_{PtP}$ = 1608 Hz, **1a**).

Synthesis of *trans*-PtX(Me)(PTA)$_2$ [X = Cl (2a); X = Br (2b); X = I (2c)]. A representative synthesis is described for complex **2a**. To a 100 mL round bottom flask equipped with a 25 mL addition funnel and a magnetic stir bar was placed PtCl(Me)(COD) (0.067 g, 0.189 mmol) dissolved in 10 mL of dichloromethane. A solution of PTA (0.060 g, 0.382 mmol) in methanol (10 mL) was added dropwise with stirring over 10 min. The reaction solution was stirred for 14-15 h at room temperature. The volatiles were removed *in vacuo* to give a white precipitate that was washed with diethyl ether (3 x 5 mL). The precipitate was filtered and dried *in vacuo* at room temperature. Complex **2a** was obtained as a white powder (0.094 g, 86% yield), Mp 278-280 ^{o}C. ^{1}H NMR (300 MHz): δ 4.50 and 4.40 (br, 12H, NCH_2), 4.24 (br, 12H, PCH_2), 0.30 (t, $^{2}J_{PtH}$ = 82 Hz, $^{3}J_{PH}$ = 7.1 Hz, 3H, Pt-CH_3). ^{31}P{^{1}H} NMR (121 MHz): δ -60.4 ($^{1}J_{PtP}$ = 2779 Hz). MS (FAB): *m/z (%)* 559 (30, M^+), 544 (25, -CH_3), 524 (35, -Cl), 307 (100), 289 (48). Anal. Calcd for $C_{13}H_{27}N_6P_2ClPt$: C, 27.89; H, 4.86. Found: C, 27.86; H, 4.77.

***trans*-PtBr(Me)(PTA)$_2$ (2b)**. Reagents used: PtBr(Me)(COD) (0.064 g, 0.16 mmol) in 10 mL of dichloromethane and PTA (0.052 g, 0.331 mmol) in 10 mL of methanol. Complex **2b** was obtained as a white powder (0.090 g, 93% yield), Mp 231 ^{o}C (dec). ^{1}H NMR (300 MHz): δ 4.50 (br, 12H, NCH_2), 4.25 (br, 12H, PCH_2), 0.36 (t, 3H, $^{2}J_{PtH}$ = 81 Hz, $^{3}J_{PH}$ = 7 Hz, Pt-CH_3). ^{31}P{^{1}H} NMR (121 MHz): δ -63.4 ($^{1}J_{PtP}$ = 2748 Hz). MS (FAB): *m/z (%)* 605 [72, $(M+H)^+$], 589 (46, -CH_3), 307 (100), 289 (58). HRMS (FAB): *m/z* calcd for $C_{13}H_{28}N_6P_2{}^{79}Br^{195}Pt$, 604.0682; found: 604.0697 [$(M+H)^+$]. Anal. Calcd for $C_{13}H_{27}N_6P_2BrPt$: C, 25.84; H, 4.50. Found: C, 25.75; H, 4.50.

***trans*-PtI(Me)(PTA)$_2$ (2c)**. Reagents used: PtI(Me)(COD) (0.040 g, 0.089 mmol) in 10 mL of dichloromethane and PTA (0.028 g, 0.178 mmol) in 10 mL of methanol. Complex **2c** was obtained as a pale yellow solid (0.050 g, 88% yield), Mp 261-263 ^{o}C. ^{1}H NMR (300 MHz): δ 4.51 and 4.48 (br, 12H, NCH_2), 4.31 (br, 12H, PCH_2), 0.47 (t, 3H, $^{2}J_{PtH}$ = 79 Hz, $^{3}J_{PH}$ = 7.1 Hz, Pt-CH_3). ^{31}P{^{1}H} NMR (121 MHz): δ -67.9 ($^{1}J_{PtP}$ = 2690 Hz). MS (FAB): *m/z (%)* 652 [53, $(M+H)^+$], 636 (58, -CH_3), 566 (19), 524 (15, -I), 307 (100), 289 (57). HRMS (FAB): *m/z* calcd for $C_{13}H_{28}N_6P_2IPt$, 652.0543; found: 652.0518 [$(M+H)^+$]: HRMS (FAB): *m/z* calcd for $C_{12}H_{24}N_6P_2IPt$, 636.0230; found: 636.0242 **[**$(M-CH_3)^+$**]**. Anal. Calcd for $C_{13}H_{27}N_6P_2IPt$: C, 23.97; H, 4.18. Found: C, 23.95; H, 4.25.

Synthesis of *trans*-PtX(Et)(PTA)$_2$ [X = Cl (3a); X = Br (3b); X = I (3c)]. A representative synthesis is described for complex **3a**. To a 100 mL round bottom flask equipped with a 25 mL addition funnel and a magnetic stir bar was placed PtCl(Et)(COD) (0.125 g, 0.340 mmol) in 10 mL of dichloromethane. A solution of PTA (0.106 g, 0.675 mmol) in 10 mL of methanol was added dropwise with stirring over 10 min. The reaction solution was stirred for 14-15 h at room temperature. The resulting colorless solution was evaporated *in vacuo* and the residue was washed with diethyl ether (3 x 5 mL). The white residue was filtered and dried *in vacuo* at room temperature. Complex **3a** was obtained as a white solid (0.268 g, 76% yield), Mp 240-242 ^{o}C. X-ray quality crystals of **3a** were obtained by slow diffusion of diethyl ether to a methylene chloride solution of **3a** at low temperature (below 0 ^{o}C). ^{1}H NMR (300 MHz): δ 4.49 (br, 12H, NCH_2), 4.26 (br, 12H, PCH_2), 1.25-0.85 (m, 5H, Pt-CH_2CH_3). ^{31}P{^{1}H} NMR (121 MHz): δ -60.3 ($^{1}J_{PtP}$ = 2961 Hz). MS (FAB): *m/z (%)* 575 [44, $(M+2H)^+$], 545 (71, -C_2H_5), 509 (71, -Cl), 307 (100), 289 (48). HRMS (FAB): *m/z* calcd for $C_{14}H_{30}N_6P_2ClPt$,

574.1343; found: 574.1337 $(M+H)^+$. HRMS(FAB): *m/z* calcd for $C_{12}H_{24}N_6P_2ClPt$, 544.0874; found: 544.0878 [$(M-C_2H_5)^+$]. Anal. Calcd for $C_{14}H_{29}N_6P_2ClPt$: C, 29.27; H, 5.09. Found: C, 28.66; H, 5.12.

***trans*-PtBr(Et)(PTA)$_2$ (3b)**. Reagents used: PtBr(Et)(COD) (0.037 g, 0.090 mmol) in 10 mL of dichloromethane and PTA (0.029 g, 0.184 mmol) in 10 mL of methanol. Complex **3b** was obtained as an off-white solid (0.042 g, 76% yield), Mp 282 ^oC (dec). NMR data were collected in anhydrous $CDCl_3$. ^1H NMR (500 MHz): δ 4.49 (br, 12H, NCH_2), 4.29 (br, 12H, PCH_2), 1.57 (s, 2H, H_2O), 1.27-0.94 (m, 5H, Pt-CH_2CH_3). $^{31}P\{^1H\}$ NMR (121 MHz): δ -63.1 ($^1J_{PtP}$ = 2926 Hz). MS (FAB): *m/z* (%) 619 [15, $(M+2H)^+$], 589 (17, -C_2H_5), 509 (15, -Br), 307 (100), 289 (56). HRMS (FAB): *m/z* calcd for $C_{14}H_{30}N_6P_2{}^{81}Br^{195}Pt$, 620.0818; found: 620.0821 [$(M+H)^+$]. Anal. Calcd for $C_{14}H_{29}N_6P_2BrPt\cdot H_2O$: C, 26.42; H, 4.91. Found: C, 26.19; H, 4.98.

***trans*-PtI(Et)(PTA)$_2$ (3c)**. Reagents used: PtI(Et)(COD) (0.050 g, 0.108 mmol) in 10 mL of dichloromethane and PTA (0.034 g, 0.218 mmol) in 10 mL of methanol. Complex **3c** was obtained as a white solid (0.044 g, 63% yield), Mp 289 ^oC (dec). $^{31}P\{^1H\}$ NMR (121 MHz): δ -67.7 ($^1J_{PtP}$ = 2867 Hz). MS (FAB): *m/z* (%) 666 [19, $(M+H)^+$], 636 (55, -C_2H_5), 566 (20), 509 (20, -I), 307 (100), 289 (58). HRMS (FAB): *m/z* calcd for $C_{14}H_{30}N_6P_2IPt$, 666.0699; found: 666.0690 [$(M+H)^+$]. Anal. Calcd for $C_{14}H_{29}N_6P_2IPt\cdot CH_2Cl_2$: C, 24.01; H, 4.16. Found: C, 23.55; H, 4.27.

***trans*-PtCl$_2$(PTA)$_2$ (4).** When **2a** was subjected to crystallization in CH_2Cl_2 solution by slow diffusion of *n*-pentane at low temperature (below 0 ^oC), X-ray quality single crystals of **4** were obtained. Mp 201 ^oC (dec). ^1H NMR (300 MHz): δ 4.47 (br, 12H,

NCH_2), 4.22 (br, 12H, PCH_2). $^{13}C\{^1H\}$ NMR (75 MHz, DMSO-d_6): δ 72.1 (vt, $^3J_{PC}$ = 4.1 Hz, NCH_2), 51.7 (m, $^1J_{PC}$ = 12 Hz, PCH_2). $^{31}P\{^1H\}$ NMR (121 MHz): δ -60.4 ($^1J_{PtP}$ = 2778 Hz).

Synthesis of *trans*-PdX(Me)(PTA)$_2$ [X = Cl (5a); X = Br (5b); X = I (5c)]. A representative synthesis is described for complex **5a**. To a 100 mL round bottom flask equipped with a 25 mL addition funnel and a magnetic stir bar was placed PdCl(Me)(COD) (0.050 g, 0.189 mmol) in 10 mL of dichloromethane. A solution of PTA (0.061 g, 0.388 mmol) in 10 mL of methanol was added dropwise with stirring over 8 min. The reaction solution was stirred for 14-15 h at room temperature. The resulting solution was evaporated *in vacuo* and the precipitate was washed with diethyl ether (3 x 5 mL). The white residue was filtered and dried *in vacuo* at room temperature. Complex **5a** was obtained as a white solid (0.065 g, 77% yield), Mp 229 ^oC (dec). Complex **5a** was stored below 0 ^oC due to slow decomposition upon standing at room temperature. ^1H NMR (300 MHz): δ 4.52 (br s, 12H, NCH_2), 4.24 (br s, 12H, PCH_2), 0.09 (t, 3H, $^3J_{PH}$ = 6.9 Hz, Pd-CH_3). $^{31}P\{^1H\}$ NMR (121 MHz): δ -62.2. MS (FAB): *m/z* (%) 473 [65, $(M+3H)^+$], 435 (68, -Cl), 307 (100), 289 (58), 278 (31). HRMS (FAB): *m/z* calcd for $C_{13}H_{28}N_6P_2ClPd$, 471.0573; found: 471.0589 [$(M+H)^+$]. Due to the thermal instability of complex **5a** no elemental analysis data were obtained.

***trans*-PdBr(Me)(PTA)$_2$ (5b)**. Reagents used: PdBr(Me)(COD) (0.050 g, 0.162 mmol) in 10 mL of dichloromethane and PTA (0.051 g, 0.324 mmol) in 10 mL of methanol. Complex **5b** was obtained as an off-white solid (0.073 g, 88% yield), Mp 250 ^oC (dec). Complex **5b** was stored below 0 ^oC due to slow decomposition upon standing at room temperature. ^1H NMR (300 MHz): δ 4.51 (s, 12H, NCH_2), 4.26 (s, 12H, PCH_2),

0.21 (t, 3H, $^3J_{PH}$ = 6.9 Hz, Pd-CH_3). $^{31}P\{^1H\}$ NMR (121 MHz): δ -64.6. MS (FAB): *m/z* (%) 517 [30, $(M+2H)^+$], 501 (22, -CH_3), 313 (26), 307 (100), 289 (49). HRMS (FAB): *m/z* calcd for $C_{13}H_{28}N_6P_2{}^{79}BrPd$, 515.0068; found: 515.0062 $[(M+H)^+]$. Due to the thermal instability of complex **5b** no elemental analysis data were obtained.

***trans*-PdI(Me)(PTA)$_2$ (5c)**. Reagents used: PdI(Me)(COD) (0.028 g, 0.078 mmol) in 10 mL of dichloromethane and PTA (0.025 g, 0.159 mmol) in 10 mL of methanol. Complex **5c** was obtained as a yellow solid (0.030 g, 68% yield), Mp 258 ^oC (dec). ^1H NMR (300 MHz): δ 4.53 and 4.51 (br s, 12H, NCH_2), 4.31 (br s, 12H, PCH_2), 0.30 (t, 3H, $^3J_{PH}$ = 6.7 Hz, Pd-CH_3). $^{31}P\{^1H\}$ NMR (121 MHz): δ -66.9. MS (FAB): *m/z (%)* 563 (64, M^+), 548 (41, -CH_3), 435 (55, -I), 419 (25), 307 (100), 289 (48). HRMS (FAB): *m/z* calcd for $C_{13}H_{28}N_6P_2IPd$, 562.9930; found: 562.9943 $[(M+H)^+]$. Anal. Calcd for $C_{13}H_{27}N_6P_2IPd$: C, 27.72; H, 4.84. Found: C, 27.32; H, 4.77.

Synthesis of *cis*- and *trans*-Pt(C$_2$Ph)$_2$(PTA)$_2$ (6a and 6b, respectively).

(i) Short reaction time optimized to produce *cis*-Pt(C$_2$Ph)$_2$(PTA)$_2$ (6a). In a 100 mL round bottom flask equipped with a 25 mL addition funnel and a magnetic stir bar was placed $Pt(C_2Ph)_2(COD)$ (0.021 g, 0.041 mmol) [8] in 10 mL of dichloromethane. A solution of PTA (0.013 g, 0.083 mmol) in 10 mL of methanol was added dropwise with stirring over 8 min. The reaction solution was stirred for 1 h at room temperature. The resulting colorless solution was evaporated *in vacuo* and the white residue formed was washed with diethyl ether (3 x 5 mL). The residue was then dried *in vacuo* at room temperature. Complex **6a** was obtained as a white powder (0.025 g, 86% yield), Mp 285 ^oC (dec). The NMR data indicated the presence of both isomers **6a** (major) and **6b**,

however when the reaction was run for a longer period of time the *trans*- isomer **6b** was the major isomer produced (see below). Attempts to crystallize **6a** by slow diffusion of diethyl ether into a methylene chloride solution of **6a** below 0 ^{o}C resulted in the isolation of crystals of *trans*-Pt(C_2Ph)$_2$(PTA)$_2$ (**6b**). X-ray quality crystals of **6b** were also isolated from the extended reaction time experiment (see below). The ^{1}H NMR spectrum data for both reactions were essentially identical and thus the ratio of the isomers could not be determined from the peak integration. The NMR data were collected in anhydrous $CDCl_3$. ^{1}H NMR (300 MHz): δ 7.45-7.15 (m, 10H, Ph, overlapping with the $CDCl_3$ signal), 4.59, 4.56, 4.54, 4.51, 4.48, 4.42 (br, 12H, NCH_2), 4.34 (br, 12H, PCH_2), 1.59 (s, 2H_2O). ^{13}C{^{1}H} NMR (125 MHz): δ 131.6 (Ph, **6a**), 131.4 (Ph, **6b**), 128.4 (Ph, **6b**), 128.1 (Ph, **6a**), 127.34 (Ph, **6a**, overlapping with shoulder for **6b** at 127.30), 126.28 (Ph, **6a**, overlapping with shoulder for **6b** at 127.33), 113.1 (s, C_a≡C_bPh, $^{2}J_{PtC}$ not resolved, **6b**), 99.7 (vt, AXX', ^{3}J (C_b, P_{trans}) + ^{3}J(C_b, P_{cis}) = 16.5 Hz, C_a≡C_bPh, $^{2}J_{PtC}$ not resolved, **6a**), 98.0 (dd, ^{2}J (C_a, P_{trans}) = 143 Hz, ^{2}J(C_a, P_{cis}) = 12.6 Hz, C_a≡C_bPh, $^{1}J_{PtC}$ not resolved, **6a**), 94.9 (s, $^{1}J_{PtC}$ not resolved, **6b**) 73.6 (NCH$_2$, **6b**), 73.5 (NCH$_2$, **6a**), 53.4 (vt, $^{1}J_{PC}$ = 12.2 Hz, PCH$_2$, **6a**), 51.7 (vt, $^{1}J_{PC}$ = 11.9 Hz, PCH$_2$, **6b**). ^{31}P{^{1}H} NMR (121 MHz): δ -69.9 ($^{1}J_{PtP}$ = 2071 Hz, **6a**) (no resonance was observed for **6b**). IR (KBr) (ν, cm^{-1}): 2103, 2042 (C≡C). MS (FAB): *m/z (%)* 712 [100, (M+H)$^{+}$], 610 (16, -C_2Ph), 509 (22, -2C_2Ph), 425 (16), 307 (100), 289 (62). HRMS (FAB): *m/z* calcd for $C_{28}H_{35}N_6P_2Pt$, 712.2045; found: 712.2033 [(M+H)$^{+}$]. Anal. Calcd for $C_{28}H_{34}N_6P_2Pt\cdot 2H_2O$: C, 44.98; H, 5.12. Found: C, 44.87; H, 4.74.

(ii) Extended reaction time to produce *trans*-Pt(C_2Ph)$_2$(PTA)$_2$ (6b). In a 100 mL three-necked round bottom flask equipped with a 25 mL addition funnel and a magnetic

stir bar was placed *cis*-$PtCl_2(PTA)_2$ (0.100 g, 0.172 mmol). Absolute ethanol (30 mL) was added to the flask and the resulting suspension was stirred for 5 min. Triethylamine (0.050 g, 0.500 mmol) was added to the suspension followed by the dropwise addition of phenylacetylene (0.035 g, 0.346 mmol) over 5 min with stirring. Absolute ethanol (5 mL) was added and the solution was stirred over 16 h and a white precipitate gradually formed. The resulting mixture was filtered using a sintered glass frit. The white solid was washed with methanol (3 x 5 mL) and dried in a vacuum desiccator for 6 h. The solid was dissolved in a minimal amount of CH_2Cl_2 and filtered. The filtrate containing **6b** was evaporated and the resultant precipitate was then washed with 5 mL of diethyl ether and dried *in vacuo*. Complex **6b** was obtained as a white solid (0.099 g, 81% yield), Mp 312 ^oC (dec). Complex **6b** slowly isomerizes to give a mixture of with the *cis* isomer **6a** upon standing for long periods in solution at room temperature. Crystals of **6b** suitable for X-ray crystallography were obtained by slow diffusion of diethyl ether to a methylene chloride solution of **6b** at low temperature (below 0 ^oC). $^{31}P\{^1H\}$ NMR (121 MHz): δ -64.3 ($^1J_{PtP}$ = 2309 Hz) (no signal was observed for **6a**). IR (KBr) (ν, cm^{-1}): 2104, 2038 (C≡C). MS (FAB): *m/z (%)* 712 [18, $(M+H)^+$], 545 (15), 307 (98), 289 (58). HRMS (FAB): *m/z* calcd for $C_{28}H_{35}N_6P_2Pt$, 712.2045; found: 712.2054 [$(M+H)^+$]. Anal. Calcd for $C_{28}H_{34}N_6P_2Pt\cdot CH_2Cl_2$: C, 43.81; H, 4.57. Found: C, 44.75; H, 4.71.

Synthesis of *trans*-$Pd(C_2Ph)_2(PTA)_2$ (7). In a 100 mL three-necked round bottom flask equipped with a 25 mL addition funnel and a magnetic stir bar was placed *cis*-$PdCl_2(PTA)_2$ (0.100 g, 0.203 mmol), in 30 mL of absolute ethanol. The resulting suspension was stirred for 5 min. Then triethylamine (0.059 g, 0.590 mmol) was added to the suspension followed by the dropwise addition of phenylacetylene (0.042 g, 0.411

mmol) over 5 min. Additional absolute ethanol (5 mL) was added and solution was stirred at room temperature for 7 h resulting in the gradual formation of a white precipitate. The solution was filtered using a sintered glass frit and the precipitate was washed with methanol (3 x 5 mL) and dried in a vacuum desiccator for 6 h. The solid was dissolved in a minimal amount of CH_2Cl_2 and filtered. The filtrate containing **7** was evaporated and the resultant precipitate was then washed with 5 mL of diethyl ether and dried *in vacuo***.** Complex **7** was obtained as a white solid (0.099 g, 86% yield), Mp 230 ^oC (dec). Complex **7** was found to be unstable in solution upon standing for extended periods of time. The NMR data were collected in anhydrous $CDCl_3$. ^1H NMR (500 MHz): δ 7.63-7.40 (m, 4H, Ph), 7.29-7.18 (m, 6H, Ph), 4.56 (br, 12H, NCH_2), 4.45 (br, 12H, PCH_2), 1.55 (s, 2H, H_2O). $^{13}C\{^1H\}$ NMR (125 MHz): δ 131.4 (Ph), 128.4 (Ph), 126.9 (Ph), 126.5 (Ph), 114.6 ($C_a{\equiv}C_b$Ph), 108.9 ($C_a{\equiv}C_b$Ph), 73.6 (NCH_2), 52.7 (vt, $^1J_{PC}$ = 8.5 Hz, PCH_2). $^{31}P\{^1H\}$ NMR (121 MHz): δ -56.3. IR (KBr) (ν, cm^{-1}): 2108, 2042 (C≡C). MS (FAB): *m/z (%)* 622 (40, M^+), 594 (25), 521 (52, -C_2Ph), 307 (100), 289 (51). HRMS (FAB): *m/z* calcd for $C_{20}H_{29}N_6P_2Pd$, 521.0963; found: 521.0966 [(M-$C_2Ph)^+$]. Anal. Calcd for $C_{28}H_{34}N_6P_2Pd{\cdot}H_2O$: C, 52.46; H, 5.66. Found: C, 52.08; H, 5.60.

Synthesis of *trans*-M($C_2SiMe_3)_2(PTA)_2$ [M = Pt (8a); M = Pd (8b)]. A representative synthesis is described for complex **8a**. In a 100 mL three-necked round bottom flask equipped with a 25 mL addition funnel and a magnetic stir bar was placed *cis*-$PtCl_2(PTA)_2$ (0.09 g, 0.155 mmol). Absolute ethanol (30 mL) was added to the flask and the resulting suspension was stirred for 5 min. Triethylamine (0.047 g, 0.465 mmol) was added to the suspension through a syringe followed by the dropwise addition of

trimethylsilylacetylene (0.152 g, 1.55 mmol) over 5 min with stirring. Absolute ethanol (5 mL) was added and the solution was stirred for 16-17 h and a white precipitate was gradually formed. The resulting mixture was filtered using a sintered glass frit. The white solid was washed with methanol (3 x 5 mL) and dried in a vacuum desiccator for 6 h. The solid was then washed with 5 mL of diethyl ether and dried *in vacuo*. Complex **8a** was obtained as a white solid (0.075 g, 69% yield), Mp 297 ^{o}C (dec). Complex **8a** was found to undergo slow decomposition and turned grey when stored at room temperature. ^{1}H NMR (300 MHz): δ 4.57, 4.53, 4.49, 4.45 (br, 12H, NCH_2), 4.30 (br, 12H, PCH_2), 0.15 (br, 18H, SiCH_3). ^{29}Si{^{1}H} NMR (99 MHz): δ -24.0. ^{31}P{^{1}H} NMR (121 MHz): δ -66.4 ($^{1}J_{PtP}$ = 2343 Hz). IR (KBr) (ν, cm^{-1}): 2112, 2054 (C≡C). MS (FAB): *m/z (%)* 704 (40, M^{+}), 606 (15, -C_2SiMe_3), 307 (100), 289 (54). HRMS (FAB): *m/z* calcd for $C_{22}H_{43}N_6P_2Si_2Pt$, 704.2210; found: 704.2237 [$(M+H)^{+}$]. Anal. Calcd for $C_{22}H_{42}N_6P_2Si_2Pt$: C, 37.54; H, 6.01. Found: C, 38.62; H, 6.15.

***trans*-Pd(C_2SiMe_3)$_2$(PTA)$_2$ (8b)**. Reagents used: *cis*-$PdCl_2(PTA)_2$ (0.075 g, 0.152 mmol), triethylamine (0.046 g, 0.458 mmol) and trimethylsilylacetylene (0.149 g, 1.52 mmol) in 35 mL of absolute ethanol. Reaction time: 76 h. Complex **8b** was obtained as a yellow solid (0.056 g, 60% yield), Mp 203 ^{o}C (dec). Complex **8b** was stored below 0 ^{o}C due to slow decomposition upon standing at room temperature. ^{1}H NMR (300 MHz): δ 4.53 (br, 12H, NCH_2), 4.33 (br, 12H, PCH_2), 0.15 (br, 18H, SiCH_3). ^{29}Si{^{1}H} NMR (99 MHz): δ -24.3. ^{31}P{^{1}H} NMR (121 MHz): δ -58.8. IR (KBr) (ν, cm^{-1}): 2108, 2042 (C≡C). MS (FAB + NaI): *m/z (%)* 669 [10, $(M\text{-}Me_3Si)^{+}$+I], 637 [18, $(M+Na)^{+}$], 517 (15), 360 (28), 326 (100), 254 (100). HRMS (FAB + NaI): *m/z* calcd for

$C_{22}H_{42}N_6P_2Si_2NaPd$, 637.1417; found: 637.1412 [$(M+Na)^+$]. Complex **8b** was not stable enough for elemental analysis.

Synthesis of *cis*-PtMe$_2$(DAPTA)$_2$ (9a). A solution of *cis*-$PtMe_2(COD)$ (0.050 g, 0.150 mmol) in dichloromethane (20 mL) was placed in a 100 mL round bottom flask equipped with a 25 mL addition funnel and a magnetic stir bar. A solution of *N,N'*-diacetyl-1,3,5-triaza-7-phosphaadamantane (DAPTA) (0.069 g, 0.301 mmol) in methanol (30 mL) was added dropwise with stirring over 10 min. The reaction solution was stirred for 14 h at room temperature. The colorless reaction mixture was then evaporated to dryness on a rotary evaporator and the resulting white residue was washed with diethyl ether (3 x 20 mL). The solid was filtered and dried under vacuum. Complex **9a** was obtained as a white solid (0.093 g, 91% yield), Mp 179-181 ^oC. ^1H NMR (300 MHz): δ 5.81 (d, J = 14.2 Hz, 2H), 5.53 (br m, 2H), 4.99 (d, J = 14.1 Hz, 2H), 4.58 (d, J = 14.1 Hz, 2H), 4.48 (br m, 2H), 4.03-3.88 (m, 4H), 3.87-3.64 (br m, 4H), 3.31 (m, 2H), 2.15, 2.12, 2.11, and 2.09 (br, 12H, $COCH_3$), 0.58 (m, $^2J_{PtH}$ = 71 Hz, 6H, Pt-CH_3). $^{13}C\{^1H\}$ NMR (75 MHz): δ 170.07 and 170.04 (s, *C*OCH_3), 169.6 (br s, *C*OCH_3), 67.3 (N*C*N), 62.1 (N*C*N), 48.3 (m, P*C*N), 44.1 (m, P*C*N), 40.4 (m, P*C*N), 21.7 and 21.3 (s, CO*C*H_3), 2.69 (dd, $^1J_{PtC}$ *ca.* 580 Hz, $^2J_{PC(trans)}$ = 9.0 Hz, $^2J_{PC(cis)}$ = 3.7 Hz, Pt-*C*H_3), 1.43 (dd, $^1J_{PtC}$ *ca.* 580 Hz, $^2J_{PC(trans)}$ = 9.8 Hz, $^2J_{PC(cis)}$ = 3.7 Hz, Pt-*C*H_3). $^{31}P\{^1H\}$ NMR (121 MHz): δ -37.8 ($^1J_{PtP}$ = 1634 Hz), -38.2 ($^1J_{PtP}$ = 1635 Hz), approximate ratio = 0.8 : 1, respectively. IR (KBr) (ν, cm^{-1}): 1617 (br, C=O). MS (FAB): *m/z (%)* 668 [15, $(M-CH_3)^+$], 460 (12), 307 (100), 289 (58). HRMS (FAB): *m/z* calcd for $C_{19}H_{35}N_6O_4P_2Pt$, 668.1832**;** found: 668.1842 [$(M-CH_3)^+$]. Anal. Calcd for $C_{20}H_{38}N_6O_4P_2Pt$: C, 35.14; H, 5.60. Found: C, 34.93; H, 5.74.

Heating a solution of **9a** in CH_2Cl_2 for 2 h resulted in isomerization to give possibly *trans*-$PtMe_2(DAPTA)_2$, **9b** assigned as the major product along with trace amounts of unassigned products. $^{31}P\{^1H\}$ NMR (121 MHz): δ -36.8 ($^1J_{PtP}$ = 2938 Hz, **9b**), -39.3 (unassigned, minor peak), -69.4 (unassigned, minor peak).

Synthesis of *trans*-PtX(Me)(DAPTA)$_2$ [X = Cl (10a); X = Br (10b); X = I (10c)]. A representative synthesis is described for complex **10a**. To a 100 mL round bottom flask equipped with a 25 mL addition funnel and a magnetic stir bar was placed PtCl(Me)(COD) (0.050g, 0.141 mmol) dissolved in 20 mL of dichloromethane. A solution of DAPTA (0.065 g, 0.282 mmol) in methanol (20 mL) was added dropwise with stirring over 10 min. The reaction solution was stirred for 14-15 h at room temperature. The volatiles were removed *in vacuo* to give a white precipitate that was washed with diethyl ether (3 x 5 mL). The precipitate was filtered and dried *in vacuo*. Complex **10a** was obtained as a white powder (0.077 g, 77% yield), Mp 240 ^oC (dec). ^1H NMR (300 MHz): δ 5.83 (d, J = 13.7 Hz, 2H), 5.64 (d, J = 16.1 Hz, 2H), 4.99 (d, J = 14.2 Hz, 2H), 4.71-4.56 (m, 4H), 4.24 (d, J = 15.6 Hz, 2H), 4.09-3.85 (m, 6H), 3.54 (d, J = 16.1 Hz, 2H), 2.14 and 2.13 (s, 12H, COCH_3), 0.48 (t, $^2J_{PtH}$ = 73 Hz, $^3J_{PH}$ = 6.9 Hz, 3H, Pt-CH_3). $^{31}P\{^1H\}$ NMR (121 MHz): δ -36.8 ($^1J_{PtP}$ = 2937 Hz). IR (KBr) (ν, cm^{-1}): 1625 (C=O). MS (FAB): *m/z (%)* 704 [56, $(M+H)^+$], 689 (62, -CH_3), 613 (35), 603 (30), 517 (25), 460 (20), 307 (100), 289 (100). HRMS (FAB): *m/z* calcd for $C_{19}H_{36}N_6O_4P_2ClPt$, 704.1609; found: 704.1609 [$(M+H)^+$]. Anal. Calcd for $C_{19}H_{35}N_6O_4P_2ClPt$: C, 32.41; H, 5.01. Found: C, 32.00; H, 5.17.

***trans*-PtBr(Me)(DAPTA)$_2$ (10b)**. Reagents used: PtBr(Me)(COD) (0.035 g, 0.088 mmol) in 10 mL of dichloromethane and DAPTA (0.040 g, 0.176 mmol) in 10 mL of

methanol. Complex **10b** was obtained as a white powder (0.055 g, 81% yield), Mp 252 ^{o}C (dec). ^{1}H NMR (300 MHz): δ 5.76 (d, J = 14.8 Hz, 2H), 5.60 (d, J = 17.1 Hz, 2H), 5.27 (s, 2H, CH_2Cl_2), 4.94 (d, J = 15 Hz, 2H), 4.70-4.50 (m, 4H), 4.19 (d, J = 14.9 Hz, 2H), 4.05-3.84 (m, 6H), 3.50 (d, J = 15.5 Hz, 2H), 2.07 and 2.06 (s, 12H, COCH_3), 0.50 (t, $^{2}J_{PtH}$ = 79 Hz, $^{3}J_{PH}$ = 6.8 Hz, 3H, Pt-CH_3). ^{31}P{^{1}H} NMR (121 MHz): δ -39.0 (br, $^{1}J_{PtP}$ = 2901 Hz). IR (KBr) (ν, cm^{-1}): 1638 (C=O). MS (FAB): *m/z (%)* 748 [54, $(M+H)^{+}$], 733 (64, -CH_3), 460 (13), 307 (100), 289 (55). HRMS (FAB): *m/z* calcd for $C_{19}H_{36}N_6O_4P_2{}^{81}BrPt$, 750.1083; found: 750.1086 [$(M+H)^{+}$]. Anal. Calcd for $C_{19}H_{35}N_6O_4P_2BrPt\cdot CH_2Cl_2$: C, 28.82; H, 4.47. Found: C, 29.26; H, 4.60.

***trans*-PtI(Me)(DAPTA)$_2$ (10c)**. Reagents used: PtI(Me)(COD) (0.036 g, 0.081 mmol) in 10 mL of dichloromethane and DAPTA (0.038 g, 0.162 mmol) in 10 mL of methanol. Complex **10c** was obtained as an off-white powder (0.044 g, 69% yield), Mp 222 ^{o}C (dec). ^{1}H NMR (300 MHz): δ 5.90 (d, J = 23.7 Hz, 2H), 5.73 (d, J = 15.1 Hz, 2H), 5.01 (d, J = 14.5 Hz, 2H), 4.74 (d, J = 15.9 Hz, 2H), 4.60 (d, J = 13.5 Hz, 2H), 4.27 (d, J = 14.7 Hz, 2H), 4.16-3.95 (m, 6H), 3.56 (d, J = 14.6 Hz, 2H), 2.14 (s, 12H, COCH_3), 0.66 (br s, $^{2}J_{PtH}$ = 76 Hz, 3H, Pt-CH_3). ^{31}P{^{1}H} NMR (121 MHz): δ -42.2 ($^{1}J_{PtP}$ = 2849 Hz). IR (KBr) (ν, cm^{-1}): 1634 (C=O). MS (FAB): *m/z (%)* 796 [20, $(M+H)^{+}$], 780 (26, -CH_3), 668 (12), 307 (100), 289 (63). HRMS (FAB): *m/z* calcd for $C_{19}H_{36}N_6O_4P_2IPt$, 796.0966; found: 796.0967 [$(M+H)^{+}$]. Anal. Calcd for $C_{19}H_{35}N_6O_4P_2IPt$: C, 28.68; H, 4.44. Found: C, 28.26; H, 4.67.

Synthesis of *trans*-PdX(Me)(DAPTA)$_2$ [X = Cl (11a); X = Br (11b); X = I (11c)]. A representative synthesis is described for complex **11a**. To a 100 mL round bottom flask equipped with a 25 mL addition funnel and a magnetic stir bar was placed

PdCl(Me)(COD) (0.034 g, 0.128 mmol) in 10 mL of dichloromethane. A solution of DAPTA (0.058 g, 0.256 mmol) in 10 mL of methanol was added dropwise with stirring over 8 min. The reaction solution was stirred for 14-15 h at room temperature. The resulting solution was evaporated *in vacuo* and the precipitate was washed with diethyl ether (3 x 5 mL). The white residue was filtered and dried *in vacuo*. Complex **11a** was obtained as a white solid (0.056 g, 72% yield), Mp 220 ^{o}C (dec). ^{1}H NMR (300 MHz): δ 5.80 (d, J = 14.6 Hz, 2H), 5.57 (d, J = 16.5 Hz, 2H), 5.28 (s, 2H, CH_2Cl_2), 4.97 (d, J = 14.2 Hz, 2H), 4.58 (d, J = 13.9 Hz, 4H), 4.24 (d, J = 15.1 Hz, 2H), 4.08-3.81 (m, 6H), 3.50 (d, J = 15.4 Hz, 2H), 2.10 and 2.09 (s, 12H, COCH_3), 0.32 (t, $^{3}J_{PH}$ = 6.5 Hz, 3H, Pd-CH_3). ^{31}P{^{1}H} NMR (121 MHz): δ -38.7. IR (KBr) (ν, cm^{-1}): 1629 (C=O). MS (FAB): *m/z (%)* 616 [32, $(M+2H)^{+}$], 601 (48, -CH_3), 579 (78), 566 (30), 508 (65), 307 (100), 289 (55). HRMS (FAB + CsI): *m/z* calcd for $C_{19}H_{35}N_6O_4P_2ICsPd$, 838.9330; found: 838.9360 [$(M-Cl)^{+}$ + CsI)]. Anal. Calcd for $C_{19}H_{35}N_6O_4P_2ClPd\cdot CH_2Cl_2$: C, 34.31; H, 5.34. Found: C, 34.68; H, 5.65.

***trans*-PdBr(Me)(DAPTA)$_2$ (11b)**. Reagents used: PdBr(Me)(COD) (0.033 g, 0.107 mmol) in 10 mL of dichloromethane and DAPTA (0.049 g, 0.214 mmol) in 15 mL of methanol. Complex **11b** was obtained as an off-white powder (0.050 g, 71% yield), Mp 199 ^{o}C (dec). ^{1}H NMR (300 MHz): δ 5.81 (d, J = 13.5 Hz, 2H), 5.60 (d, J = 15.6 Hz, 2H), 4.98 (d, J = 13.8 Hz, 2H), 4.67-4.54 (m, 4H), 4.27 (d, J = 14.1 Hz, 2H), 4.07-3.86 (m, 6H), 3.52 (dd, J = 15, 2 Hz, 2H), 2.11 and 2.09 (s, 12H, COCH_3), 0.42 (t, $^{3}J_{PH}$ = 6.5 Hz, 3H, Pd-CH_3). ^{31}P{^{1}H} NMR (121 MHz): δ -39.9. IR (KBr) (ν, cm^{-1}): 1629 (C=O). MS (FAB): *m/z (%)* 661 [78, $(M+3H)^{+}$], 643 (42, -CH_3), 579 (56), 508 (72), 307 (100), 289 (53). HRMS (FAB): *m/z* calcd for $C_{19}H_{36}N_6O_4P_2{}^{81}BrPd$, 661.0470; found: 661.0454

[$(M+H)^+$]. Anal. Calcd for $C_{19}H_{35}N_6O_4P_2BrPd$: C, 34.58; H, 5.35. Found: C, 34.93; H, 5.54.

***trans*-PdI(Me)(DAPTA)$_2$ (11c)**. Reagents used: PdI(Me)(COD) (0.028 g, 0.078 mmol) in 10 mL of dichloromethane and DAPTA (0.036 g, 0.156 mmol) in 10 mL of methanol. Complex **11c** was obtained as a yellow powder (0.035 g, 64% yield), Mp 138-140 ^oC. ^1H NMR (300 MHz): δ 5.79 (d, J = 14.4 Hz, 2H), 5.63 (d, J = 15.7 Hz, 2H), 5.27 (s, 2H, CH_2Cl_2), 4.97 (d, J = 14.1 Hz, 2H), 4.68 (d, J = 15.3 Hz, 2H), 4.56 (d, J = 13.8 Hz, 2H), 4.25 (d, J = 16.5 Hz, 2H), 4.12-3.90 (m, 6H), 3.53 (d, J = 14.3 Hz, 2H), 2.13, 2.10, and 2.08 (br, 12H, COCH_3), 0.55 (t, $^3J_{PH}$ = 6.6 Hz, 3H, Pd-CH_3). $^{31}P\{^1H\}$ NMR (121 MHz): δ -41.4. IR (KBr) (ν, cm^{-1}): 1629 (C=O). MS (FAB): *m/z (%)* 707 [61, $(M+H)^+$], 692 (40, -CH_3), 613 (22), 579 (30), 508 (40), 307 (100), 289 (56). HRMS (FAB): *m/z* calcd for $C_{19}H_{36}N_6O_4P_2IPd$, 707.0351; found: 707.0339 [$(M+H)^+$]. Anal. Calcd for $C_{19}H_{35}N_6O_4P_2IPd\cdot CH_2Cl_2$: C, 30.34; H, 4.73. Found: C, 30.57; H, 5.03.

On extending the reaction time to 48 h, the *trans*-product **11c** appears to undergo partial isomerization to *cis*-PdI(Me)(DAPTA)$_2$, **11d** resulting in a mixture containing the *cis*- and *trans*-isomers in approximately 9 : 1 ratio, respectively as a yellow powder, Mp 129 ^oC (dec). $^{31}P\{^1H\}$ NMR (121 MHz): δ -41.3 (**11c**), -47.5 (**11d**).

Synthesis of *cis*-MBr$_2$(DAPTA)$_2$ [M = Pt (12a); M = Pd (12c)] and *trans*-PtI$_2$(DAPTA)$_2$ (12d). A representative synthesis is described for complex **12a**. To a 100 mL round bottom flask equipped with a 25 mL addition funnel and a magnetic stir bar was placed $PtBr_2$(COD) (0.035 g, 0.076 mmol) in 10 mL of dichloromethane. A solution of DAPTA (0.034 g, 0.152 mmol) in 10 mL of methanol was added dropwise with

stirring over 10 min. The reaction solution was stirred for 6-7 h at room temperature. The resulting solution was evaporated *in vacuo* and the residue was dissolved in 5 mL of methanol and precipitated with the addition of an excess of *n*-pentane**.** The resulting precipitate was washed with diethyl ether (3 x 5 mL). The residue was filtered and dried *in vacuo*. Complex **12a** was obtained as an off-white solid (0.043 g, 71% yield) with a trace amount of an unassigned conformer and *trans*-$PtBr_2(DAPTA)_2$, **12b** in approximately (1 : 0.11 : 0.08) ratio, respectively, Mp 263-265 ^oC. ^1H NMR (300 MHz, DMSO-d_6): δ 5.76 (br m, 2H), 5.56 (d, J = 13.3 Hz, 2H), 5.00 (d, J = 13.3 Hz, 4H), 4.57 (d, J = 13.6 Hz, 2H), 4.37 (d, J = 15.1 Hz, 2H), 4.22 (br, 4H), 4.07 (d, J = 13.7 Hz, 2H), 3.79 (d, J = 14.3 Hz, 2H), 2.00 and 1.97 (s, 12H, COCH_3). $^{31}P\{^1H\}$ NMR (121 MHz, DMSO-d_6): δ -31.1 and -31.2 (unassigned), -31.5 ($^1J_{PtP}$ = 3307 Hz) and -31.6 ($^1J_{PtP}$ = 3311 Hz, **12a**), -32.9 and -33.1 (**12b**, $^1J_{PtP}$ not resolved), approximate ratio (0.11 : 1 : 0.08), respectively. IR (KBr) (v, cm^{-1}): 1634 (br, C=O). MS (FAB): *m/z (%)* 813 [62, $(M+2H)^+$], 733 (68, -Br), 307 (100), 289 (58). HRMS (FAB): *m/z* calcd for $C_{18}H_{33}N_6O_4P_2{}^{79}Br_2Pt$, 812.0053; found: 812.0035 [$(M+H)^+$]. Anal. Calcd for $C_{18}H_{32}N_6O_4P_2Br_2Pt$: C, 26.58; H, 3.96. Found: C, 26.24; H, 4.31.

On extending the reaction time to 15 h, complex **12a** appears to undergo slow isomerization to give a mixture of **12a** and *trans*-$PtBr_2(DAPTA)_2$, **12b** in approximately 11 : 1 ratio, respectively. $^{31}P\{^1H\}$ NMR (121 MHz, DMSO-d_6): δ -31.6, -31.7 ($^1J_{PtP}$ = 3363 Hz, **12a**), -33.0, -33.1 (**12b**, Pt satellites not resolved).

***cis*-$PdBr_2(DAPTA)_2$ (12c)**. Reagents used: $PdBr_2(COD)$ (0.036 g, 0.096 mmol) in 10 mL of dichloromethane and DAPTA (0.044 g, 0.193 mmol) in 10 mL of methanol. Reaction time: 14-15 h. Complex **12c** was obtained as a yellow powder (0.058 g, 84%

yield), Mp 210 ^{o}C (dec). ^{1}H NMR (300 MHz): δ 5.84 (d, J = 14.6 Hz, 2H), 5.76 (br d, J = 14.6 Hz, 2H), 5.00 (d, J = 15.1 Hz, 2H), 4.89 (br d, J = 15.2 Hz, 2H), 4.62 (d, J = 14.1 Hz, 2H), 4.28 (d, J = 16.5 Hz, 2H), 4.16-3.94 (m, 6H), 3.76 (m, 2H), 2.14 (br, 12H, COCH_3). ^{31}P{^{1}H} NMR (121 MHz): δ -38.9. IR (KBr) (ν, cm^{-1}): 1625 (C=O). MS (FAB): *m/z (%)* 725 [75, (M+3H)$^{+}$], 646 (33, -Br), 613 (34), 307 (100), 289 (56). HRMS (FAB): *m/z* calcd for $C_{18}H_{33}N_6O_4P_2{}^{79}Br_2Pd$, 722.9439; found: 722.9433 [(M+H)$^{+}$]. Anal. Calcd for $C_{18}H_{32}N_6O_4P_2Br_2Pd$: C, 29.79; H, 4.45. Found: C, 29.20; H, 4.63.

***trans*-PtI$_2$(DAPTA)$_2$ (12d)**. Reagents used: PtI$_2$(COD) (0.036 g, 0.064 mmol) in 10 mL of dichloromethane and DAPTA (0.029 g, 0.128 mmol) in 10 mL of methanol. Reaction time: 14-15 h. Complex **12d** was obtained as a yellow powder (0.051 g, 88% yield), Mp 263 ^{o}C (dec). X-ray quality crystals of **12d** were obtained by slow diffusion of methylene chloride to a methanol solution of **12d** below 0 ^{o}C. ^{1}H NMR (300 MHz): δ 5.91 (br d, J = 16.3 Hz, 2H), 5.80 (d, J = 15 Hz, 2H), 5.14 (br d, 2H), 4.97 (d, J = 14.8 Hz, 2H), 4.56 (d, J = 14.3 Hz, 2H), 4.27-3.93 (m, 8H), 3.61 (d, J = 15.8 Hz, 2H), 2.13, 2.10 (s, 12H, COCH_3). ^{31}P{^{1}H} NMR (121 MHz, DMSO-d_6): δ -50.3 ($^{1}J_{PtP}$ = 2369 Hz). IR (KBr) (ν, cm^{-1}): 1634 (C=O). MS (FAB): *m/z (%)* 908 [20, (M+H)$^{+}$], 780 (15, -I), 615 (20), 307 (100), 289 (58). HRMS (FAB): *m/z* calcd for $C_{18}H_{33}N_6O_4P_2I_2Pt$, 907.9776; found: 907.9790 [(M+H)$^{+}$]. Anal. Calcd for $C_{18}H_{32}N_6O_4P_2I_2Pt$: C, 23.82; H, 3.56. Found: C, 23.93; H, 3.91.

Complex **12d** was found to undergo slow decomposition in DMSO-d_6 solution at room temperature over *ca.* 3 h. On extending the reaction time to 24 h, **12d** and a mixture of two conformers of its isomer, *cis*-PtI$_2$(DAPTA)$_2$, **12e** as well as trace amounts of other unassigned products were obtained. ^{31}P{^{1}H} NMR (121 MHz, DMSO-d_6): δ

2.94 (unassigned minor product), -35.1 ($^1J_{PtP}$ = 3141 Hz, **12e**) and -35.2 ($^1J_{PtP}$ = 3144 Hz, **12e**), -35.6 and -35.7 (unassigned minor product), -37.2 and -37.3 (unassigned minor product), -48.8 (unassigned minor product), -49.4 ($^1J_{PtP}$ = 2369 Hz, **12d**).

Synthesis of *cis*-Pt(C_2Ph)$_2$(DAPTA)$_2$ (13a). In a 100 mL three-necked round bottom flask equipped with a 25 mL addition funnel and a magnetic stir bar was placed *cis*-$PtCl_2$(DAPTA)$_2$ (0.150 g, 0.207 mmol). Absolute ethanol (35 mL) was added to the flask and the resulting suspension was stirred for 5 min. Triethylamine (0.062 g, 0.620 mmol) was added to the suspension through a syringe followed by the dropwise addition of phenylacetylene (0.169 g, 1.65 mmol) over 5 min with stirring. Absolute ethanol (5 mL) was added and the solution was stirred over 14 h and an off-white precipitate gradually formed. The resulting mixture was filtered using a sintered glass frit. The solid collected was washed with methanol (3 x 5 mL) and dried in a vacuum desiccator for 6 h. The solid was then washed with 5 mL of diethyl ether and dried *in vacuo*. Complex **13a** was obtained as an off-white solid (0.120 g, 68% yield), Mp 239-241 ^oC. The NMR data were collected in anhydrous DMSO-d_6. ^1H NMR (500 MHz, DMSO-d_6): δ 7.44-7.20 (m, 10H, Ph), 5.72 (br d, J = 15.5 Hz, 2H), 5.62 (d, J = 13.8 Hz, 2H), 5.04 (d, J = 14.2 Hz, 2H), 4.85 (br m, 2H), 4.60 (d, J = 13.9 Hz, 2H), 4.21 (d, J = 15.5 Hz, 2H), 4.08-3.97 (m, 6H), 3.68-3.58 (m, 2H), 3.34 (s, 2H, H_2O), 2.06, 1.99, and 1.87 (br s, 12H, COCH_3). $^{31}P\{^1H\}$ NMR (121 MHz, DMSO-d_6): δ -41.6 ($^1J_{PtP}$ = 2145 Hz). IR (KBr) (ν, cm^{-1}): 2108, 2038 (C≡C), 1634 (C=O). MS (FAB): *m/z (%)* 856 [79, $(M+H)^+$], 683 (15), 307 (100), 289 (56). HRMS (FAB + CsI): *m/z* calcd for $C_{34}H_{42}N_6P_2O_4CsPt$, 988.1446; found: 988.1478 [$(M+Cs)^+$]. Anal. Calcd for $C_{34}H_{42}N_6P_2O_4Pt\cdot H_2O$: C, 46.74; H, 5.08. Found: C, 46.86; H, 4.96.

When the reaction was monitored after 5 h, the starting material was not consumed completely. When the reaction was extended over *ca.* 6 h, a mixture of **13a** and an unassigned product was obtained in approximately 4 : 1 ratio, respectively. $^{31}P\{^{1}H\}$ NMR (121 MHz, DMSO-d_6): δ -40.3 (unassigned product, Pt satellites not resolved), -41.5 ($^{1}J_{PtP}$ = 2144 Hz, **13a**). After 14 h, the unassigned product disappeared.

When **13a** was heated in DMSO-d_6 solution, unassigned resonances were observed in the $^{31}P\{^{1}H\}$ NMR spectrum. When **13a** was heated in $CDCl_3$ solution, due to possible isomerization, *trans*-$Pt(C_2Ph)_2(DAPTA)_2$, **13b** was obtained as a major product with trace amounts of some unassigned products. $^{31}P\{^{1}H\}$ NMR (121 MHz, $CDCl_3$): δ -39.0 (unassigned), -41.9 (br, $^{1}J_{PtP}$ = 2444 Hz, **13b**), -44.8 (d, unassigned).

Complex **13a** was also obtained (0.036 g, 71% yield) by following a similar procedure used for the synthesis of complex **6a**. Reagents used: $Pt(C_2Ph)_2(COD)$ (0.03 g, 0.059 mmol) in 10 mL of dichloromethane and DAPTA (0.027 g, 0.118 mmol) in 10 mL of methanol. Reaction time: 14-15 h. The reaction was monitored periodically and none of the *trans*-isomer, **13b** was observed.

Synthesis of *trans*-$Pd(C_2Ph)_2(DAPTA)_2$ (14). In a 100 mL three-necked round bottom flask equipped with a 25 mL addition funnel and a magnetic stir bar was placed *cis*-$PdCl_2(DAPTA)_2$ (0.090 g, 0.141 mmol). Absolute ethanol (30 mL) was added to the flask and the resulting suspension was stirred for 5 min. Triethylamine (0.043 g, 0.425 mmol) was added to the suspension through a syringe followed by the dropwise addition of phenylacetylene (0.115 g, 1.12 mmol) over 5 min with stirring. Absolute ethanol (5 mL) was added and the solution was stirred over 14 h and a yellow precipitate gradually

formed. The resulting mixture was filtered using a sintered glass frit. The yellow solid was washed with methanol (3 x 5 mL) and dried in a vacuum desiccator for 6 h. The solid was then washed with 5 mL of diethyl ether and dried *in vacuo.* Complex **14** was obtained as a yellow solid (0.070 g, 65% yield), Mp 198 ^{o}C (dec). ^{1}H NMR (300 MHz): δ 7.40-7.19 (m, 10H, Ph), 5.94-5.82 (m, 4H), 5.01 (d, J = 14 Hz, 2H), 4.89 (br d, J = 16.8 Hz, 2H), 4.65 (d, J = 13.9 Hz, 2H), 4.41 (d, J = 16.0 Hz, 2H), 4.12-3.98 (m, 6H), 3.85 (d, J = 15.8 Hz, 2H), 2.13 and 2.09 (s, 12H, COCH_3). ^{31}P{^{1}H} NMR (121 MHz): δ -35.2. IR (KBr) (v, cm^{-1}): 2112, 2046 (C≡C), 1638 (C=O). MS (FAB): *m/z (%)* 767 [10, $(M+H)^{+}$], 665 (25, -C_2Ph), 613 (42), 307 (100), 289 (57). Anal. Calcd for $C_{34}H_{42}N_6P_2O_4Pd$: C, 53.23; H, 5.51. Found: C, 52.81; H, 5.60.

Synthesis of *trans*-M($C_2Me_3Si)_2$(DAPTA)$_2$ [M = Pt (15a); M = Pd (15b)]. A representative synthesis is described for complex **15a**. In a 100 mL three-necked round bottom flask equipped with a 25 mL addition funnel and a magnetic stir bar was placed *cis*-$PtCl_2$(DAPTA)$_2$ (0.090 g, 0.124 mmol). Absolute ethanol (30 mL) was added to the flask and the resulting suspension was stirred for 5 min. Triethylamine (0.037 g, 0.373 mmol) was added to the suspension through a syringe followed by the dropwise addition of trimethylsilylacetylene (0.122 g, 1.24 mmol) over 5 min with stirring. Absolute ethanol (5 mL) was added and the solution was stirred over 14-15 h and a white precipitate gradually formed. The resulting mixture was filtered using a sintered glass frit. The solid was washed with methanol (3 x 5 mL) and dried in a vacuum desiccator for 6 h. The solid was then washed with 5 mL of diethyl ether and dried *in vacuo.* Complex **15a** was obtained as a white solid (0.071 g, 68% yield), Mp 302-304 ^{o}C. ^{1}H NMR (300 MHz): δ 5.83 (d, J = 15.4 Hz, 2H), 5.74 (d, J = 15.7 Hz, 2H), 4.99 (d, J =

13.8 Hz, 2H), 4.80 (d, *J* = 17.0 Hz, 2H), 4.66-4.55 (m, 2H), 4.26 (d, *J* = 16.0 Hz, 2H), 4.08-3.84 (m, 6H), 3.70 (d, *J* = 15.3 Hz, 2H), 2.12 and 2.10 (s, 12H, COCH_3), 0.11 (s, 18H, SiCH_3). ^{29}Si{^{1}H} NMR (99 MHz): δ -23.4. ^{31}P{^{1}H} NMR (121 MHz): δ -43.3 ($^1J_{PtP}$ = 2498 Hz). IR (KBr) (*v*, cm^{-1}): 2112, 2046 (C≡C), 1634 (C=O). MS (FAB): *m/z (%)* 847 (31, M^+), 750 (10, -C_2SiMe_3), 679 (15), 618(11), 307 (100), 289 (61). HRMS (FAB): *m/z* calcd for $C_{28}H_{51}N_6P_2O_4Si_2Pt$, 848.2639; found: 848.2655 [$(M+H)^+$]. Anal. Calcd for $C_{28}H_{50}N_6P_2O_4Si_2Pt$: C, 39.66; H, 5.94. Found: C, 39.50; H, 5.94. Complex **15a** was found to undergo slow decomposition in $CDCl_3$ and DMSO-d_6 solutions at room temperature over *ca.* 12 h.

***trans*-Pd(C$_2$Me$_3$Si)$_2$(DAPTA)$_2$ (15b)**. Reagents used: *cis*-$PdCl_2(DAPTA)_2$ (0.080 g, 0.126 mmol), triethylamine (0.038 g, 0.378 mmol) and trimethylsilylacetylene (0.123 g, 1.26 mmol) in 35 mL of absolute ethanol. Reaction time: 14-15 h. Complex **15b** was obtained as an off-white solid (0.058 g, 61% yield), Mp 307 ^{o}C (dec). Complex **15b** was stored below 0 ^{o}C due to slow decomposition upon standing at room temperature. ^{1}H NMR (300 MHz): δ 5.84 (d, *J* = 13.6 Hz, 2H), 5.75 (br d, *J* = 15.7 Hz, 2H), 5.00 (d, *J* = 13.4 Hz, 2H), 4.80 (br d, *J* = 15.8 Hz, 2H), 4.61 (d, *J* = 13.9 Hz, 2H), 4.28 (d, *J* = 16.7 Hz, 2H), 4.09-3.87 (m, 6H), 3.73 (d, *J* = 16.7 Hz, 2H), 2.13 and 2.11 (s, 12H, COCH_3), 0.16 (s, 18H, SiCH_3). ^{29}Si{^{1}H} NMR (99 MHz): δ -23.5. ^{31}P{^{1}H} NMR (121 MHz, DMSO-d_6): δ -35.1. IR (KBr) (*v*, cm^{-1}): 2103, 2046 (C≡C), 1629 (C=O). MS (FAB + NaI): *m/z (%)* 781 [24, $(M+Na)^+$], 479 (25), 329 (100), 252 (79). HRMS (FAB + NaI): *m/z* calcd for $C_{28}H_{50}N_6P_2O_4Si_2NaPd$, 781.1840; found: 781.1815 [$(M+Na)^+$]. Complex **15b** was not stable enough for elemental analysis. Complex **15b** was found to undergo slow decomposition in $CDCl_3$ and DMSO-d_6 solutions at room temperature over *ca.* 6 h.

Synthesis of *cis*-[Pt{C_2(*p*-tol)}$_2$(PTA)$_2$] (16). A solution of Pt(C_2 *p*-tol)$_2$(COD) (0.100 g, 0.187 mmol) in dichloromethane (25 mL) was placed in a 100 mL round bottom flask equipped with a 25 mL addition funnel and a magnetic stir bar. A solution of PTA (0.058 g, 0.375 mmol) in methanol (25 mL) was added dropwise with stirring over 10 min. The reaction solution was stirred for 12 h at room temperature. The reaction mixture was then evaporated to dryness on a rotary evaporator and the resulting white residue was washed with diethyl ether (3 x 10 mL). The solid was evaporated to dryness *in vacuo*. Complex **16** was obtained as an off-white solid (0.123 g, 89% yield), Mp 258-260 ^{o}C. X-ray quality crystals of **16** were obtained by layering of methanol to a CH_2Cl_2 solution of **16** at a lower temperature (below 0 ^{o}C). ^{1}H NMR (300 MHz): δ 7.29-7.25 (m, 4H, Ph), 7.06 (d, J = 7.9 Hz, 4H, Ph), 4.61-4.48 (m, 12H, NCH_2), 4.41 (br, 12H, PCH_2), 2.32 (s, 6H, CH_3), 1.57 (s, 2H, H_2O). ^{31}P{^{1}H} NMR (121 MHz): δ -70.2 ($^{1}J_{PtP}$ = 2070 Hz). IR (KBr) (ν, cm^{-1}): 2120 (C≡C). MS (FAB): *m/z (%)* 740 [31, (M+H)$^{+}$], 624 (14, -C_2tol), 307 (100), 289 (52). HRMS (FAB): *m/z* calcd for $C_{30}H_{39}N_6P_2Pt$, 740.2360; found: 740.2363 [(M+H)$^{+}$]. Anal. Calcd for $C_{30}H_{38}N_6P_2Pt\cdot H_2O$: C, 47.53; H, 5.31. Found: C, 47.78; H, 5.11.

Alternatively, complex **16** can be prepared by the following procedure:

In a 100 mL three-necked round bottom flask equipped with a 25 mL addition funnel and a magnetic stir bar was placed *cis*-$PtCl_2(PTA)_2$ (0.080 g, 0.137 mmol). Absolute ethanol (20 mL) was added to the flask and the resulting suspension was stirred for 5 min. Triethylamine (0.041 g, 0.413 mmol) was added to the suspension followed by the dropwise addition of 4-ethynyltoluene (0.079 g, 0.689 mmol) over 5 min with stirring. Absolute ethanol (5 mL) was added and the solution was stirred over *ca.* 72 h and a white

precipitate gradually formed. The resulting mixture was filtered using a sintered glass frit. The off-white solid was washed with methanol (3 x 5 mL) and dried in a vacuum desiccator for 6 h. The solid was dissolved in a minimal amount of CH_2Cl_2 and filtered. The filtrate containing **16** was evaporated and the resultant precipitate was then washed with 5 mL of diethyl ether and dried *in vacuo*. Complex **16** was obtained as an off-white solid (0.081 g, 80% yield).

Synthesis of *trans*-[Pd{C$_2$(*p*-tol)}$_2$(PTA)$_2$] (17). In a 100 mL three-necked round bottom flask equipped with a 25 mL addition funnel and a magnetic stir bar was placed *cis*-$PdCl_2(PTA)_2$ (0.080 g, 0.162 mmol). Absolute ethanol (20 mL) was added to the flask and the resulting suspension was stirred for 5 min. Triethylamine (0.049 g, 0.486 mmol) was added to the suspension followed by the dropwise addition of 4-ethynyltoluene (0.094 g, 0.810 mmol) over 5 min with stirring. Absolute ethanol (5 mL) was added and the solution was stirred over 6 h and a white precipitate gradually formed. The resulting mixture was filtered using a sintered glass frit. The off-white solid was washed with methanol (3 x 5 mL) and dried in a vacuum desiccator for 6 h. The solid was dissolved in a minimal amount of CH_2Cl_2 and filtered. The filtrate containing **17** was evaporated and the resultant precipitate was then washed with 5 mL of diethyl ether and dried *in vacuo*. Complex **17** was obtained as an off-white solid (0.086 g, 81% yield), Mp 219 ^oC (dec). Complex **17** was found to be unstable in solution on standing for long periods at room temperature. ^1H NMR (300 MHz): δ 7.30-7.25 (m, 4H, Ph), 7.06 (d, J = 7.9 Hz, 4H, Ph), 4.55 (br, 12H, NCH_2), 4.44 (br, 12H, PCH_2), 2.32 (s, 6H, CH_3). $^{31}P\{^1H\}$ NMR (121 MHz): δ -56.9. IR (KBr) (ν, cm^{-1}): 2103 (C≡C). MS (FAB): *m/z (%)* 650 (28, M^+), 535 (49, -C_2tol), 378 (32), 307 (32), 272 (100). HRMS (FAB): *m/z* calcd for

$C_{30}H_{38}N_6P_2{}^{106}Pd$, 650.1666; found: 650.1638 (M^+); *m/z* calcd for $C_{30}H_{37}N_6P_2{}^{108}Pd$, 651.1594; found: 651.1600 [$(M-H)^+$]. Anal. Calcd for $C_{30}H_{38}N_6P_2Pd$: C, 55.28; H, 5.88. Found: C, 54.74; H, 5.87.

Synthesis of *cis*-[Pt{C_2 (*m*-py)}$_2$(PTA)$_2$] (18a), *cis*-[Pt{C_2 (*o*-py)}$_2$(PTA)$_2$] (19a), and *cis*-[Pt{C_2(*m*-$C_6H_4NH_2$)}$_2$(PTA)$_2$] (20). A representative synthesis is described for complex **18a.** A solution of [Pt{C_2 (*m*-py)}$_2$(COD)] (0.100 g, 0.196 mmol) in dichloromethane (25 mL) was placed in a 100 mL round bottom flask equipped with a 25 mL addition funnel and a magnetic stir bar. A solution of PTA (0.061 g, 0.392 mmol) in methanol (25 mL) was added dropwise with stirring over 10 min. The reaction solution was stirred for 16 h at room temperature. The reaction mixture was then evaporated to dryness on a rotary evaporator and the resulting white residue was washed with diethyl ether (3 x 10 mL). The solid was evaporated to dryness *in vacuo*. Complex **18a** was obtained as a white solid (0.120 g, 86% yield), Mp 294 ^oC (dec). ^1H NMR (300 MHz): δ 8.67 (br, 2H), 8.38 (m, 2H), 7.68 (m, 2H), 7.19-7.14 (m, 2H), 4.63-4.45 (m, 12H, NCH_2), 4.33 (br, 12H, PCH_2). $^{31}P\{^1H\}$ NMR (121 MHz): δ -71.5 ($^1J_{PtP}$ = 2075 Hz). IR (KBr) (ν, cm^{-1}): 2112 (C≡C), 1613 (C=N). MS (FAB): *m/z (%)* 714 [14, $(M+H)^+$], 509 [3, -2(*m*-py)], 307 (100), 289 (54). HRMS (FAB): *m/z* calcd for $C_{26}H_{33}N_8P_2Pt$, 714.1951; found: 714.1952 [$(M+H)^+$]. Anal. Calcd for $C_{26}H_{32}N_8P_2Pt$: C, 43.75; H, 4.52. Found: C, 43.49; H, 4.62.

***cis*-[Pt{C_2 (*o*-py)}$_2$(PTA)$_2$] (19a).** Reagents used: [Pt{C_2(*o*-py)}$_2$(COD)] (0.100 g, 0.196 mmol) in dichloromethane (25 mL) and PTA (0.061 g, 0.392 mmol) in methanol (25 mL). Reaction time: 16 h. Complex **19a** was obtained as a white solid (0.115 g, 82% yield), Mp 279-281 ^oC. Complex **19a** undergoes slow isomerization on standing in

solutions. ^{1}H NMR (300 MHz): δ 8.50 (d, J = 4.3 Hz, 2H), 7.57 (m, 2H), 7.32-7.24 (m, 2H), 7.09 (m, 2H), 4.53 (br, 12H, NCH_2), 4.41 (br, 12H, PCH_2). ^{31}P{^{1}H} NMR (202 MHz): δ -70.5 ($^{1}J_{PtP}$ = 2069 Hz). IR (KBr) (ν, cm^{-1}): 2108 (C≡C), 1605 (C=N). MS (FAB): *m/z (%)* 714 [20, $(M+H)^{+}$], 460 (18), 307 (100), 289 (64). HRMS (FAB): *m/z* calcd for $C_{26}H_{33}N_8P_2Pt$, 714.1950; found: 714.1923 [$(M+H)^{+}$]. Anal. Calcd for $C_{26}H_{32}N_8P_2Pt$: C, 43.75; H, 4.52. Found: C, 43.25; H, 4.84.

Alternatively, complex **19a** can be prepared by the following procedure:

In a 100 mL three-necked round bottom flask equipped with a 25 mL addition funnel and a magnetic stir bar was placed *cis*-$PtCl_2(PTA)_2$ (0.080 g, 0.137 mmol). Absolute ethanol (20 mL) was added to the flask and the resulting suspension was stirred for 5 min. Triethylamine (0.041 g, 0.413 mmol) was added to the suspension followed by the dropwise addition of 2-ethynylpyridine (0.071 g, 0.689 mmol) over 5 min with stirring. Absolute ethanol (5 mL) was added and the solution was stirred over *ca.* 72 h and a white precipitate gradually formed. The resulting mixture was filtered using a sintered glass frit. The white solid was washed with methanol (3 x 5 mL) and dried in a vacuum desiccator for 6 h. The solid was dissolved in a minimal amount of CH_2Cl_2 and filtered. The filtrate containing **19a** was evaporated and the resultant precipitate was then washed with 5 mL of diethyl ether and dried *in vacuo.* Complex **19a** was obtained as a white solid (0.075 g, 76% yield). The reaction was found to be incomplete after 60 h and the formation of a mixture of *trans*-$[Pt\{C_2(o\text{-py})\}_2(PTA)_2]$, **19b** and an unassigned product were observed in approximately 5 : 1 ratio, respectively. ^{31}P{^{1}H} NMR (202 MHz): δ -64.3 ($^{1}J_{PtP}$ = 2287 Hz, **19b**), -60.9 (unassigned).

***cis*-[Pt{C_2(*m*-$C_6H_4NH_2$)}$_2$($PTA)_2$] (20).** Reagents used: [Pt{C_2(*m*-$C_6H_4NH_2$)}$_2$(COD)] (0.080 g, 0.149 mmol) in dichloromethane (25 mL) and PTA (0.047 g, 0.299 mmol) in methanol (25 mL). Reaction time: 12 h. Complex **20** was obtained as an off-white solid (0.086 g, 78% yield), Mp 257-259 ^{o}C. ^{1}H NMR (300 MHz, DMSO-d_6): δ 6.91(m, 2H), 6.52 (br, 2H), 6.49-6.36 (m, 4H), 5.02 (br, 4H, NH_2), 4.53-4.38 (m, 12H, NCH_2), 4.27 (br, 12H, PCH_2). ^{31}P{^{1}H} NMR (202 MHz, DMSO-d_6): δ -70.5 ($^{1}J_{PtP}$ = 2064 Hz). IR (KBr) (ν, cm^{-1}): 2095 (C≡C), 1593 (-NH_2). MS (FAB): *m/z (%)* 742, 741 [18, cluster of M^+ and $(M+H)^+$], 460 (22), 307 (100), 289 (100). Anal. Calcd for $C_{28}H_{36}N_8P_2Pt$: C, 45.34; H, 4.89. Found: C, 45.11; H, 4.99.

Alternatively, complex **20** can be prepared by the following procedure:

In a 100 mL three-necked round bottom flask equipped with a 25 mL addition funnel and a magnetic stir bar was placed *cis*-$PtCl_2(PTA)_2$ (0.080 g, 0.137 mmol). Absolute ethanol (20 mL) was added to the flask and the resulting suspension was stirred for 5 min. Triethylamine (0.041 g, 0.413 mmol) was added to the suspension followed by the dropwise addition of 3-ethynylaniline (0.080 g, 0.689 mmol) over 5 min with stirring. Absolute ethanol (5 mL) was added and the solution was stirred over *ca.* 76 h and a white precipitate gradually formed. The resulting mixture was filtered using a sintered glass frit. The off-white solid was washed with methanol (3 x 5 mL) and dried in a vacuum desiccator for 6 h. The solid was dissolved in a minimal amount of CH_2Cl_2 and filtered. The filtrate containing **20** was evaporated and the resultant precipitate was then washed with 5 mL of diethyl ether and dried *in vacuo.* Complex **20** was obtained as an off-white solid (0.072 g, 71% yield).

Synthesis of *trans*-[M{C_2(*m*-py)}$_2$(PTA)$_2$] [M = Pt (18b); M = Pd (21)], *trans*-[M{C_2(*o*-py)}$_2$(PTA)$_2$] [M = Pt (19b); M = Pd (22)], and *trans*-[Pd{C_2(*m*-$C_6H_4NH_2$)}$_2$(PTA)$_2$] (23). A representative synthesis is described for complex **18b**. In a 100 mL three-necked round bottom flask equipped with a 25 mL addition funnel and a magnetic stir bar was placed *cis*-$PtCl_2(PTA)_2$ (0.080 g, 0.137 mmol). Absolute ethanol (20 mL) was added to the flask and the resulting suspension was stirred for 5 min. Triethylamine (0.041 g, 0.413 mmol) was added to the suspension followed by the dropwise addition of 3-ethynylpyridine (0.071 g, 0.689 mmol) over 5 min with stirring. Absolute ethanol (5 mL) was added and the solution was stirred over 16 h and a white precipitate gradually formed. The resulting mixture was filtered using a sintered glass frit. The white solid was washed with methanol (3 x 5 mL) and dried in a vacuum desiccator for 6 h. The solid was dissolved in a minimal amount of CH_2Cl_2 and filtered. The filtrate containing **18b** was evaporated and the resultant precipitate was then washed with 5 mL of diethyl ether and dried *in vacuo.* Complex **18b** was obtained as a white solid (0.082 g, 84% yield), Mp 319 ^oC (dec). Complex **18b** appears to undergo isomerization to give **18a** on standing for long periods in $CDCl_3$ and DMSO-d_6 solutions. ^1H NMR (500 MHz): δ 8.63 (br, 2H), 8.42 (m, 2H), 7.62 (m, 2H), 7.19 (m, 2H), 4.59-4.50 (m, 12H, NCH_2), 4.40 (br, 12H, PCH_2). $^{13}C\{^1H\}$ NMR (150.8 MHz): δ 152.3 (Ph), 146.9 (Ph), 146.8 (Ph, **18a**), 138.3 (Ph), 138.01 (Ph, **18a**), 124.0 (Ph, **18a**), 123.1 (Ph, **18a**), 123.0 (Ph), 107.5 (C_b, $C_a{\equiv}C_b$py), 106.2 (≡*C*, **18a**), 102.5 (C_a, $C_a{\equiv}C_b$py), 100.9 (≡*C* , **18a**), 73.6 (m, **18a**), 73.5 (t, $^1J_{PC}$ = 3.4 Hz, N*C*H_2, $^2J_{PtC}$ unresolved), 53.4 (m, $^2J_{PtC}$ unresolved), 51.7 (m, P*C*H_2, $^2J_{PtC}$ unresolved, **18a**). $^{31}P\{^1H\}$ NMR (121 MHz): δ -65.3 ($^1J_{PtP}$ = 2282 Hz). IR (KBr) (ν, cm^{-1}): 2108 (C≡C), 1609 (C=N). MS (FAB): *m/z (%)*

714 (28, M^+), 535 (15), 461 (40), 401 (40), 327 (98), 281 (100). HRMS (FAB): *m/z* calcd for $C_{26}H_{33}N_8P_2Pt$, 714.1951; found: 714.1954 [$(M+H)^+$].

***trans*-[Pt{C$_2$(*o*-py)}$_2$(PTA)$_2$] (19b).** Reagents used: *cis*-$PtCl_2(PTA)_2$ (0.080 g, 0.137 mmol), triethylamine (0.041 g, 0.413 mmol), and 2-ethynylpyridine (0.071 g, 0.689 mmol), in 25 mL of absolute ethanol. Reaction time: 16 h. Complex **19b** was obtained as a white solid (0.079 g, 81% yield), Mp 304-306 ^oC. X-ray quality crystals of **19b** were obtained by layering of methanol to a $CHCl_3$ solution of **19b** at a lower temperature (below 0 ^oC). ^1H NMR (500 MHz): δ 8.50 (br, 2H), 7.55 (m, 2H), 7.32-7.26 (m, 2H), 7.08 (m, 2H), 4.53 (br, 12H, NCH_2), 4.41 (br, 12H, PCH_2). $^{31}P\{^1H\}$ NMR (202 MHz): δ -64.3 ($^1J_{PtP}$ = 2281 Hz). IR (KBr) (ν, cm^{-1}): 2103 (C≡C), 1617 (C=N). MS (FAB): *m/z (%)* 714 [15, $(M+H)^+$], 460 (25), 307 (100), 289 (100), 273 (18). HRMS (FAB): *m/z* calcd for $C_{26}H_{33}N_8P_2Pt$, 714.1950; found: 714.1937 [$(M+H)^+$].

***trans*-[Pd{C$_2$(*m*-py)}$_2$(PTA)$_2$] (21).** Reagents used: *cis*-$PdCl_2(PTA)_2$ (0.080 g, 0.162 mmol), triethylamine (0.049 g, 0.486 mmol), and 3-ethynylpyridine (0.084 g, 0.814 mmol), in 25 mL of absolute ethanol. Reaction time: 12 h. Complex **21** was obtained as a white solid (0.080 g, 79% yield), Mp 212 ^oC (dec). Complex **21** was found to be unstable in solutions on standing long at room temperature. ^1H NMR (300 MHz): δ 8.63 (br, 2H), 8.42 (m, 2H), 7.63 (dt, J = 8.7 Hz, 1.9 Hz, 2H), 7.20 (m, 2H), 4.56 (br, 12H, NCH_2), 4.43 (br, 12H, PCH_2). $^{31}P\{^1H\}$ NMR (121 MHz): δ -56.9. IR (KBr) (ν, cm^{-1}): 2108 (C≡C), 1630 (C=N). MS (FAB): *m/z (%)* 625 [56, $(M+H)^+$], 522 (15, -C_2Py), 460 (26), 307 (100), 289 (100). HRMS (FAB): *m/z* calcd for $C_{26}H_{33}N_8P_2Pd$, 625.1338; found: 625.1353 [$(M+H)^+$]. Anal. Calcd for $C_{26}H_{32}N_8P_2Pd$: C, 49.96; H, 5.16. Found: C, 49.78; H, 5.31.

***trans*-[Pd{C_2(*o*-py)}$_2$(PTA)$_2$] (22).** Reagents used: *cis*-$PdCl_2(PTA)_2$ (0.080 g, 0.162 mmol), triethylamine (0.049 g, 0.486 mmol), and 2-ethynylpyridine (0.084 g, 0.814 mmol), in 25 mL of absolute ethanol. Reaction time: 12 h. Complex **22** was obtained as a white solid (0.084 g, 83% yield), Mp 196 ^{o}C (dec). Complex **22** was found to be unstable in solutions on standing long at room temperature. X-ray quality crystals of **22** were obtained by layering of methanol to a $CHCl_3$ solution of **22** at a lower temperature (below 0 ^{o}C). ^{1}H NMR (500 MHz): δ 8.50 (d, J = 4.3 Hz, 2H), 7.56 (t, J = 7.5 Hz, 2H), 7.30 (d, J = 7.8 Hz, 2H), 7.08 (m, 2H), 4.55-4.51 (m, 12H, NCH_2), 4.45 (br, 12H, PCH_2). ^{31}P{^{1}H} NMR (121 MHz): δ -56.2. IR (KBr) (ν, cm^{-1}): 2120 (C≡C), 1629 (C=N). MS (FAB): *m/z (%)* 625 [38, $(M+H)^+$], 522 (12, -C_2Py), 460 (32), 349 (17), 307 (100), 289 (100). HRMS (FAB): *m/z* calcd for $C_{26}H_{33}N_8P_2Pd$, 625.1338; found: 625.1353 [$(M+H)^+$]. Anal. Calcd for $C_{26}H_{32}N_8P_2Pd$: C, 49.96; H, 5.16. Found: C, 49.46; H, 5.32.

***trans*-[Pd{C_2(*m*-$C_6H_4NH_2$)}$_2$(PTA)$_2$] (23)**. Reagents used: *cis*-$PdCl_2(PTA)_2$ (0.080 g, 0.162 mmol), triethylamine (0.049 g, 0.486 mmol), and 3-ethynylaniline (0.094 g, 0.814 mmol), in 25 mL of absolute ethanol. Reaction time: 16 h. Complex **23** was obtained as an off-white solid (0.078 g, 74% yield), Mp 204 ^{o}C (dec). Complex **23** was found to be unstable in solutions on standing long at room temperature. ^{1}H NMR (500 MHz): δ 7.04 (m, 2H), 6.79 (m, 2H), 6.70 (br, 2H), 6.54 (m, 2H), 4.55 (br, 12H, NCH_2), 4.42 (br, 12H, PCH_2), 3.60 (4H, NH_2). ^{31}P{^{1}H} NMR (121 MHz): δ -56.9. IR (KBr) (ν, cm^{-1}): 2099 (C≡C), 1597 (-NH_2). MS (FAB): *m/z (%)* 652 [6, M^+ and $(M+H)^+$ cluster], 536 (6, -$C_8H_4NH_2$), 460 (10), 307 (100), 289 (79). Anal. Calcd for $C_{28}H_{36}N_8P_2Pd$: C, 51.50; H, 5.55. Found: C, 51.05; H, 5.52.

Synthesis of *trans*-Pt(C_2Bz)$_2$(PTA)$_2$ (24). In a 100 mL three-necked round bottom flask equipped with a 25 mL addition funnel and a magnetic stir bar was placed *cis*-$PtCl_2(PTA)_2$ (0.080 g, 0.137 mmol). Absolute ethanol (20 mL) was added to the flask and the resulting suspension was stirred for 5 min. Triethylamine (0.041 g, 0.413 mmol) was added to the suspension followed by the dropwise addition of 3-phenyl-1-propyne (0.080 g, 0.689 mmol) over 5 min with stirring. Absolute ethanol (5 mL) was added and the solution was stirred over 36 h and a white precipitate gradually formed. The resulting mixture was filtered using a sintered glass frit. The white solid was washed with methanol (3 x 5 mL) and dried in a vacuum desiccator for 6 h. The solid was dissolved in a minimal amount of CH_2Cl_2 and filtered. The filtrate containing **24** was evaporated and the resultant precipitate was then washed with 5 mL of diethyl ether and dried *in vacuo.* Complex **24** was obtained as a white solid (0.079 g, 78% yield), Mp 244-246 ^oC. ^1H NMR (300 MHz): δ 7.40-7.35 (m, 4H, Ph), 7.33-7.27 (m, 4H, Ph), 7.22-7.15 (m, 2H, Ph), 4.48-4.22 (m, 12H, NCH_2), 4.16 (br, 12H, PCH_2), 3.68 (br, 4H), 1.62 (br, 2H, H_2O). $^{31}P\{^1H\}$ NMR (202 MHz): δ -64.4 ($^1J_{PtP}$ = 2335 Hz). IR (KBr) (ν, cm^{-1}): 2116 (C≡C). MS (FAB): *m/z (%)* 740 [48, $(M+H)^+$], 624 (14, -C_2Bz), 460 (12), 307 (100), 289 (54). HRMS (FAB + NaI): *m/z* calcd for $C_{30}H_{38}N_6P_2NaPt$, 762.2180; found: 762.2188 [$(M+Na)^+$]. Anal. Calcd for $C_{30}H_{38}N_6P_2Pt\cdot H_2O$: C, 47.55; H, 5.32. Found: C, 47.38; H, 5.19.

The reaction was found to be incomplete after 12 h and the formation of a mixture of **24** and an unassigned product was observed in approximately 1 : 1 ratio. $^{31}P\{^1H\}$ NMR (202 MHz): δ -64.4 ($^1J_{PtP}$ = 2335 Hz, **24**), -61.2 ($^1J_{PtP}$ = 2376 Hz, unassigned). Complex

24 appears to undergo slow conversion to the unassigned product (20 : 1 ratio, respectively) on standing in $CDCl_3$ solution for a few days.

Synthesis of *cis*-[Pt{C_2(*p*-tol)}$_2$(DAPTA)$_2$] (25) and *cis*-[Pt{C_2(*m*-$C_6H_4NH_2$)}$_2$(DAPTA)$_2$] (26). A representative synthesis is described for complex **25**. A solution of [Pt{C_2(*p*-tol)}$_2$(COD)] (0.100 g, 0.187 mmol) in dichloromethane (25 mL) was placed in a 100 mL round bottom flask equipped with a 25 mL addition funnel and a magnetic stir bar. A solution of DAPTA (0.086 g, 0.376 mmol) in methanol (25 mL) was added dropwise with stirring over 10 min. The reaction solution was stirred for 16 h at room temperature. The reaction mixture was then evaporated to dryness on a rotary evaporator and the resulting white residue was washed with diethyl ether (3 x 10 mL). The solid was evaporated to dryness *in vacuo*. Complex **25** was obtained as an off-white solid (0.130 g, 79% yield), Mp 261-263 ^oC. ^1H NMR (500 MHz, DMSO-d_6): δ 7.38-7.28 (m, 4H), 7.10 (m, 4H), 5.73 (br, 2H), 5.62 (d, J = 13 Hz, 2H), 5.03 (d, J = 13 Hz, 2H), 4.85 (br, 2H), 4.60 (d, J = 13 Hz, 2H), 4.20 (d, J = 14 Hz, 2H), 4.06 (br, 6H), 3.65 (d, J = 13 Hz, 2H), 3.31 (s, 4H, 2H_2O), 2.29 (s, 6H, CH_3), 1.99, 1.88 (s, 12H, COCH_3). $^{31}P\{^1H\}$ NMR (121 MHz, DMSO-d_6): δ -41.5 ($^1J_{PtP}$ = 2143 Hz). IR (KBr) (ν, cm^{-1}): 2140 (C≡C), 1642 (C=O). MS (FAB): *m/z (%)* 884 [30, M^+ and $(M+H)^+$ cluster], 654 (8, -2C_2tol), 460 (15), 307 (100), 289 (74). Anal. Calcd for $C_{36}H_{46}N_6P_2O_4Pt \cdot 2H_2O$: C, 47.00; H, 5.47. Found: C, 47.16; H, 5.34.

Alternatively, complex **25** can be prepared by the following procedure:

In a 100 mL three-necked round bottom flask equipped with a 25 mL addition funnel and a magnetic stir bar was placed *cis*-$PtCl_2(DAPTA)_2$ (0.080 g, 0.110 mmol). Absolute

ethanol (20 mL) was added to the flask and the resulting suspension was stirred for 5 min. Triethylamine (0.034 g, 0.331 mmol) was added to the suspension followed by the dropwise addition of 4-ethynyltoluene (0.064 g, 0.550 mmol) over 5 min with stirring. Absolute ethanol (5 mL) was added and the solution was stirred over *ca.* 65 h and a white precipitate gradually formed. The resulting mixture was filtered using a sintered glass frit. The off-white solid was washed with methanol (3 x 5 mL) and dried in a vacuum desiccator for 6 h. The solid was dissolved in a minimal amount of CH_2Cl_2 and filtered. The filtrate containing **25** was evaporated and the resultant precipitate was then washed with 5 mL of diethyl ether and dried *in vacuo.* Complex **25** was obtained as an off-white solid (0.073 g, 75% yield).

***cis*-[Pt{C_2 (*m*-$C_6H_4NH_2$)}$_2$(DAPTA)$_2$] (26)**. Reagents used: [Pt{C_2 (*m*-$C_6H_4NH_2$)}$_2$(COD)] (0.075 g, 0.140 mmol) in dichloromethane (25 mL) and DAPTA (0.064 g, 0.280 mmol) in methanol (25 mL). Reaction time: 16 h. Complex **26** was obtained as a yellow solid (0.084 g, 68% yield), Mp 246-248 ^oC. ^1H NMR (300 MHz, DMSO-d_6): δ 6.91 (t, J = 7.8 Hz, 2H), 6.60 (m, 4H), 6.41 (d, J = 8.0 Hz, 2H), 5.61 (d, J = 13 Hz, 4H), 5.05-4.96 [m, 6H, NH_2 (4H) and NCH_2N (2H) peaks overlap], 4.85 (br, 2H), 4.58 (d, J = 13 Hz, 2H), 4.20 (d, J = 15 Hz, 2H), 4.08-3.95 (m, 6H), 3.65 (d, J = 14.8 Hz, 2H), 3.34 (s, 3H, 1.5H_2O), 1.99, 1.92 (s, 12H, COCH_3). $^{31}P\{^1H\}$ NMR (121 MHz, DMSO-d_6): δ -41.2 ($^1J_{PtP}$ = 2141 Hz). IR (KBr) (v, cm^{-1}): 2103 (C≡C), 1638 (C=O), 1589 (-NH_2). MS (FAB in NBA): *m/z (%)* 1153 [14, (M^+ + 2NBA) - 2NH_3], 1019 [36, (M^+ + NBA) - NH_3], 885 [35, M^+ and $(M+H)^+$ cluster], 460 (17), 307 (100), 289 (94). Anal. Calcd for $C_{34}H_{44}N_8P_2O_4Pt\cdot1.5H_2O$: C, 44.74; H, 5.19. Found: C, 45.02; H, 5.08.

Synthesis of *cis*-[Pt{C_2 (*m*-py)}$_2$(DAPTA)$_2$] (27), *trans*-[Pt{C_2 (*o*-py)}$_2$(DAPTA)$_2$] (28), and *trans*-[Pd{C_2(*p*-tol)}$_2$(DAPTA)$_2$] (29). A representative synthesis is described for complex **27**. In a 100 mL three-necked round bottom flask equipped with a 25 mL addition funnel and a magnetic stir bar was placed *cis*-$PtCl_2(DAPTA)_2$ (0.080 g, 0.110 mmol). Absolute ethanol (20 mL) was added to the flask and the resulting suspension was stirred for 5 min. Triethylamine (0.034 g, 0.331 mmol) was added to the suspension followed by the dropwise addition of 3-ethynylpyridine (0.057 g, 0.553 mmol) over 5 min with stirring. Absolute ethanol (5 mL) was added and the solution was stirred over *ca.* 48 h and a white precipitate gradually formed. The resulting mixture was filtered using a sintered glass frit. The off-white solid was washed with methanol (3 x 5 mL) and dried in a vacuum desiccator for 6 h. The solid was dissolved in a minimal amount of CH_2Cl_2 and filtered. The filtrate containing **27** was evaporated and the resultant precipitate was then washed with 5 mL of diethyl ether and dried *in vacuo.* Complex **27** was obtained as an off-white solid (0.076 g, 80% yield), Mp 226-228 ^oC. On extending the reaction time to *ca.* 76 h, complex **27** wasn't found to undergo isomerization. ^1H NMR (300 MHz): δ 8.70 (br, 2H), 8.41 (m, 2H), 7.78 (m, 2H), 7.23-7.14 (m, 2H), 5.84 (d, J = 14.4 Hz, 4H), 5.03 (d, J = 15 Hz, 2H), 4.84 (br m, 2H), 4.64 (d, J = 14.1 Hz, 2H), 4.38-4.23 (m, 2H), 4.15-3.91(m, 6H), 3.54 (br m, 2H), 2.16-2.04 (m, 12H, COCH_3), 1.65 (br, 2H, H_2O). $^{31}P\{^1H\}$ NMR (121 MHz): δ -45.0 ($^1J_{PtP}$ = 2124Hz) and -45.2 ($^1J_{PtP}$ = 2123 Hz) (approximate ratio = 1 : 1). IR (KBr) (ν, cm^{-1}): 2123 (C≡C), 1625 (C=O). MS (FAB): *m/z (%)* 857 (11, M^+), 460 (21), 307 (100), 289 (100), 273 (17). HRMS (FAB): *m/z* calcd for $C_{32}H_{41}N_8P_2O_4Pt$, 858.2373; found: 858.2399 [$(M+H)^+$]. Anal. Calcd for $C_{32}H_{40}N_8P_2O_4Pt \cdot H_2O$: C, 43.88; H, 4.83. Found: C, 44.17; H, 4.80.

Alternatively, complex **27** can be prepared by the following procedure:

A solution of [Pt{C_2(*m*-py)}$_2$(COD)] (0.070 g, 0.137 mmol) in dichloromethane (25 mL) was placed in a 100 mL round bottom flask equipped with a 25 mL addition funnel and a magnetic stir bar. A solution of DAPTA (0.063 g, 0.275 mmol) in methanol (25 mL) was added dropwise with stirring over 10 min. The reaction solution was stirred for 16 h at room temperature. The reaction mixture was then evaporated to dryness on a rotary evaporator and the resulting white residue was washed with diethyl ether (3 x 10 mL). The solid was evaporated to dryness *in vacuo*. Complex **27** was obtained as an off-white solid (0.099 g, 84% yield).

***trans*-[Pt{C_2(*o*-py)}$_2$(DAPTA)$_2$] (28).** Reagents used: *cis*-$PtCl_2(DAPTA)_2$ (0.080 g, 0.110 mmol), triethylamine (0.034 g, 0.331 mmol), and 2-ethynylpyridine (0.057 g, 0.553 mmol) in 25 mL of absolute ethanol. Reaction time: *ca.* 48 h. Complex **28** was obtained as an off-white solid (0.077 g, 82% yield), Mp 196-198 ^oC. On extending the reaction time to *ca.* 76 h, complex **28** wasn't found to undergo isomerization. ^1H NMR (300 MHz, DMSO-d_6): δ 8.44 (br, 2H), 7.73-7.66 (m, 2H), 7.49 (m, 2H), 7.19 (br, 2H), 5.61 (d, J = 13.0 Hz, 4H), 5.02 (d, J = 13 Hz, 2H), 4.87 (br, 2H), 4.62 (d, J = 13.2 Hz, 2H), 4.28 (d, J = 15.0 Hz, 2H), 4.21-4.02 (m, 6H), 3.73 (br d, J = 15.2 Hz, 2H), 2.05-1.89 (m, 12H, COCH_3). $^{31}P\{^1H\}$ NMR (121 MHz): δ -41.5 ($^1J_{PtP}$ = 2441 Hz). IR (KBr) (ν, cm^{-1}): 2120 (C≡C), 1642 (C=O). MS (FAB): *m/z (%)* 857 (18, M^+), 460 (15), 307 (100), 289 (79). HRMS (FAB): *m/z* calcd for $C_{32}H_{41}N_8P_2O_4Pt$, 858.2373; found: 858.2375 [$(M+H)^+$]. Anal. Calcd for $C_{32}H_{40}N_8P_2O_4Pt$: C, 44.80; H, 4.70. Found: C, 44.74; H, 4.99.

Complex **28** can also be prepared by applying similar alternative procedure as described for complex **27**. Reagents used: [Pt{C_2(*o*-py)}$_2$(COD)] (0.070 g, 0.137 mmol) in dichloromethane (25 mL) and DAPTA (0.063 g, 0.275 mmol) in methanol (25 mL). Reaction time: 16 h. Complex **28** was obtained as an off-white solid (0.098 g, 83% yield).

***trans*-[Pd{C_2(*p*-tol)}$_2$(DAPTA)$_2$] (29).** Reagents used: *cis*-$PdCl_2(DAPTA)_2$ (0.070 g, 0.110 mmol), triethylamine (0.034 g, 0.336 mmol), and 4-ethynyltoluene (0.063 g, 0.550 mmol) in absolute ethanol (25 mL). Reaction time: *ca.* 18 h. Complex **29** was obtained as a yellow solid (0.070 g, 80% yield), Mp 228 ^{o}C (dec). Complex **29** was found to be unstable in solutions on standing long at room temperature. ^{1}H NMR (300 MHz): δ 7.30-7.24 (m, 4H), 7.08 (d, J = 8.0 Hz, 4H), 5.84 (m, 4H), 5.00 (d, J = 14.7 Hz, 2H), 4.88 (br d, J = 14.4 Hz, 2H), 4.63 (d, J = 13.2 Hz, 2H), 4.39 (d, J = 15.2 Hz, 2H), 4.11-4.00 (m, 6H), 3.84 (d, J = 16.0 Hz, 2H), 2.32 (s, 6H, CH_3), 2.12, 2.08 (s, 12H, COCH_3). ^{31}P{^{1}H} NMR (202 MHz): δ -35.0. IR (KBr) (ν, cm^{-1}): 2103 (C≡C), 1650 (C=O). MS (FAB): *m/z (%)* 794 [9, M^+ and $(M+H)^+$ cluster], 679 (11, -C_2tol), 460 (20), 307 (100), 289 (100). Anal. Calcd for $C_{36}H_{46}N_6P_2O_4Pd$: C, 54.46; H, 5.79. Found: C, 54.97; H, 5.70.

3.1.3 Synthesis of additional PTA complexes including a chelating PTA complex

Synthesis of *cis,cis*-[$PtMe_2(\mu$-P,P)$_2PtMe_2]^{4+}$ 4Br$^-$, 30. In a 250 mL three-necked round bottom flask equipped with a 25 mL addition funnel and a magnetic stir bar was placed 1,1'-[1,3-phenylenebis(methylene)]bis-[3,5-diaza-1-azonia-7-phosphatricyclo[3.3.1.1]decane dibromide[16] (0.057 g, 0.099 mmol) and stirred with dry

methanol (100 mL) for 15 min. To this, a solution of $PtMe_2(COD)$ (0.033 g, 0.099 mmol) in dry dichloromethane (20 mL) was added dropwise with stirring over 10 min. The reaction solution was stirred for 16 h at room temperature. The reaction mixture was then evaporated to dryness on a rotary evaporator and the resulting white residue was washed with diethyl ether (3 x 10 mL) and dichloromethane (2 x 10 mL). The solid was evaporated to dryness *in vacuo*. Complex **30** was obtained as a white solid (0.085 g, 54% yield), Mp 325 ^{o}C (dec). $^{31}P\{^{1}H\}$ NMR (202 MHz, D_2O): δ -35.9 (d, $^{1}J_{PtP}$ = 1694 Hz, $^{2}J_{PP}$ = 9.5 Hz,), -38.0 (d, $^{1}J_{PtP}$ = 1701 Hz, $^{2}J_{PP}$ = 9.3 Hz),. HPLC/MS (API-ESI): *m/z* (%) 1011.9 [100, M^{+} – (P, P + CH_3)].

Synthesis of $PtI(Me)(OPTA)_2$, 31. To a 100 mL round bottom flask equipped with a 25 mL addition funnel and a magnetic stir bar was placed incompletely dried $PtI(Me)(COD)$[2] (0.100 g, 0.224 mmol) and 20 mL of dichloromethane was added to it. To this was added PTA (0.070 g, 0.448 mmol) in 20 mL of methanol. The reaction mixture was stirred overnight and the resulting solution was evaporated *in vacuo*. The residue was washed with diethyl ether (3 x 5 mL) and evaporated to dryness *in vacuo*. Formation of the oxidized product (**31**) was observed as an off-white solid, Mp 322 ^{o}C (dec). ^{1}H NMR (300 MHz): δ 4.55-4.44 (br m, NCH_2), 4.30 (br s, PCH_2), 0.47 (t, $^{2}J_{PtH}$ = 39 Hz, 3H, CH_3). $^{31}P\{^{1}H\}$ NMR (121 MHz): δ -12.2 (P=O). MS (FAB): *m/z (%)* 683 (24, M^{+}), 651 (45), 636 (57), 566 (20), 524 (24), 307 (100), 289 (57), 232 (31).

Synthesis of *trans*-$PdI_2(PTA)_2$, 32. To a 100 mL three-necked round bottom flask equipped with 25 mL addition funnel and a magnetic stirrer were placed $PdI_2(TMEDA)$[17] (0.060 g, 0.100 mmol) (TMEDA = tetramethylethylenediamine) and dissolved in dichloromethane (10 mL). The solution of PTA (0.033 g, 0.210 mmol) in methanol (10

mL) was added to it dropwise through the addition funnel with continuous stirring. The solution was stirred for 6 h at 0 ^{o}C. The resulting yellow solution formed was evaporated *in vacuo* and the yellow powder obtained was washed with (3 x 5 mL) of diethyl ether. The residue was then evaporated to dryness *in vacuo*. Complex **32** was obtained as a yellow solid (0.046 g, 68% yield), Mp 238 ^{o}C (dec). ^{1}H NMR (300 MHz): δ 4.56-4.45 (br m, NCH_2), 4.41 (br s, PCH_2). ^{31}P{^{1}H}NMR (121 MHz): δ -68.5. MS (FAB): *m/z (%)* 674 (17, M^+), 547 (10, -I), 157 (100), 115 (65), 86 (46). HRMS (FAB): *m/z* calcd for $C_{12}H_{24}N_6P_2I_2Pd$, 673.8661; found: 673.8643 (M^+).

3.1.4 Synthesis of some PTA-derivatized ligands

Synthesis of *N*-methyl-3,5-diaza-1-azonia-7-phosphatricyclo[3.3.1.1]decane-7-(4-methylpentan-2-one) triflate (ipac mPTA), L1 triflate. In a 250 mL three-necked round bottom flask equipped with a 25 mL addition funnel and a magnetic stir bar was placed PTA (0.126 g, 0.800 mmol) and was dissolved in 60 mL of bulk acetone or acetone/water mixture (*ca.* 20 : 1) at 45 ^{o}C. To this solution was added methyl triflate (0.131 g, 0.800 mmol) dropwise through the addition funnel with continuous stirring over 5 min. After stirring the solution for 20 min, an additional amount of methyl triflate (0.131 g, 0.800 mmol) was added. The resulting solution was refluxed for 2 h. The resulting solution was then evaporated *in vacuo* until *ca.* 90% of the original solution had been evaporated, then 5 mL of chloroform was added and the solution was cooled to 0 ^{o}C. A white precipitate was formed which was filtered through a sintered glass frit. The residue was washed with (3 x 10 mL) of *n*-pentane, dried over anhydrous $MgSO_4$ for 24 h, filtered, and finally dried *in vacuo*. The novel phosphine **L1** was obtained as a white solid (0.273 g, 60% yield), Mp 282-284 ^{o}C. X-ray quality crystals of **L1** were obtained

by layering methanol over the solution of **L1** in acetone below 0 ^{o}C. ^{1}H NMR (300 MHz, DMSO-d_6): δ 5.10 (br, 4H, NCH_2NC), 4.98 (d, J = 9.0 Hz, 2H, NCH_2N), 4.76-4.61 (m, 4H, PCH_2N), 4.45 (dd, J = 45.0 Hz, 13.8 Hz, 2H, PCH_2NC), 3.17 (d, J = 21.0 Hz, 2H, CH_2), 2.89 (d, J = 6.3 Hz, 3H, NCH_3), 2.23 (s, 3H, COCH_3), 1.31 (d, J = 19.2 Hz, 6H, CH_3). ^{13}C{^{1}H} NMR (75 MHz, DMSO-d_6): δ 206.5 (CO), 120.5 (q, J_{CF} = 315 Hz, CF$_3$), 77.7 (NCH$_2$NC), 77.0 (NCH$_2$N), 53.8 (d, J_{CP} = 32.2 Hz, PCH$_2$NC), 51.6 (NCH$_3$), 45.0 (d, J_{CP} = 28.5 Hz, PCH$_2$N), 42.2 (d, J_{CP} = 22.5 Hz, CH$_2$), 33.1 (d, J_{CP} = 22.5 Hz, C), 30.6 (COCH$_3$), 21.2 (CH$_3$). ^{31}P{^{1}H} NMR (121 MHz, DMSO-d_6): δ -14.0. IR (KBr) (v, cm^{-1}): 1613 (C=O). MS (FAB + NaI): *m/z (%)* 717 (100, (M^{+}+NaI)), 633 (45, -Me$_2$CH$_2$COMe), 420 (100, (M^{+}-OTf)), 336 (35, -CH$_3$, -COCH$_3$, -CH$_2$), 270 (92, (M^{+}-2OTf)), 227 (50, -COCH$_3$).

Synthesis of *N,N'*-diacetyl-1,3,5-triaza-7-phosphaadamantane (DAPTA), L2. DAPTA was synthesized following a modified literature procedure.[10] In a 500 mL three-necked round bottom flask equipped with a 25 mL addition funnel and a magnetic stir bar, was dissolved PTA (0.500 g, 3.18 mmol) in 300 mL of acetone. To this solution, maintained at 0 ^{o}C, was added acetic anhydride (0.974 g, 9.55 mmol) dropwise through the addition funnel with stirring over a period of 15 min. The mixture was stirred at 0 ^{o}C for 3 h and the solution was then allowed to stand for 30 min. The colorless reaction mixture was then evaporated to dryness on a rotary evaporator. The residue was then dissolved in a minimal quantity of acetone and precipitated with 50 mL of *n*-pentane. The resulting solution was left overnight at room temperature and the solvent was decanted off. The resulting white solid was washed with (3 x 20 mL) of diethyl ether. The sample was dried under vacuum for 30 min. **L2** was obtained as a crystalline white

solid (0.482 g, 66% yield), Mp 167-169 ^{o}C. ^{1}H NMR (300 MHz): δ 5.87 (d, J = 14 Hz, 2H), 5.35 (d, J = 18 Hz, 2H), 5.01 (d, J = 14 Hz, 2H), 4.61 (d, J = 14 Hz, 2H), 4.37 (d, J = 15 Hz, 2H), 4.02 (d, J = 14 Hz, 2H), 3.87 (m, 2H), 3.59 (d, J = 12 Hz, 4H), 3.27 (m, 2H), 2.11 and 2.12 (s, 12H, COCH_3). ^{31}P{^{1}H} NMR (121 MHz): δ -79.2. IR (KBr) (v, cm^{-1}): 1628 (C=O).

X-Ray Structure Determination of Complexes 1a, 3a, 4, 6b, 11d, 16, 19b, and 22. Crystals of the ligand **L1** and the complexes, **1a**, **3a**, **4**, **6b**, **11d**, **16**, **19b**, and **22** of appropriate dimensions were mounted on a Mitgen cryoloop in a random orientation. Preliminary examination and data collection were performed using a Bruker Kappa Apex II Charge Coupled Device (CCD) Detector system single crystal X-ray diffractometer equipped with an Oxford Cryostream LT device. All data were collected using graphite monochromated Mo Kα radiation (λ = 0.71073 Å) from a fine focus sealed tube X-ray source. Preliminary unit cell constants were determined with a set of 36 narrow frame scans. Typical data sets consist of combinations of ϖ and ϕ scan frames with typical scan width of 0.5^{o} and counting time of 15 sec/frame at a crystal to detector distance of 4.0 cm. The collected frames were integrated using an orientation matrix determined from the narrow frame scans. Apex II and SAINT software packages[18] were used for data collection and data integration. Analysis of the integrated data did not show any decay. Final cell constants were determined by global refinement of xyz centroids from the complete data set. Collected data were corrected for systematic errors using SADABS[12] based on the Laue symmetry using equivalent reflections.

Selected crystal data are listed in the Tables **2.1.1**, **2.1.4**, **2.1.5**, **2.1.7**, **2.1.9**, **2.1.10**, **2.1.11**, and **2.1.16** and intensity data collection parameters are listed in Tables **2.1.3** and **2.1.8**. Structure solution and refinement were carried out using the SHELXTL- PLUS software package.[19] The structures were solved by direct methods and refined successfully in the space groups; P-1, Pbca, $P2_1/c$, and $P2_1/n$. Full matrix least-squares refinement was carried out by minimizing $\Sigma w(F_O^2-F_C^2)^2$. The non-hydrogen atoms were refined anisotropically to convergence. A 0.5 molecule of disordered $CHCl_3$ solvate was located in the lattice of *cis*-$PtMe_2(PTA)_2$ (**1a**). One molecule of CH_2Cl_2 was found as a solvent in the lattice of *trans*-$PtCl(Et)((PTA)_2$ (**3a**) and *cis*-$[Pt\{C_2(p\text{-tol})\}_2(PTA)_2]$ (**16**) and a molecule of $CHCl_3$ was found as a solvent in the lattice of *trans*-$[Pd\{C_2(o\text{-py})\}_2(PTA)_2]$ (**22**). The complex, *trans*-$PtI_2(PTA)_2$ (**12d**) crystallizes as a hydrate with 1.75 molecules of water per Pt. There are some large residual peaks in this structure that could not be modeled successfully. The ligand, **L1** crystallizes along with a molecule of acetone and two molecules of triflate counter-anion. Various geometrical and displacement parameters restraints were used for disorder solvents (SADI, SIMU, DELU and EADP) to improve the model. Hydrogen atoms were treated using appropriate riding model (AFIX m3).

Complete listings of geometrical parameters, positional and isotropic displacement coefficients for hydrogen atoms, and anisotropic displacement coefficients for the non-hydrogen atoms within the associated CIF files and thermal ellipsoid plots are listed in Appendix II.1-II.9.

3.2 Hydrosilylation Reactions Catalyzed by cis-$PtMe_2(PTA)_2$

3.2.1 Hydrosilylation reactions of unsaturated hydrocarbons using Ph_2MeSiH (S1) and cis-$PtMe_2(PTA)_2$ (1a) as a pre-catalyst.

A representative reaction is described for the hydrosilylation reaction of 1-octyne with the hydrosilane, Ph_2MeSiH (**S1**). Unless otherwise stated, the ^1H and $^{13}C\{^1H\}$ NMR spectral data for the major isomer have been reported here.

Hydrosilylation reaction of 1-octyne. *cis*-$PtMe_2(PTA)_2$, **1a** (0.030 g, 0.25 mole%) was taken in a 100 mL three-necked round bottom flask fitted with the condenser. Both 1-octyne (1.30 g, 11.8 mmol) and **S1** (2.20 g, 11.8 mmol) were injected into the flask, then 20 mL of *n*-hexane was added. The reaction mixture was refluxed under argon with continuous stirring and monitored periodically by GC. The color started to turn red after 2 h and the reaction was carried out overnight. The reaction mixture was distilled under reduced pressure using a Kugelrohr distillation set-up and the fractions were collected at 95 ^oC and 1 mm/Hg pressure. The resulting product mixture was run through a silica gel column using hexane and CH_2Cl_2 as the eluent (1 : 1) followed by evaporation *in vacuo*. The hydrosilylated products, **H1** were obtained as a colorless oil (3.08 g, 85% yield). The product ratio (*β-trans* : *α*) = 87% : 13%. ^1H NMR (300 MHz): δ 7.81-7.49 (m, 10H), 6.40 (dt, J = 18.5 Hz, 6.0 Hz, 1H), 6.18 (dt, J = 18.5 Hz, 1.0 Hz, 1H), 2.40 (q, J = 6.2 Hz, 2H), 1.65-1.35 (m, 8H), 1.14-1.05 (m, 3H), 0.82 (s, 3H). $^{13}C\{^1H\}$ NMR (75 MHz): δ 151.9 (=CH), 137.4 (=C), 135.4 (=CH), 135.2 (=CH), 129.4 (=CH), 128.1 (=CH), 125.6 (=CH), 37.3 (CH_2), 32.1 (CH_2), 29.2 (CH_2), 28.9 (CH_2), 23.0 (CH_2), 14.5 (CH_3), -3.1 (CH_3). $^{13}C\{^1H\}$ NMR (75 MHz, DEPT): δ 151.7 (=CH), 135.2 (=C), 135.0 (=CH), 129.3 (=CH), 127.9 (=CH), 125.7 (=CH), 37.1 (CH_2), 31.9 (CH_2), 29.1 (CH_2),

28.7 (CH_2), 22.8 (CH_2), 14.3 (CH_3), -3.3 (CH_3). $^{29}Si\{^1H\}$NMR (99 MHz, DEPT): δ -11.0 (α-isomer), -14.8. MS (EI^+): *m/z* (%) 308 (9, M^+), 293 (9, -CH_3), 223 (10), 197 (14), 154 (100), 77 (8). HRMS (EI^+): *m/z* calcd for $C_{21}H_{28}Si$, 308.1960; found: 308.1953 (M^+). GC/MS (EI^+, 70 eV): *m/z* (%) 293 [17, $(M\text{-}CH_3)^+$], 223 (49), 197 (40), 183 (65), 145 (50), 121 (91), 105 (100), 93 (16), 53 (13).

Hydrosilylation reaction of 1-hexene. Reagents used: complex **1a** (0.020 g, 0.5 mole%), 1-hexene (0.630 g, 7.50 mmol), and **S1** (1.47 g, 7.50 mmol), 20 mL of *n*-hexane. Reaction time: 12 h. The solution gradually turned red. The reaction mixture was distilled under reduced pressure using a Kugelrohr distillation set-up and the fractions were collected at 95 ^oC and 1 mm/Hg pressure. The hydrosilylated product, **H2** was isolated as a colorless oil after column chromatography on silica gel using *n*-hexane as the eluent followed by evaporation *in vacuo* (1.30 g, 62% yield). The product ratio (β : α) = mainly β-isomer with a small amount of α-isomer. ^1H NMR (300 MHz, C_6D_6): δ 7.45-7.39 (m, 4H), 7.27-7.20 (m, 6H), 1.29-1.11 (m, 8H), 1.00-0.94 (m, 2H), 0.80-0.73 (m, 3H), 0.43 (s, 3H). $^{13}C\{^1H\}$ NMR (75 MHz): δ 137.6 (CH), 134.5 (CH), 129.1 (CH), 128.9 (CH), 33.4 (CH_2), 31.6 (CH_2), 23.9 (CH_2), 22.7 (CH_2), 14.3 (d, J_{CSi} = 6.0 Hz, CH_2), 1.2 (CH_3), -4.2 (CH_3). $^{29}Si\{^1H\}$ NMR (99 MHz, DEPT): δ -7.1. GC/MS (EI^+, 70 eV): *m/z* (%) 267 [1, $(M\text{-}CH_3)^+$], 204 (11), 197 (100), 183 (10), 105 (16).

Hydrosilylation reaction of phenylacetylene. Reagents used: complex **1a** (0.030 g, 0.5 mole%), phenylacetylene (1.53 g, 15.0 mmol), and **S1** (2.97 g, 15.0 mmol), 20 mL of *n*-hexane. Reaction time: 36 h. The reaction mixture was evaporated on a rotary evaporator and then distilled under reduced pressure using a Kugelrohr distillation set-up and the fractions were collected at 95 ^oC and 1 mm/Hg pressure. The hydrosilylated

products, **H3** were isolated as a colorless oil by column chromatography on silica gel using *n*-hexane and dichloromethane (1 : 1) as the eluents followed by evaporation *in vacuo* (2.51 g, 56% yield). The product ratio (*β-trans* : *α*) = 88% : 12%. ^{1}H NMR (300 MHz): *δ* 7.56-7.50 (m, 4H), 7.42-7.37 (m, 2H), 7.34-7.14 (m, 9H), 6.93 (d, *J* = 19.1 Hz, 1H), 6.72 (d, *J* = 19.1 Hz, 1H), 0.67 (s, 3H). ^{13}C{^{1}H} NMR (75 MHz): *δ* 147.8 (=CH), 138.6 (=C), 137.0 (=CH), 135.5 (=CH), 129.9 (=CH), 128.9 (=CH), 128.7 (=CH), 128.5 (=CH), 128.2 (=CH), 125.4 (=CH), -3.0 (CH_3). ^{13}C{^{1}H} NMR (75 MHz, DEPT): *δ* 148.0 (=CH), 135.5 (=CH), 130.1 (=CH), 129.2 (=CH), 129.0 (=CH), 128.6 (=CH), 125.5 (=CH), -3.2 (CH_3), -4.2 (*α*-isomer, CH_3). ^{29}Si{^{1}H} NMR (99 MHz, DEPT): *δ* -11.4 (*α*-isomer), -13.6. GC/MS (EI^{+}, 70 eV): *m/z* (%) 300 (12, M^{+}), 285 (34, -CH_3), 222 (40), 207 (85), 197 (13), 181 (24), 145 (21), 121 (31), 105 (100), 93 (16), 77 (22), 53 (24).

Hydrosilylation reaction of 3-phenyl-1-propyne. Reagents used: complex **1a** (0.5 mole%), 3-phenyl-1-propyne (0.384 g, 3.30 mmol), and **S1** (0.656 g, 3.30 mmol), 20 mL of *n*-hexane. Reaction time: 25 h. The reaction mixture was distilled under reduced pressure in a Kugelrohr distillation set-up and the fractions were collected at 95 ^{o}C and 1 mm/Hg pressure. After distillation, the residual solid was dissolved in a a small amount of CH_2Cl_2. Then an excess of *n*-hexane was added and the resulting precipitate was filtered. The residue was washed with *n*-hexane and evaporated in a rotary evaporator. The product was isolated as a colorless oil after column chromatography on silica gel using *n*-hexane and CH_2Cl_2 as the eluents (1 : 1) followed by evaporation *in vacuo*. A colorless semi-solid, **H4** was obtained (0.673 g, 65% yield). The product ratio (*β-trans* : *α*) = 86% : 14%. ^{1}H NMR (300 MHz): *δ* 7.7-7.1 (m, 15H), 6.40 (dt, *J* = 18.4 Hz, 6.2 Hz, 1H), 6.12 (dt, *J* = 18.4 Hz, 1.4 Hz, 1H), 3.65-3.57 (m, 2H), 0.69 (s, 3H). ^{13}C{^{1}H} NMR

(75 MHz, DEPT): δ 135.5 (=CH), 135.2 (=C), 129.9 (=CH), 129.7 (=CH), 129.6 (=CH), 129.2 (=CH), 128.9 (=CH), 128.6 (=CH), 128.2 (=CH), 127.6 (=CH), 126.6 (=CH), 43.8 (CH_2), 42.8 (α-isomer, CH_2), -3.2 (CH_3), -3.5 (α-isomer, CH_3). $^{29}Si\{^1H\}$ NMR (99 MHz, DEPT): δ -11.1 (α-isomer), -15.3. GC/MS (EI^+, 70 eV): *m/z* (%) 299 [7, $(M\text{-}CH_3)^+$], 223 (100), 197 (27), 183 (34), 145 (53), 121 (41), 105 (71), 91 (26), 53 (15). MS (EI^+): *m/z* (%) 314 (30, M^+), 299 (35, -CH_3), 236 (34, -Ph), 223 (100), 197 (75), 183 (50). HRMS (EI^+): *m/z* calcd for $C_{22}H_{22}Si$, 314.1491; found: 314.1484 (M^+).

Hydrosilylation reaction of 1,7-octadiyne. Reagents used: complex **1a** (0.5 mole%) in 20 mL of *n*-hexane, and **S1** (1.66 g, 8.40 mmol), and 1,7-octadiyne (0.400 g, 4.20 mmol). Reaction time: 26 h. The crude product was purified by silica gel column using *n*-hexane and dichloromethane (1 : 1) as the eluents. The hydrosilylated products, **H5** were obtained as a colorless oil (3.01 g, 71% yield). The product ratio (β-*trans* : α) = 87% : 13%. ^1H NMR (300 MHz): δ 7.67-7.39 (m, 20H), 6.27 (dt, J = 18.6 Hz, 6.0 Hz, 2H), 6.07 (dt, J = 18.6 Hz, 1.3 Hz, 2H), 2.36-2.26 (m, 4H), 1.61-1.52 (m, 4H), 0.73 (s, 6H). $^{13}C\{^1H\}$ NMR (75 MHz): δ 151.4 (=CH), 137.2 (=C), 135.2 (=CH), 135.0 (=CH), 129.3 (=CH), 127.9 (=CH), 125.5 (=CH), 36.9 (CH_2), 28.2 (CH_2), -3.4 (CH_3). $^{13}C\{^1H\}$ NMR (75 MHz, DEPT): δ 151.8 (=CH), 135.5 (=CH), 135.3 (=CH), 129.7 (=CH), 128.3 (=CH), 125.8 (=CH), 37.2 (CH_2), 28.8 (CH_2), -3.0 (CH_3). $^{29}Si\{^1H\}$ NMR (99 MHz, DEPT): δ -11.5 (α-isomer), -15.3. MS (FAB^+): *m/z* (%) 505 [10, $(M+2H)^+$], 434 (14), 393 (55), 322 (100), 282 (20), 250 (28), 210 (12). GC/MS (EI^+, 70 eV): *m/z* (%) 289 [12, (M^+-Ph_2Me_2Si)], 226 (8), 211 (29), 197 (55), 183 (52), 145 (32), 131 (18), 121 (70), 105 (100), 91 (20), 53 (18).

Hydrosilylation reaction of 1,9-decadiene. Reagents used: complex **1a** (0.5 mole%) in 20 mL of *n*-hexane, **S1** (0.914 g, 4.62 mmol), 1,9-decadiene (0.320 g, 2.30 mmol). Reaction time: 32 h (45% conversion with respect to **S1**). The crude product was purified by silica gel column using *n*-hexane and dichloromethane (1 : 1) as the eluents. A colorless oily product, **H6** was obtained (0.502 g, 65% yield with respect to 1,9-decadiene). The product ratio (β : α) = β-isomer only. ^{1}H NMR (300 MHz): δ 7.65-7.39 (m, 10H), 5.77-5.55 (m, 1H), 4.92-4.80 (m, 2H), 1.93-1.88 (m, 2H), 1.17-1.12 (m, 10H), 0.44 (br s, 7H). ^{13}C{^{1}H} NMR (75 MHz): δ 139.3 (=CH), 137.7 (=C), 134.6 (=CH), 129.2 (=CH), 127.9 (=CH), 114.3 (=CH_2), 34.0 (CH_2), 33.8 (CH_2), 29.6 (CH_2), 29.3 (m, CH_2), 29.1 (CH_2), 24.0 (CH_2), 14.3 (*C*H_2-Si), -4.2 (*C*H_3-Si). ^{13}C{^{1}H} NMR (75 MHz, DEPT): δ 140.0 (=CH), 135.3 (=CH), 129.9 (=CH), 128.6 (=CH), 115.0 (=CH_2), 34.7 (CH_2), 34.5 (CH_2), 30.3 (CH_2), 30.1 (m, CH_2), 30.0 (CH_2), 24.7 (CH_2), 14.2 (*C*H_2-Si), -3.5 (*C*H_3-Si). ^{29}Si{^{1}H} NMR (99 MHz, DEPT): δ -7.1. GC/MS (EI^{+}, 70 eV): *m/z* (%) 258 [5, (M-Ph)$^{+}$], 197 (100), 183 (20), 121 (20), 105 (30), 55 (24).

3.2.2 Hydrosilylation reactions of 1-heptyne using sterically hindered hydrosilanes and HSi(C≡CPh)$_3$ in the presence of (1a) as a pre-catalyst.

A representative reaction is described for the hydrosilylation of 1-heptyne (**A1**) using diisopropyloctylsilane (**S2**).

Hydrosilylation reaction of 1-heptyne (A1) using diisopropyloctylsilane (S2). Complex **1a (**0.5 mole%) was placed in a 100 mL three-necked round bottom flask fitted with a condenser and stirred with 20 mL of *n*-hexane. Then **A1** (0.270 g, 2.80 mmol) and **S2** (0.600 g, 2.60 mmol) were injected into the flask. The reaction mixture was refluxed under argon with continuous stirring. The reaction was run overnight (*ca.* 16 h) and

monitored periodically by GC. The crude product was purified by silica gel column chromatography using hexane/dichloromethane as the eluents (1 : 1) followed by evaporation *in vacuo*. A colorless oil, **H7** was obtained (0.656 g, 77% isolated yield). Product ratio (*β-trans* : *α*): mainly *β-trans* isomer with a small amount of the *α*-isomer. The product ratio before isolation (*β-trans* : *α*) = 93% : 7%. ^{1}H NMR (300 MHz): δ 5.95 (dt, J_{HH} = 18.7 Hz, 6.3 Hz, 1H), 5.41(dt, J_{HH} = 18.7 Hz, 1.4 Hz, J_{SiH} = 114 Hz, 1H), 2.08-1.96 (m, 2H), 1.28-1.16 (m, 18H), 0.96-0.87 (m, 12H), 0.84-0.79 (m, 8H), 0.55-0.49 (m, 2H). ^{13}C{^{1}H} NMR (75 MHz): δ 149.7 (=CH), 124.3 (=CH), 37.6 (CH_2), 34.6 (CH_2), 32.4 (CH_2), 31.7 (CH_2), 29.77 (CH), 29.70 (CH), 28.9 (CH_2), 24.5 (CH_2), 23.1 (CH_2), 22.9 (CH_2), 18.6 (CH_3), 18.5 (CH_3), 14.5 (CH_2), 14.4 (CH_2), 11.5 (CH_3), 9.9 (CH_3). ^{29}Si{^{1}H} NMR (99 MHz, DEPT): δ -1.5. GC/MS (EI^{+}, 70 eV): *m/z* (*%*) 281 [46, (M-^{i}Pr)$^{+}$], 169 (100), 141 (41), 127 (39), 113 (40), 99 (99), 85 (87), 71 (51), 69 (51), 59 (87).

Reaction using dimethyloctadecylsilane (S3). Reagents used: complex **1a** (0.5 mole%) in 20 mL of *n*-hexane, **A1** (0.210 g, 2.10 mmol), and **S3** (0.600 g, 1.92 mmol). Reaction time: 16 h. The hydrosilylated products, **H8** were obtained as a colorless oil (0.783 g, 85% yield). The product ratio (*β-trans* : *α*) = 97% : 3%. ^{1}H NMR (300 MHz): δ 6.03 (dt, *J* = 18.6 Hz, 6.2 Hz, 1H), 5.60 (d, *J* = 18.6 Hz, 1.4 Hz, 1H), 2.11 (q, *J* = 6.3 Hz, 2H), 2.11 (q, *J* = 6.4 Hz, 2H), 1.35-1.23 (br m, 38H), 0.96-0.85 (m, 6H), 0.56-0.47 (m, 2H, C*H*$_2$-Si), -0.01 (s, 6H). ^{13}C{^{1}H} NMR (75 MHz): δ 147.9 (=CH), 128.8 (=CH), 37.1 (CH_2), 33.9 (CH_2), 32.2 (CH_2), 31.7 (CH_2), 30.0 (CH_2), 29.6 (m, CH_2), 28.7 (CH_2), 24.2 (CH_2), 23.0 (CH_2), 22.8 (CH_2), 16.0 (CH_3), 14.3 (*C*H_2-Si), -2.7 (*C*H_3-Si). ^{29}Si{^{1}H}NMR (99 MHz, DEPT): δ -3.8 (*α*-isomer), -7.0. GC/MS (EI^{+}, 70 eV): *m/z* (*%*) 393 [1, (M-CH_3)$^{+}$], 155 (100), 141 (27), 127 (41), 99 (29), 73 (19), 59 (80).

Reaction using dimethylphenethylsilane (S4). Reagents used: complex **1a** (0.5 mole%) in 20 mL of *n*-hexane, **A1** (0.400 g, 4.10 mmol), and **S4** (0.600 g, 3.70 mmol). Reaction time: 16 h. The hydrosilylated products, **H9** were obtained as a colorless oil (0.609 g, 67% yield). The product ratio (*β-trans* : *α*) = 96% : 4%. ^{1}H NMR (300 MHz): *δ* 7.47-7.29 (m, 5H), 6.27 (dt, *J* = 18.5 Hz, 6.2 Hz, 1H), 5.82 (dt, *J* = 18.5 Hz, 1.4 Hz, 1H), 2.86-2.78 (m, 2H), 2.35-2.28 (m, 2H), 1.63-1.48 (m, 6H and *α*-isomer), 1.24-1.08 (m, 3H and *α*-isomer), 0.41-0.26 (m, 6H and *α*-isomer). ^{13}C{^{1}H} NMR (75 MHz): *δ* 148.4 (=CH), 145.4 (=CH), 128.4 (=CH), 128.1 (=CH), 128.0 (=CH), 125.6 (=CH), 37.0 (CH_2), 31.6 (CH_2), 30.3 (CH_2), 28.6 (CH_2), 22.8 (CH_2), 18.1 (CH_2), 14.3 (CH_3), -2.8 (CH_3). ^{13}C{^{1}H}NMR (75 MHz, DEPT): *δ* 148.5 (=CH), 128.5 (=CH), 128.1 (=CH), 128.0 (=CH), 125.6 (=CH), 36.9 (CH_2), 31.8 (CH_2), 30.4 (CH_2), 28.6 (CH_2), 22.8 (CH_2), 18.1 (CH_2), 14.3 (CH_3), -2.8 (CH_3). ^{29}Si{^{1}H}NMR (99 MHz, DEPT): *δ* -3.5 (*α*-isomer), -6.6. GC/MS (EI^{+}, 70 eV): *m/z* (%) 245 [15, (M-CH_3)$^{+}$], 162 (100), 155 (72), 147 (32), 135 (17), 99 (18), 85 (17), 59 (85).

Reaction using $HSi(C{\equiv}CPh)_3$ (S5). Reagents used: complex **1a** (0.5 mole%) in 20 mL of toluene, **S5** (0.600 g, 1.80 mmol) in 10 mL of toluene, and **A1** (0.200 g, 2.00 mmol). Reaction time: 18 h. The hydrosilylated products, **H10** were obtained as a colorless solid (0.423 g, 55% yield), Mp 65-68 ^{o}C. The product ratio (*β-trans* : *α*) = 67% : 33%. ^{1}H NMR (300 MHz): *δ* 7.65-7.34 (m, 15H), 6.77 (dt, *J* = 18.2 Hz, 6.2 Hz, 1H), 6.08 (m, *α*-isomer), 5.93 (m, *α*-isomer), 5.81 (dt, *J* = 18.3 Hz, 1.5 Hz, 1H), 2.51 (m, *α*-isomer), 2.30 (q, *J* = 7.2 Hz, 2H), 1.79-1.67 (m, *α*-isomer), 1.59-1.48 (m, 2H), 1.46-1.30 (m, 4H and *α*-isomer), 0.97-0.87 (m, 3H and *α*-isomer). ^{13}C{^{1}H} NMR (75 MHz): *δ* 154.5 (=C), 132.5 (=CH), 129.4 (=CH), 128.4 (=CH), 122.5 (=CH), 121.0 (=CH), 107.3

(≡C, α-isomer), 107.1 (≡C), 87.3 (≡C), 87.0 (≡C, α-isomer), 36.7 (CH_2), 35.5 (CH_2, α-isomer), 31.7 (CH_2), 28.8 (CH_2, α-isomer), 28.0 (CH_2), 22.7 (CH_2), 14.2 (CH_3). $^{13}C\{^1H\}$ NMR (75 MHz, DEPT): δ 154.5 (=CH), 131.5 (=CH), 129.3 (=CH), 128.24 (=CH), 120.9 (=CH), 36.7 (CH_2), 35.5 (CH_2), 31.8 (CH_2), 31.7 (CH_2), 28.8 (CH_2), 28.0 (CH_2), 22.8 (CH_2), 22.7 (CH_2), 14.2 (CH_3). $^{29}Si\{^1H\}$ NMR (99 MHz, DEPT): δ -70.0. GC/MS (EI^+, 70 eV): *m/z* (%) 428 (6, M^+), 371 (10), 357 (12), 331 (20), 283 (19), 231 (23), 207 (45), 153 (25), 129 (100), 103 (20), 96 (10).

3.2.3 Hydrosilylation reaction of 1-heptyne using Ph_2MeSiH in the presence of some polydentate phosphine complexes of platinum as pre-catalysts.

A representative reaction is described for $Pt_2(\mu\text{-dppm})_3$ (**B1**) used as a pre-catalyst for the hydrosilylation reaction of 1-heptyne (**A1**) with Ph_2MeSiH (**S1**). The pre-catalysts, **B1** and **B2** were prepared previously by a former graduate student following literature procedures (see the references in "**General remarks**" in this section).

Hydrosilylation reaction of 1-heptyne using Ph_2MeSiH (S1) in the presence of $Pt_2(\mu\text{-dppm})_3$ (B1) [dppm = 1,1-bis(diphenylphosphino)methane]. A sample of **B1** (0.5 mole%) was placed in a 100 mL three-necked round bottom flask fitted with a condenser and stirred with 20 mL of *n*-hexane. Then **A1** (0.316 g, 3.30 mmol) and **S1** (0.600 g, 3.00 mmol) were injected into the flask. The reaction mixture was refluxed under argon with continuous stirring and monitored periodically by means of GC. The reaction was carried out overnight (*ca*. 16 h). The reaction mixture was distilled under reduced pressure using a Kugelrohr distillation set-up and the fractions were collected at 95 ^oC and 1 mm/Hg pressure. The product was purified by silica gel column chromatography using *n*-hexane and dichloromethane (1 : 1) as the eluents, and then

evaporated *in vacuo*. The hydrosilylated products, **H11** were obtained as a colorless oil (0.661 g, 75% yield). The product ratio (*β-trans* : *α*) = 89% : 11%. ^{1}H NMR (300 MHz): *δ* 7.44-7.41 (m, 4H), 7.27-7.22 (m, 6H), 6.07 (dt, *J* = 18.5 Hz, 6.1 Hz, 1H), 5.85 (dt, *J* = 18.5 Hz, 1.3 Hz, 1H), 2.08 (m, 2H), 1.38-1.12 (m, 8H), 0.79 (m, 3H), 0.50 (s, 3H). ^{13}C{^{1}H} NMR (75 MHz): *δ* 151.8 (=CH), 137.3 (=C), 135.2 (*α*-isomer), 135.0 (=CH), 129.3 (=CH), 127.9 (=CH), 125.3 (=CH), 37.1 (CH_2), 31.6 (CH_2), 28.4 (CH_2), 22.7 (CH_2), 14.3 (CH_3), -3.4 (CH_3). ^{13}C{^{1}H} NMR (75 MHz, DEPT): *δ* 151.8 (=CH), 135.0 (=CH), 129.3 (=CH), 127.9 (=CH), 125.2 (=CH), 37.1 (CH_2), 31.7 (CH_2), 28.4 (CH_2), 22.8 (CH_2), 14.2 (CH_3), -3.4 (CH_3). ^{29}Si{^{1}H} NMR (99 MHz, DEPT): *δ* -11.4 (*α*-isomer), -15.2. GC/MS (EI^+, 70 eV): *m/z* (%) 294 (12, M^+), 279 (11, -CH_3), 223 (12), 197 (100), 183 (20), 160 (14), 121 (36), 105 (56), 93 (14), 53 (22).

Reaction in the presence of $Pt_3(nbe)_2(dppa)_4$ (B2) [nbe = norbornene; dppa = 1,2-bis(diphenylphosphino)acetylene]. Reagents used: **B2** (0.5 mole%) in 20 mL of *n*-hexane, **A1** (0.316 g, 3.30 mmol), and **S1** (0.600 g, 3.00 mmol). Reaction time: 16 h. A colorless oil, **H11** was formed (0.652 g, 74% yield). The product ratio (*β-trans* : *α*) = 90% : 10%. ^{1}H NMR (300 MHz): *δ* 7.46-7.42 (m, 4H), 7.28-7.24 (m, 6H), 6.08 (dt, *J* = 18.5 Hz, 6.1 Hz, 1H), 5.85 (m, 1H), 2.10 (m, 2H), 1.39-1.12 (m, 8H), 0.78 (m, 3H), 0.51 (s, 3H). ^{13}C{^{1}H} NMR (75 MHz): *δ* 151.9 (=CH), 137.3 (=C), 135.2 (*α*-isomer), 135.0 (=CH), 129.3 (=CH), 127.9 (=CH), 125.2 (=CH), 37.1 (CH_2), 31.6 (CH_2), 28.4 (CH_2), 22.7 (CH_2), 14.2 (CH_3), -3.4 (CH_3). ^{13}C{^{1}H} NMR (75 MHz, DEPT): *δ* 151.9 (=CH), 135.0 (=CH), 129.3 (=CH), 127.9 (=CH), 125.2 (=CH), 36.2 (CH_2), 31.8 (CH_2), 28.7 (CH_2), 22.7 (CH_2), 14.2 (CH_3), -3.4 (CH_3). ^{29}Si{^{1}H} NMR (99 MHz, DEPT): *δ* -11.6 (*α*-

isomer), -15.4. GC/MS (EI^+, 70 eV): *m/z* (%) 294 (5, M^+), 279 (23, -Me), 223 (56), 197 (39), 183 (100), 145 (61), 121 (83), 105 (87), 53 (15).

Reaction in the presence of $PtMe_2$(dppp) (B3) [dppp = 1,3-bis(diphenylphosphino)propane]. Reagents used: **B3** (0.5 mole%) in 20 mL of *n*-hexane, **A1** (0.316 g, 3.30 mmol), and **S1** (0.600 g, 3.00 mmol). Reaction time: 16 h. A colorless oil, **H11** was formed (0.635 g, 72% yield). The product ratio (β-*trans* : α) = 87% : 13%. ^{1}H NMR (500 MHz): δ 7.65-7.60 (m, 4H), 7.47-7.42 (m, 6H), 6.29 (dt, *J* = 18.5 Hz, 6.2 Hz, 1H), 6.07 (dt, *J* = 18.5 Hz, 1.4 Hz, 1H), 2.32-2.27 (m, 2H), 1.56-1.38 (m, 6H), 1.01 (m, 3H), 0.72 (s, 3H). ^{13}C{^{1}H} NMR (125 MHz): δ 151.8 (=C), 137.4 (=CH), 135.2 (α-isomer), 135.0 (=CH), 129.4 (=CH), 127.9 (=CH), 125.3 (=CH), 37.1 (CH_2), 31.8 (CH_2), 28.4 (CH_2), 22.7 (CH_2), 14.3 (CH_3), -3.4 (CH_3). ^{29}Si{^{1}H} NMR (99 MHz, DEPT): δ -11.5 (α-isomer), -15.3. GC/MS (EI^+, 70 eV): *m/z* (%) 294 (3, M^+), 279 (16, -CH_3), 223 (40), 197 (21), 183 (67), 145 (47), 121 (96), 105 (100), 91 (14), 53 (19).

Reaction in the presence of $PtMe_2$(dppe) (B4) [dppe = 1,2-bis(diphenylphosphino)ethane]. Reagents used: **B4** (0.5 mole%) in 20 mL of *n*-hexane, **A1** (0.316 g, 3.30 mmol), and **S1** (0.600 g, 3.00 mmol). Reaction time: 16 h. A colorless oil, **H11** was formed (0.740 g, 84% yield). The product ratio (β-*trans* : α) = 90% : 10%. ^{1}H NMR (300 MHz): δ 7.77-7.67 (m, 4H), 7.54-7.49 (m, 6H), 6.39 (dt, *J* = 18.5 Hz, 6.1 Hz, 1H), 6.17 (dt, *J* = 18.5 Hz, 1.3 Hz, 1H), 2.40 (m, 2H), 1.70-1.45 (m, 6H), 1.08 (m, 3H), 0.81 (s, 3H). ^{13}C{^{1}H} NMR (75 MHz): δ 151.8 (=CH), 137.3 (=C), 135.2 (α-isomer), 135.0 (=CH), 129.3 (=CH), 127.9 (=CH), 125.3 (=CH), 37.1 (CH_2), 31.8 (CH_2), 28.4 (CH_2), 22.7 (CH_2), 14.3 (CH_3), -3.4 (CH_3). ^{29}Si{^{1}H} NMR (99 MHz,

DEPT): δ -11.4 (α-isomer), -15.2. GC/MS (EI^+, 70 eV): *m/z* (%) 294 (3, M^+), 279 (11, -Me), 223 (33), 197 (25), 183 (68), 145 (61), 121 (85), 105 (100), 91 (12), 53 (12).

Reaction in the presence of (1a). Reagents used: **1a** (0.5 mole%) in 20 mL of *n*-hexane, **A1** (0.316 g, 3.30 mmol), and **S1** (0.600 g, 3.00 mmol). Reaction time: 16 h. A colorless oil, **H11** was formed (0.746 g, 85% yield). The product ratio (β-*trans* : α) = 89% : 11%. ^{1}H NMR (500 MHz): δ 7.77-7.70 (m, 4H), 7.60-7.45 (m, 6H), 6.36 (dt, *J* = 18.5 Hz, 6.2 Hz, 1H), 6.15 (dt, *J* = 18.5 Hz, 1.4 Hz, 1H), 2.34 (m, 2H), 1.63-1.37 (m, 8H), 1.14 (m, 3H), 0.78 (s, 3H). ^{29}Si{^{1}H} NMR (99 MHz, DEPT): δ -11.5 (α-isomer), -15.3.

3.2.4 Hydrosilylation reactions using a variety of siloles and silafluorenes in the presence of (1a) as a pre-catalyst.

A representative reaction is described for the hydrosilylation reaction of 1-heptyne (**A1**) using 1-hydrido-1,2,5-triphenylsilole (**S6**) in the presence of (**1a**).

Hydrosilylation of 1-heptyne using 1-hydrido-1,2,5-triphenylsilole (S6). Complex **1a** (0.5 mole%) was stirred in 10 mL of benzene in a 100 mL three-necked round bottom flask. The solution of **S6** (0.400 g, 1.22 mmol) in 30 mL of benzene and **A1** (0.150 g, 1.50 mmol) were injected into the flask. The reaction mixture was refluxed under argon with continuous stirring for 26 h and monitored by GC periodically. The crude product was purified by silica gel column chromatography using *n*-hexane/dichloromethane as the eluents (1 : 1) and then evaporated *in vacuo*. A yellow viscous liquid, **H12** was obtained which converted into a yellow solid on standing at room temperature (0.302 g, 61% yield), Mp 133-135 ^{o}C. The product ratio (β-*trans* : α) = 84% : 16%. ^{1}H NMR (300

MHz): δ 7.64-7.12 (m, 21H), 6.38 (dt, J = 18.5 Hz, 6.2 Hz, 1H), 6.07 (m, 1H), 2.15 (m, 2H), 1.38-1.20 (br m, 6H), 0.88-0.80 (m, 5H). $^{13}C\{^{1}H\}$ NMR (75 MHz, DMSO-d_6): δ 154.5 (=CH), 142.5 (=C), 139.9 (=C), 137.8 (=C), 134.5 (=CH), 132.2 (=CH), 130.2 (=CH), 128.6 (=CH), 128.4 (=CH), 127.1 (=CH), 126.4 (=CH), 120.2 (=CH), 36.3 (CH_2), 30.5 (CH_2), 27.4 (CH_2), 21.8 (CH_2), 13.8 (CH_3). $^{13}C\{^{1}H\}$ NMR (75 MHz, DEPT, DMSO-d_6): δ 140.0 (=CH), 134.5 (=CH), 130.2 (=CH), 129.0 (=CH), 128.7 (=CH), 128.5 (=CH), 127.2 (=CH), 126.4 (=CH), 36.3 (CH_2), 30.5 (CH_2), 27.4 (CH_2), 21.8 (CH_2), 13.9 (CH_3). $^{29}Si\{^{1}H\}$ NMR (99 MHz, DEPT): δ -10.0 (α-isomer), -12.2. GC/MS (EI^+, 70 eV): *m/z* (%) 406 (13, M^+), 322 (22), 245 (16), 207 (44), 129 (14), 105 (100), 85 (19), 55 (14).

Hydrosilylation reaction of trimethylsilylacetylene using 1-hydrido-1-methyl(tetraphenyl)silole (S7). Reagents used: complex **1a** (3 mole%) in 10 mL of toluene, **S7** (0.600 g, 1.50 mmol) in 10 mL of toluene and trimethylsilylacetylene (0.147 g, 1.50 mmol). Reaction time: 24 h. The products ratio (β-*trans* : α) = *ca.* 2 : 1. After purification by silica gel column chromatography using dichloromethane and hexane (1 : 1) as the eluents followed by evaporation *in vacuo*, the residue was dissolved in 1 mL of THF and reprecipitated using 10 mL of methanol. The residue was filtered using a sintered glass frit and then dried in air. The hydrosilylated β-*trans* product, **H13** was obtained as a yellow powder (0.373 g, 50% yield), Mp 115-117 ^{o}C (lit.[13d] 118-119 ^{o}C). ^{1}H NMR (mixture of isomers) (300 MHz): δ 7.88 (d, J = 7.5 Hz, 4H), 7.84-7.03 (m, 17H), 6.51 (d, J = 18.9 Hz, 1H), 0.60 (m, 3H, CH_3-Si, α-isomer), 0.37 (br m, 3H, CH_3-Si, β-*trans* isomer), 0.07 (s, 9H, Me_3-Si). ^{1}H NMR (β-*trans* isomer) (300 MHz): δ 7.18-6.68 (m, 22H), 0.40 (br s, 3H, CH_3-Si), 0.07 (br s, 9H, Me_3-Si). $^{13}C\{^{1}H\}$ NMR (75 MHz): δ

153.7 (=CH), 139.0 (=C), 138.5 (=C), 137.2 (=C), 130.0 (=CH), 129.3 (=CH), 128.0 (=CH), 127.6 (=CH), 126.5 (=CH), 125.9 (=CH), 1.2 (CH_3-Si), -1.6 (Me_3-Si). $^{29}Si\{^1H\}$ NMR (99 MHz, DEPT): δ -1.0, -7.4. GC/MS (EI^+, 70 eV): *m/z* (%) 499 [20, $(M+H)^+$], 484 (35, -CH_3), 428 (16), 357 (14), 303 (18), 226 (15), 207 (100), 162 (24), 139 (14), 104 (34), 71 (42), 54 (20). UV-Vis (CH_2Cl_2, 10^{-3} M): λ_{abs} = 278.9, 289.0 nm; Fluorescence (CH_2Cl_2, 10^{-3} M): λ_{em} = 416.0 nm, λ_{ex} = 345.0 nm.

Hydrosilylation reaction of 1,4-diethynylbenzene using 1-hydrido-1-methylsilafluorene (S8). Complex **1a** (3 mole%) was stirred in 10 mL of toluene in a 100 mL three-necked round bottom flask equipped with a bent tube. The solution of **S8** (0.101 g, 1.60 mmol) in 20 mL of toluene was injected into the flask and stirred for 2 min. A sample of 1,4-diethynylbenzene (0.315 g, 0.800 mmol) was introduced into the solution through the bent tube. The reaction mixture was stirred under argon for 20 h at room temperature and monitored by GC periodically. The light yellow solution was filtered through a sintered glass frit and evaporated *in vacuo*. The reaction mixture was purified by silica gel column chromatography using *n*-hexane/dichloromethane as the eluents (1 : 1) and then evaporated *in vacuo*. The residue was dissolved in 2 mL of THF and reprecipitated using 10 mL of methanol. The precipitate was filtered by vacuum filtration using a sintered glass frit and then dried in air. The hydrosilylated products, **H14** were obtained as an off-white powder (0.770 g, 52% yield), Mp 338-342 ^oC. The product ratio (β-*trans* : α) = 87% : 13%. ^1H NMR (500 MHz): δ 7.84 (m, 4H), 7.66 (m, 4H), 7.44 (m, 4H), 7.35 (s, 4H), 7.34-7.24 (m, 4H, overlapping with solvent), 7.06 (br d, *J* = 18.9 Hz, 2H), 6.50 (d, *J* = 18.9 Hz, 2H), 0.69 (s, 6H). $^{13}C\{^1H\}$ NMR (125 MHz): δ 148.4 (=CH), 146.9 (=CH), 137.5 (=C), 134.5 (=C), 133.5 (=CH), 130.6 (=CH), 128.2

(=CH), 128.1 (=CH), 128.0 (=CH), 127.8 (=CH), 127.7 (=CH), 127.6 (=CH), 127.0 (=CH), 123.4 (=CH), 121.1 (=CH), -5.0 (CH_3). $^{29}Si\{^1H\}$ NMR (99 MHz, DEPT): δ -4.9 (α-isomer), -12.9.

Hydrogermylation reaction of 1,4-diethynylbenzene using 1,1-dihydrido(tetraphenyl)germole (S9). Reagents used: complex **1a** (6 mole%) in 10 mL of toluene, **S9** (0.025 g, 0.056 mmol) in 20 mL of toluene, and 1,4-diethynylbenzene (0.085 g, 0.067 mmol). Reaction time: 24 h (refluxed). The residue was dissolved in 1 mL of THF and reprecipitated using 10 mL of methanol. The procedure of precipitation was repeated three times to remove low molecular weight oligomers. The resulting precipitate was filtered using a sintered glass frit and then dried in air. A yellow-powdered oligomeric product, **H15** was obtained. ^1H NMR (300 MHz): δ 7.32-6.69 (br, 28H). IR (KBr) (ν, cm^{-1}): 2251 (C≡C). UV-Vis (CH_2Cl_2, 10^{-3} M): λ_{abs} = 279 nm; Fluorescence (CH_2Cl_2, 10^{-3} M): λ_{ex} = 358 nm, λ_{em} = 420 nm.

Hydrosilylation reaction of 2,4-pentanedione using 1-hydrido-1-methylsilafluorene, S8. A sample of 2 mole % of Wilkinson's catalyst or 1 mole% of Speier's catalyst was placed in a 100 mL three-necked round bottom flask. A solution of **S8** (0.400 g, 2.0 mmol) was prepared in 20 mL of toluene. This solution and 2,4-pentanedione (0.102 g, 1.0 mmol) in 10 mL of toluene were injected into the flask. The reaction mixture was stirred under argon for 20 h at room temperature. The reaction was monitored by GC (46% conversion with respect to **S8**). The resulting brownish solution was filtered through a sintered glass frit and immediately evaporated *in vacuo*. The colorless solid, **H16** was then characterized by GC-MS. GC-MS: *m/z* (%) 281 (25, -CH_3), 207 (100), 191 (24), 133 (32), 96 (43), 73 (38).

3.3 Cross-Coupling Reactions Catalyzed by Palladium(II)-PTA Complexes

3.3.1 Suzuki-Miyaura cross-coupling reactions of a variety of substrates with phenylboronic acid catalyzed by trans-PdCl(Me)(PTA)$_2$, 5a.

A representative reaction is described for the reaction of 4-bromoacetophenone with phenylboronic acid.

Reaction of 4-bromoacetophenone. The following reagents, 4-bromoacetophenone, **R1** (0.100 g, 0.505 mmol), K_2CO_3 (0.210 g, 1.50 mmol), and *trans*-PdCl(Me)(PTA)$_2$, **5a** (3 mole%) were placed in a 100 mL three-necked round bottom flask equipped with a 25 mL addition funnel and a magnetic stir bar and degassed for 20 min under argon atmosphere. To this was added phenylboronic acid, **T1** (0.081 g, 0.651 mmol) in 20 mL of toluene or methanol or isopropanol dropwise through the addition funnel over a period of 5 min with continuous stirring. The reaction mixture was refluxed under argon with continuous stirring for about 20 min. About 1 mL of the mixture was filtered using a silica gel plug, followed by washing the plug with 1 mL of the respective solvent. The resulting products were analyzed by GC. The reaction mixture was then refluxed for 3 h and then cooled at room temperature. The product was purified on a silica gel column using CH_2Cl_2/MeOH as the eluents (1 : 1) followed by evaporation *in vacuo*. The cross-coupled product, 4-phenylacetophenone, **P1** was obtained as a white solid (0.083 g, 82% yield with respect to **R1**; when isopropanol was used as a solvent), Mp 116-119 ^oC (lit.[14a] 118-123 ^oC). ^1H NMR (300 MHz): δ 8.04 (m, 2H), 7.71-7.58 (m, 4H), 7.50-7.35 (m, 3H), 2.64 (s, 3H). $^{13}C\{^1H\}$ NMR (125 MHz): δ 197.2 (C=O), 136.0 (=C), 135.9 (=C), 132.9 (=CH), 132.1 (=CH), 130.1 (=CH), 128.5 (=CH), 128.2 (=CH), 26.7 (CH_3). IR

(KBr) (ν, cm^{-1}): 1674 (C=O). GC/MS (EI^+, 70 eV): *m/z* (%) 196 (75, M^+), 181 (100, -CH_3), 152 (87), 90 (26), 76 (97), 51 (38).

Reaction of 4-iodotoluene. Reagents used: 4-iodotoluene, **R2** (0.050 g, 0.229 mmol), K_2CO_3 (0.094 g, 0.687 mmol), **T1** (0.033 g, 0.274 mmol) in 20 mL of methanol or isopropanol, and **5a** (3 mole%). Reaction time: 3 h. The cross-coupled product, 4-phenyltoluene, **P2** was obtained as a white solid (0.033 g, 86% yield; when isopropanol was used as a solvent), Mp 42-45 ^oC (lit.[14b] 44-47 ^oC). ^1H NMR (300 MHz): δ 7.86 (d, *J* = 7.6 Hz, 2H), 7.60-7.22 (m, 7H), 2.53 (s, 3H). $^{13}C\{^1H\}$ NMR (75 MHz): δ 136.9 (=C), 135.8 (=C), 132.9 (=CH), 131.4 (=CH), 131.0 (=CH), 128.2 (=CH), 119.2 (=CH), 21.1 (CH_3). GC/MS (EI^+, 70 eV): *m/z* (%) 168 (93, M^+), 139 (100), 125 (46), 109 (41), 79 (25), 69 (31), 63 (13), 51 (10).

Reaction of 4-bromotoluene. Reagents used: 4-bromotoluene, **R3** (0.046 g, 0.270 mmol), K_2CO_3 (0.113 g, 0.820 mmol), **T1** (0.040 g, 0.330 mmol) in 10 mL of isopropanol, and **5a** (8 mole%). Reaction time: 48 h. The cross-coupled product, 4-phenyltoluene, **P2** was obtained as a white solid (0.015 g, 34% yield), Mp 41-44 ^oC (lit.[14b] 44-47 ^oC). ^1H NMR (300 MHz): δ 7.96-7.92 (m, 2H), 7.63-7.22 (m, 7H), 2.55 (s, 3H). $^{13}C\{^1H\}$ NMR (125 MHz): δ 137.0 (=C), 135.9 (=C), 132.9 (=CH), 131.5 (=CH), 131.0 (=CH), 128.2 (=CH), 119.3 (=CH), 21.1 (CH_3). GC/MS (EI^+, 70 eV): *m/z* (%) 168 (91, M^+), 139 (100), 125 (24), 109 (24), 69 (15).

Reaction of 4-bromobenzonitrile. Reagents used: 4-bromobenzonitrile, **R4** (0.050 g, 0.270 mmol), K_2CO_3 (0.113 g, 0.820 mmol), **T1** (0.040 g, 0.330 mmol) in 10 mL of isopropanol, and **5a (**3 mole%). Reaction time: 3 h. The cross-coupled product,

4-phenylbenzonitrile, **P3** was obtained as a pale yellow solid (0.038 g, 80% yield), Mp 84-86 ^{o}C (lit.[14c] 84-85 ^{o}C). ^{1}H NMR (500 MHz): δ 7.74-7.68 (m, 4H), 7.60 (m, 2H), 7.50-7.33 (m, 3H). ^{13}C{^{1}H} NMR (125 MHz): δ 135.8 (=C), 133.5 (=CH), 132.9 (=C), 132.8 (=CH), 128.1 (=CH), 118.2 (C≡N), 111.4 (=C). IR (KBr) (ν, cm^{-1}): 2222 (C≡N). GC/MS (EI^{+}, 70 eV): *m/z* (%) 179 (100, M^{+}), 151 [22, -(C≡N)], 76 (30), 63 (21), 51 (22).

3.3.2 Analysis of residual Pd species in Suzuki-Miyaura cross-coupling reaction.

A part of the reaction mixture consisting of the residual catalytic species and product from the reaction of **R1** and **T1** in the presence of **5a** was analyzed with the ^{31}P{^{1}H} NMR spectroscopy. The reaction mixture was then filtered through a small silica gel column in a disposable pipette and the resulting filtrate was analyzed with ^{31}P{^{1}H} NMR spectroscopy. ^{31}P{^{1}H} NMR (121 MHz, DMSO-d_6): δ -10.5 (major), -66.3 (minor) [ratio of the peaks: 3 : 1 (before filtration)]; δ -7.3 [after filtration]. Finally, the pure cross-coupled product obtained after column chromatography was also analyzed with the ^{31}P{^{1}H} NMR spectroscopy while no signal was observed.

A part of the reaction mixture which consists of the catalyst and product was filtered through a filter paper. The crude residue was dried *in vacuo*. A part of the dried residue was washed with dichloromethane (5 mL), methanol (5 mL), and finally with distilled water (10 mL). The resulting residue was dried *in vacuo* and then in air. The crude and washed dry residues were analyzed by SEM and EDS experiments.

3.3.3 Copper-free Sonogashira cross-coupling reactions of a variety of substrates with phenylacetylene and trimethylsilylacetylene catalyzed by cis-$PdCl_2(PTA)_2$, M1.

A representative reaction is described for the reaction of 4-bromoacetophenone with phenylacetylene.

Reaction of 4-bromoacetophenone with phenylacetylene. 4-bromoacetophenone, **R1** (0.400 g, 2.02 mmol) and **M1** (3 mole%) were placed in a 100 mL three-necked round bottom flask equipped with a 25 mL addition funnel and a magnetic stir bar and degassed for 20 min under argon atmosphere. The mixture was stirred with 10 mL of piperidine for *ca.* 5 min. To this was added phenylacetylene, **A4** (0.206 g, 2.02 mmol) dropwise through the addition funnel with continuous stirring over a period of 5 min. An additional 10 mL of piperidine was added to the reaction mixture, and then it was refluxed under argon for 3 h. The resulting product mixture was analyzed by GC. The product was purified on a silica gel column using CH_2Cl_2/MeOH as the eluents (1 : 1) followed by evaporation *in vacuo*. The cross-coupled product, 4-(phenylethynyl)acetophenone, **P4** was obtained as a pale yellow solid (0.320 g, 72% yield), Mp 97-99 ^oC (lit.[14d] 95-96 ^oC). ^1H NMR (300 MHz): δ 8.04 (m, 2H), 7.71-7.62 (m, 4H), 7.51-7.41 (m, 3H), 2.65 (s, 3H). $^{13}C\{^1H\}$ NMR (75 MHz): δ 197.0 (C=O), 135.9 (=C), 132.0 (=CH), 131.7 (=CH), 129.9 (=CH), 128.5 (=CH), 128.4 (=CH), 123.3 (=C), 89.5 (≡C), 26.6 (CH_3). IR (KBr) (ν, cm^{-1}): 1671 (C=O). GC/MS (EI^+, 70 eV): *m/z* (%) 220 (68, M^+), 205 (100, -CH_3), 176 (60), 151 (25), 102 (17), 88 (34).

Reaction of 4-bromoacetophenone with trimethylsilylacetylene. Reagents used: 4-bromoacetophenone, **R1** (0.400 g, 2.02 mmol), trimethylsilylacetylene, **A2** (0.198 g,

2.02 mmol), and **M1** (3 mole%) in 20 mL of piperidine. Reaction time: 3 h. The crude product was distilled. The pure cross-coupled product, 4-[(trimethylsilyl)ethynyl]acetophenone, **P5** was obtained as a brownish oily liquid which upon standing slowly solidified to a light brown solid (0.266 g, 61% yield). ^{1}H NMR (300 MHz): δ 7.66 (d, J = 8.5 Hz, 2H), 7.44 (d, J = 8.5 Hz, 2H), 2.50 (s, 3H), 0.35 (s, 9H). ^{13}C{^{1}H} NMR (125 MHz): δ 197.2 (C=O), 136.0 (=C), 132.1 (=CH), 130.0 (=CH), 128.5 (=C), 93.2 (≡C), 90.3 (≡C), 26.7 (CH_3), -0.05 (CH_3Si). GC/MS (EI$^+$, 70 eV): *m/z* (%) 216 (19, M^+), 201 (100, -CH_3), 158 (9), 143 (7), 93 (8).

Reaction of 4-iodotoluene with phenylacetylene. Reagents used: 4-iodotoluene, **R2** (0.400 g, 1.83 mmol), **M1** (3 mole%), and phenylacetylene, **A4** (0.187 g, 1.83 mmol) in 20 mL of piperidine. Reaction time: 4 h. The cross-coupled product, 4-(phenylethynyl)toluene, **P6** was obtained as a white solid (0.267 g, 76% yield), Mp 68-70 ^{o}C (lit.[14d] 70-72 ^{o}C). ^{1}H NMR (300 MHz): δ 7.68-7.13 (m, 9H), 2.35 (s, 3H). ^{13}C{^{1}H} NMR (75 MHz): δ 137.9 (=C), 137.5 (=CH), 130.3 (=CH), 129.1 (=CH), 128.3 (=CH), 127.5 (=CH), 125.4 (=C), 94.6 (≡C), 21.6 (CH_3). GC/MS (EI$^+$, 70 eV): *m/z* (%) 192 (100, M^+), 165 (19), 115 (8), 94 (5).

Reaction of 4-iodotoluene with trimethylsilylacetylene. Reagents used: 4-iodotoluene, **R2** (0.400 g, 1.83 mmol), **M1** (3 mole%), and trimethylsilylacetylene, **A2** (0.179 g, 1.83 mmol) in 20 mL of piperidine. Reaction time: 4 h. The crude product was distilled. The cross-coupled product, 4-[(trimethylsilyl)ethynyl]toluene, **P7** was obtained as a yellow oily liquid (0.278 g, 81% yield). ^{1}H NMR (300 MHz): δ 7.60 (d, J = 8.2 Hz, 2H), 6.95 (d, J = 7.9 Hz, 2H), 2.33 (s, 3H), 0.32 (s, 9H). ^{13}C{^{1}H} NMR (75 MHz): δ 138.0 (=C), 132.5 (=CH), 131.0 (=CH), 127.5 (=CH), 127.4 (=CH), 125.1 (=C), 93.2

(≡C), 90.2 (≡C), 23.1 (CH_3), -0.09 (CH_3Si). GC/MS (EI^+, 70 eV): *m/z* (%) 188 (16, M^+), 173 (100, -CH_3), 143 [11, (-3CH_3)], 119 (11), 98 (24), 86 (13), 53 (14).

Reaction of 4-bromotoluene with trimethylsilylacetylene. Reagents used: 4-bromotoluene, **R3** (0.400 g, 2.35 mmol), **M1** (3 mole%), and trimethylsilylacetylene, **A2** (0.230 g, 2.35 mmol) in 20 mL of piperidine. Reaction time: 18 h. The crude product was distilled. The cross-coupled product, 4-[(trimethylsilyl)ethynyl]toluene, **P7** was obtained as a yellow oily liquid (0.190 g, 43% yield). ^1H NMR (300 MHz): δ 7.63-7.56 (m, 2H), 6.95 (d, J = 7.8 Hz, 2H), 2.32 (s, 3H), 0.32 (s, 9H). $^{13}C\{^1H\}$ NMR (75 MHz): δ 138.0 (=C), 132.5 (=CH), 131.1 (=CH), 127.5 (=CH), 127.4 (=CH), 125.1 (=C), 93.2 (≡C), 90.2 (≡C), 23.1 (CH_3), -0.09 (CH_3Si). GC/MS (EI^+, 70 eV): *m/z* (%) 189 [(35, $M+H)^+$], 174 (100, -CH_3), 130 (10), 120 (10), 87 (13), 77 (13), 53 (9).

Reaction of 4-bromobenzonitrile with phenylacetylene. Reagents used: 4-bromobenzonitrile, **R4** (0.400 g, 2.21 mmol), **M1** (3 mole%), and phenylacetylene, **A4** (0.225 g, 2.21 mmol) in 20 mL of piperidine. Reaction time: 5 h. The cross-coupled product, 4-(phenylethynyl)benzonitrile, **P8** was obtained as an off-white solid (0.318 g, 71% yield), Mp 110-112 ^oC (lit.[14d] 108-110 ^oC). ^1H NMR (300 MHz): δ 7.68-7.65 (m, 4H), 7.54-7.38 (m, 5H). $^{13}C\{^1H\}$ NMR (125 MHz): δ 133.5 (=CH), 132.7 (=CH), 131.7 (=CH), 128.5 (=CH), 128.4 (=CH), 128.1 (minor, unassigned), 123.4 (=C), 118.2 (C≡N), 118.0 (minor, unassigned), 111.3 (=C), 89.5 (≡C). IR (KBr) (ν, cm^{-1}): 2230 (C≡N). GC/MS (EI^+, 70 eV): *m/z* (%) 203 (69, M^+), 171 (33), 155 (85), 145 (71), 92 (13), 76 (100), 63 (19), 50 (32).

Reaction of 4-bromobenzonitrile with trimethylsilylacetylene. Reagents used: 4-bromobenzonitrile, **R4** (0.400 g, 2.21 mmol), **M1** (3 mole%), and trimethylsilylacetylene, **A2** (0.216 g, 2.21 mmol) in 20 mL of piperidine. Reaction time: 5 h. The crude product was distilled. The cross-coupled product, 4-[(trimethylsilyl)ethynyl]benzonitrile, **P9** was obtained as a tan solid (0.277 g, 63% yield), Mp 105-108 ^{o}C (lit.[14g] 107-111 ^{o}C). ^{1}H NMR (500 MHz): δ 7.57 (d, J = 8.5 Hz, 2H), 7.46 (d, J = 8.5 Hz, 4H), 0.37 (s, 9H). ^{13}C{^{1}H} NMR (125 MHz): δ 133.6 (=CH), 132.9 (=CH), 128.2 (=C), 118.3 (*C*≡N), 111.5 (=C), 93.2 (≡C), 90.3 (≡C), -0.03 (*C*H$_3$Si). IR (KBr) (ν, cm^{-1}): 2218 (C≡N), 2153 (C≡C). GC/MS (EI^{+}, 70 eV): *m/z* (%) 199 (10, M^{+}), 184 (100, -CH$_3$), 154 [12, (-3CH$_3$)], 130 (12), 92 (9), 77 (11), 53 (21).

3.4 References

[1] Kim, H.-J.; Lee, S. W. *Bull. Korean Chem. Soc.* **1999**, *20*, 1089.

[2] Clark, H. C.; Manzer, L. E. *J. Organomet. Chem.* **1973**, *59*, 411.

[3] (a) Hassan, F. S. M.; Higgins, S. J.; Jacobsen, G. B.; Shaw, B. L.; Thornton-Pett, M. *J. Chem. Soc., Dalton Trans.* **1988**, 3011. (b) Cotton, F. A. *Inorg. Synth. XIII* **1972**, 52.

[4] Rulke, R. E.; Ernsting, J. M.; Spek, A. L.; Elsevier, C. J.; van Leeuwen, P. W. N. M.; Vrieze, K. *Inorg. Chem.* **1993**, *32*, 5769.

[5] Cross, R. J.; Davidson, M. F. *J. Chem. Soc, Dalton Trans.* **1986**, 1987.

[6] Krogstad, D. A.; Owens, S. B.; Halfen, J. A.; Young, V. G. Jr. *Inorg. Chem. Commun*. **2005**, *8*, 65.

[7] (a) Krogstad, D. A.; Cho, J.; DeBoer, A. J.; Klitzke, J. A.; Sanow, W. R.; Williams, H. A.; Halfen, J. A. *Inorg. Chim. Acta* **2006**, *359*, 136. (b) Meij, A. M. M.; Otto, S.; Roodt, A. *Inorg. Chim. Acta* **2005**, *358*, 1005.

[8] (a) Miranda, S.; Vergara, E.; Mohr, F; de Vos, D.; Cerrada, E.; Mendia, A.; Laguna, M. *Inorg. Chem.* **2008**, *47*, 5641. (b) Vergara, E.; Miranda, S.; Mohr, F.; Cerrada, E.; Tiekink, E. R. T.; Romero, P.; Mendía, A.; Laguna, M. *Eur. J. Inorg. Chem.* **2007**, 2926.

[9] Evrard, D.; Lucas, D.; Mugnier, Y.; Meunier, P.; Hierso, J.-C. *Organometallics* **2008**, *27*, 2643.

[10] (a) Darensbourg, D. J.; Ortiz, C. G.; Kamplain, J. W. *Organometallics* **2004**, *23*, 1747. (b) Elena Vergara, E.; Miranda, S.; Mohr, F.; Cerrada, E.; Tiekink, E. R. T.; Romero, P.; Mendía, A.; Laguna, M. *Eur. J. Inorg. Chem.* **2007**, 2926.

[11] (a) Spivak, G. J.; Holah, D. G.; Hughes, A. N.; Krysa, E.; Havighurst, M. D.; Magnuson,V. R. *Polyhedron* **1997**, *16*, 2353. (b) Romeo, R.; D'Amico, G. *Organometallics* **2006**, *25*, 3435. (c) Procelewska, J.; Zahl, A.; Liehr, G.; van Eldik, R.; Smythe, N. A.; Williams, B. S.; Goldberg, K. I. *Inorg. Chem.* **2005**, *44*, 7732.

[12] (a) Ruehlmann, K. *Z. Chem.* **1965**, *5*, 354. (b) Toal, S. J.; Sohn, H.; Zakarov, L. N.; Kassel, W. S.; Golen, J. A.; Rheingold, A. L.; Trogler, W. C. *Organometallics* **2005**, *24*, 3081. (c) Becker, B.; Corriu, R. J. P.; Henner, B. J. L.; Wojnowski, W.; Peters, K.; von Schnering, H. G. *J. Organomet. Chem.* **1986**, *312*, 305.

[13] (a) Motoda, D.; Shinokubo, H.; Oshima, K. *Synlett* **2002**, *9*, 1529. (b) Caseri, W.; Pregosin, P. S. *Organometallics* **1988**, *7*, 1373. (c) Rivera-Claudio, M.; Rozell, J.; Ramirez-Oliva, E.; Cervantes, J.; Pannell, K. H. *J. Organomet. Chem.* **1996**, *521*, 267. (d) Sanchez, J. C.; Urbas, S.; Toal, S.; DiPasquale, A. G.; Rheingold, A. L.; Trogler, W. C. *Macromolecules* **2008**, *41*, 1237.

[14] (a) http://www.chemexper.com/chemicals/supplier/cas/92-91-1.html. (b) Leadbeater, N. E.; Resouly, S. M. *Tetrahedron* **1999**, *55*, 11889. (c) Seganish, W. M.; Deshong, P. *J. Org. Chem.* **2004**, *69*, 1137. (d) Komáromi, A.; Novák, Z. *Chem. Commun.* **2008**, 4968. (e) Thorand, S.; Krause, N. *J. Org. Chem.* **1998**, *63*, 8551. (f) Leadbeater, N. E.; Marko, M.; Tominack, B. J. *Org. Lett.* **2003**, *5*, 3919. (g) http://www.sigmaaldrich.com/catalog/product/aldrich/658391.

[15] Foley, S. R.; Stockland, R. A. Jr.; Shen, H.; Jordan, R. F. *J. Am. Chem. Soc.* **2003**, *125*, 4350.

[16] Krogstad, D. A.; Gohmann, K. E.; Sunderland, T. L.; Geis, A. L.; Bergamini, P.; Marvelli, L.; Young Jr., V. G. *Inorg. Chim. Acta* **2009**, *362*, 3049.

[17] De Graaf, W.; Boersma, J.; Smeets, W. W. J.; Spek, A. L.; van Koten, G. *Organometallics*, **1989**, *8*, 2907.

[18] Bruker Analytical X-Ray, Madison, WI, 2010.

[19] Sheldrick, G.M. *Acta Crystallogr.* **2008**, *A64*, 112.

4. Appendices

4.1. Appendix I. NMR Spectra

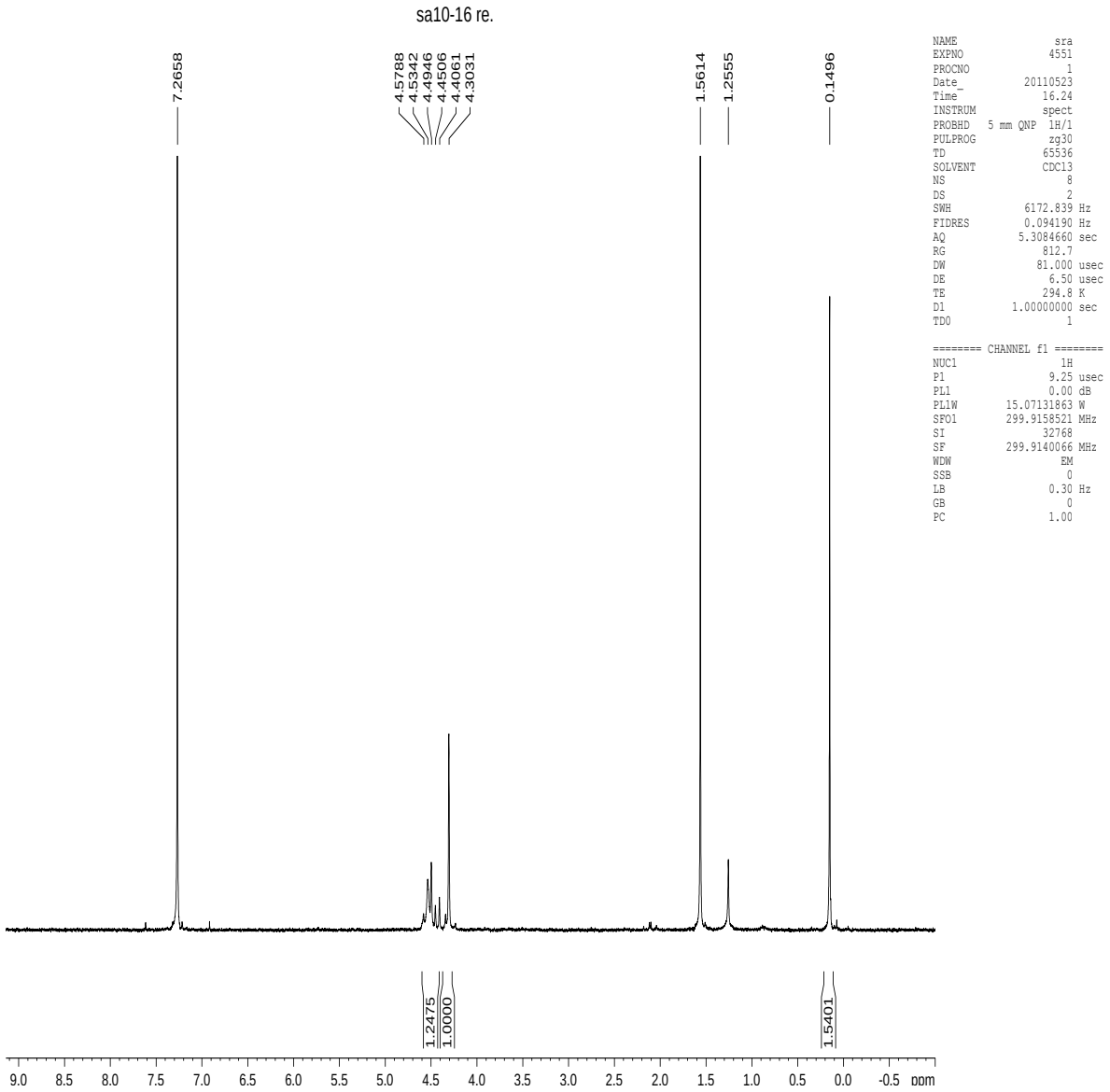

Appendix I.1. ^{1}H NMR spectrum of trans-$Pt(C_2SiMe_3)_2(PTA)_2$, 8a.

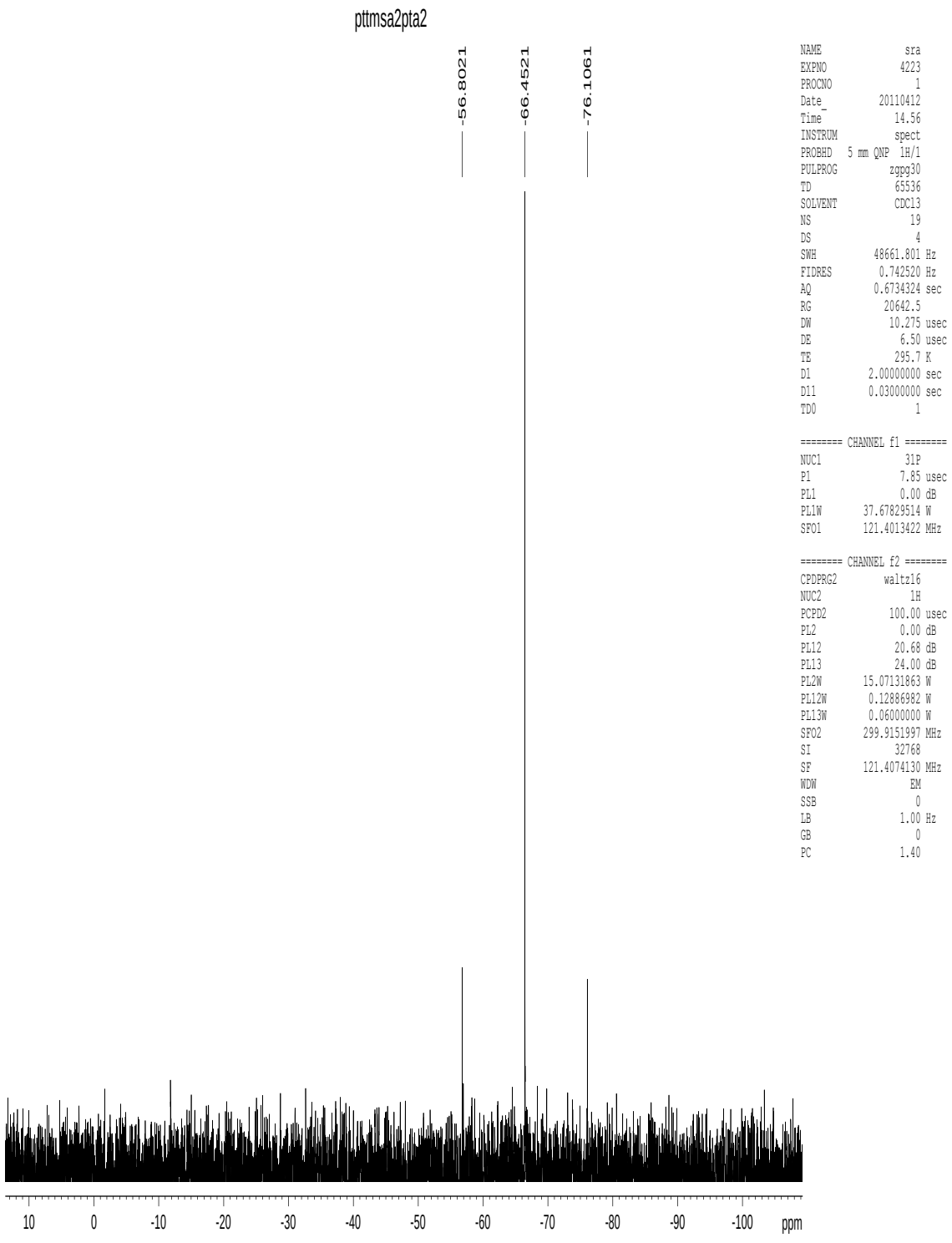

Appendix I.2. $^{31}P\{^{1}H\}$ NMR spectrum of trans-$Pt(C_2SiMe_3)_2(PTA)_2$, 8a.

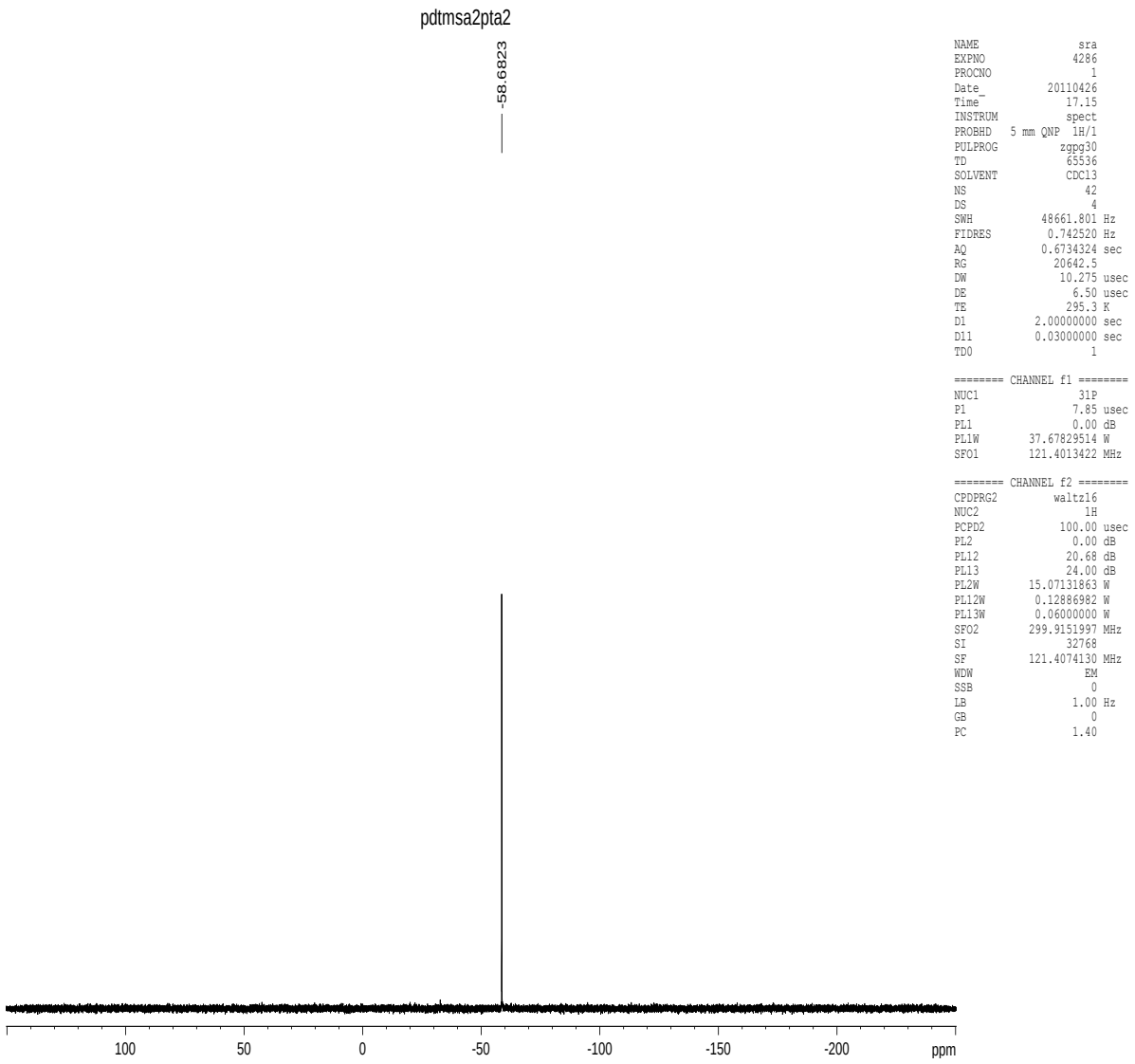

Appendix I.3. $^{31}P\{^{1}H\}$ NMR spectrum of trans-$Pd(C_2SiMe_3)_2(PTA)_2$, 8b.

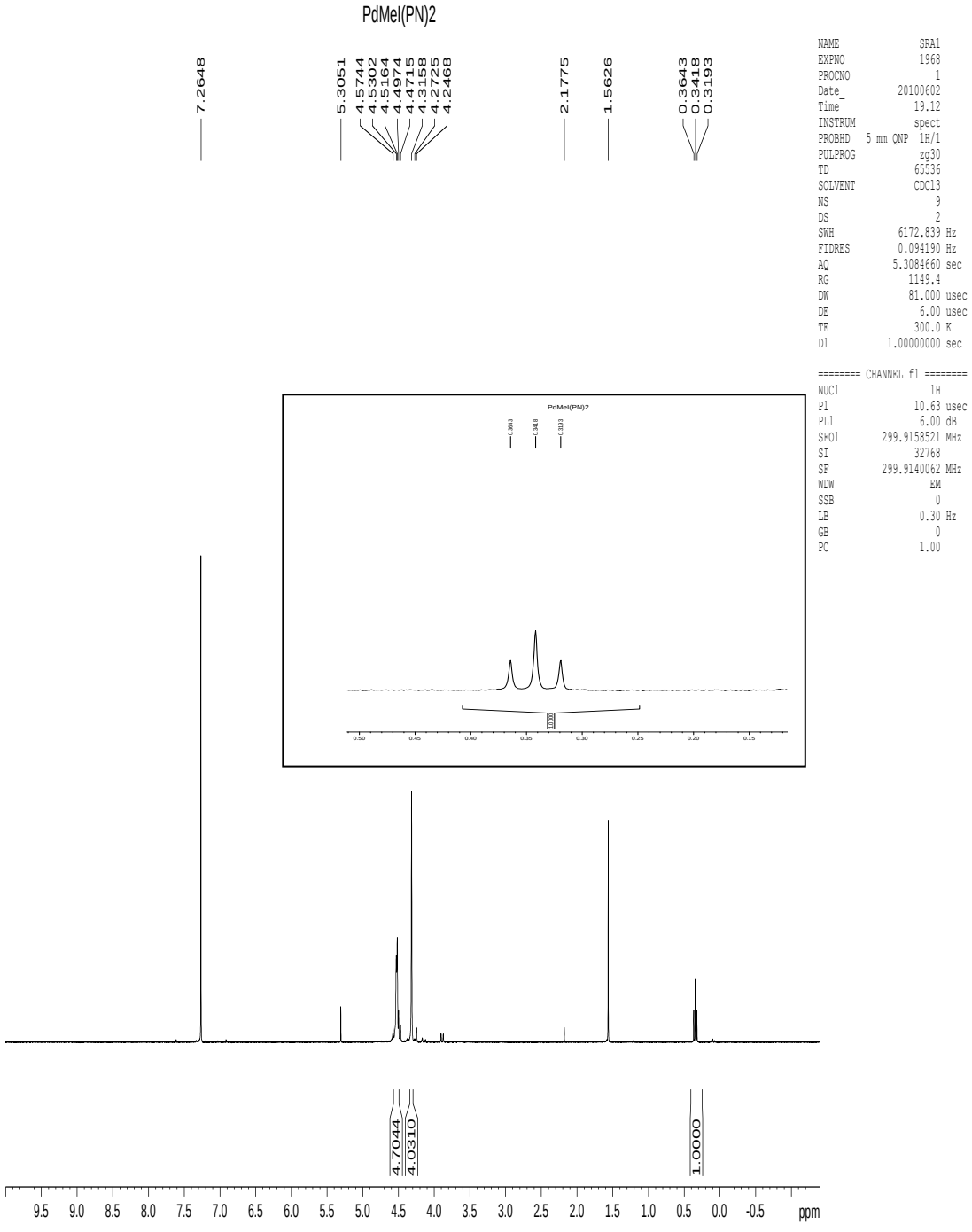

Appendix I.4. ^{1}H NMR spectrum of trans-PdI(Me)(PTA)$_2$, 5c.

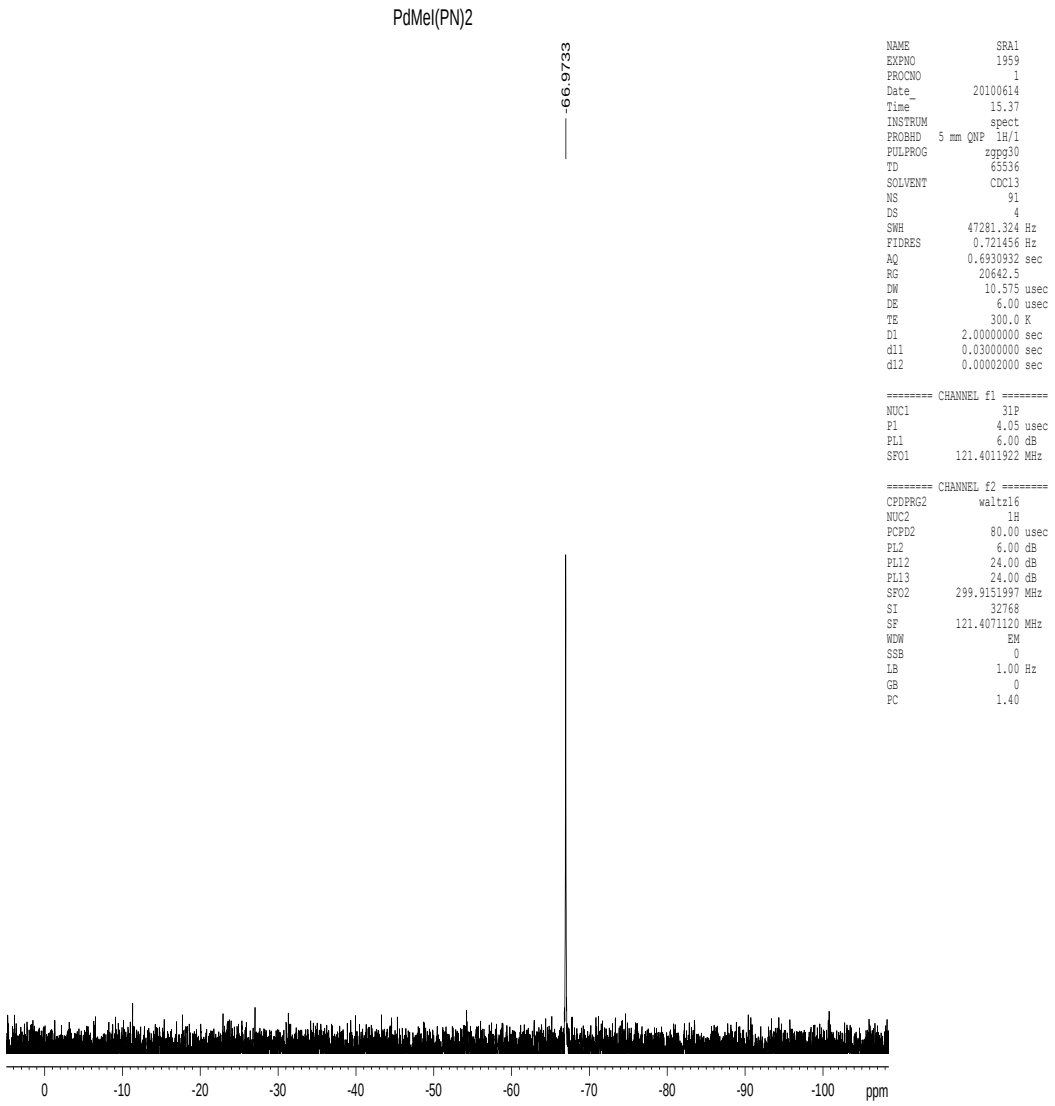

Appendix I.5. $^{31}P\{^{1}H\}$ NMR spectrum of trans-PdI(Me)(PTA)$_2$, 5c.

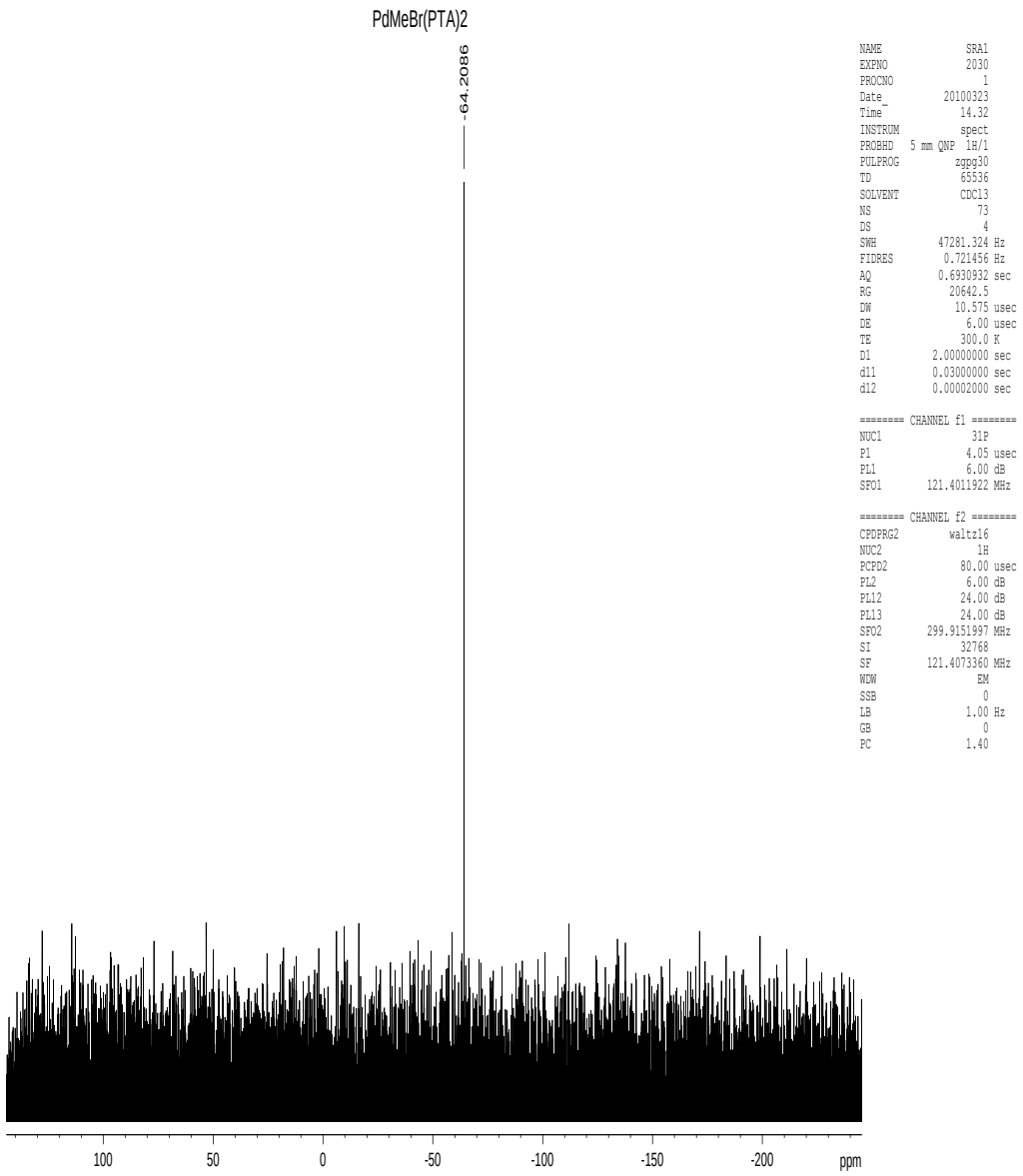

Appendix I.6. $^{31}P\{^{1}H\}$ NMR spectrum of trans-PdBr(Me)(PTA)$_2$, 5b.

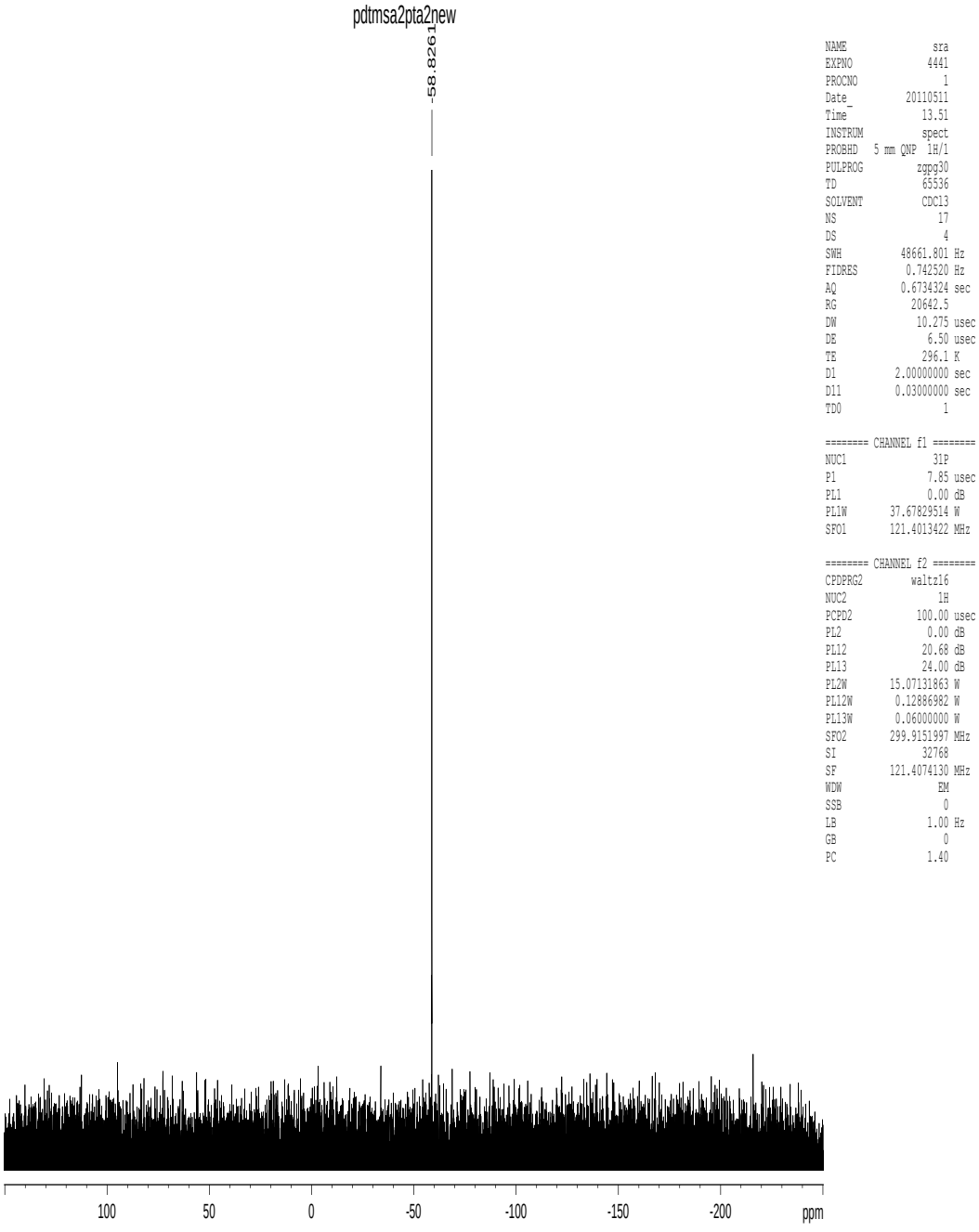

Appendix I.7. $^{31}P\{^{1}H\}$ NMR spectrum of trans-$Pd(C_2SiMe_3)_2(PTA)_2$, 8b.

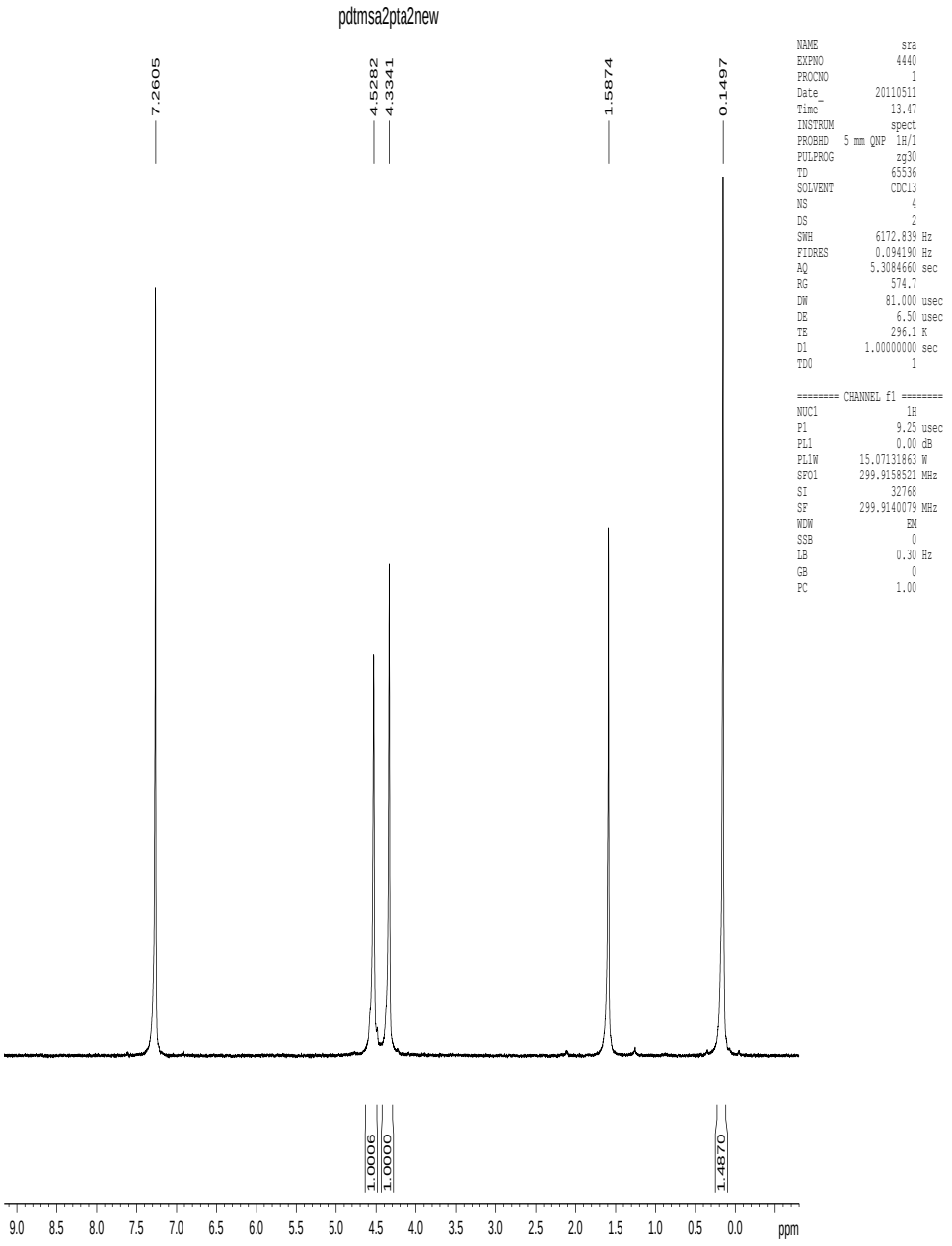

Appendix I.8. ^{1}H NMR spectrum of trans-$Pd(C_2SiMe_3)_2(PTA)_2$, 8b.

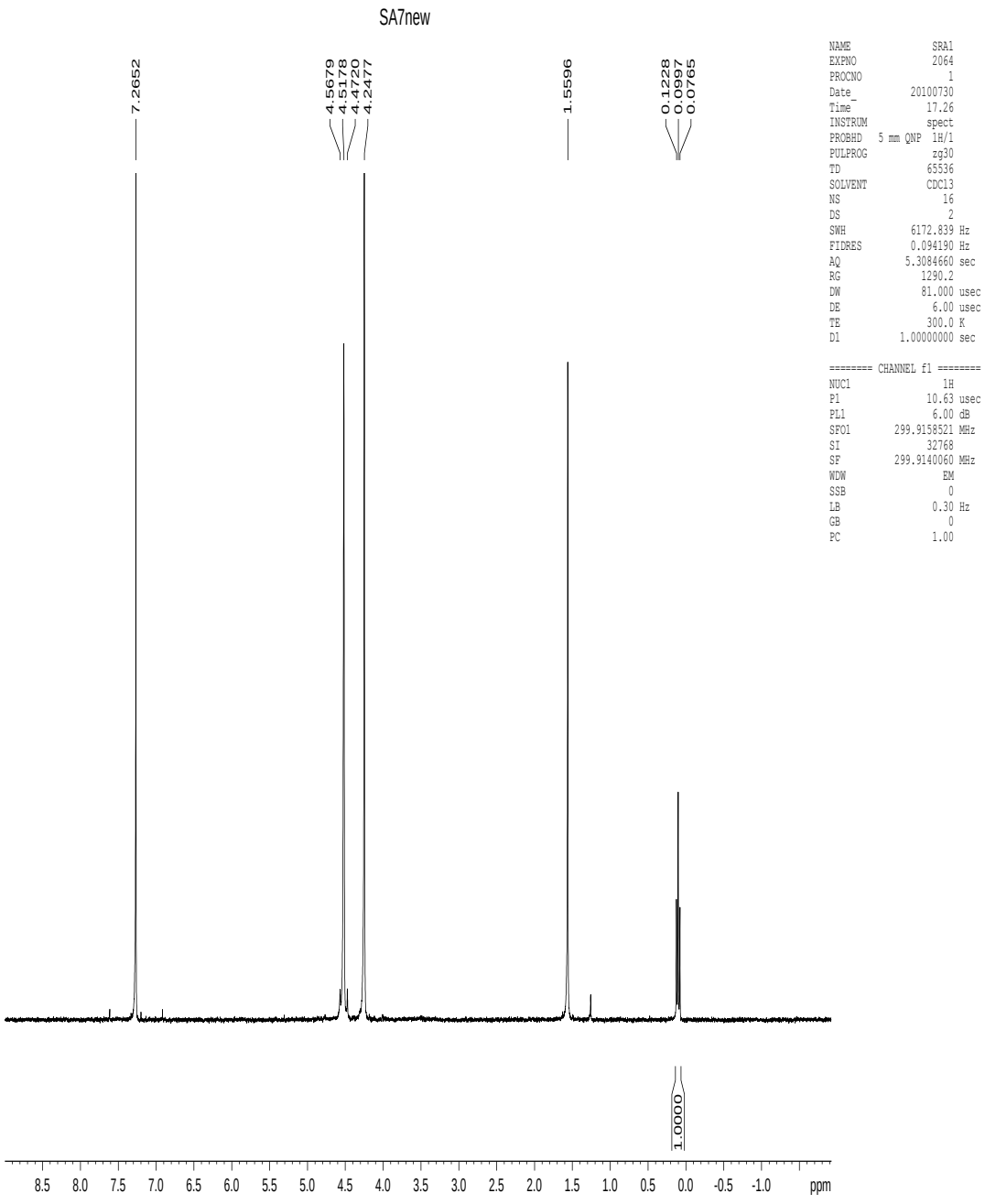

Appendix I.9. ^{1}H NMR spectrum of trans-PdCl(Me)(PTA)$_2$, 5a.

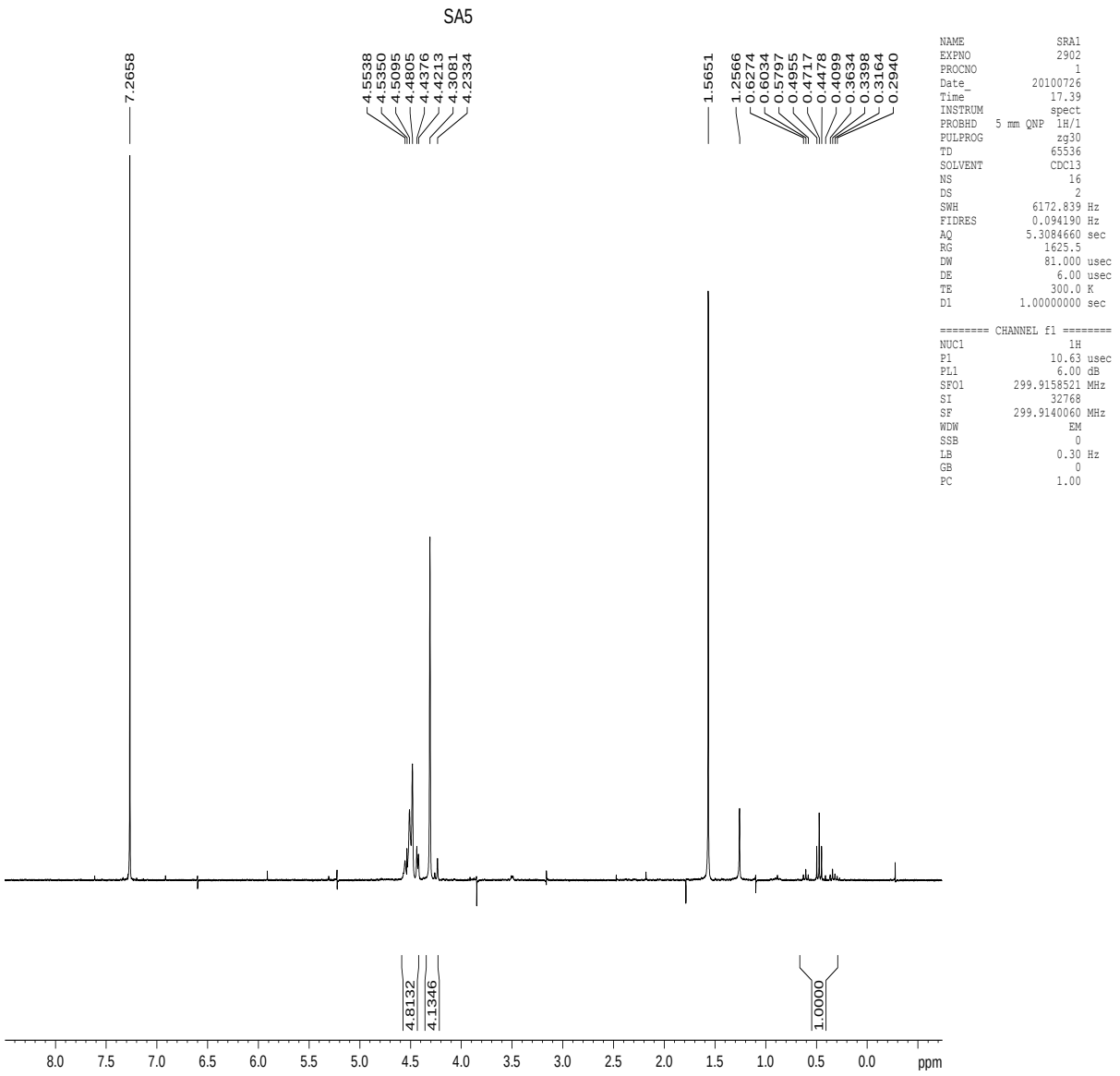

Appendix I.10. ^{1}H NMR spectrum of trans-PtI(Me)(PTA)$_2$, 2c.

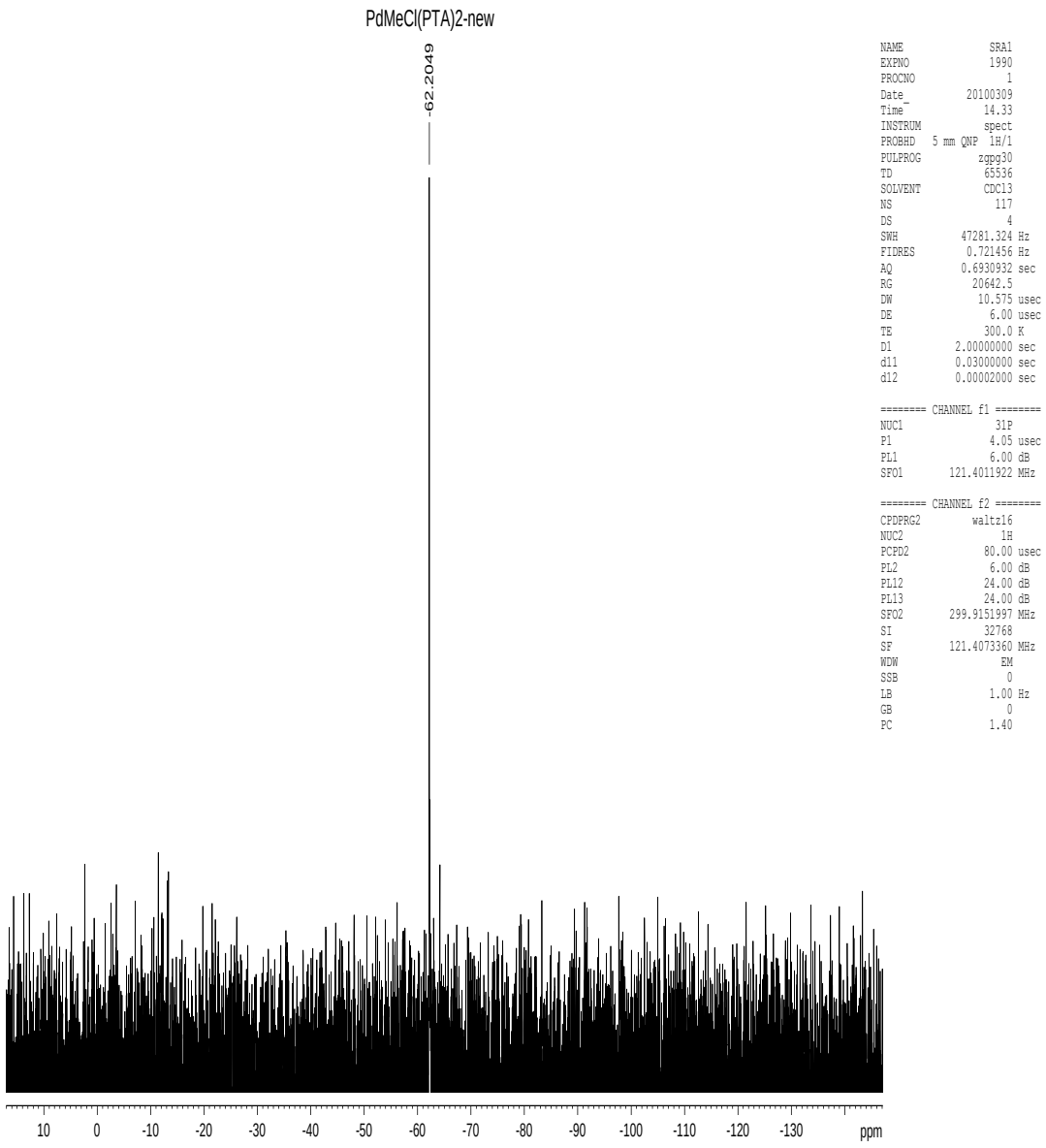

Appendix I.11. $^{31}P\{^{1}H\}$ NMR spectrum of trans-PdCl(Me)(PTA)$_2$, 5a.

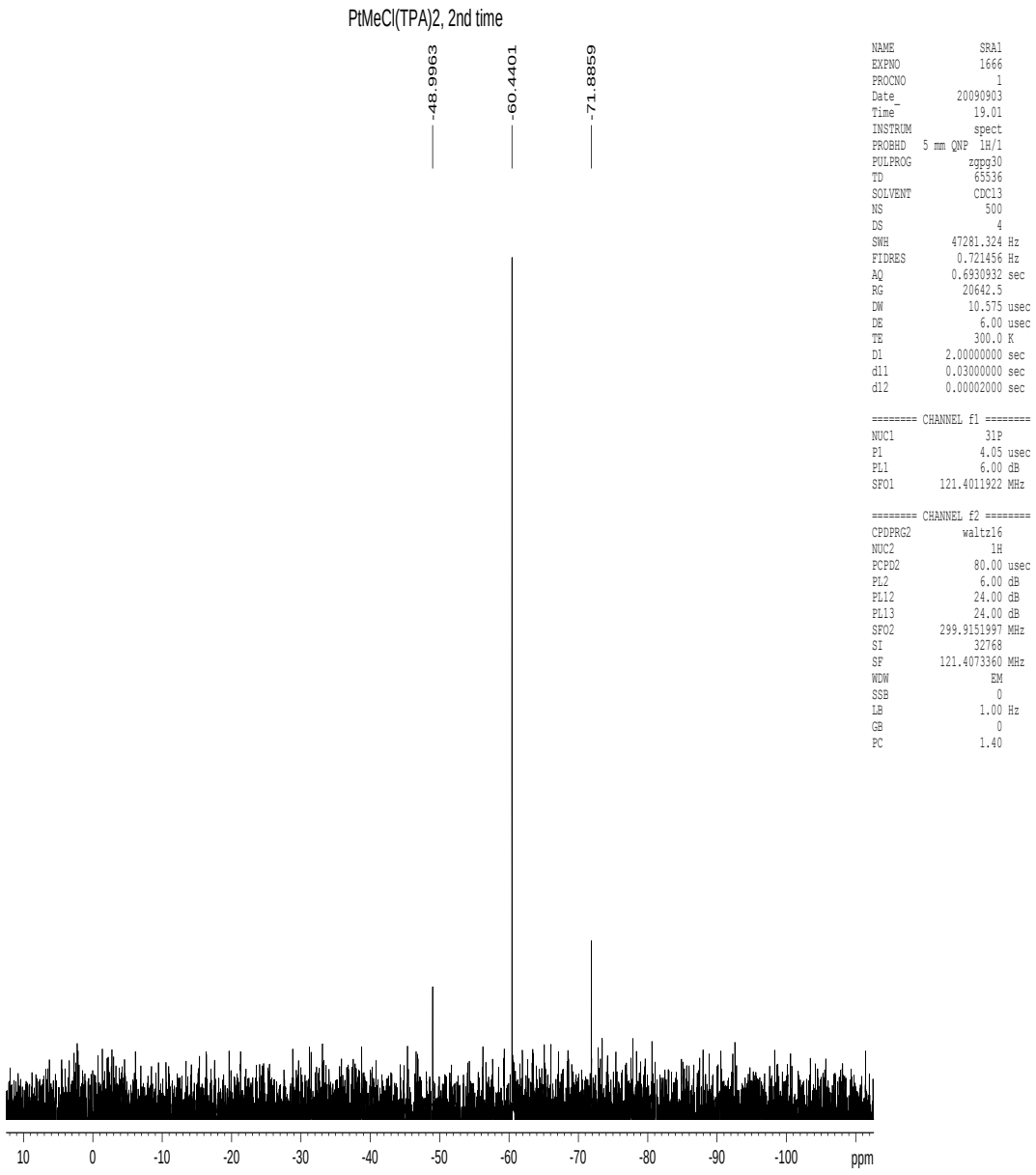

Appendix I.12. $^{31}P\{^{1}H\}$ NMR spectrum of trans-PtCl(Me)(PTA)$_2$, 2a.

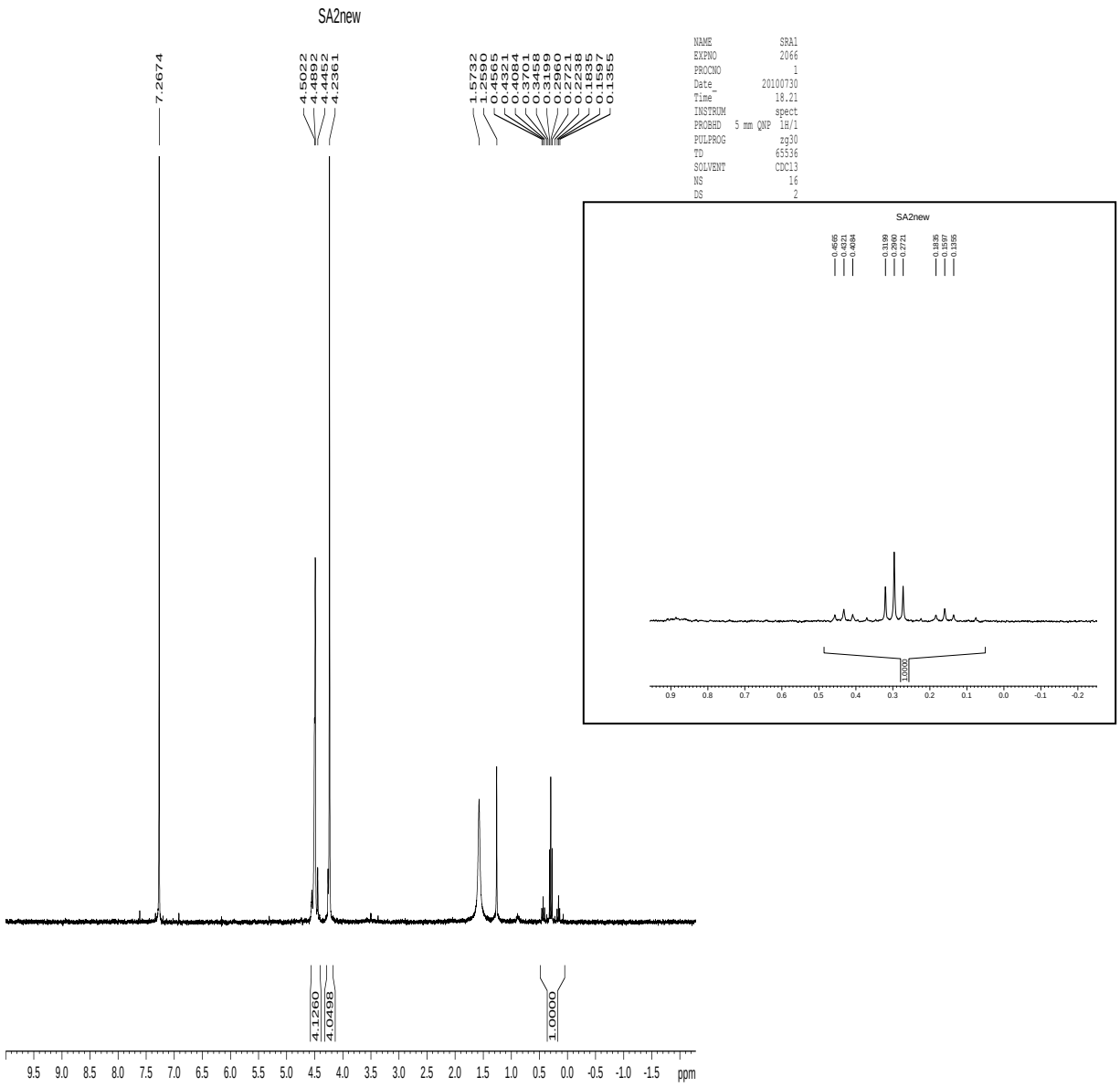

Appendix I.13. ^{1}H NMR spectrum of trans-PtCl(Me)(PTA)$_2$, 2a.

Appendix I.14. $^{31}P\{^{1}H\}$ NMR spectrum of trans-PtBr(Me)(PTA)$_2$, 2b.

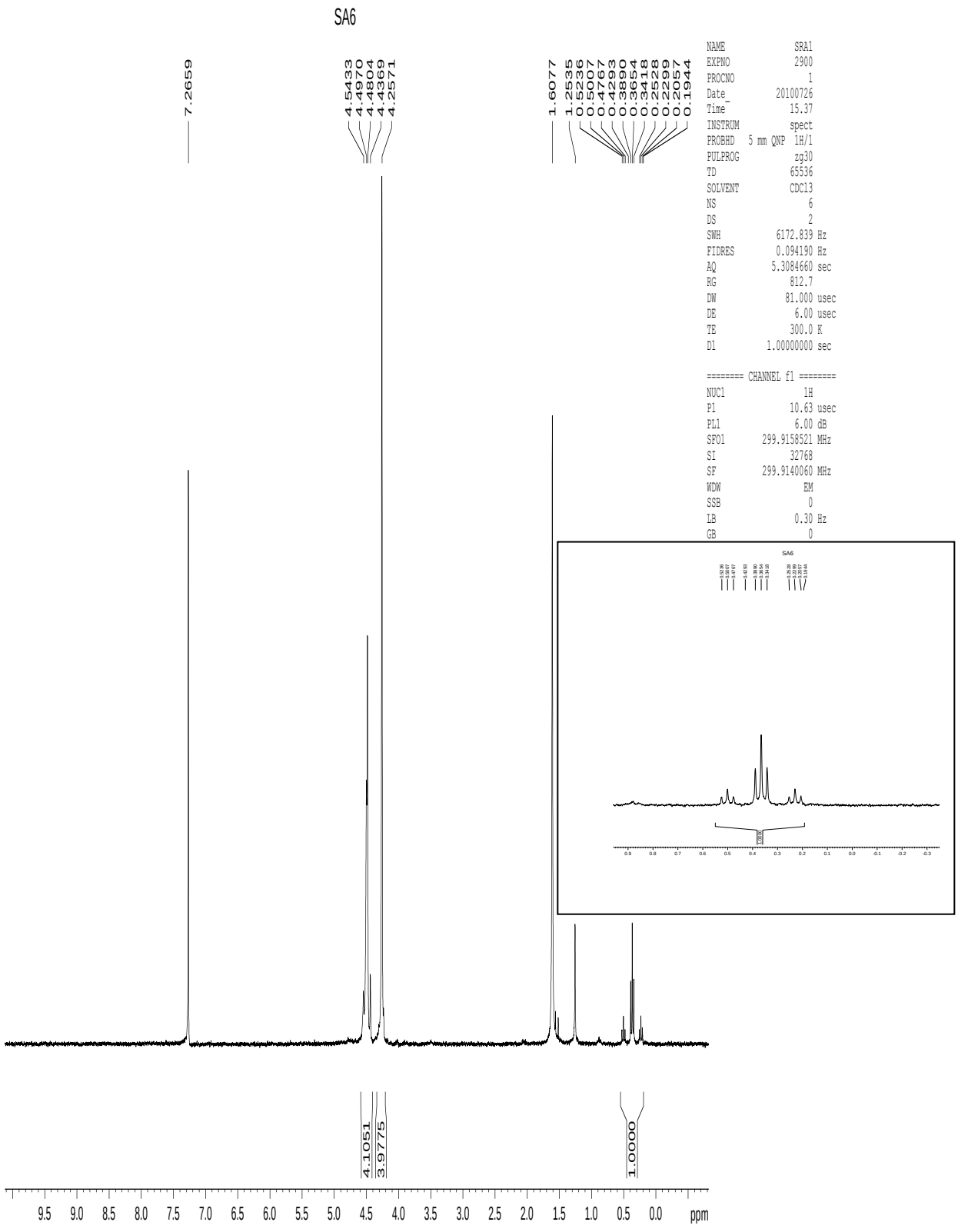

Appendix I.15. ^{1}H NMR spectrum of trans-PtBr(Me)(PTA)$_2$, 2b.

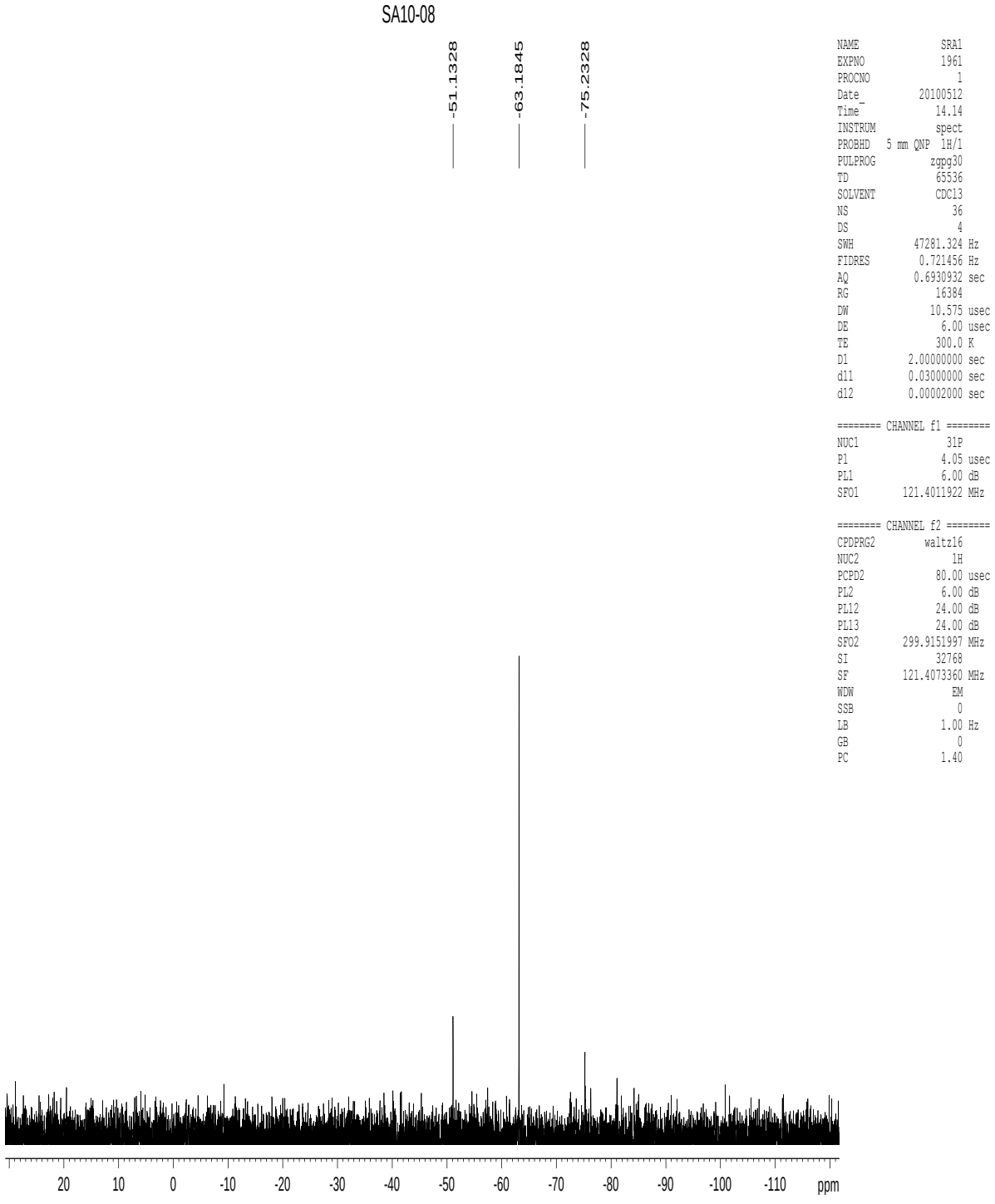

Appendix I.16. $^{31}P\{^{1}H\}$ NMR spectrum of trans-PtBr(Et)(PTA)$_2$, 3b.

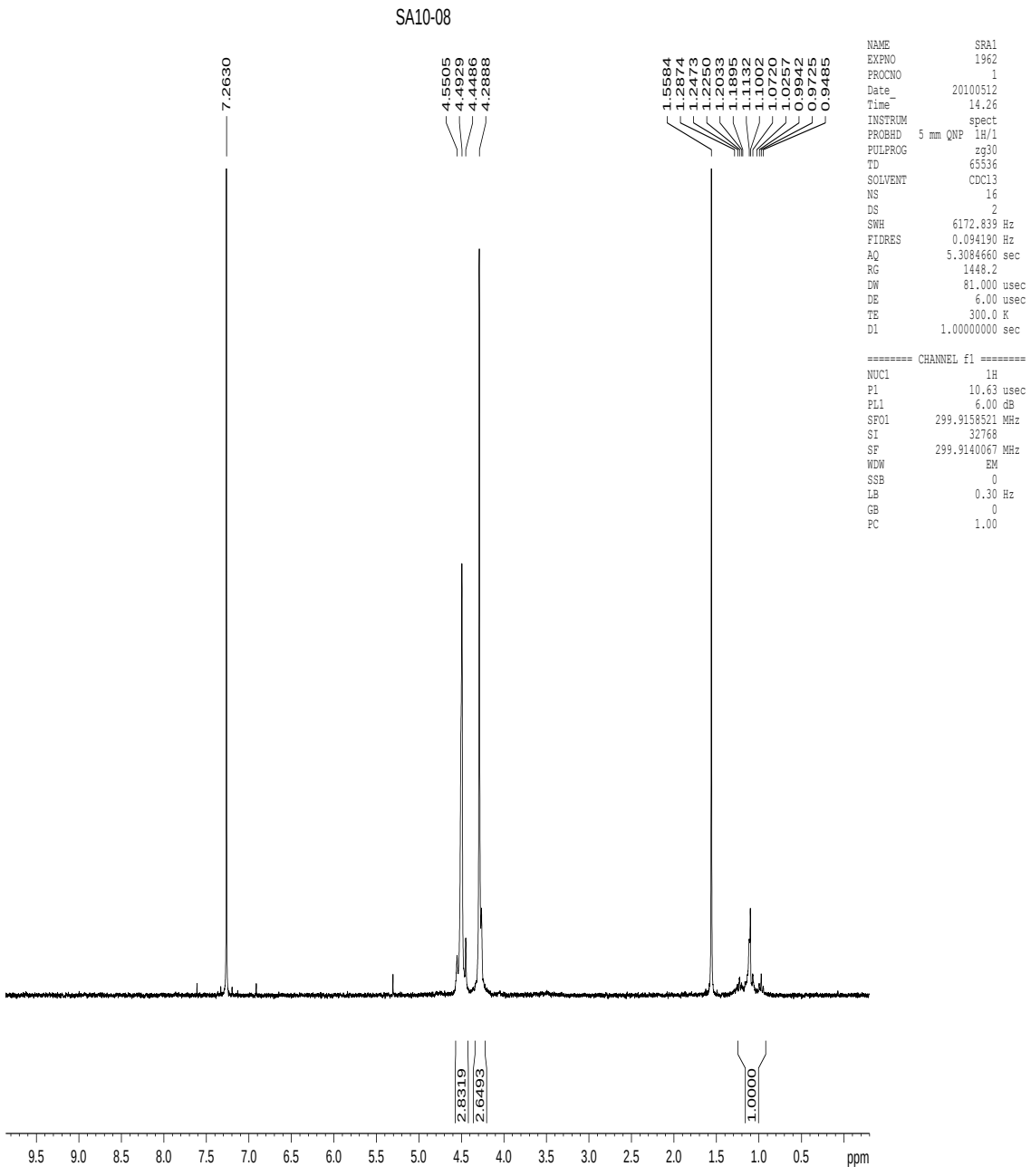

Appendix I.17. ^{1}H NMR spectrum of trans-PtBr(Et)(PTA)$_2$, 3b.

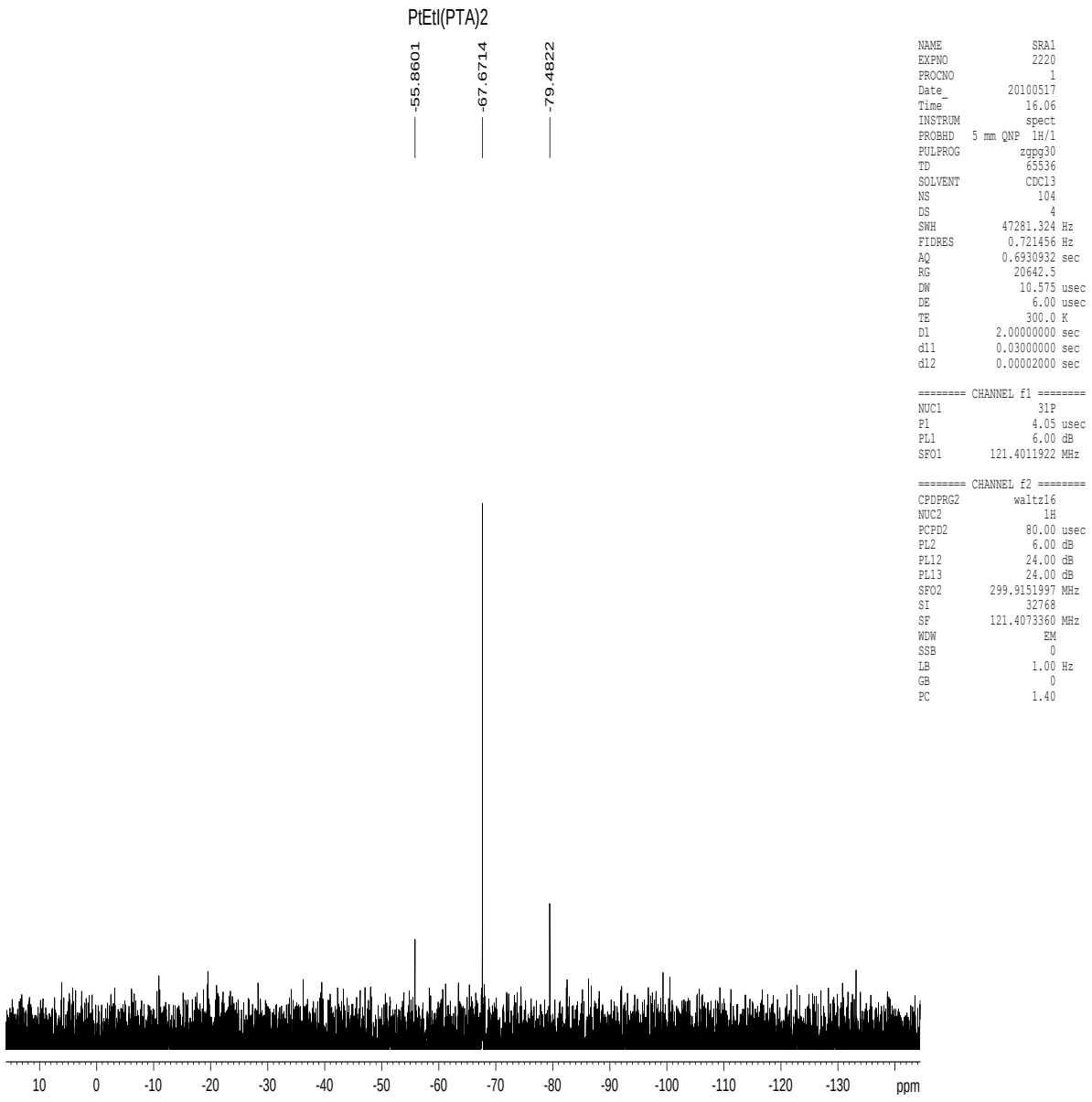

Appendix I.18. $^{31}P\{^{1}H\}$ NMR spectrum of trans-PtI(Et)(PTA)$_2$, 3c.

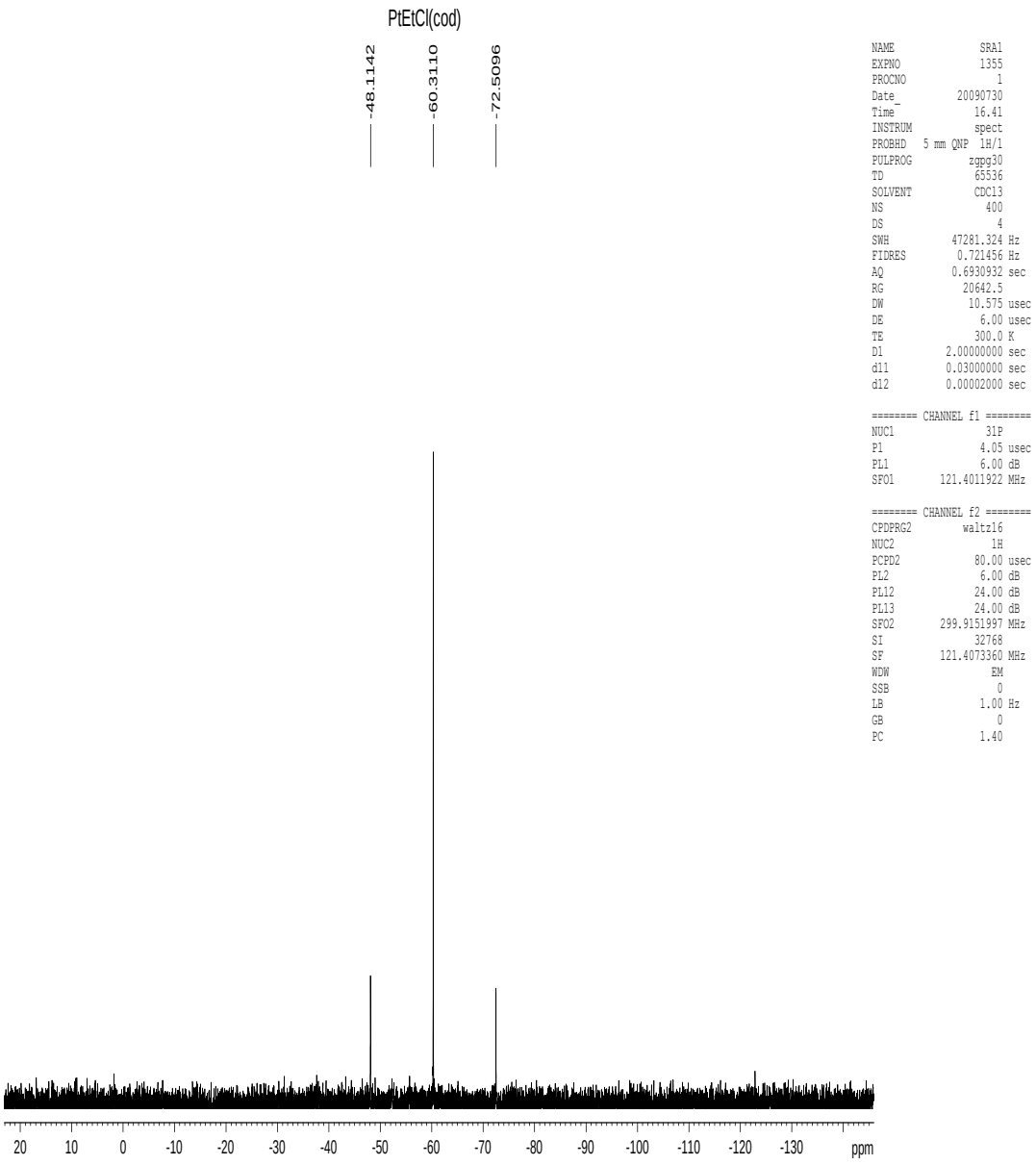


```
NAME                SRA1
EXPNO               1355
PROCNO                 1
Date_           20090730
Time                16.41
INSTRUM             spect
PROBHD   5 mm QNP  1H/1
PULPROG           zgpg30
TD                  65536
SOLVENT             CDCl3
NS                    400
DS                      4
SWH            47281.324 Hz
FIDRES          0.721456 Hz
AQ              0.6930932 sec
RG                20642.5
DW                10.575 usec
DE                 6.00 usec
TE                 300.0 K
D1            2.00000000 sec
d11           0.03000000 sec
d12           0.00002000 sec

======== CHANNEL f1 ========
NUC1                 31P
P1                  4.05 usec
PL1                 6.00 dB
SFO1         121.4011922 MHz

======== CHANNEL f2 ========
CPDPRG2          waltz16
NUC2                 1H
PCPD2              80.00 usec
PL2                 6.00 dB
PL12               24.00 dB
PL13               24.00 dB
SFO2         299.9151997 MHz
SI                 32768
SF           121.4073360 MHz
WDW                  EM
SSB                   0
LB                 1.00 Hz
GB                    0
PC                 1.40
```

Appendix I.19. $^{31}P\{^{1}H\}$ NMR spectrum of trans-PtCl(Et)(PTA)$_2$, 3a.

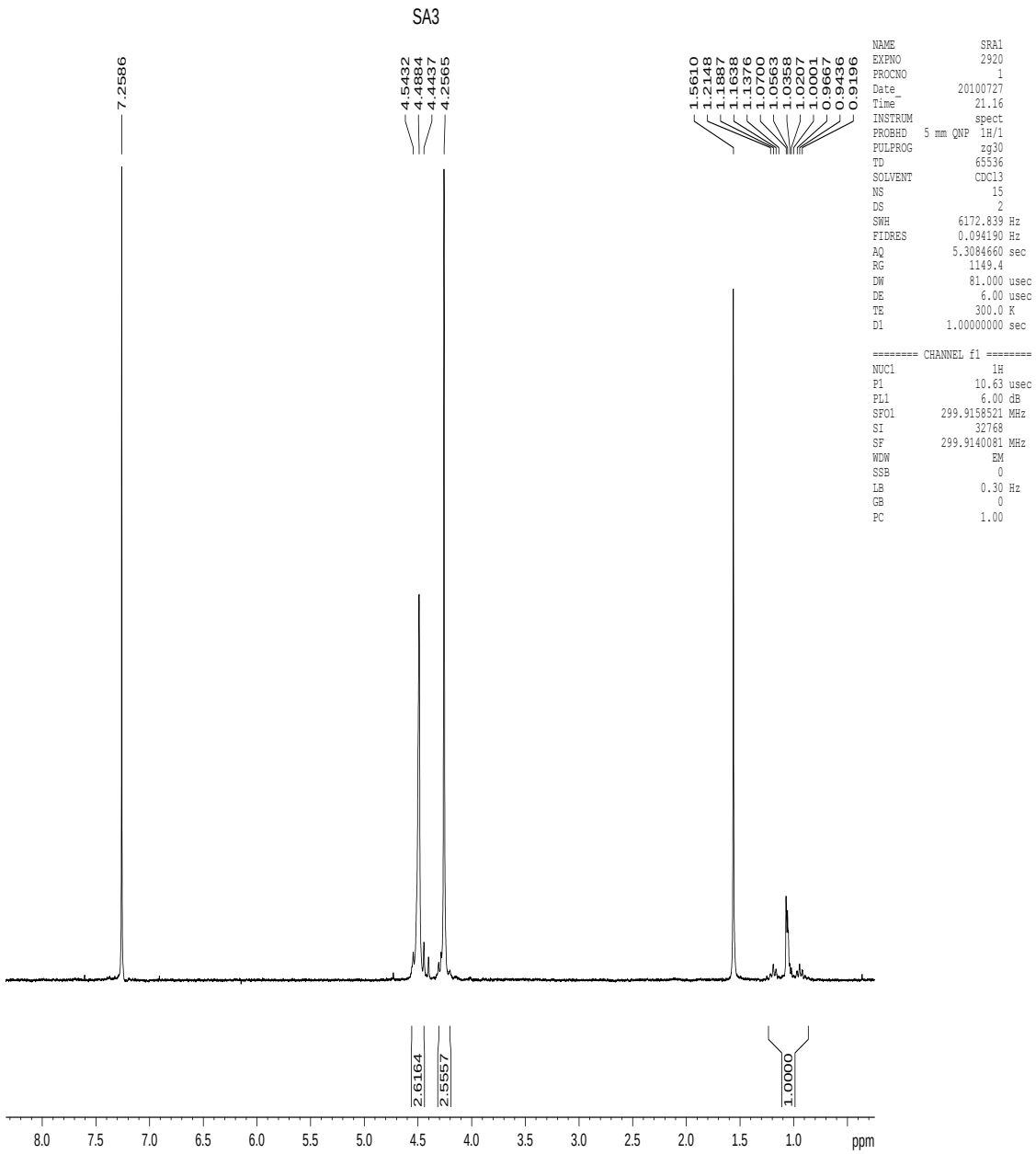

Appendix I.20. ^{1}H NMR spectrum of trans-PtCl(Et)(PTA)$_2$, 3a.

Appendix I.21. $^{31}P\{^{1}H\}$ NMR spectrum of trans-$PtCl_2(PTA)_2$, 4.

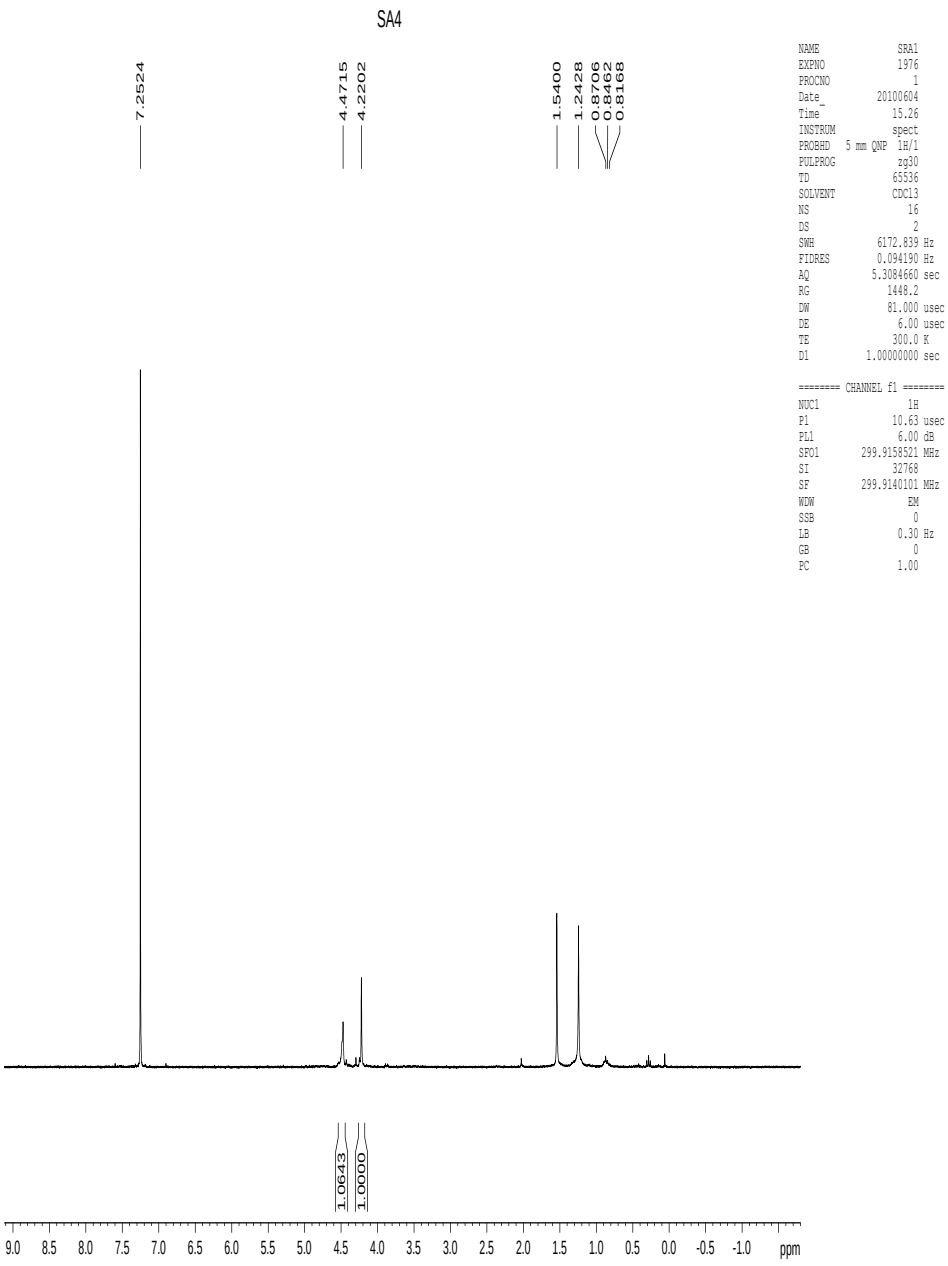

Appendix I.22. ^{1}H NMR spectrum of trans-$PtCl_2(PTA)_2$, 4.

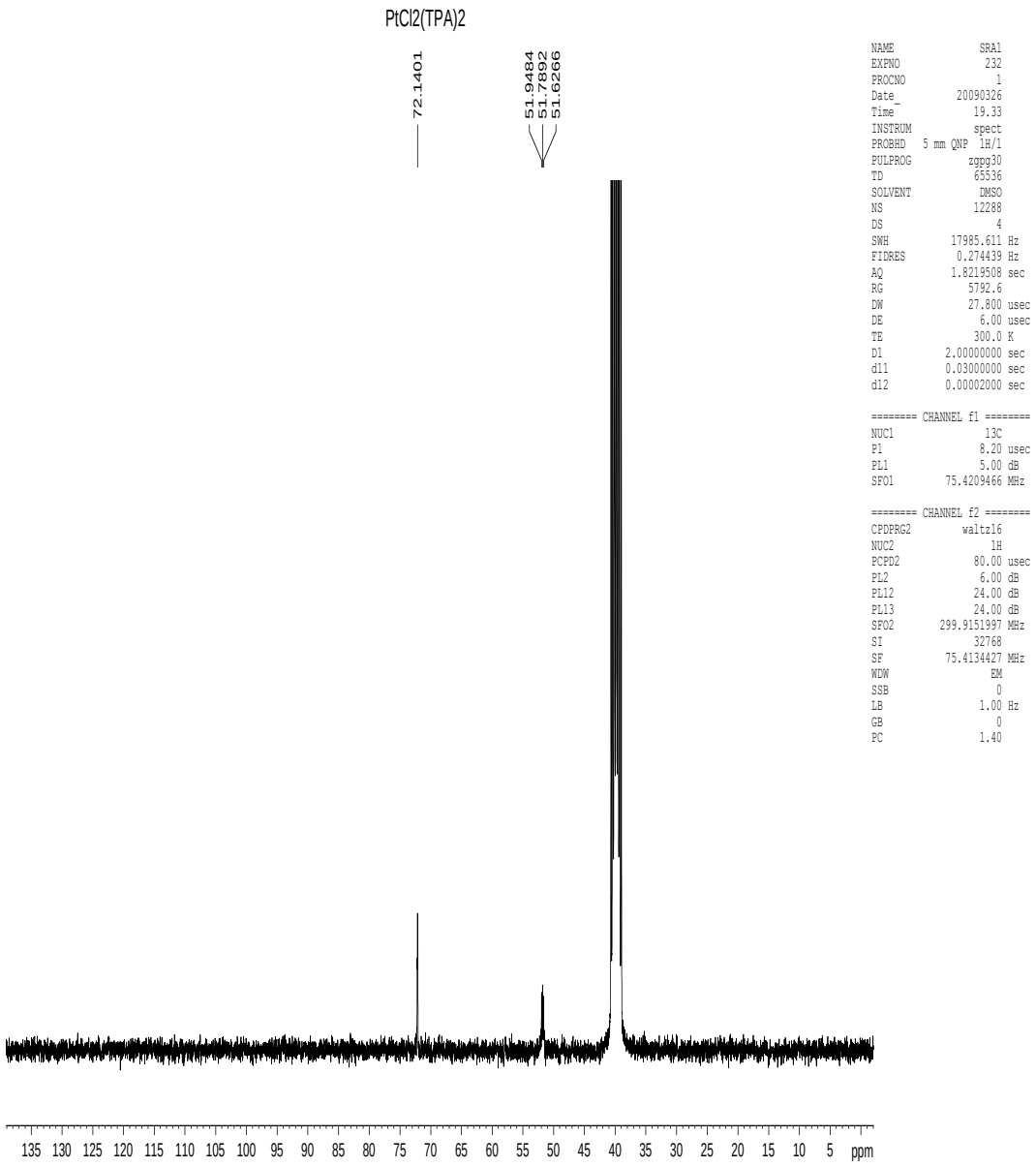

Appendix I.23. $^{13}C\{^{1}H\}$ NMR spectrum of trans-$PtCl_2(PTA)_2$, 4.

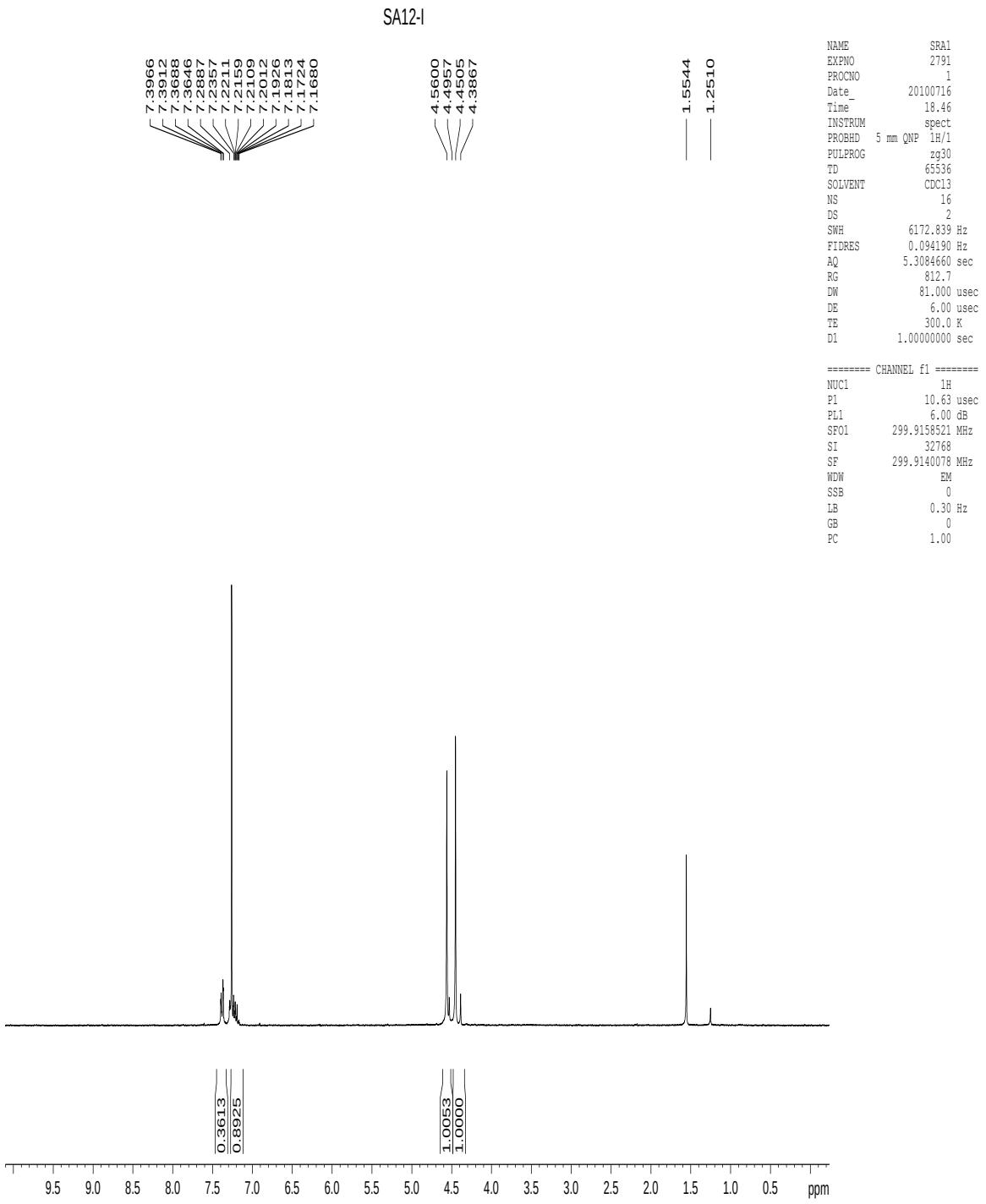

Appendix I.24. ^{1}H NMR spectrum of trans-Pd(C$_2$Ph)$_2$(PTA)$_2$, 7.

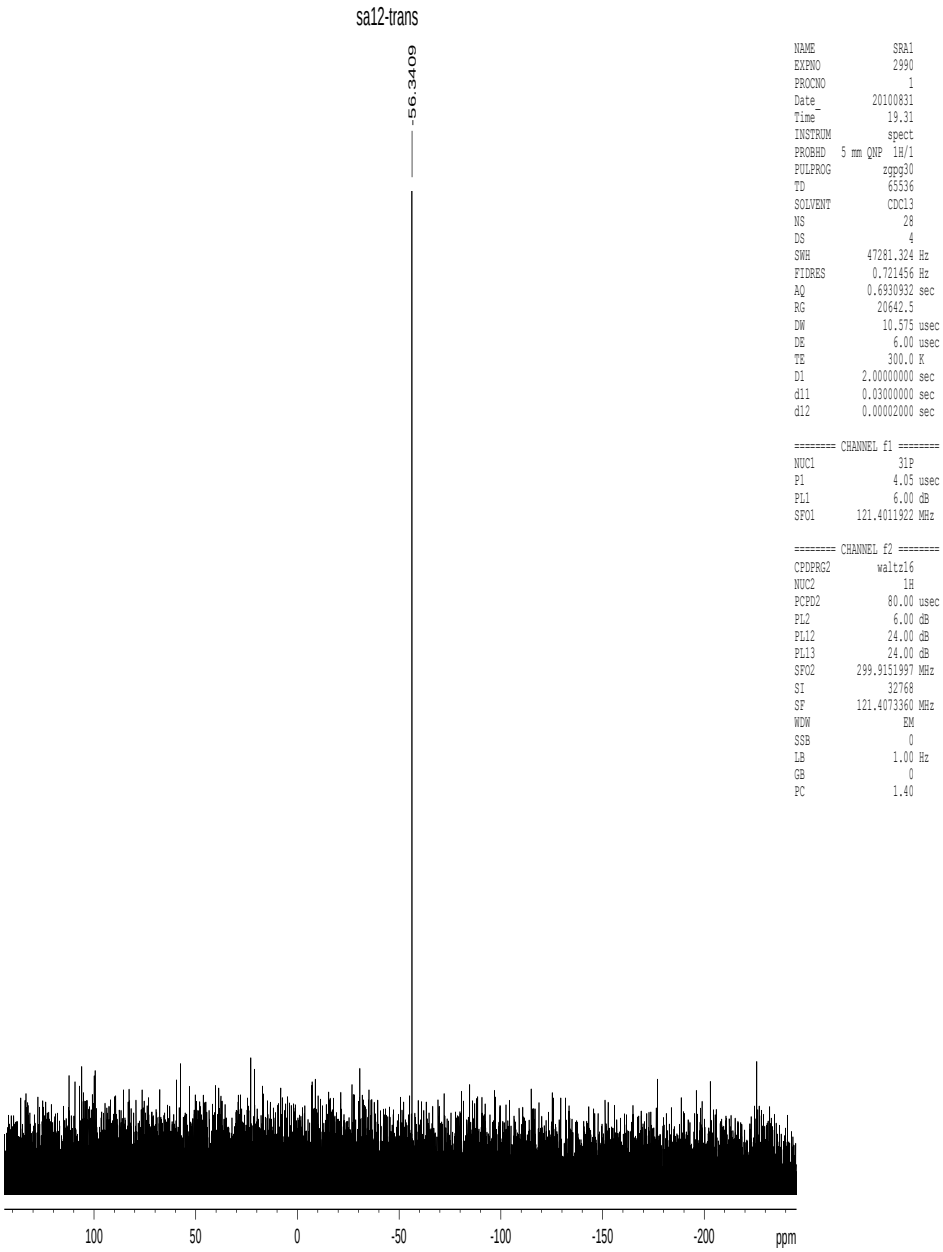

Appendix I.25. $^{31}P\{^{1}H\}$ NMR spectrum of trans-$Pd(C_2Ph)_2(PTA)_2$, 7.

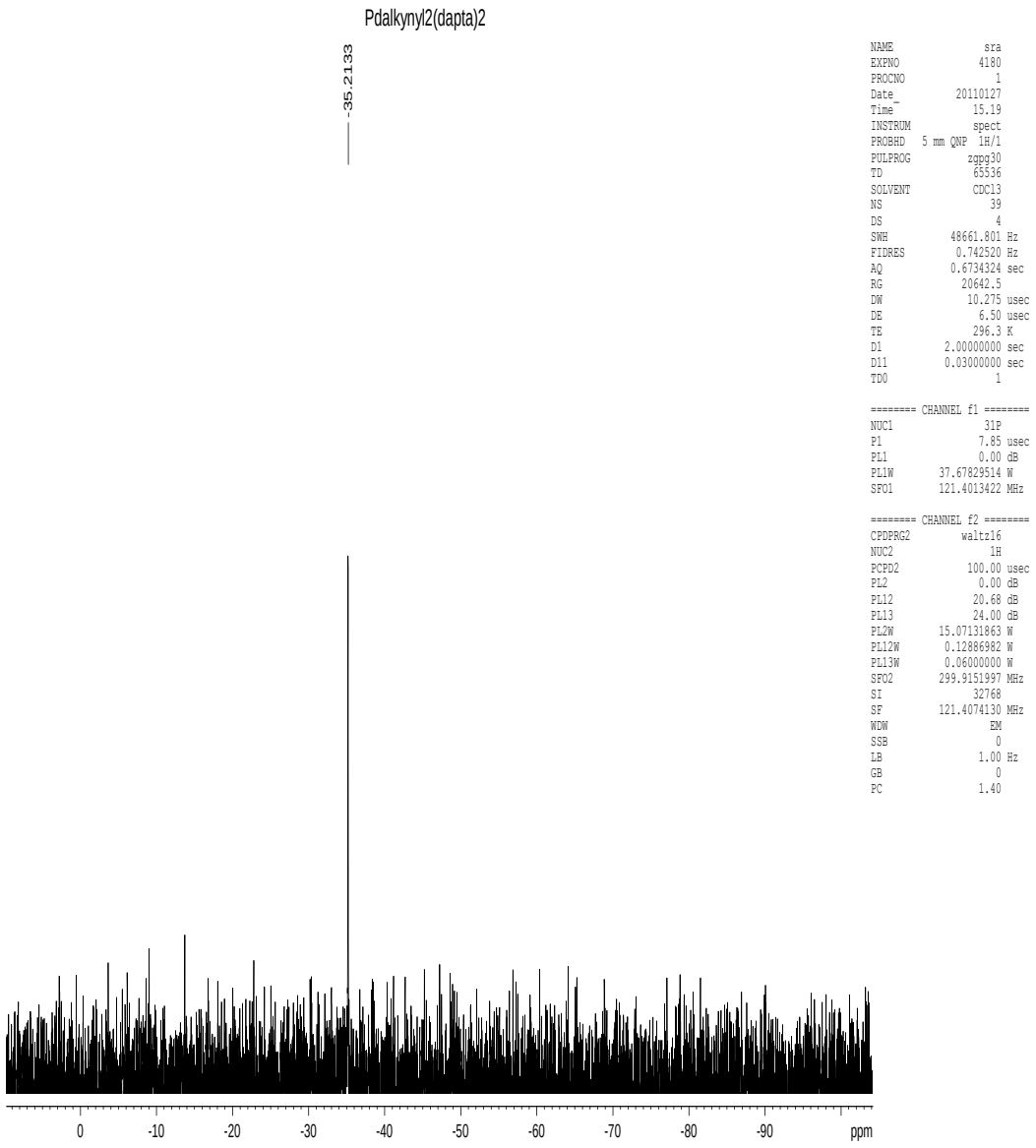

Appendix I.26. $^{31}P\{^{1}H\}$ NMR spectrum of trans-$Pd(C_2Ph)_2(DAPTA)_2$, 14.

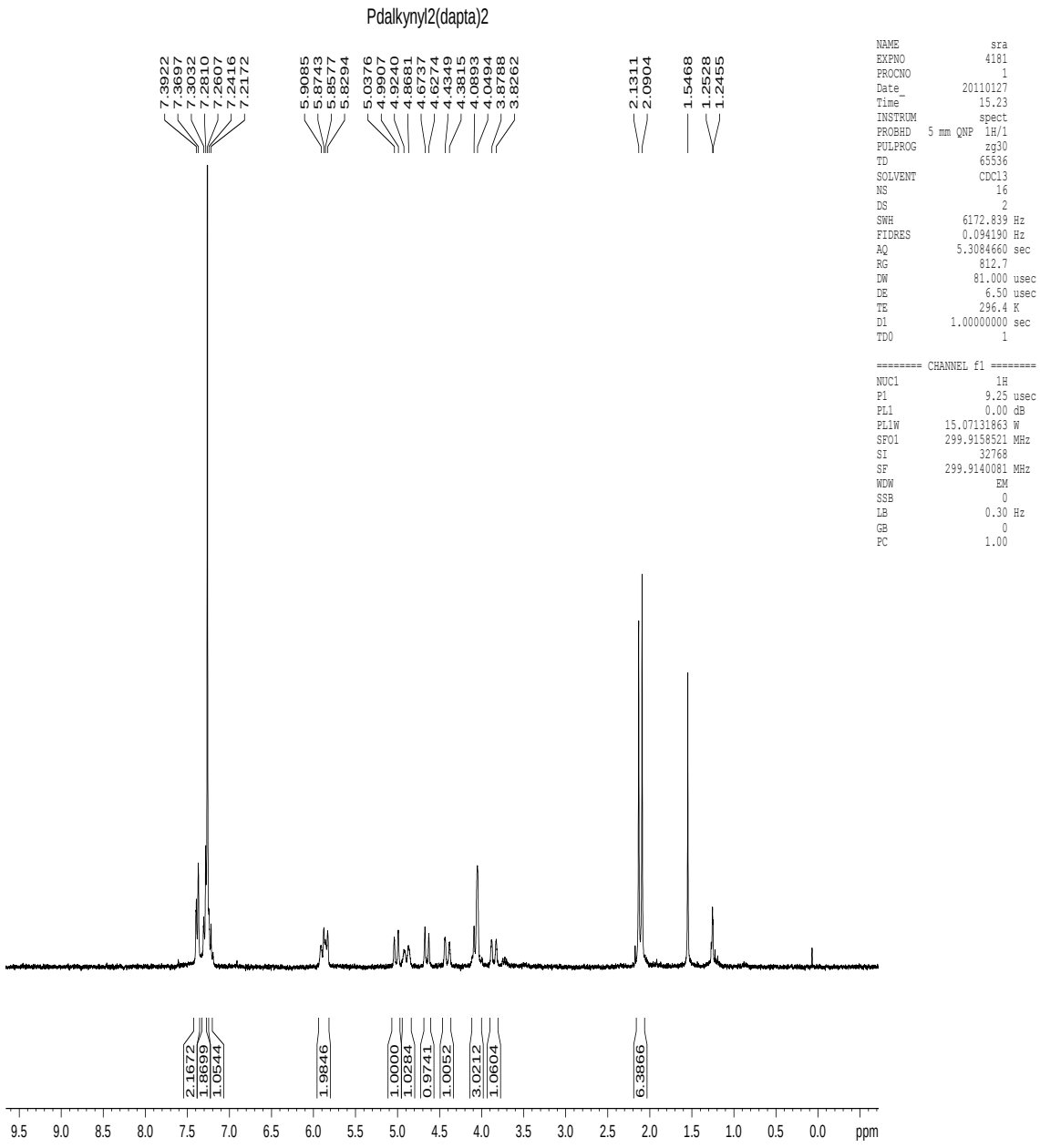

Appendix I.27. ^{1}H NMR spectrum of trans-Pd(C$_2$Ph)$_2$(DAPTA)$_2$, 14.

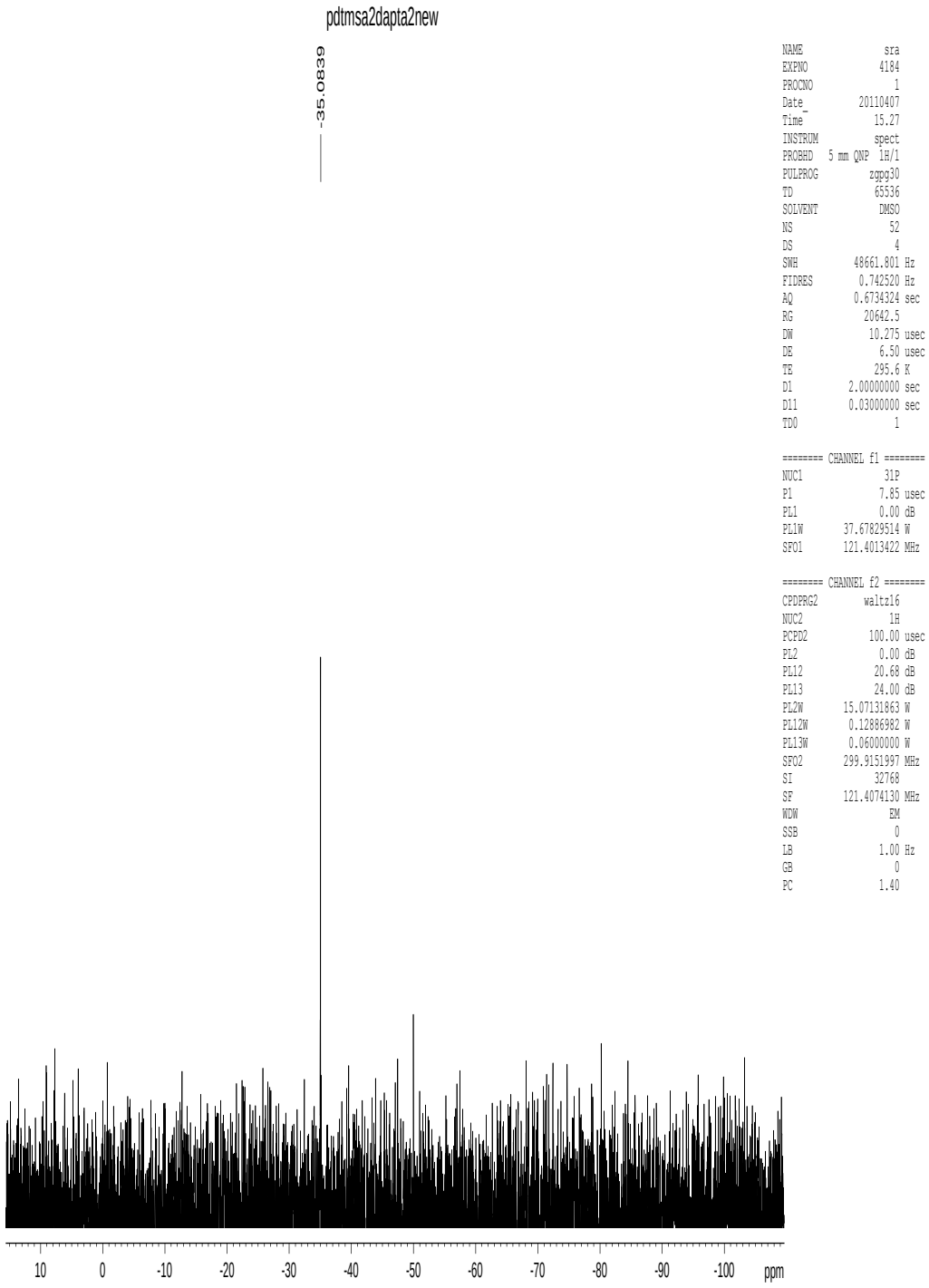

Appendix I.28. $^{31}P\{^{1}H\}$ NMR spectrum of trans-$Pd(C_2SiMe_3)_2(DAPTA)_2$, 15b.

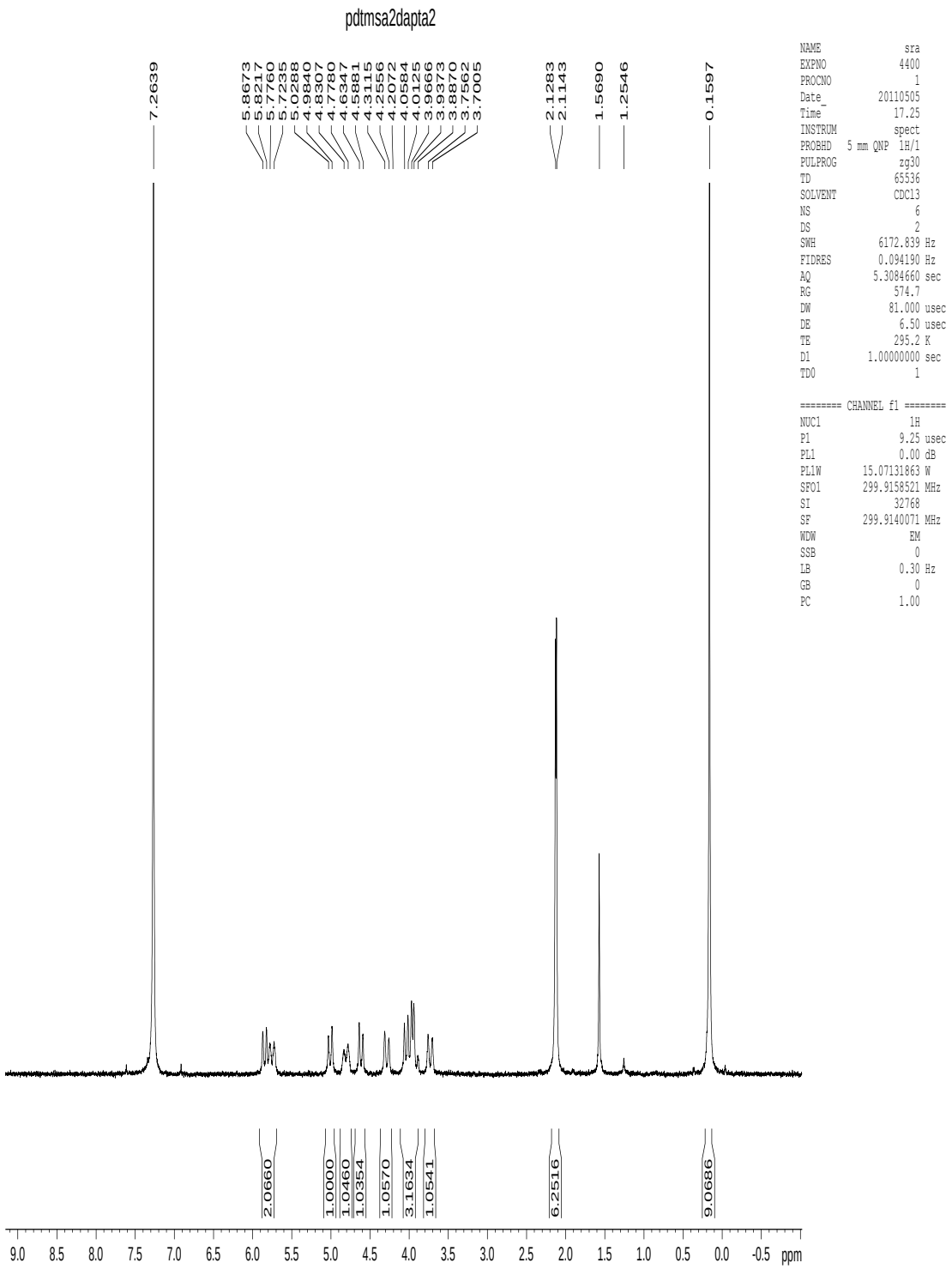

Appendix I.29. ^{1}H NMR spectrum of trans-$Pd(C_2SiMe_3)_2(DAPTA)_2$, 15b.

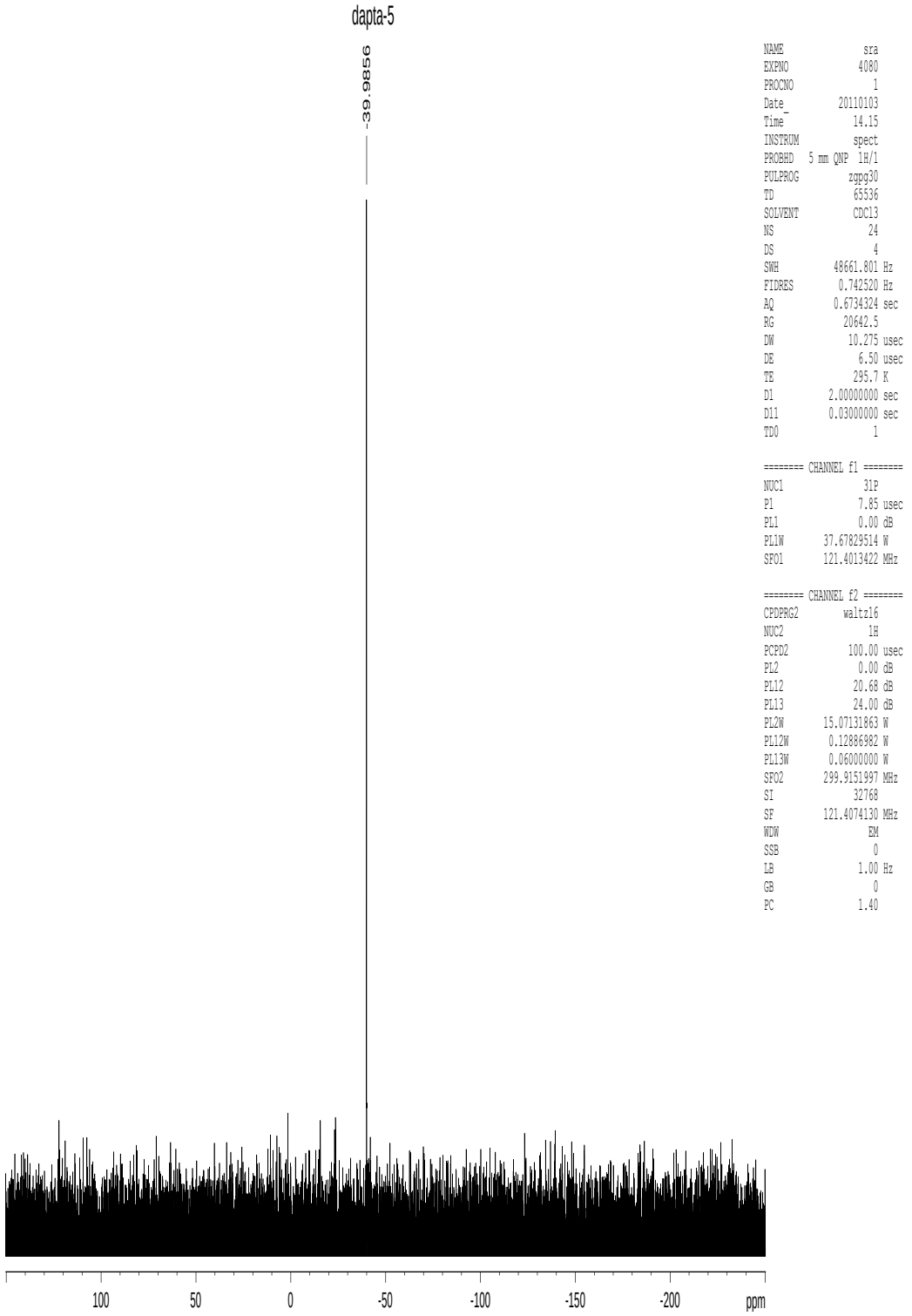

Appendix I.30. $^{31}P\{^{1}H\}$ NMR spectrum of trans-PdBr(Me)(DAPTA)$_2$, 11b.

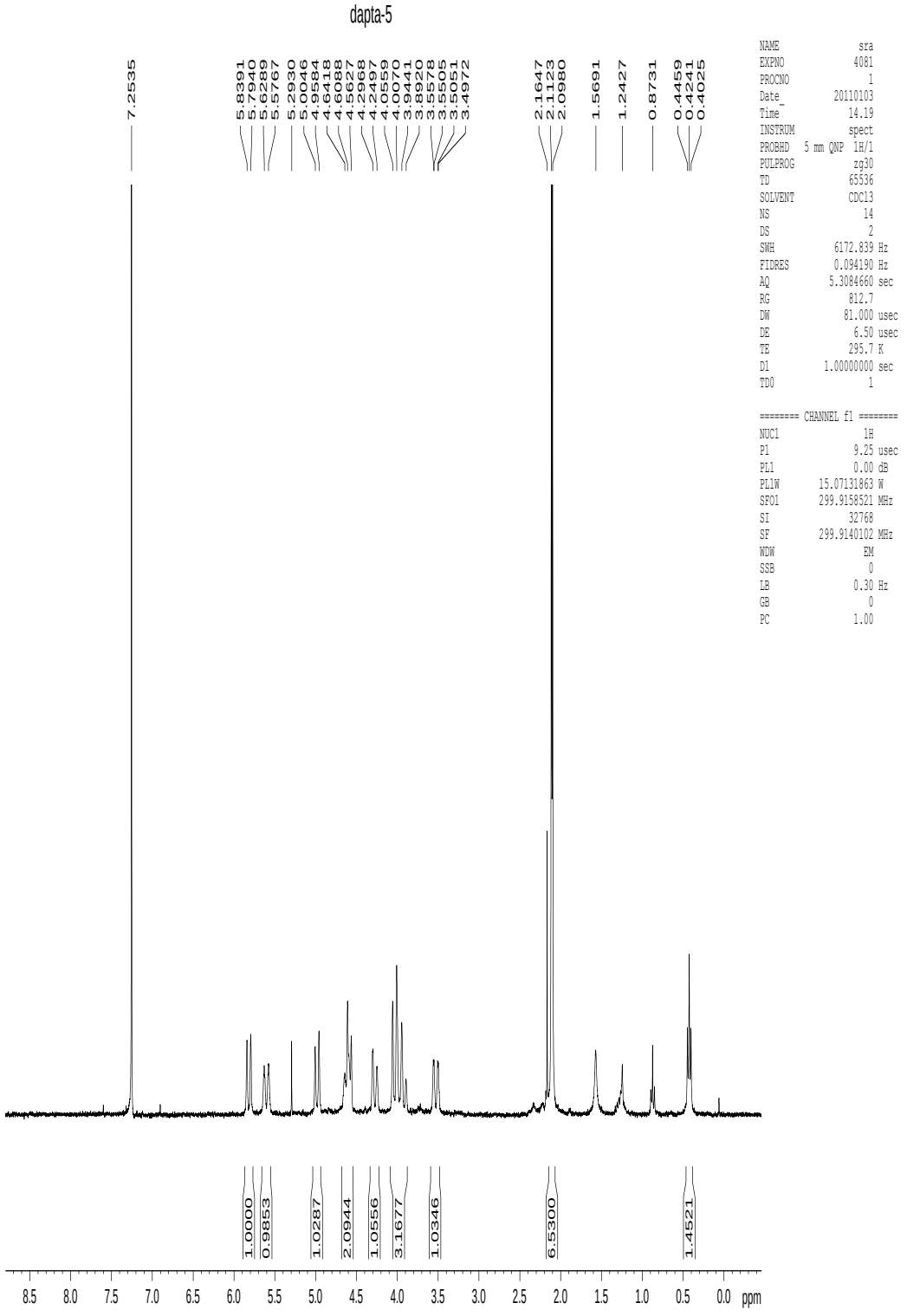

Appendix I.31. ^{1}H NMR spectrum of trans-PdBr(Me)(DAPTA)$_2$, 11b.

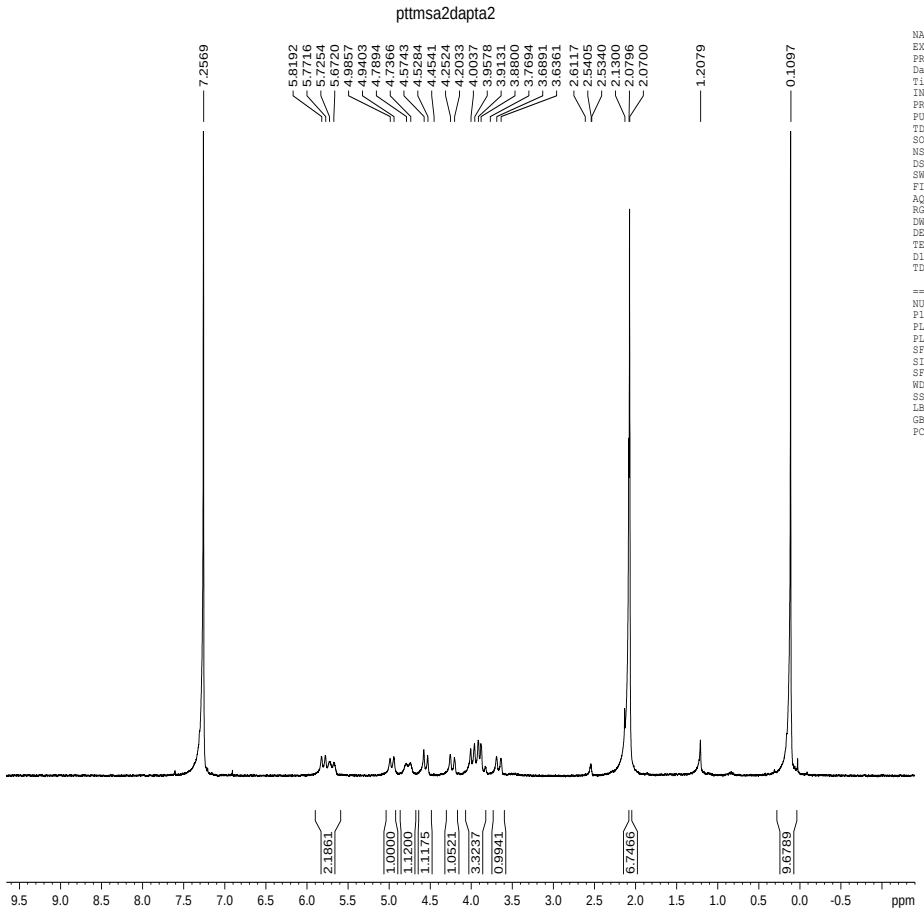

Appendix I.32. ^{1}H NMR spectrum of trans-Pt(C_2SiMe_3)$_2$(DAPTA)$_2$, 15a.

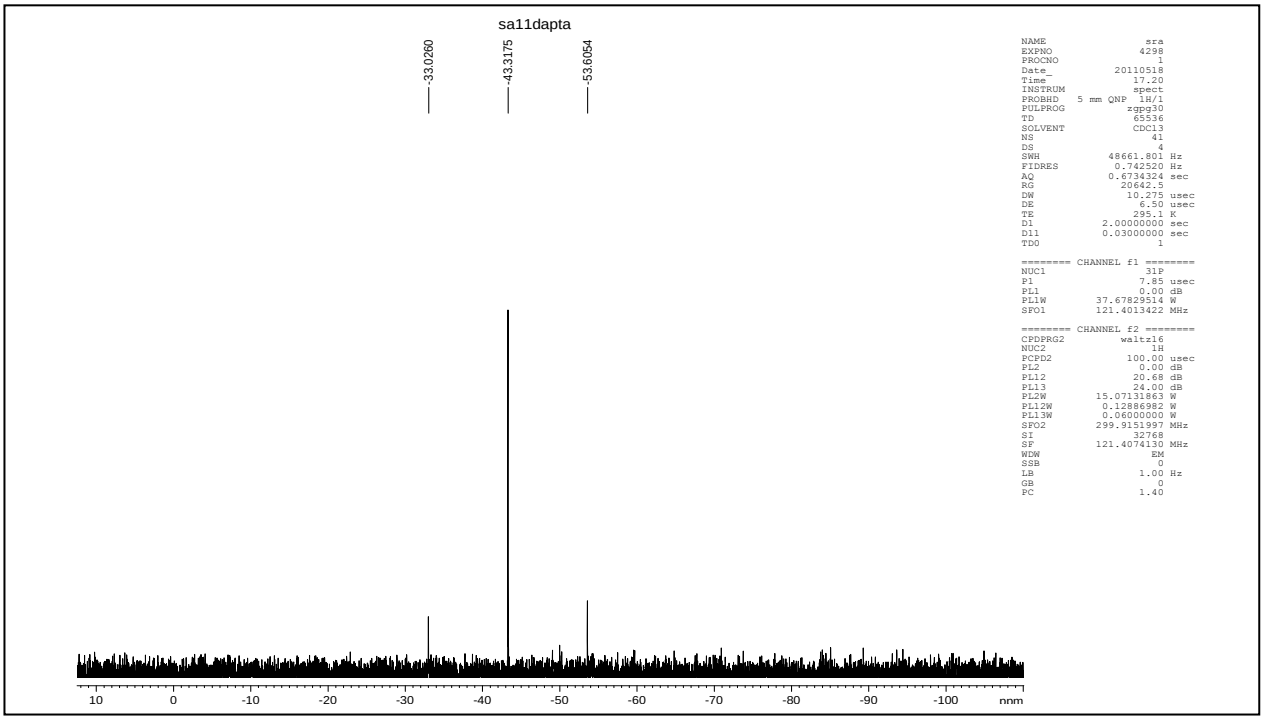

Appendix I.33. $^{31}P\{^{1}H\}$ NMR spectrum of trans-Pt(C_2SiMe_3)$_2$(DAPTA)$_2$, 15a.

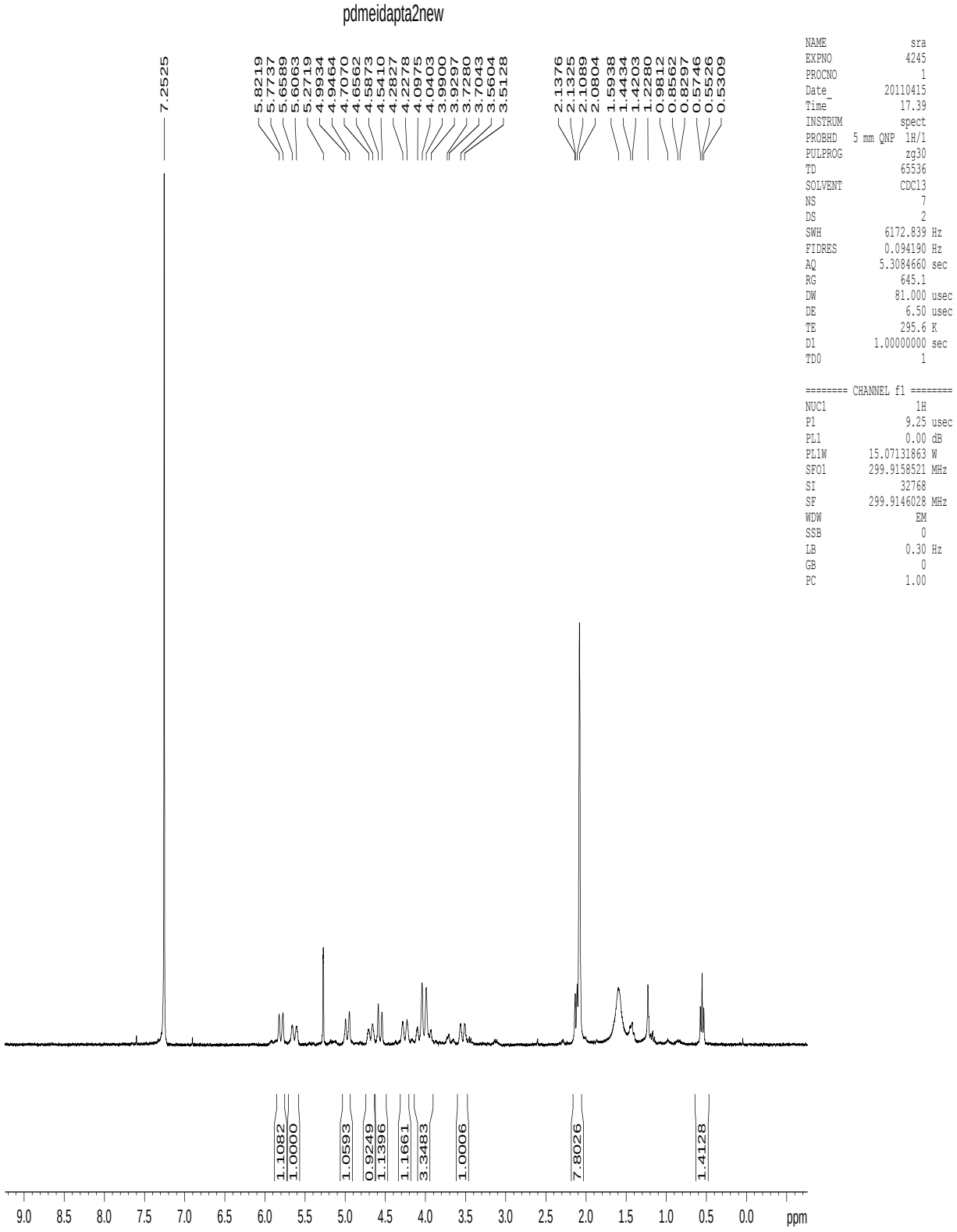

Appendix I.34. ^{1}H NMR spectrum of trans-PdI(Me)(DAPTA)$_2$, 11c.

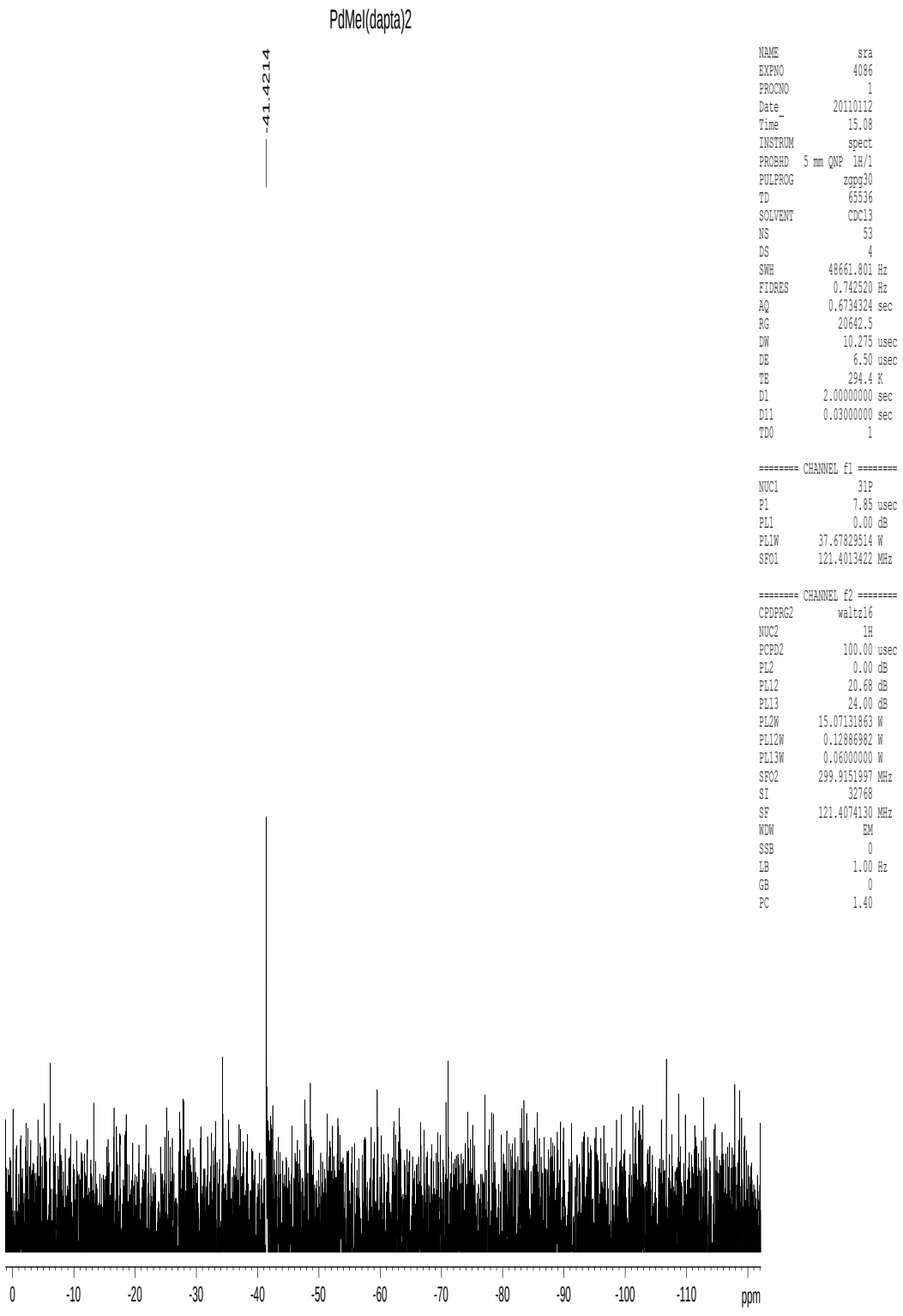

Appendix I.35. $^{31}P\{^{1}H\}$ NMR spectrum of trans-PdI(Me)(DAPTA)$_2$, 11c.

Appendix I.36. $^{31}P\{^{1}H\}$ NMR spectrum of trans-$Pt(C_2Ph)_2(DAPTA)_2$, 13a.

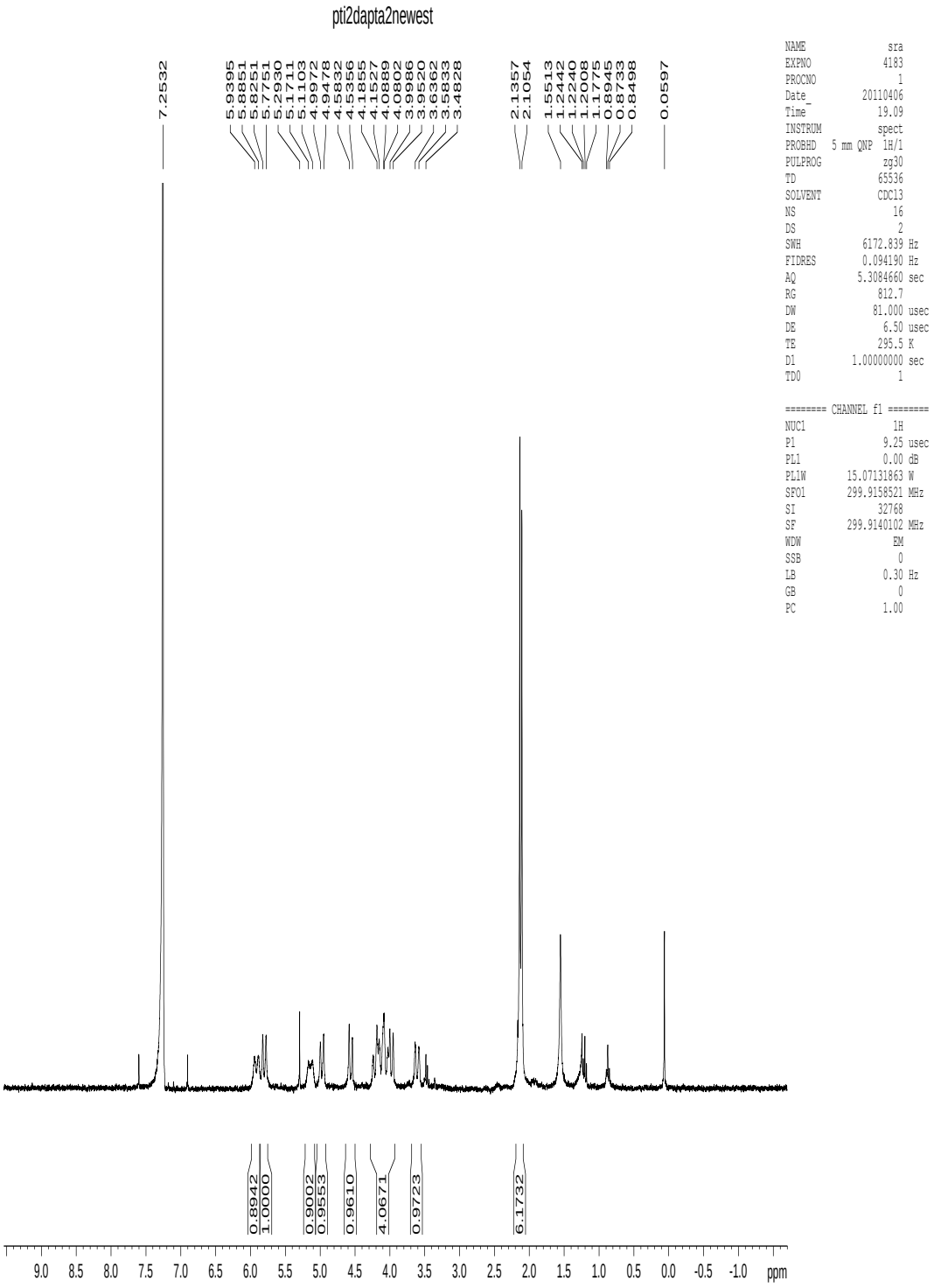

Appendix I.37. ^{1}H NMR spectrum of trans-$PtI_2(DAPTA)_2$, 12d.

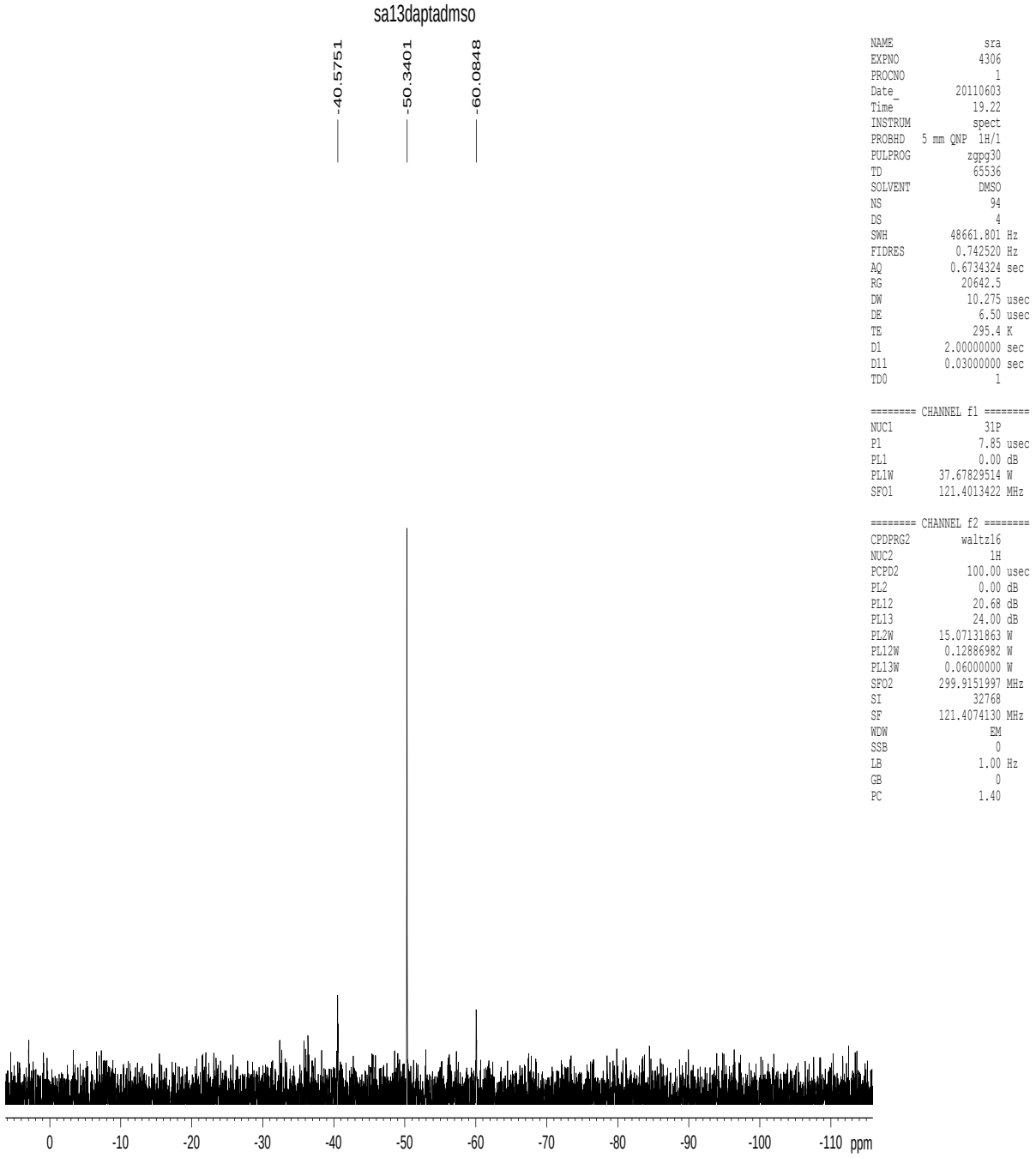

Appendix I.38. $^{31}P\{^{1}H\}$ NMR spectrum of trans-$PtI_2(DAPTA)_2$, 12d.

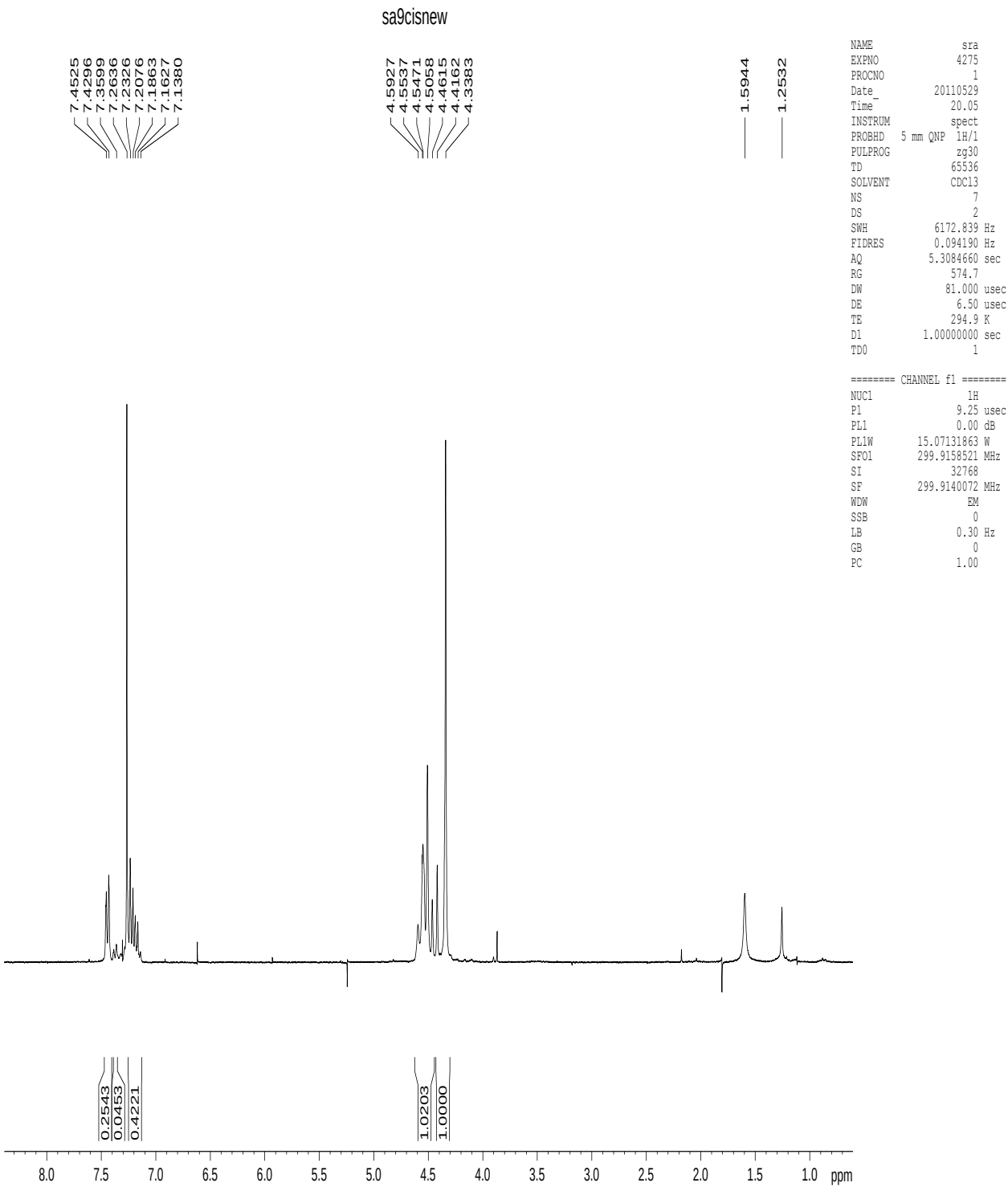

Appendix I.39. ^{1}H NMR spectrum of cis-$Pt(C_2Ph)_2(PTA)_2$, 6a.

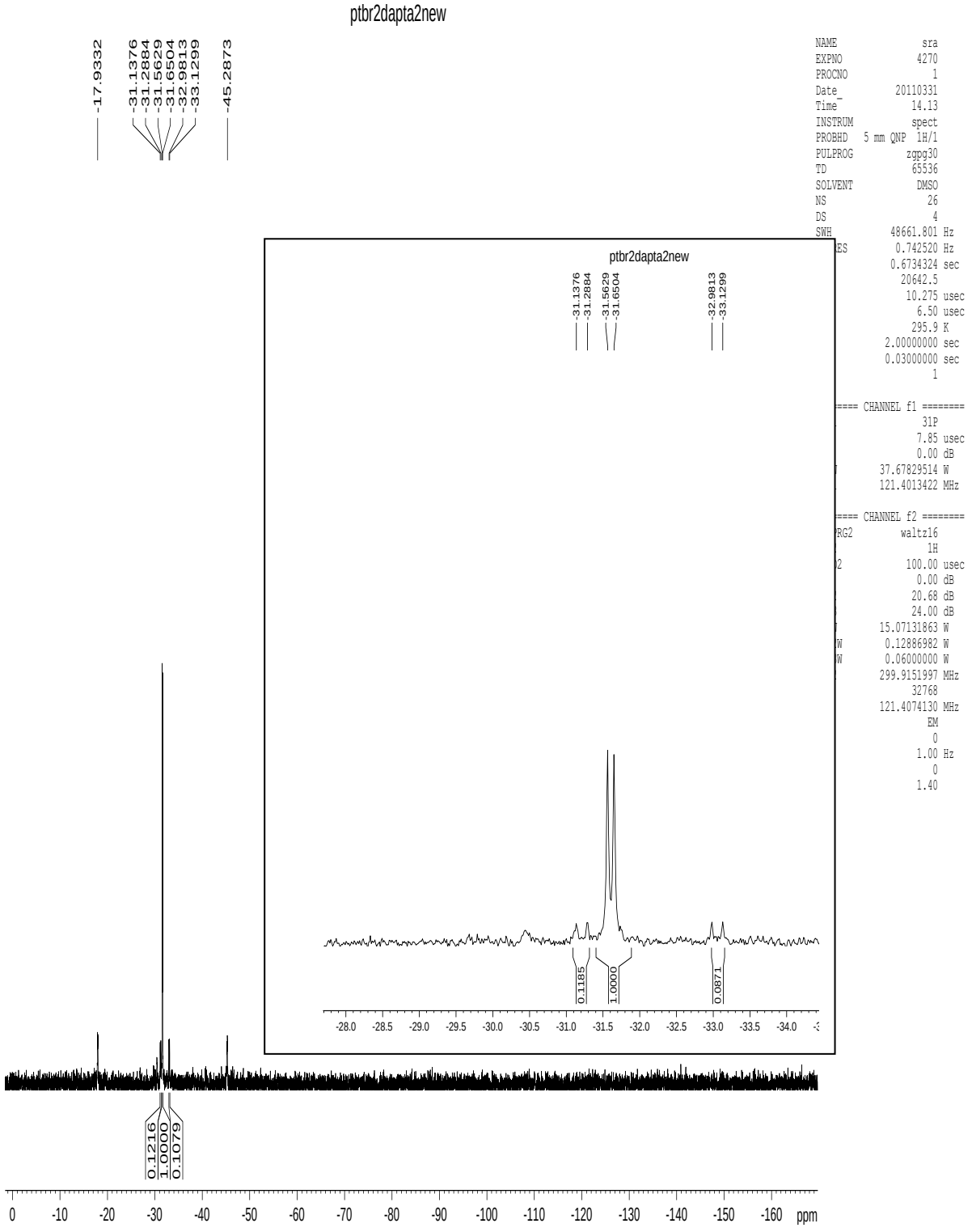

Appendix I.40. $^{31}P\{^{1}H\}$ NMR spectrum of cis-$PtBr_2(DAPTA)_2$, 12a.

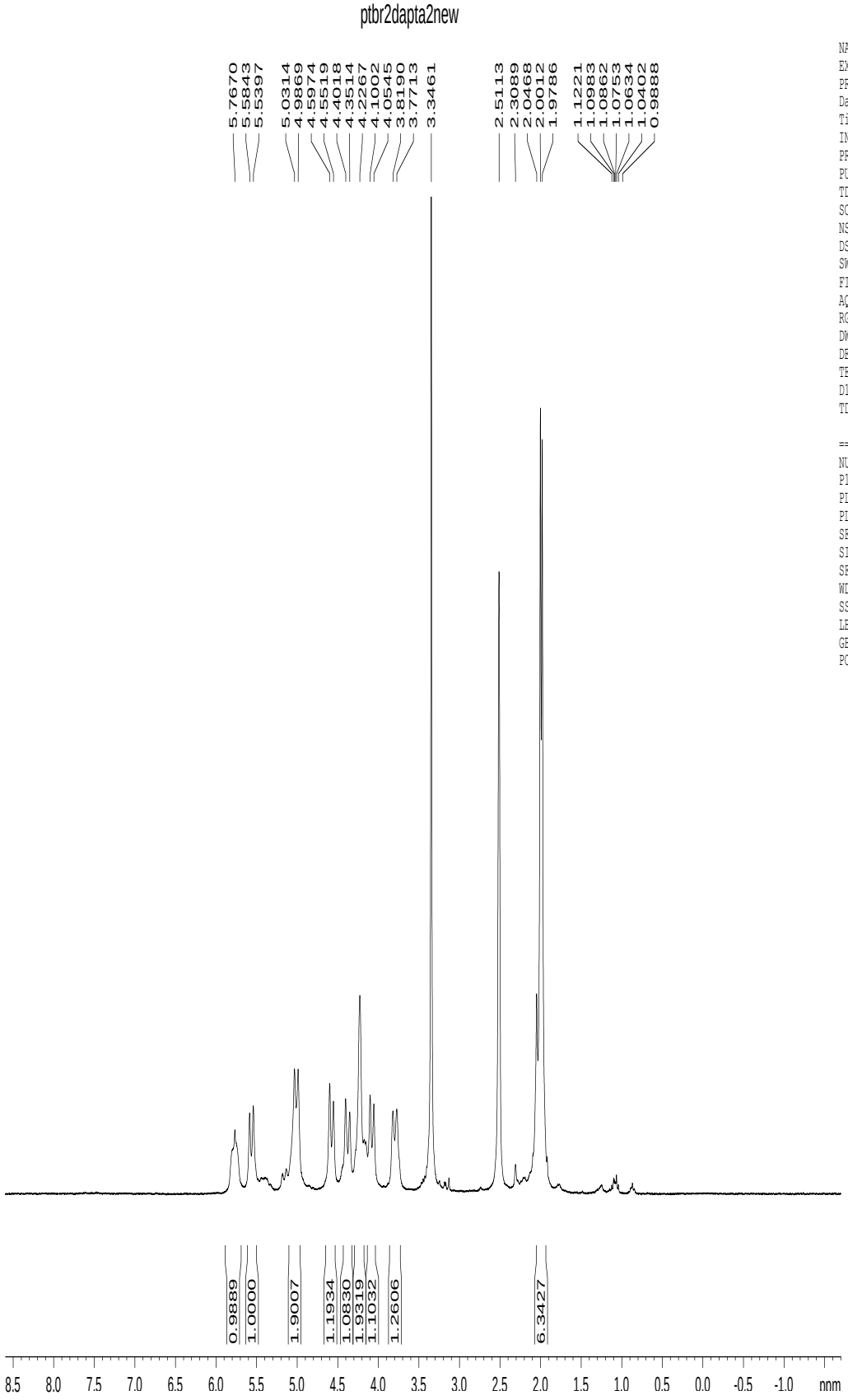

Appendix I.41. ^{1}H NMR spectrum of cis-$PtBr_2(DAPTA)_2$, 12a.

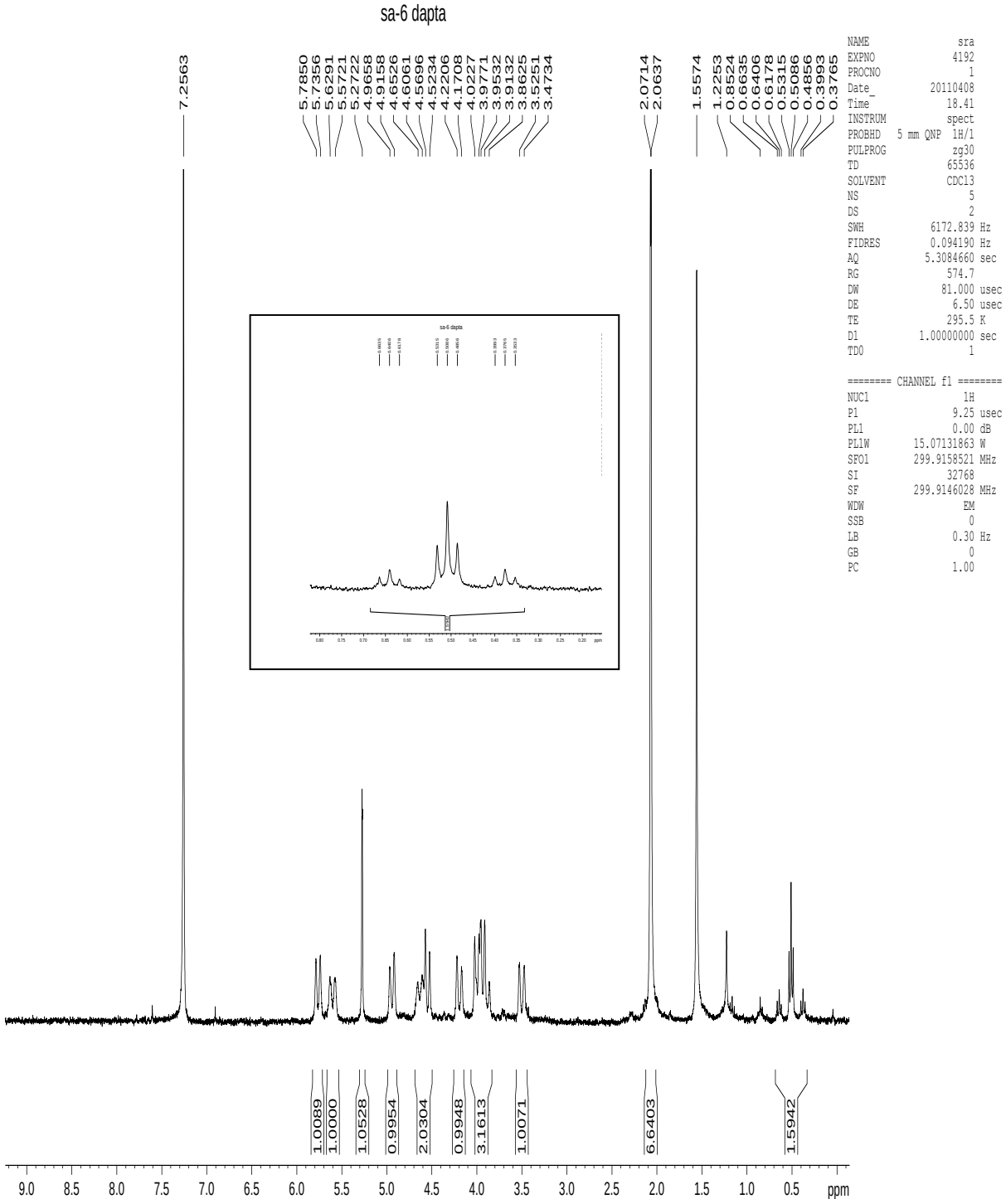

Appendix I.42. ^{1}H NMR spectrum of trans-PtBr(Me)(DAPTA)$_2$, 10b.

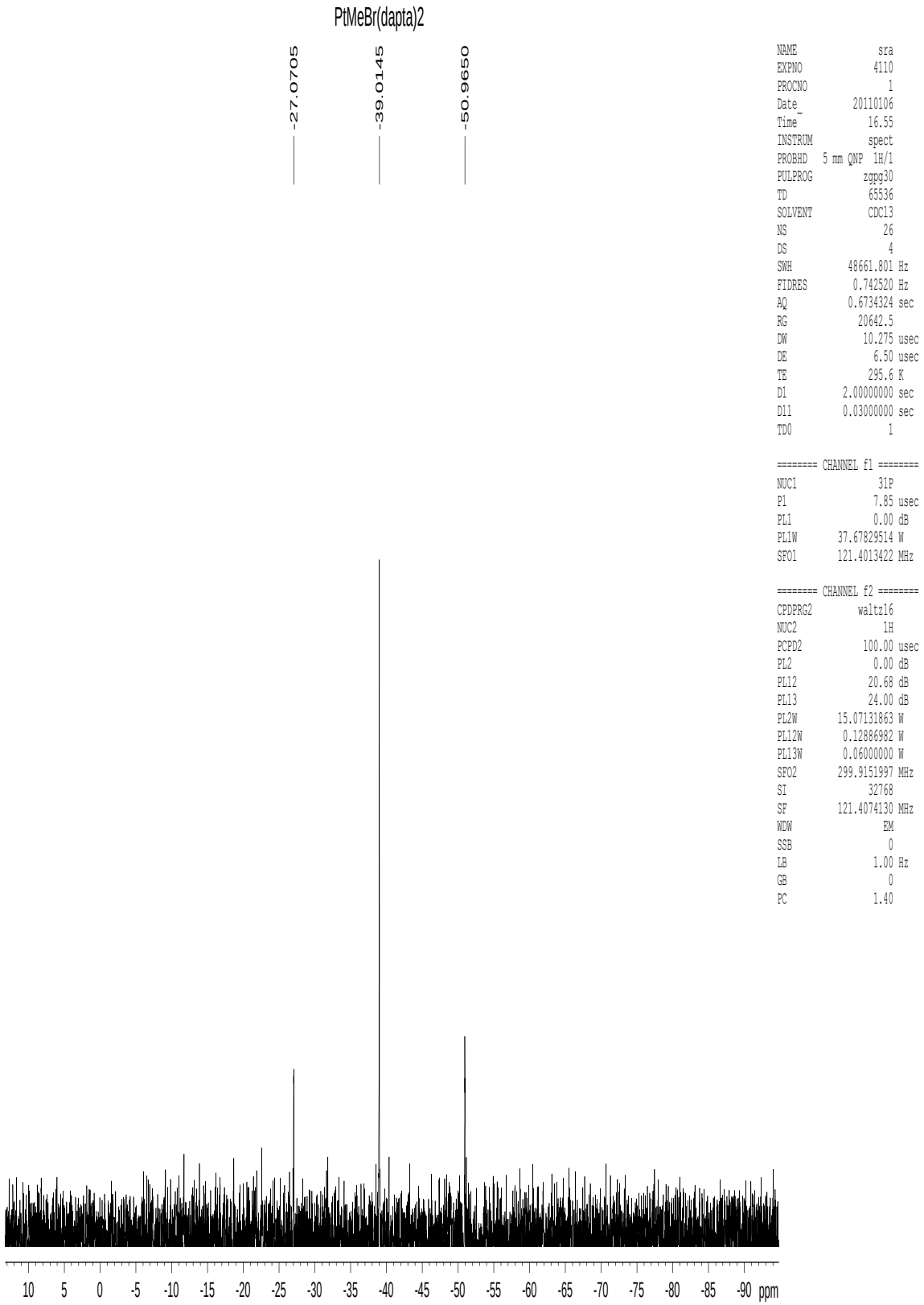

Appendix I.43. $^{31}P\{^{1}H\}$ NMR spectrum of trans-PtBr(Me)(DAPTA)$_2$, 10b.

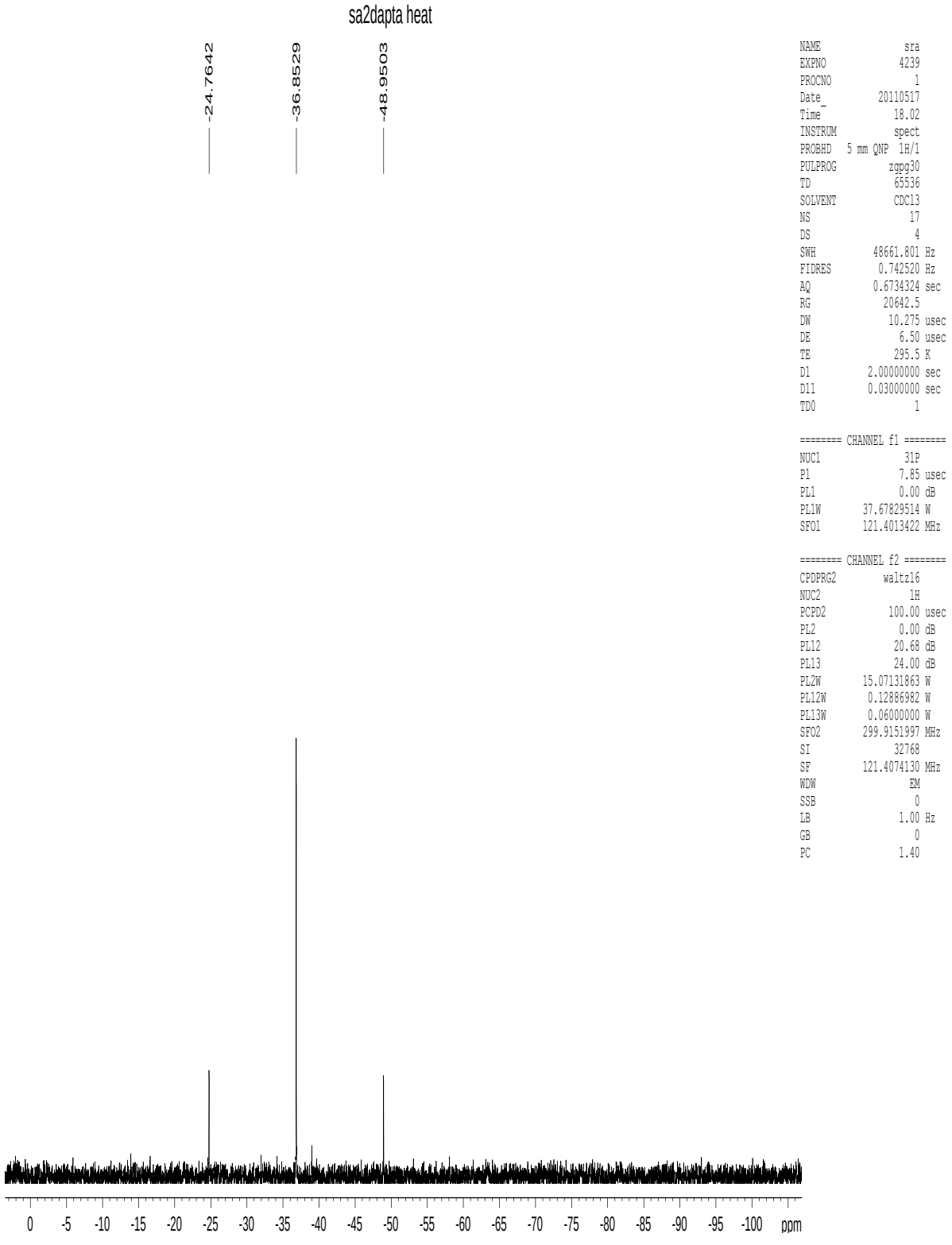

Appendix I.44. $^{31}P\{^{1}H\}$ NMR spectrum of trans-PtCl(Me)(DAPTA)$_2$, 10a.

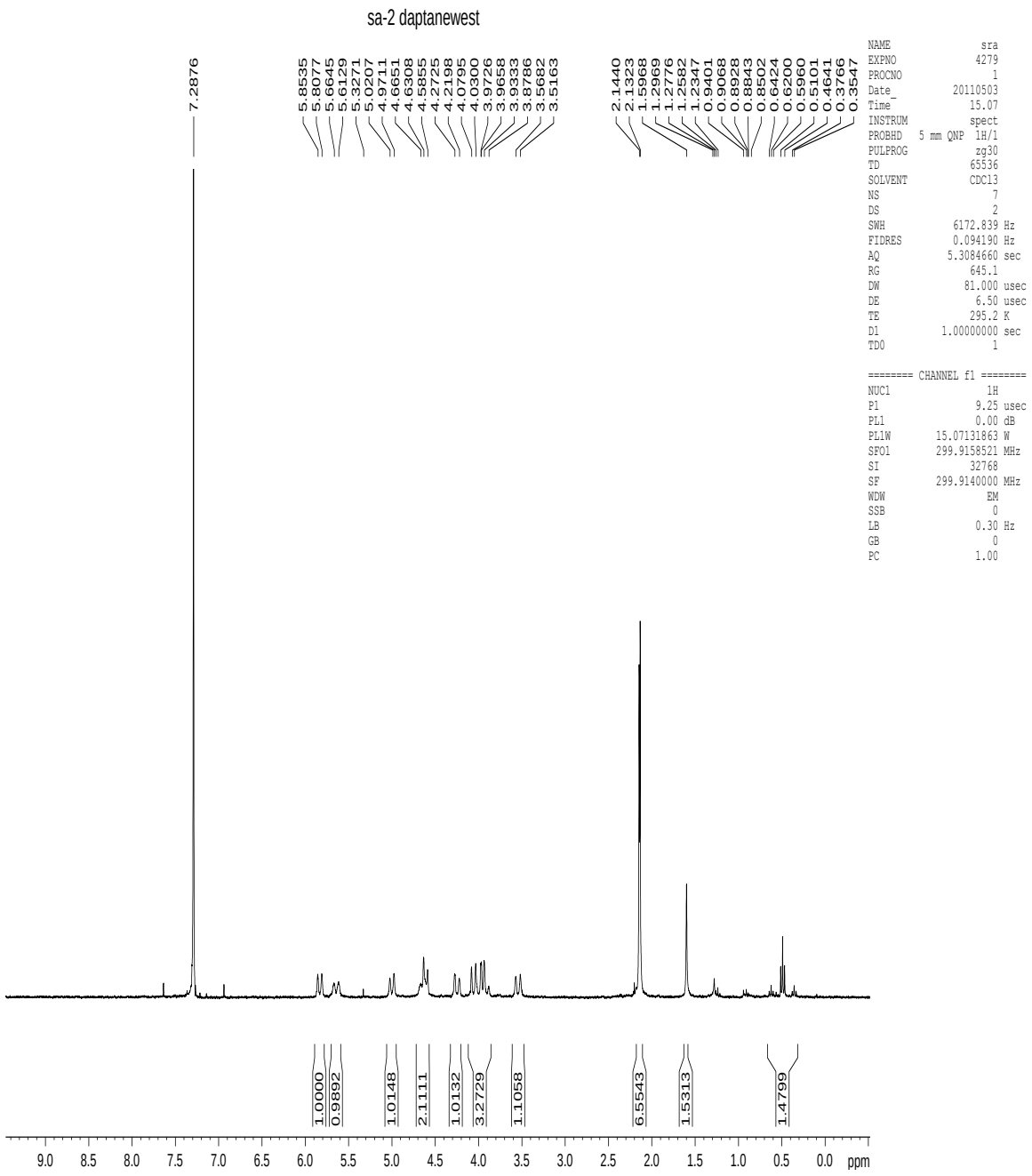

Appendix I.45. ^{1}H NMR spectrum of trans-PtCl(Me)(DAPTA)$_2$, 10a.

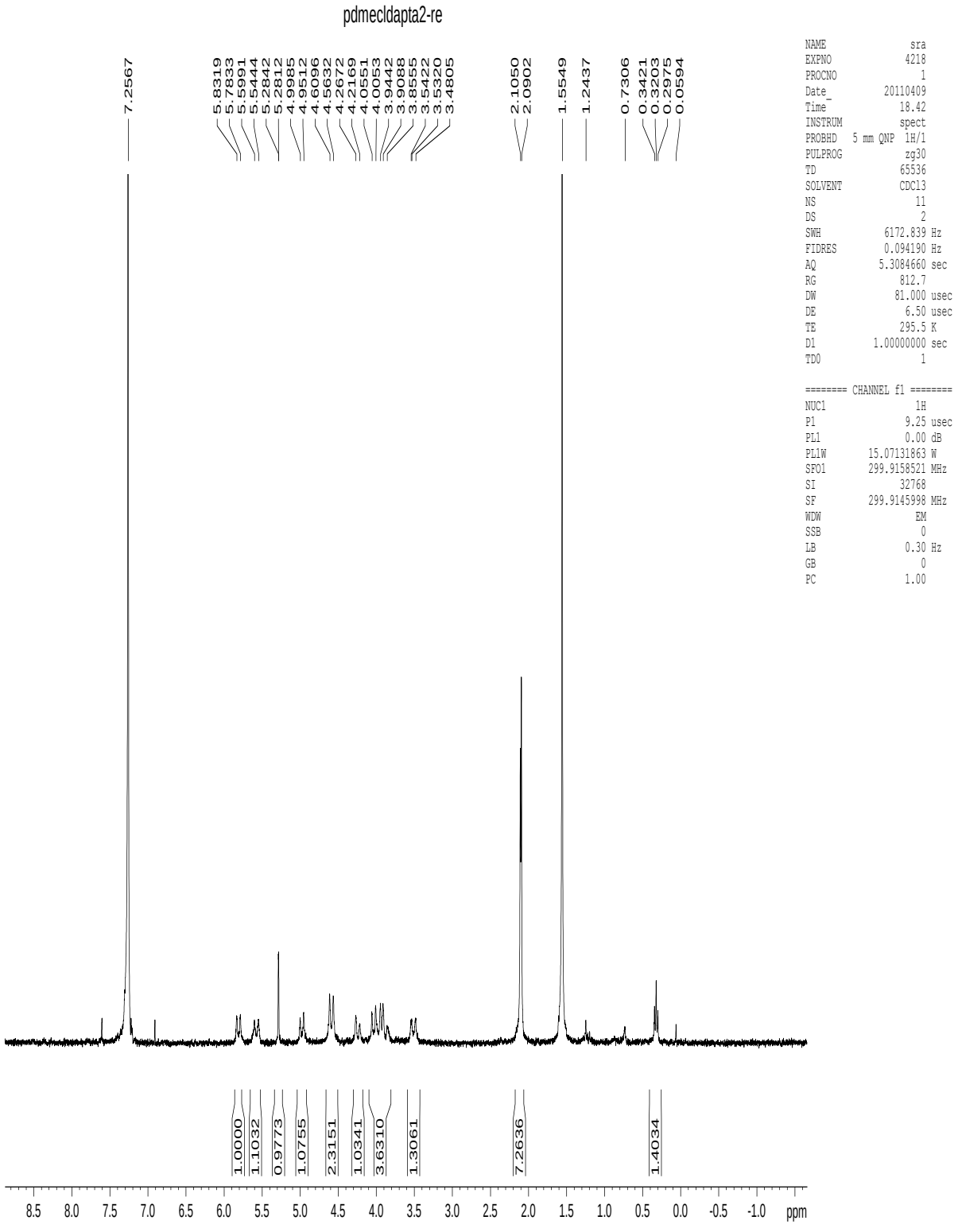

Appendix I.46. ^{1}H NMR spectrum of trans-PdCl(Me)(DAPTA)$_2$, 11a.

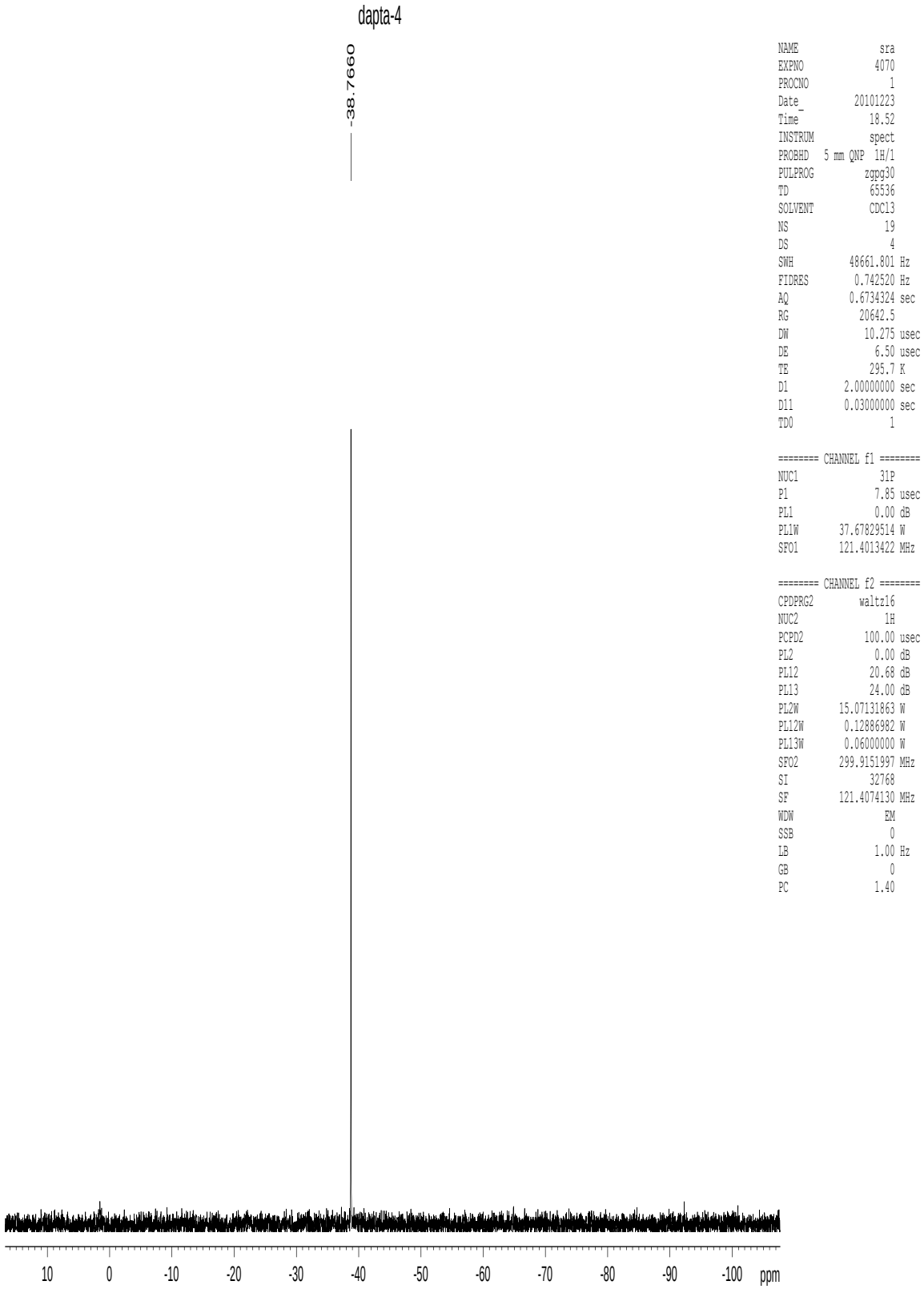

Appendix I.47. $^{31}P\{^{1}H\}$ NMR spectrum of trans-PdCl(Me)(DAPTA)$_2$, 11a.

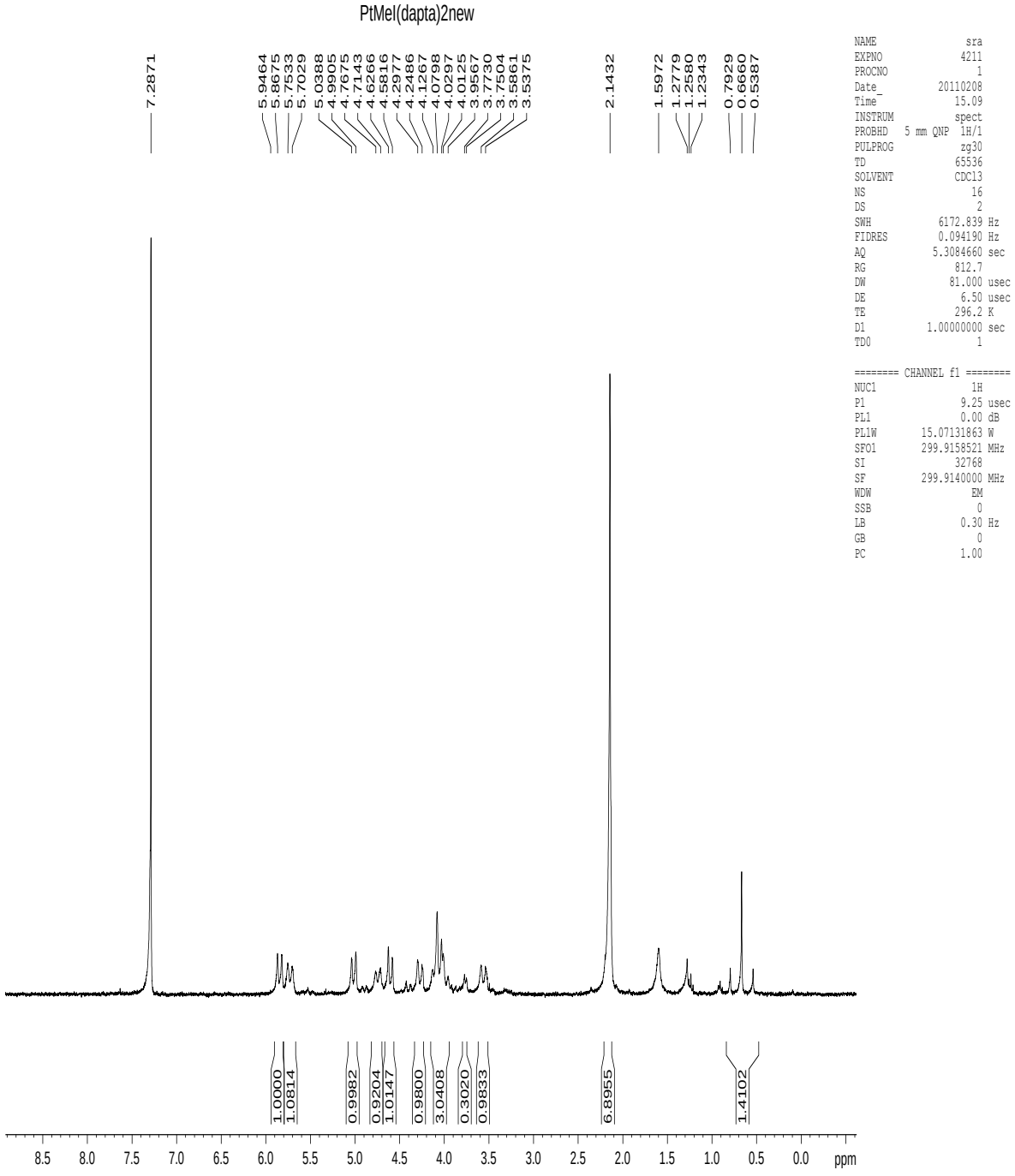

Appendix I.48. ^{1}H NMR spectrum of trans-PtI(Me)(DAPTA)$_2$, 10c.

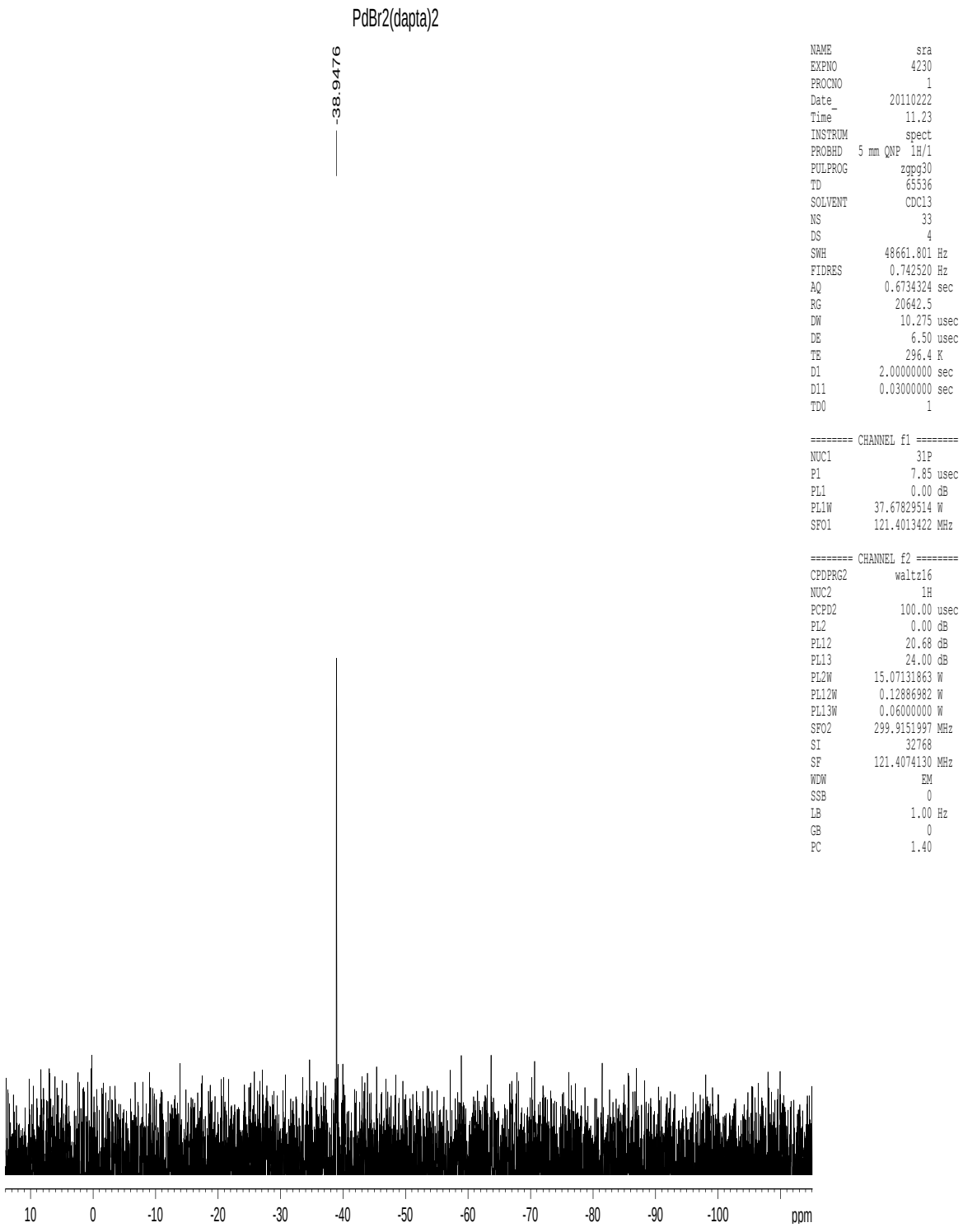

Appendix I.49. $^{31}P\{^{1}H\}$ NMR spectrum of cis-$PdBr_2(DAPTA)_2$, 12c.

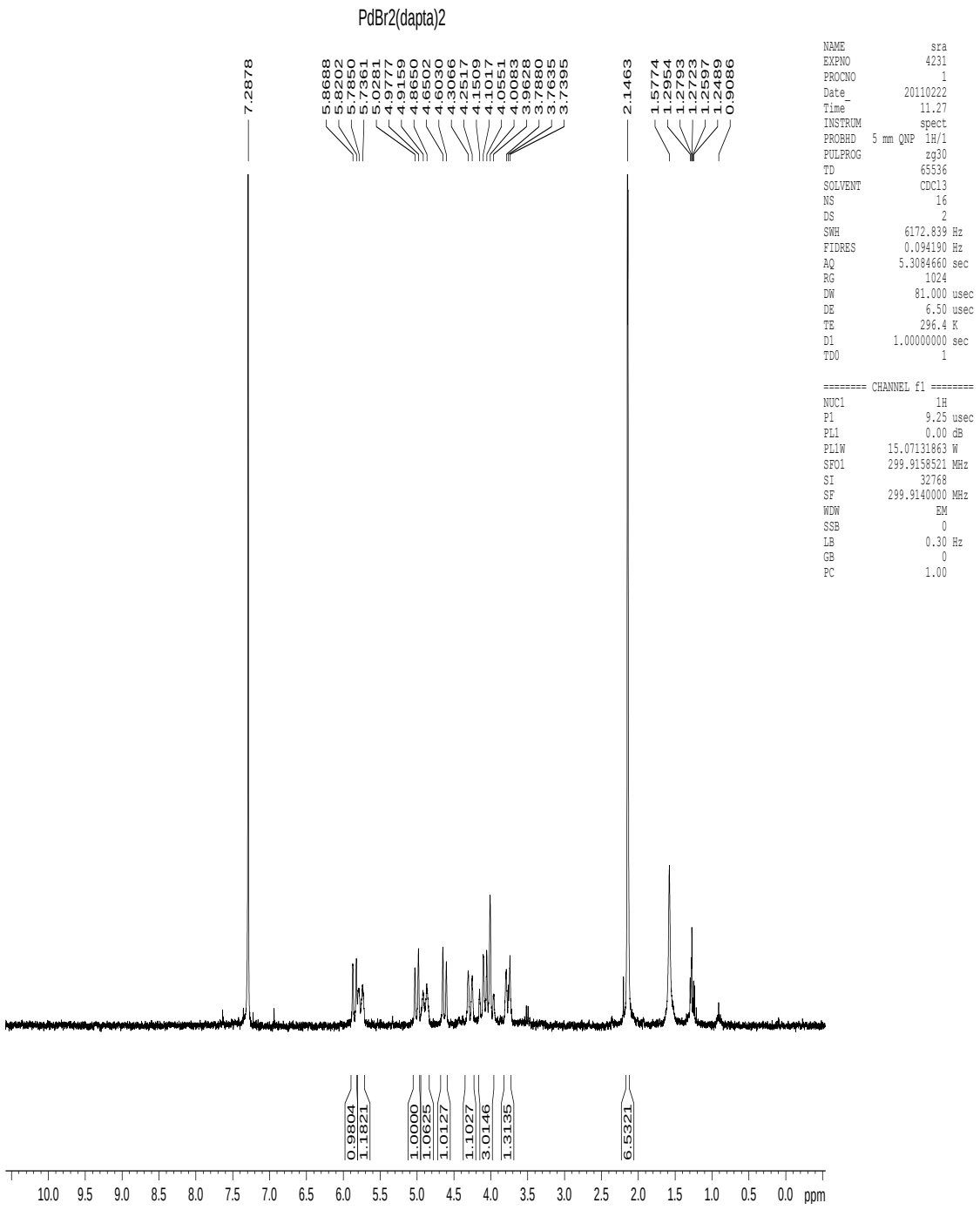

Appendix I.50. ^{1}H NMR spectrum of cis-PdBr$_2$(DAPTA)$_2$, 12c.

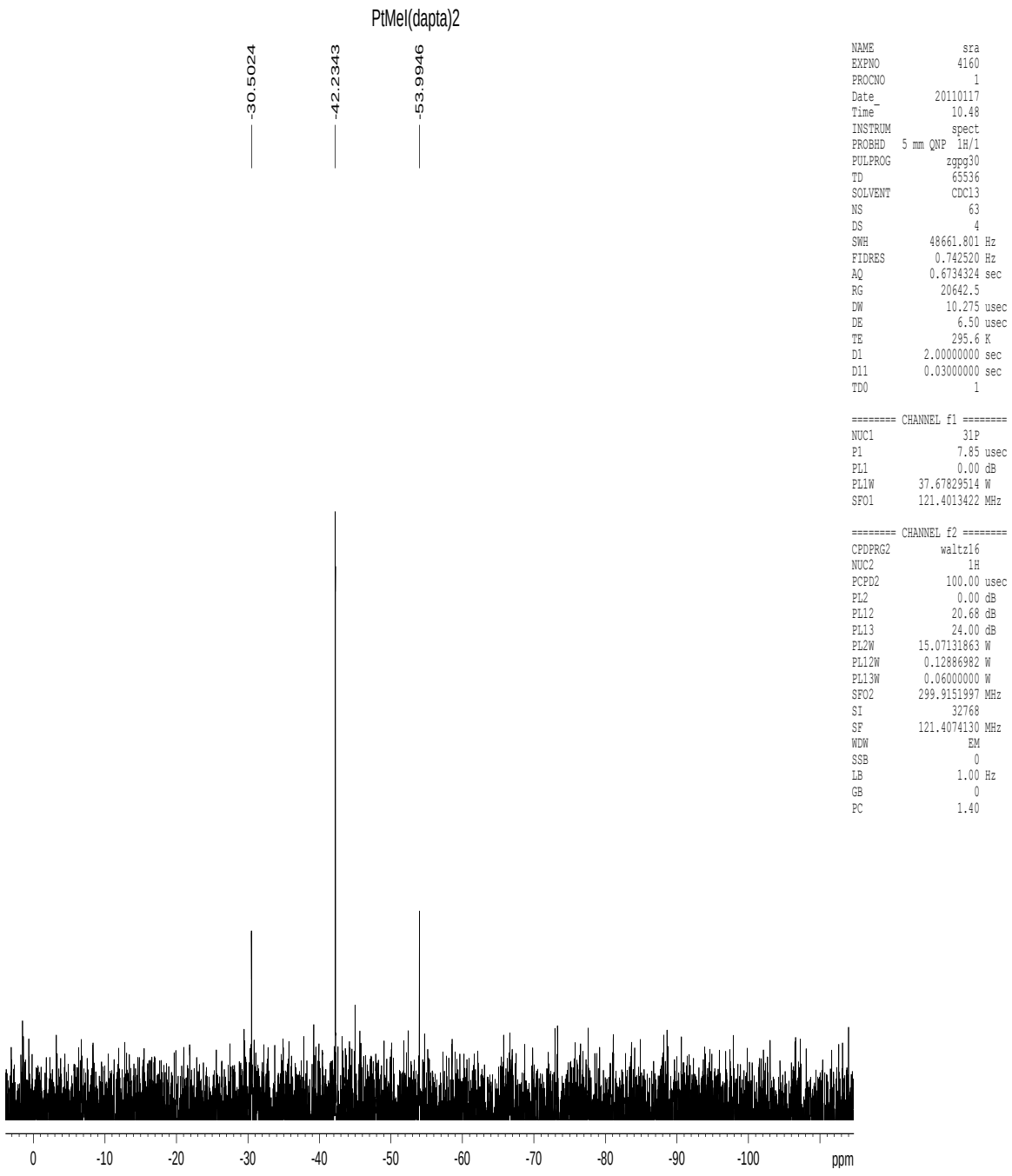

Appendix I.51. $^{31}P\{^{1}H\}$ NMR spectrum of trans-PtI(Me)(DAPTA)$_2$, 10c.

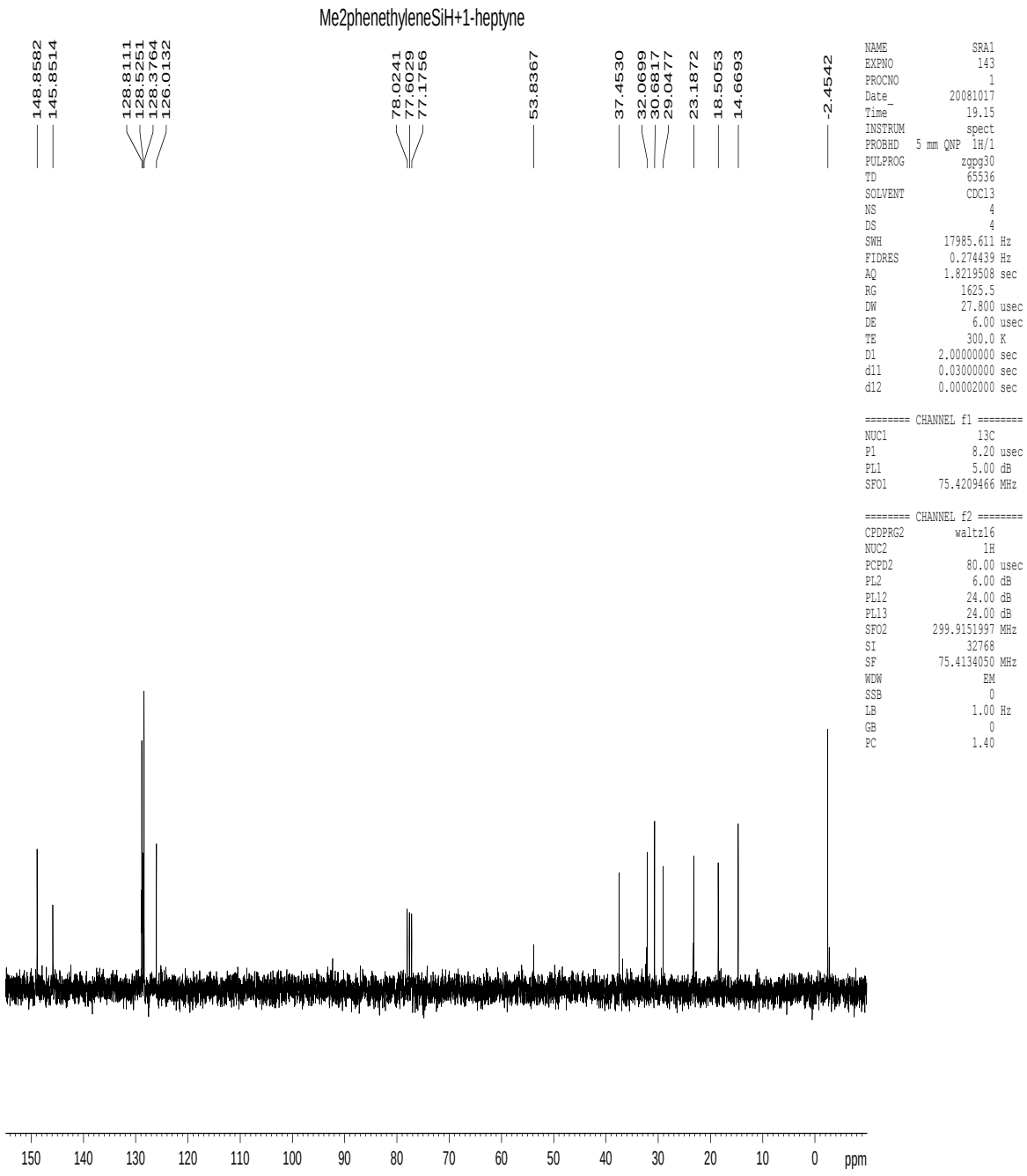

Appendix I.52. $^{13}C\{^{1}H\}$ NMR spectrum of the product from hydrosilylation reaction of dimethylphenethylsilane (S4) and 1-heptyne (A1) in the presence of (1a).

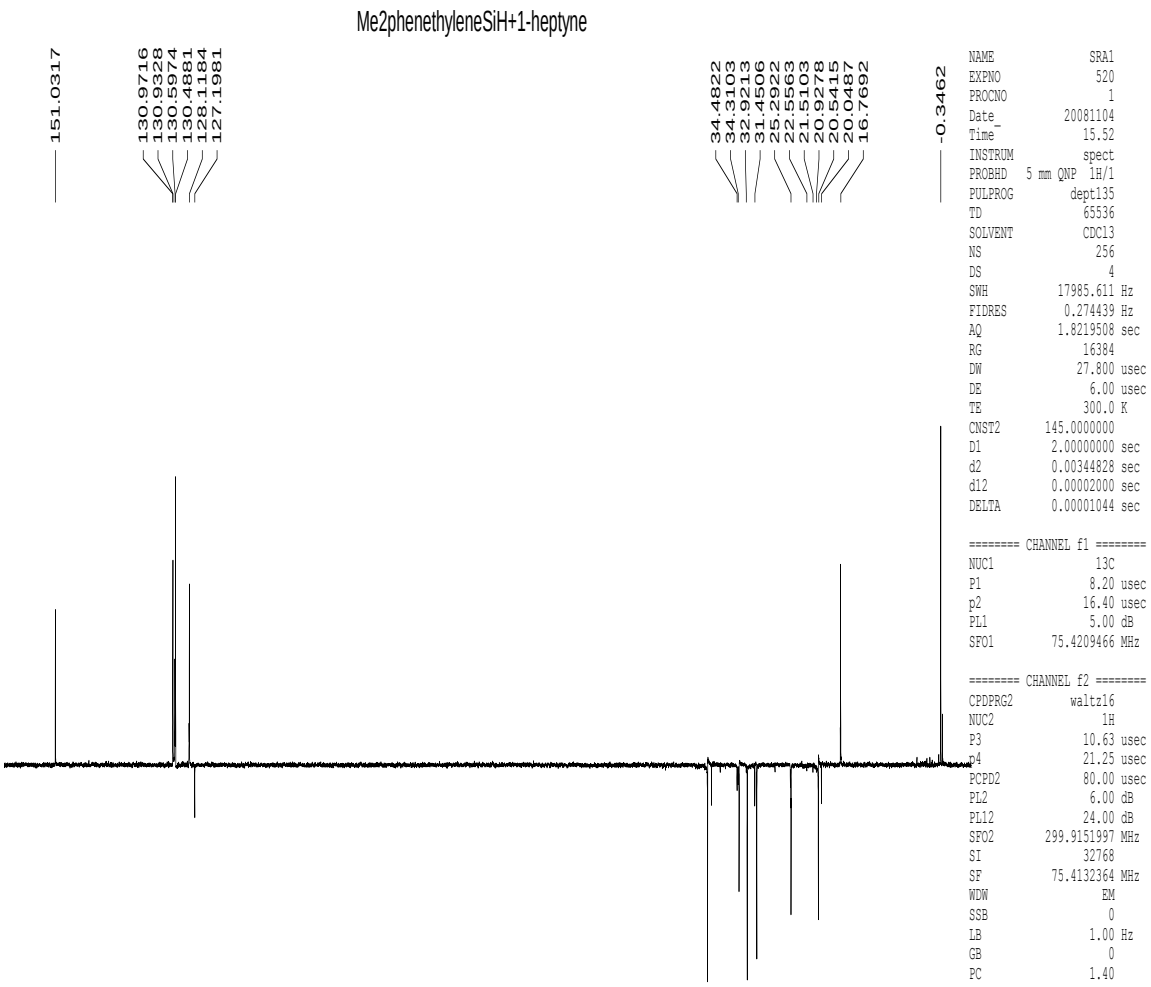

Appendix I.53. $^{13}C\{^{1}H\}$ (DEPT) NMR spectrum of the product from hydrosilylation reaction of dimethylphenethylsilane (S4) and 1-heptyne (A1) in the presence of (1a).

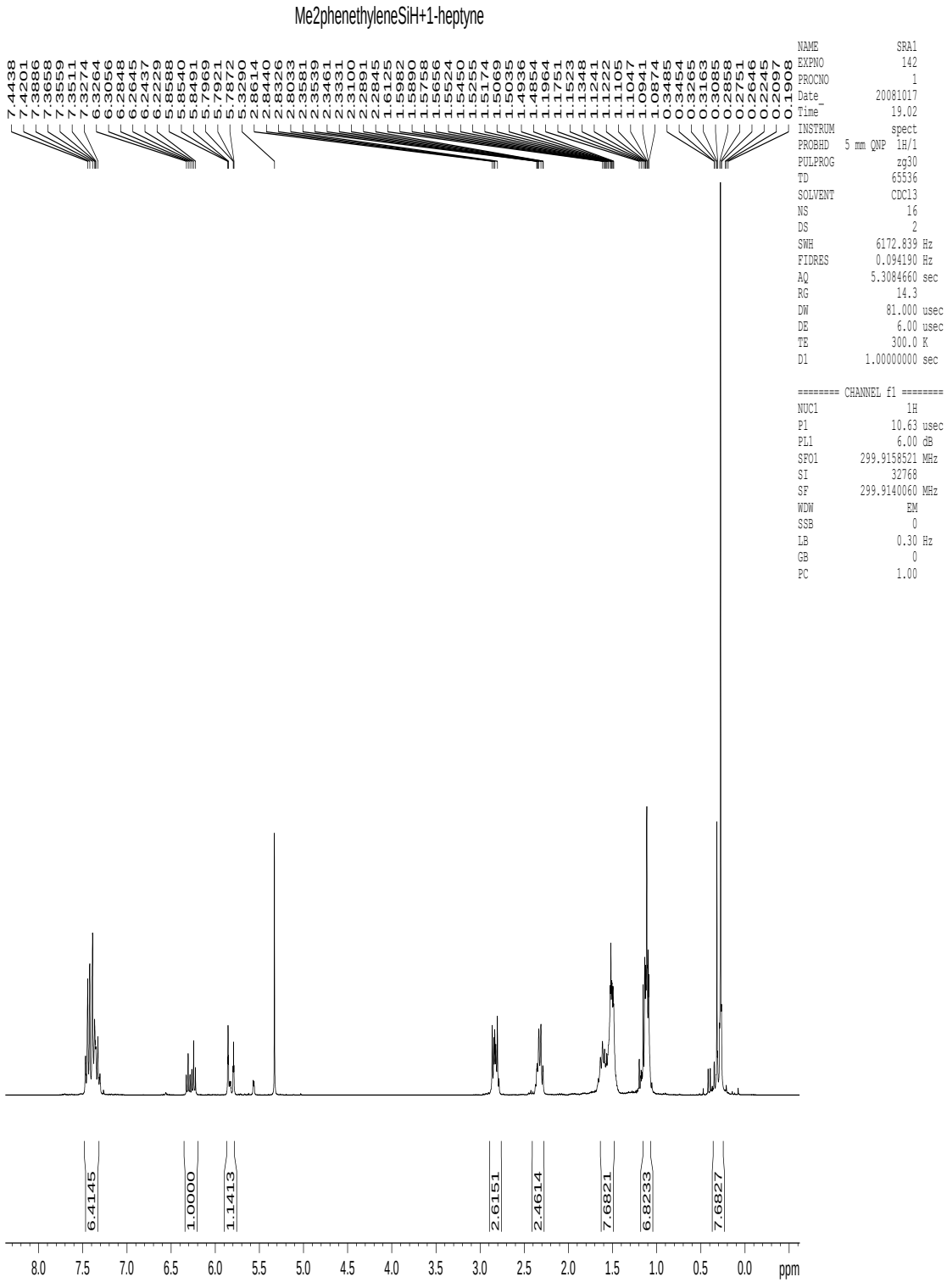

Appendix I.54. ^{1}H NMR spectrum of the product from hydrosilylation reaction of dimethylphenethylsilane (S4) and 1-heptyne (A1) in the presence of (1a).

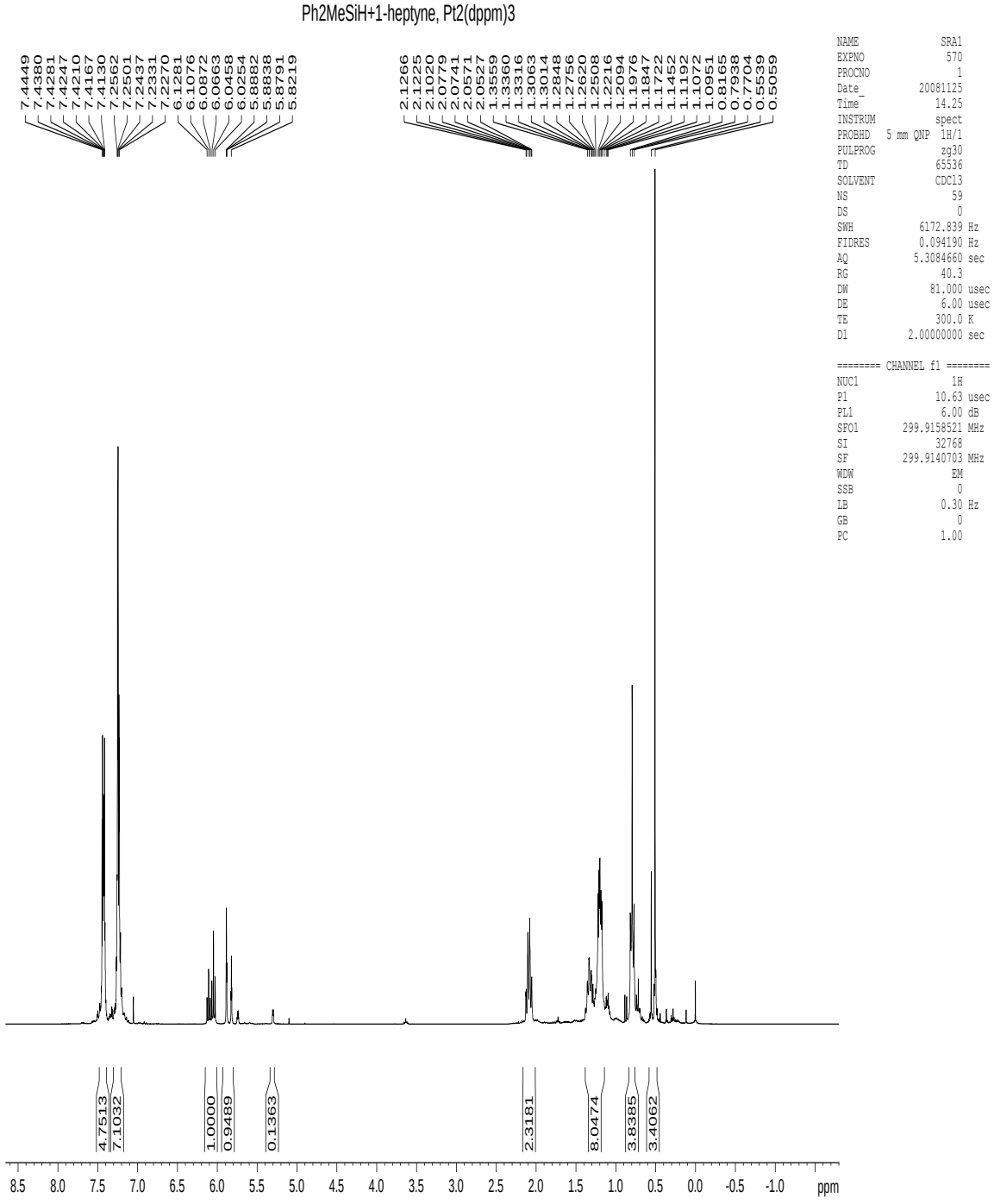

Appendix I.55. ^{1}H NMR spectrum of the product from hydrosilylation reaction of methyldiphenylsilane (S1) and 1-heptyne (A1) in the presence of $Pt_2(\mu\text{-dppm})_3$ (B1).

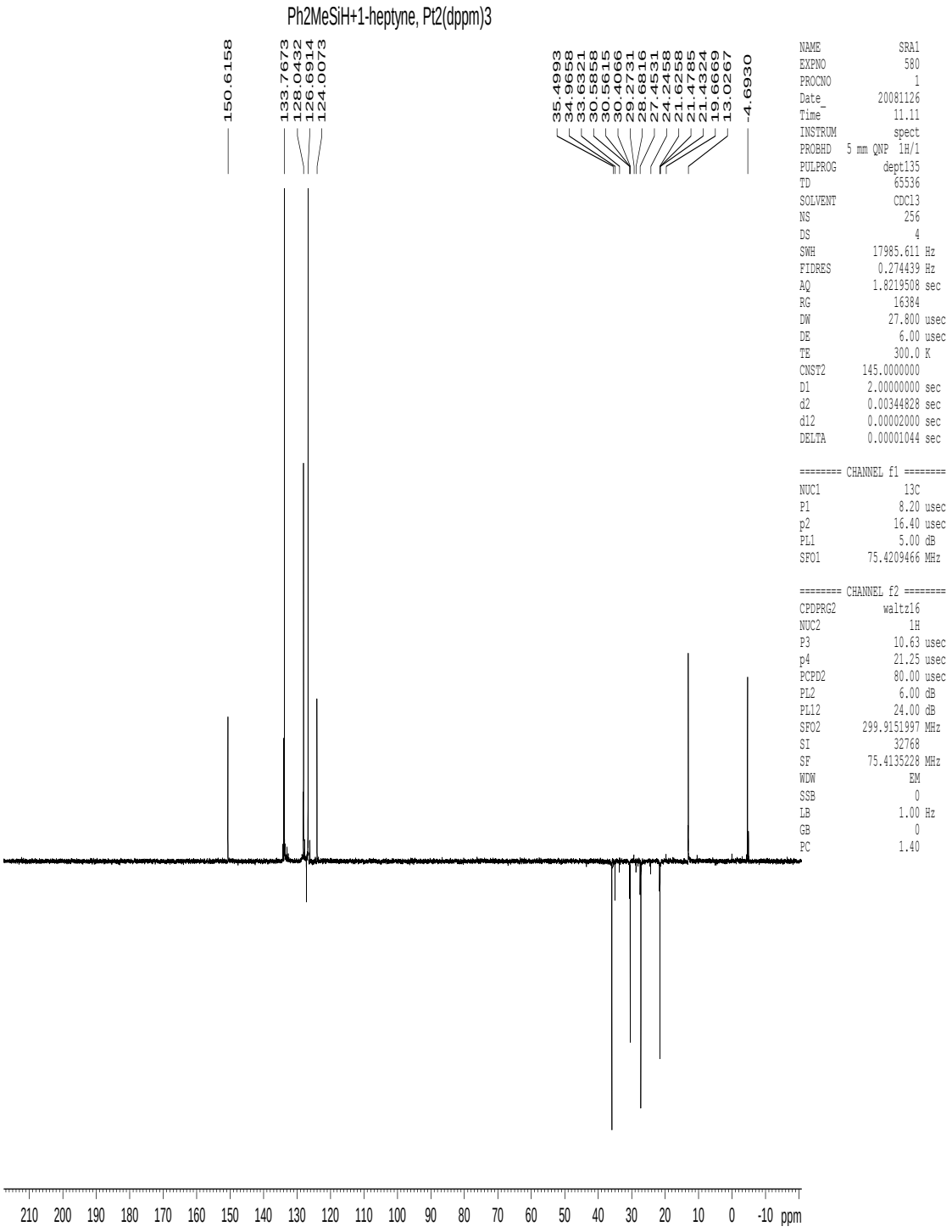

Appendix I.56. $^{13}C\{^{1}H\}$ (DEPT) NMR spectrum of the product from hydrosilylation reaction of methyldiphenylsilane (S1) and 1-heptyne (A1) in the presence of $Pt_2(\mu\text{-dppm})_3$ (B1).

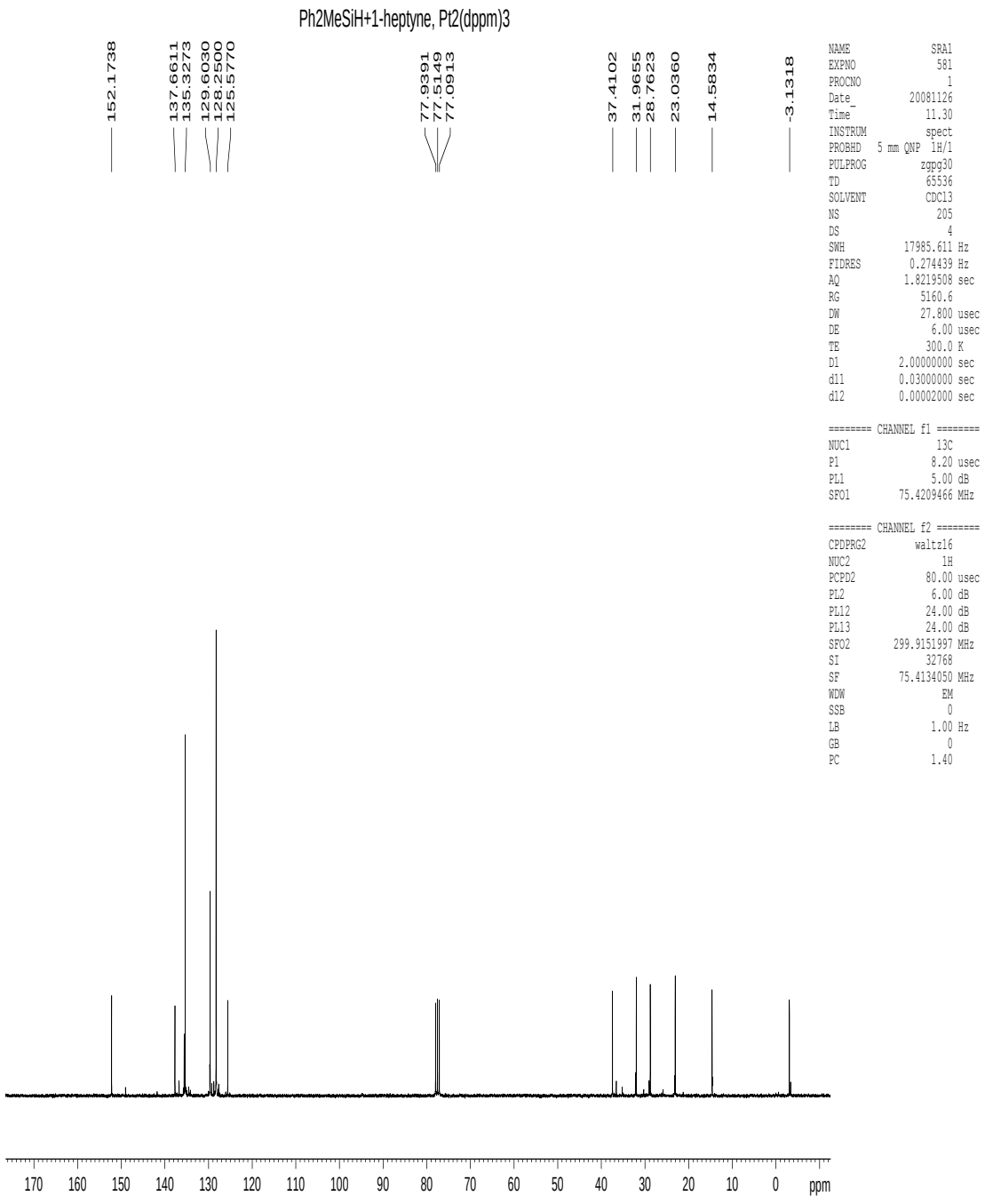

Appendix I.57. $^{13}C\{^{1}H\}$ NMR spectrum of the product from hydrosilylation reaction of methyldiphenylsilane (S1) and 1-heptyne (A1) in the presence of $Pt_2(\mu\text{-dppm})_3$ (B1).

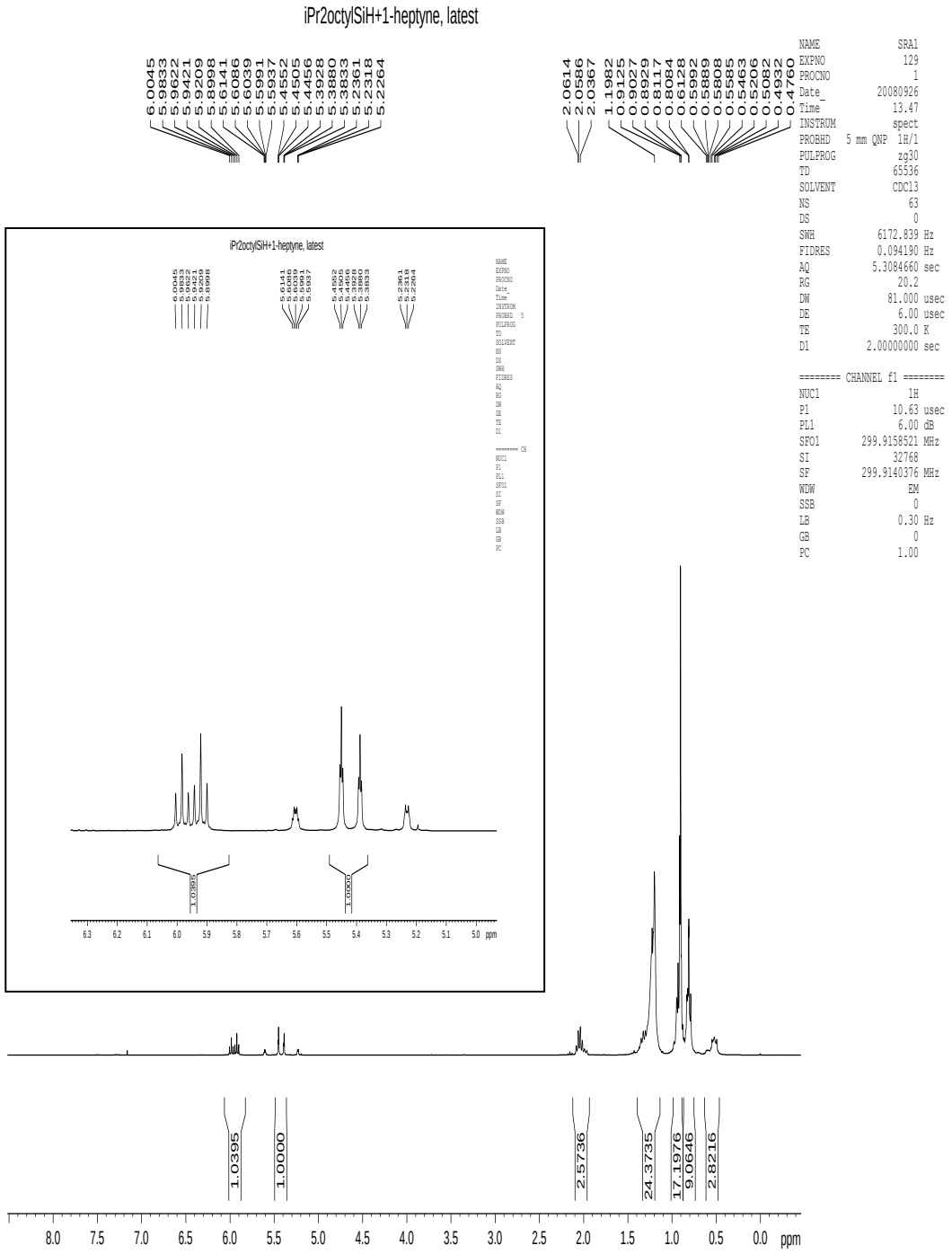

Appendix I.58. ^{1}H NMR spectrum of the product from hydrosilylation reaction of diisopropyloctylsilane (S2) and 1-heptyne (A1) in the presence of (1a).

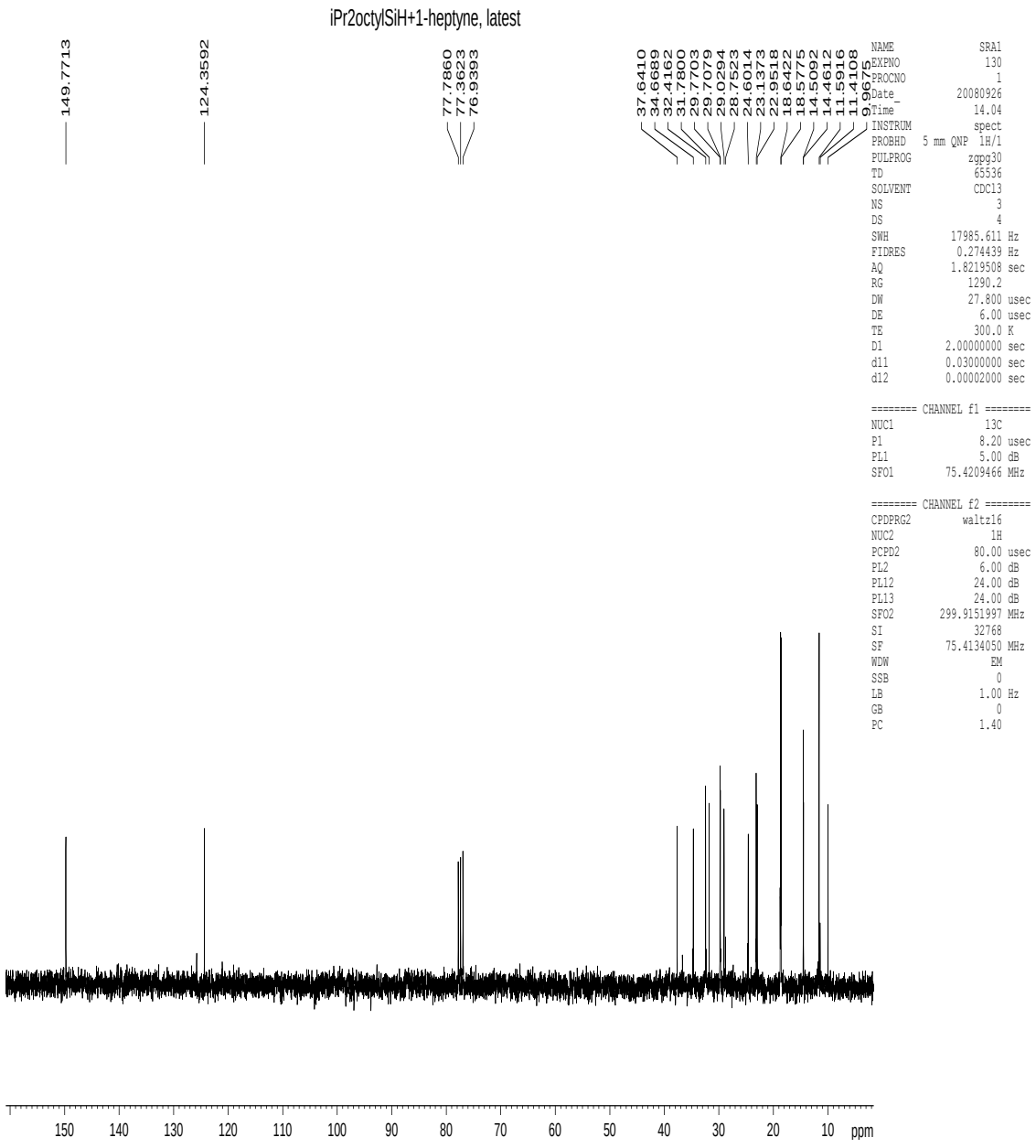

Appendix I.59. $^{13}C\{^{1}H\}$ NMR spectrum of the product from hydrosilylation reaction of diisopropyloctylsilane (S2) and 1-heptyne (A1) in the presence of (1a).

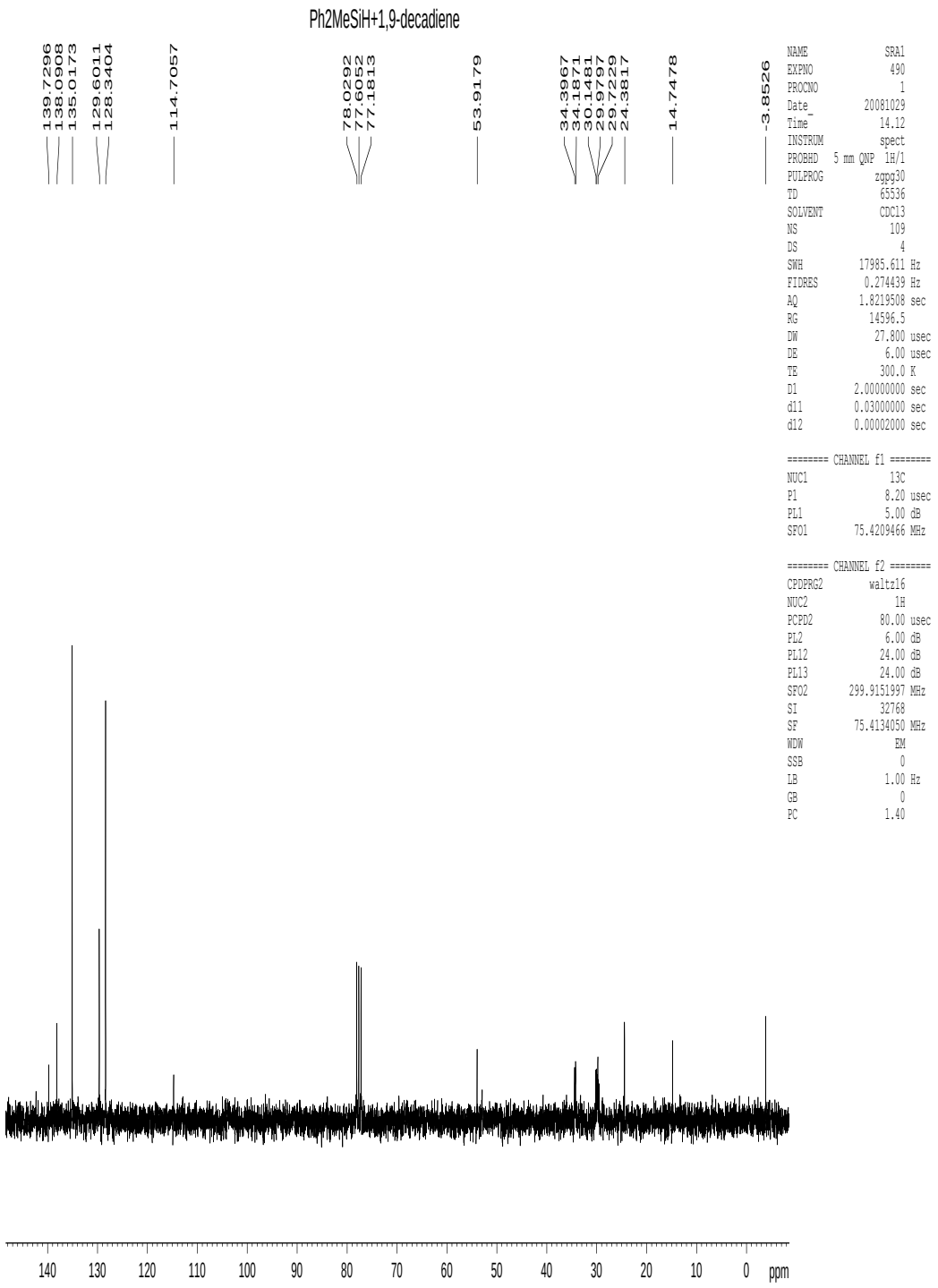

Appendix I.60. $^{13}C\{^{1}H\}$ NMR spectrum of the product from hydrosilylation reaction of methyldiphenylsilane (S1) and 1,9-decadiene in the presence of (1a).

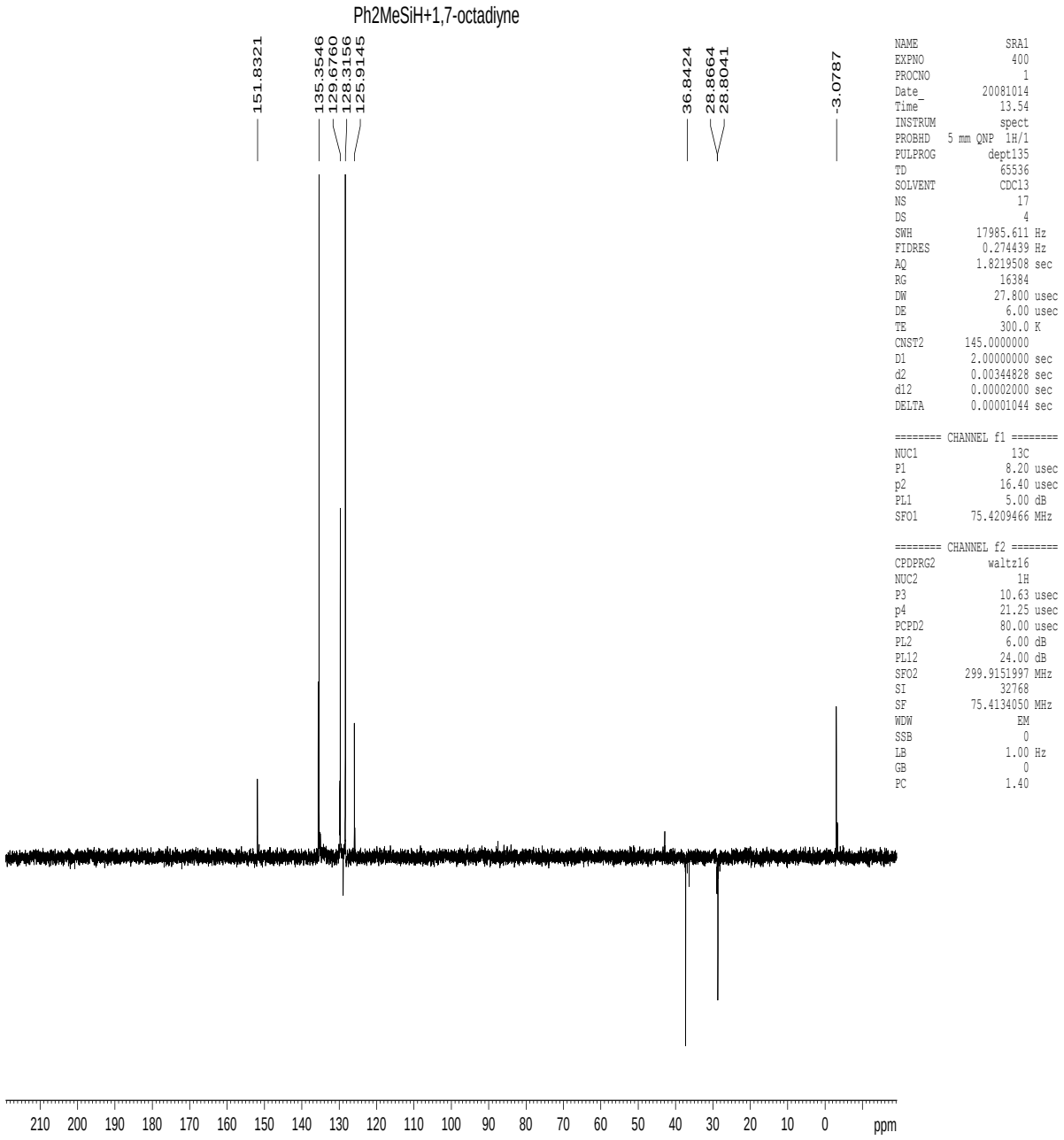

Appendix I.61. $^{13}C\{^{1}H\}$ (DEPT) NMR spectrum of the product from hydrosilylation reaction of methyldiphenylsilane (S1) and 1,7-octadiyne in the presence of (1a).

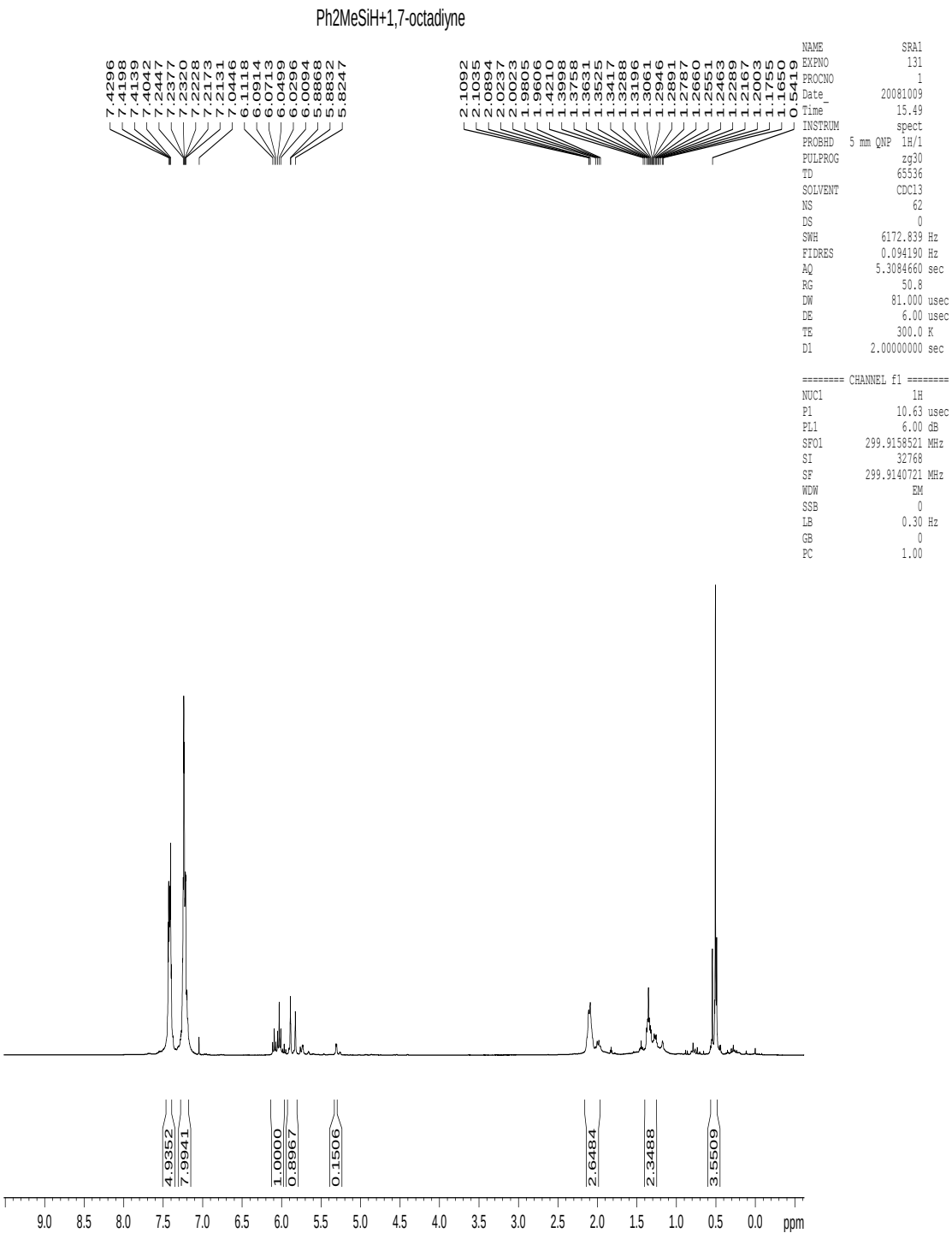

Appendix I.62. ^{1}H NMR spectrum of the product from hydrosilylation reaction of methyldiphenylsilane (S1) and 1,7-octadiyne in the presence of (1a).

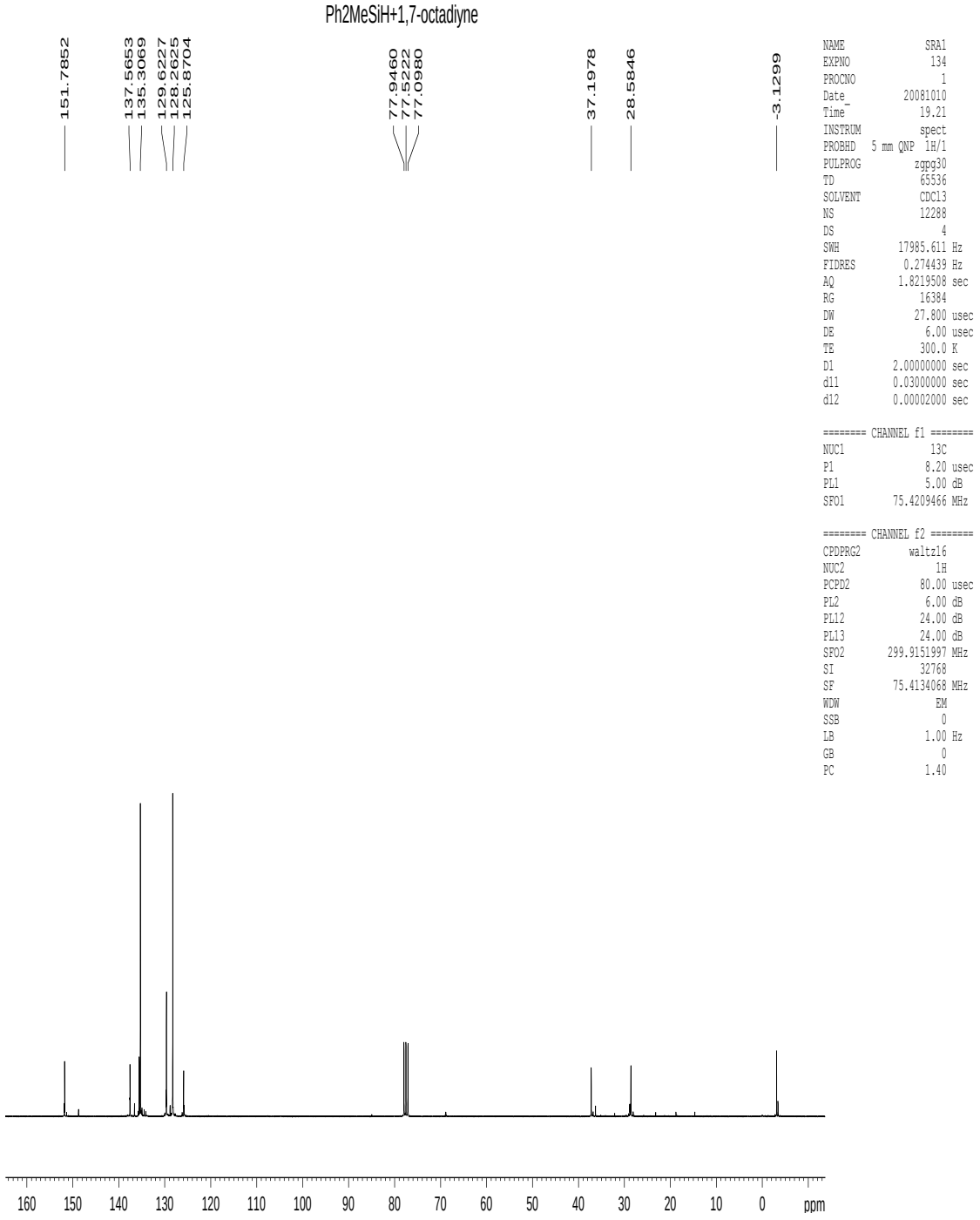

Appendix I.63. $^{13}C\{^{1}H\}$ NMR spectrum of the product from hydrosilylation reaction of methyldiphenylsilane (S1) and 1,7-octadiyne in the presence of (1a).

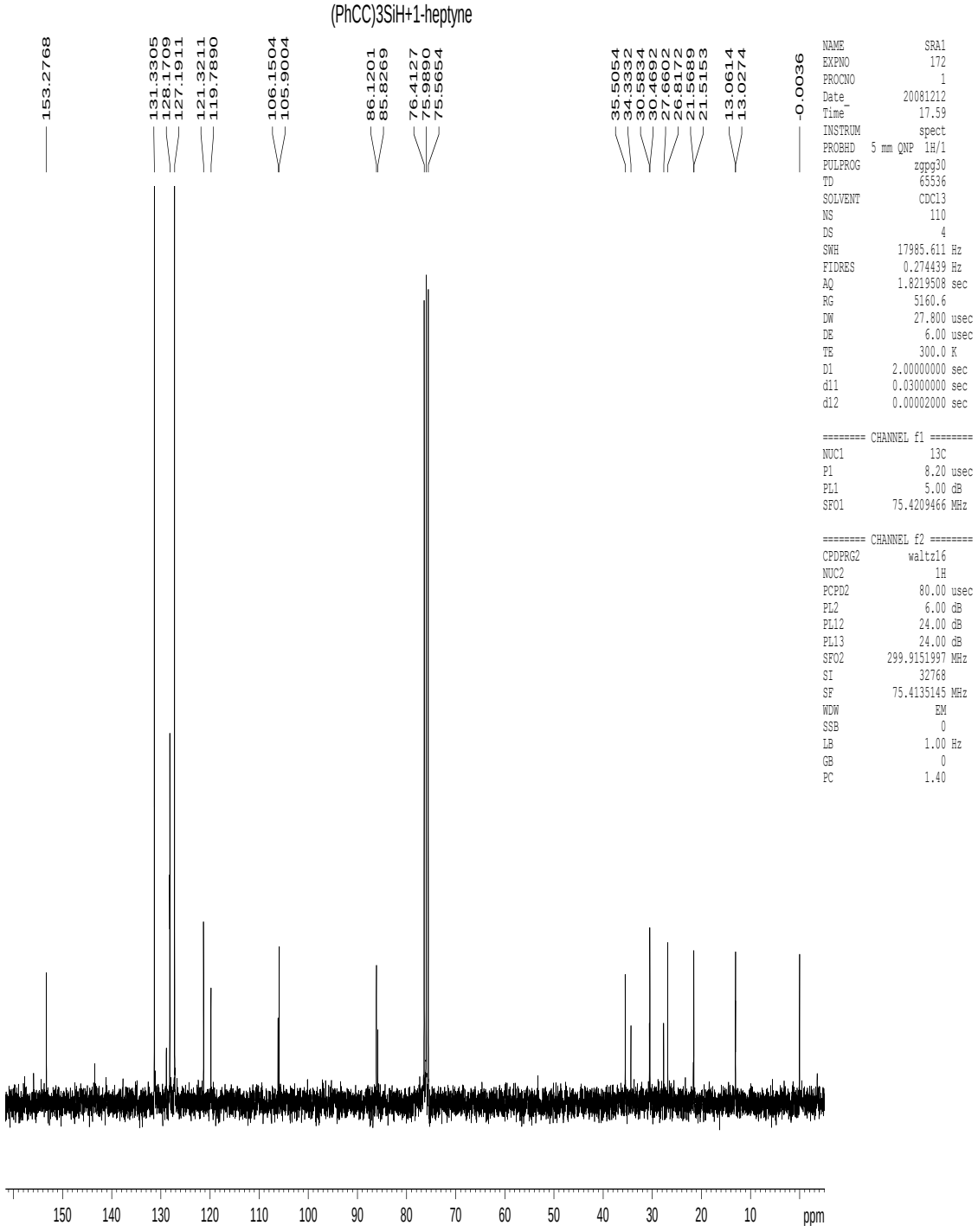

Appendix I.64. ***$^{13}C\{^{1}H\}$ NMR spectrum of the product from hydrosilylation reaction of $(C_2Ph)_3SiH$ (S5) and 1-heptyne (A1) in the presence of (1a).***

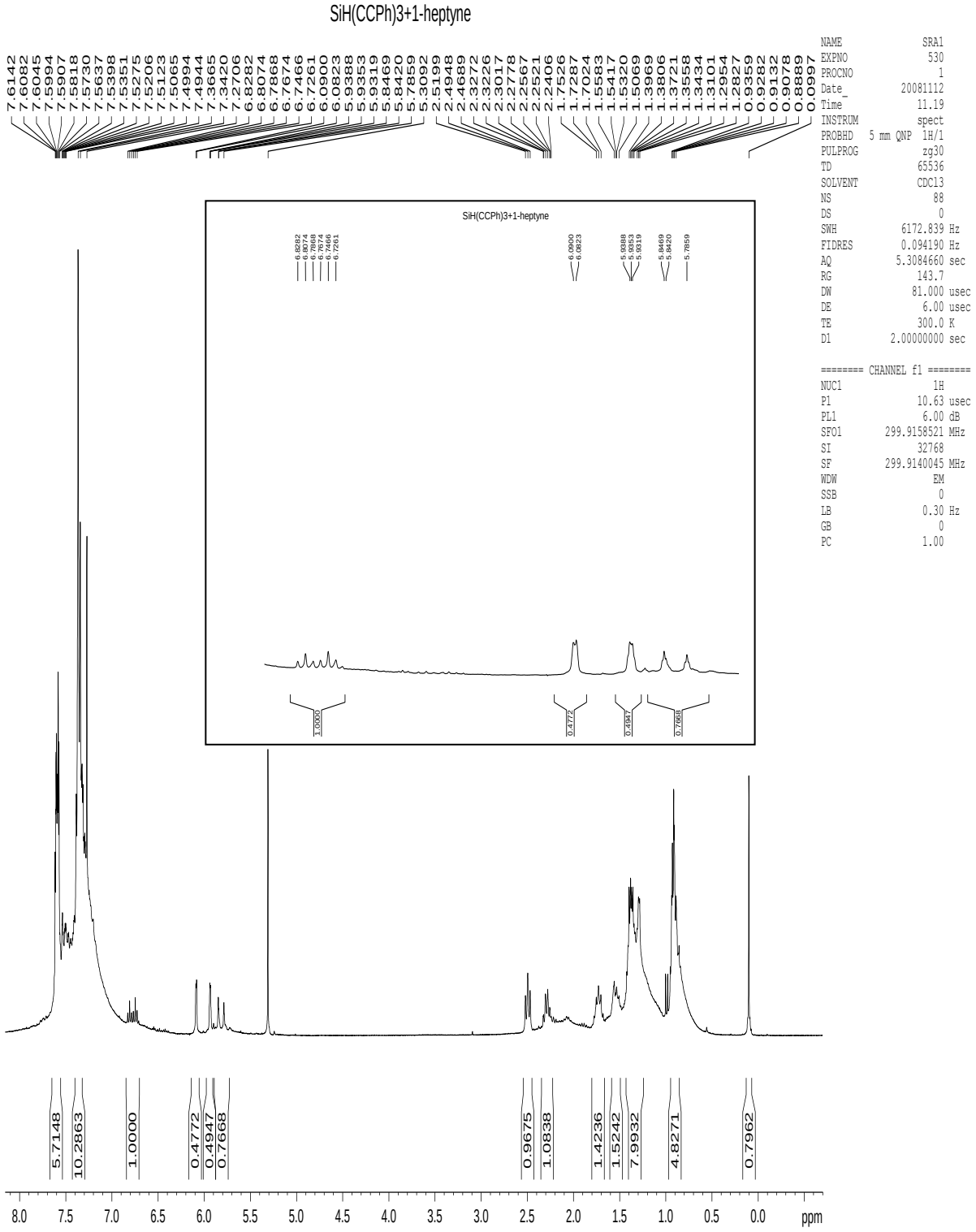

Appendix I.65. ^{1}H NMR spectrum of the product from hydrosilylation reaction of $(C_2Ph)_3SiH$ (S5) and 1-heptyne (A1) in the presence of (1a).

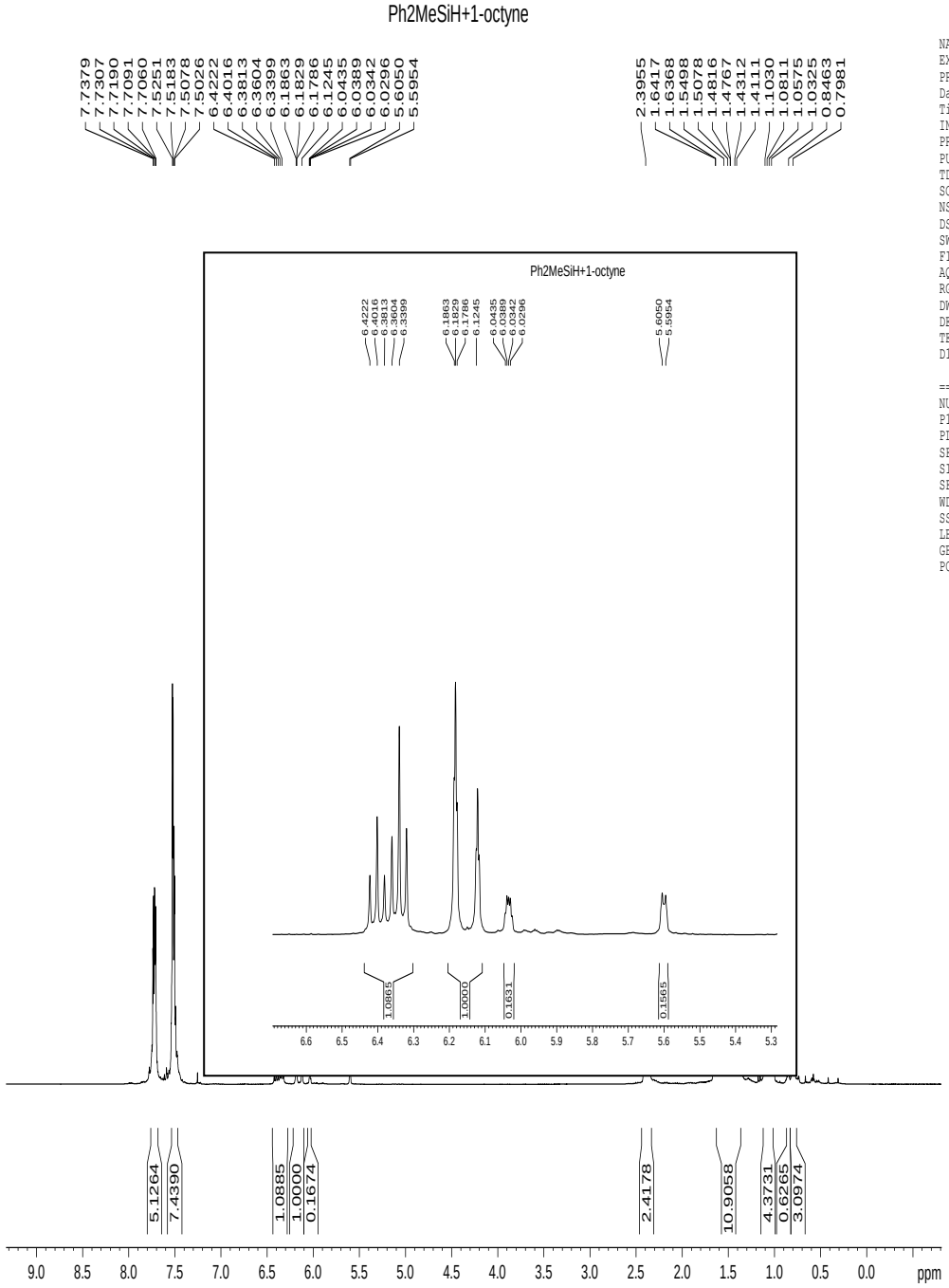

Appendix I.66. ^{1}H NMR spectrum of the product from hydrosilylation reaction of methyldiphenylsilane (S1) and 1-octyne in the presence of (1a).

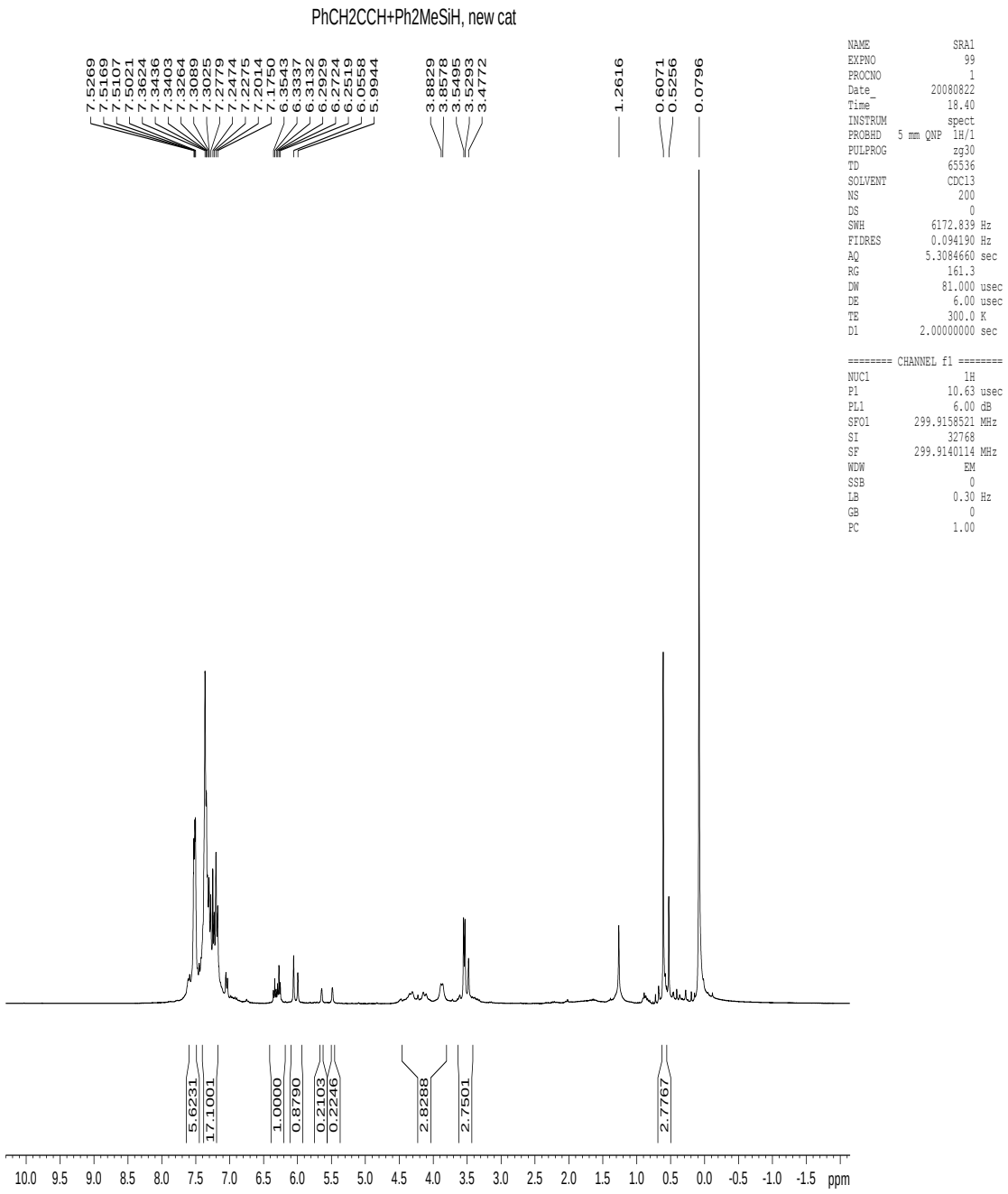

Appendix I.67. ^{1}H NMR spectrum of the product from hydrosilylation reaction of methyldiphenylsilane (S1) and 3-phenyl-1-propyne in the presence of (1a).

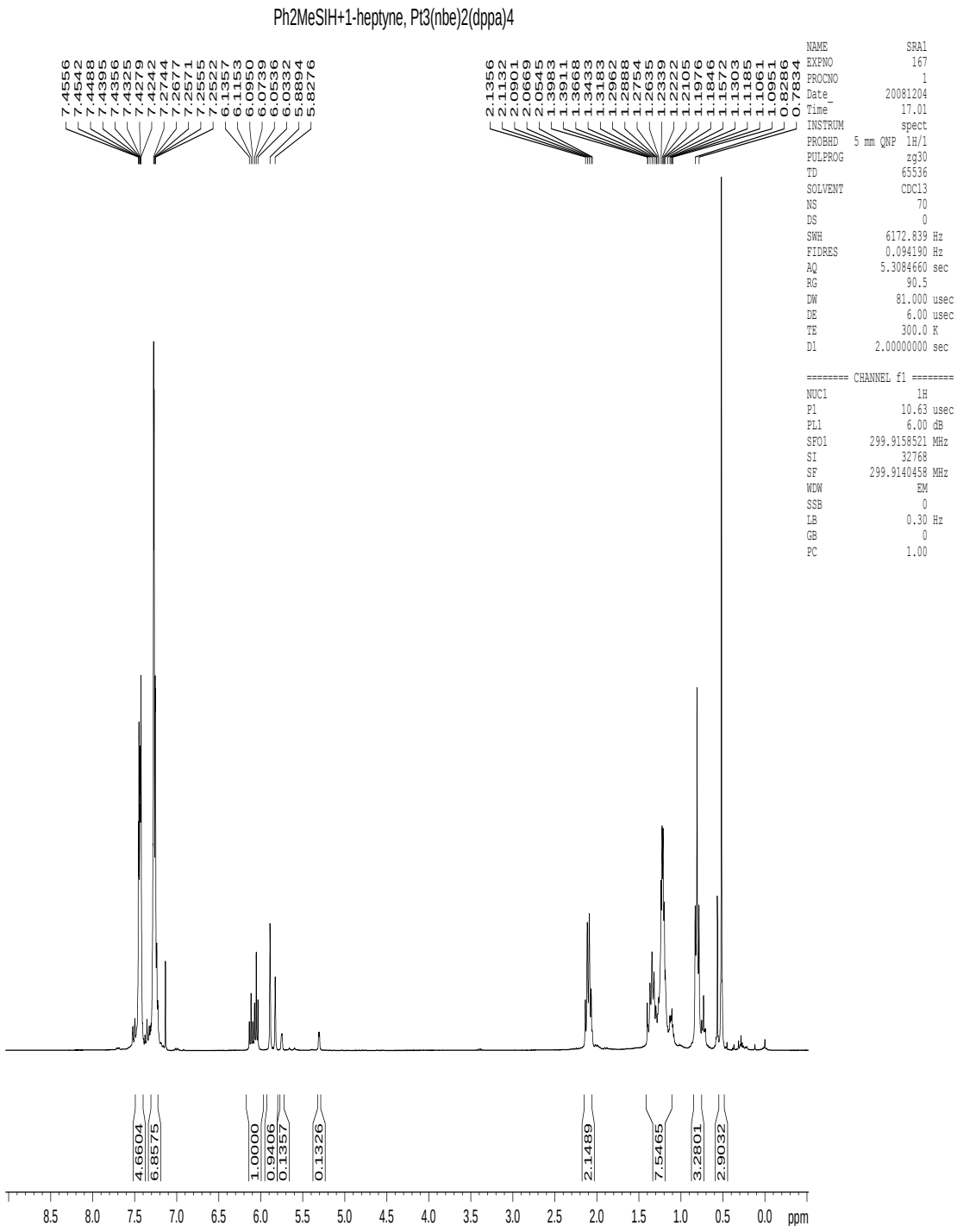

Appendix I.68. ^{1}H NMR spectrum of the product from hydrosilylation reaction of methyldiphenylsilane (S1) and 1-heptyne (A1) in the presence of $Pt_3(nbe)_2(dppa)_4$, B2.

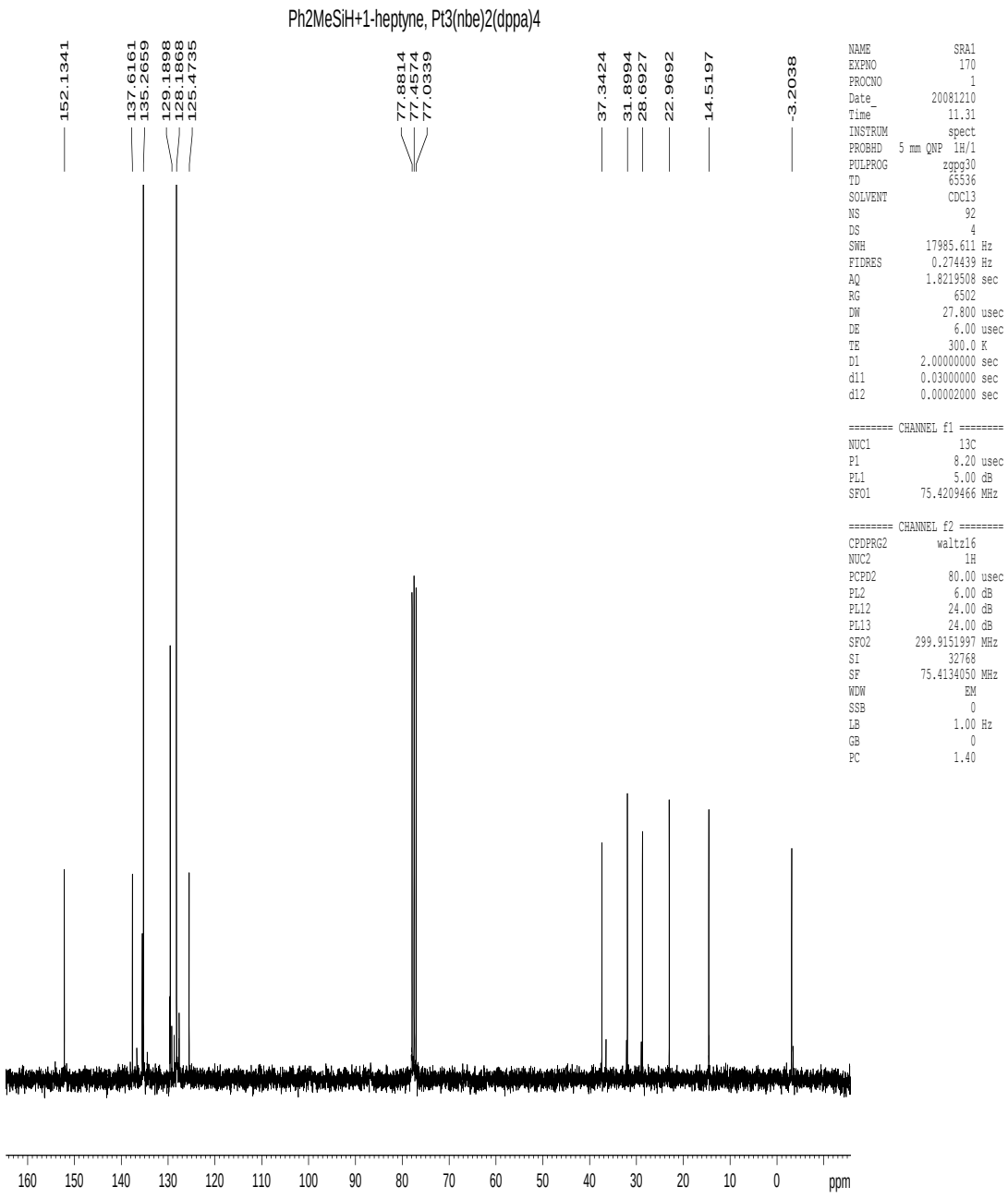

Appendix I.69. $^{13}C\{^{1}H\}$ NMR spectrum of the product from hydrosilylation reaction of methyldiphenylsilane (S1) and 1-heptyne (A1) in the presence of $Pt_3(nbe)_2(dppa)_4$, B2.

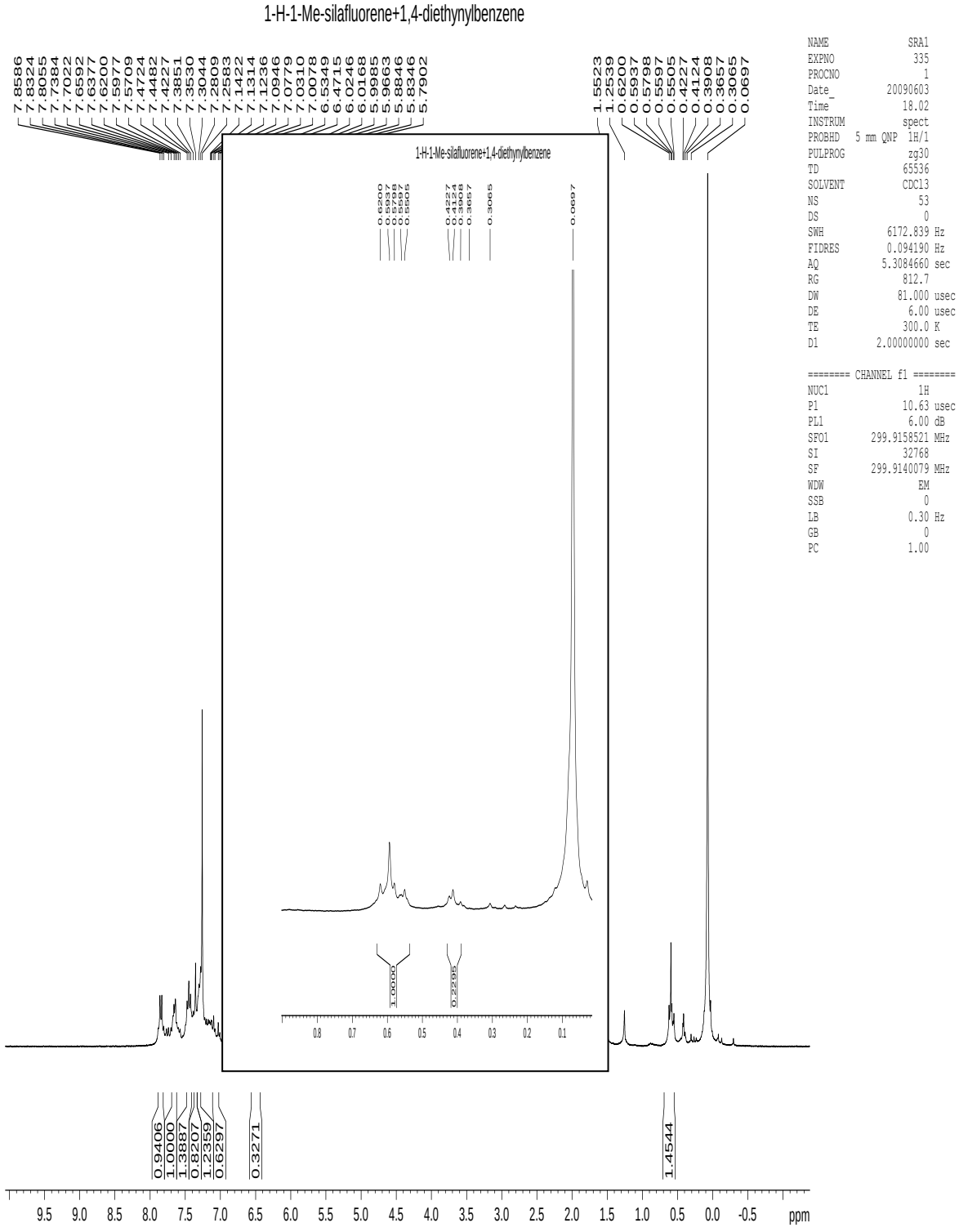

Appendix I.70. ^{1}H NMR spectrum of the product from hydrosilylation reaction of 1-hydrido-1-methylsilafluorene (S8) and 1,4-diethynylbenzene (A3) in the presence of (1a).

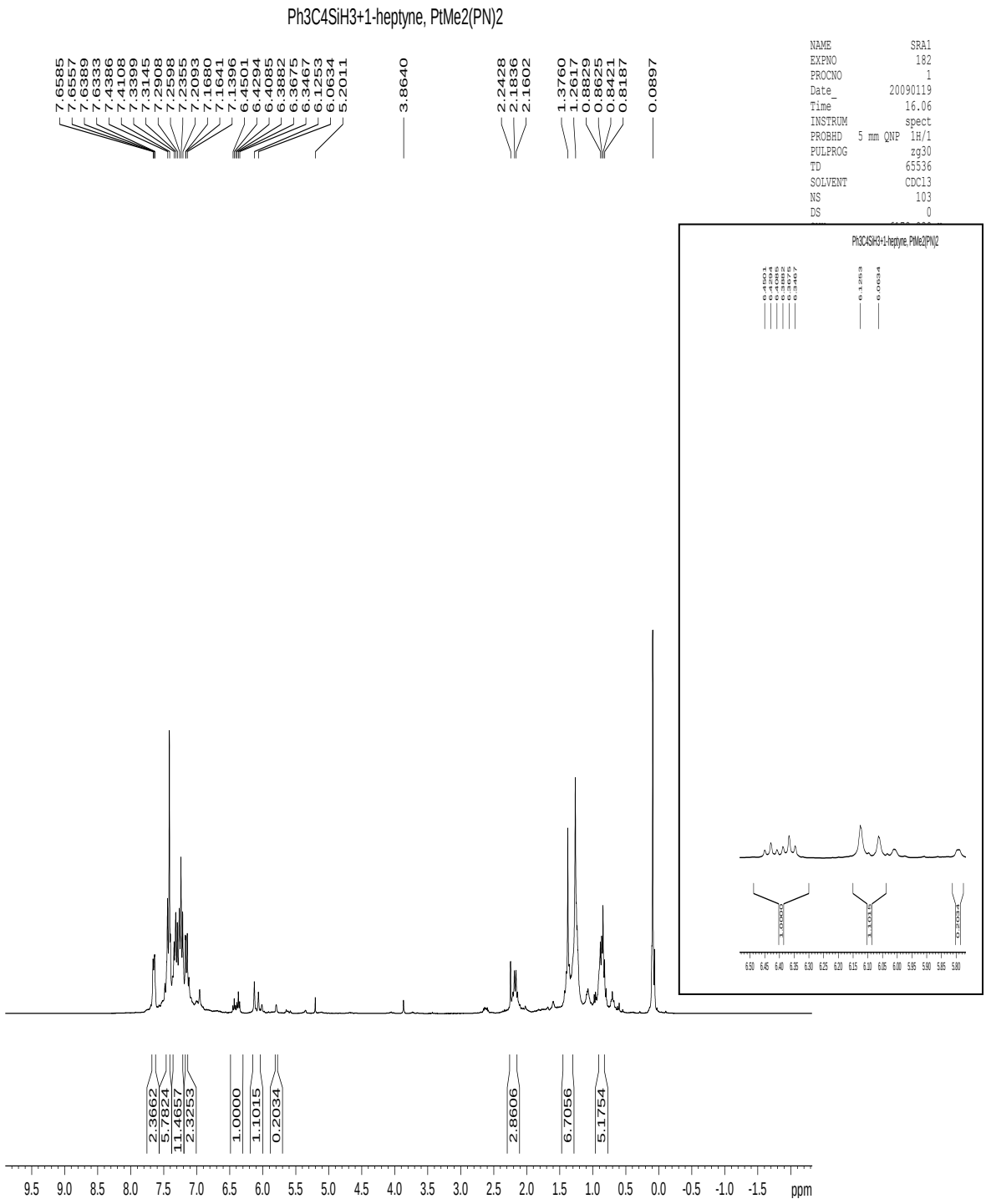

Appendix I.71. ^{1}H NMR spectrum of the product from hydrosilylation reaction of 1-hydrido-1,2,5-triphenylsilole (S6) and 1-heptyne (A1) in the presence of (1a).

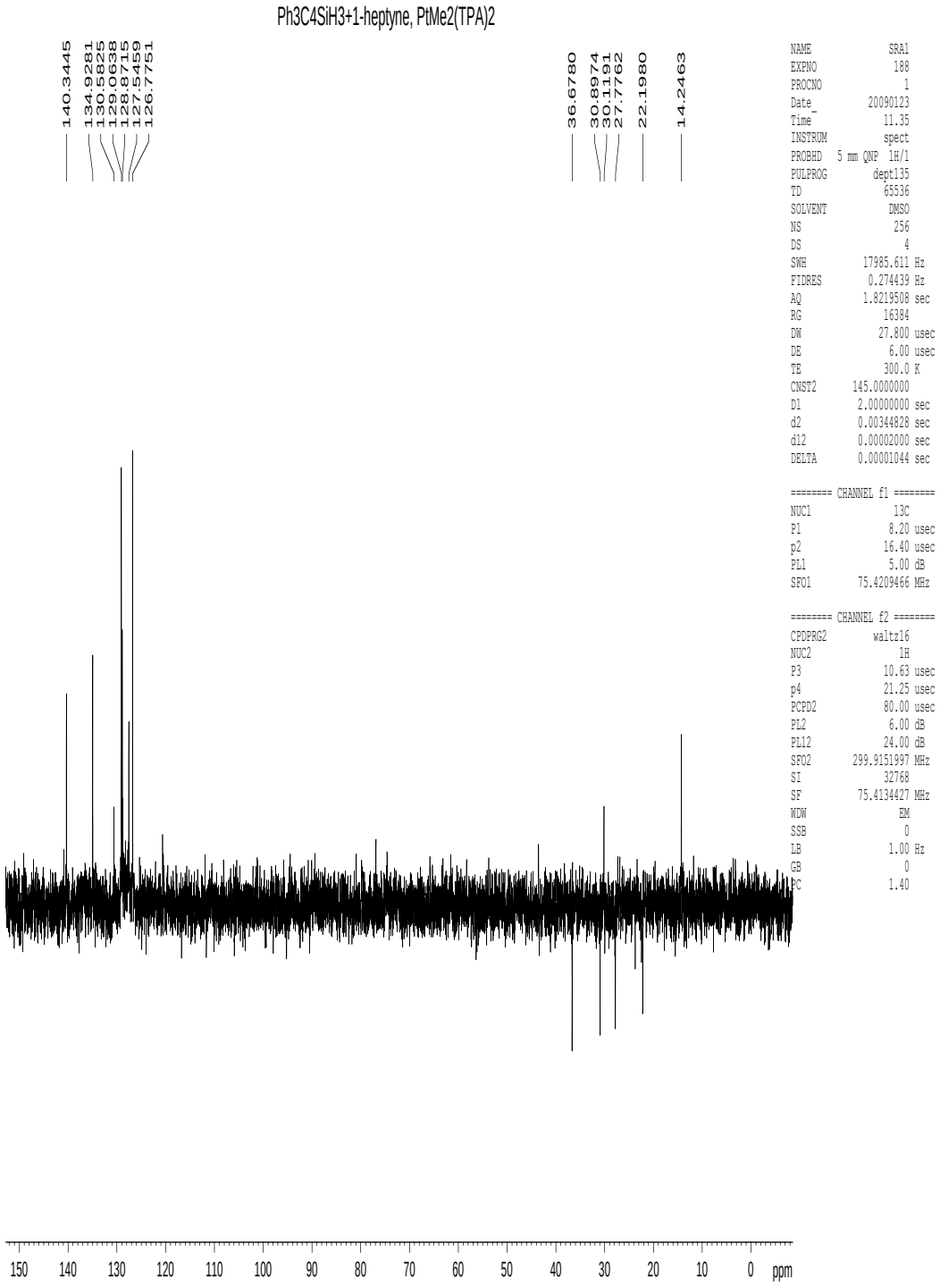

Appendix I.72. $^{13}C\{^{1}H\}$ (DEPT) NMR spectrum of the product from hydrosilylation reaction of 1-hydrido-1,2,5-triphenylsilole (S6) and 1-heptyne (A1) in the presence of (1a).

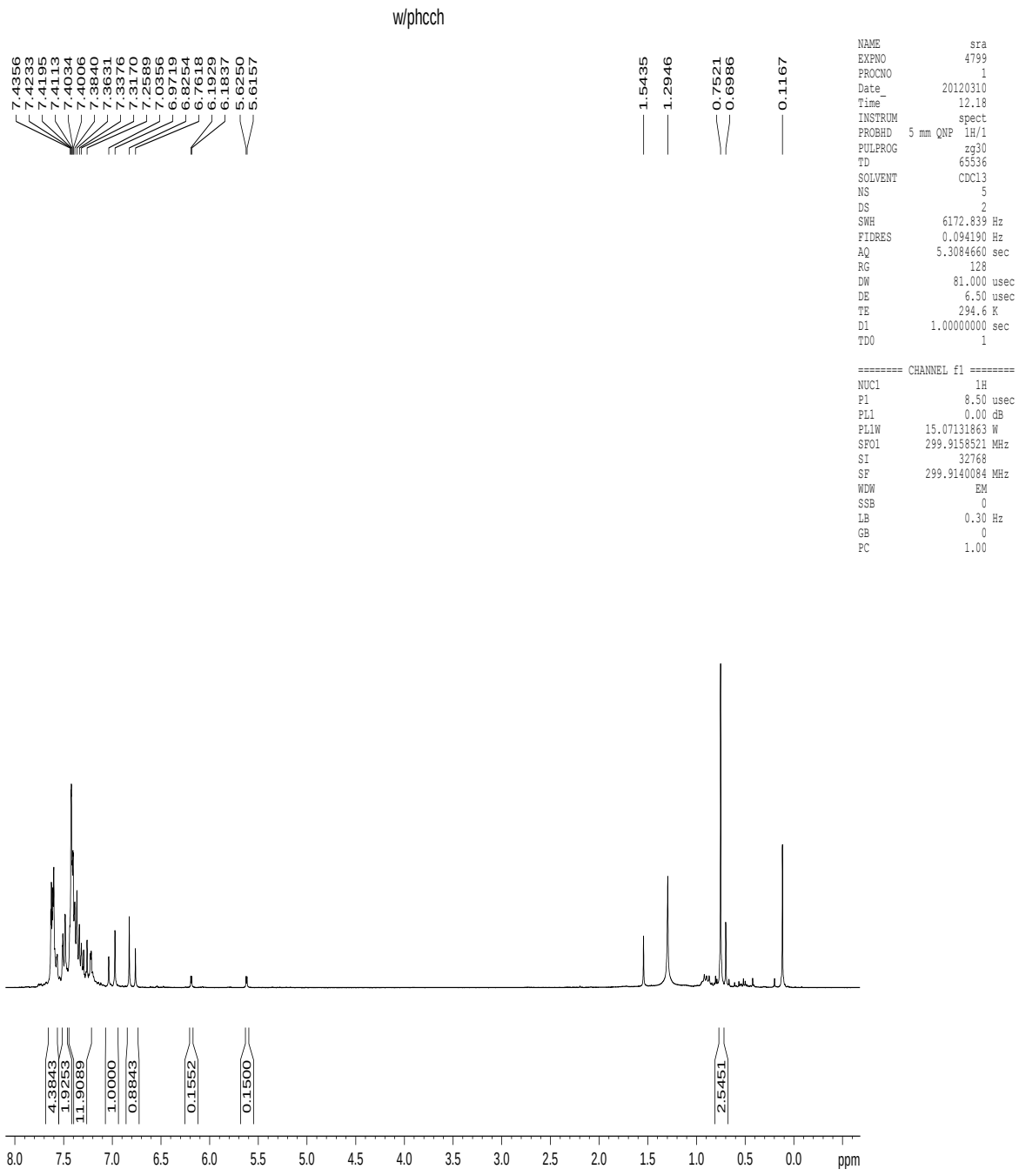

Appendix I.73. ^{1}H NMR spectrum of the product from hydrosilylation reaction of methyldiphenylsilane (S1) and phenylacetylene in the presence of (1a).

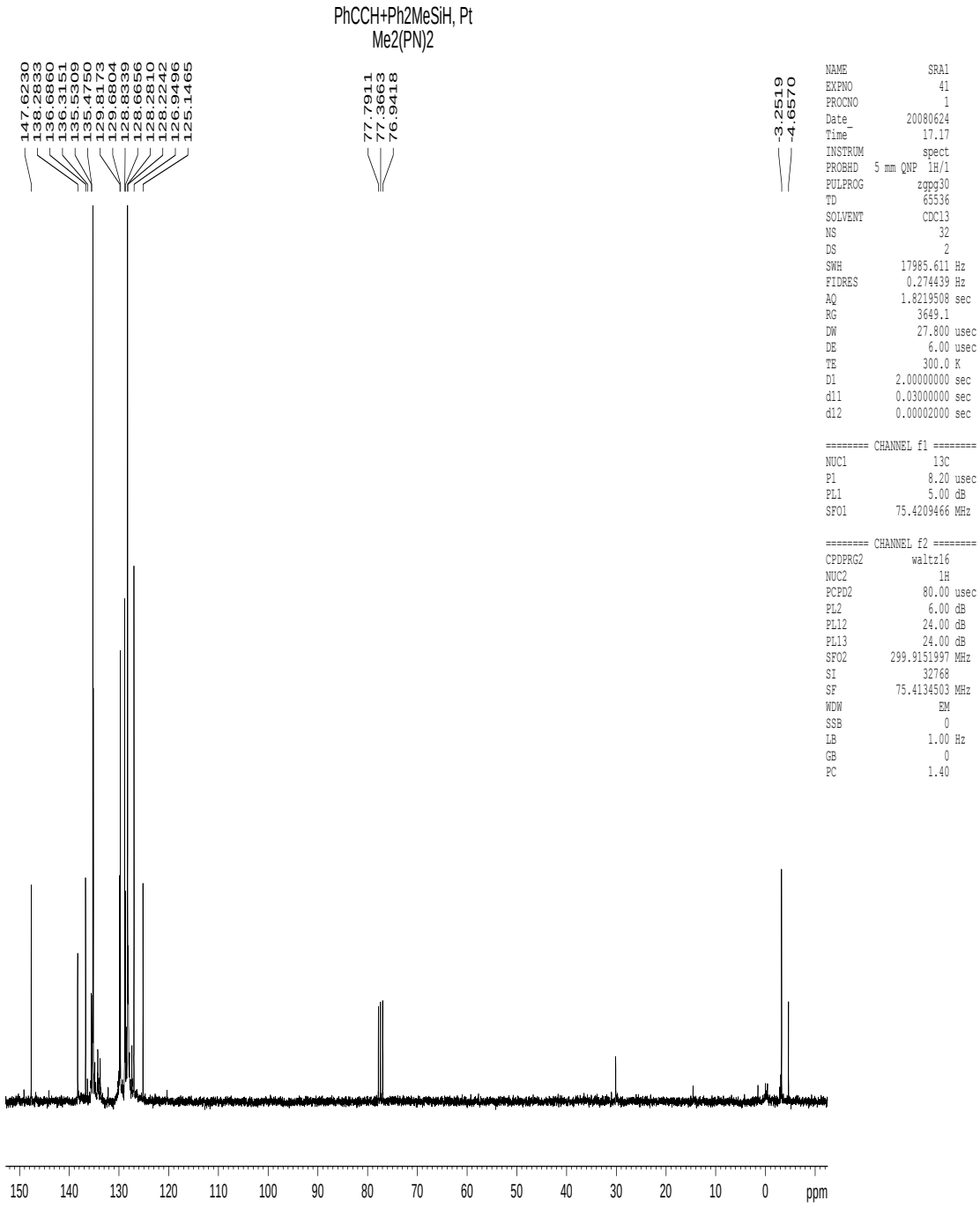

Appendix I.74. $^{13}C\{^{1}H\}$ NMR spectrum of the product from hydrosilylation reaction of methyldiphenylsilane (S1) and phenylacetylene in the presence of (1a).

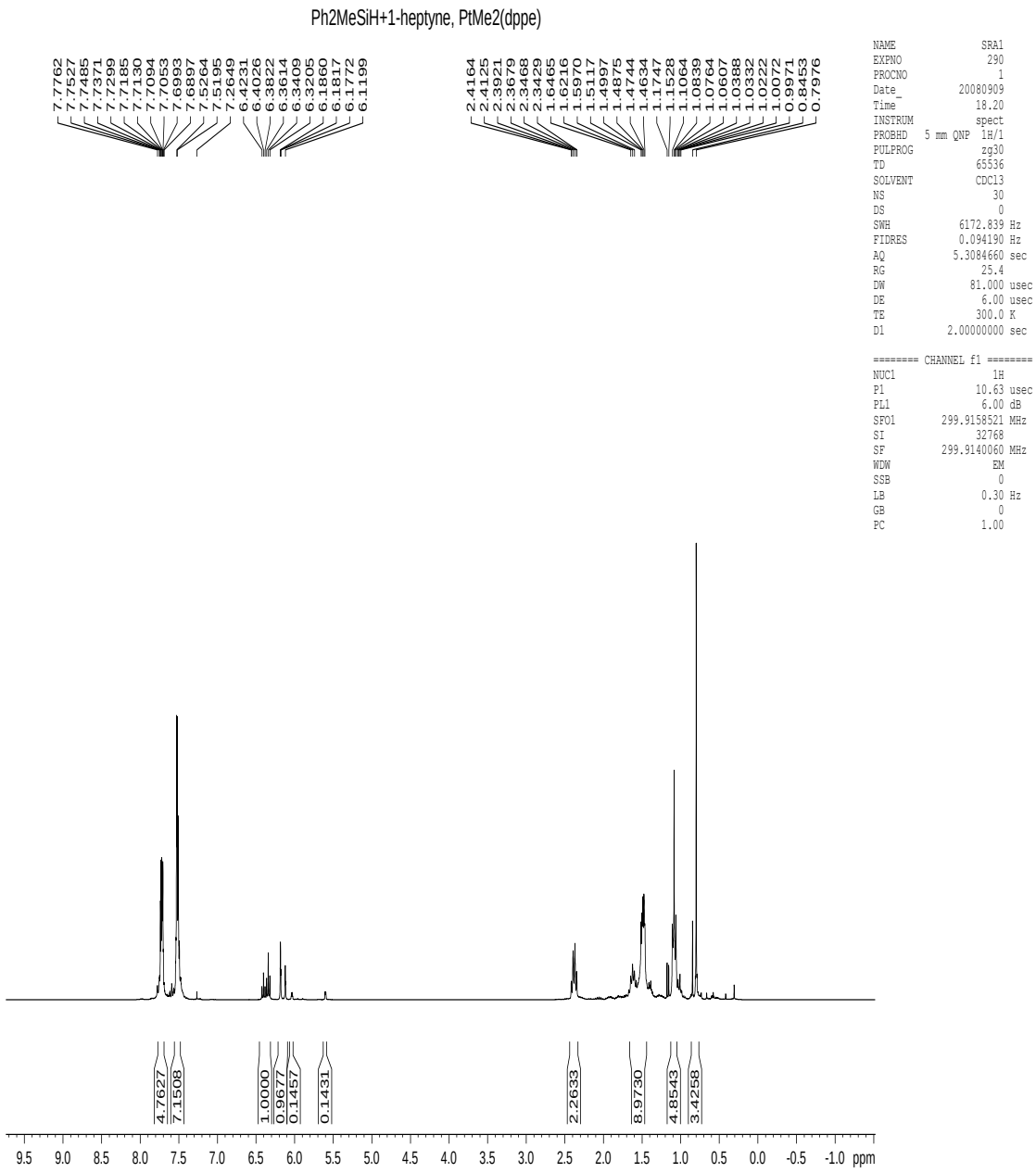

Appendix I.75. ^{1}H NMR spectrum of the product from hydrosilylation reaction of methyldiphenylsilane (S1) and 1-heptyne (A1) in the presence of $PtMe_2$(dppe), B4.

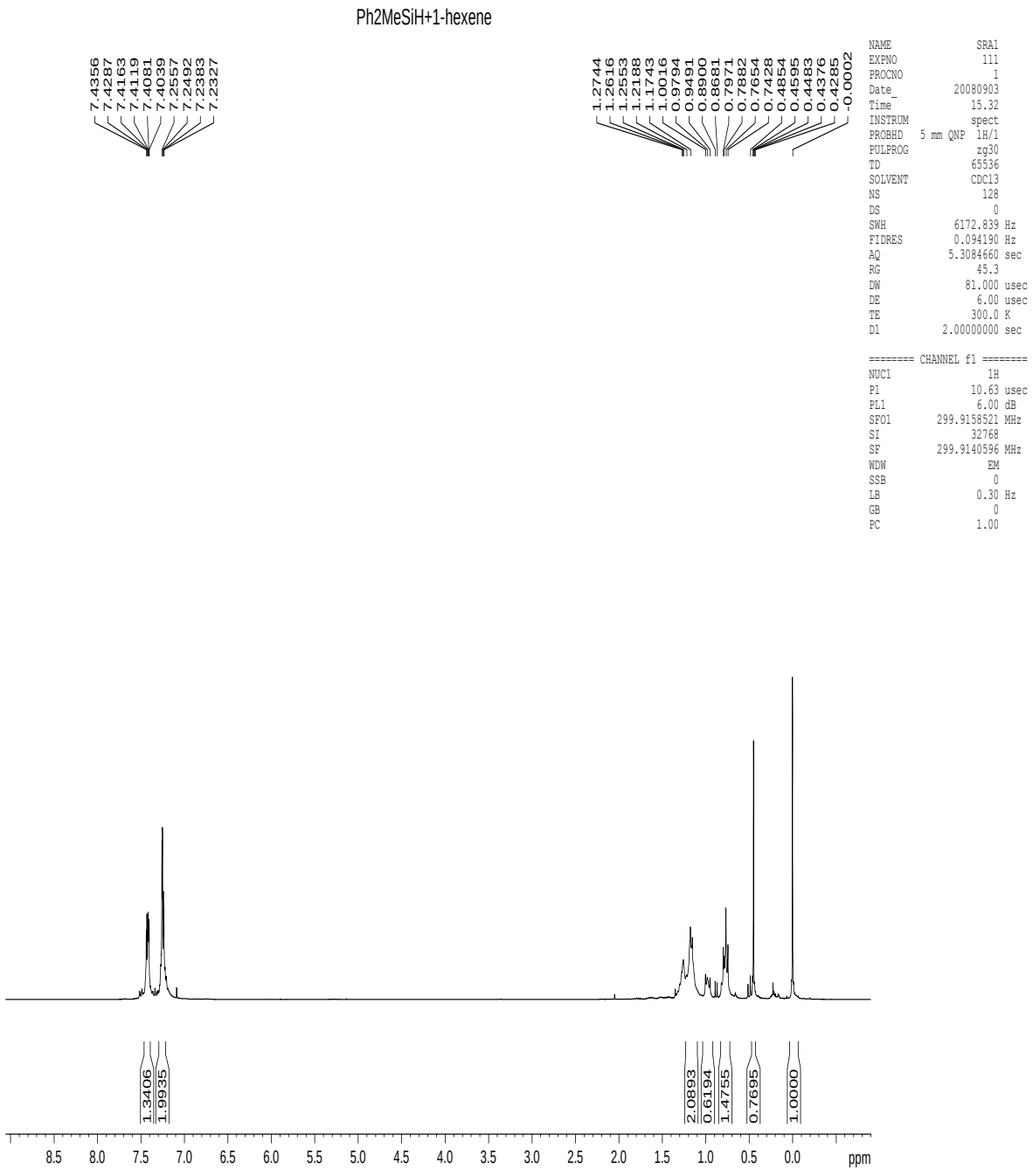

Appendix I.76. ^{1}H NMR spectrum of the product from hydrosilylation reaction of methyldiphenylsilane (S1) and 1-hexene in the presence of (1a).

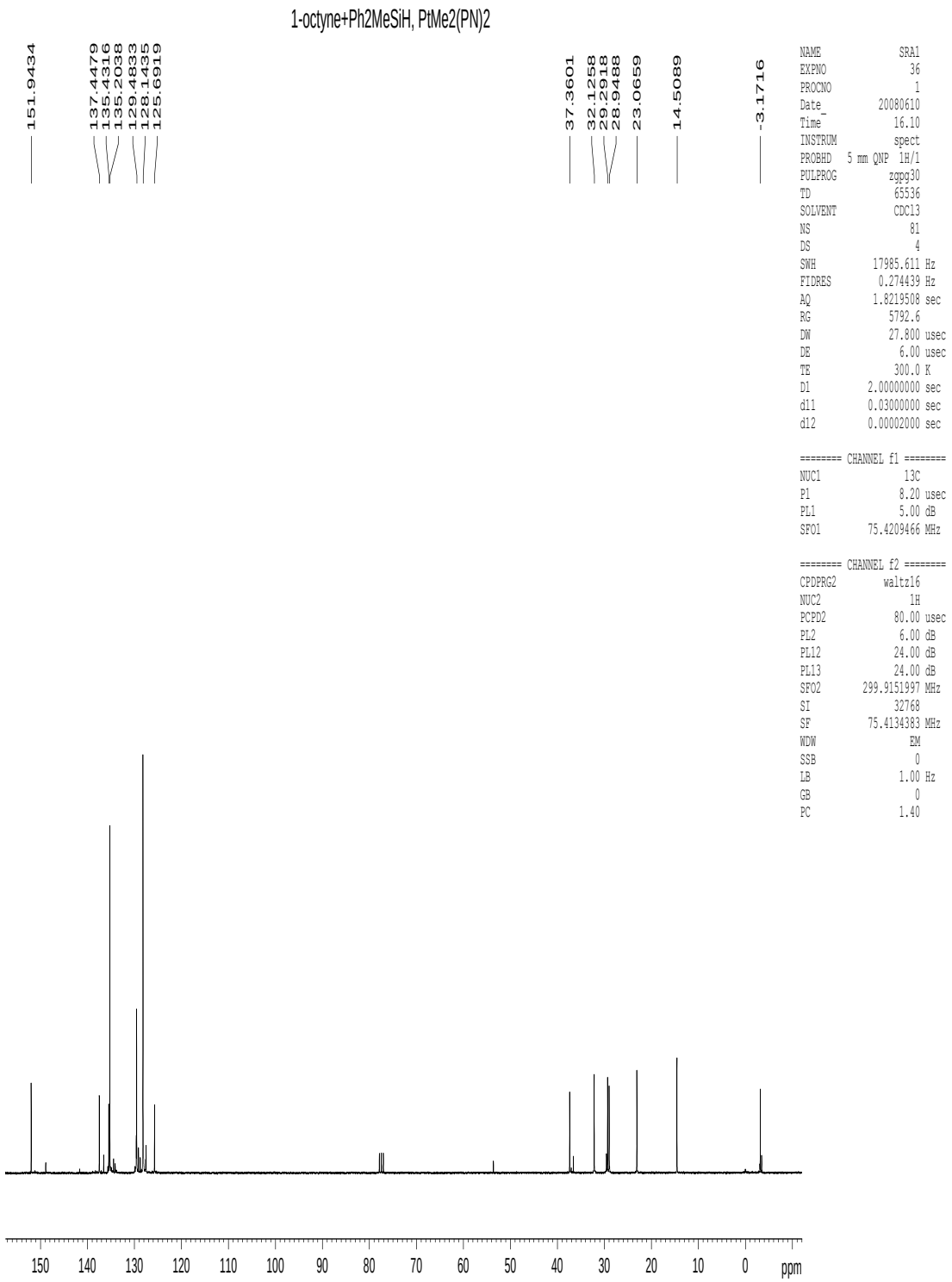

Appendix I.77. $^{13}C\{^{1}H\}$ NMR spectrum of the product from hydrosilylation reaction of methyldiphenylsilane (S1) and 1-octyne in the presence of (1a).

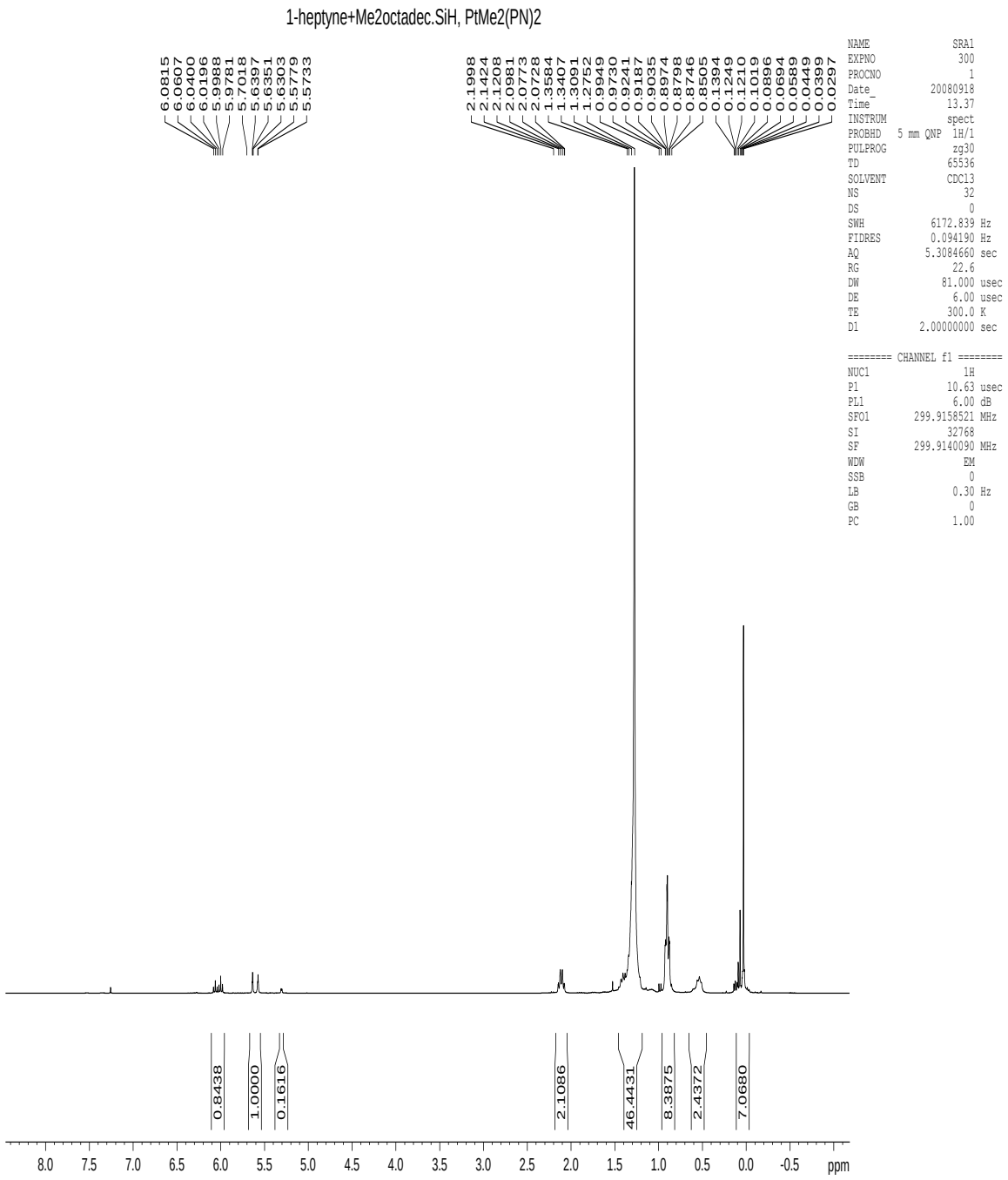

Appendix I.78. ^{1}H NMR spectrum of the product from hydrosilylation reaction of dimethyloctadecylsilane (S3) and 1-heptyne (A1) in the presence of (1a).

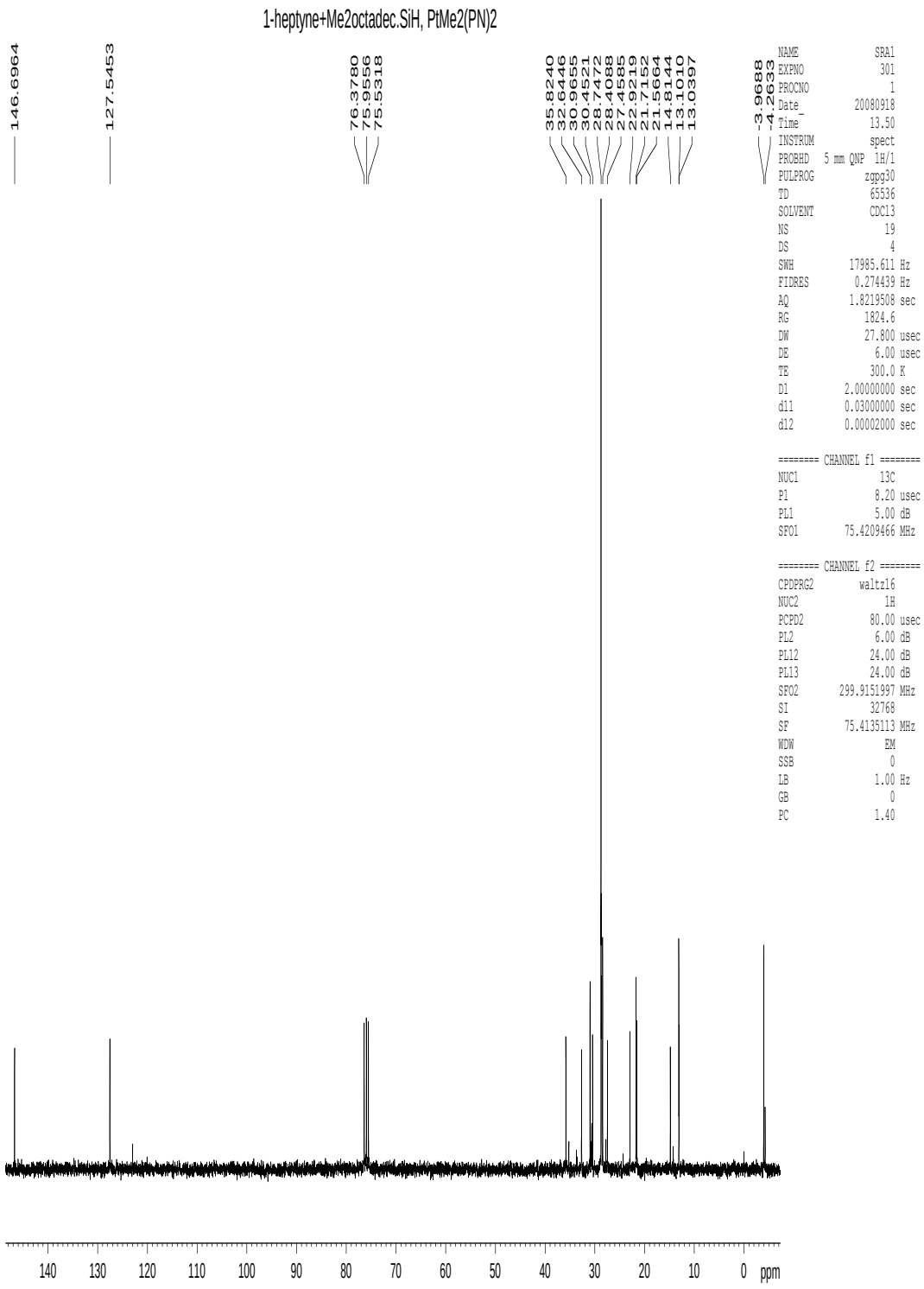

Appendix I.79. $^{13}C\{^{1}H\}$ NMR spectrum of the product from hydrosilylation reaction of dimethyloctadecylsilane (S3) and 1-heptyne (A1) in the presence of (1a).

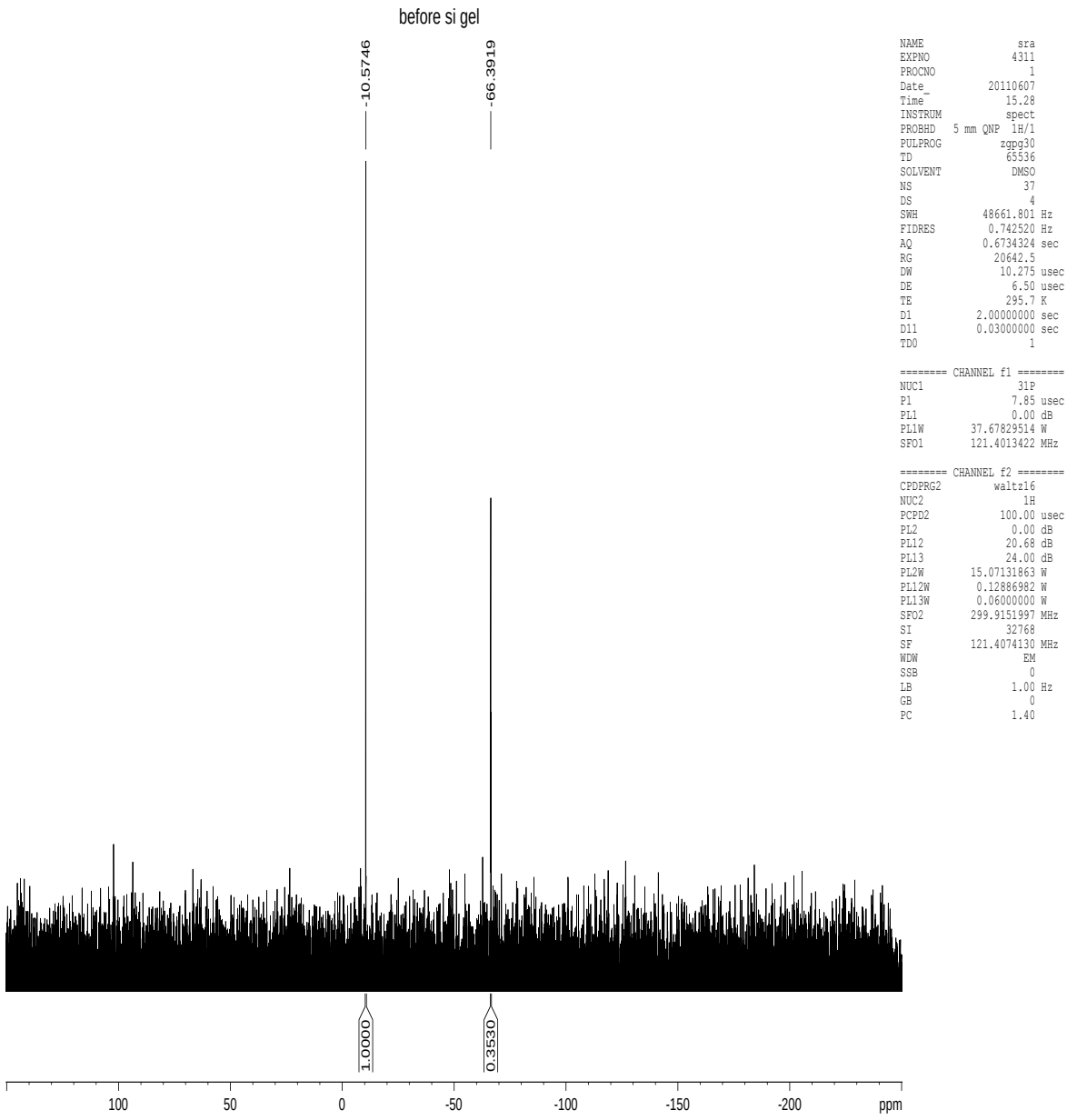

Appendix I.80. $^{31}P\{^{1}H\}$ NMR spectrum of the residual metal species after Suzuki-Miyaura cross-coupling reaction in the presence of (5a).

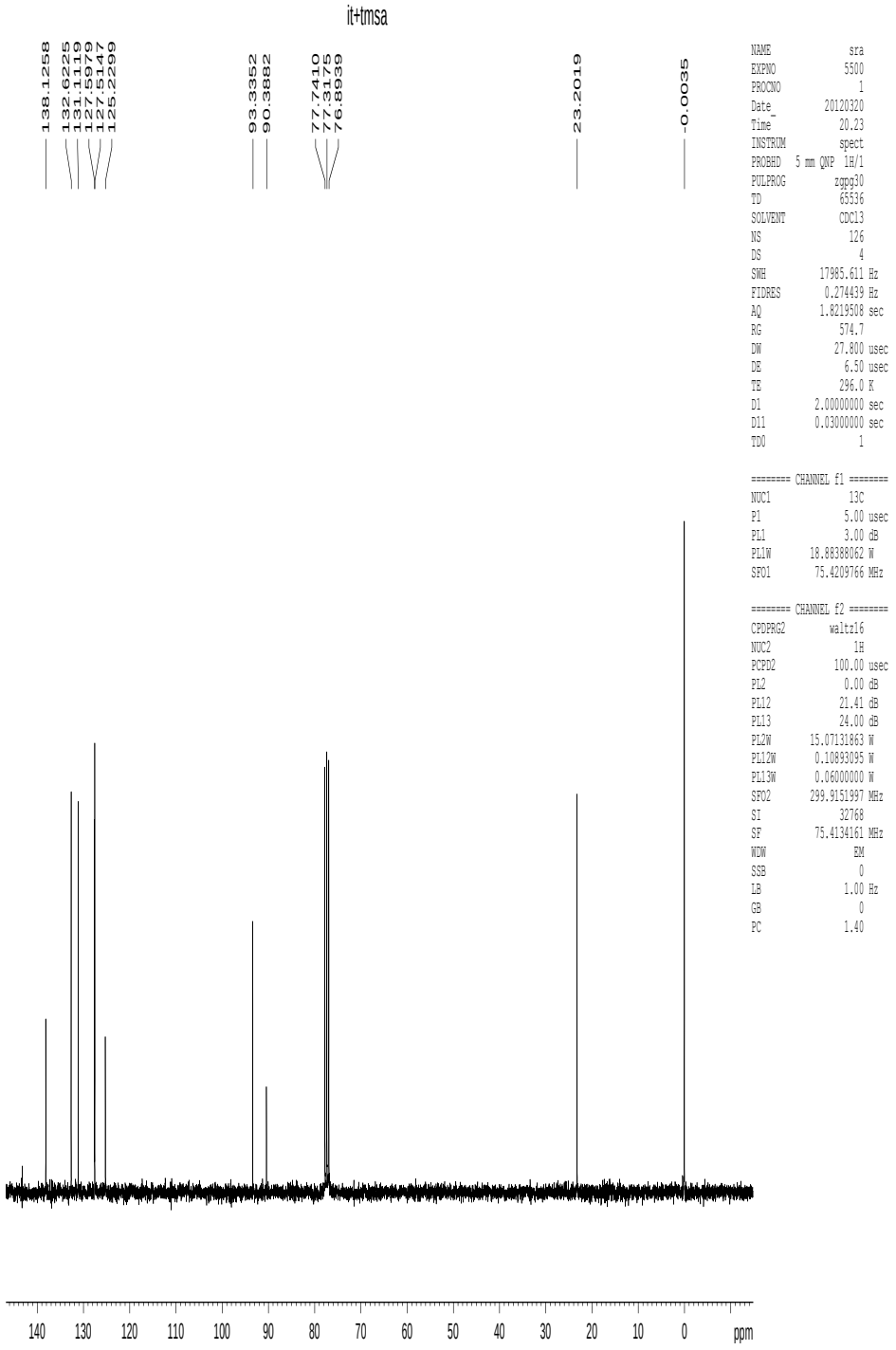

Appendix I.81. $^{13}C\{^{1}H\}$ NMR spectrum of the product from Sonogashira cross-coupling reaction of 4-iodotoluene (R2) and trimethylsilylacetylene (A2) in the presence of (M1).

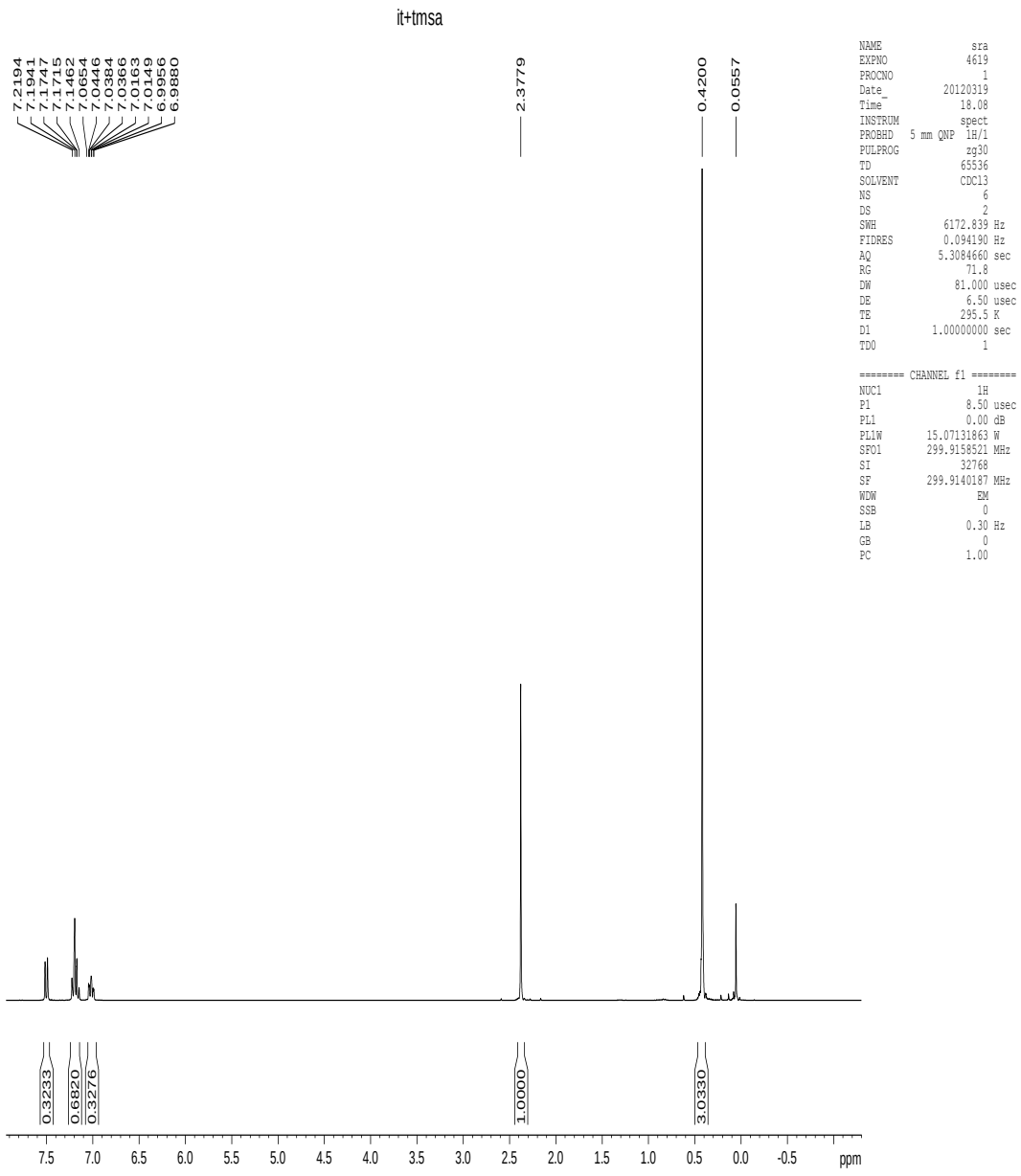

Appendix I.82. ^{1}H NMR spectrum of the product from Sonogashira cross-coupling reaction of 4-iodotoluene (R2) and trimethylsilylacetylene (A2) in the presence of (M1).

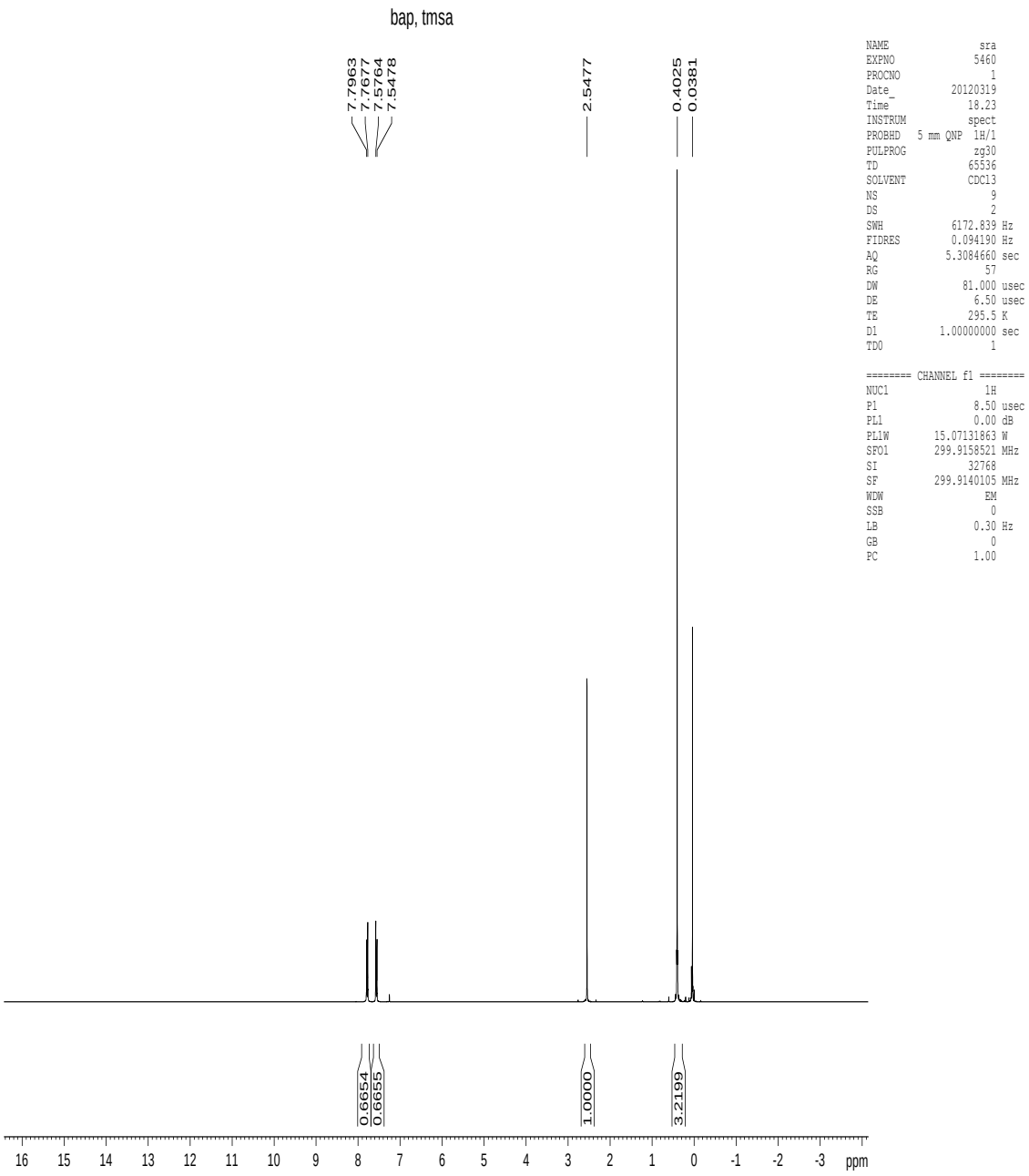

Appendix I.83. $^{13}C\{^{1}H\}$ NMR spectrum of the product from Sonogashira cross-coupling reaction of 4-bromoacetophenone (R1) and trimethylsilylacetylene (A2) in the presence of (M1).

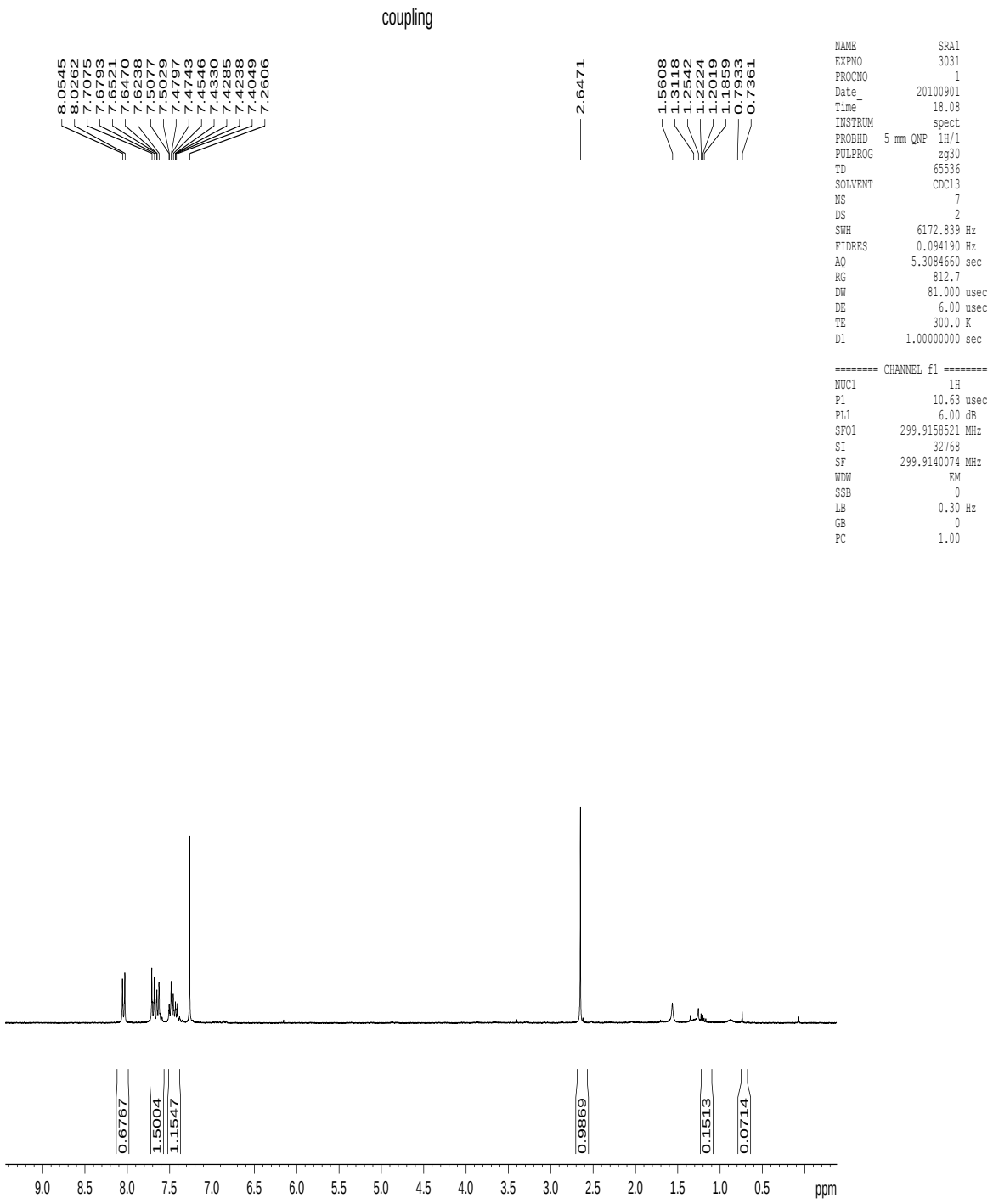

Appendix I.84. ^{1}H NMR spectrum of the product from Suzuki-Miyaura cross-coupling reaction of 4-bromoacetophenone (R1) and phenylboronic acid (T1) in the presence of (5a).

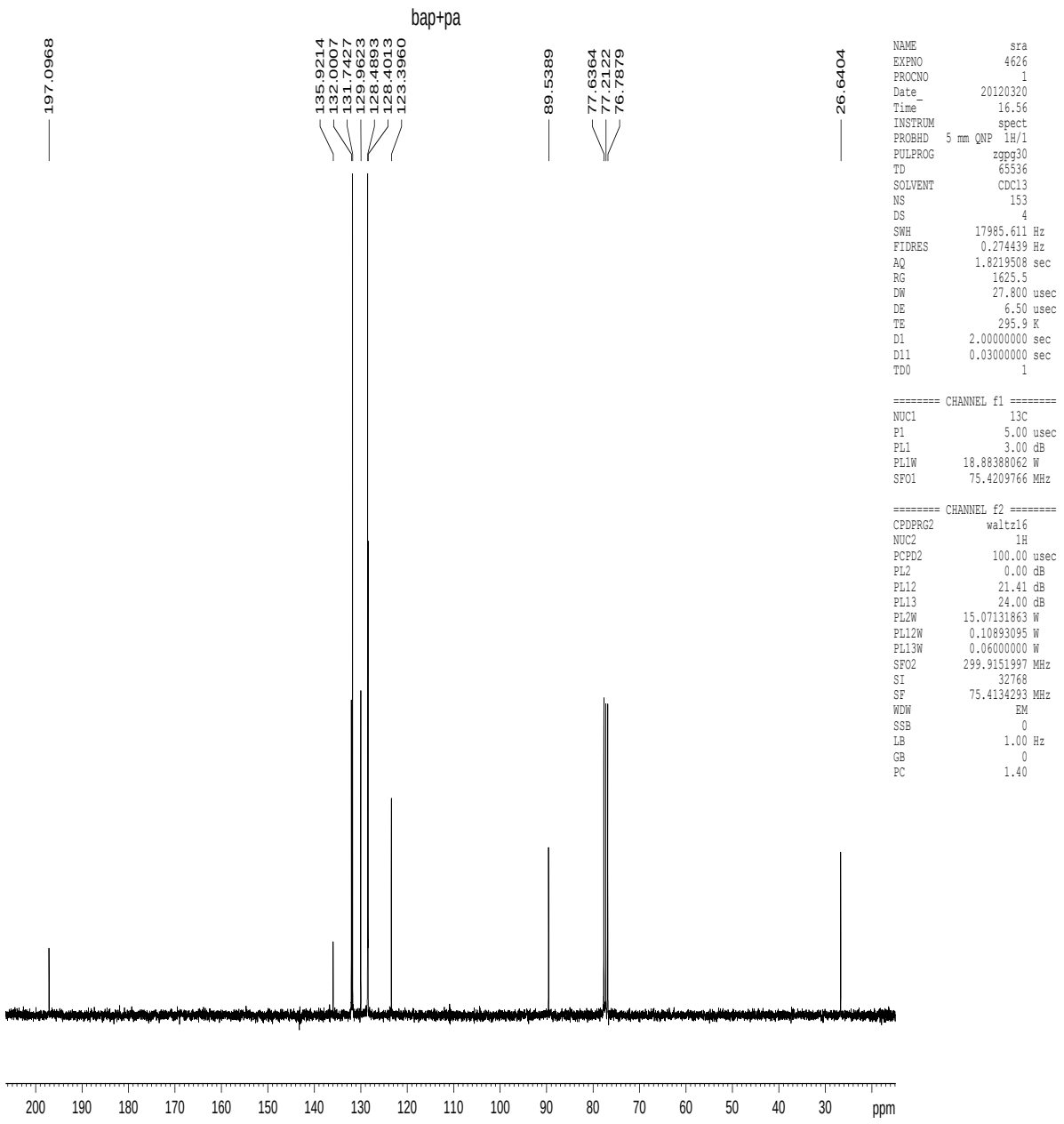

Appendix I.85. $^{13}C\{^{1}H\}$ NMR spectrum of the product from Sonogashira cross-coupling reaction of 4-bromoacetophenone (R1) and phenylacetylene (A4) in the presence of (M1).

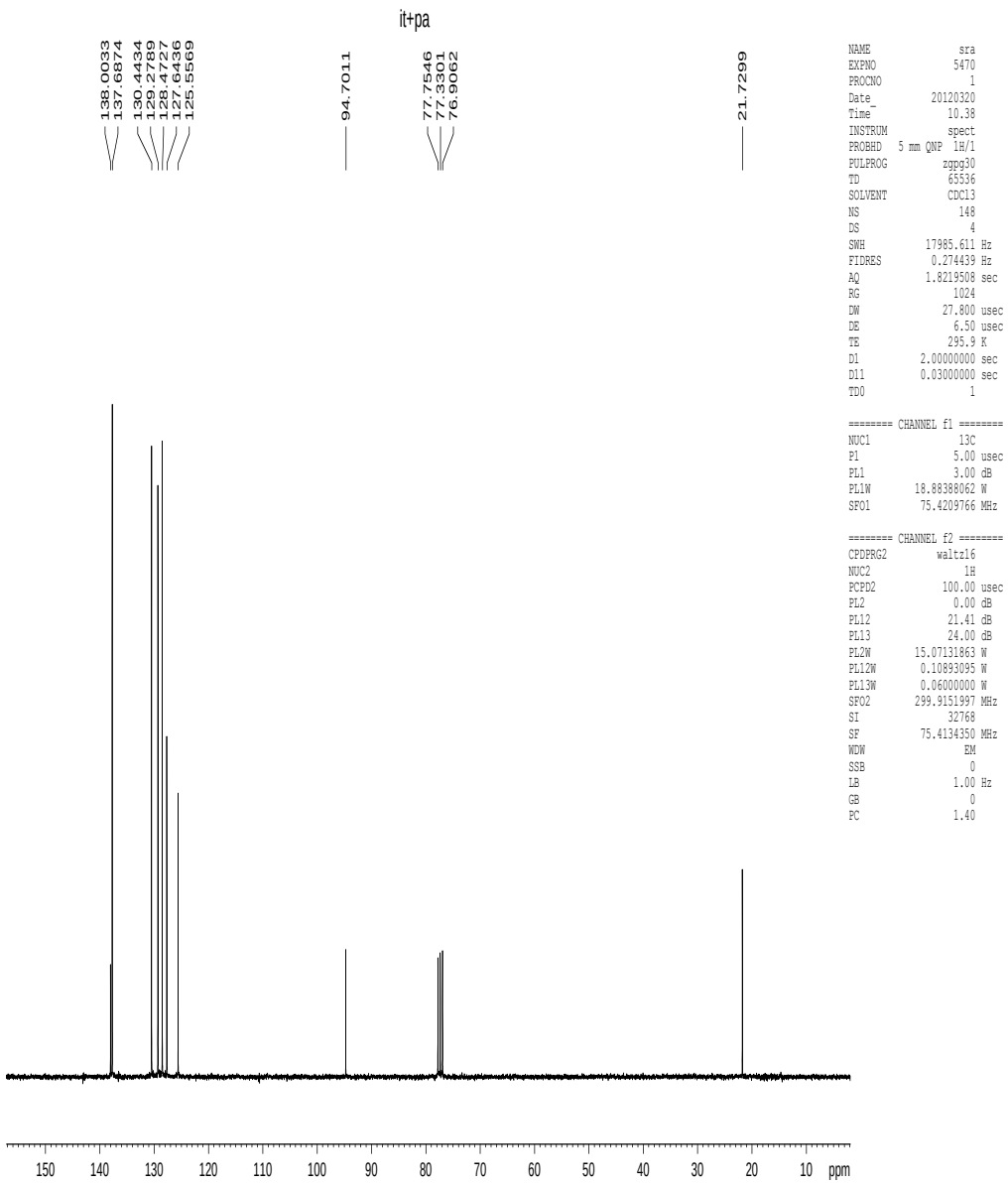

Appendix I.86. $^{13}C\{^{1}H\}$ NMR spectrum of the product from Sonogashira cross-coupling reaction of 4-bromoacetophenone (R1) and phenylacetylene (A4) in the presence of (M1).

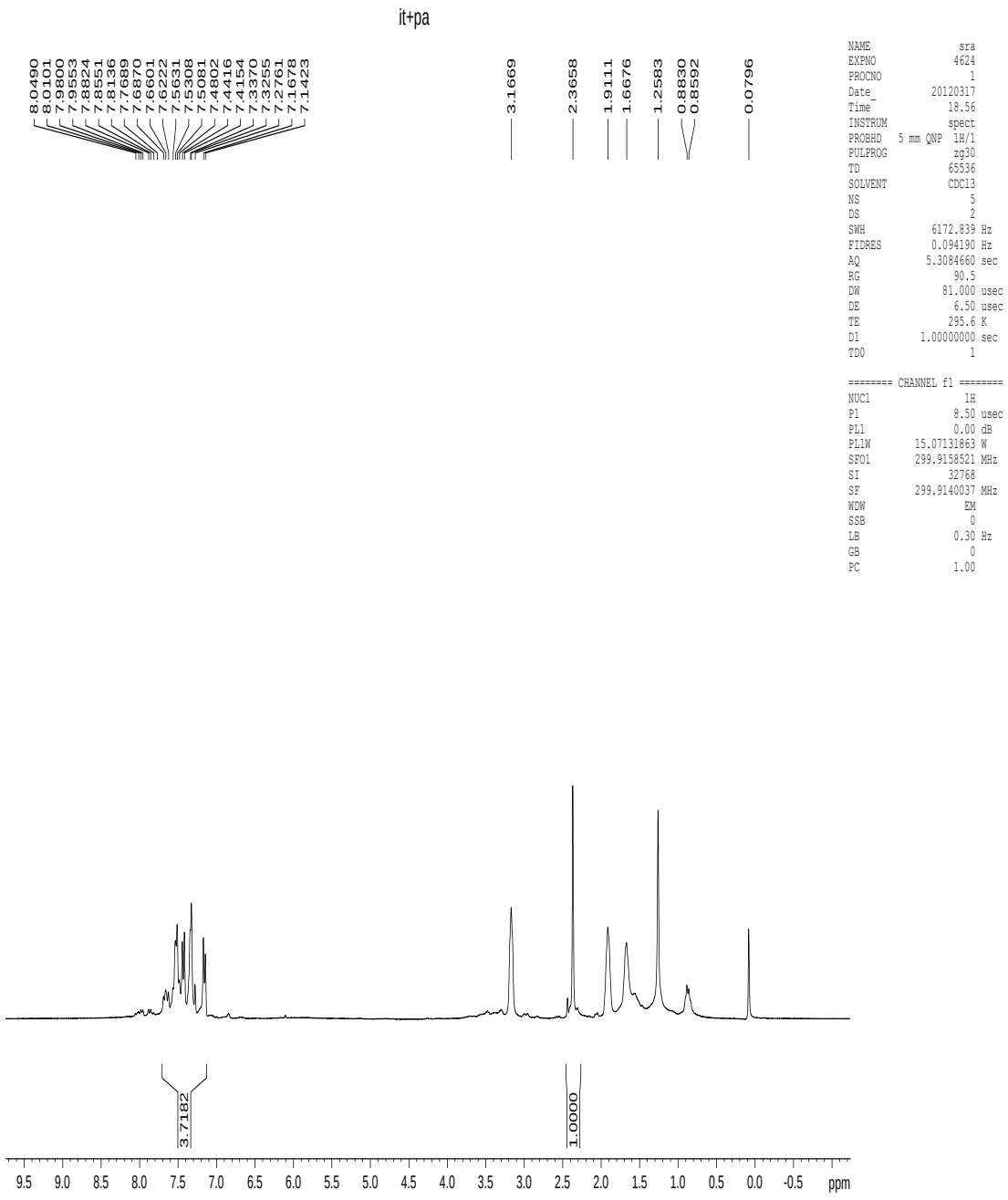

Appendix I.87. ^{1}H NMR spectrum of the product from Sonogashira cross-coupling reaction of 4-iodotoluene (R2) and phenylacetylene (A4) in the presence of (M1).

The signals at 3.16, 1.91, and 1.66 ppm are from piperidine.

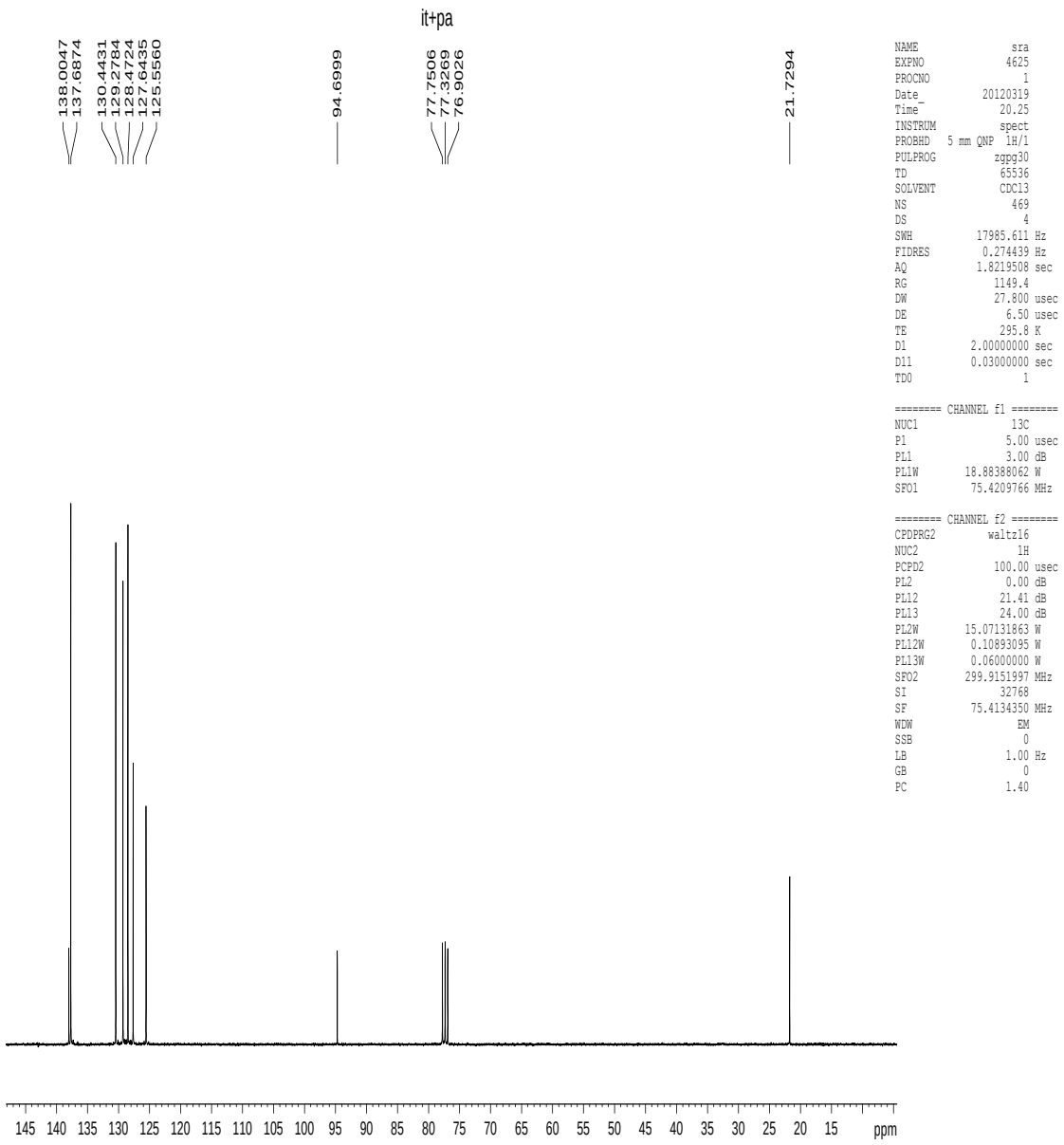

Appendix I.88a. $^{13}C\{^{1}H\}$ NMR spectrum of the product from Sonogashira cross-coupling reaction of 4-iodotoluene (R2) and phenylacetylene (A4) in the presence of (M1).

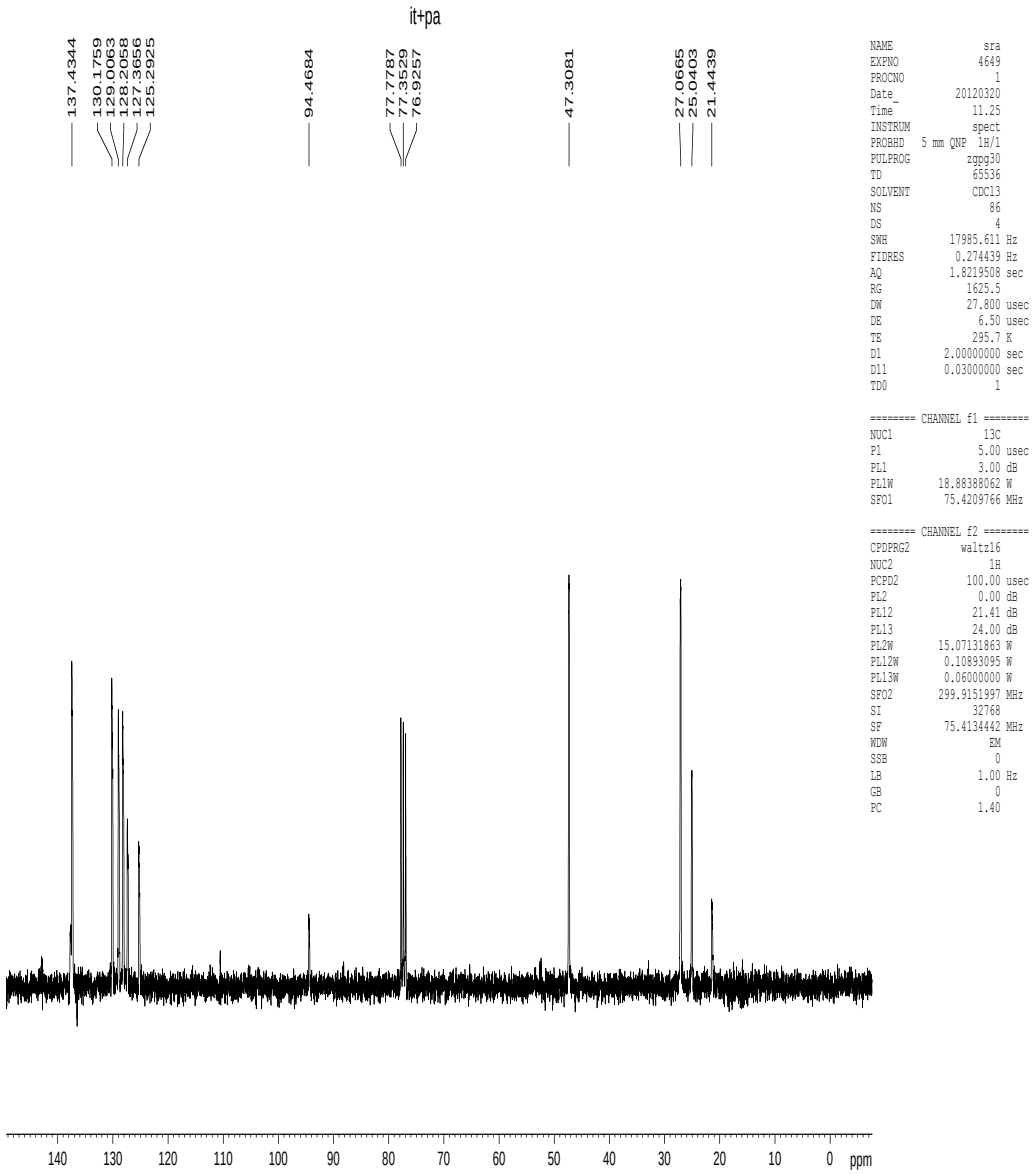

Appendix I.88b. $^{13}C\{^{1}H\}$ NMR spectrum of the product from Sonogashira cross-coupling reaction of 4-iodotoluene (R2) and phenylacetylene (A4) in the presence of (M1).

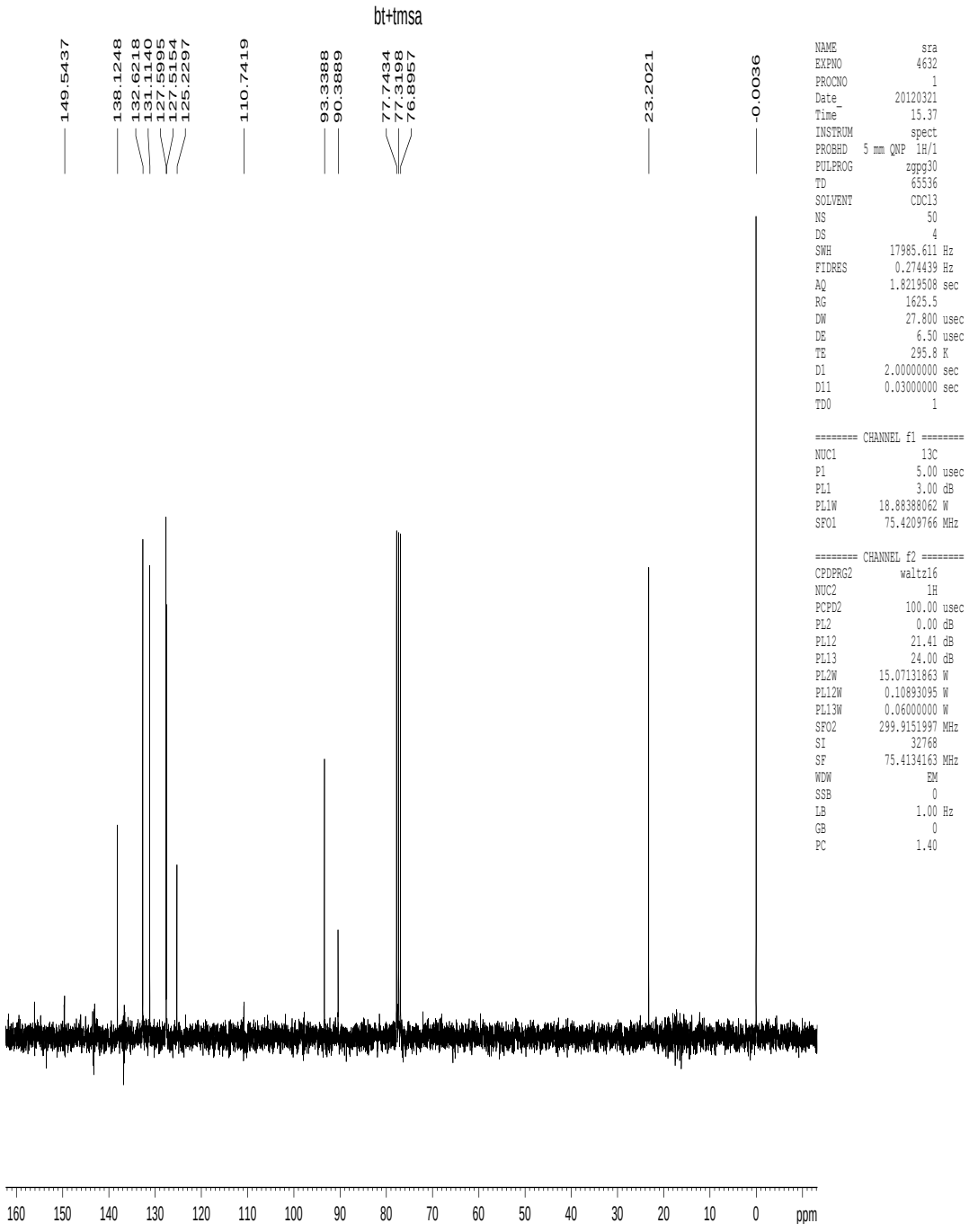

Appendix I.89. $^{13}C\{^{1}H\}$ NMR spectrum of the product from Sonogashira cross-coupling reaction of 4-bromotoluene (R2) and trimethylsilylacetylene (A2) in the presence of (M1).

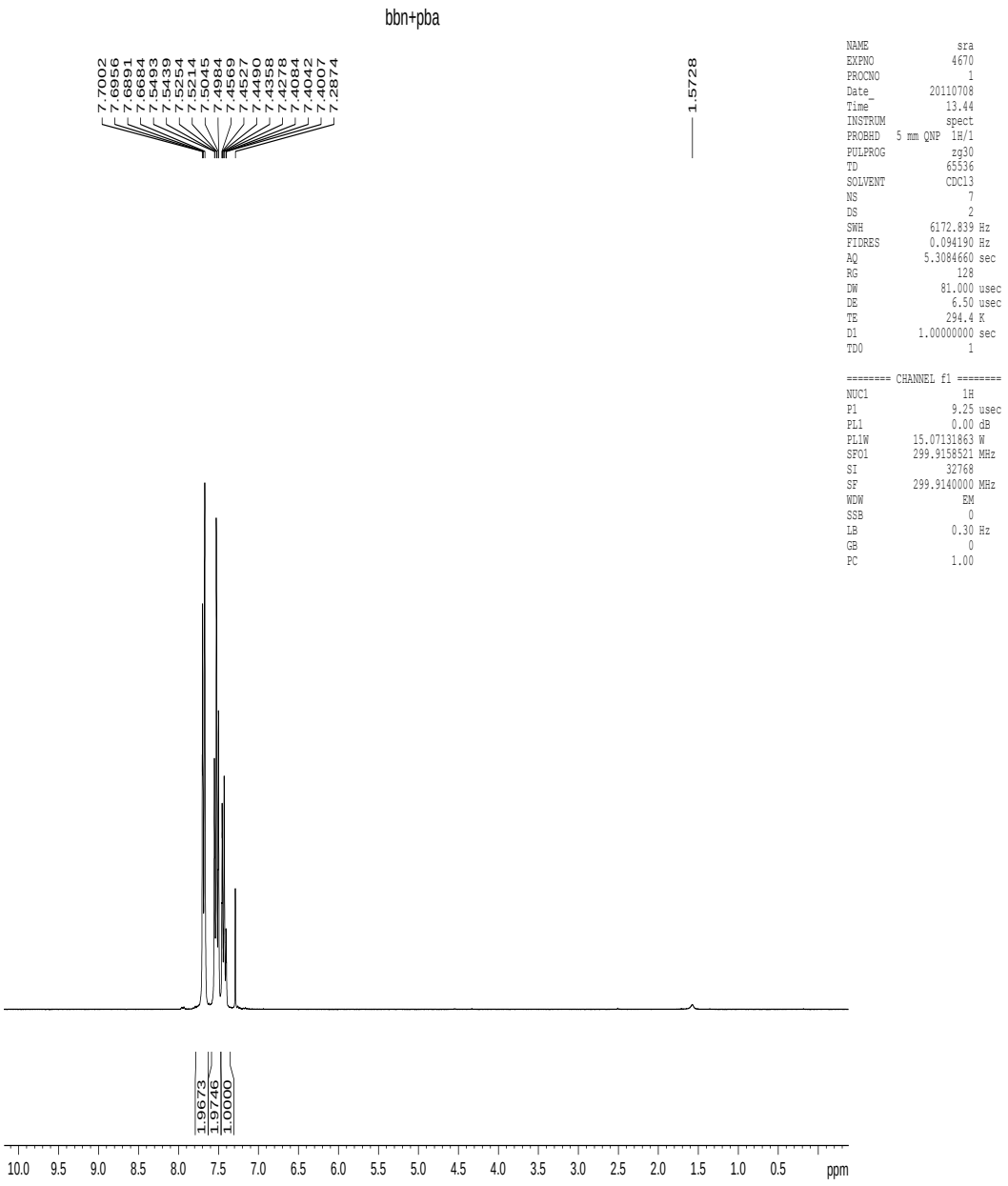

Appendix I.90. ^{1}H NMR spectrum of the product from Suzuki-Miyaura cross-coupling reaction of 4-bromobenzonitrile (R4) and phenylboronic acid (T1) in the presence of (5a).

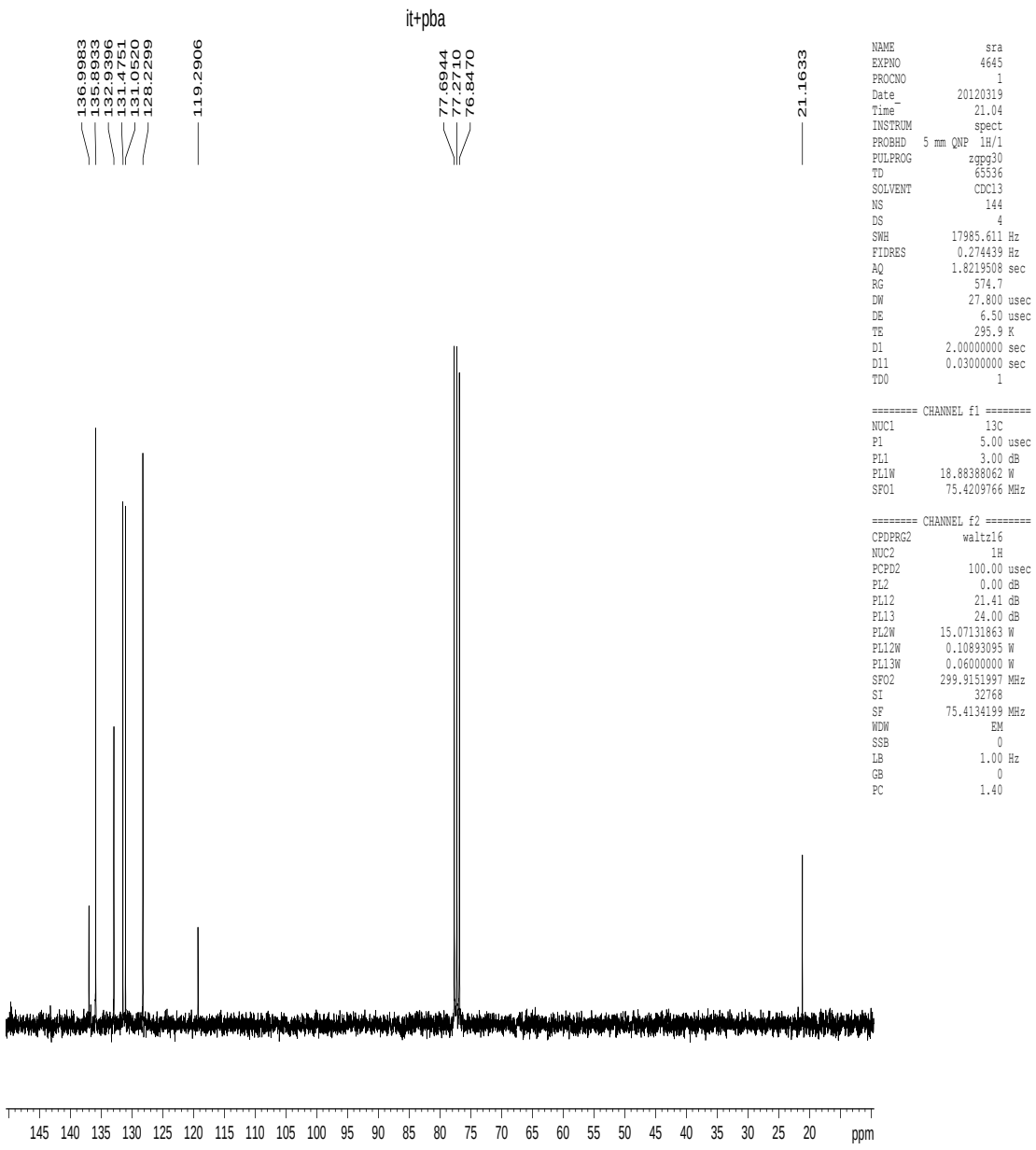

Appendix I.91. $^{13}C\{^{1}H\}$ NMR spectrum of the product from Suzuki-Miyaura cross-coupling reaction of 4-iodotoluene (R2) and phenylboronic acid (T1) in the presence of (5a).

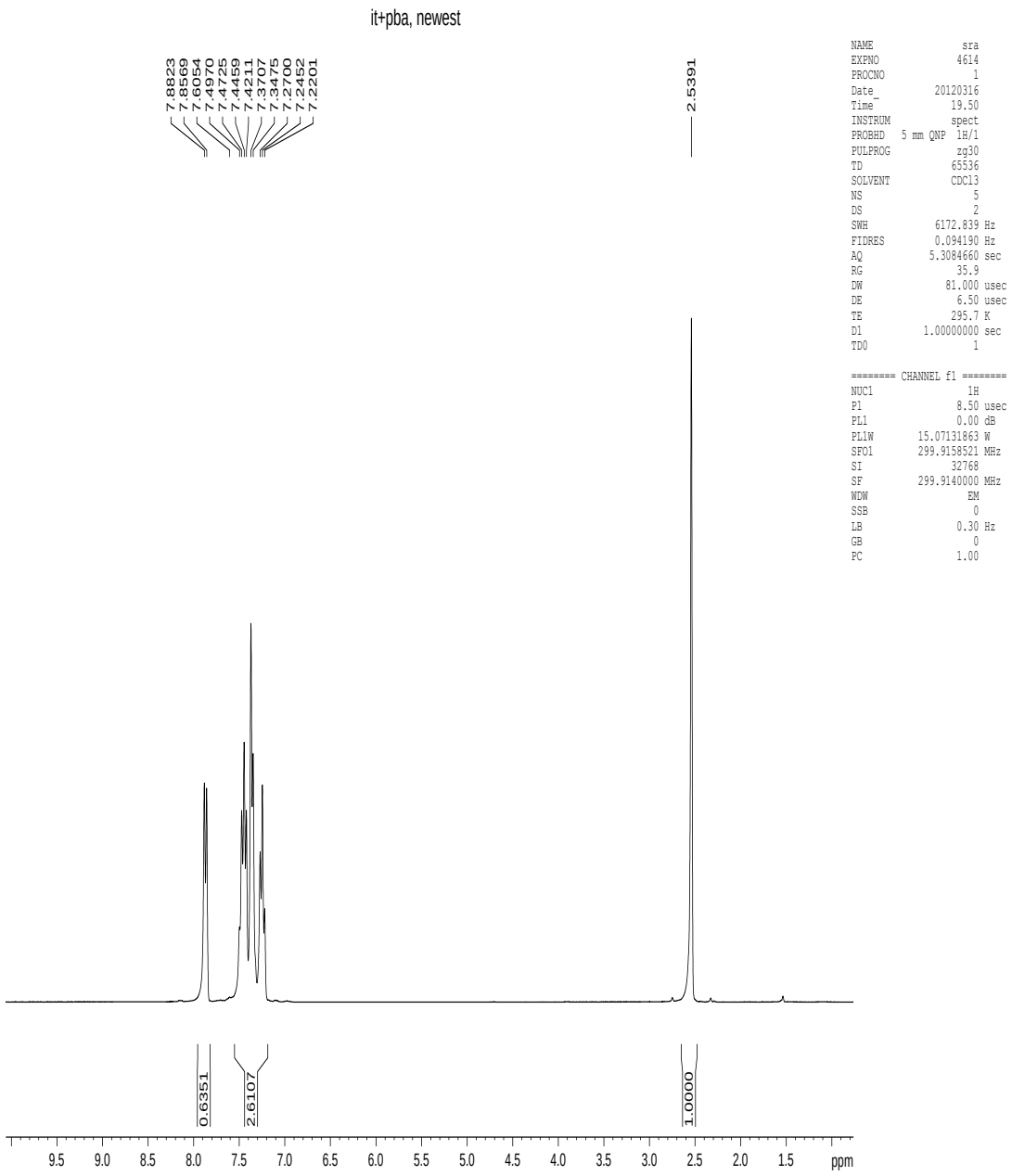

Appendix I.92. ^{1}H NMR spectrum of the product from Suzuki-Miyaura cross-coupling reaction of 4-iodotoluene (R2) and phenylboronic acid (T1) in the presence of (5a).

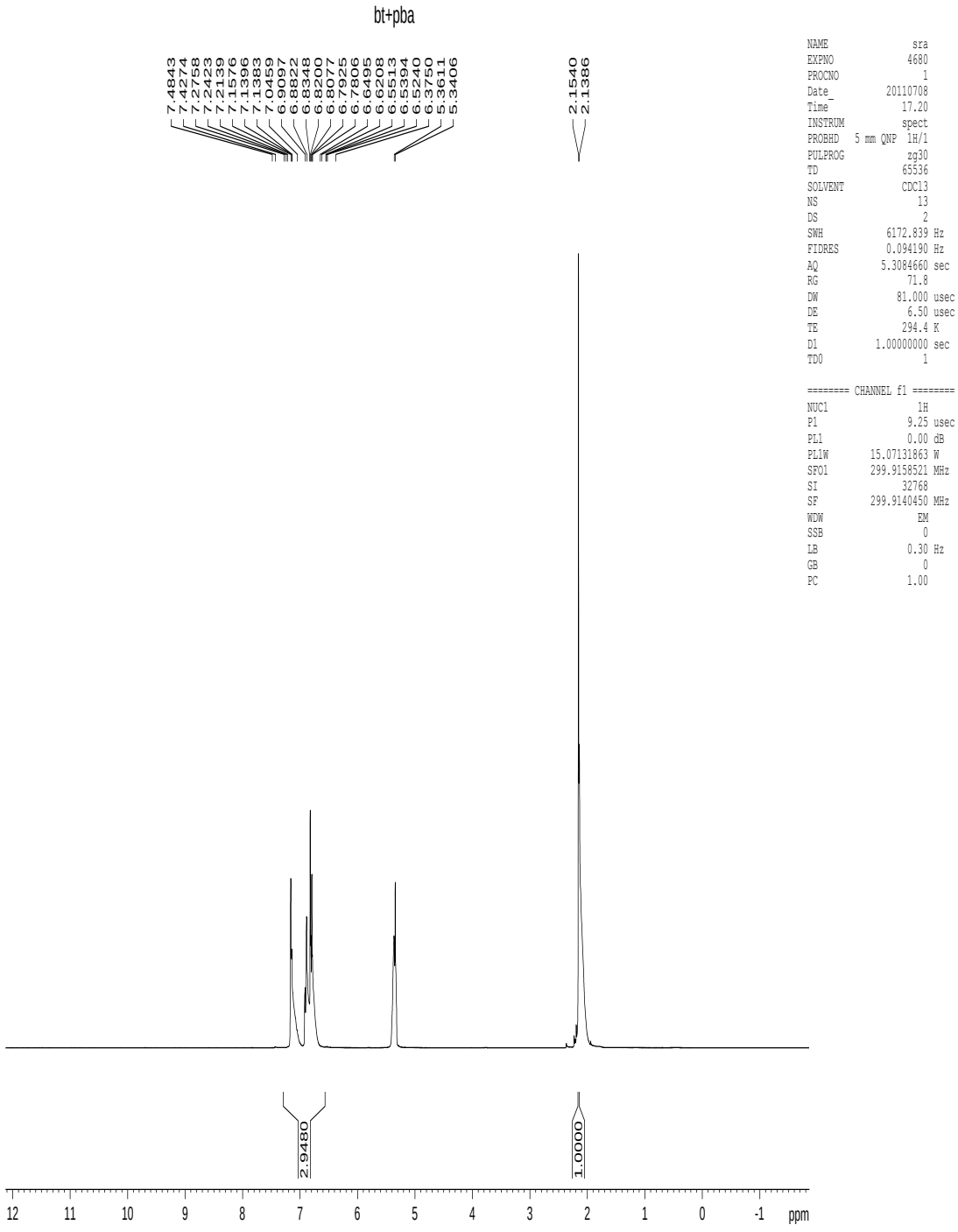

Appendix I.93. ^{1}H NMR spectrum of the product from Suzuki-Miyaura cross-coupling reaction of 4-bromotoluene (R3) and phenylboronic acid (T1) in the presence of (5a).

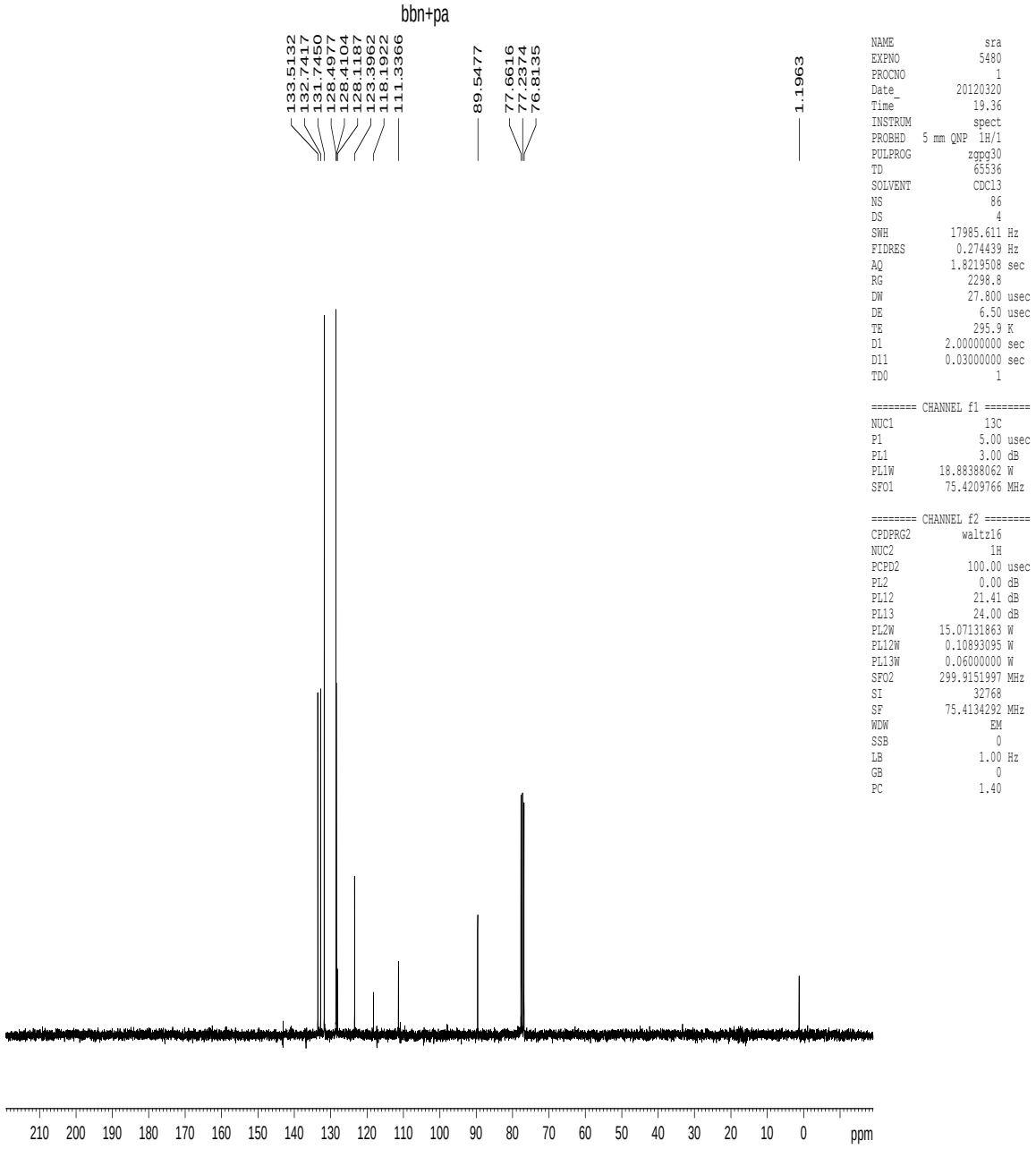

Appendix I.94. $^{13}C\{^{1}H\}$ NMR spectrum of the product from Sonogashira cross-coupling reaction of 4-bromobenzonitrile (R4) and phenylacetylene (A4) in the presence of (M1).

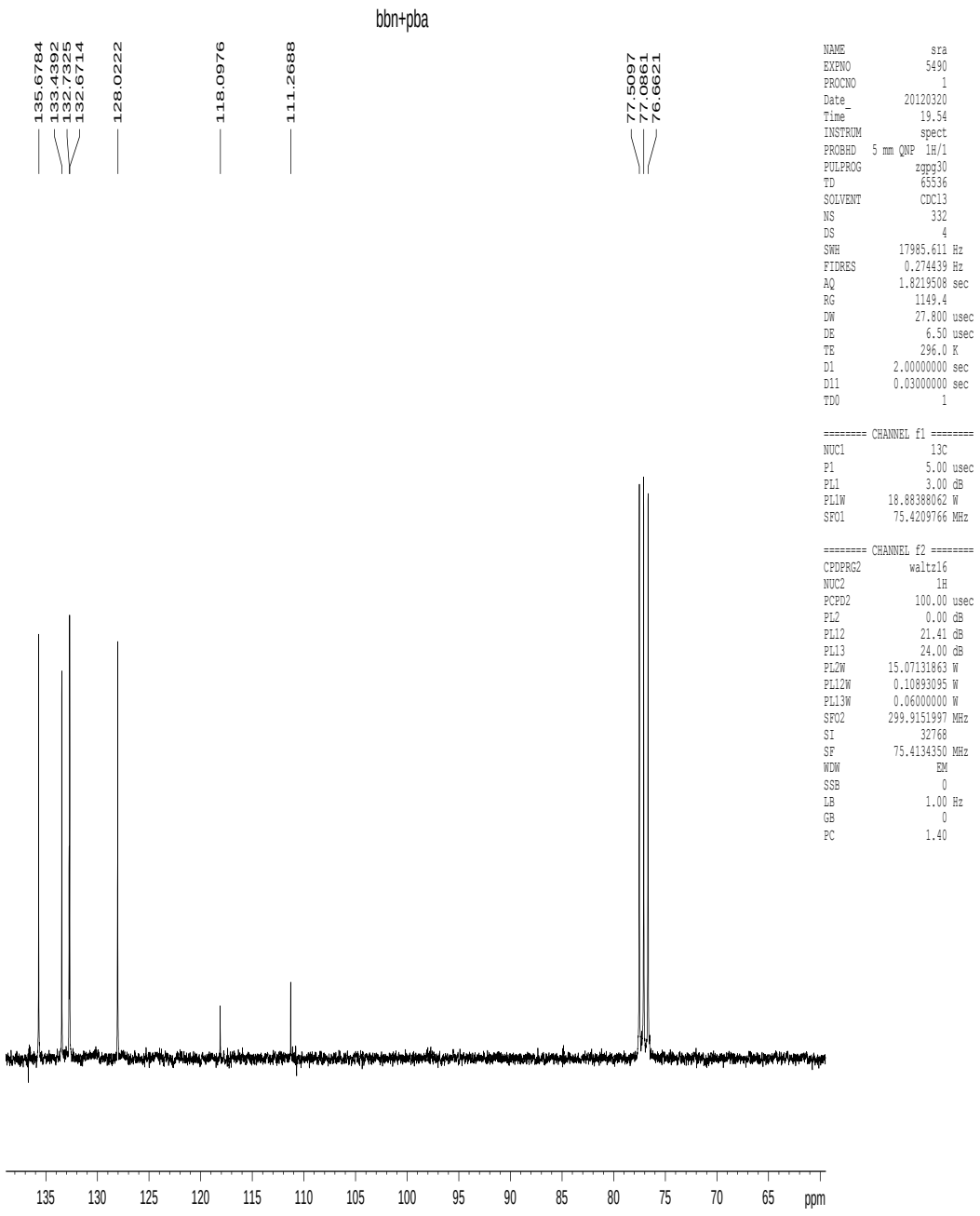

Appendix I.95. $^{13}C\{^{1}H\}$ NMR spectrum of the product from Suzuki-Miyaura cross-coupling reaction of 4-bromobenzonitrile (R4) and phenyboronic acid (T1) in the presence of (5a).

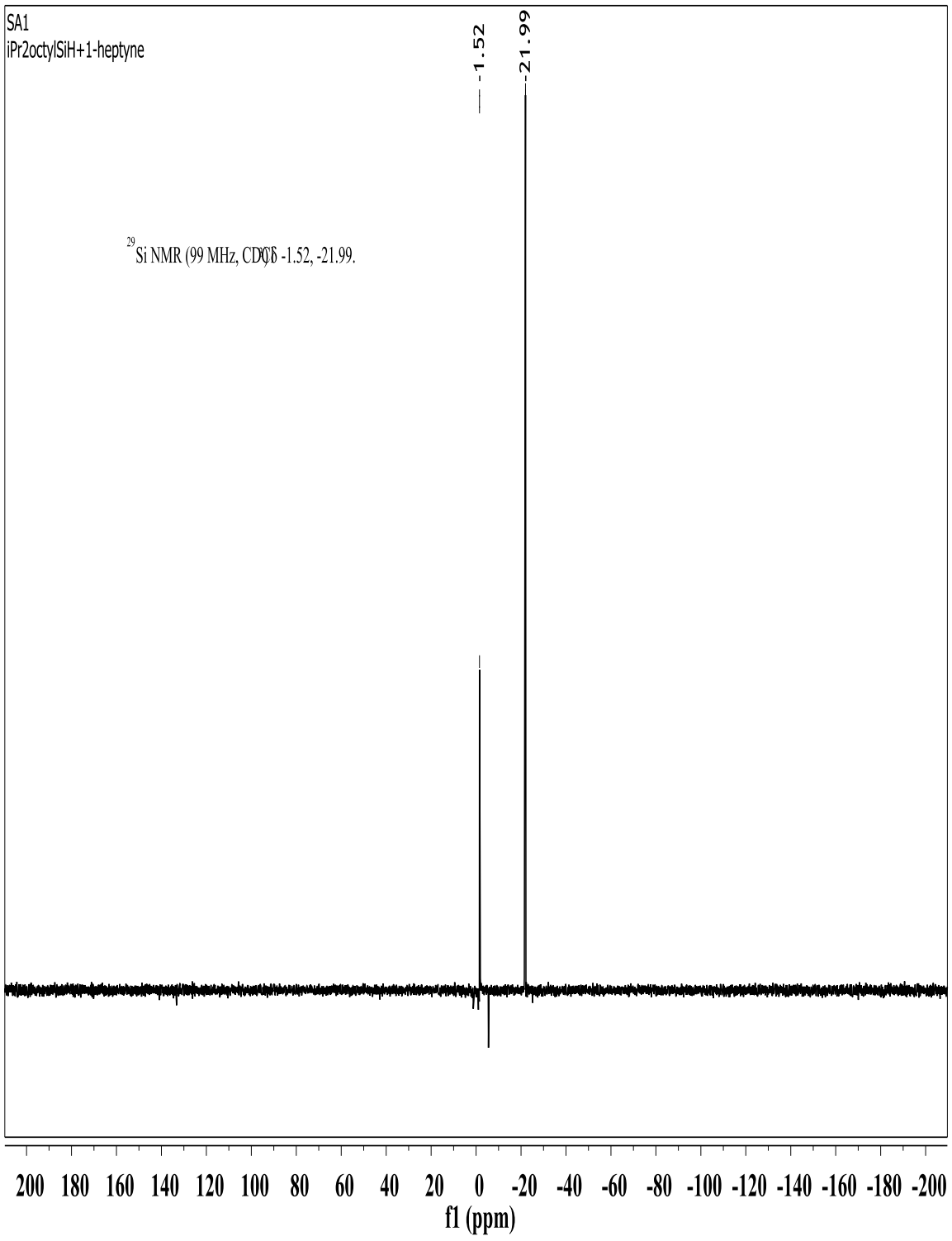

Appendix I.96. $^{29}Si\{^{1}H\}$ NMR spectrum of the product from hydrosilylation reaction of diisopropyloctylsilane (S2) and 1-heptyne (A1) in the presence of (1a).

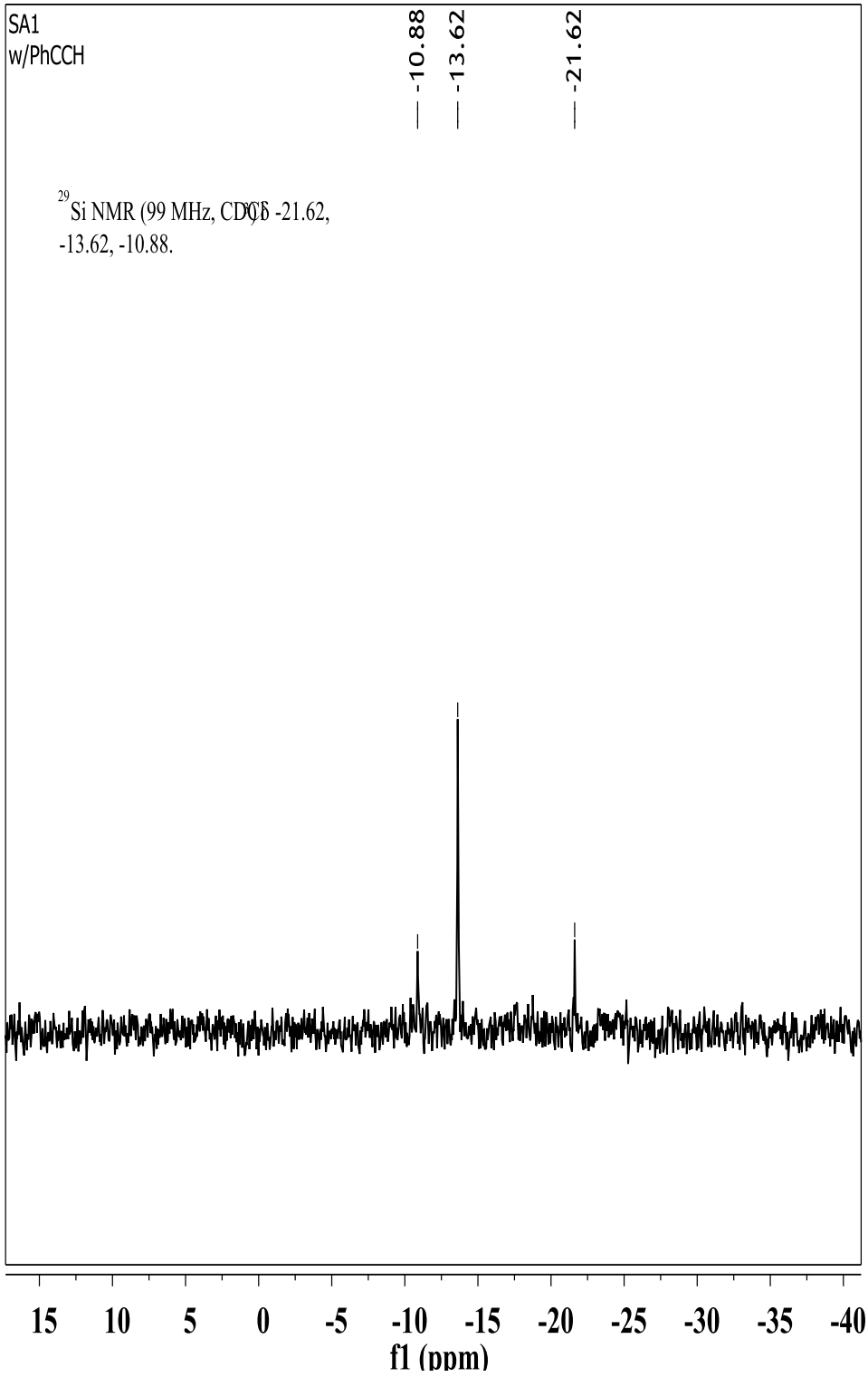

Appendix I.97. $^{29}Si\{^{1}H\}$ NMR spectrum of the product from hydrosilylation reaction of methyldiphenylsilane (S1) and phenylacetylene (A4) in the presence of (1a).

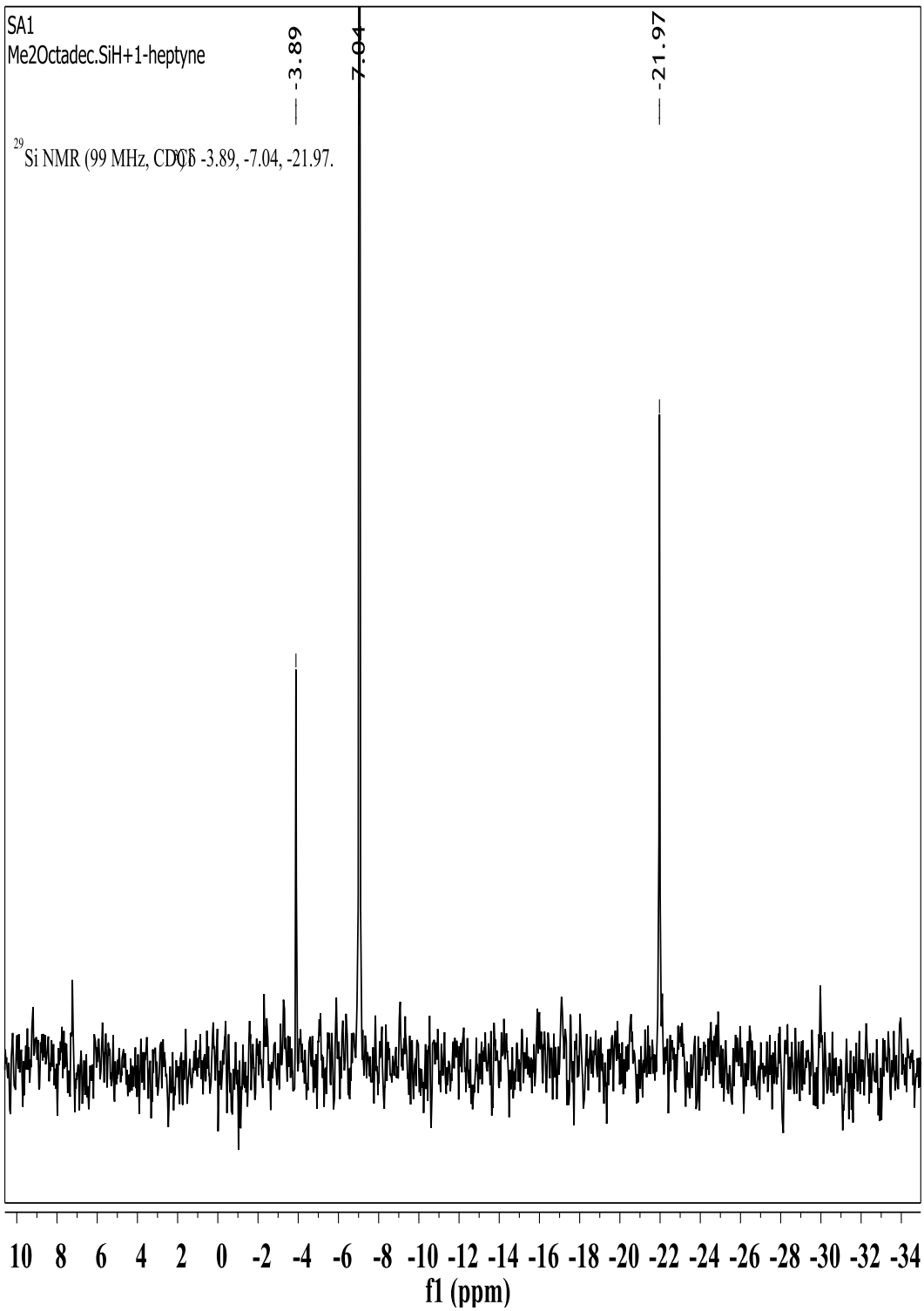

Appendix I.98. $^{29}Si\{^{1}H\}$ NMR spectrum of the product from hydrosilylation reaction of dimethyloctadecylsilane (S2) and 1-heptyne (A1) in the presence of (1a).

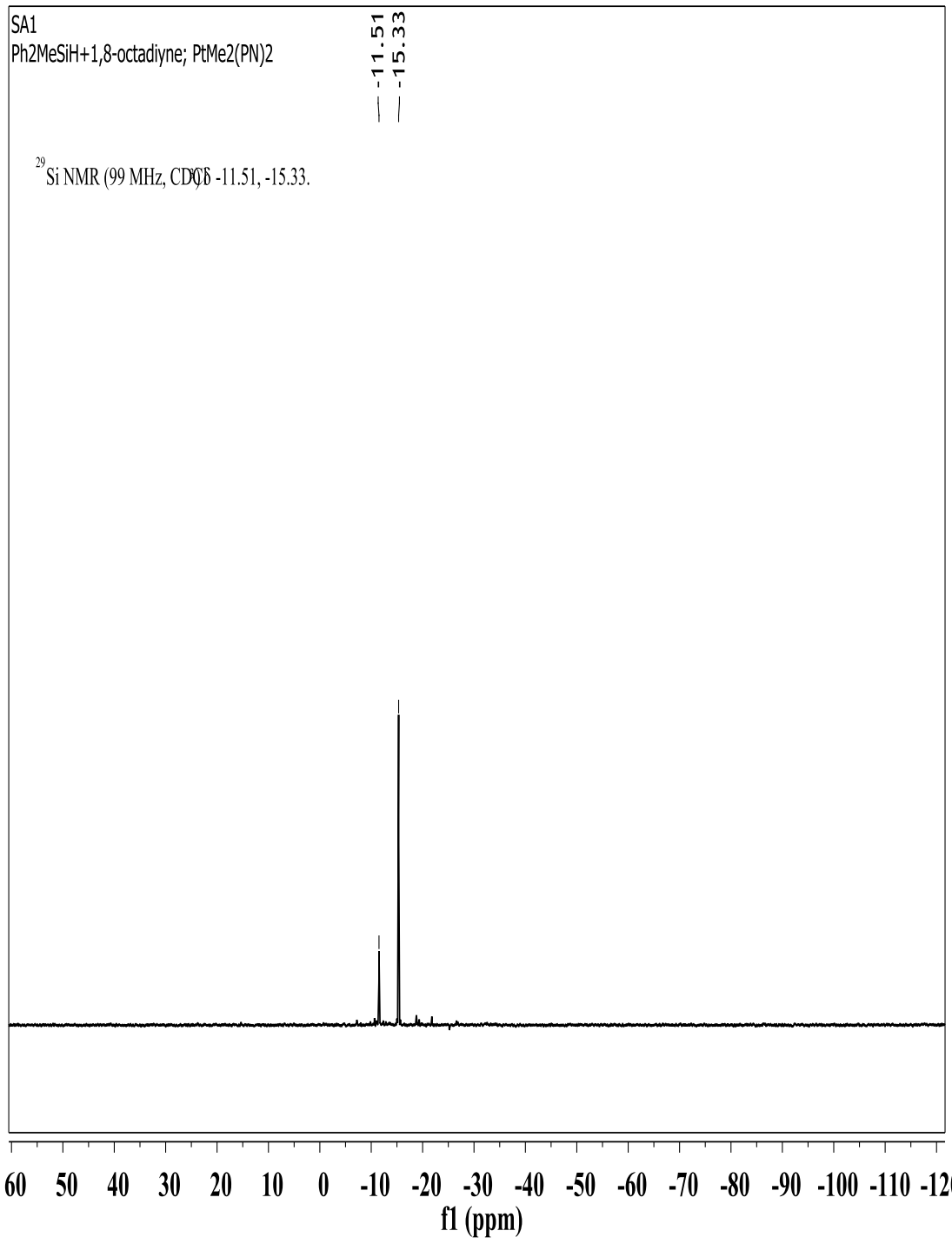

Appendix I.99. $^{29}Si\{^{1}H\}$ NMR spectrum of the product from hydrosilylation reaction of 1,7-octadiyne and methydiphenylsilane (S1) in the presence of (1a).

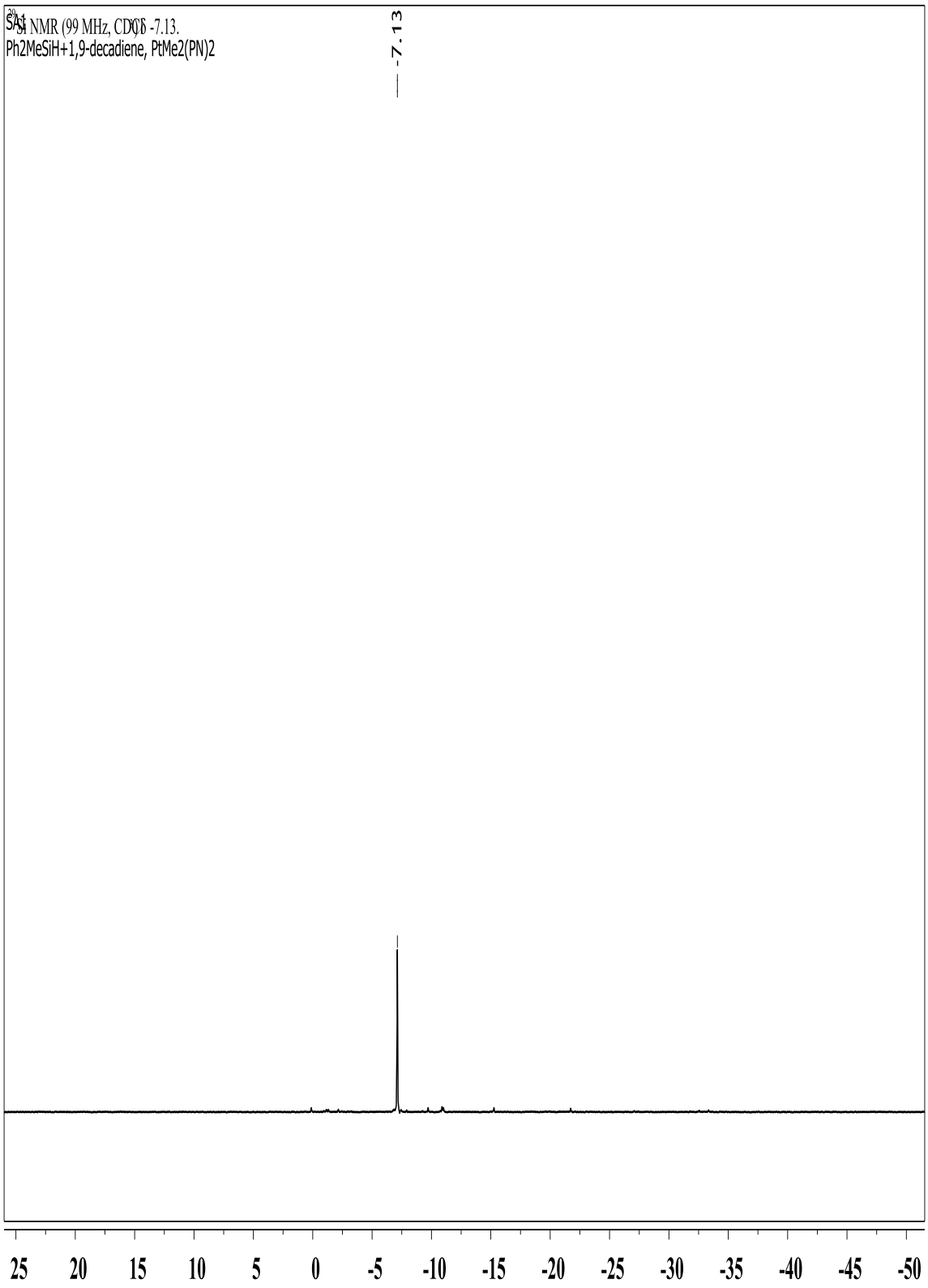

Appendix I.100. $^{29}Si\{^{1}H\}$ NMR spectrum of the product from hydrosilylation reaction of methyldiphenylsilane (S1) and 1,9-decadiene in the presence of (1a).

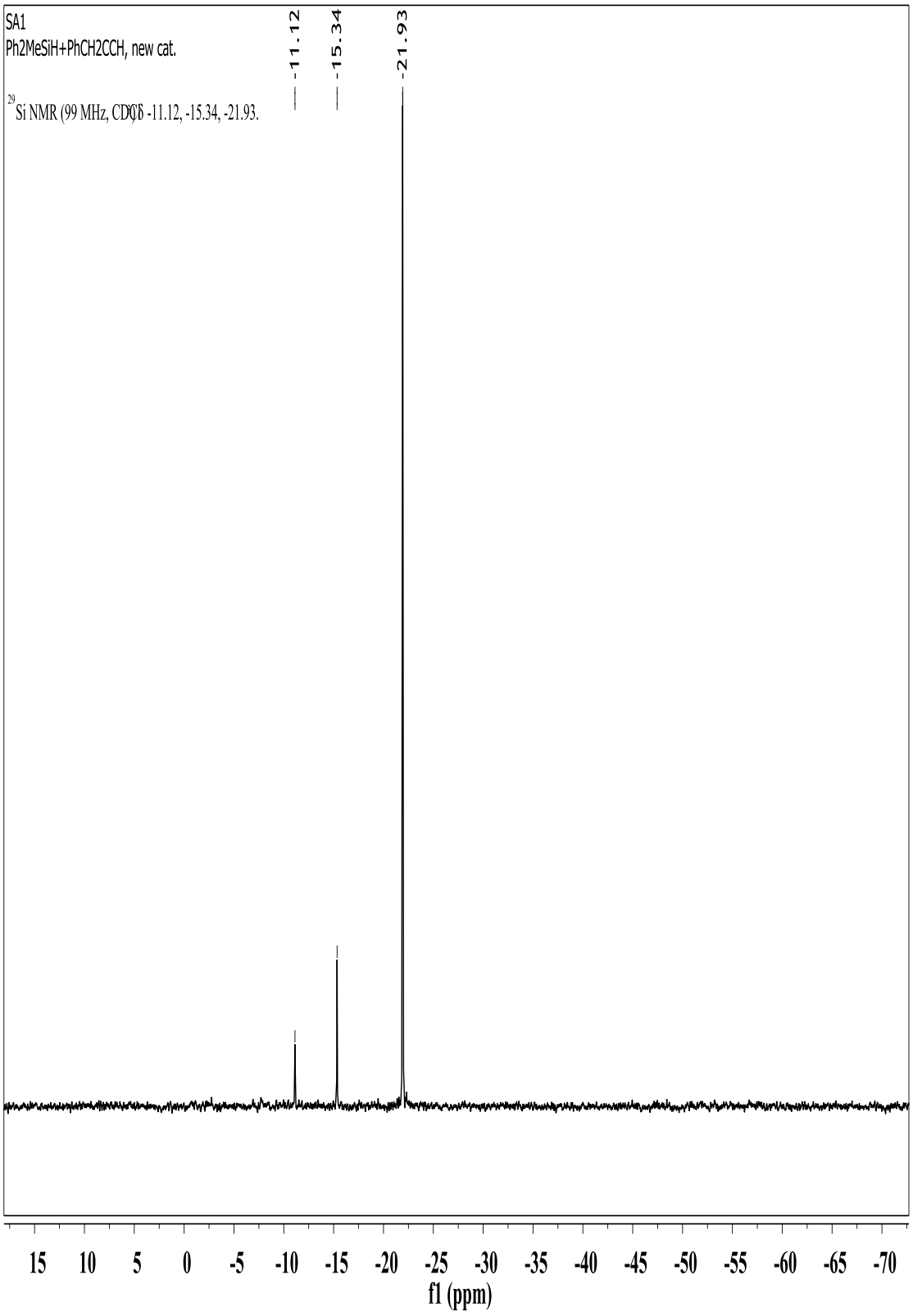

Appendix I.101. $^{29}Si\{^{1}H\}$ NMR spectrum of the product from hydrosilylation reaction of methyldiphenylsilane (S1) and 3-phenyl-1-propyne in the presence of (1a).

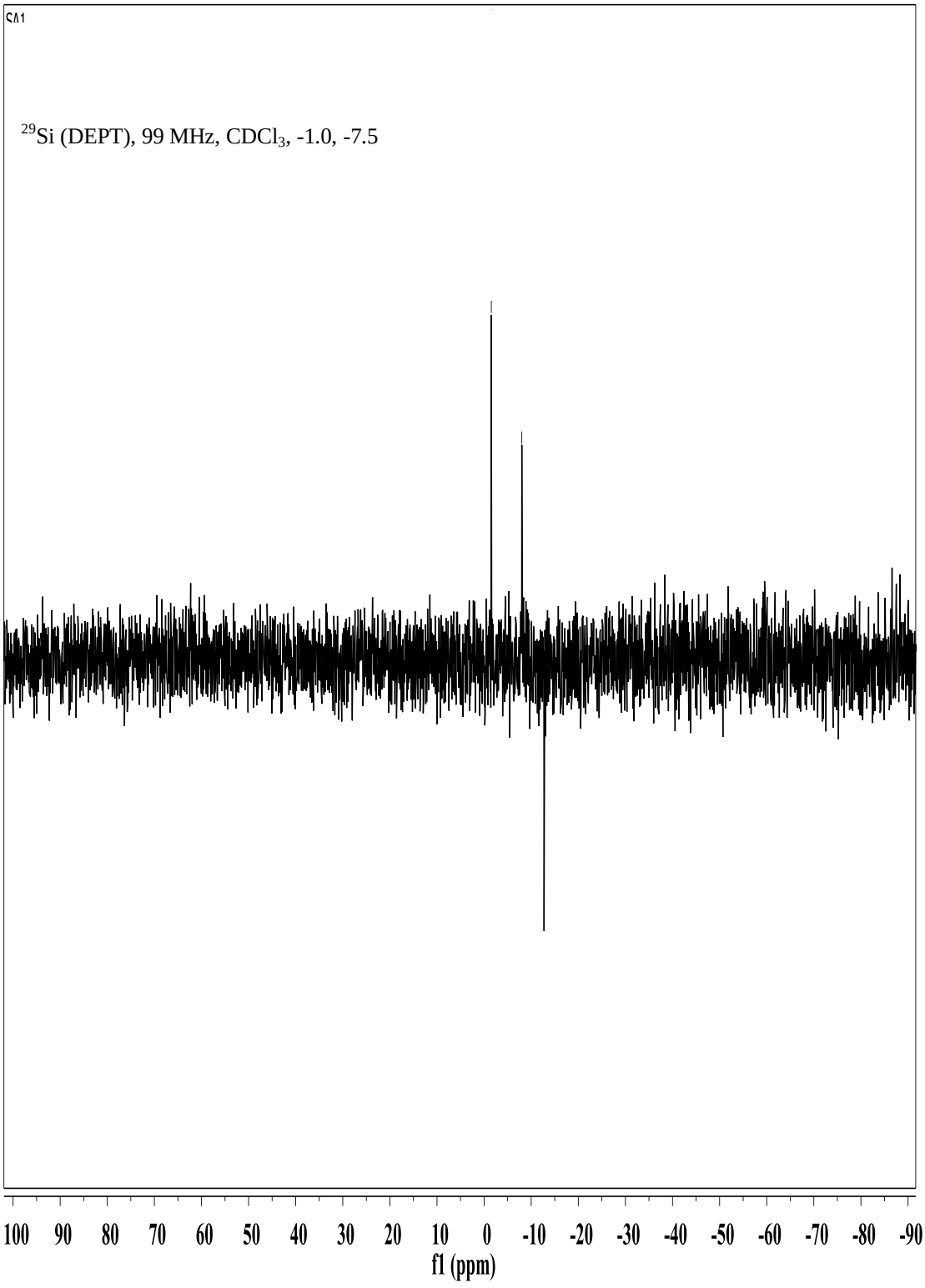

Appendix I.102. $^{29}Si\{^{1}H\}$ NMR spectrum of the product from hydrosilylation reaction of 1-hydrido-1-methyl(tetraphenyl)silole (S7) and trimethylsilylacetylene (A2) in the presence of (1a).

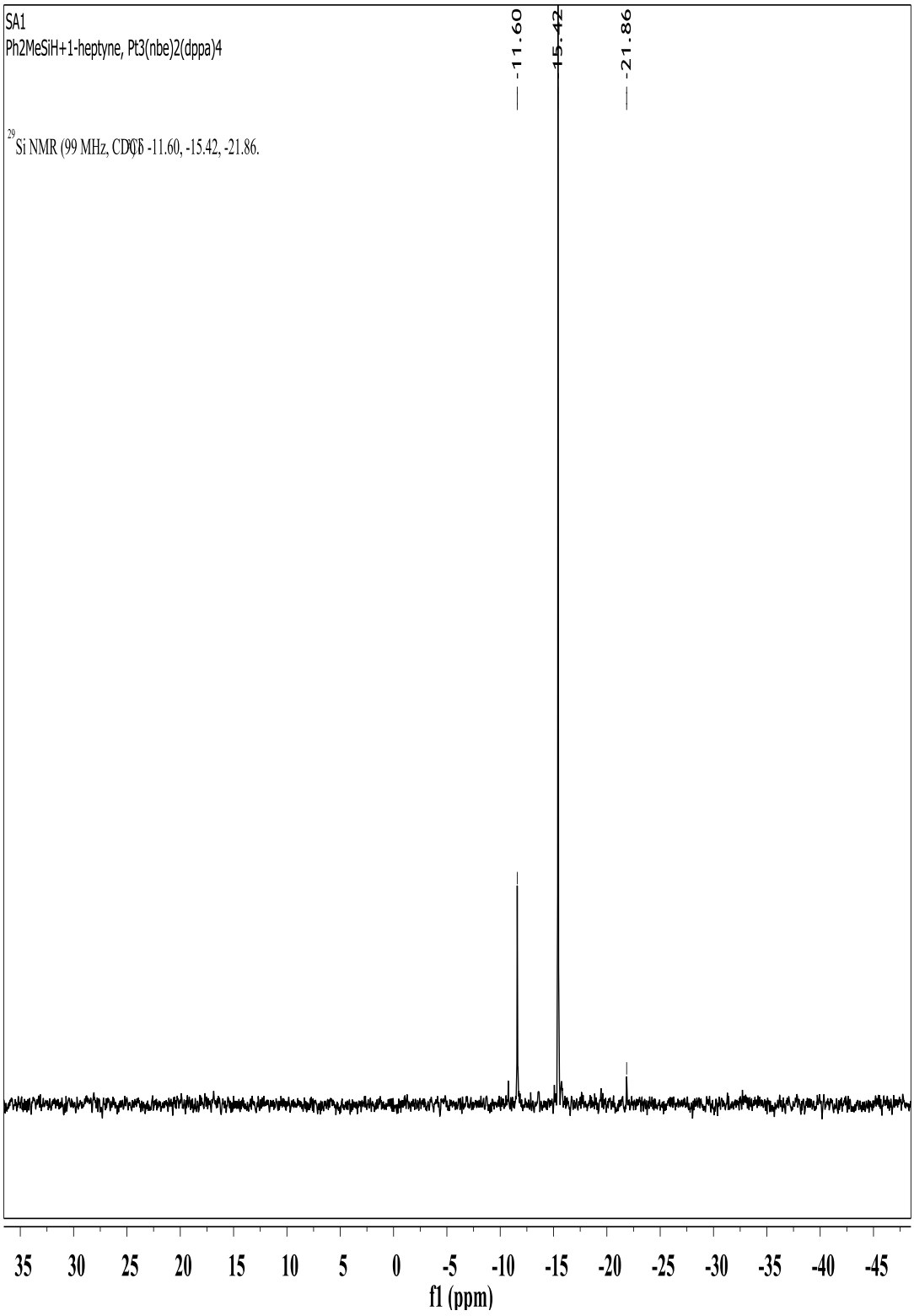

Appendix I.103. $^{29}Si\{^{1}H\}$ NMR spectrum of the product from hydrosilylation reaction of methyldiphenylsilane (S1) and 1-heptyne (A1) in the presence of (B2).

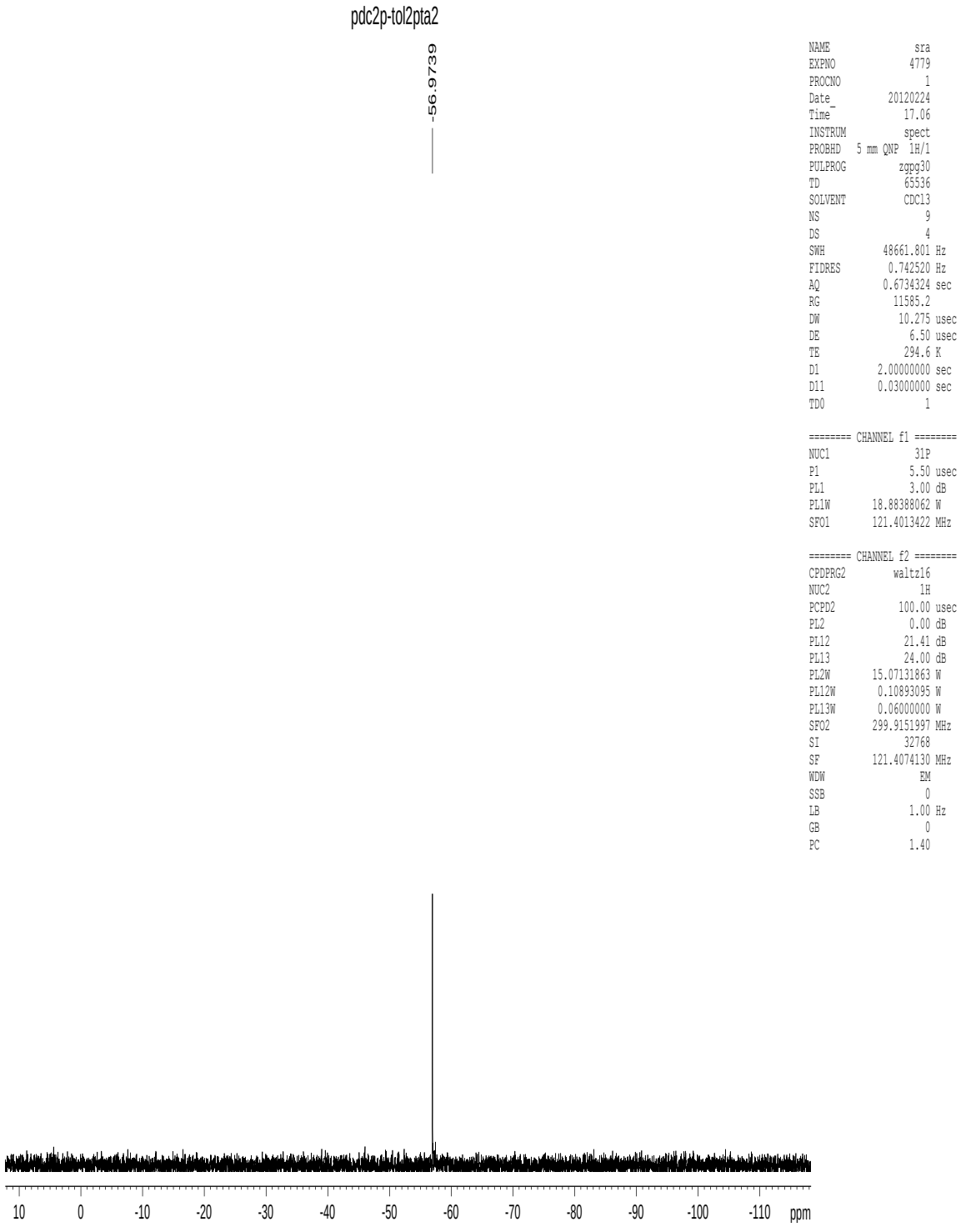

Appendix I.104. $^{31}P\{^{1}H\}$ NMR spectrum of trans-[Pd{C_2(p-tol)}$_2$(PTA)$_2$], 17.

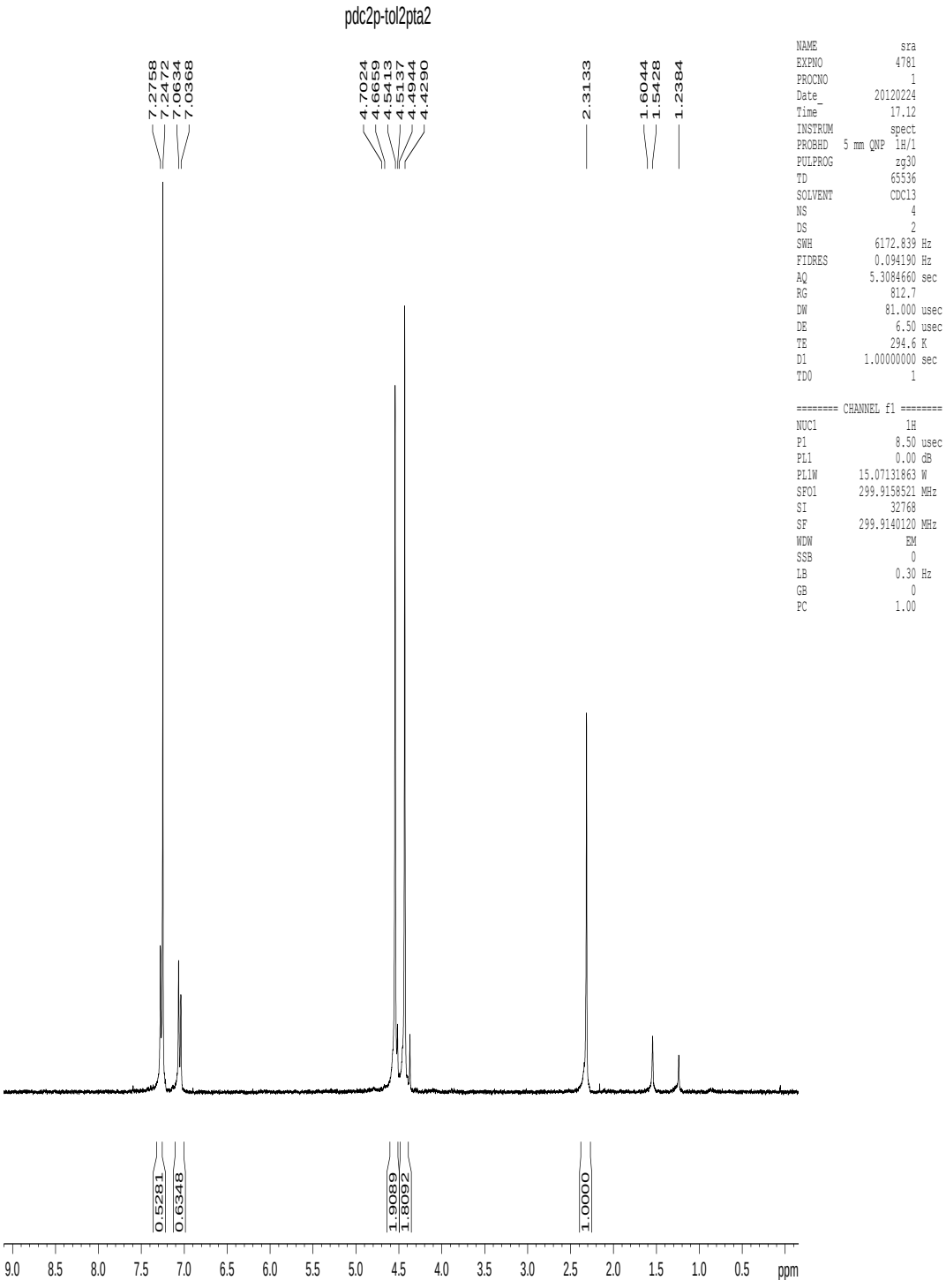

Appendix I.105. ^{1}H NMR spectrum of trans-[Pd{C_2(p-tol)}$_2$($PTA)_2$], 17.

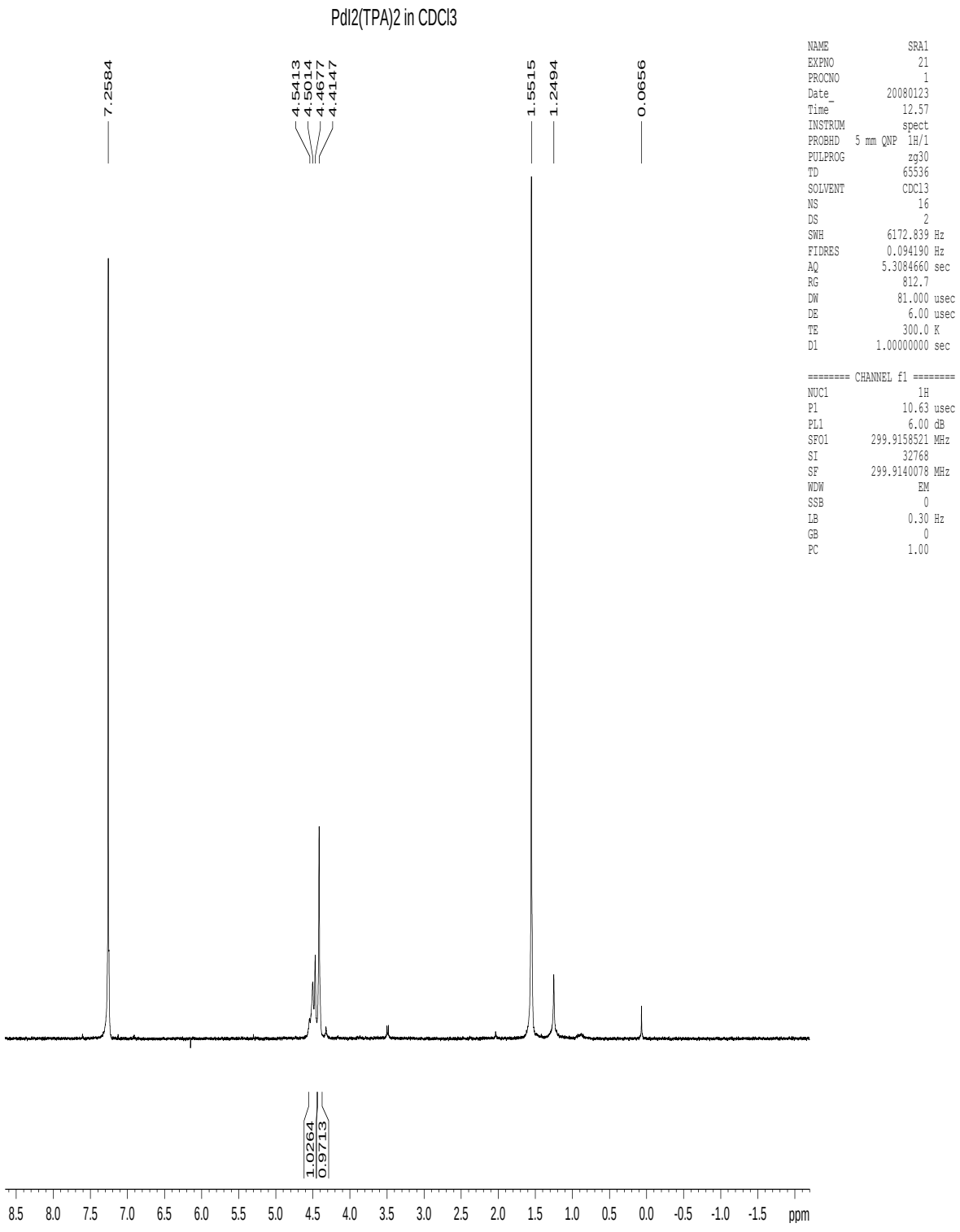

Appendix I.106. ^{1}H NMR spectrum of trans-PdI$_2$(PTA)$_2$, 32.

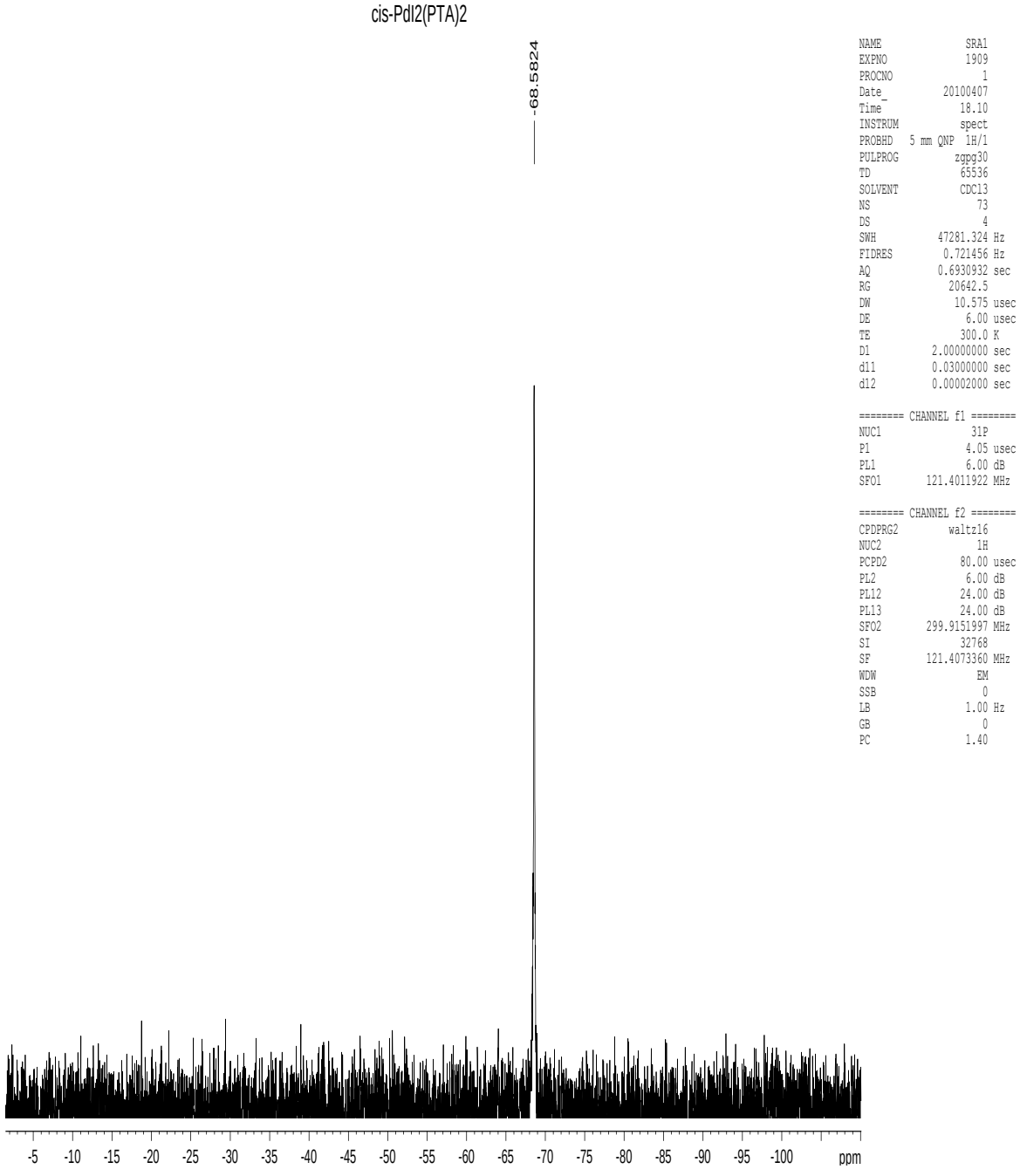

Appendix I.107. $^{31}P\{^{1}H\}$ NMR spectrum of trans-$PdI_2(PTA)_2$, 32.

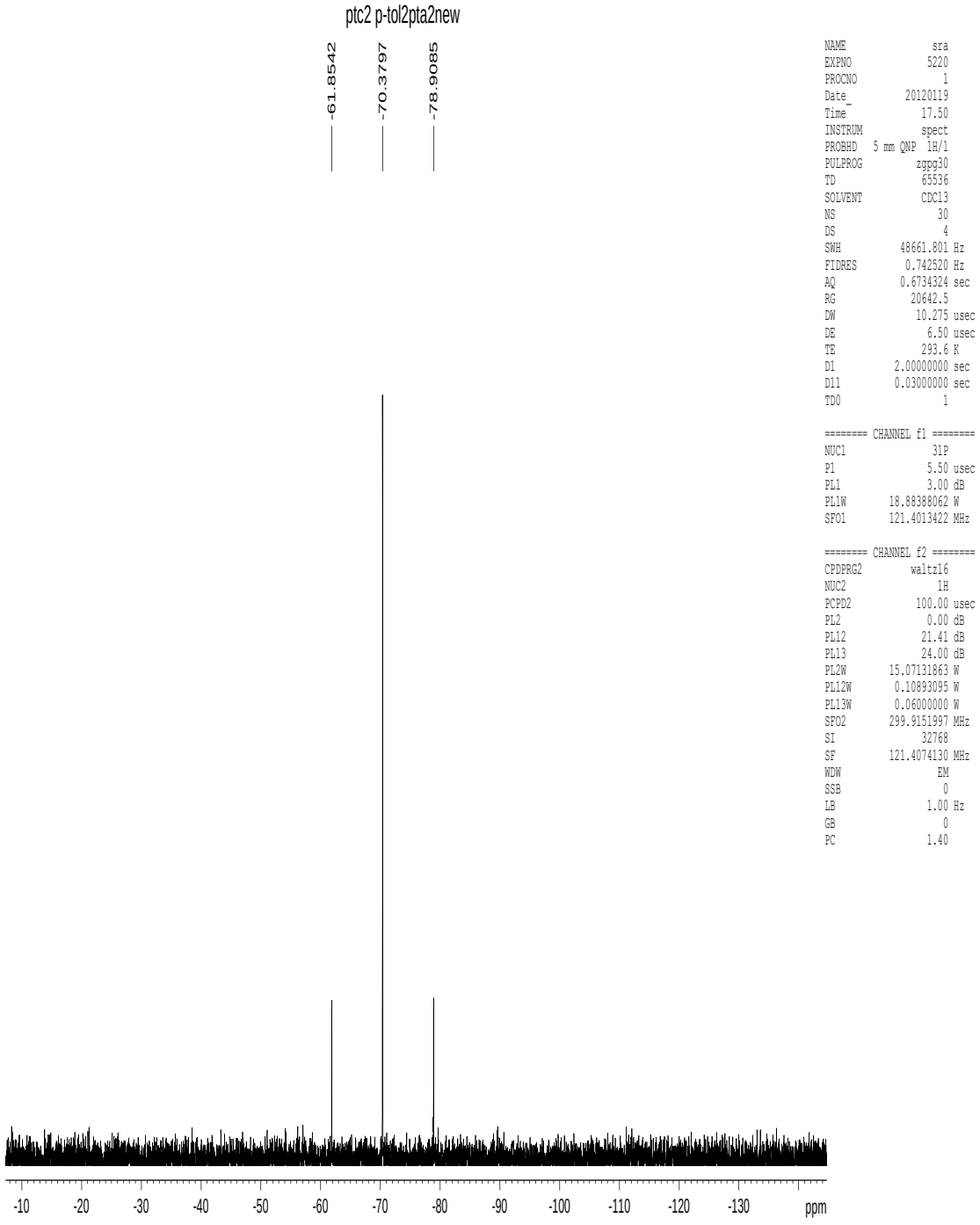

Appendix I.108. $^{31}P\{^{1}H\}$ NMR spectrum of cis-[Pt{C_2(p-tol)}$_2$($PTA)_2$], 16.

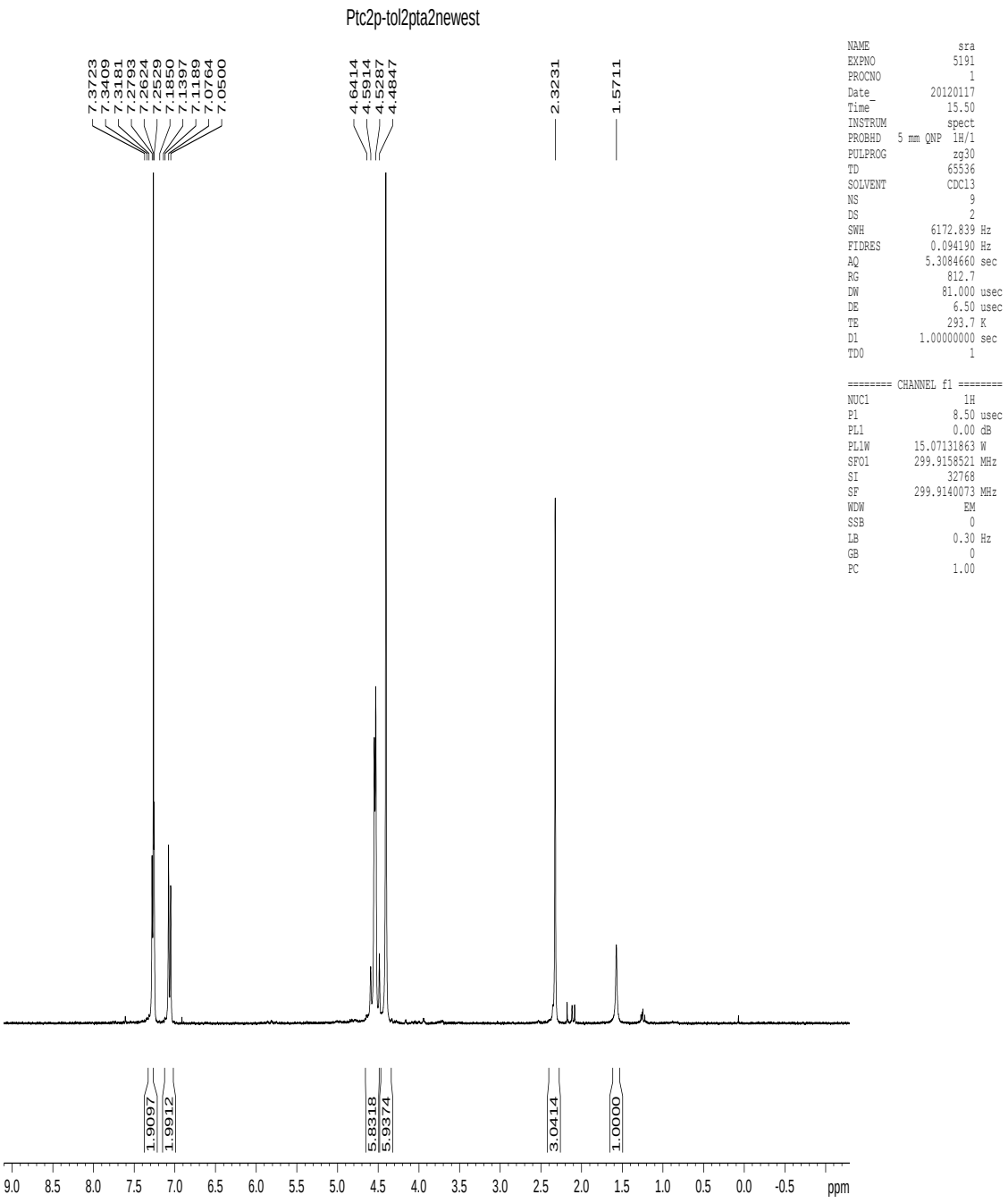

Appendix I.109. ^{1}H NMR spectrum of cis-[Pt{C$_2$(p-tol)}$_2$(PTA)$_2$], 16.

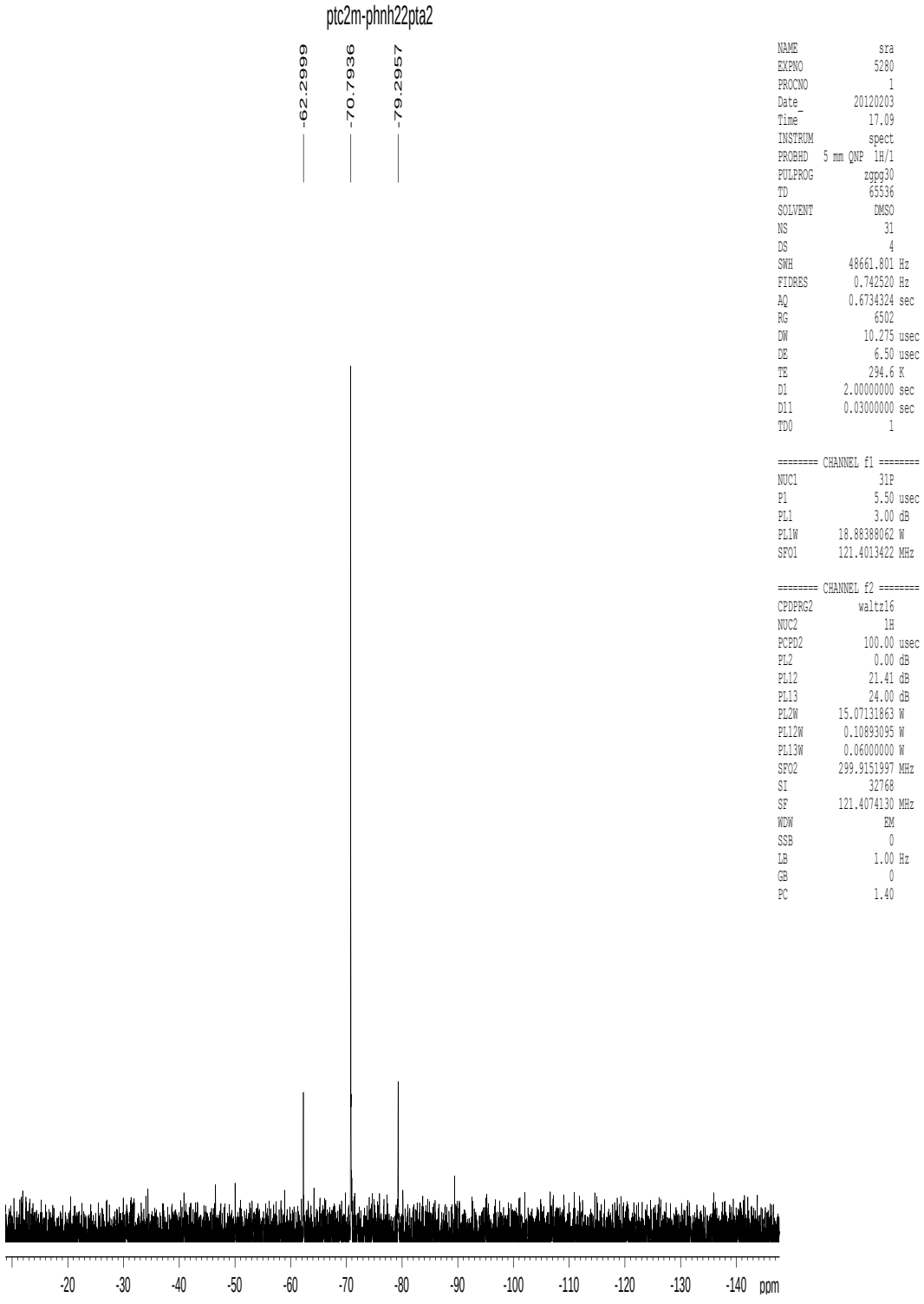

Appendix I.110. $^{31}P\{^{1}H\}$ NMR spectrum of cis-[Pt{C_2(m-$C_6H_4NH_2$)}$_2$(PTA)$_2$], 20.

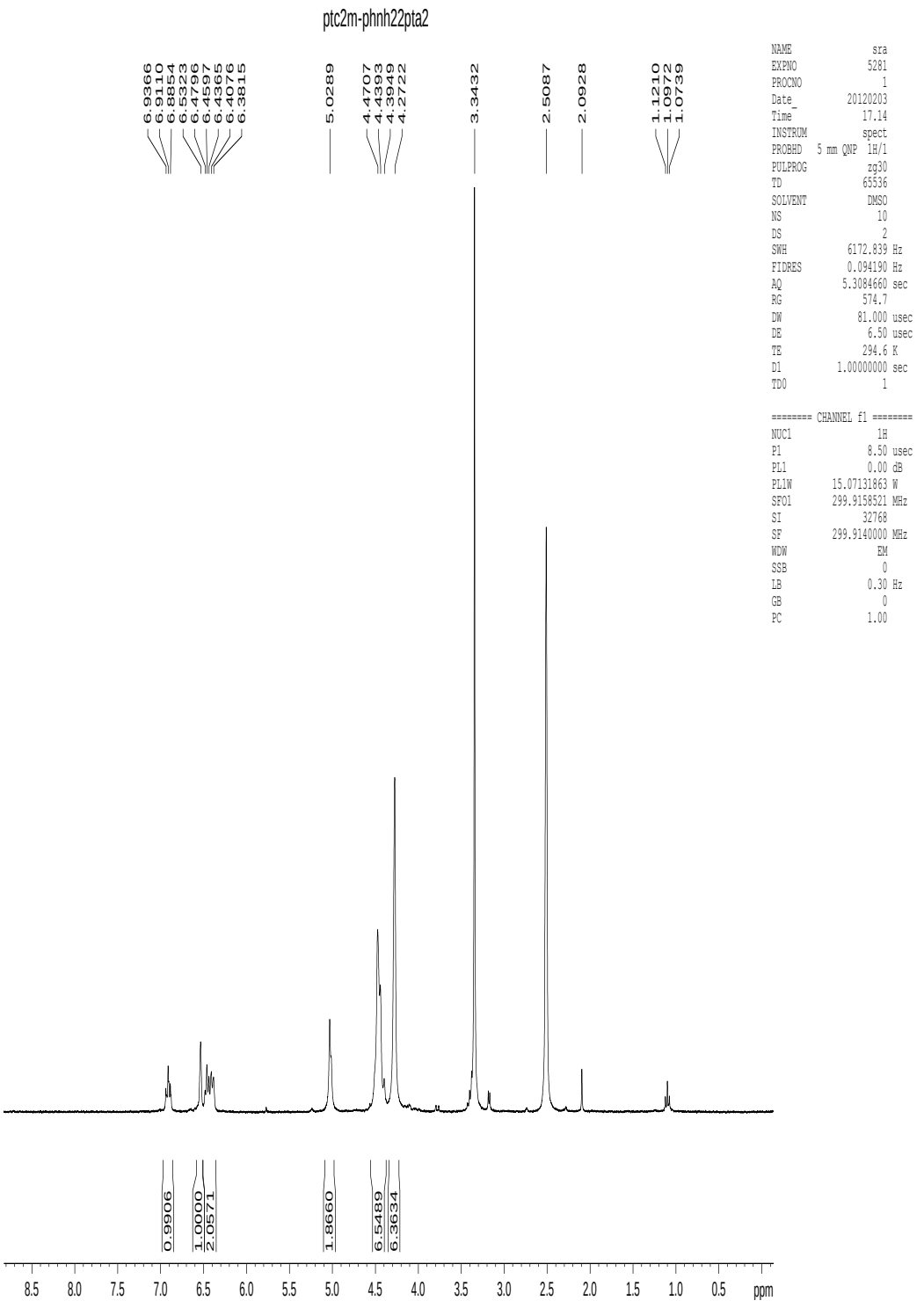

Appendix I.111. ^{1}H NMR spectrum of cis-[Pt{C_2(m-$C_6H_4NH_2$)}$_2$($PTA)_2$], 20.

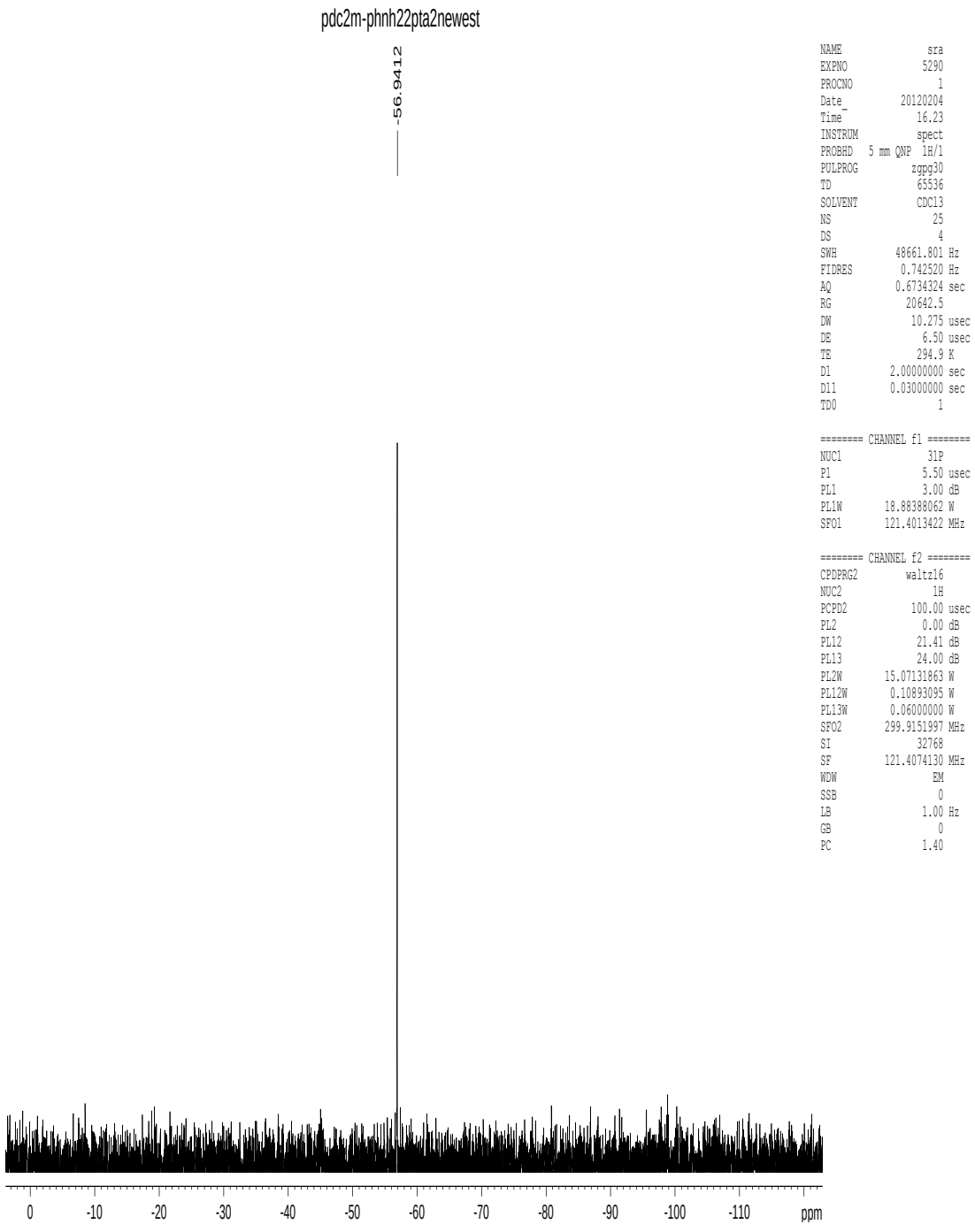

Appendix I.112. $^{31}P\{^{1}H\}$ NMR spectrum of trans-[Pd{C_2(m-$C_6H_4NH_2$)}$_2$(PTA)$_2$], 23.

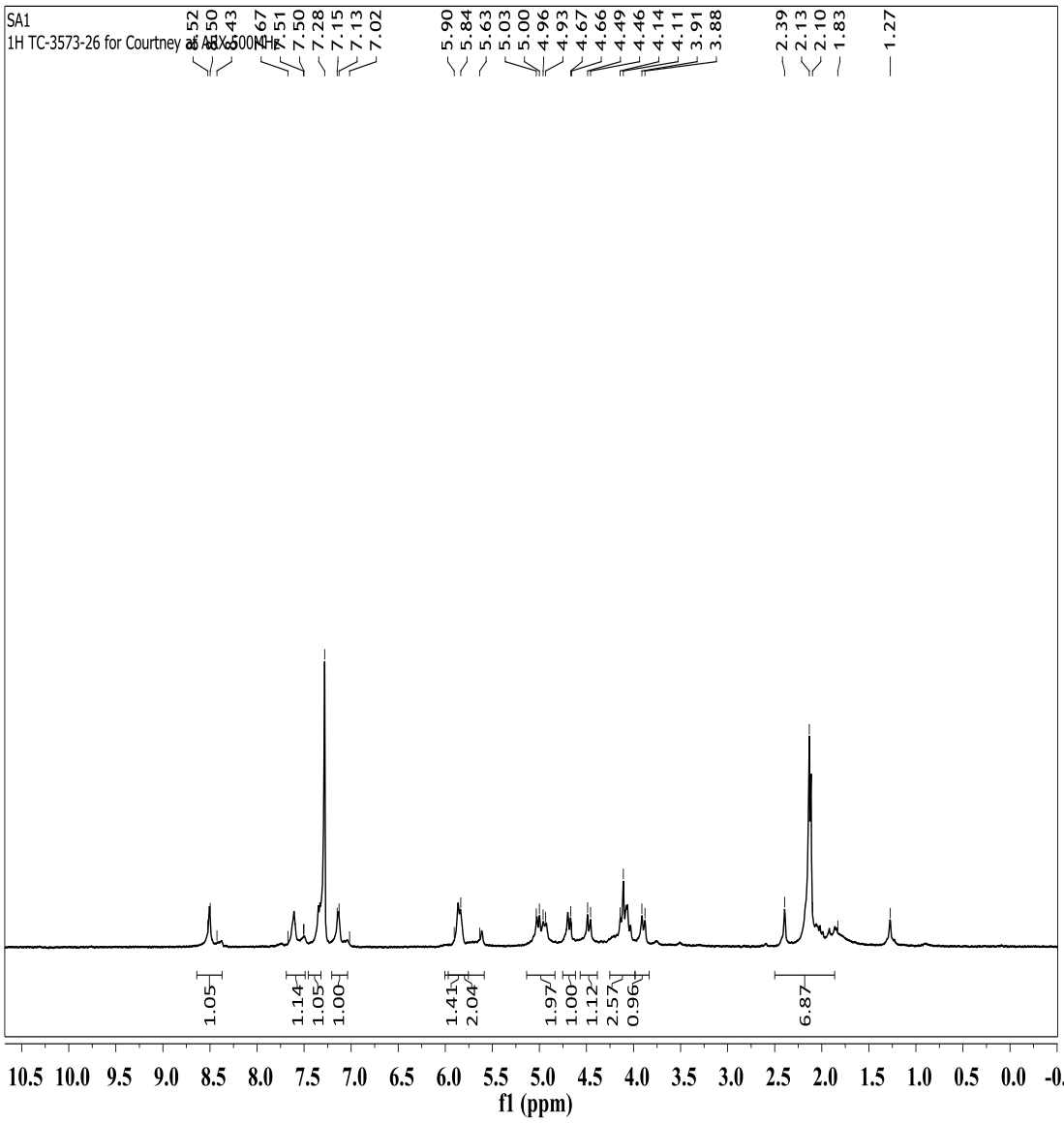

Appendix I.113. ^{1}H NMR spectrum of trans-[Pt{C_2(o-py)}$_2$(DAPTA)$_2$], 28.

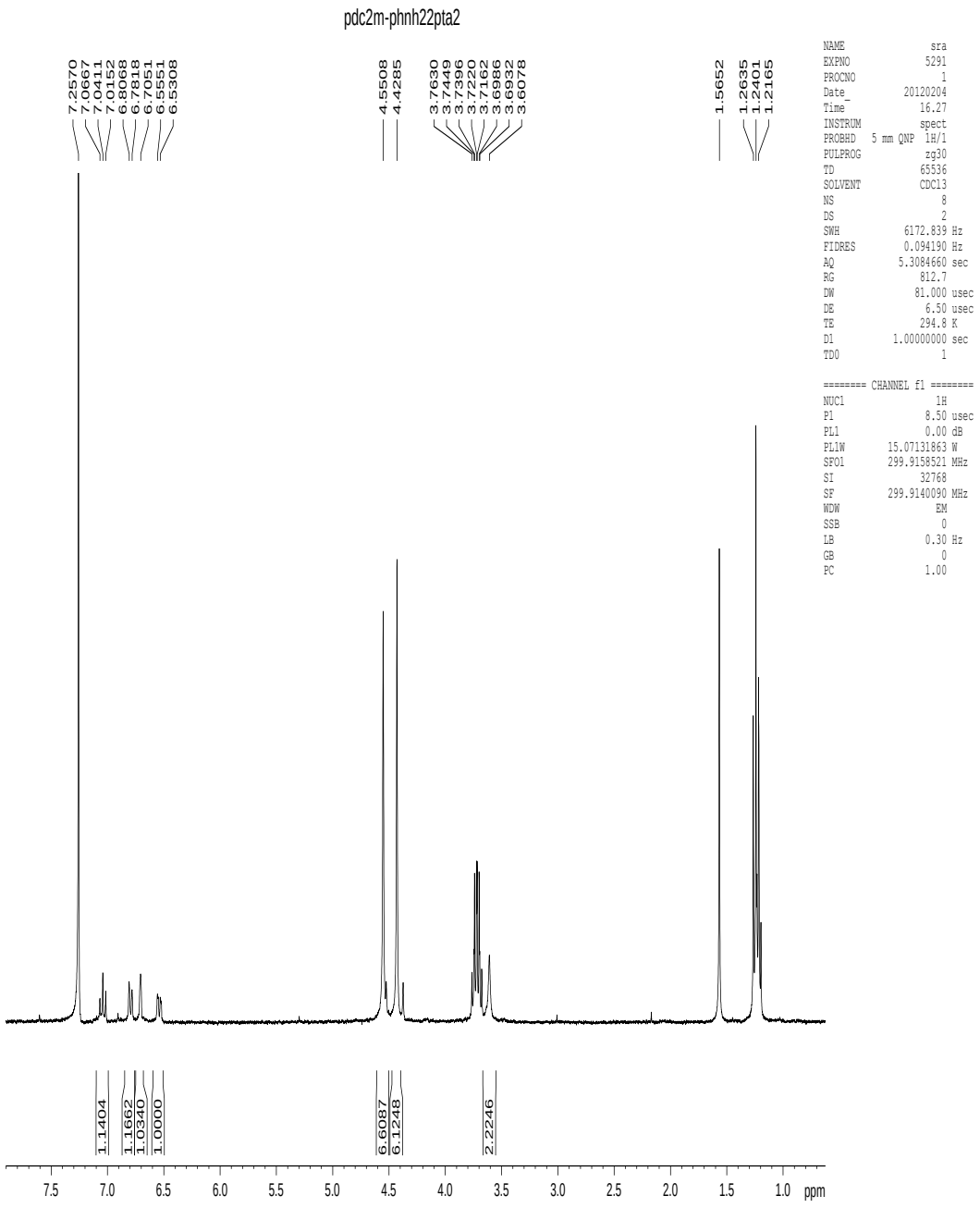

Appendix I.114. ^{1}H NMR spectrum of trans-[Pd{C$_2$(m-C$_6$H$_4$NH$_2$)}$_2$(PTA)$_2$], 23.

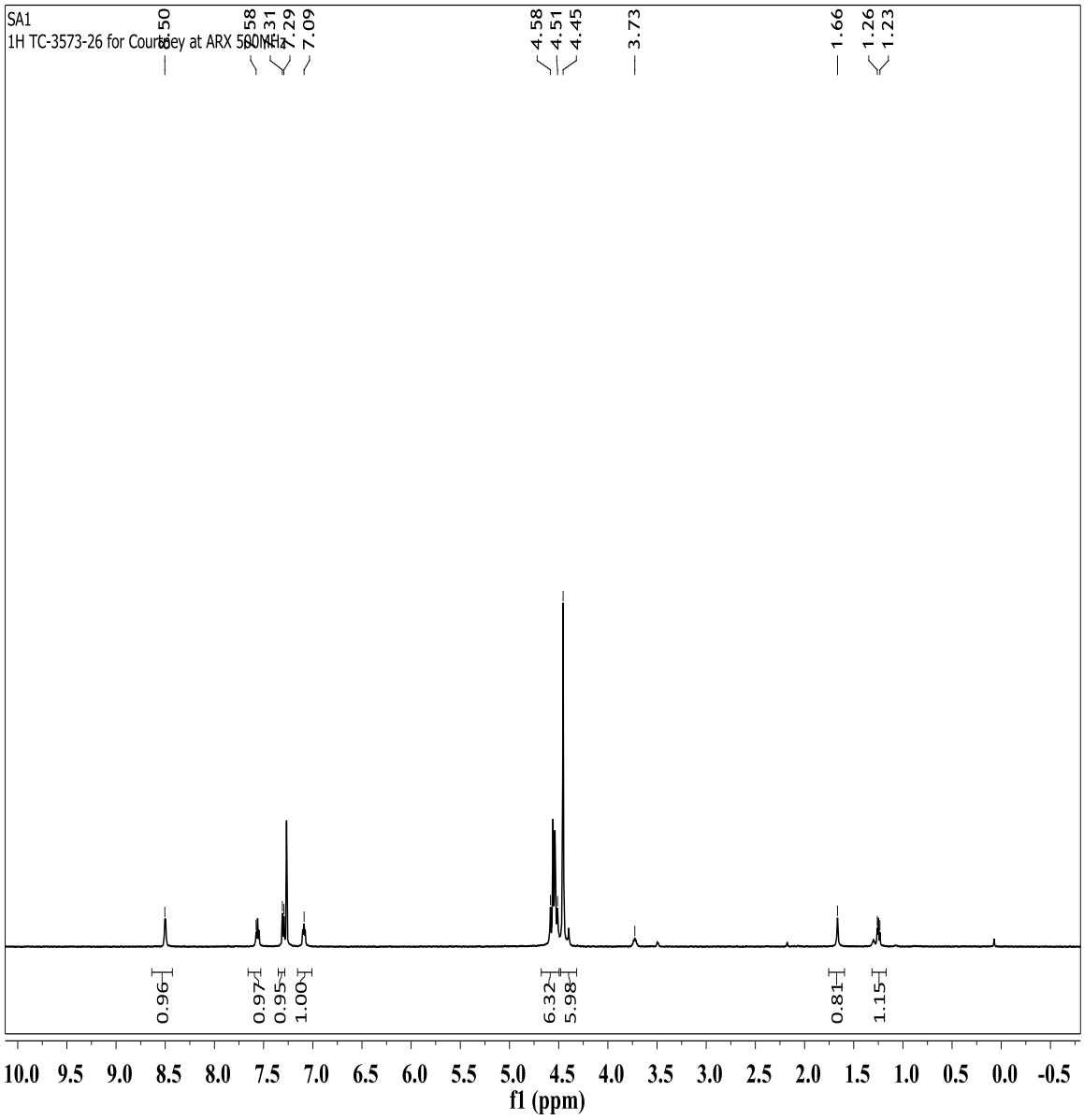

Appendix I.115. ^{1}H NMR spectrum of trans-[Pd{C_2(o-py)}$_2$(PTA)$_2$], 22.

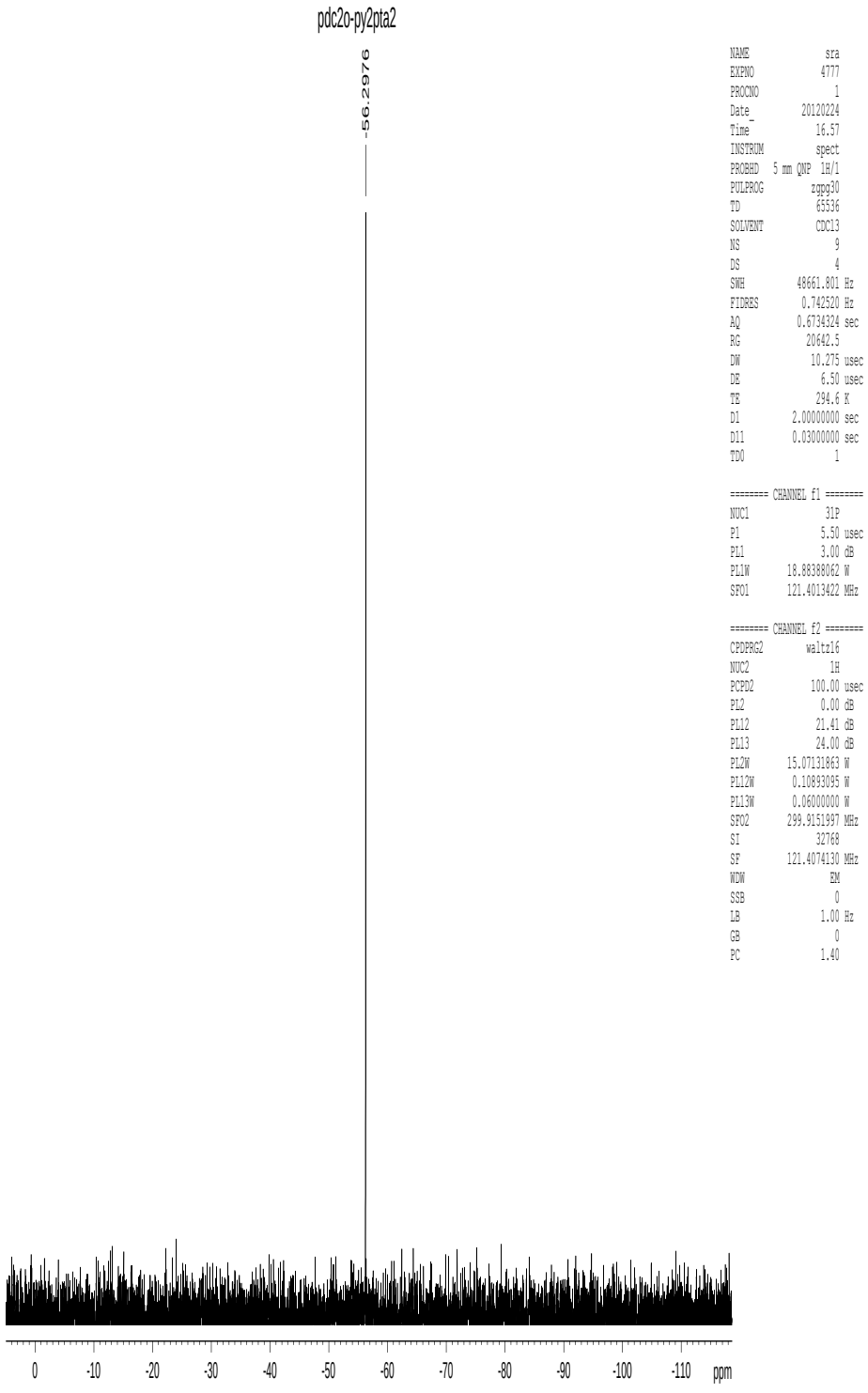

Appendix I.116. $^{31}P\{^{1}H\}$ NMR spectrum of trans-[Pd{C_2(o-py)}$_2$($PTA)_2$], 22.

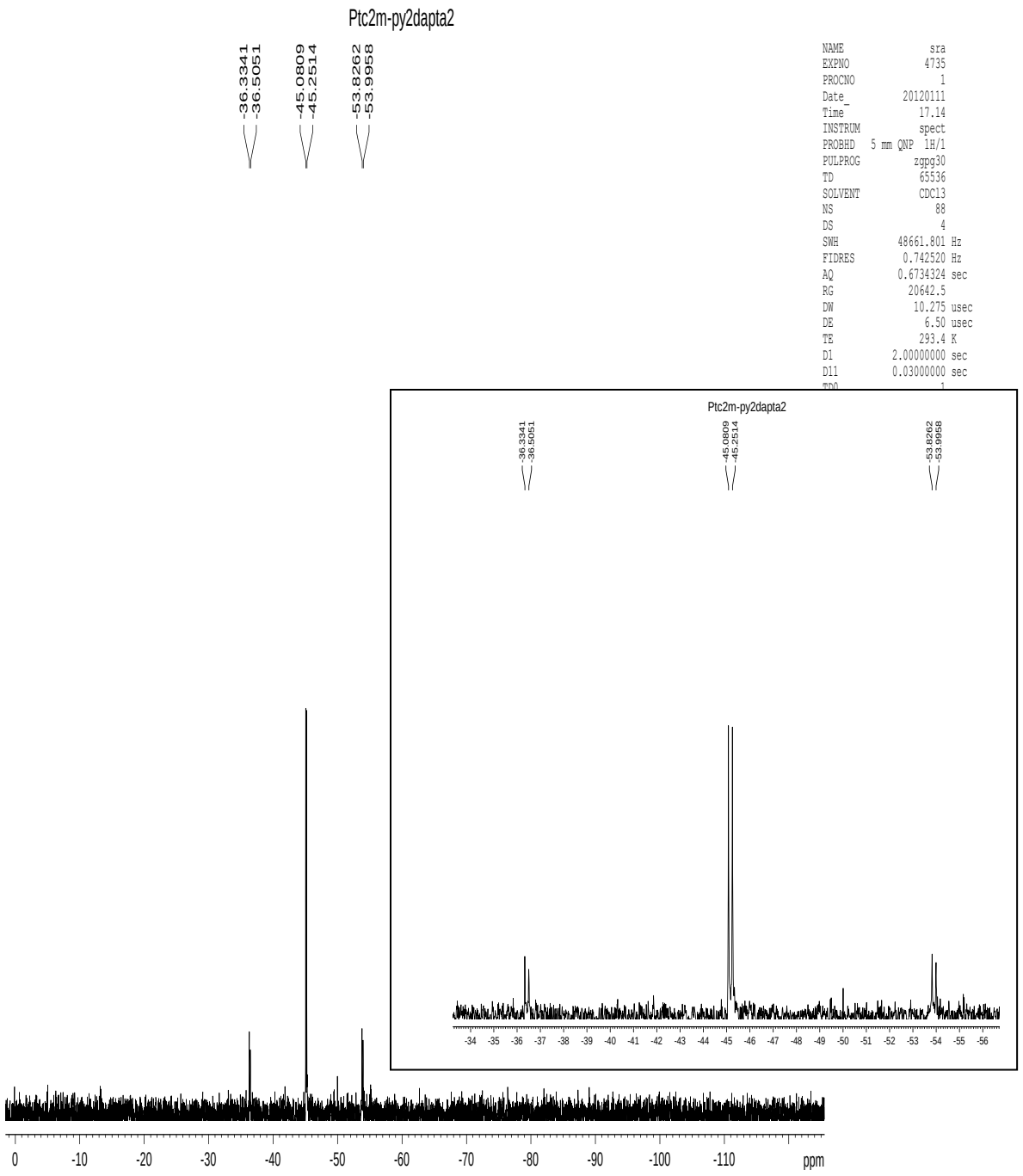

Appendix I.117. $^{31}P\{^{1}H\}$ NMR spectrum of trans-[Pt{C_2(m-py)}$_2$(DAPTA)$_2$], 27.

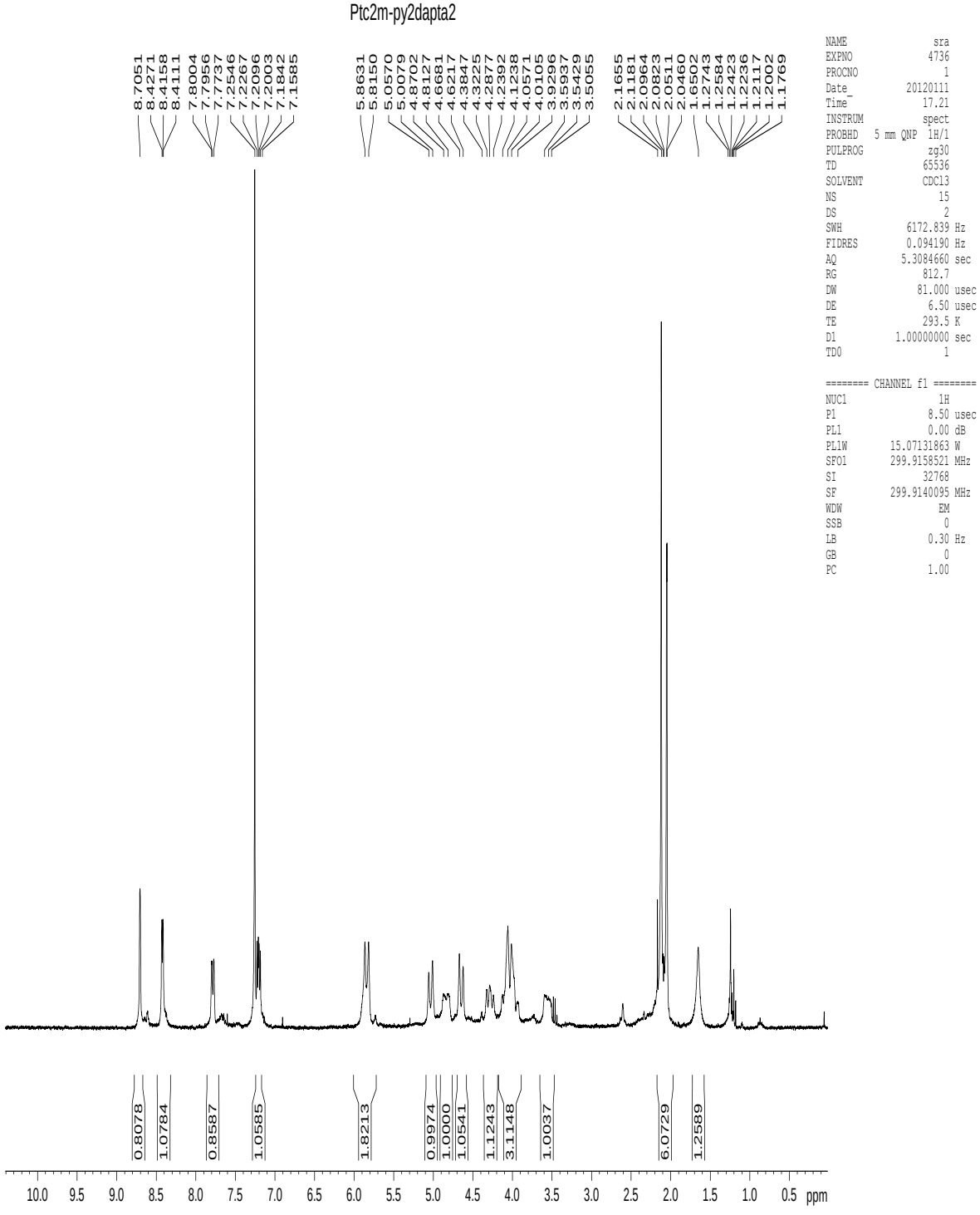

Appendix I.118. ^{1}H NMR spectrum of trans-[Pt{C_2(m-py)}$_2$(DAPTA)$_2$], 27.

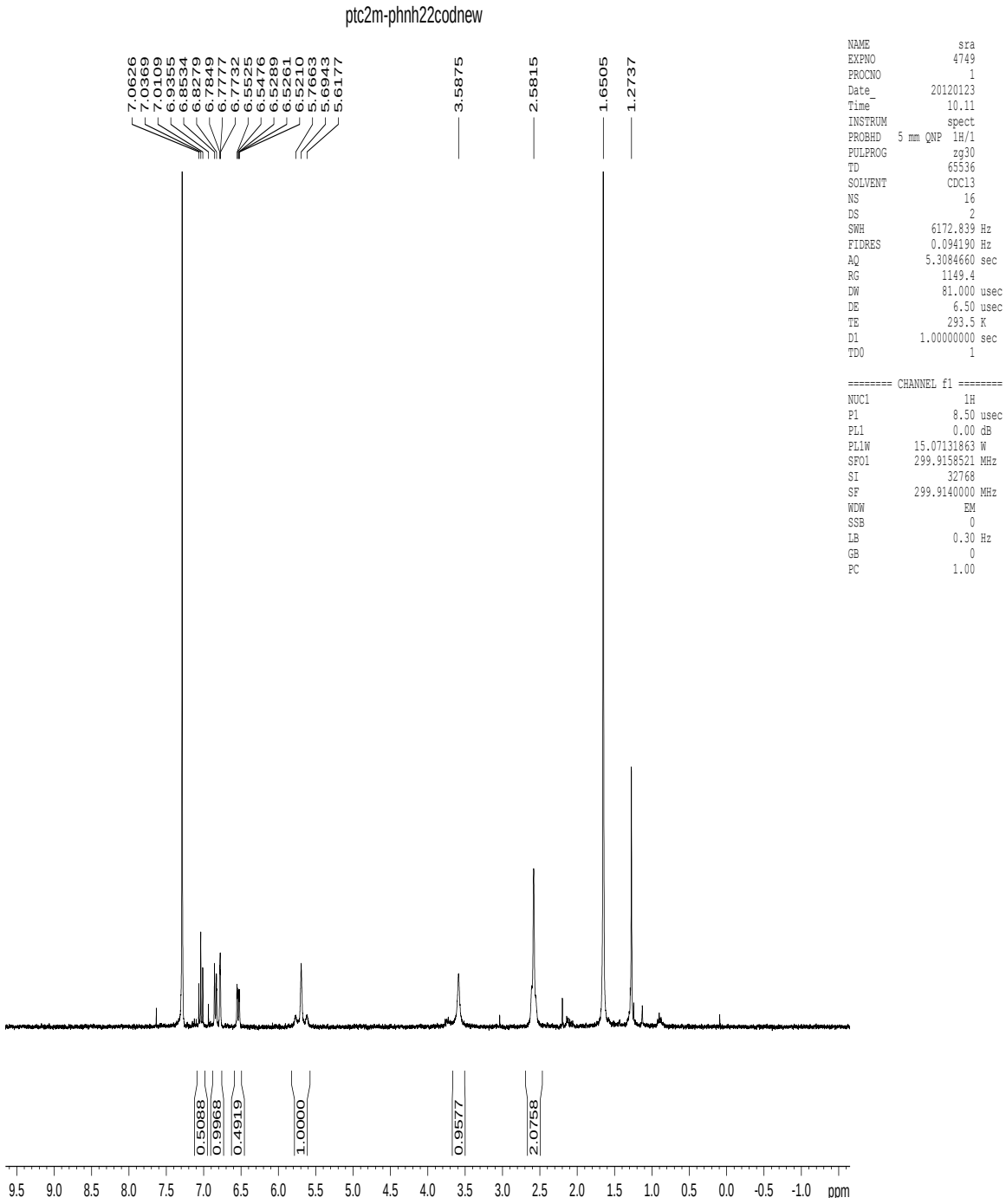

Appendix I.119. ^{1}H NMR spectrum of [Pt{C_2(m-$C_6H_4NH_2$)}$_2$(COD), C2.

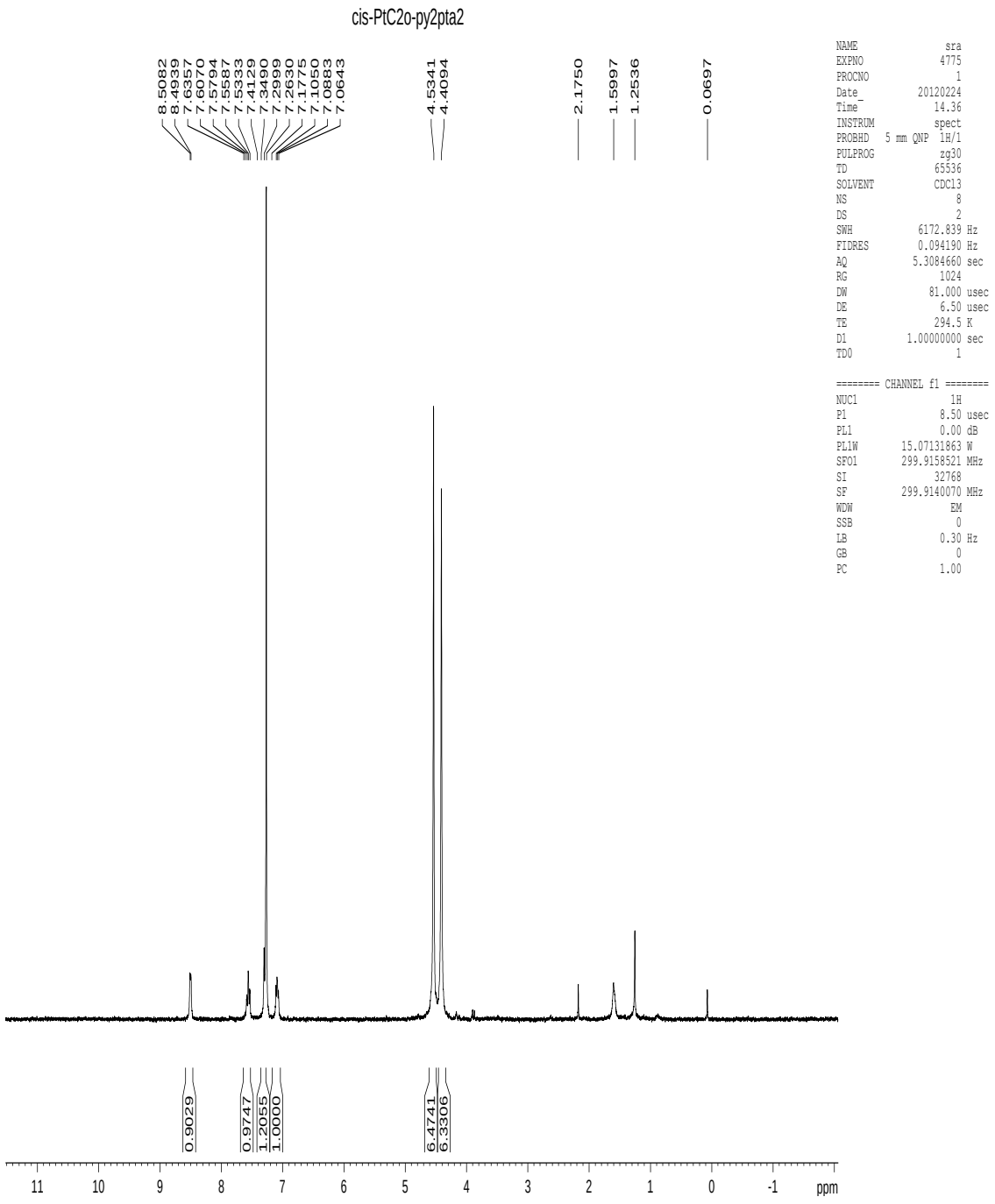

Appendix I.120. ^{1}H NMR spectrum of cis-[Pt{C$_2$(o-py)}$_2$(PTA)$_2$], 19a.

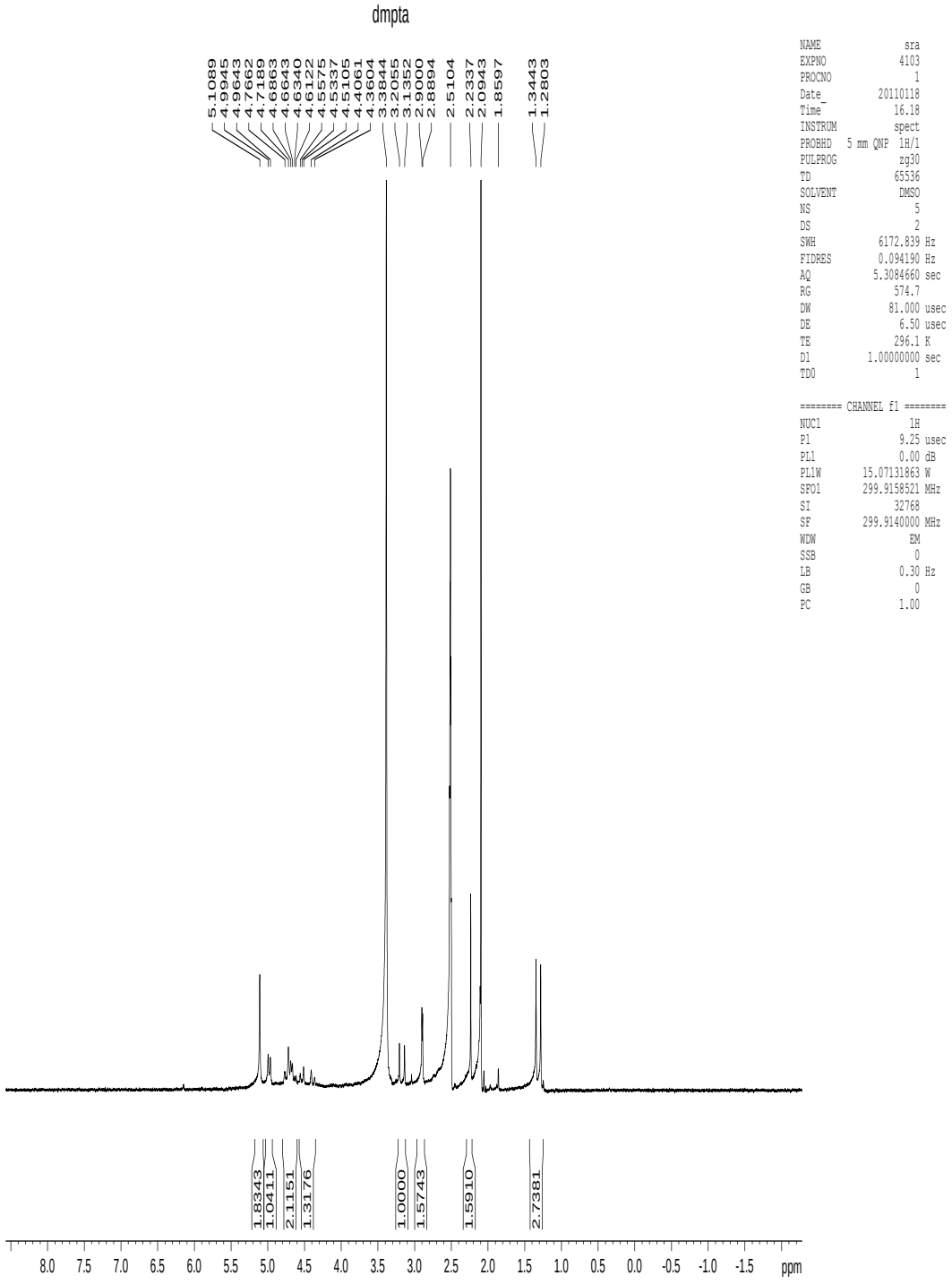

Appendix I.121a. ^{1}H NMR spectrum of ipac mPTA (L1) triflate.

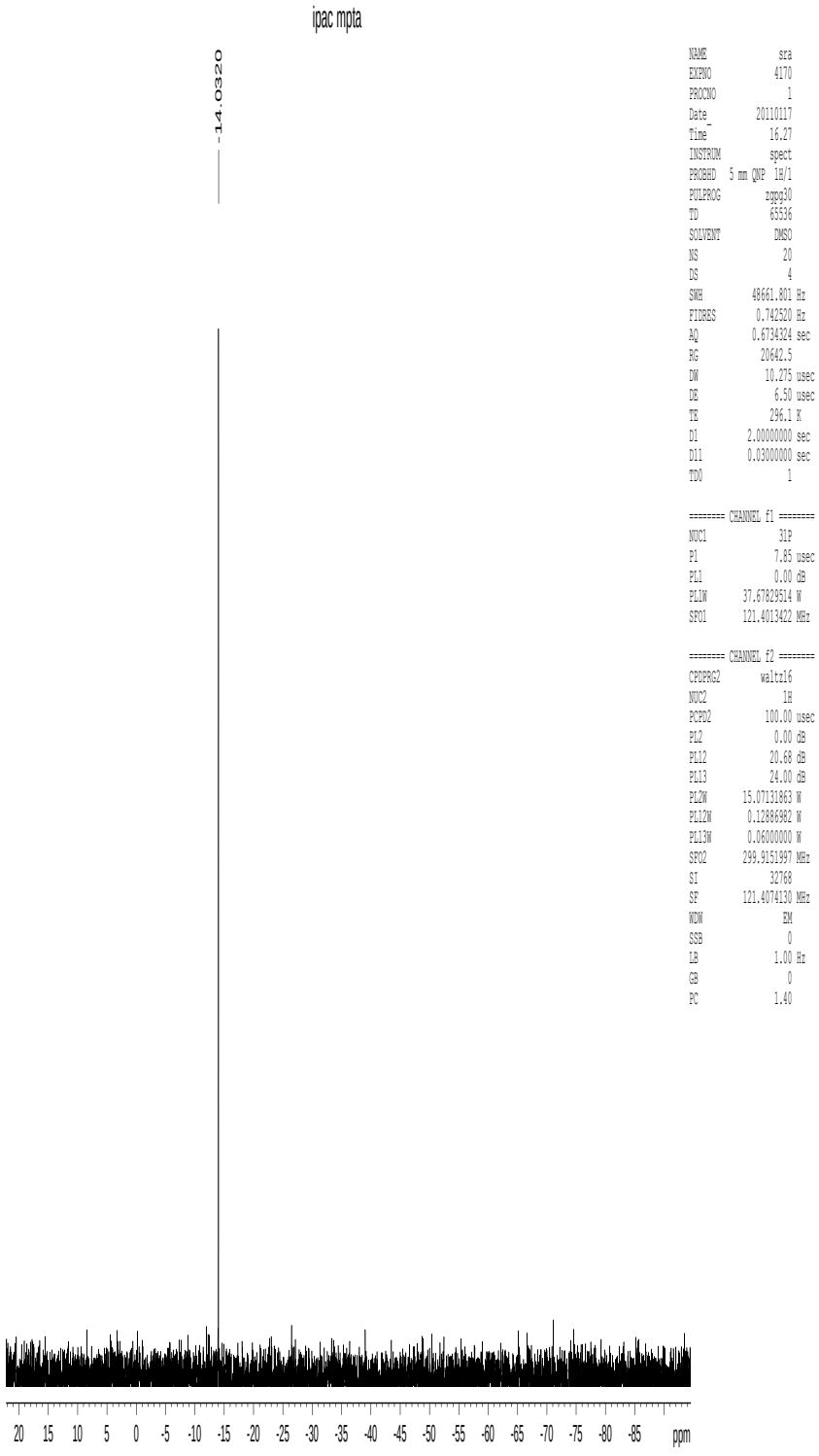

Appendix I.121b. $^{31}P\{^{1}H\}$ NMR spectrum of ipac mPTA, L1.

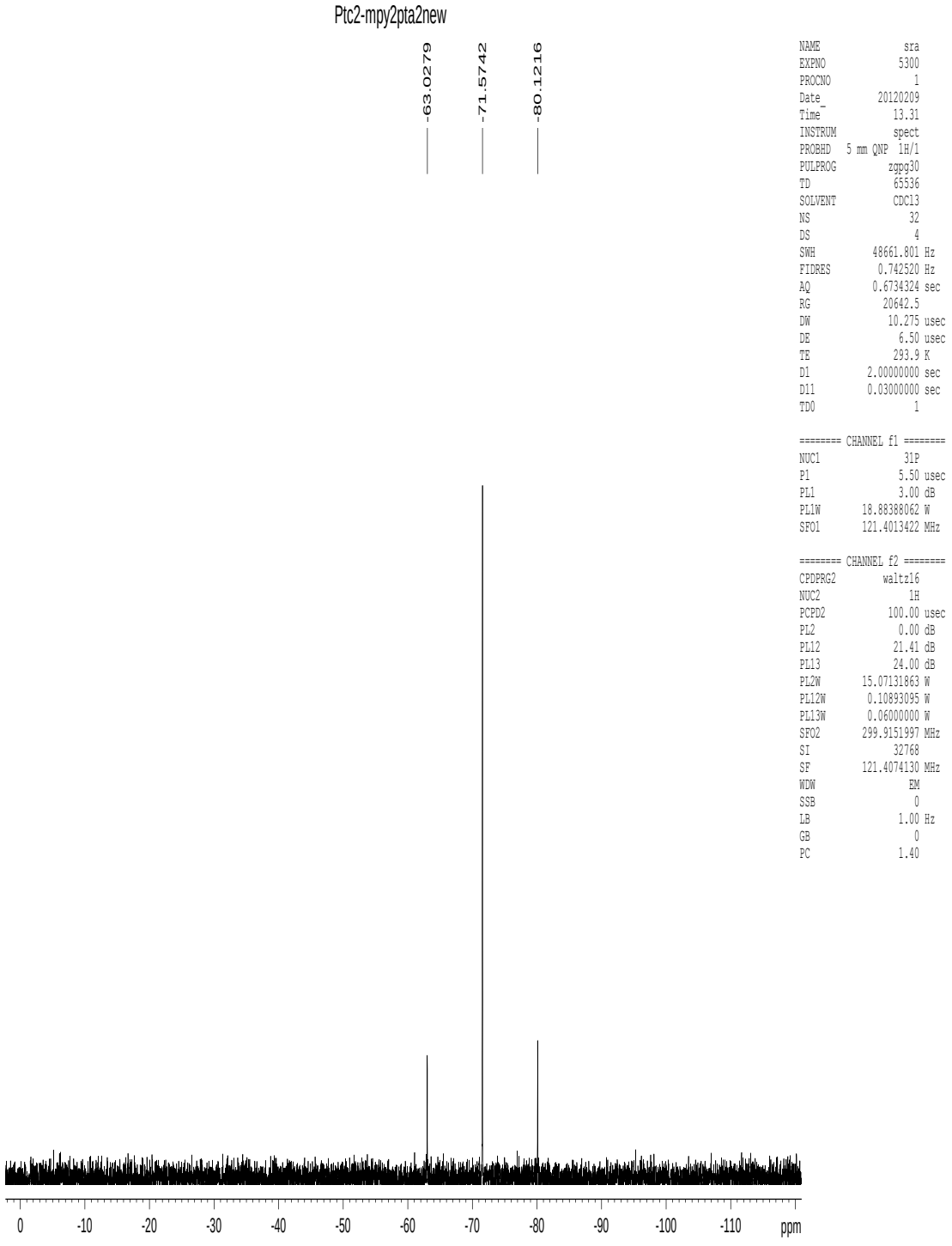

NAME	sra
EXPNO	5300
PROCNO	1
Date_	20120209
Time	13.31
INSTRUM	spect
PROBHD	5 mm QNP 1H/1
PULPROG	zgpg30
TD	65536
SOLVENT	CDCl3
NS	32
DS	4
SWH	48661.801 Hz
FIDRES	0.742520 Hz
AQ	0.6734324 sec
RG	20642.5
DW	10.275 usec
DE	6.50 usec
TE	293.9 K
D1	2.00000000 sec
D11	0.03000000 sec
TD0	1
======== CHANNEL f1 ========	
NUC1	31P
P1	5.50 usec
PL1	3.00 dB
PL1W	18.88388062 W
SFO1	121.4013422 MHz
======== CHANNEL f2 ========	
CPDPRG2	waltz16
NUC2	1H
PCPD2	100.00 usec
PL2	0.00 dB
PL12	21.41 dB
PL13	24.00 dB
PL2W	15.07131863 W
PL12W	0.10893095 W
PL13W	0.06000000 W
SFO2	299.9151997 MHz
SI	32768
SF	121.4074130 MHz
WDW	EM
SSB	0
LB	1.00 Hz
GB	0
PC	1.40

Appendix I.122. $^{31}P\{^{1}H\}$ NMR spectrum of cis-[Pt{C_2(m-py)}$_2$(PTA)$_2$], 18a.

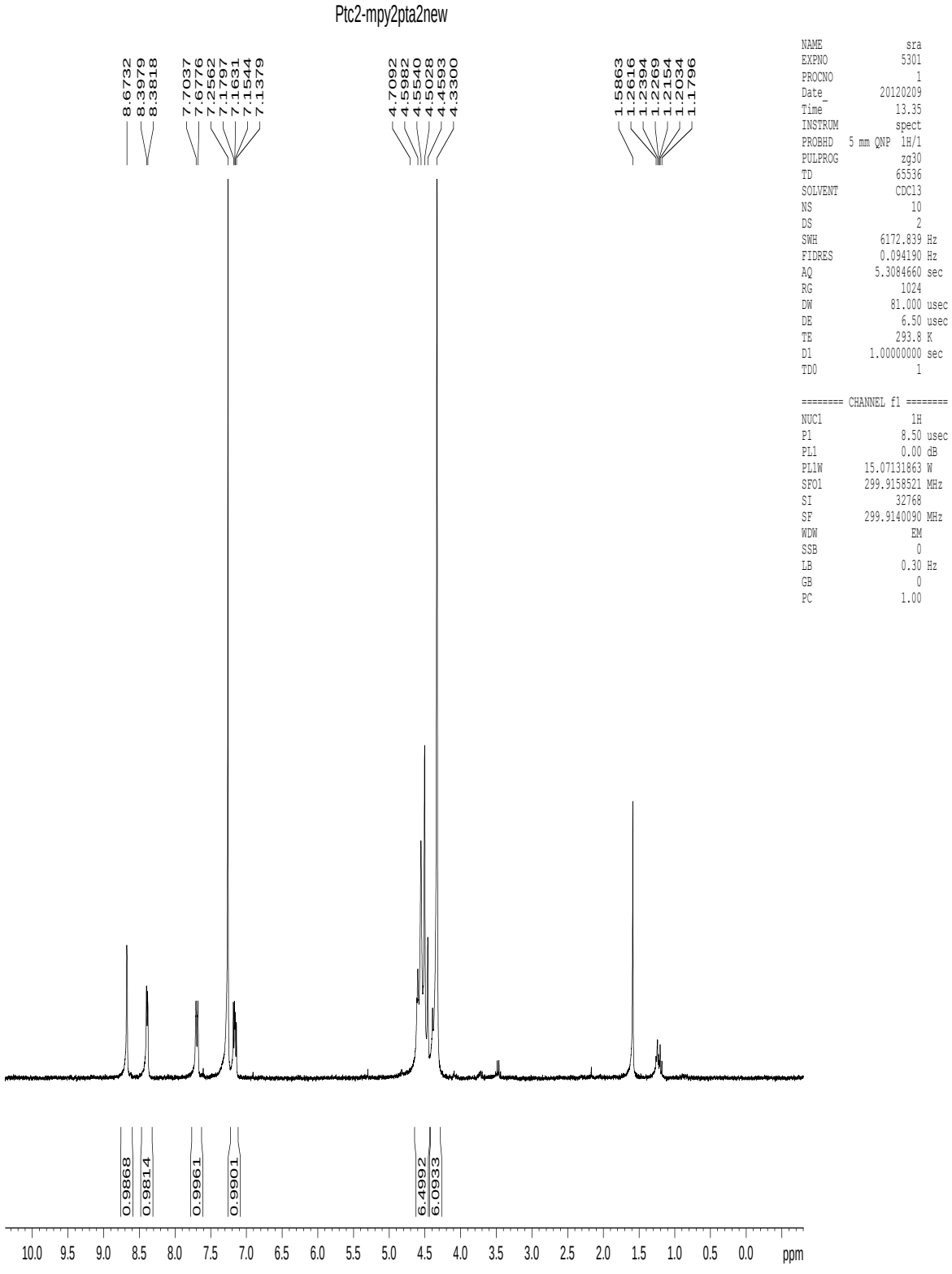

Appendix I.123. ^{1}H NMR spectrum of cis-[Pt{C_2(m-py)}$_2$($PTA)_2$], 18a.

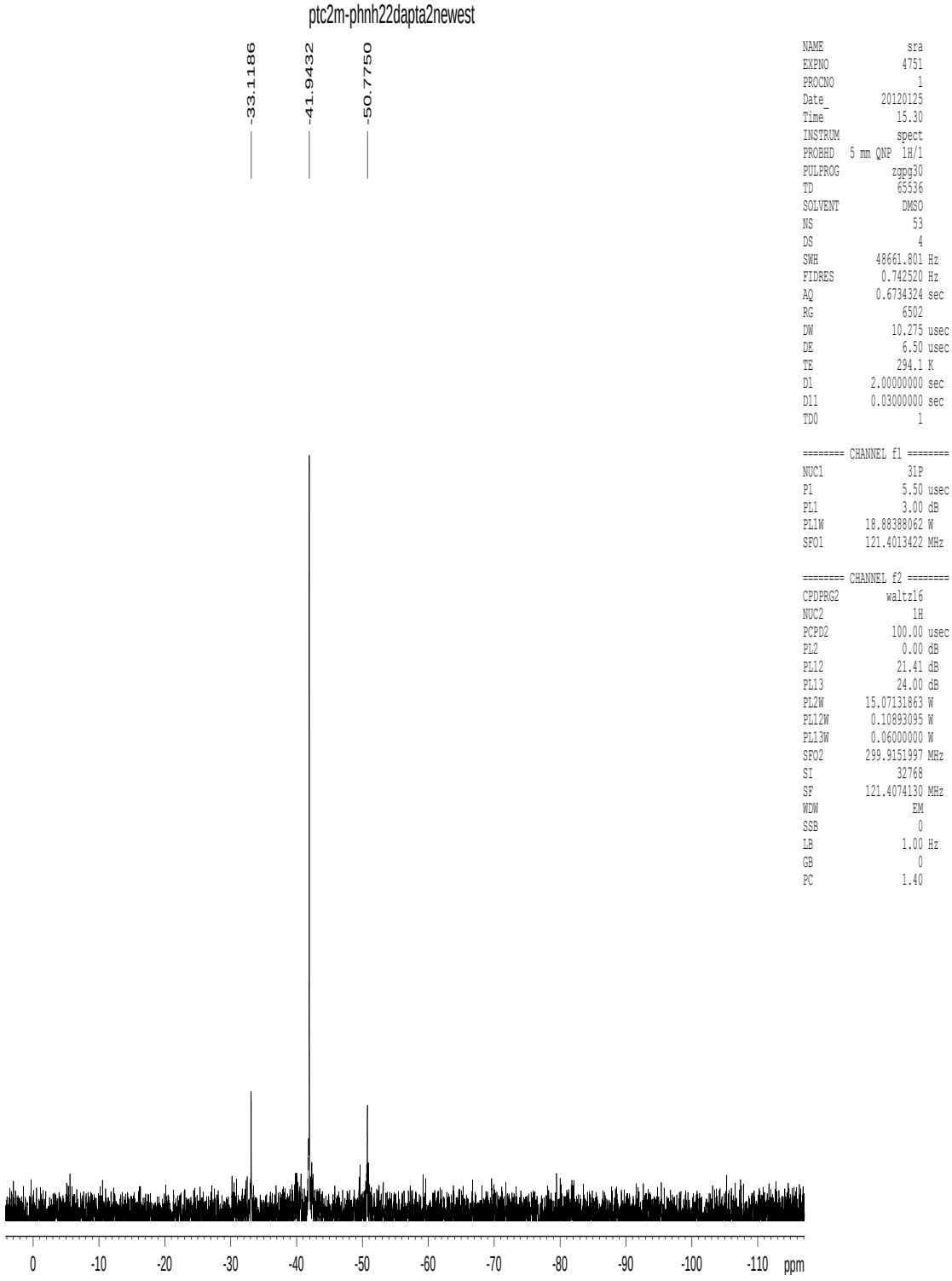

Appendix I.124. $^{31}P\{^{1}H\}$ NMR spectrum of cis-[Pt{C_2(m-$C_6H_4NH_2$)}$_2$(DAPTA)$_2$], 26.

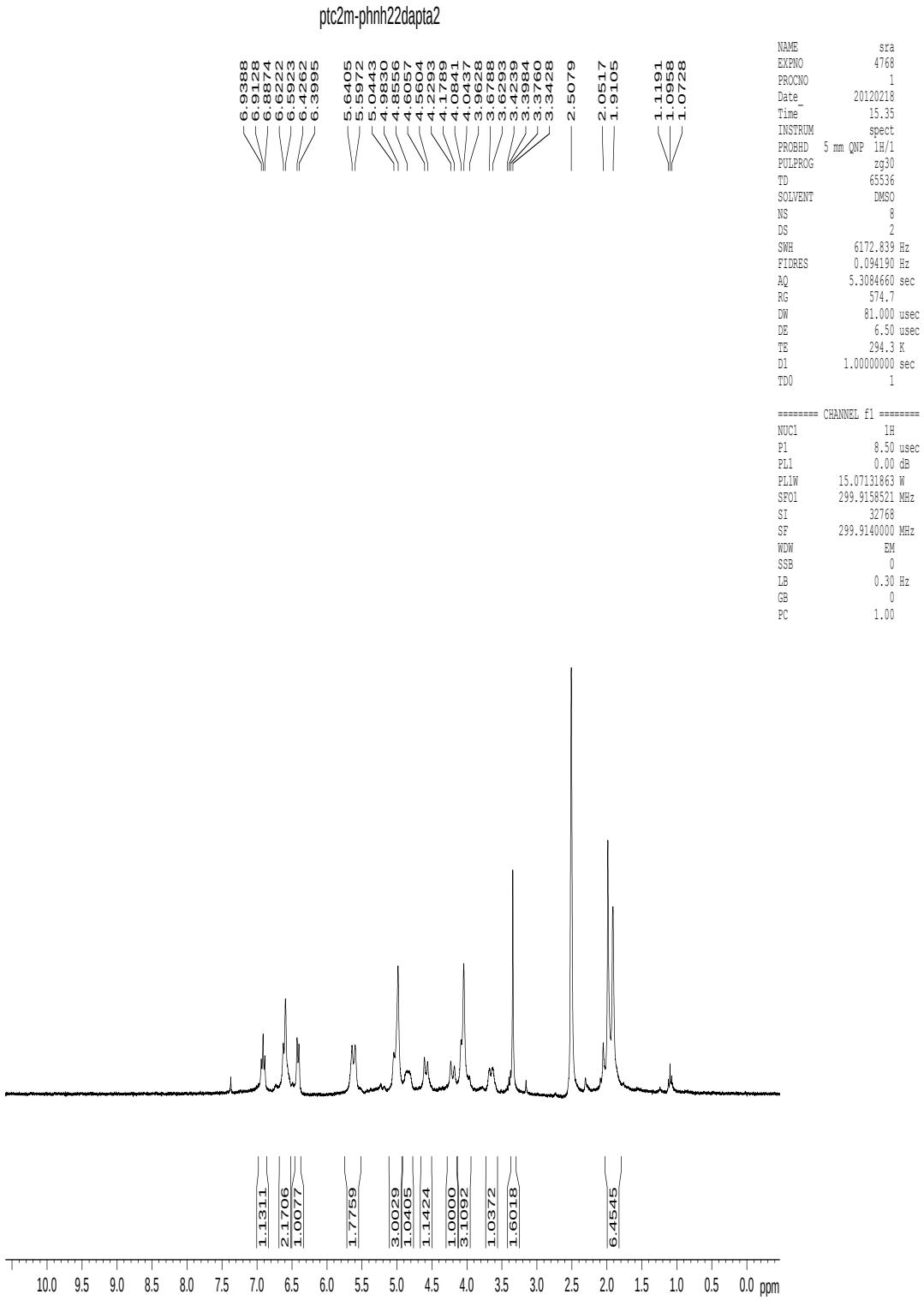

Appendix I.125. ^{1}H NMR spectrum of cis-[Pt{C_2(m-$C_6H_4NH_2$)}$_2$(DAPTA)$_2$], 26.

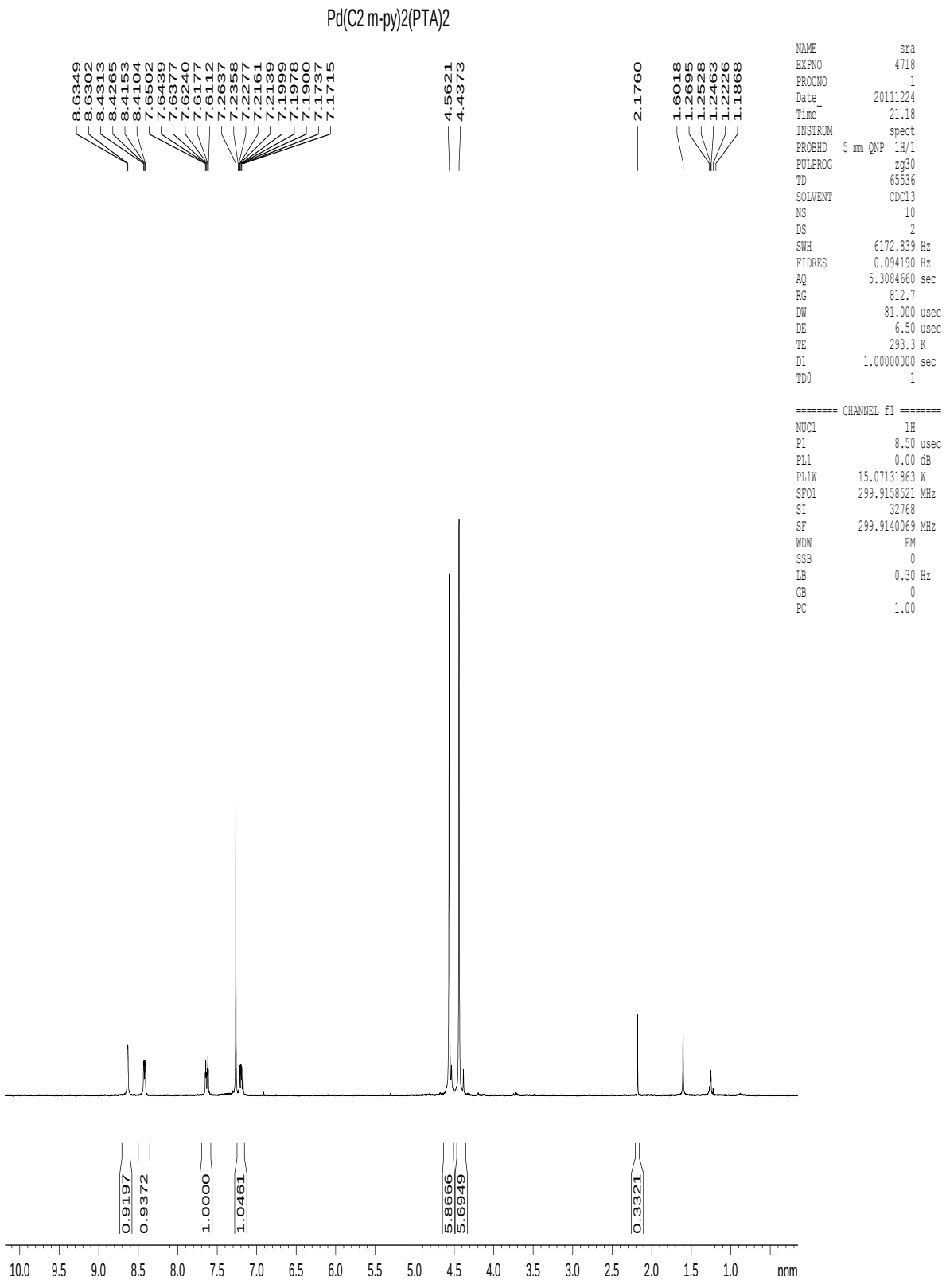

Appendix I.126. ^{1}H NMR spectrum of trans-[Pd{C_2(m-py)}$_2$($PTA)_2$], 21.

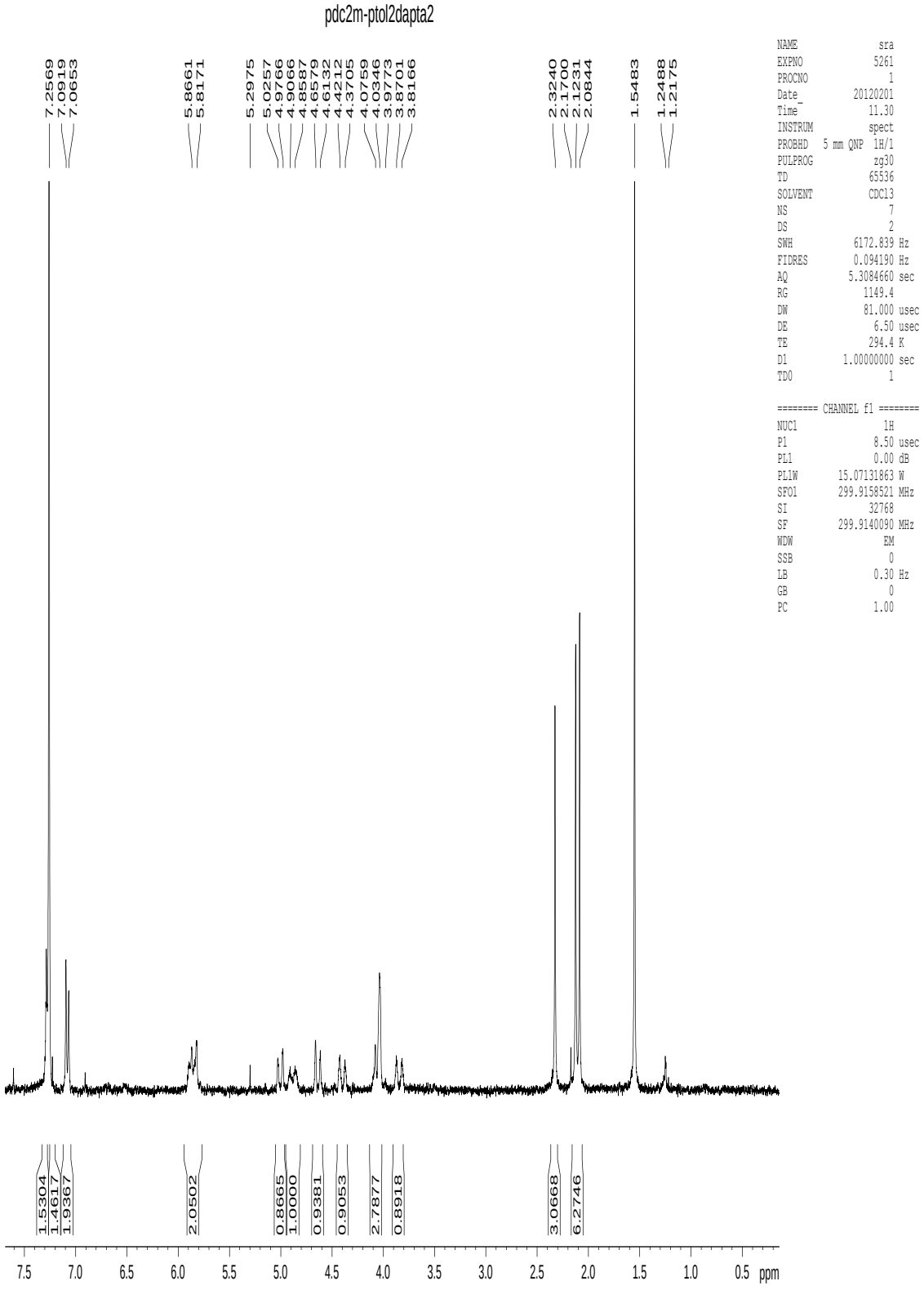

Appendix I.127. ^{1}H NMR spectrum of trans-[Pd{C$_2$(p-tol)}$_2$(DAPTA)$_2$], 29.

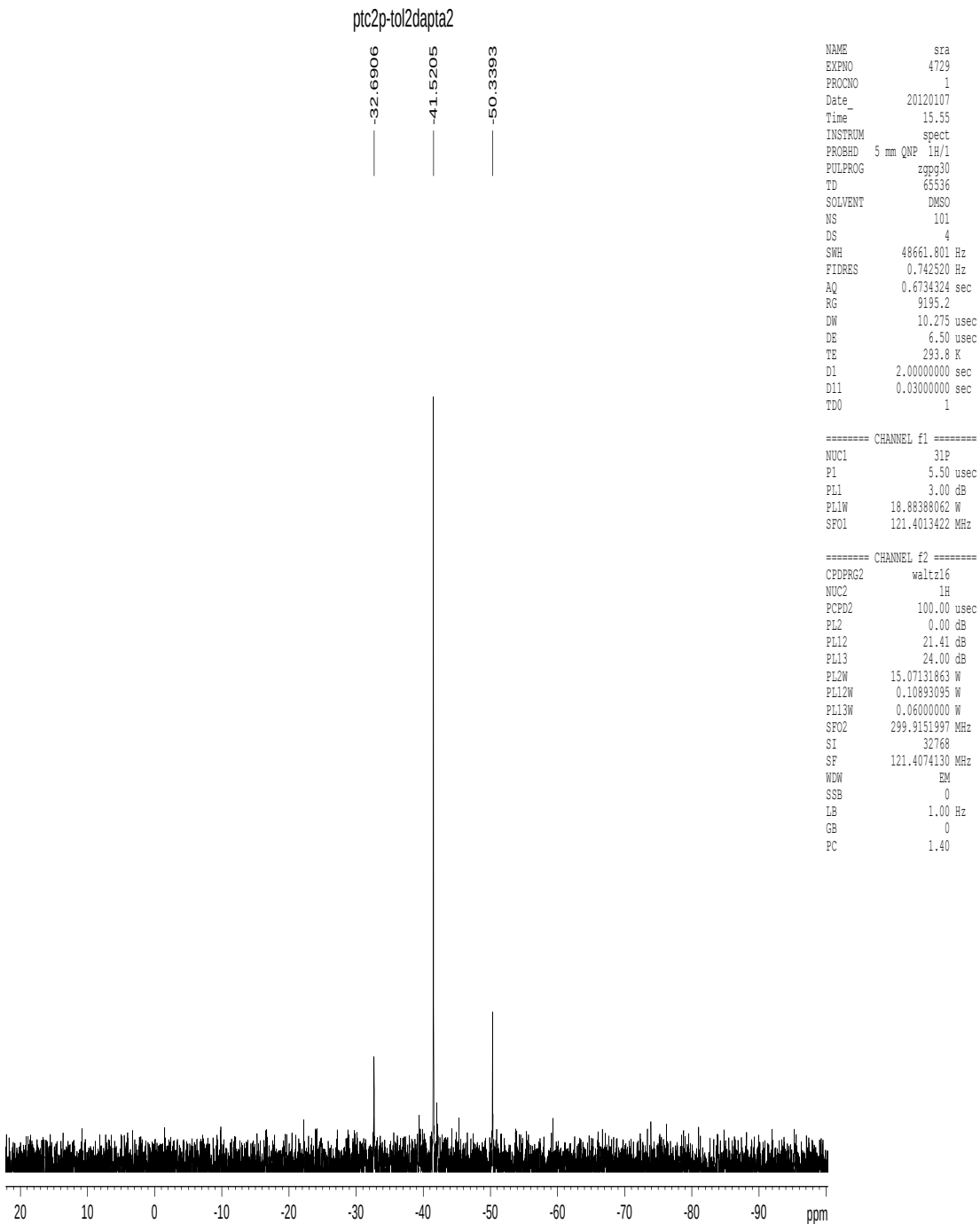

Appendix I.128. $^{31}P\{^{1}H\}$ NMR spectrum of cis-[Pt{C_2(p-tol)}$_2$(DAPTA)$_2$], 25.

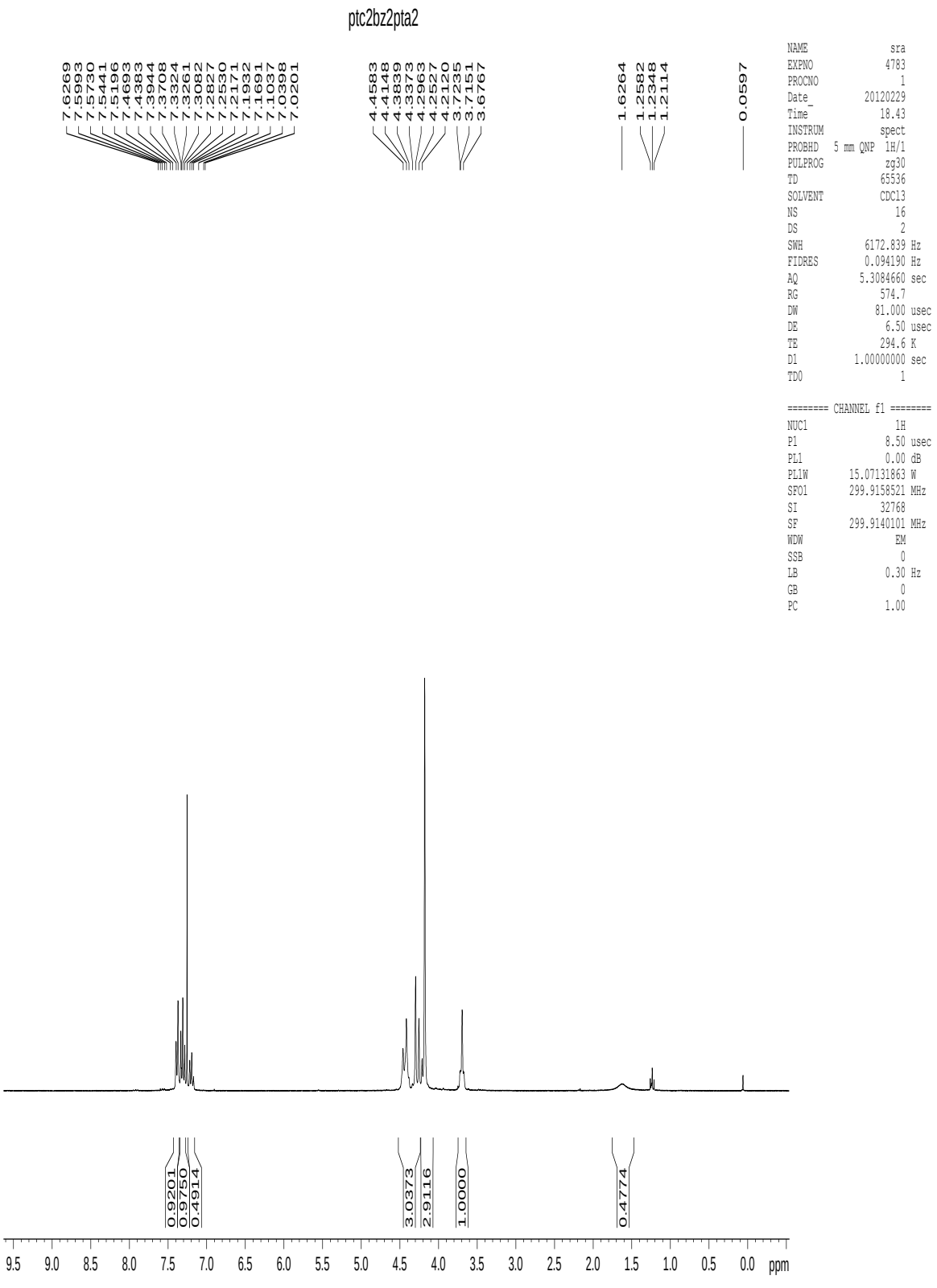

Appendix I.129. ^{1}H NMR spectrum of trans-$Pt(C_2Bz)_2(PTA)_2$, 24.

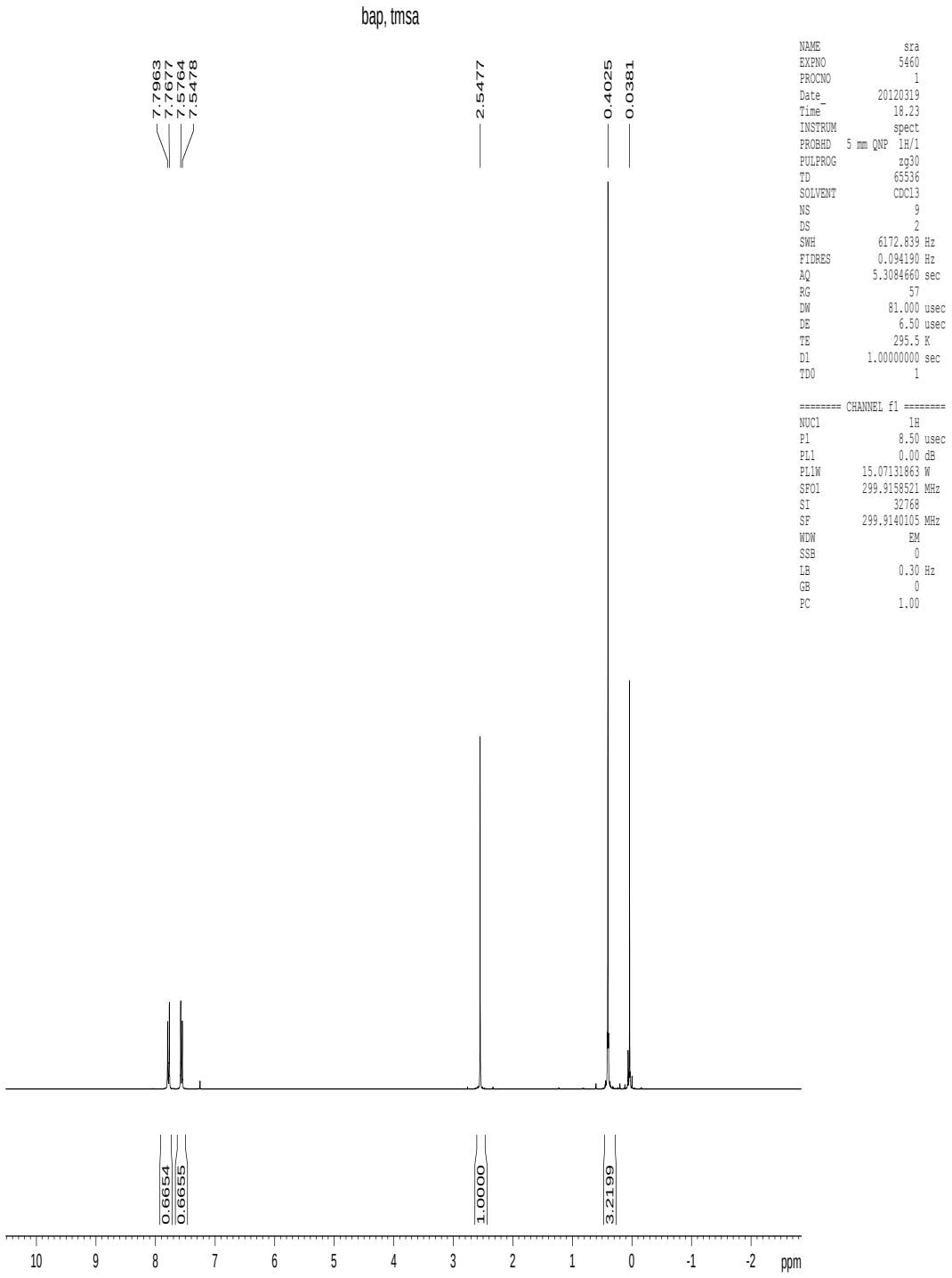

Appendix I.130. ^{1}H NMR spectrum of the product from Sonogashira cross-coupling reaction of 4-bromoacetophenone (R1) and trimethylsilylacetylene

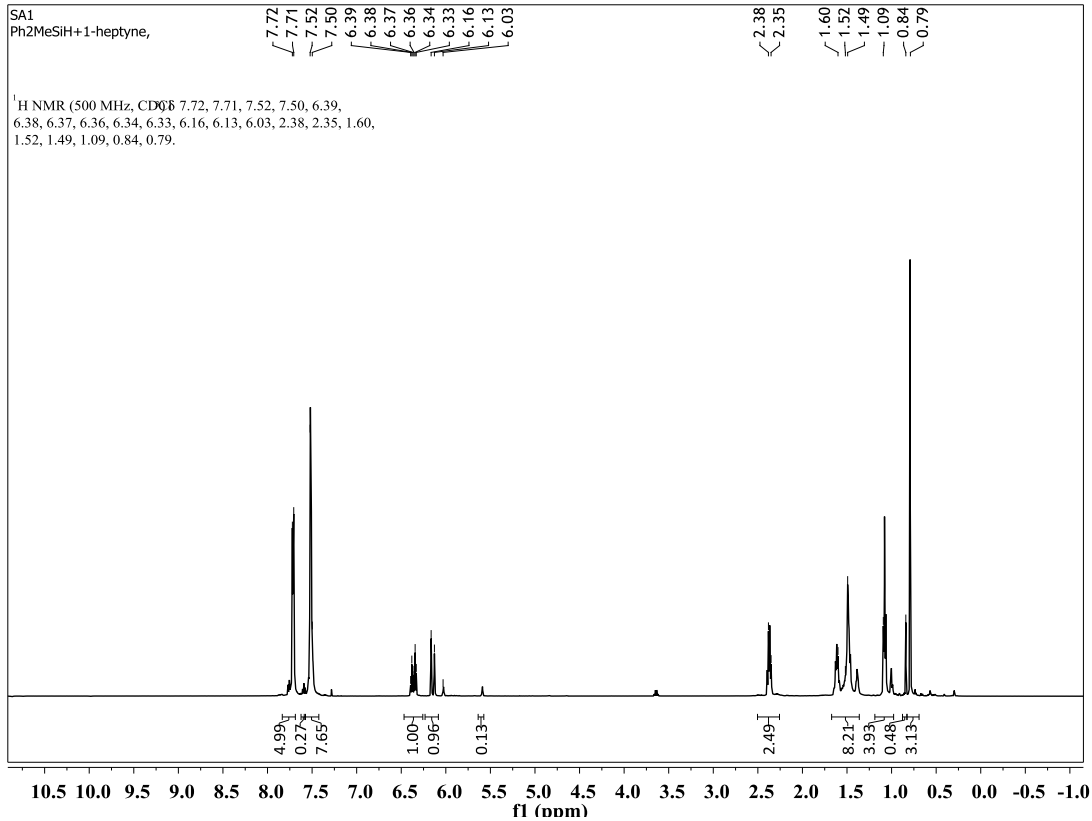

Appendix I.131. ^{1}H NMR spectrum of the product from hydrosilylation reaction of methyldiphenylsilane (S1) and 1-heptyne (A1) in the presence of (1a).

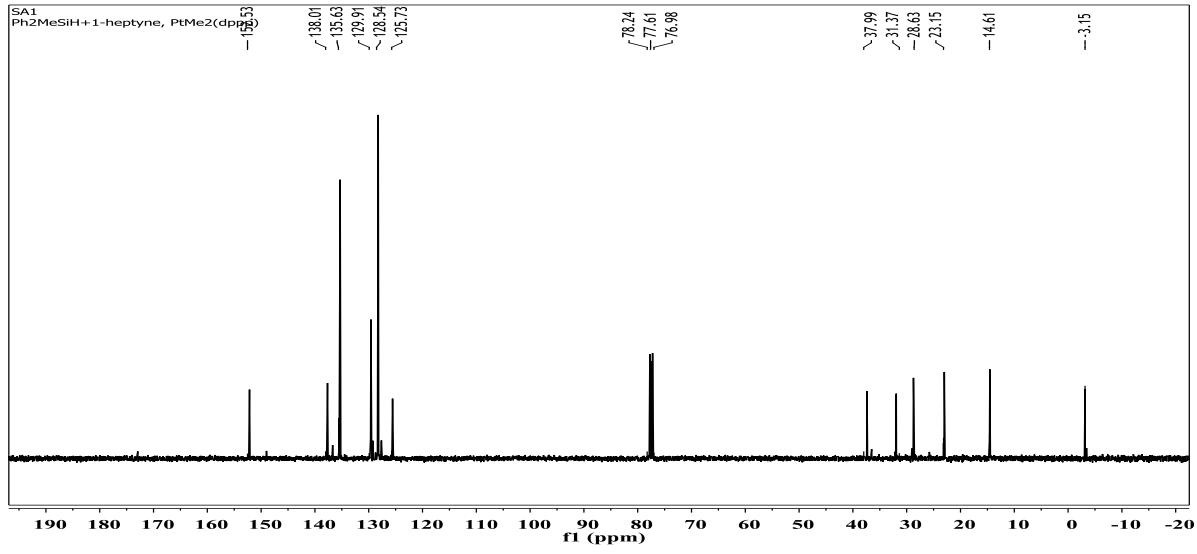

Appendix I.132. $^{13}C\{^{1}H\}$ NMR spectrum of the product from hydrosilylation reaction of methyldiphenylsilane (S1) and 1-heptyne (A1) in the presence of $PtMe_2$(dppp) (B3).

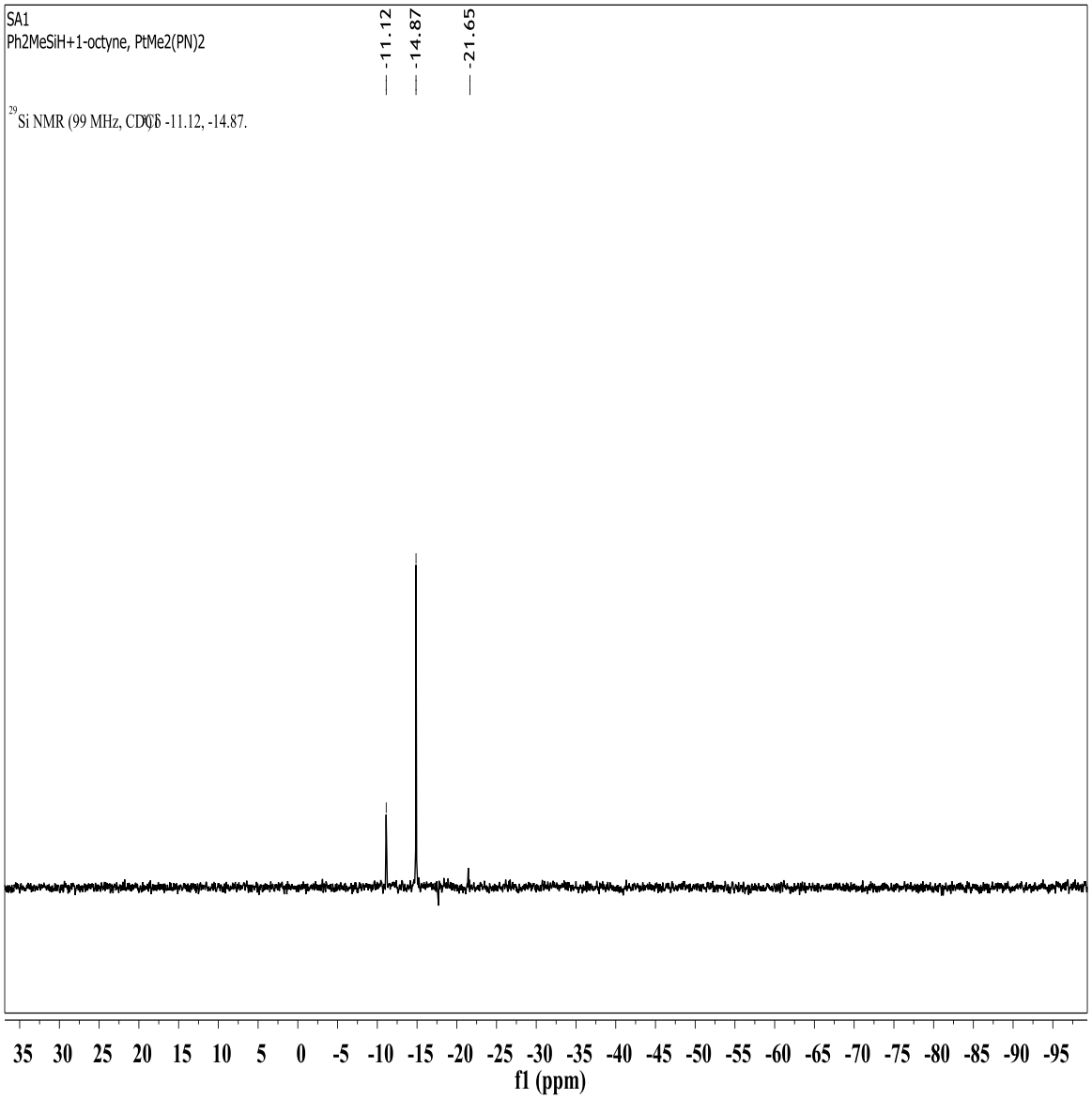

Appendix I.133. $^{29}Si\{^{1}H\}$ NMR spectrum of the product from hydrosilylation reaction of methyldiphenylsilane (S1) and 1-octyne in the presence of (1a).

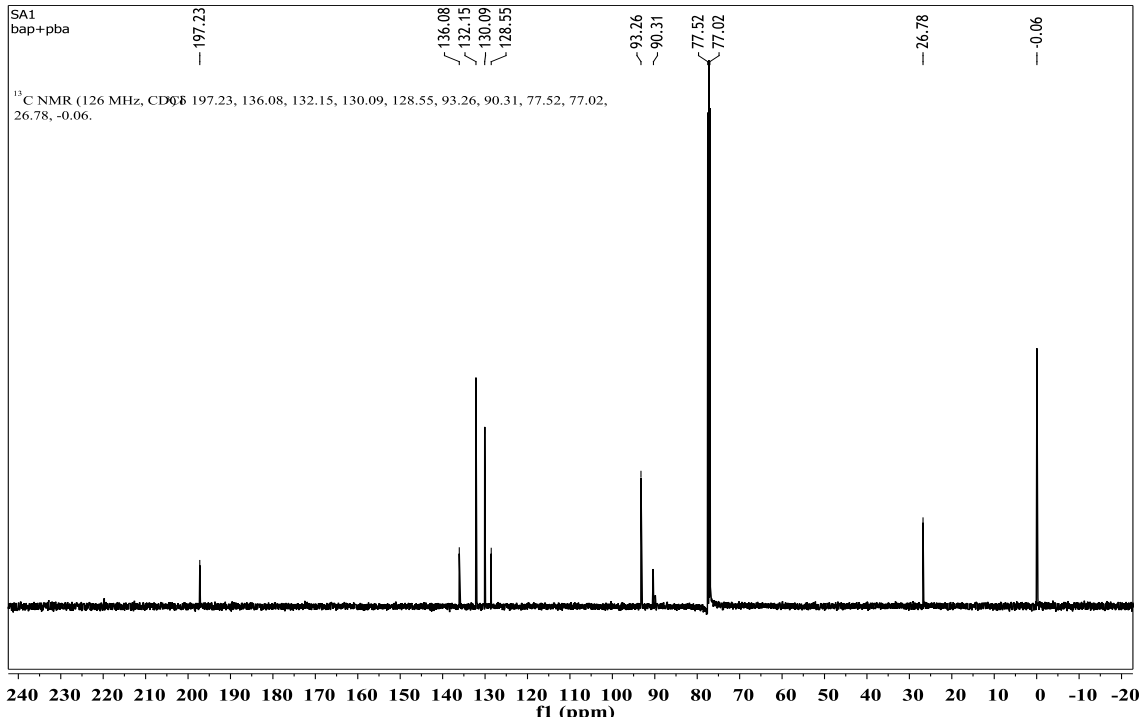

Appendix I.134. $^{13}C\{^{1}H\}$ NMR spectrum of the product from Suzuki-Miyaura cross-coupling reaction of 4-bromoacetophenone (R1) and phenylboronic acid (T1) in the presence of (5a).

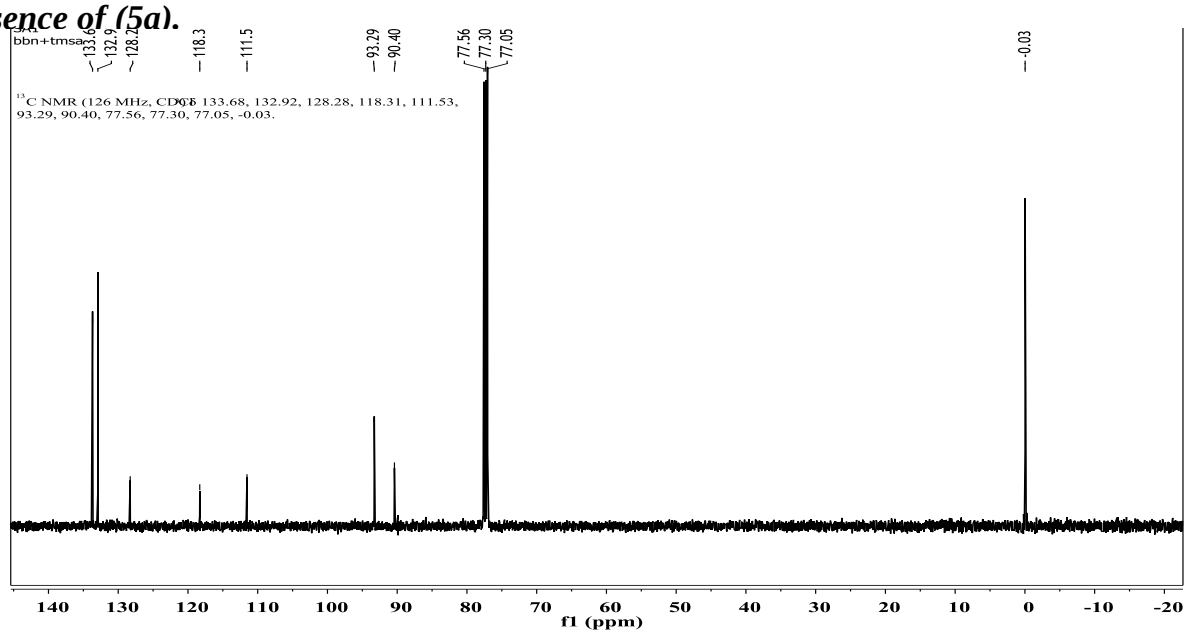

Appendix I.135. $^{13}C\{^{1}H\}$ NMR spectrum of the product from Sonogashira cross-coupling reaction of 4-bromobenzonitrile (R4) and trimethylsilylacetylene (A2) in the presence of (M1).

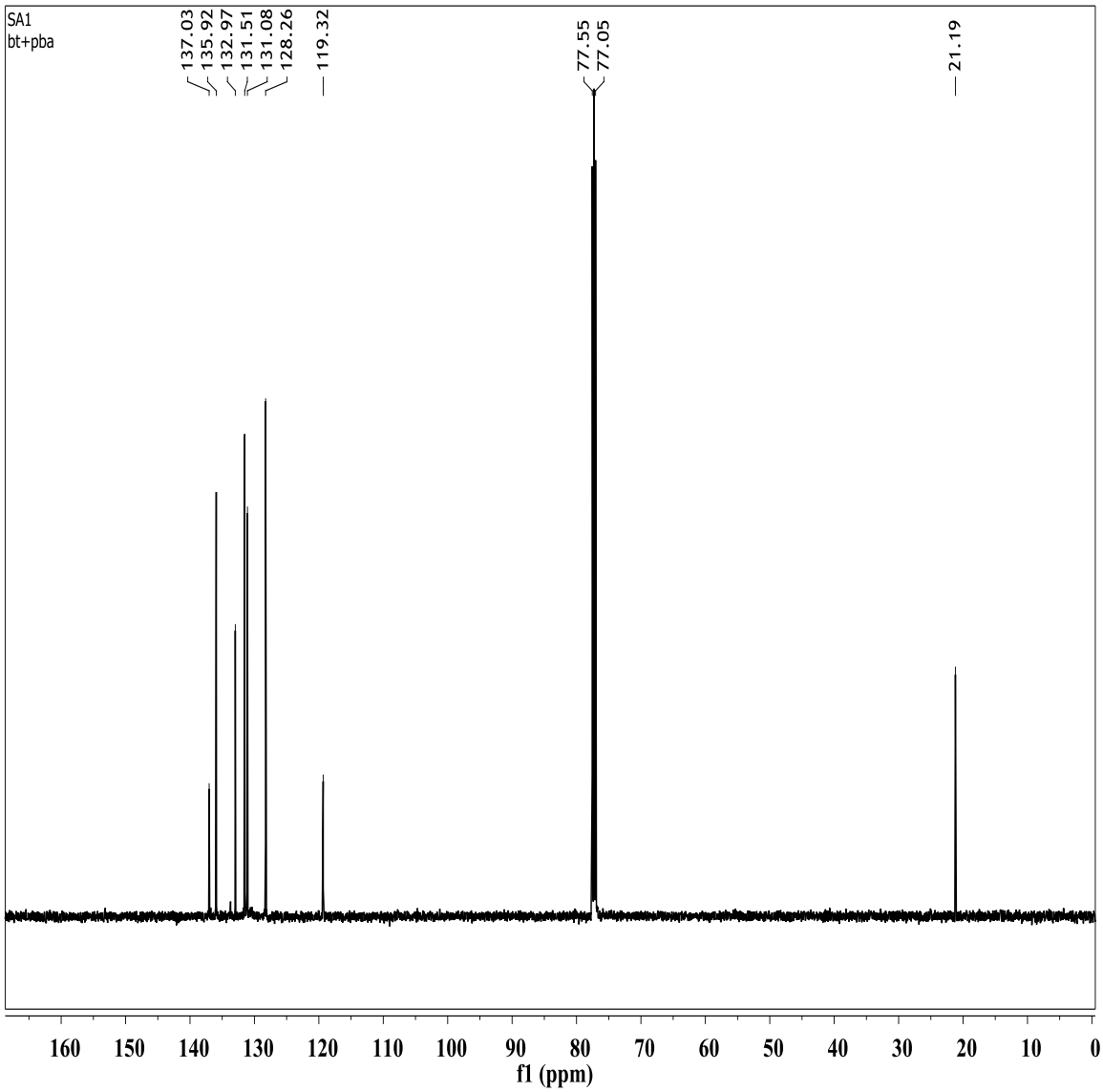

Appendix I.136. $^{13}C\{^{1}H\}$ NMR spectrum of the product from Suzuki-Miyaura cross-coupling reaction of 4-bromotoluene (R3) and phenylboronic acid (T1) in the presence of (5a).

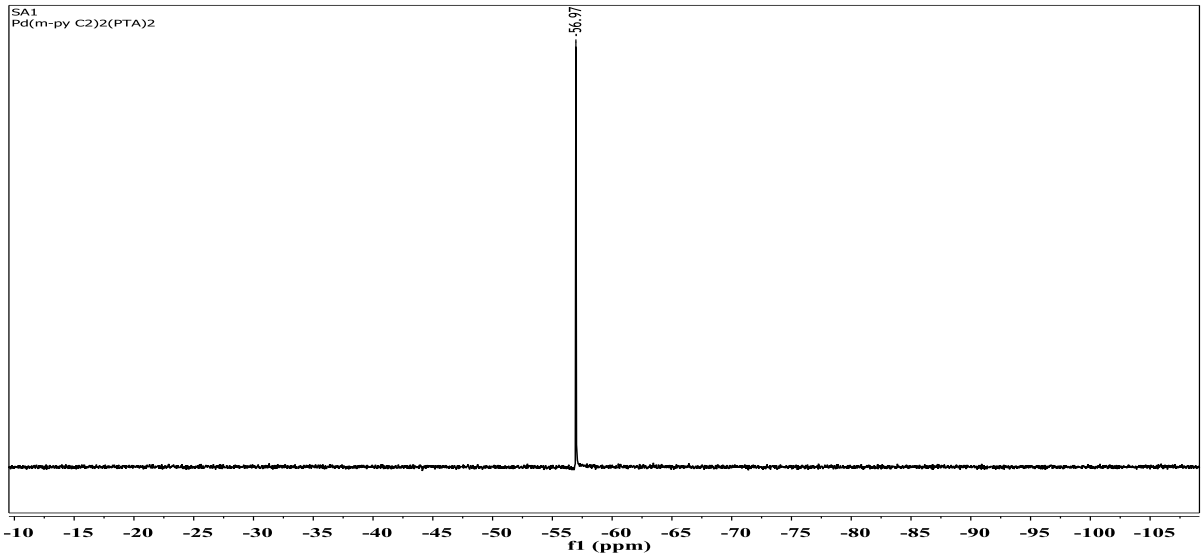

Appendix I.137. $^{31}P\{^{1}H\}$ NMR spectrum of trans-[Pd{C_2(m-py)}$_2$(PTA)$_2$], 21.

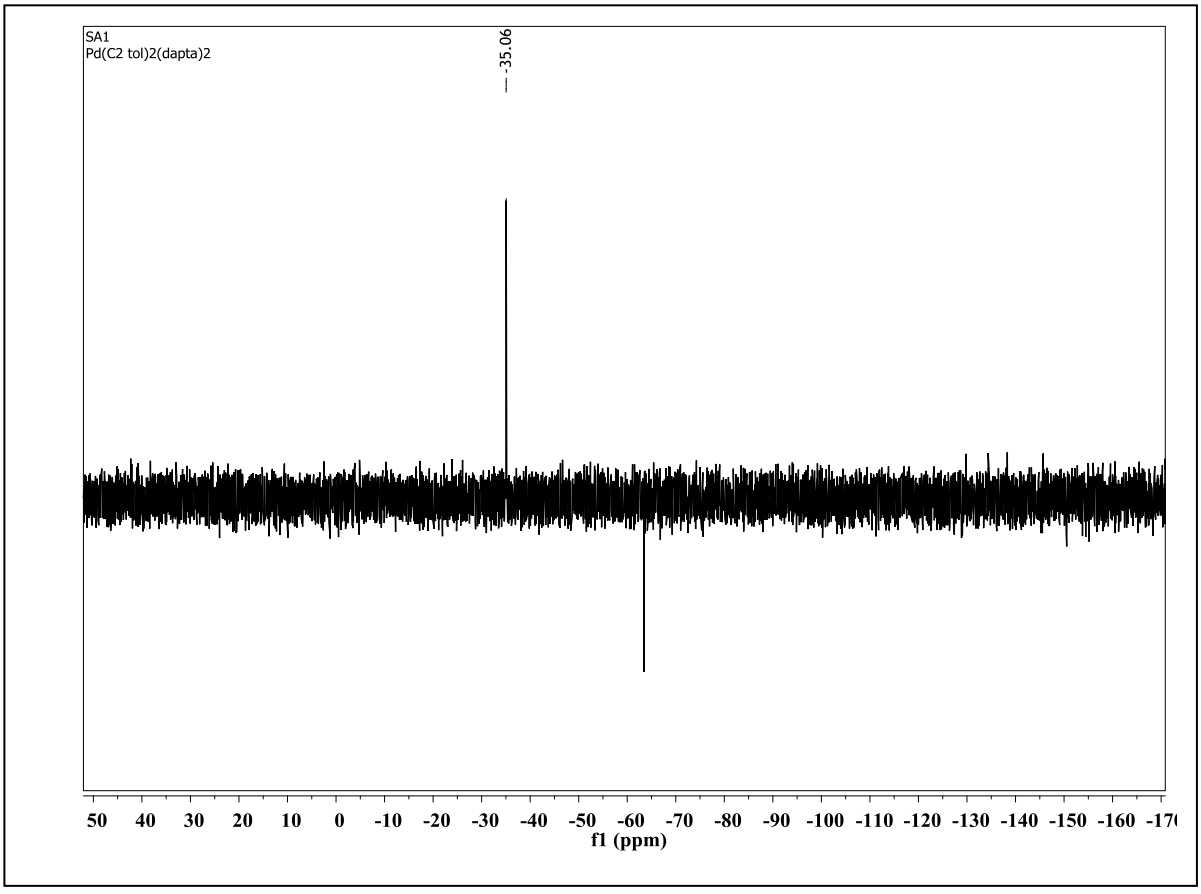

Appendix I.138. $^{31}P\{^{1}H\}$ NMR of trans-[Pd{C_2(p-tol)}$_2$(DAPTA)$_2$], 26.

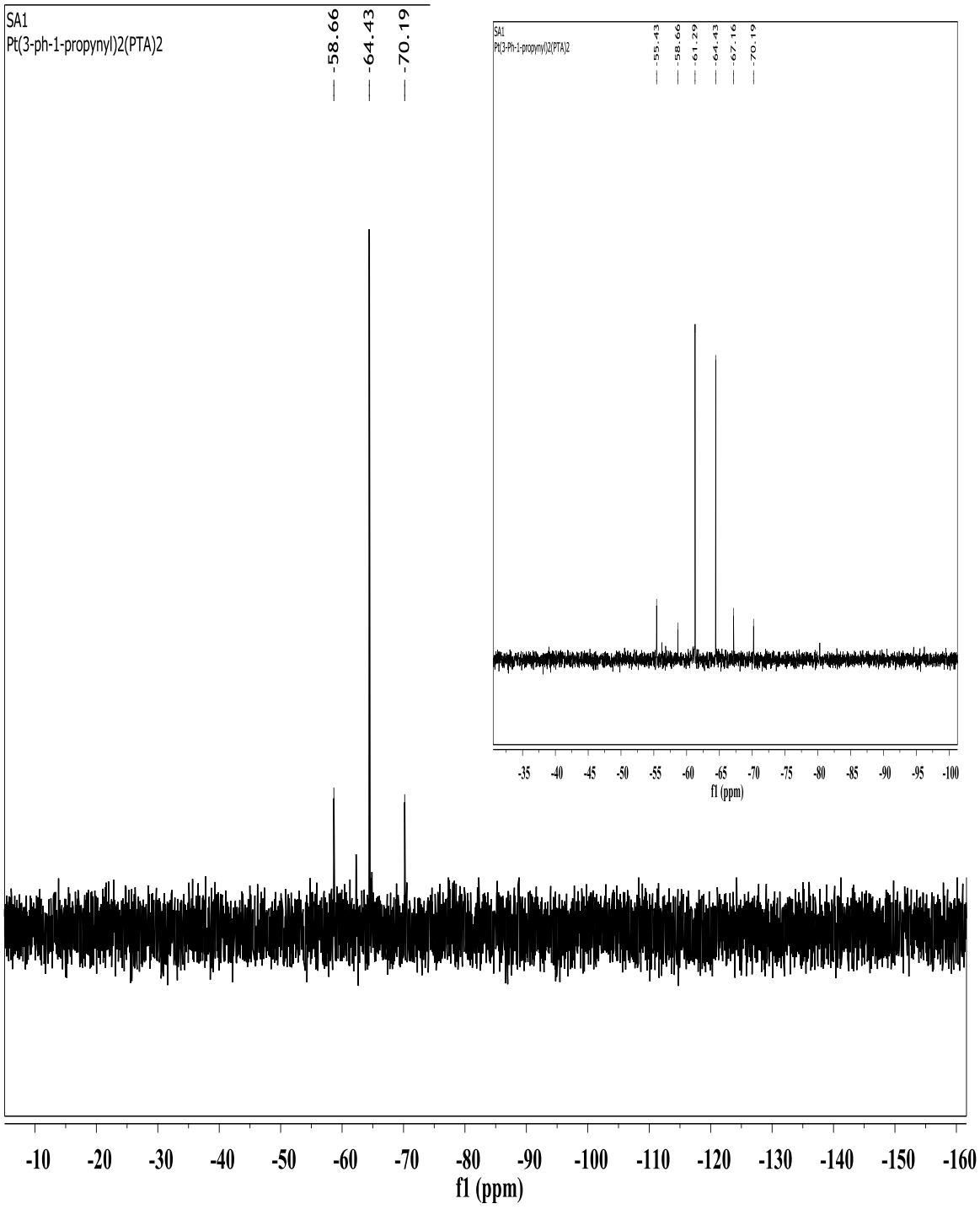

Appendix I.139. $^{31}P\{^{1}H\}$ NMR spectrum of trans-$Pt(C_2Bz)_2(PTA)_2$, 24.

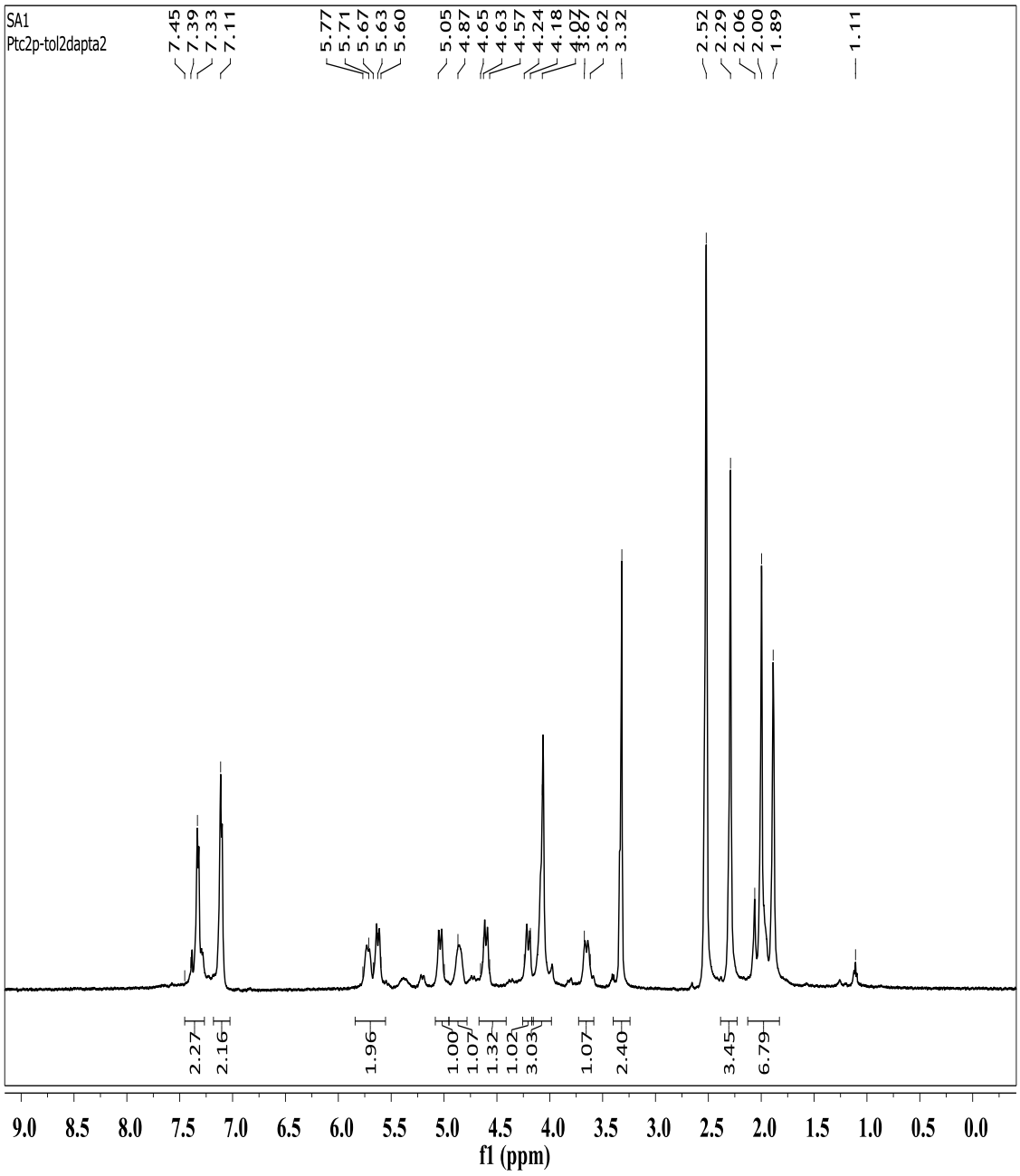

Appendix I.140. ^{1}H NMR spectrum of cis-[Pt{C_2(p-tol)}$_2$(PTA)$_2$], 25.

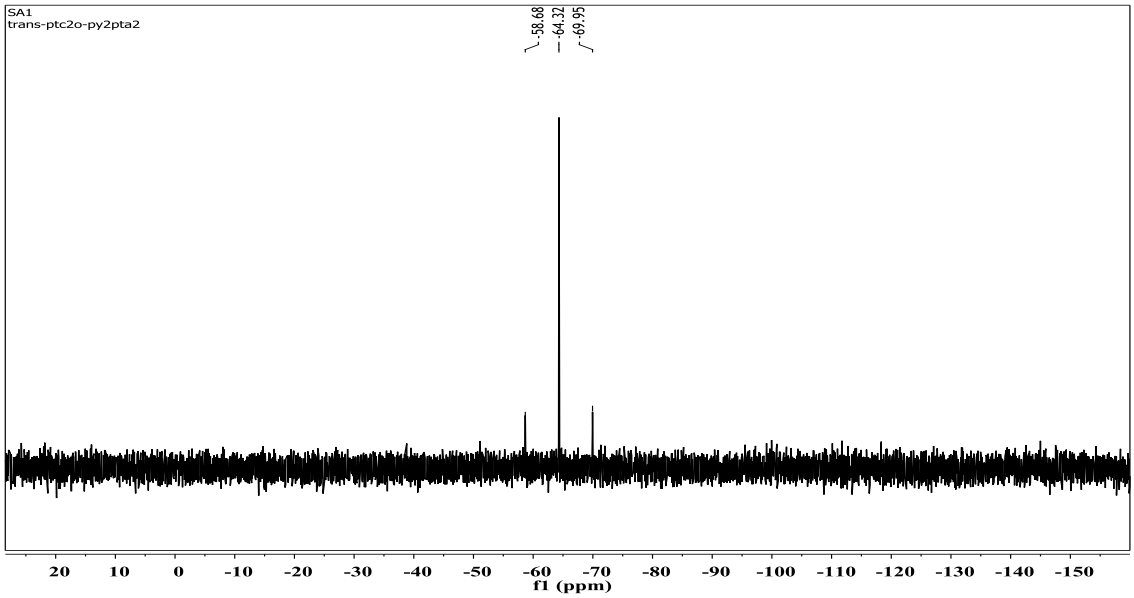

Appendix I.141. $^{31}P\{^{1}H\}$ NMR spectrum of trans-[Pt{C_2(o-py)}$_2$(PTA)$_2$], 19b.

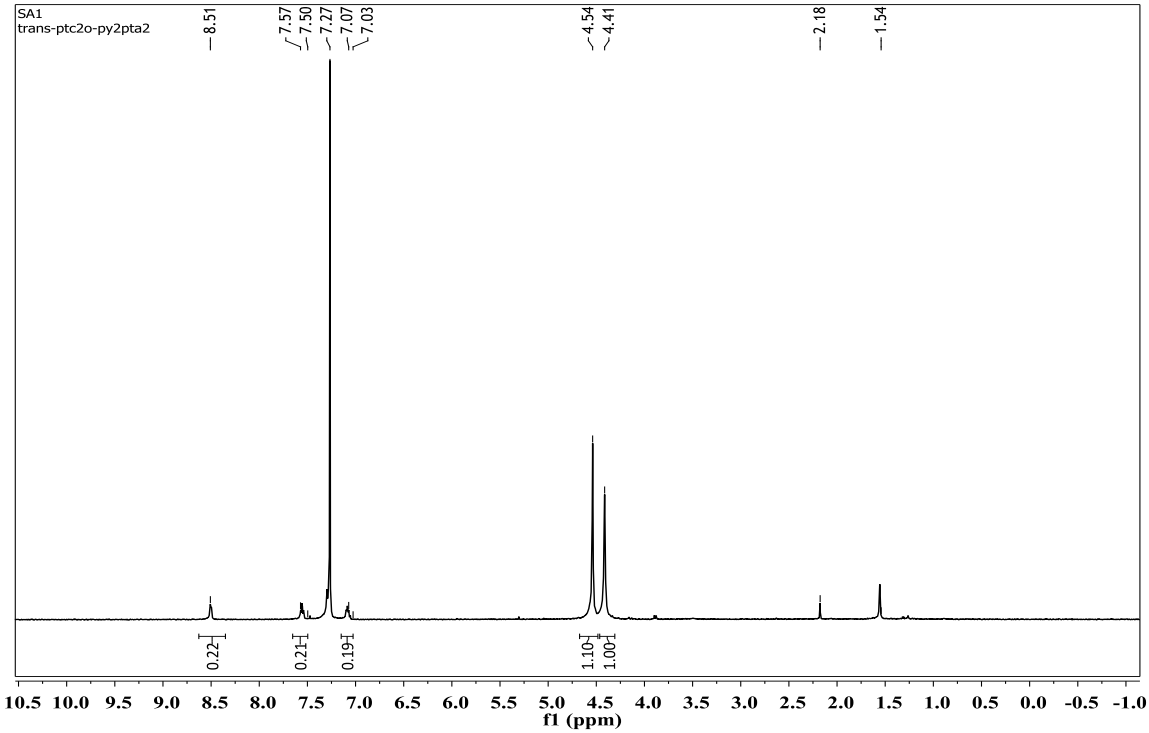

Appendix I.142. ^{1}H NMR spectrum of trans-[Pt{C_2(o-py)}$_2$(PTA)$_2$], 19b.

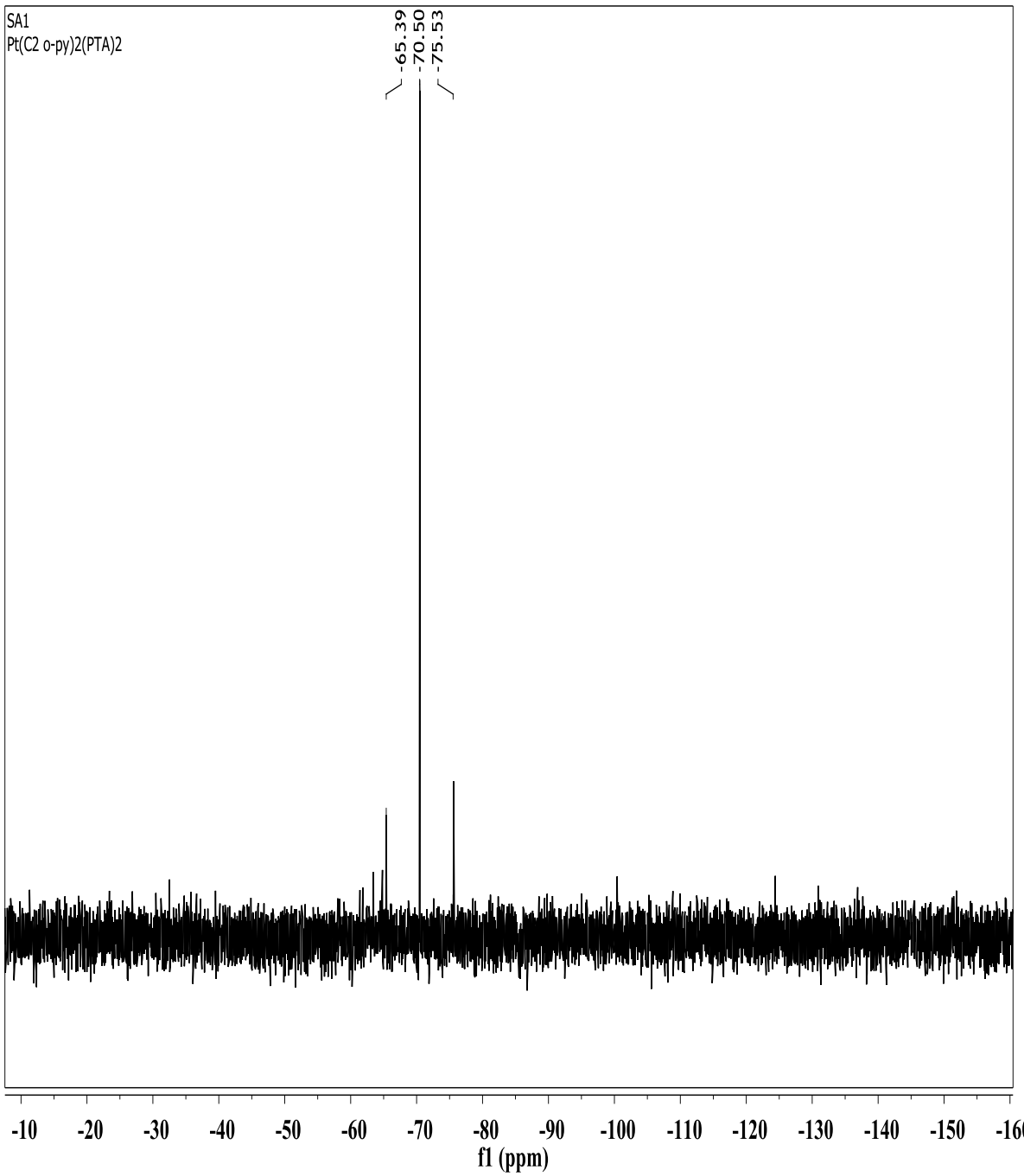

Appendix I.143. $^{31}P\{^{1}H\}$ NMR spectrum of cis-[Pt{C_2(o-py)}$_2$(PTA)$_2$], 19a.

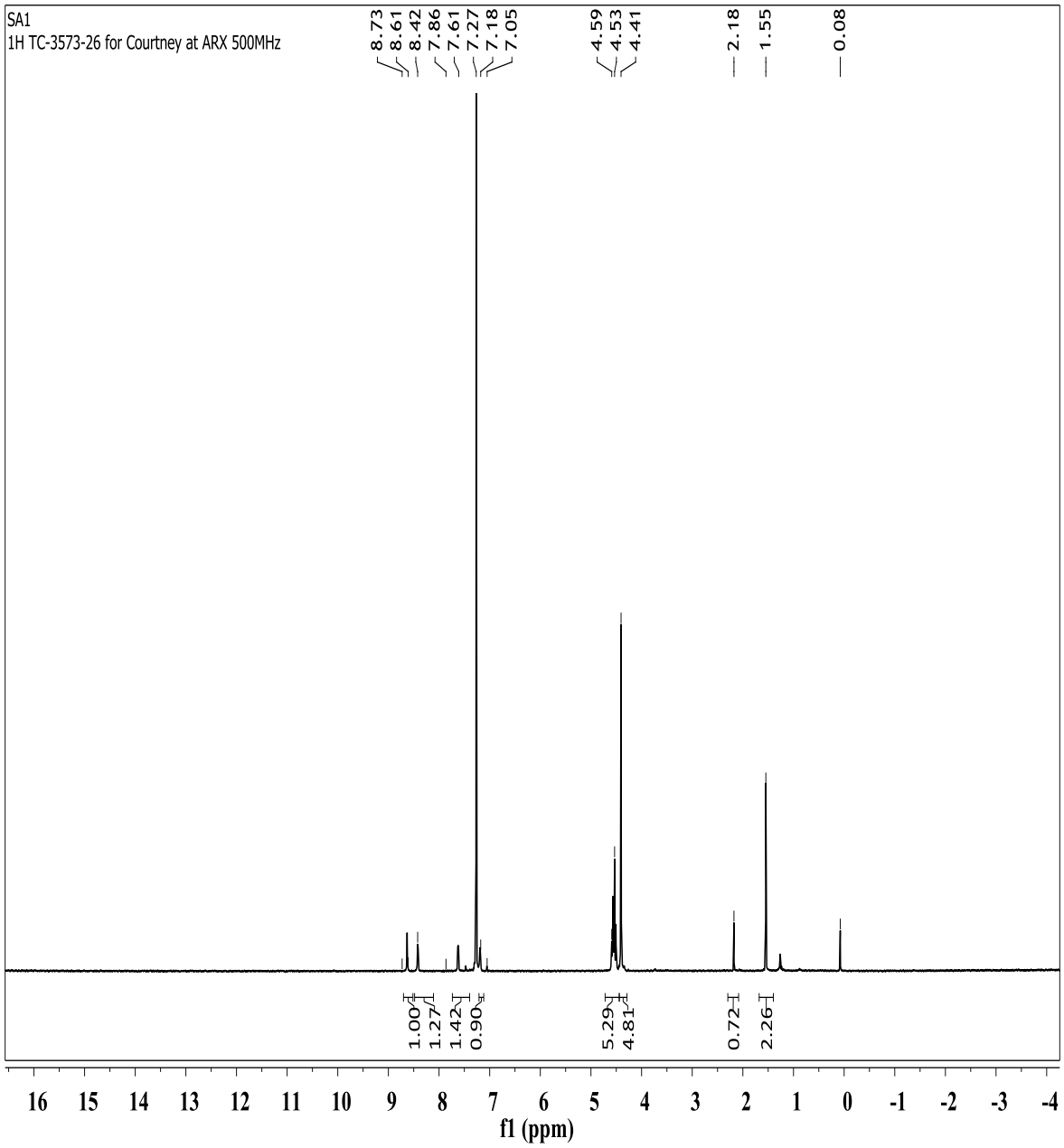

Appendix I.144. ^{1}H NMR spectrum of trans-[Pt{C$_2$(m-py)}$_2$(PTA)$_2$], 18b.

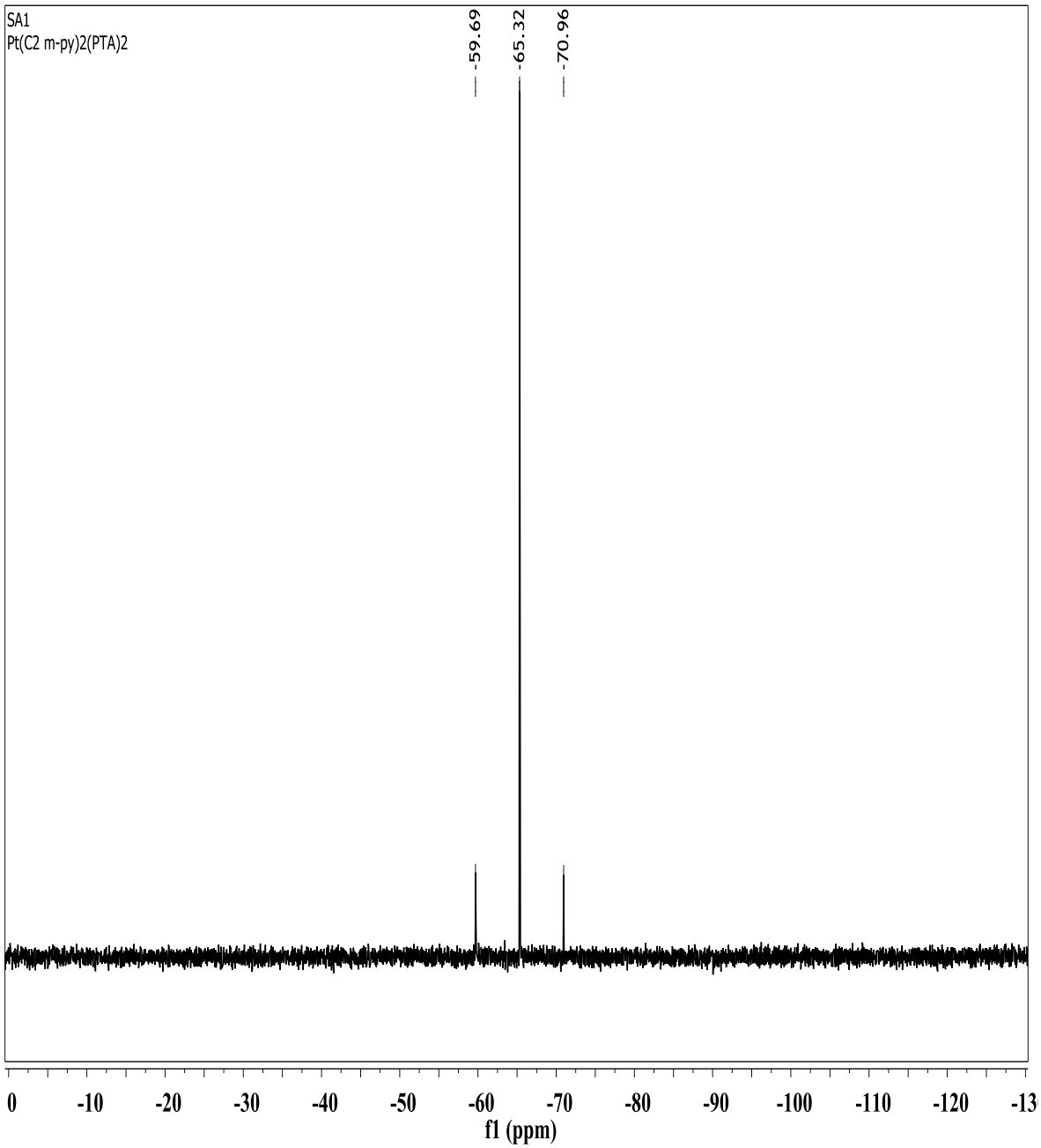

Appendix I.145. $^{31}P\{^{1}H\}$ NMR spectrum of trans-[Pt{C_2(m-py)}$_2$($PTA)_2$], 18b.

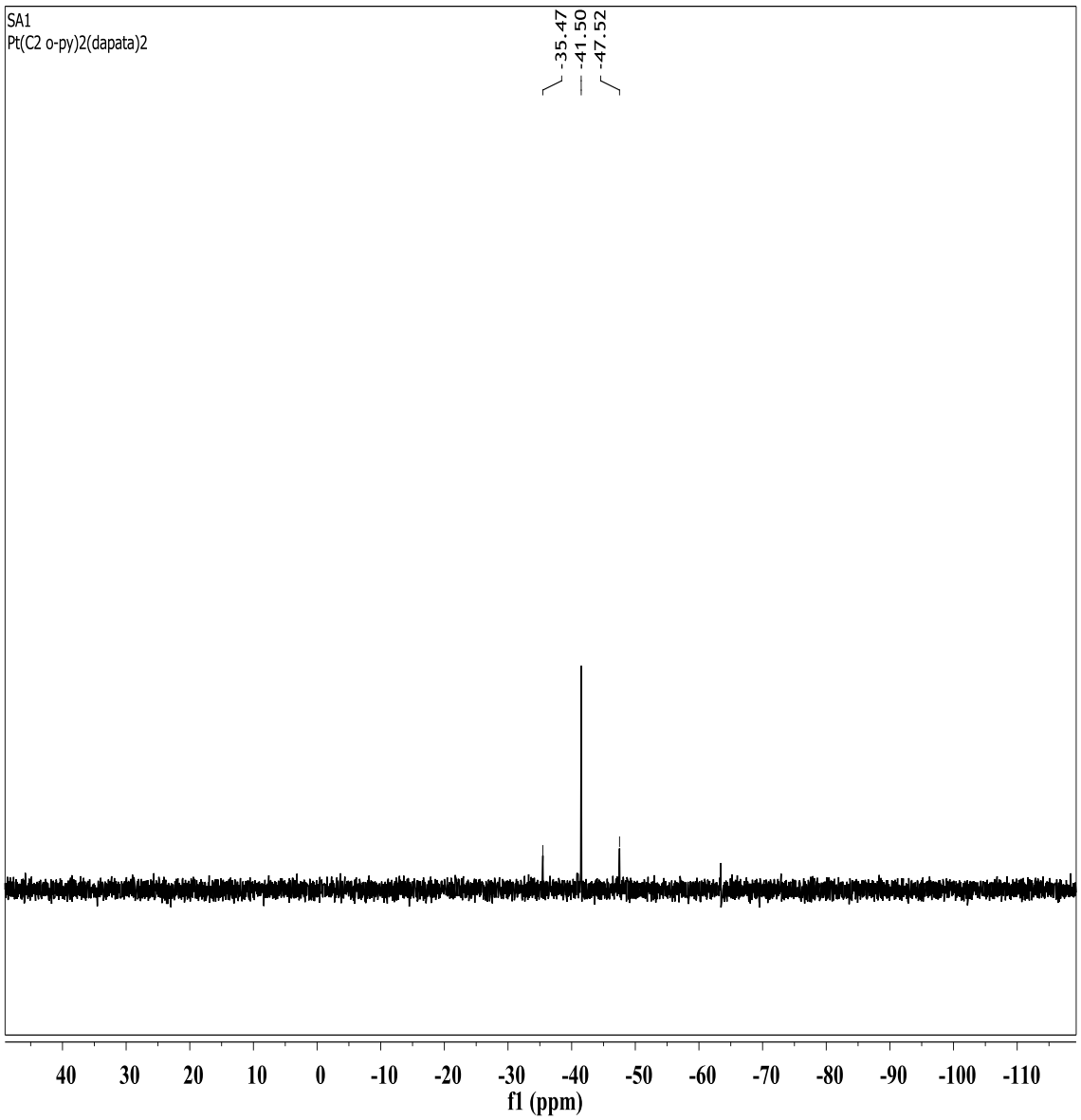

Appendix I.146. $^{31}P\{^{1}H\}$ NMR spectrum of trans-[Pt{C_2(o-py)}$_2$(DAPTA)$_2$], 28.

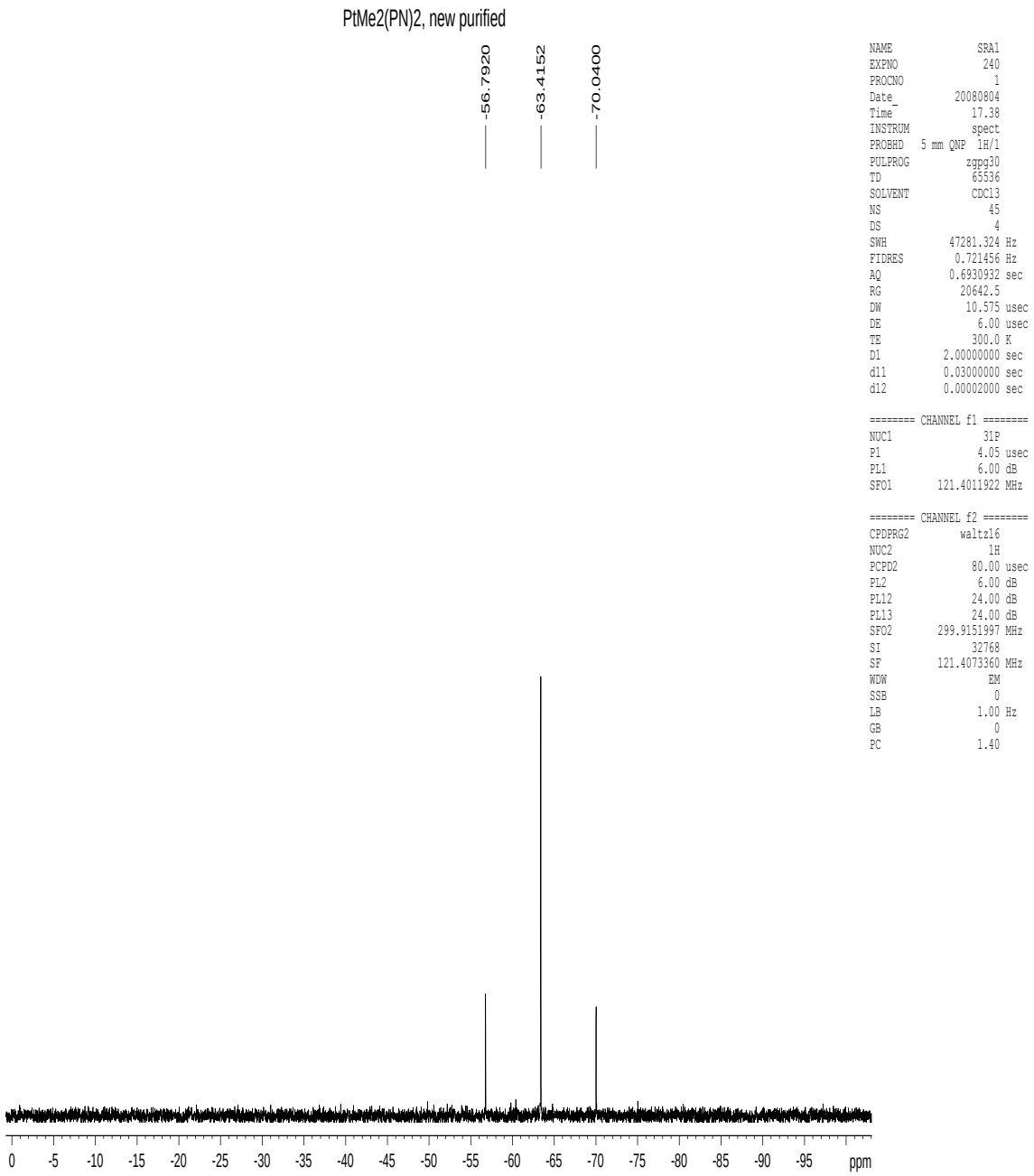

Appendix I.147. $^{31}P\{^{1}H\}$ NMR spectrum of cis-$PtMe_2(PTA)_2$, 1a.

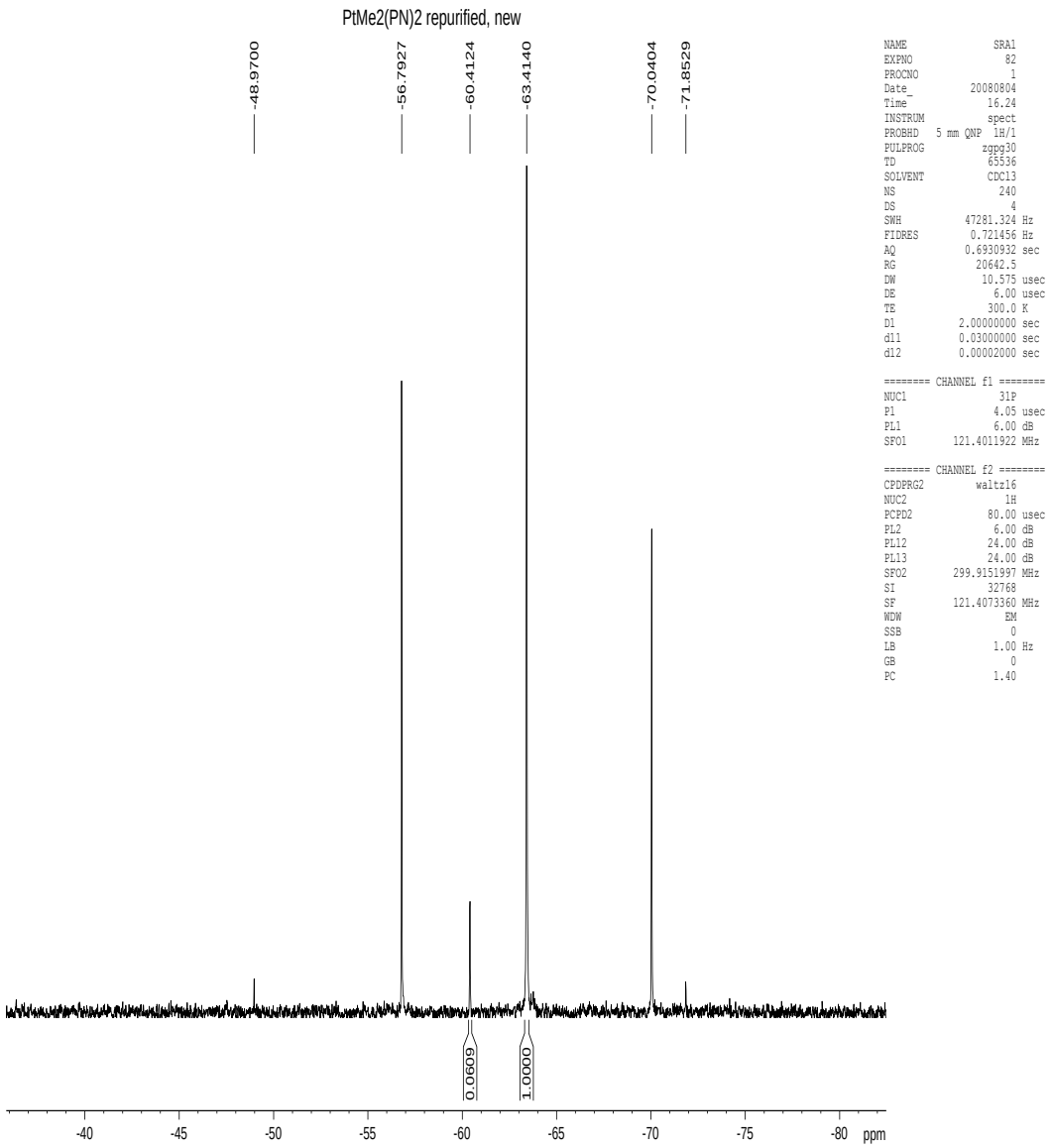

Appendix I.148. $^{31}P\{^{1}H\}$ NMR spectrum of mixture of cis-$PtMe_2(PTA)_2$, 1a and trans-$PtMe_2(PTA)_2$, 1b.

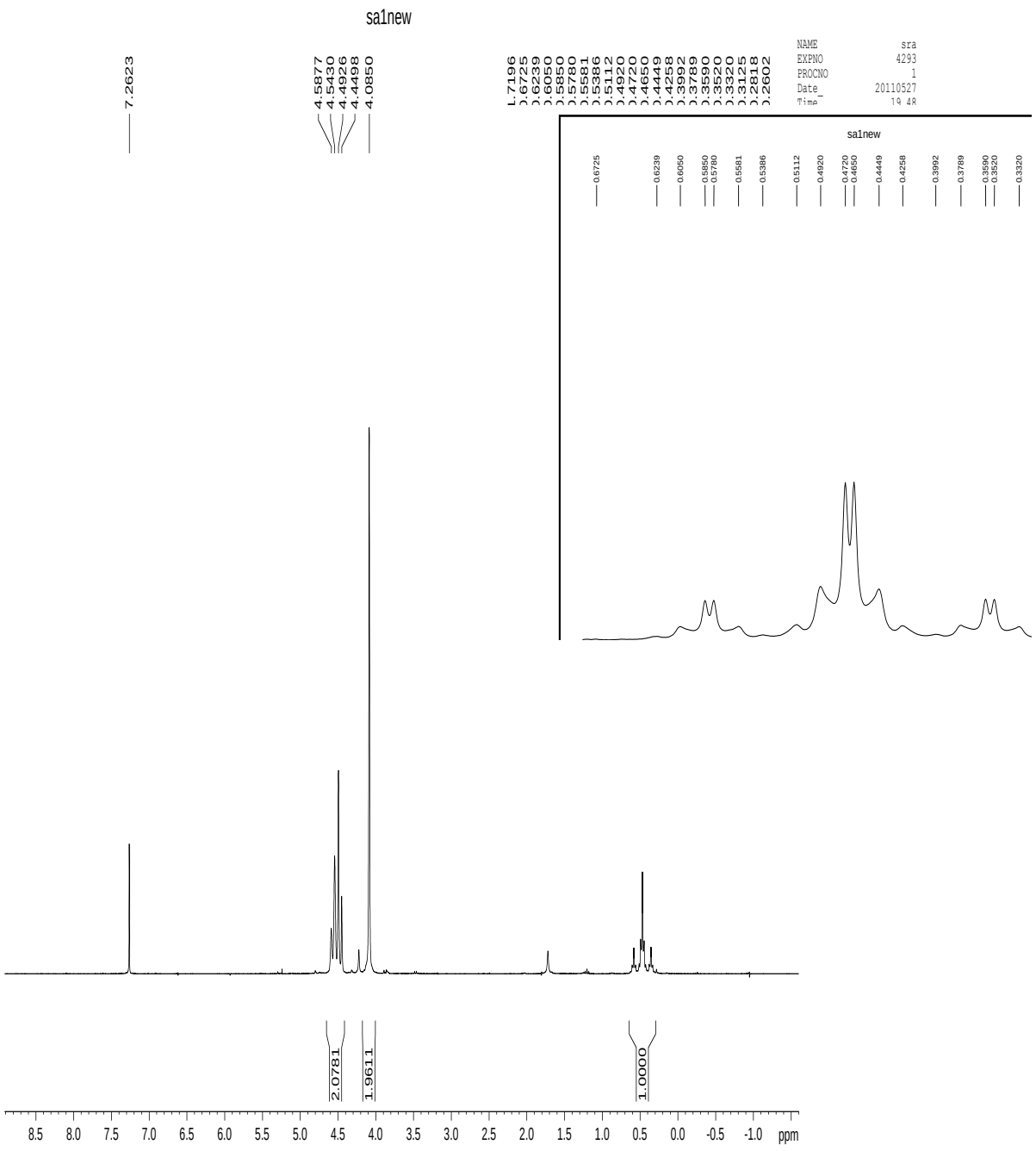

Appendix I.149. ^{1}H NMR spectrum of cis-PtMe$_2$(PTA)$_2$, 1a.

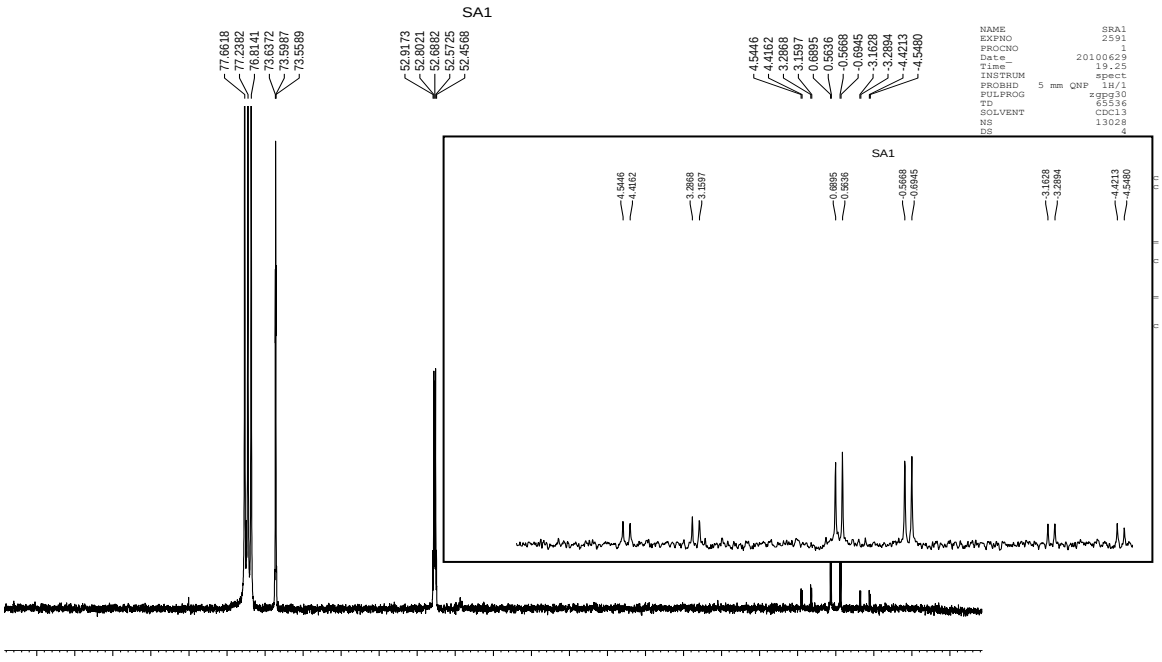

Appendix I.150. $^{13}C\{^{1}H\}$ NMR spectrum of cis-PtMe$_2$(PTA)$_2$, 1a.

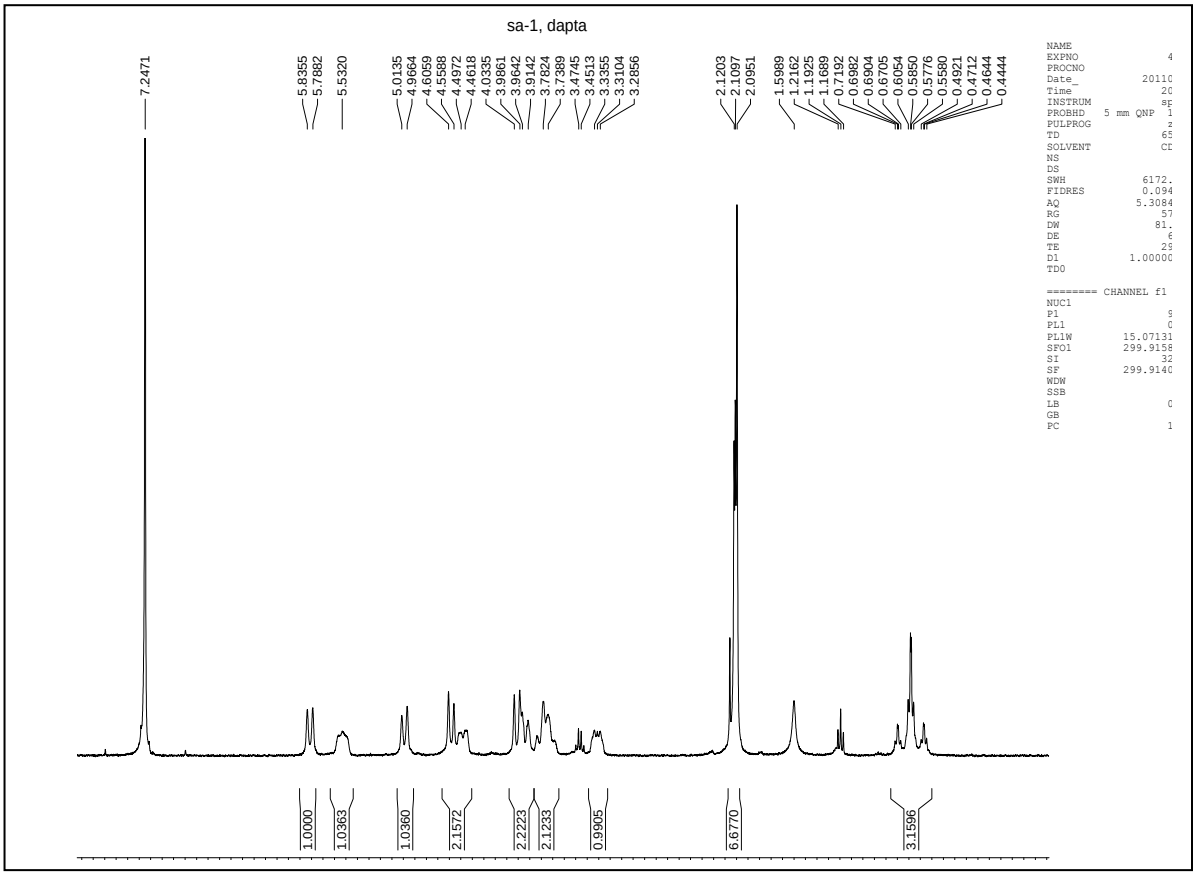

Appendix I.151. ^{1}H NMR spectrum of cis-PtMe$_2$(DAPTA)$_2$, 9a.

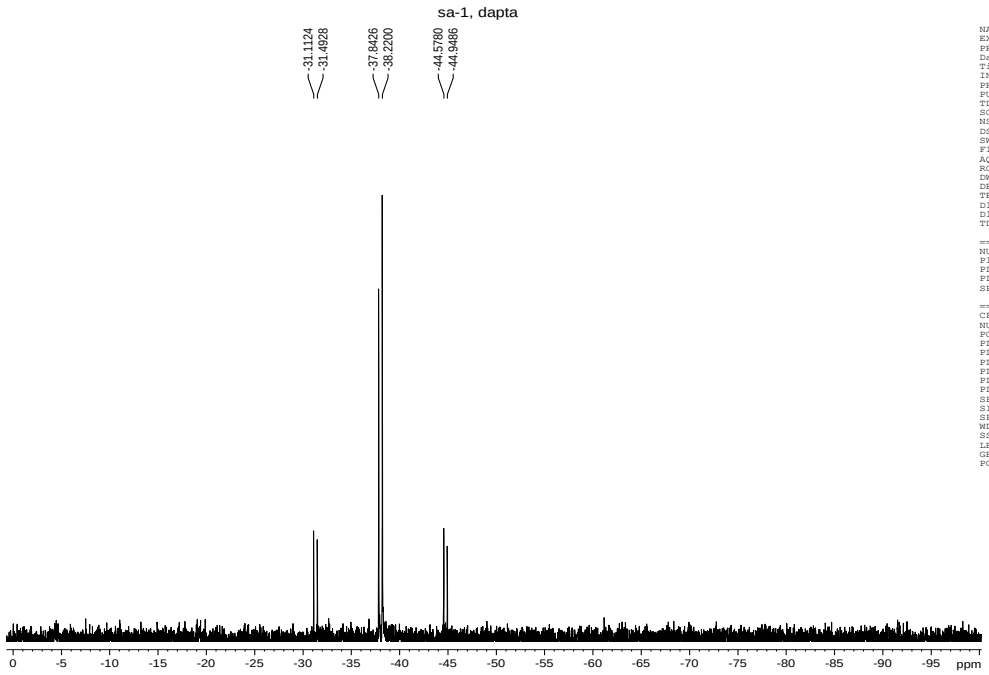

Appendix I.153. $^{31}P\{^{1}H\}$ NMR spectrum of cis-$PtMe_2(DAPTA)_2$, 9a.

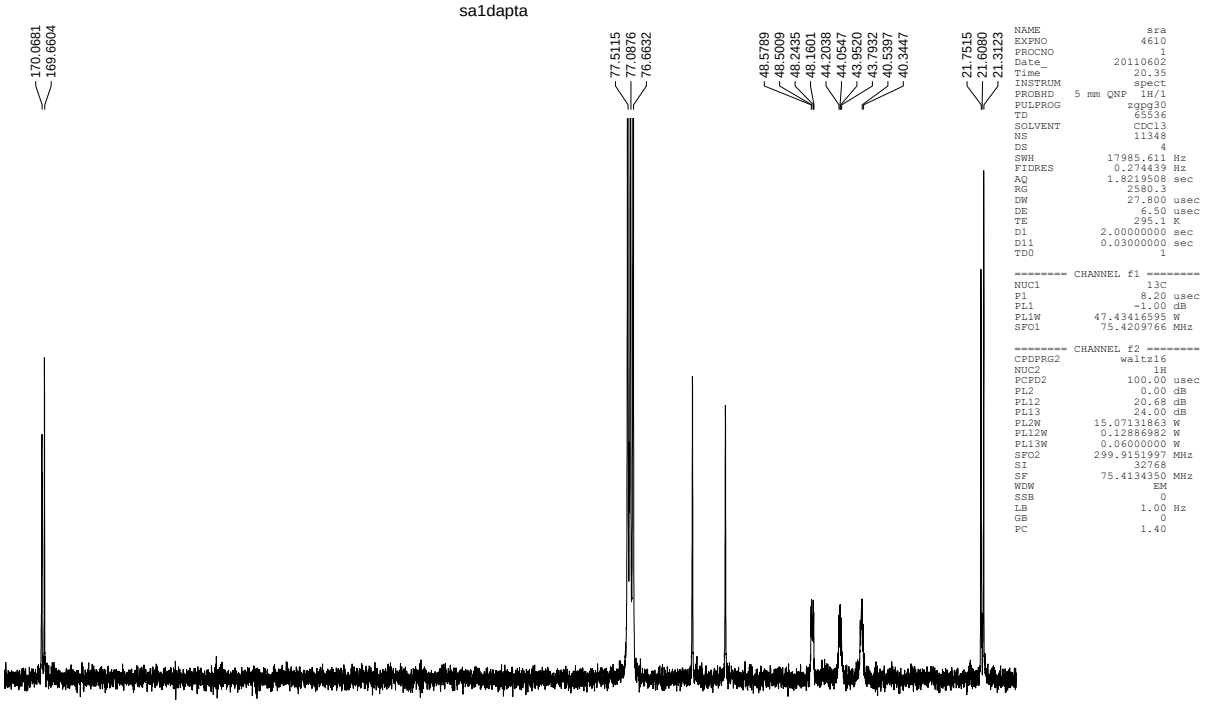

Appendix I.153. $^{13}C\{^{1}H\}$ NMR spectrum of cis-$PtMe_2(DAPTA)_2$, 9a.

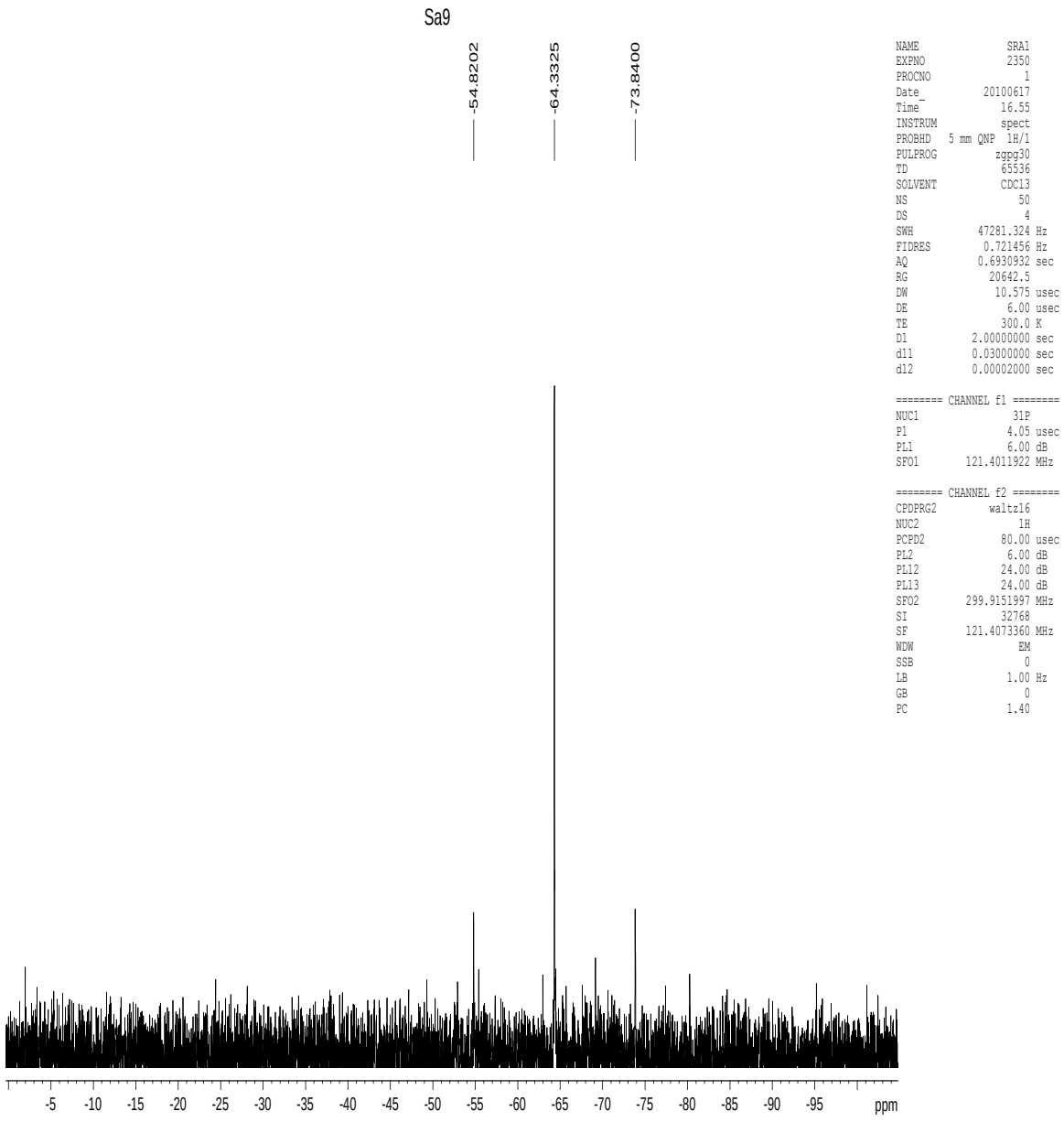

Appendix I.154. $^{31}P\{^{1}H\}$ NMR spectrum of trans-$Pt(C_2Ph)_2(PTA)_2$, 6b.

Appendix I.155. $^{31}P\{^{1}H\}$ NMR spectrum of cis-$Pt(C_2Ph)_2(PTA)_2$, 6a.

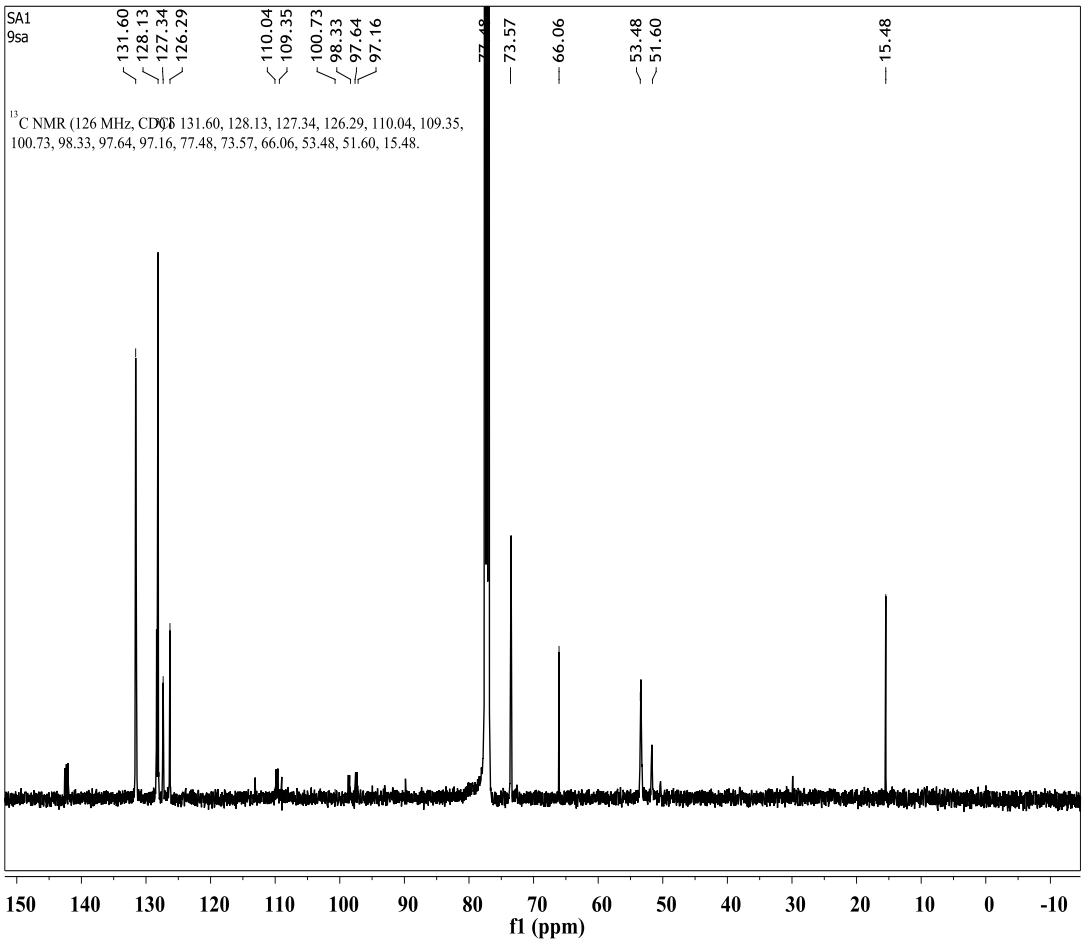

Appendix I.156. $^{13}C\{^{1}H\}$ NMR spectrum of cis-$Pt(C_2Ph)_2(PTA)_2$, 6a.

4.2. Appendix II. X-Ray Crystallography Data and Files

Appendix II.1. Crystal data and parameters for cis-$PtMe_2(PTA)_2$ (1a)

Table II.1.1. Atomic coordinates (x 10^4) and equivalent isotropic displacement parameters ($Å^2$x 10^3) for (**1a**). U(eq) is defined as one third of the trace of the orthogonalized U^{ij} tensor.

	x	y	z	U(eq)
Pt(1)	3157(1)	15932(1)	6988(1)	20(1)
Pt(2)	2527(1)	10111(1)	-74(1)	11(1)
P(1)	2727(2)	18079(2)	6414(1)	15(1)
P(2)	1254(3)	15520(2)	6806(2)	18(1)
P(3)	2422(2)	8055(2)	-10(1)	12(1)
P(4)	2787(2)	9971(2)	1222(1)	12(1)
N(1)	3591(8)	20368(9)	5795(5)	21(2)
N(2)	1399(9)	20541(8)	6405(5)	22(2)
N(3)	1845(8)	20080(8)	5088(5)	19(2)
N(4)	-1337(9)	16160(9)	6514(5)	22(2)
N(5)	-542(10)	14035(9)	7454(6)	32(2)
N(6)	-59(11)	14381(10)	6003(7)	37(3)
N(7)	3454(8)	5808(8)	-467(5)	19(2)
N(8)	2146(8)	5560(8)	781(5)	17(2)
N(9)	1107(8)	6533(8)	-509(5)	17(2)
N(10)	3179(9)	8705(8)	2826(5)	20(2)
N(11)	4185(8)	10594(8)	2257(5)	19(2)
N(12)	1841(8)	10907(8)	2530(5)	18(1)
C(1)	4028(10)	18977(10)	6205(6)	20(2)
C(2)	2093(10)	18659(9)	5401(6)	17(2)
C(3)	1566(10)	19190(10)	6882(6)	19(2)
C(4)	927(10)	20696(10)	5613(6)	22(2)
C(5)	2605(11)	20985(11)	6293(7)	25(2)
C(6)	3031(11)	20546(10)	5024(6)	22(2)
C(7)	-263(10)	16729(10)	6592(6)	19(2)
C(8)	610(11)	14358(12)	7641(7)	34(3)
C(9)	1169(12)	14748(11)	6008(7)	29(3)

C(10)	-1110(12)	15531(13)	5870(7)	31(3)
C(11)	-1584(11)	15176(10)	7258(7)	28(2)
C(12)	-323(14)	13473(12)	6772(9)	42(4)
C(13)	4954(11)	16057(14)	7296(8)	39(3)
C(14)	3797(12)	13912(12)	7442(9)	41(3)
C(15)	3726(9)	7073(10)	-484(6)	18(2)
C(16)	2270(10)	6783(9)	925(6)	16(2)
C(17)	1079(9)	7884(10)	-525(6)	17(2)
C(18)	3293(10)	5036(10)	354(7)	21(2)
C(19)	1034(10)	5742(10)	314(6)	19(2)
C(20)	2295(10)	5979(10)	-892(6)	21(2)
C(21)	3018(10)	8472(9)	2053(6)	17(2)
C(22)	4152(9)	10587(10)	1418(6)	19(2)
C(23)	1509(9)	10929(10)	1730(6)	18(1)
C(24)	4303(10)	9267(10)	2787(6)	22(2)
C(25)	3012(10)	11406(10)	2498(7)	21(2)
C(26)	2056(10)	9588(10)	3044(6)	20(2)
C(27)	2300(10)	10541(10)	-1313(6)	20(2)
C(28)	2588(11)	12078(9)	-307(6)	21(2)
C(1S)	4999(6)	14996(5)	4998(4)	370(30)
Cl(1)	3905(6)	16058(5)	4362(4)	94(2)
Cl(2)	4411(6)	13354(4)	5194(4)	95(2)
Cl(3)	6041(10)	15028(8)	5263(8)	201(7)

Table II.1.2. Anisotropic displacement parameters ($Å^2 x\ 10^3$) for jbw4609. The anisotropic displacement factor exponent takes the form: $-2\pi^2[\ h^2\ a^{*2}U^{11} + ...\ + 2\ h\ k\ a^*\ b^*\ U^{12}\ ]$

	U^{11}	U^{22}	U^{33}	U^{23}	U^{13}	U^{12}
Pt(1)	17(1)	19(1)	15(1)	2(1)	1(1)	6(1)
Pt(2)	13(1)	10(1)	11(1)	-3(1)	-1(1)	-3(1)
P(1)	15(1)	16(1)	13(1)	-4(1)	-3(1)	1(1)
P(2)	22(1)	11(1)	16(1)	-1(1)	5(1)	1(1)
P(3)	13(1)	11(1)	12(1)	-3(1)	-1(1)	-4(1)
P(4)	13(1)	11(1)	12(1)	-5(1)	-2(1)	-2(1)

N(1)	23(4)	19(4)	24(5)	-8(4)	-4(4)	-6(3)
N(2)	23(4)	18(4)	23(4)	-8(4)	-3(4)	1(3)
N(3)	23(4)	18(4)	14(4)	0(3)	-5(3)	-6(3)
N(4)	29(5)	20(4)	16(4)	0(3)	2(4)	-9(4)
N(5)	29(5)	17(4)	35(5)	6(4)	16(4)	2(4)
N(6)	45(6)	34(6)	45(6)	-25(5)	25(5)	-28(5)
N(7)	19(4)	18(4)	27(5)	-14(4)	3(3)	-6(3)
N(8)	23(4)	12(4)	17(4)	-3(3)	-4(3)	-7(3)
N(9)	19(4)	18(4)	18(4)	-4(3)	-4(3)	-9(3)
N(10)	28(5)	19(4)	15(4)	-7(3)	-7(3)	0(4)
N(11)	18(4)	23(4)	22(4)	-15(4)	-6(3)	-2(3)
N(12)	17(3)	21(3)	14(3)	-9(2)	-4(2)	2(2)
C(1)	16(5)	22(5)	25(5)	-9(4)	-5(4)	-3(4)
C(2)	23(5)	17(5)	13(4)	-3(4)	-5(4)	-6(4)
C(3)	20(5)	20(5)	14(5)	-6(4)	-2(4)	1(4)
C(4)	23(5)	17(5)	21(5)	0(4)	-7(4)	0(4)
C(5)	31(6)	20(5)	27(6)	-11(4)	-2(5)	-7(4)
C(6)	28(6)	20(5)	20(5)	-5(4)	1(4)	-10(4)
C(7)	24(5)	12(4)	21(5)	-2(4)	-4(4)	0(4)
C(8)	29(6)	27(6)	25(6)	11(5)	11(5)	9(5)
C(9)	36(6)	22(5)	36(6)	-17(5)	22(5)	-14(5)
C(10)	35(6)	40(7)	28(6)	-13(5)	5(5)	-23(5)
C(11)	29(6)	16(5)	26(6)	4(4)	11(5)	1(4)
C(12)	43(7)	18(6)	64(9)	-17(6)	31(7)	-13(5)
C(13)	20(6)	45(8)	34(7)	11(6)	-7(5)	3(5)
C(14)	28(6)	28(6)	44(8)	10(5)	7(5)	12(5)
C(15)	17(5)	19(5)	21(5)	-11(4)	5(4)	-8(4)
C(16)	25(5)	13(4)	12(4)	-3(4)	-3(4)	-7(4)
C(17)	17(5)	18(5)	19(5)	-3(4)	-4(4)	-8(4)
C(18)	21(5)	13(5)	30(6)	-8(4)	-5(4)	-2(4)
C(19)	21(5)	17(5)	21(5)	-5(4)	-1(4)	-9(4)
C(20)	26(5)	24(5)	18(5)	-12(4)	1(4)	-10(4)
C(21)	23(5)	14(4)	14(4)	-7(4)	-6(4)	-1(4)
C(22)	16(5)	21(5)	23(5)	-11(4)	-3(4)	-5(4)
C(23)	17(3)	21(3)	14(3)	-9(2)	-4(2)	2(2)
C(24)	23(5)	19(5)	25(5)	-12(4)	-13(4)	5(4)

C(25)	20(5)	20(5)	28(5)	-15(4)	-6(4)	0(4)
C(26)	24(5)	25(5)	14(5)	-8(4)	0(4)	-4(4)
C(27)	26(5)	18(5)	15(5)	-1(4)	-2(4)	-7(4)
C(28)	32(6)	13(5)	19(5)	-2(4)	-3(4)	-7(4)
C(1S)	330(40)	280(40)	500(50)	0(40)	-350(40)	-70(40)
Cl(1)	90(4)	101(5)	96(4)	-36(4)	-3(3)	-17(4)
Cl(2)	81(4)	87(4)	115(5)	-32(4)	4(3)	-11(3)
Cl(3)	179(11)	161(10)	244(15)	53(10)	-77(10)	-103(9)

Table II.1.3. Hydrogen coordinates (x 10^4) and isotropic displacement parameters (Å^{2}x 10^3) for (**1a**).

	x	y	z	U(eq)
H(1A)	4410	18899	6715	24
H(1B)	4702	18581	5868	24
H(2A)	2714	18267	5035	21
H(2B)	1287	18360	5411	21
H(3A)	730	18926	6957	22
H(3B)	1860	19117	7416	22
H(4A)	148	20328	5687	26
H(4B)	676	21634	5345	26
H(5A)	2954	20826	6825	30
H(5B)	2425	21934	6048	30
H(6A)	2863	21481	4739	27
H(6B)	3667	20087	4695	27
H(7A)	-473	17164	7027	23
H(7B)	-146	17398	6090	23
H(8A)	1273	13553	7797	41
H(8B)	420	14728	8105	41
H(9A)	1321	15355	5485	35
H(9B)	1861	13963	6074	35
H(10A)	-916	16167	5369	38

H(10B)	-1905	15271	5795	38
H(11A)	-1732	15583	7707	33
H(11B)	-2375	14894	7204	33
H(12A)	-1087	13142	6722	50
H(12B)	409	12723	6884	50
H(13A)	5166	16879	6977	58
H(13B)	5604	15333	7191	58
H(13C)	4933	16018	7865	58
H(14A)	4689	13726	7595	61
H(14B)	3739	13481	7030	61
H(14C)	3262	13590	7910	61
H(15A)	3861	7561	-1045	21
H(15B)	4527	6926	-203	21
H(16A)	3033	6618	1244	20
H(16B)	1510	7097	1241	20
H(17A)	263	8234	-270	21
H(17B)	1103	8409	-1088	21
H(18A)	4054	4972	652	25
H(18B)	3256	4148	346	25
H(19A)	268	6150	587	23
H(19B)	912	4879	307	23
H(20A)	2223	5125	-946	25
H(20B)	2384	6550	-1437	25
H(21A)	2269	8066	2100	20
H(21B)	3783	7854	1927	20
H(22A)	4957	10041	1273	23
H(22B)	4105	11481	1072	23
H(23A)	1323	11839	1398	21
H(23B)	721	10585	1776	21
H(24A)	5054	8700	2601	26
H(24B)	4468	9278	3333	26
H(25A)	2894	12281	2119	25
H(25B)	3127	11500	3033	25
H(26A)	1291	9229	3041	25
H(26B)	2142	9617	3598	25
H(27A)	2208	9760	-1448	30

H(27B)	3052	10840	-1602	30
H(27C)	1533	11223	-1465	30
H(28A)	2491	12497	-880	32
H(28B)	3411	12153	-147	32
H(28C)	1891	12501	-4	3

Appendix II.2. Crystal data and parameters for trans-PtCl(Et)(PTA)$_2$ (3a)

Table II.2.1. Atomic coordinates (x 10^4) and equivalent isotropic displacement parameters (Å^{2}x 10^3) for **3a**. U(eq) is defined as one third of the trace of the orthogonalized U^{ij} tensor.

	x	y	z	U(eq)
Pt(1)	4522(1)	9420(1)	2181(1)	9(1)
P(1)	5648(1)	9452(1)	1480(1)	12(1)
P(2)	3448(1)	9572(1)	2885(1)	11(1)
Cl(1)	1503(1)	9874(1)	1894(1)	14(1)
Cl(2)	6677(2)	4329(2)	204(1)	42(1)
Cl(3)	9792(2)	2885(1)	-106(1)	32(1)
N(1)	5052(5)	9600(4)	564(1)	21(1)
N(2)	7572(4)	10936(3)	877(1)	17(1)
N(3)	7816(4)	8469(4)	822(1)	19(1)
N(4)	3862(5)	9603(4)	3806(1)	21(1)
N(5)	1086(5)	8605(3)	3500(1)	20(1)
N(6)	1529(5)	11066(3)	3485(1)	17(1)
C(1)	7018(5)	8886(4)	2427(1)	13(1)
C(2)	7203(5)	7360(4)	2468(1)	17(1)
C(3)	4102(5)	9450(4)	991(1)	18(1)
C(4)	6960(5)	10955(4)	1346(1)	15(1)
C(5)	7241(5)	8174(4)	1283(1)	17(1)
C(6)	6296(6)	8493(5)	502(1)	22(1)
C(7)	6059(6)	10868(4)	554(1)	21(1)
C(8)	8730(5)	9771(4)	801(1)	19(1)
C(9)	4908(5)	9462(5)	3393(1)	19(1)

C(10)	2258(5)	11129(4)	3030(1)	16(1)
C(11)	1743(5)	8358(4)	3044(1)	18(1)
C(12)	2555(6)	8529(4)	3838(1)	24(1)
C(13)	271(6)	9945(4)	3528(1)	20(1)
C(14)	2957(6)	10904(4)	3826(1)	19(1)
C(1S)	8785(6)	3651(5)	359(2)	26(1)

Table II.2.2. Anisotropic displacement parameters ($Å^2 x\ 10^3$) for **3a**. The anisotropic displacement factor exponent takes the form: $-2\pi^2[\ h^2\ a^{*2}U^{11} + ...\ + 2\ h\ k\ a^*\ b^*\ U^{12}\ ]$

	U^{11}	U^{22}	U^{33}	U^{23}	U^{13}	U^{12}
Pt(1)	8(1)	10(1)	11(1)	0(1)	0(1)	0(1)
P(1)	10(1)	14(1)	12(1)	0(1)	1(1)	0(1)
P(2)	9(1)	11(1)	12(1)	0(1)	0(1)	0(1)
Cl(1)	8(1)	19(1)	15(1)	0(1)	-1(1)	2(1)
Cl(2)	36(1)	43(1)	46(1)	0(1)	1(1)	11(1)
Cl(3)	35(1)	30(1)	32(1)	4(1)	5(1)	3(1)
N(1)	17(2)	32(2)	14(2)	-3(1)	0(1)	-1(1)
N(2)	15(2)	21(2)	14(2)	5(1)	1(1)	-3(1)
N(3)	16(2)	24(2)	16(2)	-3(1)	3(1)	-1(1)
N(4)	22(2)	29(2)	12(2)	0(1)	-1(1)	6(1)
N(5)	25(2)	15(2)	20(2)	1(1)	8(1)	-4(1)
N(6)	18(2)	17(2)	15(2)	-1(1)	2(1)	1(1)
C(1)	10(2)	14(2)	14(2)	0(1)	-1(1)	2(1)
C(2)	15(2)	14(2)	20(2)	2(1)	-5(1)	3(1)
C(3)	12(2)	28(2)	16(2)	-2(2)	0(1)	0(2)
C(4)	16(2)	16(2)	13(2)	2(1)	1(1)	-2(1)
C(5)	16(2)	17(2)	18(2)	-1(1)	3(1)	0(1)
C(6)	21(2)	29(2)	16(2)	-6(2)	1(2)	-3(2)
C(7)	21(2)	27(2)	14(2)	6(2)	-1(1)	-3(2)
C(8)	14(2)	28(2)	16(2)	0(2)	3(1)	-3(2)
C(9)	14(2)	31(2)	13(2)	1(2)	-2(1)	4(2)
C(10)	18(2)	15(2)	14(2)	1(1)	3(1)	5(1)

C(11)	20(2)	16(2)	18(2)	-3(1)	7(1)	-5(2)
C(12)	34(2)	21(2)	19(2)	8(2)	4(2)	2(2)
C(13)	19(2)	24(2)	17(2)	-3(2)	5(2)	-2(2)
C(14)	22(2)	19(2)	15(2)	-6(1)	2(2)	-2(2)
C(1S)	31(2)	26(2)	21(2)	0(2)	-6(2)	-2(2)

Table II.2.3. Hydrogen coordinates (x 10^4) and isotropic displacement parameters ($Å^2$x 10^3) for **3a**.

	x	y	z	U(eq)
H(1A)	7931	9237	2223	15
H(1B)	7223	9305	2726	15
H(2A)	6313	7014	2674	25
H(2B)	8396	7137	2585	25
H(2C)	7021	6945	2171	25
H(3A)	3423	8592	985	22
H(3B)	3245	10203	1020	22
H(4A)	6230	11774	1392	18
H(4B)	8005	11005	1554	18
H(5A)	8292	8157	1490	20
H(5B)	6678	7269	1290	20
H(6A)	6755	8547	193	26
H(6B)	5642	7628	527	26
H(7A)	5241	11626	616	25
H(7B)	6509	10998	247	25
H(8A)	9265	9863	501	23
H(8B)	9709	9781	1029	23
H(9A)	5530	8579	3398	23
H(9B)	5816	10185	3385	23
H(10A)	3081	11907	3012	19
H(10B)	1276	11277	2808	19

H(11A)	734	8411	2825	22
H(11B)	2240	7432	3031	22
H(12A)	2046	8554	4142	29
H(12B)	3165	7648	3806	29
H(13A)	-323	10026	3821	24
H(13B)	-655	10026	3287	24
H(14A)	3840	11634	3787	22
H(14B)	2449	11010	4128	22
H(1S1)	9561	4384	477	31
H(1S2)	8644	2973	600	31

Appendix II.3. Crystal data and parameters for trans-$PtCl_2(PTA)_2$ (4)

Table II.3.1. Atomic coordinates (x 10^4) and equivalent isotropic displacement parameters ($Å^2$x 10^3) for **4**. U(eq) is defined as one third of the trace of the orthogonalized U^{ij} tensor.

	x	y	z	U(eq)
Pt(1)	0	0	0	10(1)
P(1)	-1613(3)	839(1)	-934(3)	8(1)
Cl(1)	2390(6)	330(1)	3318(6)	54(1)
N(1)	-2770(12)	1646(3)	-4135(11)	12(1)
N(2)	-5529(12)	1494(3)	-1780(12)	15(2)
N(3)	-1775(12)	1958(3)	-244(11)	13(1)
C(1)	-1607(15)	1104(4)	-3676(14)	15(2)
C(2)	-4720(13)	931(3)	-1045(14)	12(2)
C(3)	-484(14)	1460(3)	686(14)	12(2)
C(4)	-5211(14)	1610(4)	-3986(15)	16(2)
C(5)	-1587(14)	2059(3)	-2496(14)	13(2)
C(6)	-4247(15)	1910(3)	-233(14)	15(2)

Table II.3.2. Anisotropic displacement parameters ($Å^2 x\ 10^3$) for **4**. The anisotropic displacement factor exponent takes the form: $-2\pi^2[\ h^2\ a^{*2}U^{11} + ... + 2\ h\ k\ a^*\ b^*\ U^{12}\ ]$

	U^{11}	U^{22}	U^{33}	U^{23}	U^{13}	U^{12}
Pt(1)	8(1)	10(1)	10(1)	0(1)	1(1)	1(1)
P(1)	6(1)	9(1)	8(1)	0(1)	2(1)	1(1)
Cl(1)	59(2)	49(2)	51(2)	2(2)	10(2)	10(2)
N(1)	12(3)	13(3)	11(3)	0(3)	3(3)	1(3)
N(2)	12(3)	12(3)	21(4)	2(3)	6(3)	3(3)
N(3)	12(3)	13(3)	13(3)	-1(3)	2(3)	-3(3)
C(1)	16(4)	18(4)	11(4)	0(3)	6(3)	5(3)
C(2)	8(4)	14(4)	13(4)	3(3)	1(3)	1(3)
C(3)	11(4)	12(4)	12(4)	-1(3)	0(3)	-1(3)
C(4)	11(4)	16(4)	19(4)	2(4)	-3(4)	1(3)
C(5)	13(4)	10(4)	17(4)	1(3)	4(3)	-3(3)
C(6)	15(4)	12(4)	19(4)	1(3)	8(4)	3(3)

Table II.3.3. Hydrogen coordinates ($x\ 10^4$) and isotropic displacement parameters ($Å^2 x\ 10^3$) for **4**.

	x	y	z	U(eq)
H(1A)	28	1138	-3798	17
H(1B)	-2408	835	-4803	17
H(2A)	-5643	657	-2074	14
H(2B)	-4987	863	437	14
H(3A)	-612	1410	2225	15
H(3B)	1189	1508	714	15
H(4A)	-5997	1965	-4504	20
H(4B)	-6001	1317	-5002	20
H(5A)	89	2069	-2500	16
H(5B)	-2251	2428	-2964	16

H(6A)	-5006	2274	-611	18
H(6B)	-4361	1815	1277	18

Appendix II.4. Crystal data and parameters for trans-Pt(C_2Ph)$_2$(PTA)$_2$ (6b)

Table II.4.1. Atomic coordinates (x 10^4) and equivalent isotropic displacement parameters (Å^{2}x 10^3) for **6b**. U(eq) is defined as one third of the trace of the orthogonalized U^{ij} tensor.

	x	y	z	U(eq)
Pt(1)	0	5000	5000	39(1)
Pt(2)	10000	0	0	39(1)
P(1)	520(6)	3383(2)	4783(2)	32(1)
P(2)	11670(6)	1414(3)	748(2)	38(1)
N(1)	3410(20)	2046(9)	4508(8)	46(3)
N(2)	-160(20)	1613(9)	3808(8)	51(3)
N(3)	160(20)	1527(10)	5187(8)	54(4)
N(4)	12510(30)	2594(11)	2154(8)	62(4)
N(5)	12080(20)	3436(10)	1057(10)	80(5)
N(6)	15440(20)	2706(10)	1243(7)	64(4)
C(1)	2020(20)	5291(8)	4188(7)	34(3)
C(2)	3310(20)	5450(10)	3722(9)	52(4)
C(3)	4870(20)	5744(10)	3175(8)	44(4)
C(4)	4480(30)	6407(13)	2704(13)	69(5)
C(5)	5990(40)	6653(16)	2203(14)	86(7)
C(6)	7930(40)	6246(17)	2140(14)	81(7)
C(7)	8300(30)	5578(13)	2583(14)	71(6)
C(8)	6820(30)	5317(12)	3116(11)	57(4)
C(9)	3320(20)	3133(10)	4674(10)	45(4)
C(10)	-750(30)	2649(10)	3897(10)	50(4)
C(11)	-360(30)	2558(10)	5445(9)	48(4)
C(12)	2170(30)	1633(12)	3798(10)	59(5)
C(13)	2480(30)	1556(12)	5117(10)	56(4)

C(14)	-970(30)	1116(11)	4419(11)	59(5)
C(15)	7920(20)	-264(13)	798(7)	52(3)
C(16)	6740(20)	-470(13)	1285(7)	52(3)
C(17)	5160(20)	-652(11)	1853(8)	44(4)
C(18)	3010(30)	-1064(12)	1646(10)	49(4)
C(19)	1520(30)	-1266(12)	2175(11)	57(4)
C(20)	2200(40)	-1109(14)	2936(12)	73(6)
C(21)	4320(30)	-735(13)	3173(10)	60(5)
C(22)	5790(30)	-511(11)	2626(9)	47(4)
C(23)	11360(30)	1619(13)	1776(10)	62(5)
C(24)	10910(30)	2550(11)	563(12)	74(6)
C(25)	14650(20)	1749(12)	749(10)	60(5)
C(27)	14840(30)	2671(13)	2034(9)	60(5)
C(26)	11510(90)	3340(30)	1839(15)	84(7)
C(28)	14470(30)	3550(30)	1030(40)	84(7)
C(26')	11870(90)	3450(30)	1872(15)	84(7)
C(28')	14400(40)	3440(30)	890(40)	84(7)
O(1)	1170(130)	5400(60)	120(40)	89(8)
C(29)	2420(190)	6280(80)	640(70)	89(8)
C(29')	1470(80)	5150(30)	-146(19)	89(8)
O(1')	1950(50)	5870(20)	593(17)	89(8)

Table II.4.2. Anisotropic displacement parameters ($Å^2 x\ 10^3$) for **6b**. The anisotropic displacement factor exponent takes the form: $-2\pi^2[\ h^2\ a^{*2}U^{11} + ... + 2\ h\ k\ a^*\ b^*\ U^{12}\ ]$

	U^{11}	U^{22}	U^{33}	U^{23}	U^{13}	U^{12}
Pt(1)	39(1)	18(1)	59(1)	1(1)	-6(1)	9(1)
Pt(2)	27(1)	55(1)	29(1)	-6(1)	5(1)	-4(1)
P(1)	35(2)	20(1)	41(2)	5(1)	-3(2)	4(1)
P(2)	28(2)	46(2)	35(2)	0(2)	3(1)	-7(2)
N(1)	33(7)	37(6)	68(9)	6(6)	-5(6)	11(5)
N(2)	47(8)	37(7)	58(8)	-6(6)	-10(6)	-4(6)
N(3)	67(10)	39(7)	63(9)	20(6)	20(7)	17(6)
N(4)	59(10)	60(9)	53(8)	-16(7)	5(7)	-9(7)

N(5)	70(12)	46(9)	116(15)	8(9)	-25(11)	-4(8)
N(6)	34(8)	81(11)	64(9)	-12(8)	-6(7)	-2(7)
C(1)	30(7)	15(5)	59(9)	11(6)	7(6)	11(5)
C(2)	50(10)	25(7)	79(12)	-3(7)	-14(9)	10(7)
C(3)	38(9)	29(7)	60(10)	-1(7)	-12(7)	-2(6)
C(4)	60(12)	51(10)	101(16)	20(10)	2(11)	19(9)
C(5)	98(18)	62(13)	104(18)	42(12)	14(14)	5(12)
C(6)	60(14)	72(14)	100(17)	-5(13)	22(12)	-10(11)
C(7)	36(10)	45(10)	119(18)	-18(11)	5(10)	2(8)
C(8)	41(9)	40(8)	85(13)	-1(8)	-9(9)	5(7)
C(9)	32(8)	28(7)	71(10)	0(7)	-6(7)	7(6)
C(10)	42(9)	34(7)	72(11)	26(7)	-27(8)	-10(6)
C(11)	79(12)	25(7)	44(8)	17(6)	13(8)	5(7)
C(12)	71(12)	39(8)	63(11)	-4(8)	18(9)	6(8)
C(13)	68(12)	42(8)	63(11)	20(8)	-4(9)	18(8)
C(14)	52(10)	25(7)	97(14)	17(8)	-2(9)	-8(7)
C(15)	43(7)	74(8)	28(5)	-7(5)	-4(4)	-8(6)
C(16)	43(7)	74(8)	28(5)	-7(5)	-4(4)	-8(6)
C(17)	46(9)	39(8)	44(8)	1(7)	17(7)	2(7)
C(18)	40(9)	52(9)	54(9)	13(8)	4(7)	-2(7)
C(19)	47(10)	47(9)	79(13)	24(9)	15(9)	-5(7)
C(20)	95(17)	62(11)	79(14)	39(11)	60(13)	30(11)
C(21)	76(14)	61(11)	52(10)	19(8)	15(9)	31(10)
C(22)	49(9)	46(8)	47(9)	5(7)	3(7)	14(7)
C(23)	62(11)	56(10)	51(10)	-11(8)	15(8)	-29(9)
C(24)	64(12)	38(9)	114(17)	23(10)	-38(12)	-14(8)
C(25)	25(8)	77(12)	65(11)	-17(9)	0(7)	-3(8)
C(27)	55(11)	51(10)	62(11)	-10(8)	-18(8)	-4(8)
C(26)	60(12)	71(12)	95(15)	-21(11)	-6(10)	-34(9)
C(28)	60(12)	71(12)	95(15)	-21(11)	-6(10)	-34(9)
C(26')	60(12)	71(12)	95(15)	-21(11)	-6(10)	-34(9)
C(28')	60(12)	71(12)	95(15)	-21(11)	-6(10)	-34(9)
O(1)	90(14)	100(20)	95(15)	65(19)	36(13)	20(12)
C(29)	90(14)	100(20)	95(15)	65(19)	36(13)	20(12)
C(29')	90(14)	100(20)	95(15)	65(19)	36(13)	20(12)
O(1')	90(14)	100(20)	95(15)	65(19)	36(13)	20(12)

Table II.4.3. Hydrogen coordinates (x 10^4) and isotropic displacement parameters ($Å^2$x 10^3) for **6b**.

	x	y	z	U(eq)
H(4A)	3190	6687	2728	83
H(5A)	5711	7110	1889	103
H(6A)	8959	6436	1798	97
H(7A)	9564	5281	2533	85
H(8A)	7113	4865	3432	69
H(9A)	3928	3445	4258	54
H(9B)	4206	3423	5142	54
H(10A)	-2338	2615	3900	60
H(10B)	-261	2961	3466	60
H(11A)	356	2820	5949	58
H(11B)	-1938	2526	5490	58
H(12A)	2703	2012	3407	71
H(12B)	2457	958	3644	71
H(13A)	2796	877	5036	67
H(13B)	3231	1889	5601	67
H(14A)	-815	419	4294	70
H(14B)	-2527	1156	4448	70
H(18A)	2549	-1211	1127	59
H(19A)	57	-1508	2019	69
H(20A)	1200	-1262	3296	87
H(21A)	4776	-630	3691	72
H(22A)	7247	-259	2786	56
H(23A)	9805	1578	1869	75
H(23B)	11926	1099	2000	75
H(24A)	11162	2608	33	89
H(24B)	9342	2530	624	89
H(25A)	15361	1234	928	72

H(25B)	15058	1788	228	72
H(27A)	15382	2106	2201	72
H(27B)	15586	3266	2360	72
H(26A)	11952	3981	2168	100
H(26B)	9922	3183	1844	100
H(28A)	15114	4149	1373	100
H(28B)	14854	3627	513	100
H(26C)	10352	3492	1983	100
H(26D)	12766	4046	2150	100
H(28C)	15206	4099	1084	100
H(28D)	14515	3310	343	100
H(1)	638	4987	369	133
H(29A)	1421	6723	836	133
H(29B)	3512	6623	367	133
H(29C)	3126	6057	1065	133
H(29D)	1257	5502	-562	133
H(29E)	159	4691	-109	133
H(29F)	2681	4784	-237	133
H(1')	2828	6351	523	133

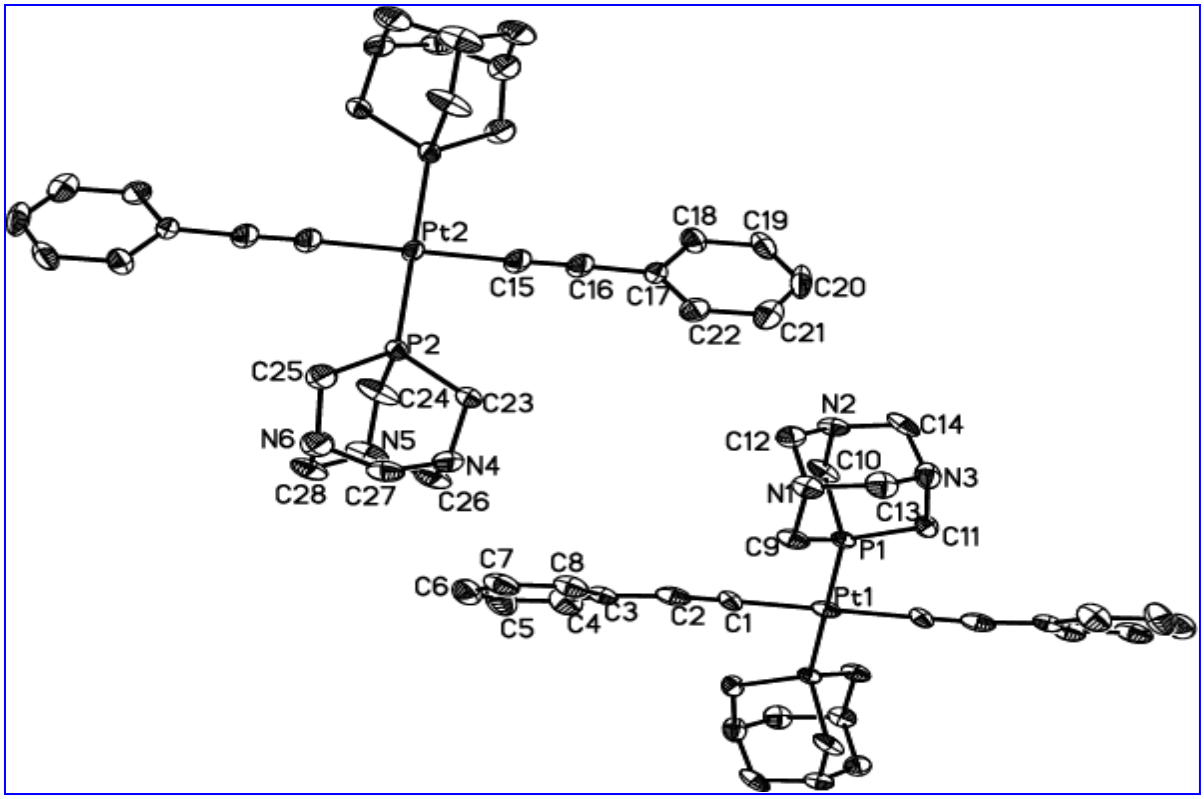

Figure II.1. ORTEP diagram of **6b**. Projection view with 30% thermal ellipsoids: disorder atoms, H atoms and solvent omitted.

Appendix II.5. Crystal data and parameters for trans-$PtI_2(DAPTA)_2$ (12d)

Table II.5.1. Atomic coordinates (x 10^4) and equivalent isotropic displacement parameters ($Å^2$x 10^3) for **12d**. U(eq) is defined as one third of the trace of the orthogonalized U^{ij} tensor.

	x	y	z	U(eq)
Pt(1)	5000	0	5000	10(1)
I(1)	1708(1)	-2567(1)	4900(1)	16(1)
P(1)	3678(1)	781(1)	3542(1)	13(1)
O(1)	6869(2)	2538(2)	1263(1)	26(1)
O(2)	3280(2)	5694(2)	1805(1)	28(1)
N(1)	3069(2)	3758(2)	2888(1)	19(1)
N(2)	3905(2)	801(2)	1441(1)	18(1)
N(3)	759(2)	713(2)	2052(1)	23(1)
C(1)	3832(2)	3230(2)	3812(1)	18(1)

C(2)	4795(2)	296(2)	2353(1)	16(1)
C(3)	1062(2)	-157(2)	2928(1)	20(1)
C(4)	1034(2)	2662(3)	2379(2)	26(1)
C(5)	1737(3)	157(3)	1184(1)	25(1)
C(6)	5085(2)	1926(2)	940(1)	16(1)
C(7)	4143(3)	2366(2)	-24(1)	20(1)
C(8)	4071(2)	5205(2)	2530(1)	18(1)
C(9)	6192(3)	6193(2)	3030(2)	22(1)
O(1S)	9308(3)	5867(3)	1039(2)	34(1)
O(2S)	10040(20)	4815(19)	-188(11)	34(1)

Table II.5.2. Anisotropic displacement parameters ($Å^2 x\ 10^3$) for **12d**. The anisotropic displacement factor exponent takes the form: $-2\pi^2[\ h^2\ a^{*2}U^{11} + ... + 2\ h\ k\ a^*\ b^*\ U^{12}\ ]$

	U^{11}	U^{22}	U^{33}	U^{23}	U^{13}	U^{12}
Pt(1)	11(1)	9(1)	11(1)	4(1)	4(1)	3(1)
I(1)	12(1)	15(1)	21(1)	9(1)	4(1)	2(1)
P(1)	13(1)	12(1)	14(1)	6(1)	2(1)	3(1)
O(1)	18(1)	30(1)	32(1)	18(1)	6(1)	6(1)
O(2)	31(1)	27(1)	29(1)	17(1)	4(1)	6(1)
N(1)	16(1)	18(1)	26(1)	12(1)	3(1)	6(1)
N(2)	18(1)	20(1)	13(1)	8(1)	0(1)	2(1)
N(3)	15(1)	28(1)	27(1)	17(1)	-1(1)	1(1)
C(1)	20(1)	13(1)	22(1)	7(1)	3(1)	7(1)
C(2)	20(1)	18(1)	13(1)	6(1)	4(1)	7(1)
C(3)	14(1)	21(1)	24(1)	12(1)	2(1)	0(1)
C(4)	14(1)	31(1)	37(1)	21(1)	3(1)	7(1)
C(5)	20(1)	29(1)	18(1)	10(1)	-5(1)	-4(1)
C(6)	20(1)	15(1)	16(1)	6(1)	5(1)	7(1)
C(7)	28(1)	20(1)	17(1)	10(1)	5(1)	8(1)
C(8)	20(1)	15(1)	21(1)	6(1)	7(1)	6(1)
C(9)	22(1)	18(1)	25(1)	5(1)	7(1)	4(1)
O(1S)	27(1)	25(1)	50(1)	17(1)	6(1)	6(1)
O(2S)	27(1)	25(1)	50(1)	17(1)	6(1)	6(1)

Table II.5.3. Hydrogen coordinates (x 10^4) and isotropic displacement parameters ($Å^2$x 10^3) for **12d**.

	x	y	z	U(eq)
H(1A)	3080	3501	4386	21
H(1B)	5228	3978	4064	21
H(2A)	6221	975	2522	19
H(2B)	4660	-1030	2159	19
H(3A)	707	-1503	2658	24
H(3B)	219	106	3456	24
H(4A)	128	2868	2881	31
H(4B)	668	3104	1751	31
H(5A)	1317	629	579	30
H(5B)	1296	-1199	957	30
H(7A)	5175	3030	-364	30
H(7B)	3302	3130	190	30
H(7C)	3341	1225	-526	30
H(9A)	6821	6966	2581	33
H(9B)	6891	5294	3104	33
H(9C)	6244	6961	3730	33
H(1S1)	8510(50)	4830(30)	1030(30)	50
H(2S1)	11028	5775	-392	50
H(2S2)	8908	4267	-764	50

Appendix II.6. Crystal data and parameters for trans-[Pd{C_2(o-py)}$_2$($PTA)_2$] (22)

Table II.6.1. Atomic coordinates (x 10^4) and equivalent isotropic displacement parameters ($Å^2$x 10^3) for **22**. U(eq) is defined as one third of the trace of the orthogonalized U^{ij} tensor.

	x	y	z	U(eq)

Pd(1)	5000	5000	10000	11(1)
P(1)	5526(2)	5264(1)	8388(1)	12(1)
N(1)	8494(6)	5555(2)	7124(3)	16(1)
N(2)	4800(6)	6082(2)	6792(3)	16(1)
N(3)	4968(5)	5022(2)	6290(2)	15(1)
N(4)	9713(6)	7006(2)	11580(3)	17(1)
C(1)	7217(7)	5653(2)	10564(3)	12(1)
C(2)	8538(7)	6044(2)	10834(3)	14(1)
C(3)	10204(7)	6520(2)	11042(3)	13(1)
C(4)	12200(7)	6479(2)	10660(3)	16(1)
C(5)	13694(7)	6955(2)	10790(3)	19(1)
C(6)	13177(8)	7465(2)	11305(3)	20(1)
C(7)	11186(7)	7457(2)	11686(3)	20(1)
C(8)	8453(7)	5374(2)	8210(3)	18(1)
C(9)	7275(7)	6116(2)	6855(3)	18(1)
C(10)	7418(7)	5098(2)	6372(3)	18(1)
C(11)	3876(7)	5606(2)	6053(3)	17(1)
C(12)	4286(7)	5970(2)	7829(3)	14(1)
C(13)	4476(7)	4776(2)	7267(3)	15(1)
C(1S)	7443(7)	8127(2)	8555(3)	17(1)
Cl(1)	8329(2)	7398(1)	8936(1)	28(1)
Cl(2)	4750(2)	8267(1)	8844(1)	24(1)
Cl(3)	9455(2)	8647(1)	9210(1)	24(1)

Table II.6.2. Anisotropic displacement parameters ($Å^2 \times 10^3$) for **22**. The anisotropic displacement factor exponent takes the form: $-2\pi^2[h^2 a^{*2}U^{11} + ... + 2 h k a^* b^* U^{12}]$

	U^{11}	U^{22}	U^{33}	U^{23}	U^{13}	U^{12}
Pd(1)	13(1)	11(1)	9(1)	1(1)	3(1)	-2(1)
P(1)	14(1)	12(1)	10(1)	0(1)	4(1)	-1(1)
N(1)	14(2)	22(2)	11(2)	-2(2)	4(2)	-2(2)
N(2)	21(2)	17(2)	13(2)	2(2)	9(2)	-2(2)

N(3)	18(2)	18(2)	8(2)	4(2)	2(1)	1(2)
N(4)	18(2)	17(2)	16(2)	-3(2)	4(2)	-1(2)
C(1)	9(2)	16(2)	14(2)	2(2)	4(2)	3(2)
C(2)	16(2)	17(2)	11(2)	6(2)	6(2)	6(2)
C(3)	15(2)	12(2)	13(2)	2(2)	3(2)	2(2)
C(4)	16(2)	14(2)	18(2)	-3(2)	4(2)	-3(2)
C(5)	15(2)	23(2)	19(2)	1(2)	5(2)	0(2)
C(6)	19(3)	19(2)	22(3)	-3(2)	1(2)	-2(2)
C(7)	22(3)	20(2)	16(2)	-6(2)	2(2)	0(2)
C(8)	15(2)	27(3)	12(2)	2(2)	4(2)	1(2)
C(9)	27(3)	14(2)	14(2)	2(2)	9(2)	-7(2)
C(10)	17(2)	21(3)	16(2)	-2(2)	7(2)	1(2)
C(11)	20(2)	22(3)	9(2)	5(2)	0(2)	-1(2)
C(12)	17(2)	15(2)	12(2)	1(2)	6(2)	1(2)
C(13)	18(2)	13(2)	15(2)	-2(2)	6(2)	-4(2)
C(1S)	17(2)	18(2)	15(2)	0(2)	3(2)	-1(2)
Cl(1)	39(1)	19(1)	26(1)	0(1)	8(1)	4(1)
Cl(2)	19(1)	30(1)	27(1)	-4(1)	9(1)	-3(1)
Cl(3)	21(1)	24(1)	28(1)	-4(1)	7(1)	-4(1)

Table II.6.3. Hydrogen coordinates (x 10^4) and isotropic displacement parameters ($Å^2$x 10^3) for **22**.

	x	y	z	U(eq)
H(4)	12533	6129	10315	19
H(5)	15060	6934	10531	23
H(6)	14148	7802	11389	25
H(7)	10842	7799	12052	24
H(8A)	9205	5683	8705	21
H(8B)	9322	5001	8377	21
H(9A)	7543	6255	6167	21
H(9B)	7926	6417	7389	21
H(10A)	7688	5199	5667	21

H(10B)	8180	4713	6581	21
H(11A)	4027	5727	5338	21
H(11B)	2228	5565	6042	21
H(12A)	2611	5959	7764	17
H(12B)	4900	6298	8311	17
H(13A)	5206	4382	7404	18
H(13B)	2809	4723	7183	18
H(1S)	7321	8167	7779	20

Appendix II.7. Crystal data and parameters for trans-[Pt{C_2(o-py)}$_2$(PTA)$_2$] (19b)

Table II.7.1. Atomic coordinates (x 10^4) and equivalent isotropic displacement parameters (Å^{2}x 10^3) for **19b**. U(eq) is defined as one third of the trace of the orthogonalized U^{ij} tensor.

	x	y	z	U(eq)
Pt(1)	0	10000	10000	10(1)
P(1)	981(1)	8954(1)	7900(1)	10(1)
N(1)	214(2)	6834(1)	5457(1)	13(1)
N(2)	3987(1)	7668(1)	6259(1)	12(1)
N(3)	1866(2)	9221(1)	5525(1)	12(1)
N(4)	4243(2)	6759(1)	12194(1)	18(1)
C(1)	1862(2)	8821(1)	10593(1)	13(1)
C(2)	3014(2)	8083(1)	10915(1)	14(1)
C(3)	4533(2)	7240(1)	11183(1)	12(1)
C(4)	6298(2)	6972(1)	10409(1)	15(1)
C(5)	7809(2)	6199(1)	10688(1)	17(1)
C(6)	7525(2)	5706(1)	11727(1)	19(1)
C(7)	5735(2)	6014(2)	12439(1)	21(1)
C(8)	-679(2)	7333(1)	6760(1)	13(1)
C(9)	3588(2)	8276(1)	7670(1)	12(1)
C(10)	1163(2)	10034(1)	6826(1)	12(1)
C(11)	2365(2)	6443(1)	5550(1)	14(1)

C(12)	328(2)	7939(1)	4841(1)	13(1)
C(13)	3971(2)	8760(1)	5633(1)	14(1)

Table II.7.2. Anisotropic displacement parameters ($Å^2 x\ 10^3$) for **19b**. The anisotropic displacement factor exponent takes the form: $-2\pi^2[\ h^2\ a^{*2}U^{11} + ... + 2\ h\ k\ a^*\ b^*\ U^{12}\ ]$

	U^{11}	U^{22}	U^{33}	U^{23}	U^{13}	U^{12}
Pt(1)	9(1)	12(1)	10(1)	6(1)	2(1)	3(1)
P(1)	10(1)	12(1)	10(1)	5(1)	1(1)	3(1)
N(1)	13(1)	11(1)	15(1)	5(1)	-2(1)	0(1)
N(2)	10(1)	14(1)	12(1)	4(1)	1(1)	2(1)
N(3)	14(1)	11(1)	10(1)	4(1)	0(1)	1(1)
N(4)	21(1)	23(1)	14(1)	9(1)	4(1)	11(1)
C(1)	13(1)	15(1)	12(1)	6(1)	2(1)	3(1)
C(2)	13(1)	15(1)	14(1)	6(1)	0(1)	4(1)
C(3)	12(1)	13(1)	11(1)	3(1)	-2(1)	4(1)
C(4)	13(1)	16(1)	16(1)	6(1)	2(1)	3(1)
C(5)	13(1)	15(1)	20(1)	4(1)	1(1)	4(1)
C(6)	19(1)	17(1)	19(1)	5(1)	-1(1)	9(1)
C(7)	27(1)	27(1)	16(1)	12(1)	4(1)	15(1)
C(8)	10(1)	14(1)	16(1)	8(1)	0(1)	0(1)
C(9)	10(1)	16(1)	12(1)	6(1)	0(1)	3(1)
C(10)	16(1)	11(1)	11(1)	5(1)	1(1)	2(1)
C(11)	14(1)	11(1)	16(1)	4(1)	0(1)	3(1)
C(12)	16(1)	13(1)	12(1)	4(1)	-3(1)	1(1)
C(13)	13(1)	15(1)	12(1)	6(1)	3(1)	1(1)

Table II.7.3. Hydrogen coordinates ($x\ 10^4$) and isotropic displacement parameters ($Å^2 x\ 10^3$) for **19b**.

	x	y	z	U(eq)

H(4)	6420(30)	7329(19)	9730(15)	15(4)
H(5)	9020(20)	6040(20)	10220(20)	29(5)
H(6)	8490(30)	5190(20)	11970(20)	24(5)
H(7)	5530(40)	5680(20)	13126(17)	30(6)
H(8A)	-700(30)	6540(18)	7081(19)	19(4)
H(8B)	-2100(20)	7570(20)	6640(20)	23(5)
H(9A)	4720(30)	9060(20)	8140(20)	20(5)
H(9B)	3570(30)	7540(20)	7985(18)	12(4)
H(10A)	-210(20)	10300(20)	6736(18)	14(4)
H(10B)	2140(30)	10876(16)	7252(18)	15(4)
H(11A)	2730(30)	5996(19)	4658(13)	13(4)
H(11B)	2290(30)	5711(16)	5935(16)	8(4)
H(12A)	770(30)	7500(19)	3957(14)	14(4)
H(12B)	-1070(20)	8250(20)	4821(19)	16(4)
H(13A)	5010(30)	9586(17)	6138(18)	19(5)
H(13B)	4470(30)	8342(19)	4744(14)	12(4)

Appendix II.8. Crystal data and parameters for cis-[Pt{C_2(p-tol)}$_2$($PTA)_2$] (16)

Table II.8.1. Atomic coordinates (x 10^4) and equivalent isotropic displacement parameters (Å^2 x 10^3)

for **16**. U(eq) is defined as one third of the trace of the orthogonalized U^{ij} tensor.

	x	y	z	U(eq)
Pt(1)	4174(1)	1342(1)	7248(1)	12(1)
P(1)	3285(1)	655(1)	7825(1)	13(1)
P(2)	4998(1)	2054(1)	7824(1)	14(1)
N(1)	3560(2)	-565(1)	8274(1)	18(1)
N(2)	1549(2)	-263(1)	8002(1)	19(1)
N(3)	2419(2)	264(1)	8767(1)	17(1)
N(4)	6148(2)	2321(1)	8732(1)	20(1)
N(5)	4637(2)	3119(1)	8461(1)	19(1)
N(6)	6547(2)	3077(1)	8008(1)	21(1)

C(1)	3447(2)	754(1)	6709(1)	16(1)
C(2)	2954(2)	402(1)	6403(1)	18(1)
C(3)	2309(2)	-4(1)	6045(1)	19(1)
C(4)	1730(2)	-576(1)	6200(1)	20(1)
C(5)	1101(2)	-958(1)	5851(1)	24(1)
C(6)	1037(3)	-793(2)	5335(1)	27(1)
C(7)	1605(3)	-222(2)	5180(1)	40(1)
C(8)	2230(3)	166(2)	5524(1)	35(1)
C(9)	359(3)	-1206(2)	4952(1)	38(1)
C(10)	5016(2)	1820(1)	6686(1)	17(1)
C(11)	5580(2)	2068(1)	6340(1)	16(1)
C(12)	6262(2)	2307(1)	5912(1)	14(1)
C(13)	6454(2)	1896(1)	5486(1)	21(1)
C(14)	7105(2)	2116(1)	5069(1)	22(1)
C(15)	7610(2)	2738(1)	5062(1)	18(1)
C(16)	7431(3)	3142(1)	5490(1)	20(1)
C(17)	6760(2)	2934(1)	5907(1)	18(1)
C(18)	8321(3)	2973(2)	4608(1)	24(1)
C(19)	4177(2)	-87(1)	7946(1)	16(1)
C(20)	1895(2)	257(1)	7636(1)	19(1)
C(21)	2867(2)	853(1)	8497(1)	17(1)
C(22)	2445(3)	-777(1)	8040(1)	21(1)
C(23)	3295(2)	-265(1)	8778(1)	19(1)
C(24)	1346(2)	12(1)	8516(1)	20(1)
C(25)	5740(2)	1765(1)	8415(1)	20(1)
C(26)	4009(2)	2672(1)	8112(1)	17(1)
C(27)	6162(2)	2619(1)	7599(1)	21(1)
C(28)	5176(2)	2751(1)	8887(1)	22(1)
C(29)	7023(2)	2717(1)	8452(1)	23(1)
C(30)	5561(2)	3486(1)	8187(1)	22(1)
C(31)	5166(6)	212(3)	5338(2)	27(1)
Cl(1)	4933(8)	-637(3)	5325(2)	49(2)
Cl(2)	4931(7)	572(3)	4712(2)	45(1)

Table II.8.2. Anisotropic displacement parameters ($Å^2 x\ 10^3$) for **16**. The anisotropic displacement factor exponent takes the form: $-2\pi^2[\ h^2\ a^{*2}U^{11} + ...\ + 2\ h\ k\ a^*\ b^*\ U^{12}\ ]$

	U^{11}	U^{22}	U^{33}	U^{23}	U^{13}	U^{12}
Pt(1)	12(1)	11(1)	14(1)	1(1)	1(1)	0(1)
P(1)	12(1)	12(1)	14(1)	0(1)	1(1)	0(1)
P(2)	13(1)	12(1)	17(1)	0(1)	2(1)	0(1)
N(1)	20(1)	14(1)	18(1)	3(1)	2(1)	1(1)
N(2)	15(1)	22(1)	20(1)	3(1)	1(1)	-6(1)
N(3)	17(1)	19(1)	15(1)	1(1)	3(1)	-1(1)
N(4)	17(1)	20(1)	23(1)	-1(1)	-4(1)	-1(1)
N(5)	17(1)	17(1)	23(1)	-5(1)	-2(1)	1(1)
N(6)	18(1)	20(1)	24(1)	-4(1)	1(1)	-7(1)
C(1)	16(1)	15(1)	17(1)	4(1)	3(1)	2(1)
C(2)	17(1)	18(1)	18(1)	1(1)	2(1)	2(1)
C(3)	20(1)	20(1)	17(1)	-2(1)	-1(1)	3(1)
C(4)	21(1)	20(1)	20(1)	-4(1)	0(1)	2(1)
C(5)	20(1)	23(1)	29(1)	-6(1)	-1(1)	2(1)
C(6)	25(2)	30(2)	27(1)	-10(1)	-8(1)	3(1)
C(7)	56(2)	45(2)	19(1)	1(1)	-12(1)	-11(2)
C(8)	51(2)	32(2)	21(1)	5(1)	-7(1)	-12(1)
C(9)	33(2)	42(2)	37(2)	-15(1)	-14(1)	1(1)
C(10)	17(1)	16(1)	17(1)	0(1)	-1(1)	0(1)
C(11)	16(1)	16(1)	17(1)	0(1)	-1(1)	2(1)
C(12)	13(1)	17(1)	14(1)	1(1)	-1(1)	1(1)
C(13)	21(1)	20(1)	22(1)	-4(1)	4(1)	-3(1)
C(14)	20(1)	27(1)	19(1)	-8(1)	4(1)	-1(1)
C(15)	15(1)	24(1)	15(1)	0(1)	2(1)	1(1)
C(16)	23(1)	17(1)	20(1)	1(1)	2(1)	-3(1)
C(17)	22(1)	18(1)	15(1)	-1(1)	3(1)	-2(1)
C(18)	23(1)	33(2)	18(1)	-2(1)	7(1)	-4(1)
C(19)	15(1)	14(1)	19(1)	2(1)	4(1)	2(1)
C(20)	15(1)	24(1)	17(1)	3(1)	0(1)	-5(1)
C(21)	19(1)	15(1)	17(1)	0(1)	5(1)	1(1)
C(22)	26(1)	14(1)	22(1)	0(1)	4(1)	-6(1)
C(23)	21(1)	20(1)	16(1)	4(1)	2(1)	-1(1)
C(24)	14(1)	25(1)	20(1)	4(1)	4(1)	-2(1)

C(25)	18(1)	16(1)	26(1)	2(1)	-4(1)	0(1)
C(26)	14(1)	16(1)	21(1)	-2(1)	0(1)	2(1)
C(27)	20(1)	23(1)	21(1)	-4(1)	6(1)	-9(1)
C(28)	21(1)	25(1)	18(1)	-3(1)	-2(1)	0(1)
C(29)	16(1)	24(1)	30(1)	-4(1)	-1(1)	-2(1)
C(30)	23(1)	15(1)	29(1)	-1(1)	-2(1)	-2(1)
C(31)	36(3)	21(2)	24(2)	-4(2)	-13(2)	4(2)
Cl(1)	66(3)	21(1)	61(3)	-14(1)	-30(2)	2(1)
Cl(2)	66(3)	50(3)	20(1)	-6(1)	-18(1)	32(2)

Table II.8.3. Hydrogen coordinates (x 10^4) and isotropic displacement parameters ($Å^2$x 10^3) for **16**.

	x	y	z	U(eq)
H(4)	1765	-708	6552	24
H(5)	704	-1343	5970	28
H(7)	1566	-92	4828	48
H(8)	2613	554	5404	42
H(9A)	70	-1608	5122	56
H(9B)	876	-1328	4664	56
H(9C)	-310	-951	4820	56
H(13)	6134	1462	5482	25
H(14)	7209	1832	4780	26
H(16)	7776	3570	5496	24
H(17)	6640	3224	6191	22
H(18A)	8753	2599	4459	37
H(18B)	8880	3312	4722	37
H(18C)	7795	3161	4346	37
H(19A)	4377	-298	7613	19
H(19B)	4922	45	8116	19
H(20A)	1266	595	7619	22
H(20B)	1983	62	7288	22

H(21A)	3560	1028	8684	20
H(21B)	2253	1201	8496	20
H(22A)	2610	-947	7688	25
H(22B)	2123	-1148	8245	25
H(23A)	3013	-616	9014	23
H(23B)	4033	-85	8925	23
H(24A)	996	-336	8737	24
H(24B)	768	376	8489	24
H(25A)	5188	1491	8619	24
H(25B)	6420	1485	8320	24
H(26A)	3635	2933	7833	20
H(26B)	3378	2442	8305	20
H(27A)	6845	2357	7480	26
H(27B)	5866	2878	7302	26
H(28A)	5469	3071	9146	26
H(28B)	4563	2478	9055	26
H(29A)	7377	3040	8695	28
H(29B)	7660	2421	8331	28
H(30A)	5871	3834	8420	27
H(30B)	5204	3710	7885	27
H(31A)	5982	303	5451	32
H(31B)	4623	418	5590	32

Appendix II.9. Crystal data and parameters for ipac mPTA (L1) triflate

Table II.9.1. Cryatal data parameters for **L1**.

Bond precision: C-C = 0.0044 Å Wavelength = 0.71073 Å

Cell: a = 8.2446(3), b = 10.3581(5), c = 16.4757(7)

Alpha = 108.059(2), beta = 99.716(2), gamma = 91.297(3). Temperature: 100 K

Volume: 1314.28(10), 1314.27(10) $Å^3$ Space group P-1

Sum formula C_{18} H_{32} F_6 $N_3O_8PS_2$	MW = 627.58, 627.56
Dx, g cm^{-3} 1.586, 1.586	Z = 2
Mu (mm^{-1}) 0.354, 0.354	F000 652.0, 652.0
F000' 653.15	N_{ref} 6049, 5829
T_{min},T_{max} 0.938, 0.969, 0.831, 0.969	T_{min}' 0.826
Data completeness = 0.964	Theta (max) = 27.500

R (reflections) = 0.0506(4721) wR2 (reflections) = 0.1327(5829) S = 1.068 Npar = 347

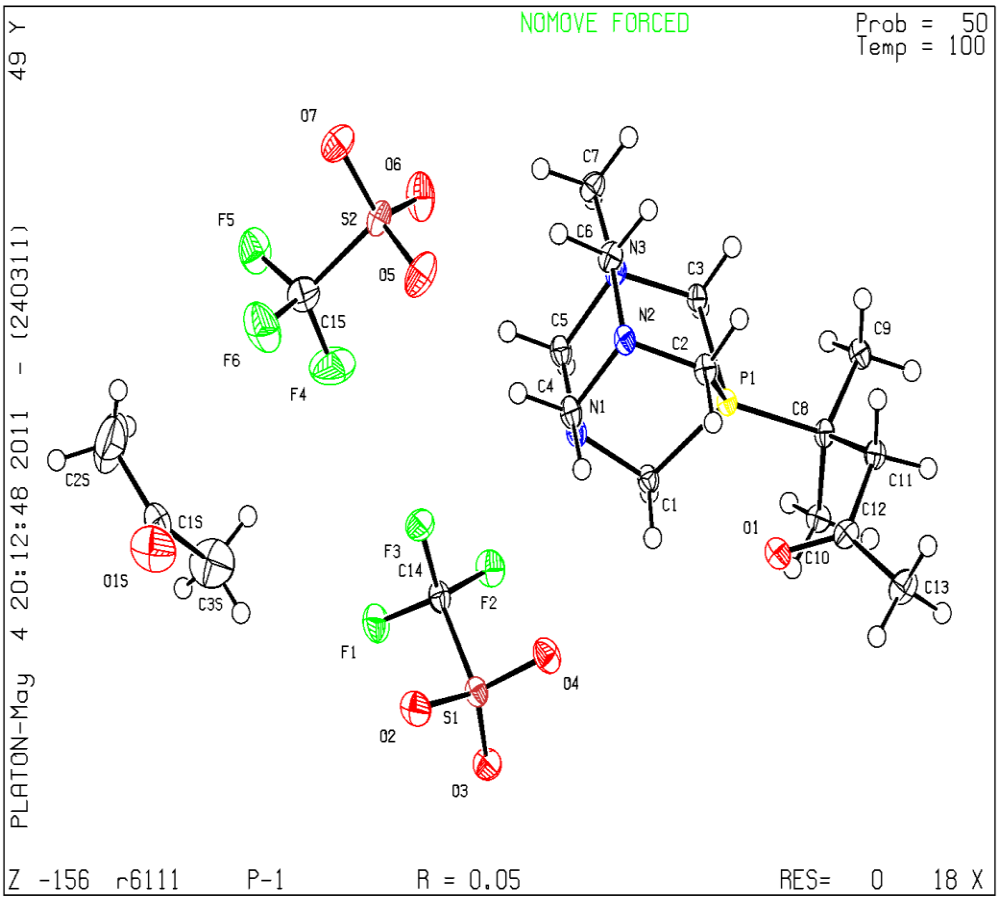

Figure II.2. CheckCIF file of **L1** triflate.

4.3. Appendix III. SEM Images and EDS Spectra

Appendix III.1. SEM images

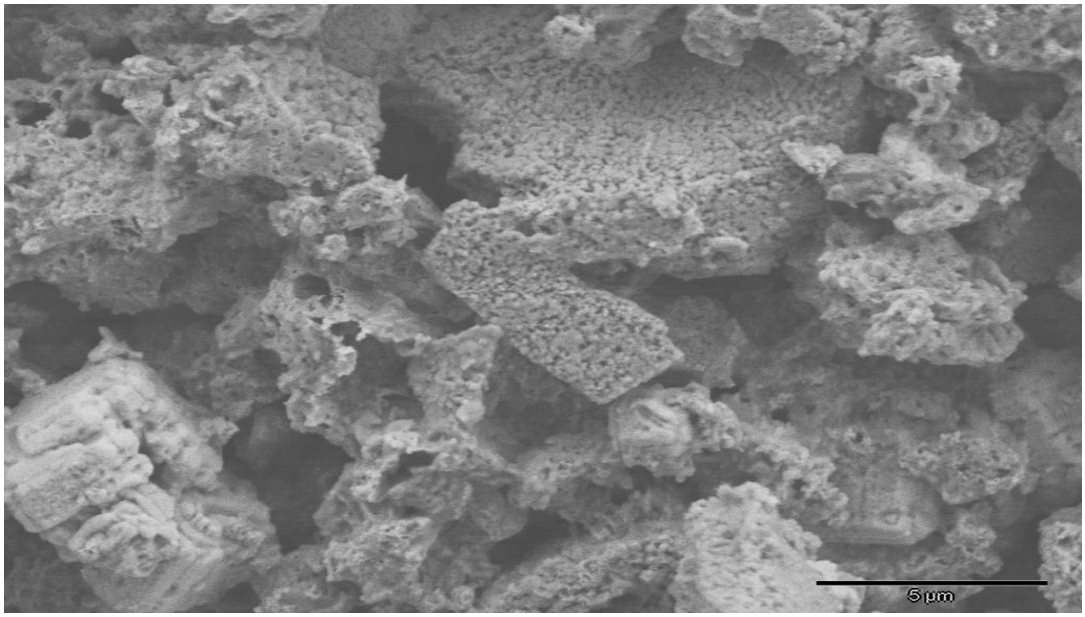

(a) SEM magnification @ 5,000X

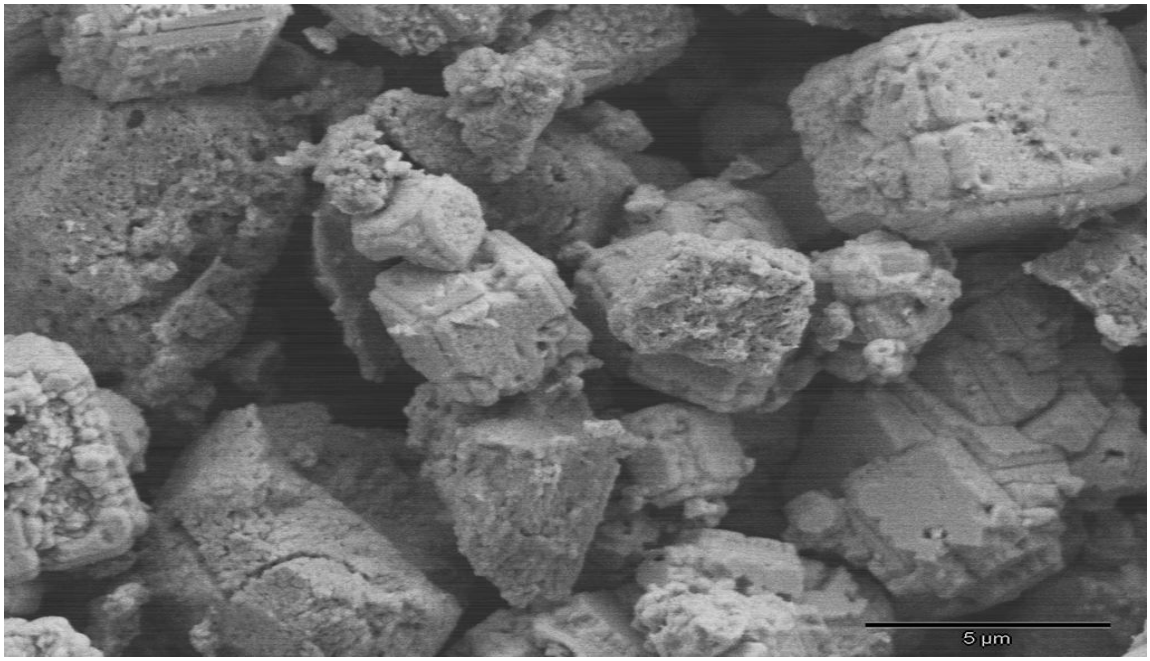

(b) SEM magnification @ 5,000X

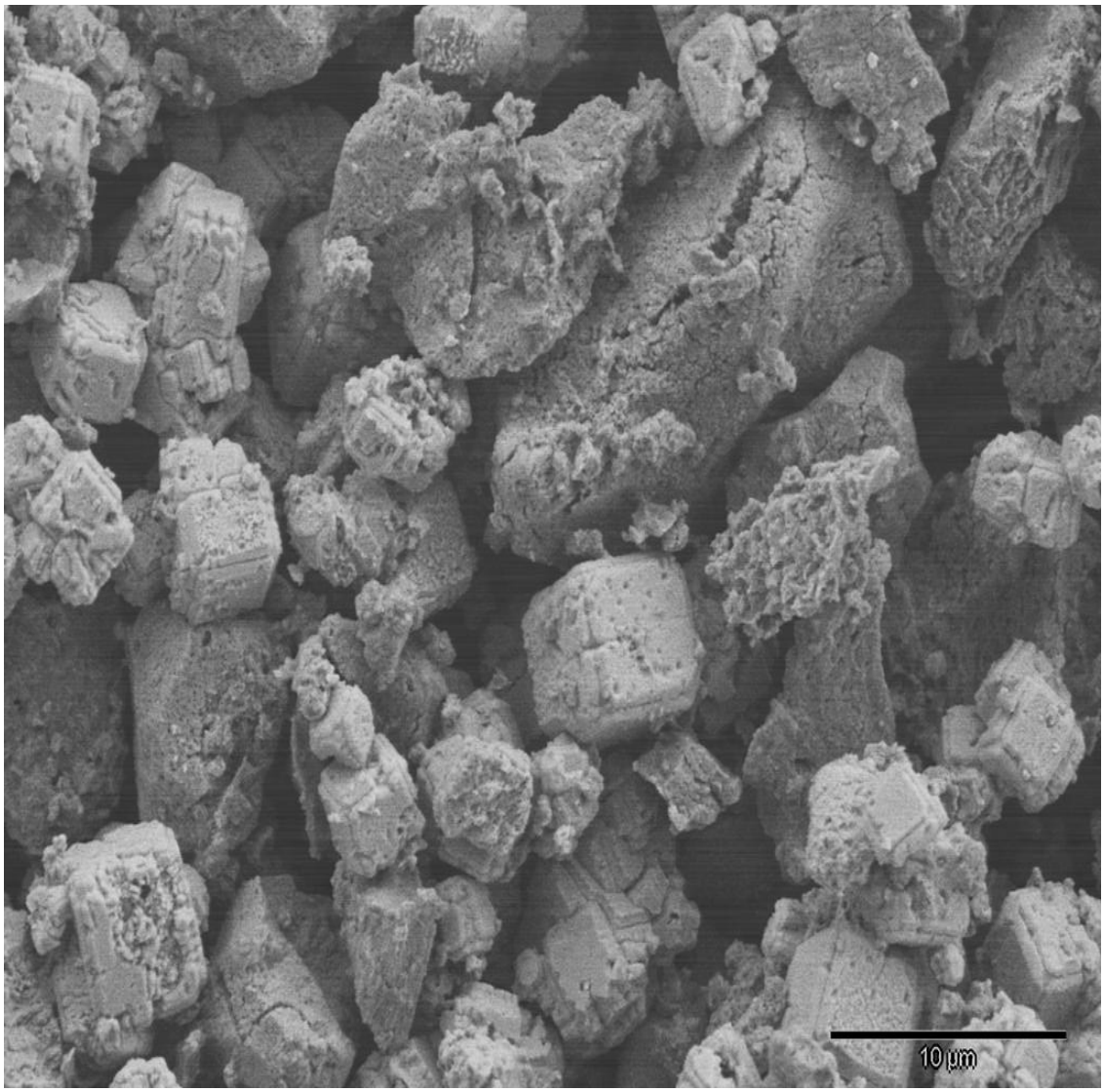

(c) SEM magnification @ 2500X

Figure III.1. SEM images of residual Pd species in Suzuki-Miyaura cross-coupling reaction of 4-bromoacetophenone (**R1**) and phenylboronic acid (**T1**) in ^{i}PrOH (a) before washing and (b) & (c) after washing the residual species with water.

Appendix III.2. EDS spectra

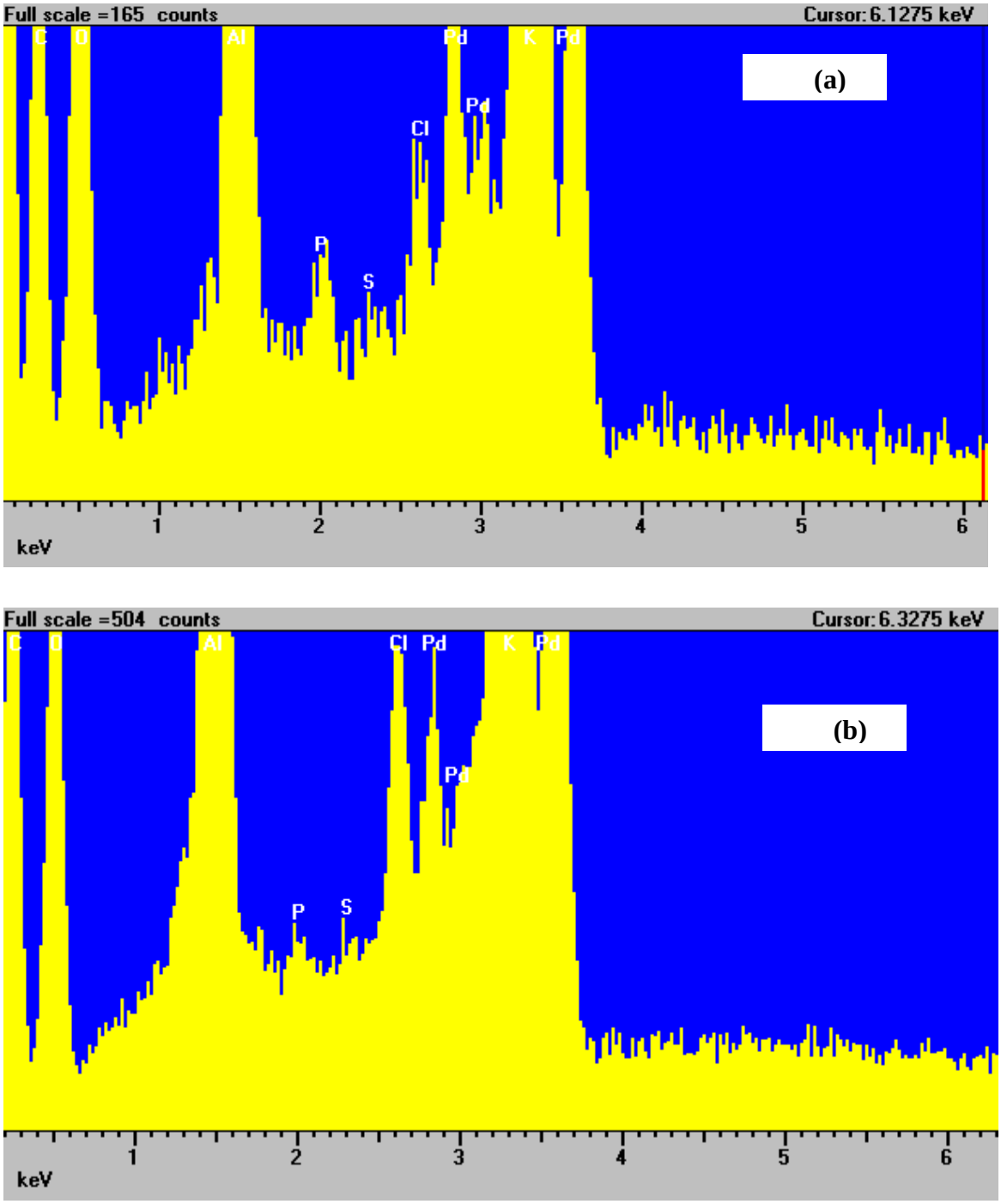

Figure III.2. EDS spectra of residual Pd species in Suzuki-Miyaura cross-coupling reaction of 4-bromoacetophenone (**R1**) and phenylboronic acid (**T1**) in ^{i}PrOH (a) before washing and (b) after washing the residual species with water. The presence of Al is from the sample holder.

4.4 Appendix IV. IR Spectra

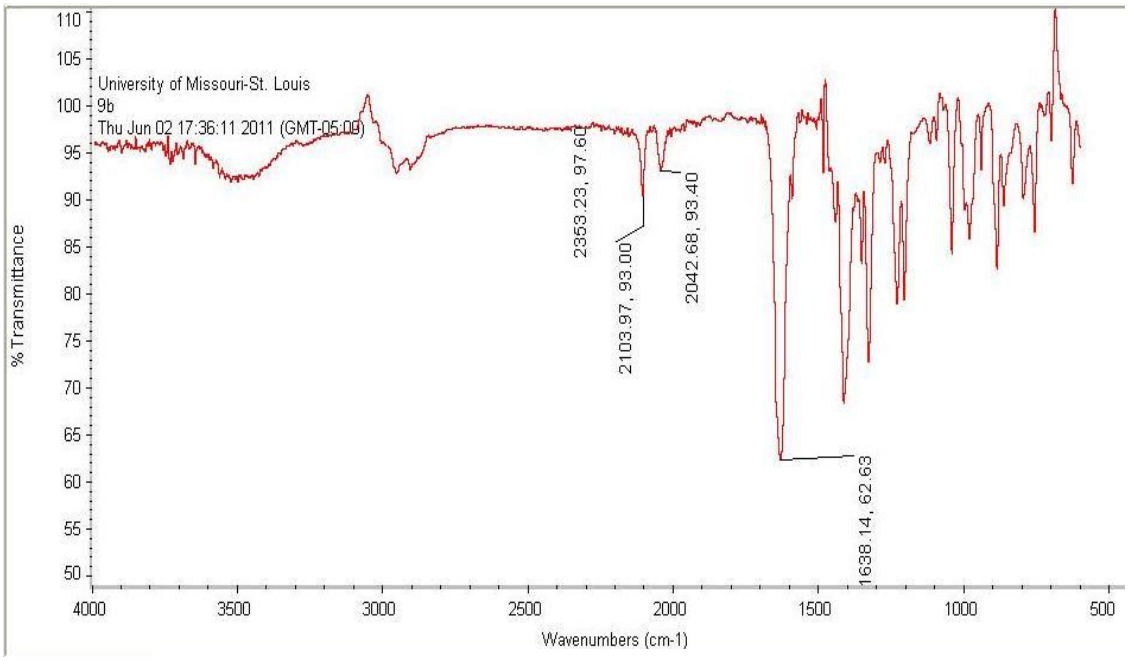

Appendix IV.1. IR spectrum of cis-Pt(C₂Ph)₂(PTA)₂, 6a.

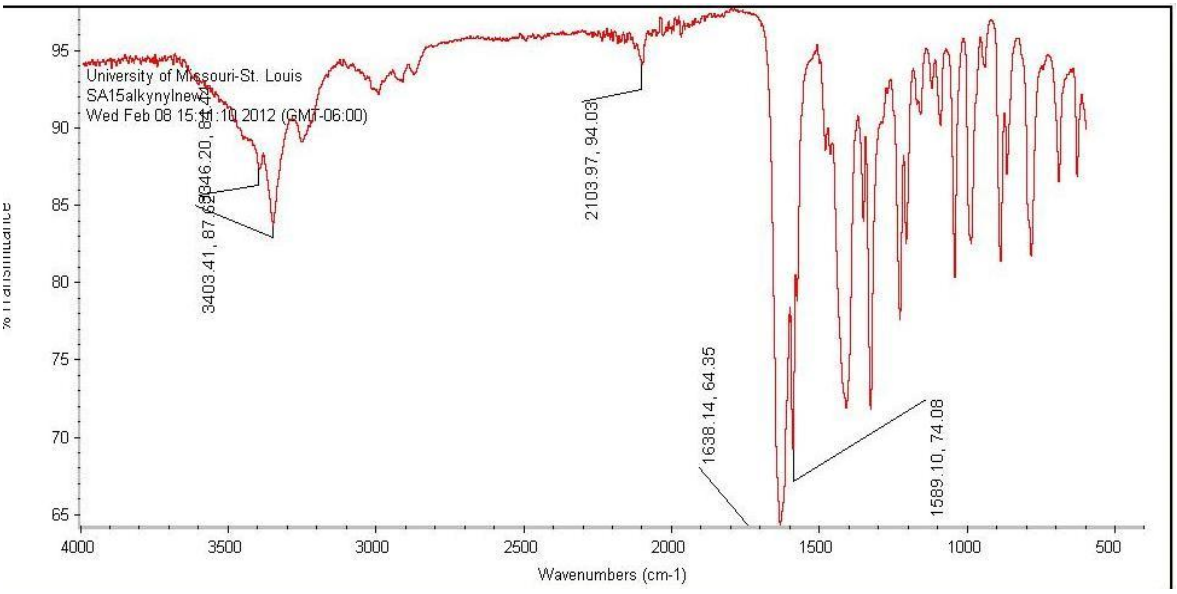

Appendix IV.2. IR spectrum of cis-[Pt{C₂(m-C₆H₄NH₂)}₂(DAPTA)₂], 26.

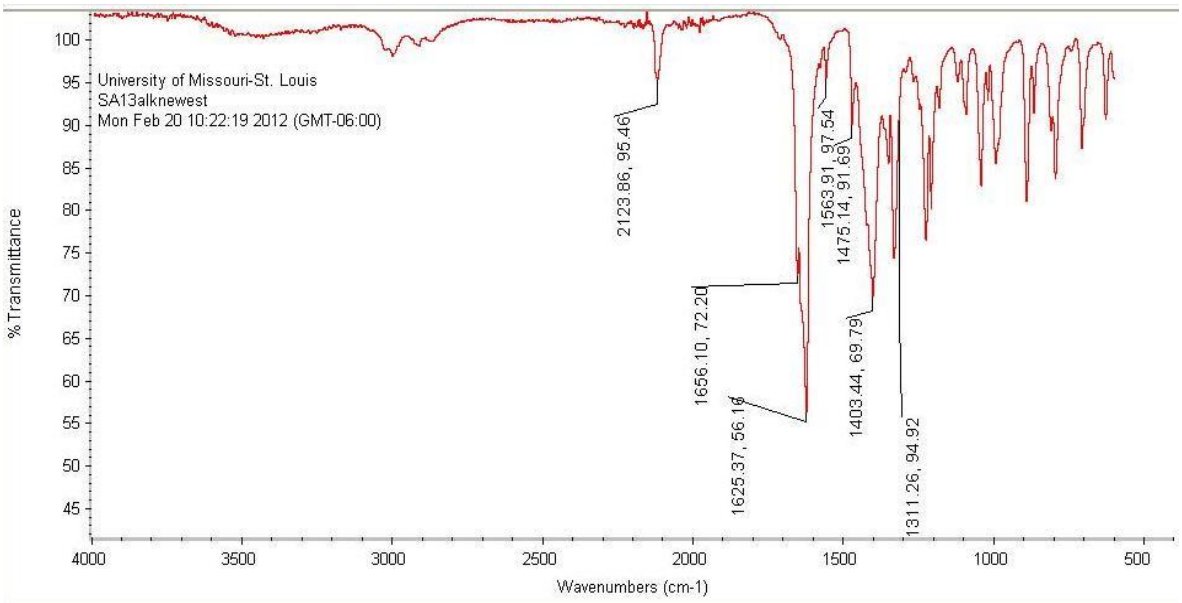

Appendix IV.3. IR spectrum of cis-[Pt{C_2(m-py)}$_2$(DAPTA)$_2$], 27.

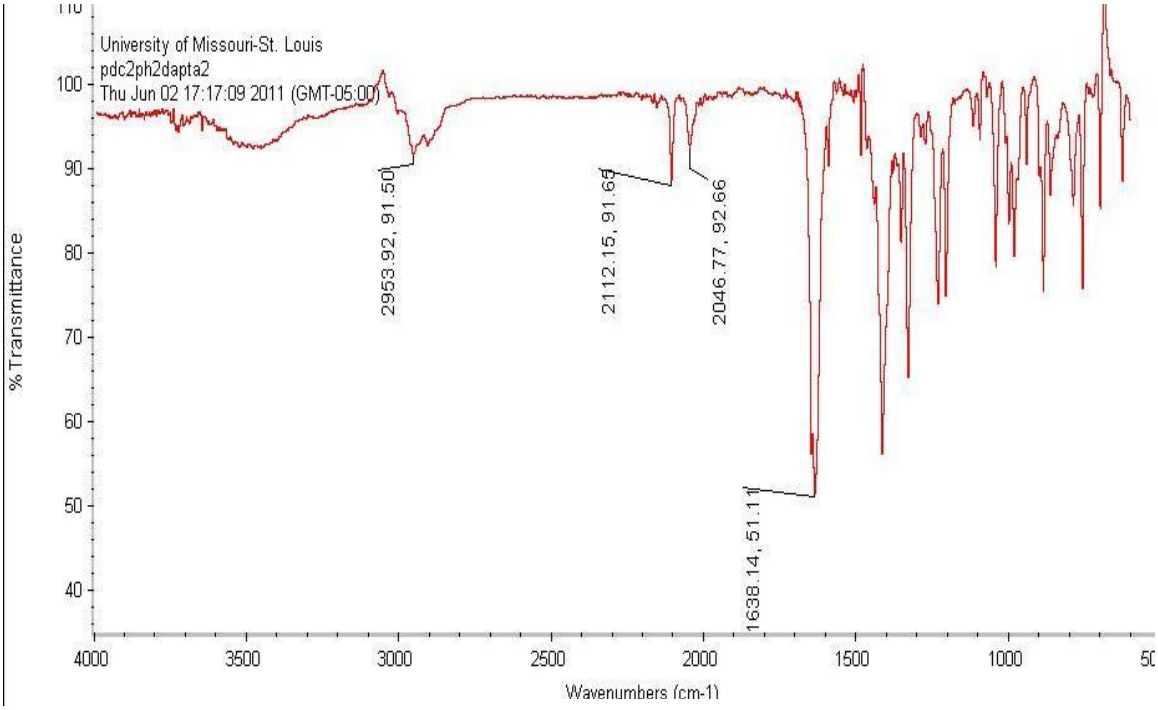

Appendix IV.4. IR spectrum of trans-Pd(C_2Ph)$_2$(DAPTA)$_2$, 14.

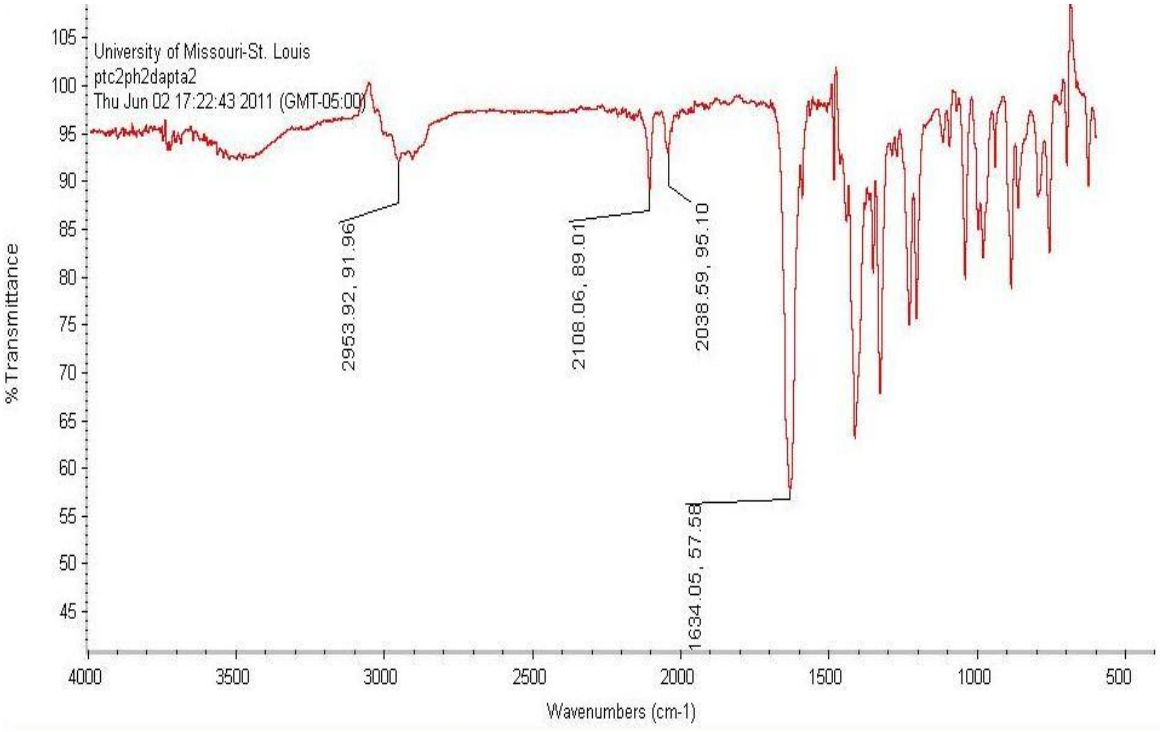

Appendix IV.5. IR spectrum of cis-Pt(C_2Ph)$_2$(DAPTA)$_2$, 13a.

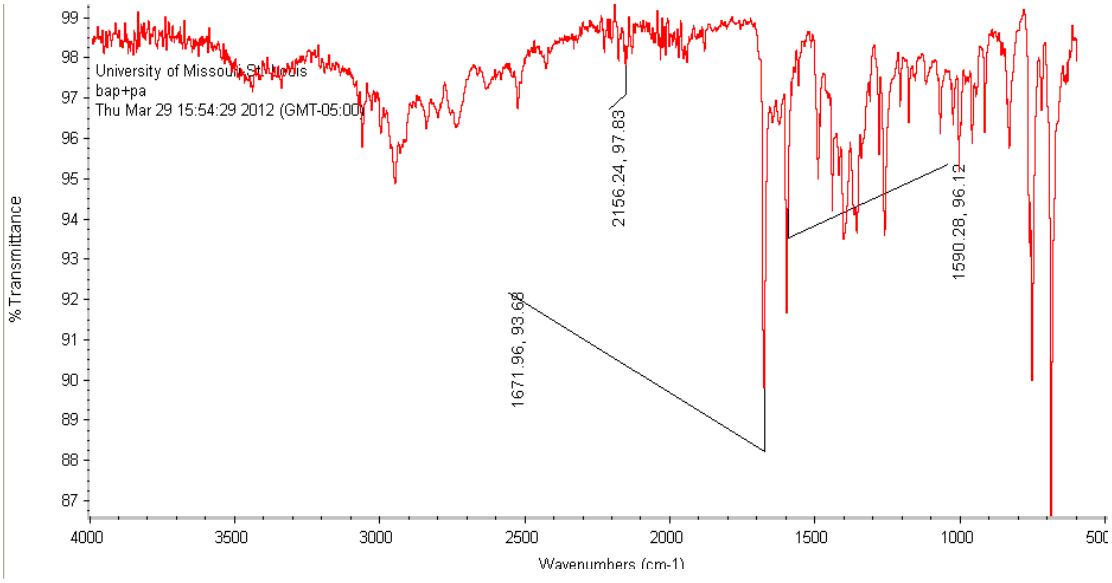

Appendix IV.6. IR spectrum of the product from Sonogashira cross-coupling reaction of 4-bromoacetophenone (R1) and phenylacetylene (A4) in the presence of (M1).

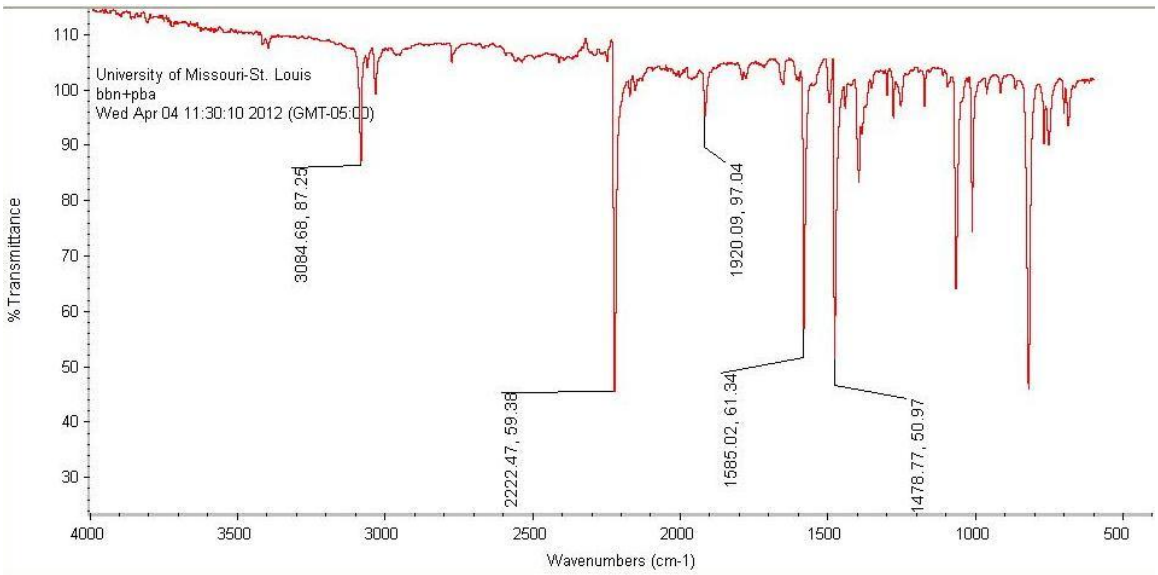

Appendix IV.7. IR spectrum of the product from Suzuki-Miyaura cross-coupling reaction of 4-bromobenzonitrile (R4) and phenylboronic acid (T1) in the presence of (5a).

4.5 Appendix V. Mass Spectra

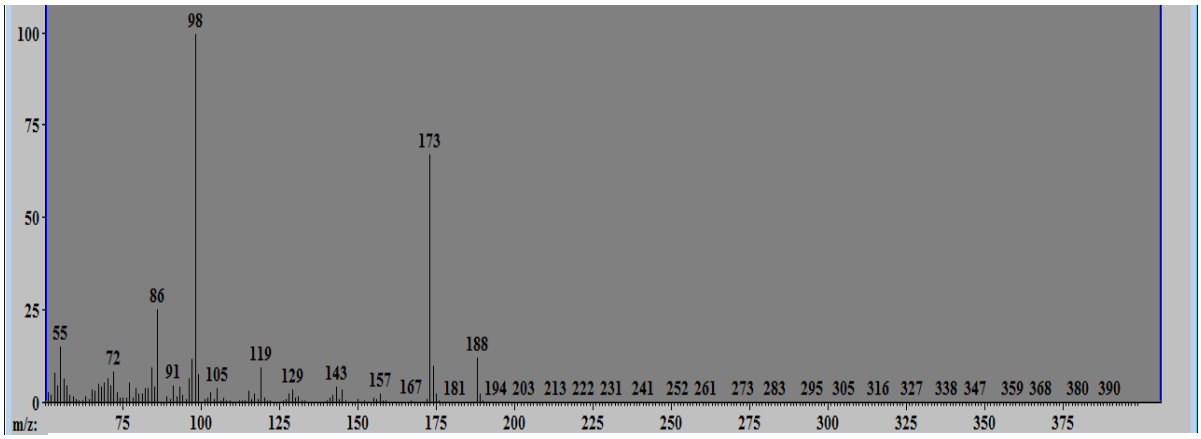

Appendix V.1. GC-MS spectra of the product from Sonogashira cross-coupling reaction of 4-iodotoluene (R3) and trimethylsilylacetylene (A2) in the presence of (M1).

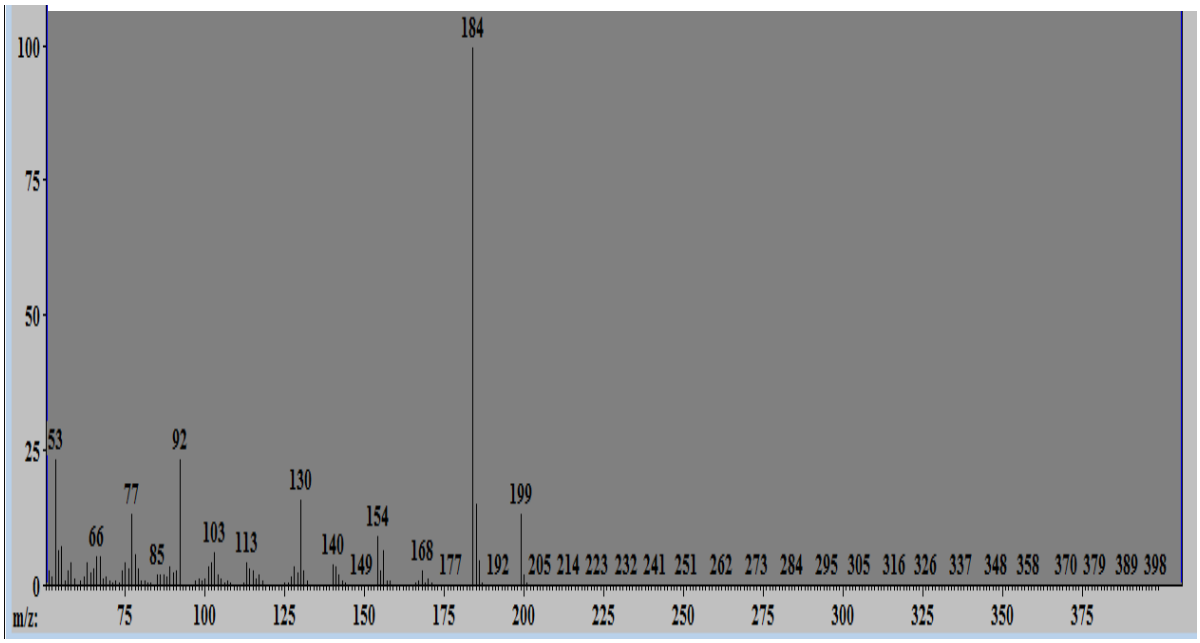

Appendix V.2. GC-MS spectra of the product from Sonogashira cross-coupling reaction of 4-bromobenzonitrile (R4) and trimethylsilylacetylene (A2) in the presence of (M1).

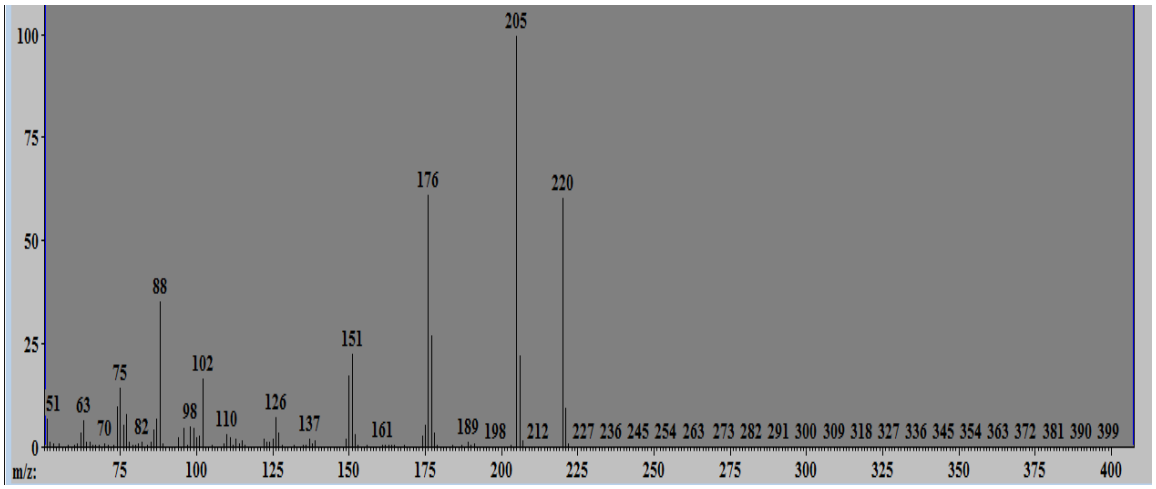

Appendix V.3. GC-MS spectra of the product from Sonogashira cross-coupling reaction of 4-bromoacetophenone (R1) and phenylacetylene (A4) in the presence of (M1).

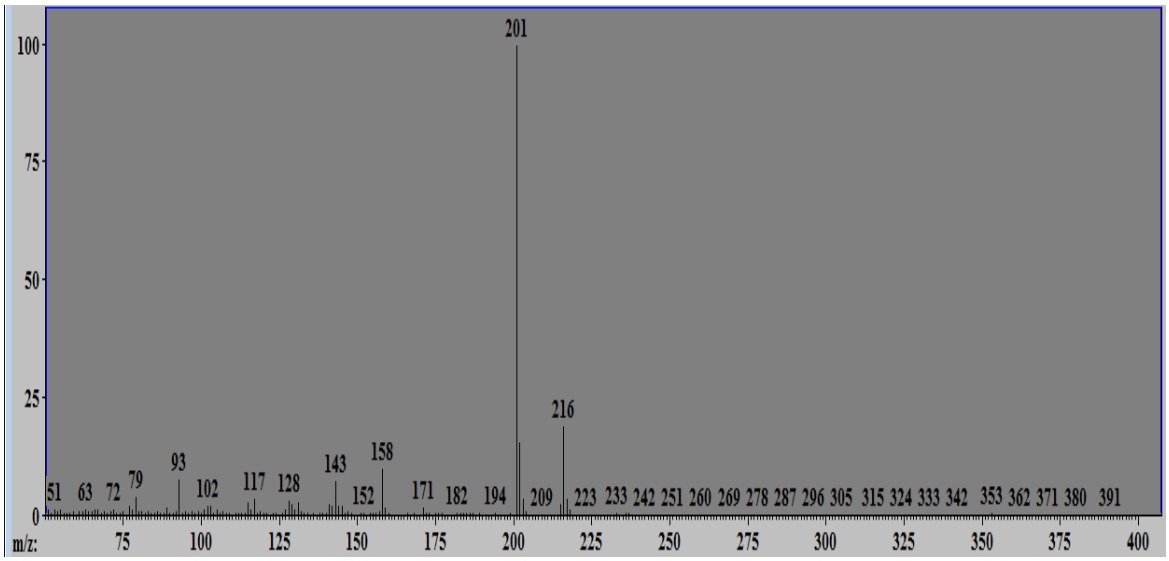

Appendix V.4. GC-MS spectra of the product from Sonogashira cross-coupling reaction of 4-bromobenzonitrile (R1) and trimethylsilylacetylene (A2) in the presence of (M1).

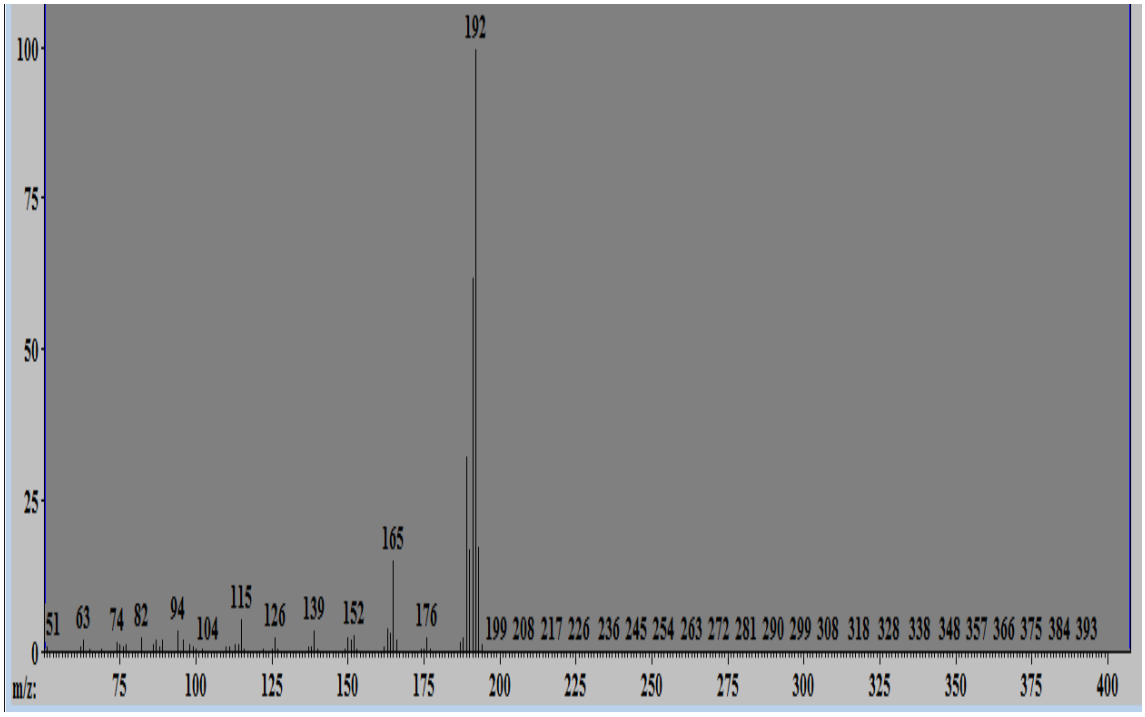

Appendix V.5. GC-MS spectra of the product from Sonogashira cross-coupling reaction of 4-iodotoluene (R3) and phenylacetylene (A4) in the presence of (M1).

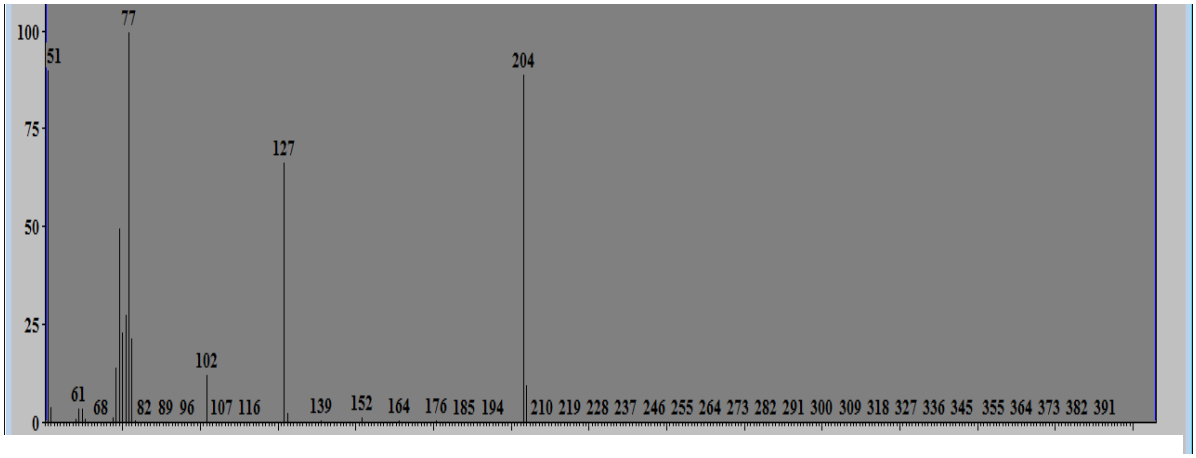

Appendix V.6. GC-MS spectra of the product from Sonogashira cross-coupling reaction of 4-bromobenzonitrile (R4) and phenylacetylene (A4) in the presence of (M1).

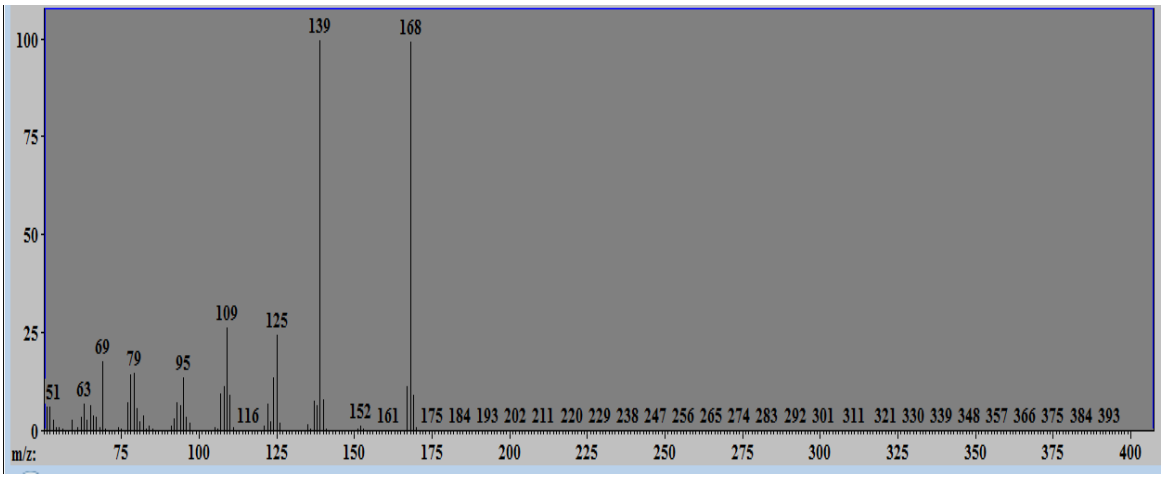

Appendix V.7. GC-MS spectra of the product from Suzuki-Miyaura cross-coupling reaction of 4-iodotoluene (R3) and phenylboronic acid (T1) in the presence of (5a).

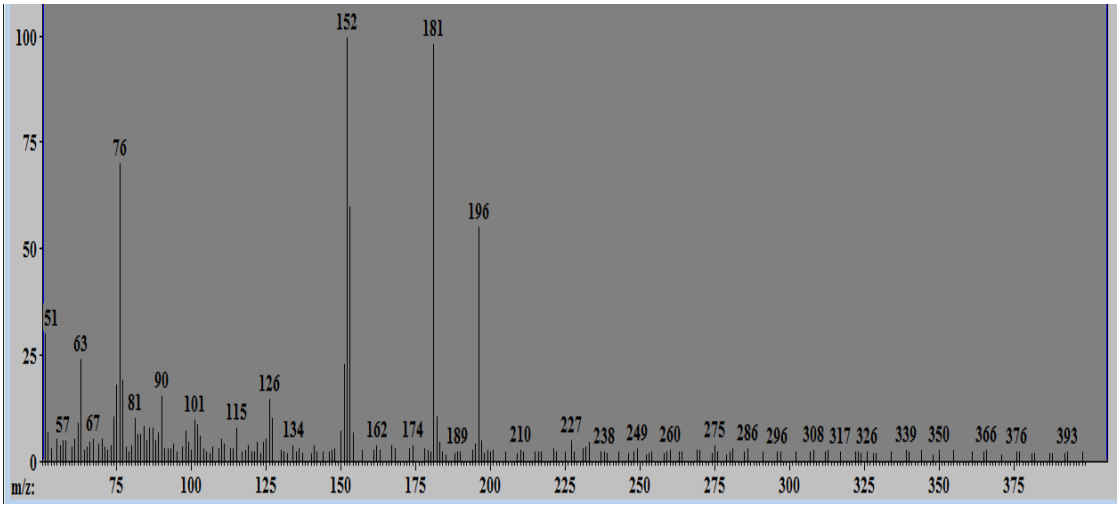

Appendix V.8. GC-MS spectra of the product from Suzuki-Miyaura cross-coupling reaction of 4-bromoacetophenone (R1) and phenylboronic acid (T1) in the presence of (5a).

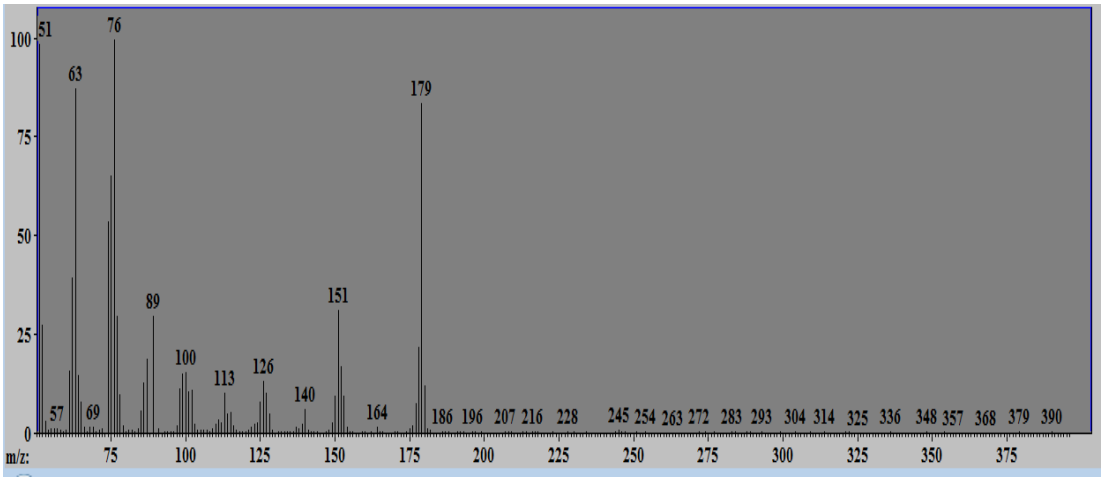

Appendix V.9. GC-MS spectra of the product from Suzuki-Miyaura cross-coupling reaction of 4-bromobenzonitrile (R4) and phenylboronic acid (T1) in the presence of (5a).

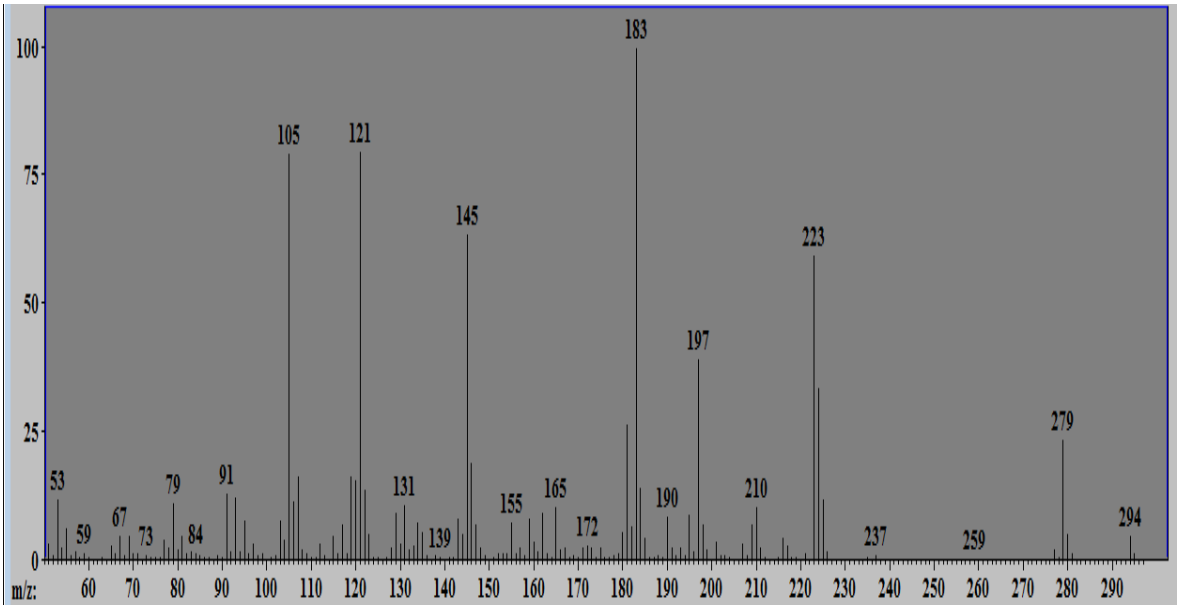

Appendix V.10. GC-MS spectra of the product from hydrosilylation reaction of 1-heptyne (A1) and methyldiphenylsilane (S1) in the presence of (B2).

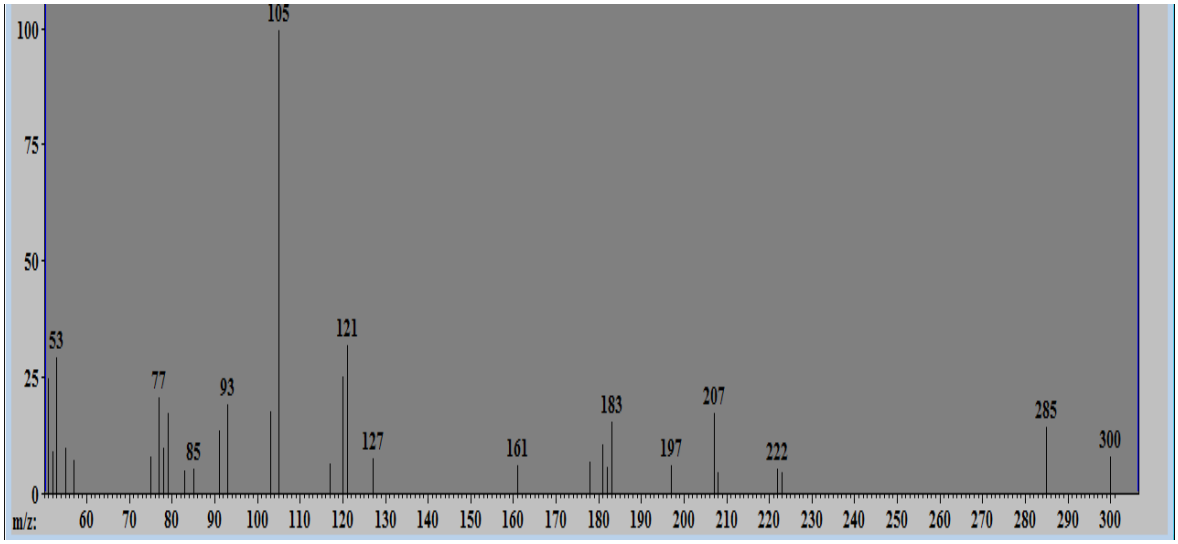

Appendix V.11. GC-MS spectra of the product from hydrosilylation reaction of phenylacetylene and methyldiphenylsilane (S1) in the presence of (1a).